Universitat
de les Illes Balears

DOCTORAL THESIS

MESOPHYLL CONDUCTANCE ADAPTATION AND ACCLIMATIZATION BY ANATOMICAL ADJUSTMENTS

Marc Carriquí Alcover

2019

Universitat
de les Illes Balears

DOCTORAL THESIS

2019

Doctoral Programme of Plant Biology

MESOPHYLL CONDUCTANCE ADAPTATION AND ACCLIMATIZATION BY ANATOMICAL ADJUSTMENTS

Marc Carriquí Alcover

Thesis Supervisor: Jaume Flexas Sans

Thesis tutor: Jaume Flexas Sans

Doctor by the Universitat de les Illes Balears

Universitat de les Illes Balears

Dr. Jaume Flexas Sans, Professor Titular de la Universitat de les Illes Balears

DECLARO:

Que la tesi doctoral que porta per títol *Mesophyll conductance adaptation and acclimatization by anatomical adjustments*, presentada per Marc Carriquí Alcover per a l'obtenció del títol de doctor, ha estat realitzada sota la meva supervisió i que compleix amb els requisits necessaris per optar al títol de Doctor.

I perquè quedi constància d'això signo aquest document.

Signatura

Palma, 3 de maig del 2019

Al meu pare

Acknowledgements

Per a que es puguin assolir les grans fites que un es proposa a la vida és imprescindible comptar amb 'els teus'. Aquest conjunt de persones, 'els teus', són aquells que sempre hi són, aquells que et recolzen o t'ofereixen una oportunitat, aquells que t'ajuden a millorar, aquells que t'aprecien per com ets. Realitzar i escriure la tesi doctoral ha estat per a mi una d'aquestes grans fites. Per això, després de gairebé cinc anys d'intensa dedicació, passió, però també alhora sacrificis, estic immensament agraït de poder escriure aquestes línies per adreçar-me 'als meus'.

Especialment, a en Jaume Flexas així com a en Jeroni Galmés, però també a tots i cadascun dels integrants del Grup de Recerca en Biologia de les Plantes de la Universitat de les Illes Balears, els estic agraït per diversos motius. Primer de tot, per obrir-me les portes al fascinant món de la investigació i de la fisiologia vegetal des que tot just començava els meus estudis en el Grau en Biologia fins a l'actualitat. Al llarg d'aquests anys heu sabut encetar i alimentar la meva curiositat científica, que és el que em va dur a decidir-me a començar la tesi. Gràcies també per transmetre'm la vostra passió i entrega a la ciència, demostrant que és realment possible fer d'una afició la teva feina. Durant aquesta tesi he tengut la gran sort de poder treballar en equip i tenir alhora la total llibertat per experimentar en el que volgués per a poder resoldre les meves preguntes. També, però, fer la tesi amb vosaltres m'ha permès complir almenys dos dels somnis que nasqueren ja durant la meva infantesa. Per una banda, poder explorar alguns dels límits del coneixement científic envoltat de diversos dels millors investigadors de l'actualitat. Per altra banda, tenir la possibilitat de ser com un d'aquells investigadors que sortien als meus documentals de National Geographic per treballar en algunes de les darreres regions més prístines del planeta, com ho han estat la meves experiències a l'Antàrtida i als gegantins i antics boscs de Tasmània.

Estic agraït, també, a en Tim Brodribb, de la Universitat de Tasmània, a en León Bravo, de la Universitat de la Frontera, i a n'Ichiro Terashima i a en Yusuke Mizokami, de la Universitat de Tòquio, per haver-me acollit de la millor manera possible als seus respectius laboratoris. Fruit d'aquestes estades investigadores he pogut avançar en el desenvolupament de la meva tesi, iniciar-

me en diverses disciplines de la fisiologia vegetal, així com també enriquir-me personalment descobrint noves formes de pensar. Alhora, també, amb ells he tengut l'oportunitat de congriar noves i valuoses amistats.

Per descomptat, estic summament agraït a la meva família, especialment a na Cati, la meva mare. Gràcies per haver-hi estat sempre que m'heu fet falta. Sense el vostre recolzament aquesta tesi no seria la mateixa.

Finalment, estic extremament agraït a na Maria, la meva companya de viatge. Gràcies per estimar-me així com som. Sense el teu continuat suport, el qual, com bé saps, m'ha infós l'alè a continuar endavant en els moments més difícils, molts cops a costa de la teva paciència i sacrificis personals. Definitivament aquesta etapa que comprèn la realització de la tesi no hauria estat, ni de bon tros, tan dolça.

Funding

This work was supported by the PhD grants provided by the Universitat de les Illes Balears and by Conselleria d'Educació, Cultura i Universitats (Govern de les Illes Balears) and European Social Fund (FPI/1700/2014), consecutively, the projects BFU2011-23294 and CTM2014-53902-C2-1-P from the Ministerio de Economía y Competitividad (MINECO, Spain) and the European Regional Development Fund (FEDER), the travel grant provided by La Caixa Banking Foundation (2016), and the travel grant provided by the Vicepresidència i Conselleria d'Innovació, Recerca i Turisme del Govern de les Illes Balears (2017).

Symbols and abbreviations used along this Thesis

Symbols	Meaning
α	leaf absorptance
A_{area}	net assimilation per unit area
ABA	abscisic acid
A_{mass}	net assimilation per unit mass
A_N	net CO_2 assimilation rate
A_N/g_s	intrinsic water use efficiency
β	fraction of absorbed light that reaches photosystem II
C	cellulose
C_a	atmospheric CO_2 concentration
CA	carbonic anhydrases
C_c	chloroplast CO_2 concentration
Chl	chlorophyll
C_i	sub-stomatal CO_2 concentration
CMA	projected canopy mass per area
CO_2	carbon dioxide
C_s	leaf surface CO_2 concentration
ΔL_i	diffusion path length
ΔL_{ias}	diffusion path length in the gas-phase
D_a	diffusion coefficient for CO_2 in the gas-phase
D_L	leaf density
D_w	aqueous phase diffusion coefficient for CO_2
ETR	electron transport rate
Φ_{PSII}	effective photosystem II quantum yield
F	curvature correction factor
f_{ias}	fraction of mesophyll occupied by intercellular air spaces
F_m'	maximum fluorescence under illumination

F_s	steady-state fluorescence
Γ^*	CO_2 compensation point in absence of mitochondrial respiration
g_{ct}	cytosol conductance
g_{cw}	cell wall conductance
g_{en}	chloroplast envelope conductance
g_{ias}	gas phase conductance
g_{lip}	lipid phase conductance
g_{liq}	liquid phase conductance
g_m	mesophyll conductance to CO_2
$g_{m,anat}$	mesophyll conductance inferred by anatomy measurements
g_{nsd}	nonstomatal diffusion conductance to CO_2
g_{nsd_ANAT}	nonstomatal diffusion conductance to CO_2 modelled from foliage anatomical characteristics
g_{nsd_FLU}	nonstomatal diffusion conductance to CO_2 estimated from Chl fluorescence
g_{pl}	plasmalemma conductance
g_s	stomatal conductance
g_{st}	chloroplast stroma conductance
g_{tot}	total conductance to CO_2
H	Henry's law constant
H	hemicellulose
IRGA	infrared gas analyser
J_{max}	maximum electron transport rate
λ	lateral path lengthening
l_b	biochemical relative limitation
L_{chl}	chloroplast length
LES	leaf economics spectrum
l_i	liquid phase limitations to photosynthesis
l_{ias}	gas phase limitations to photosynthesis

l_m	mesophyll conductance relative limitation
LMA	leaf mass area
l_{nsd}	nonstomatal diffusion conductance limitation
l_s	stomatal relative limitation
Myr	million years
N	nitrogen
N_{area}	nitrogen content per area
N_{mass}	nitrogen content per mass
O_2	oxygen
P	pectin
PAR	photosynthetic active radiation
p_{cw}	cell wall porosity
p_i	effective porosity
PPFD	photosynthetic photon flux density
P_r	photorespiration
PSII	photosystem II
R	gas constant
R_d	Respiration in the light
$r_{f,i}$	decrease of diffusion conductance compared to free diffusion in water
R_n	dark-adapted mitochondrial respiration
Rubisco	ribulose 1·5-bisphosphate carboxylase/oxygenase
ς	diffusion path tortuosity
$S_{C/O}$	specificity factor of Rubisco
S_c/S	chloroplast surface area exposed to intercellular air spaces per unit of leaf area
S_c/S_m	ratio between mesophyll and chloroplast surface area exposed to intercellular air spaces per leaf area
S_m/S	mesophyll surface area exposed to intercellular air spaces per unit of leaf area
T_{chl}	chloroplast thickness

T_{cw}	cell wall thickness
T_{cyt}	cytoplasm thickness
T_k	absolute temperature
T_L	leaf temperature
T_{leaf}	leaf thickness
T_{mes}	mesophyll thickness
$V_{c,max}$	maximum velocity of carboxylation
VPD	vapour pressure deficit

Publications derived from the present Thesis

The present PhD Thesis is presented as a compendium of six manuscripts, either published, submitted or in preparation.

Carriquí M[*]**,** Douthe C[*], Molins A, Flexas J (2019) Leaf anatomy does not explain apparent short-term responses of mesophyll conductance to light and CO_2 in tobacco. Physiologia Plantarum 165(3), 604-618. Q2, IF 2.58.

Carriquí M, Nadal M, Flexas J. Acclimation of mesophyll anatomy and photosynthesis to light during leaf ageing in *Arabidopsis thaliana* (in preparation).

Carriquí M, Cabrera HM, Conesa MÀ, Coopman RE, Douthe C, Gago J, Gallé A, Galmés J, Ribas-Carbó M, Tomás M, Flexas J (2015) Diffusional limitations explain the lower photosynthetic capacity of ferns as compared with angiosperms in a common garden study. Plant, Cell and Environment 38, 448-460. Q1, IF 6.16.

Carriquí M, Roig-Oliver M, Brodribb TJ, Coopman R, Gill W, Mark K, Niinemets Ü, Perera-Castro AV, Ribas-Carbó M, Sack L, Tosens T, Waite M, Flexas J (2019) Anatomical constraints to nonstomatal diffusion conductance and photosynthesis in lycophytes and bryophytes. New Phytologist, 222(3), 1256-1270. Q1, IF 7.43.

Carriquí M, Nadal M, Flexas J. *Thuja plicata*, a conifer species with very thick leaves and cell walls, compensates low CO_2 diffusion by extremely high exposure of chloroplasts to intercellular air spaces. Tree Physiology (submitted). Q1, IF 3.38.

Carriquí M[*]**,** Nadal M[*], Clemente-Moreno MJ, Gago J, Miedes E, Molina A, Flexas J. Cell wall composition is a key determinant of mesophyll conductance in conifers (in preparation).

[*] These authors contributed equally to the present study.

Contents

Summary

Mesophyll (internal) conductance to CO_2 (g_m) is a key photosynthetic trait. Despite it has been traditionally considered infinite, g_m limits the diffusion of CO_2 from the substomatal cavity to the sites of carboxylation in the chloroplast and varies in response to environmental factors, either in the short- (i.e. seconds to minutes) and long-term, along leaf ontogeny and differs between genotypes and phylogenetic groups. However, although several structural and biochemical determinants regulating g_m have been identified, the mechanistic basis of g_m variability are not fully understood. Among them, the mechanisms explaining the immediate changes of g_m to environmental variations are unknown. Moreover, the extent of the effect of such variations on g_m is reduced to a few species, notably crops and plant model species, being the information available on g_m and its anatomical determinants in important groups of terrestrial plants (such as pteridophytes, lycophytes or bryophytes) very scarce. To determine these mechanistic bases and the different anatomical strategies that exist in photosynthetic organs is crucial for improving photosynthesis models and pinpointing targets for engineering leaf structure to enhance photosynthetic capacity in crops.

The objectives of the present thesis are (1) to provide further insights on how the environment modulates the relationship between leaf anatomy and mesophyll conductance to CO_2, and (2) to determine the main leaf anatomy traits influencing mesophyll conductance to CO_2 across the land plant phylogeny.

The results show that typically observed changes in g_m in response to short-term variations in ambient CO_2 concentrations or light intensity are not explained by anatomical mechanisms in tobacco. Instead, anatomical mechanisms largely explain the acclimation of g_m to different light growth conditions in *Arabidopsis*. Leaves developed under higher irradiances present thicker leaves, allowing space for more mesophyll cells, which improves the mesophyll and chloroplast surface area exposed to intercellular airspaces per leaf area (S_m/S and S_c/S, respectively) and positively affecting g_m. The role of cell walls on setting g_m increases its relevance along *Arabidopsis* leaf ageing due to the increase of cell wall thickness (T_{cw}) regardless of the light intensity.

Concerning different phylogenetic groups, the present PhD thesis represents the first exhaustive analysis of g_m and the anatomical features that determines it in three of the most primitive embryophyte groups: pteridophytes, lycophytes and bryophytes. These land plant groups are distinguished by their low g_m values, generally explained by their low S_c/S and their thick cell walls. These findings demonstrate a phylogenetic trend —whether due to evolutionary adaptation and/or adaptation to different habitats or life forms— towards decreased CO_2 diffusion resistance inside photosynthetic organs mainly thanks to increased S_c/S and decreased T_{cw} along the land plant's phylogeny.

For a deeper understanding of the leaf structural strategies that allow to increase S_c/S, and therefore decrease total CO_2 diffusion resistance in the mesophyll, the exceptional nature of *Thuja plicata* is investigated. *T. plicata* proves to be able to achieve the highest S_c/S ever reported by developing thick leaves and mesophyll cells, revealing another biologically viable target for manipulating the leaf structure in order to increase plants' photosynthetic capacity.

Finally, the study of physiological traits and cell wall properties in seven conifers reveals that, at least in species with thick cell walls, cell wall chemical properties are strong determinants of g_m. Specifically, the pectin fraction content seems to have a crucial role in regulating g_m.

Resum

La conductància del mesòfil (interna) al CO_2 (g_m) és un tret fotosintètic clau. La g_m, malgrat haver estat considerada tradicionalment com a infinita, limita la difusió del CO_2 des de la cavitat subestomàtica fins als llocs de carboxilació en el cloroplast i, a més, varia en resposta de factors ambientals, tant a curt (és a dir, de segons a minuts) com a llarg termini, durant l'ontogènia foliar, i entre genotips i grups filogenètics. No obstant això, tot i que s'han identificat diversos determinants estructurals i bioquímics que regulen la g_m, les bases mecanicistes de la variabilitat de la g_m no són completament compreses. Entre aquestes bases, es desconeixen els mecanismes que expliquen els canvis immediats de la g_m a variacions ambientals. A més, l'abast de l'efecte d'aquestes variacions sobre la g_m es redueix a unes poques espècies, principalment a cultius i espècies de plantes model, de tal manera que és molt escassa la informació disponible sobre la g_m i els seus determinants anatòmics en grups importants de plantes terrestres (com els pteridòfits, els licòfits o els briòfits). Determinar aquestes bases mecanicistes i les diferents estratègies anatòmiques que existeixen en els òrgans fotosintètics és crucial per millorar els models fotosintètics i per identificar les dianes per a redissenyar l'estructura de les fulles i millorar la capacitat fotosintètica dels cultius.

Els objectius d'aquesta tesi són (1) proporcionar més informació sobre com l'ambient modula la relació entre l'anatomia de les fulles i la conductància del mesòfil al CO_2, i (2) determinar els principals trets anatòmics foliars que influencien la conductància del mesòfil al CO_2 al llarg de la filogènia de les plantes terrestres.

Els resultats mostren que els canvis típicament observats en g_m en resposta a variacions a curt termini de les concentracions ambientals de CO_2 o de la intensitat lumínica no s'expliquen per mecanismes anatòmics en el tabac. En canvi, els mecanismes anatòmics expliquen en gran mesura l'aclimatació de la g_m a diferents condicions lumíniques de creixement en el cas de l'*Arabidopsis*. Les fulles desenvolupades sota irradiacions superiors presenten fulles més gruixudes, fet que permet més espai per a cèl·lules del mesòfil i augmenta l'àrea de superfície del mesòfil i cloroplàstica exposada als espais aeris intercel·lulars

per unitat d'àrea foliar (S_m/S i S_c/S, respectivament). Conseqüentment, això afecta positivament a la g_m. El paper de les parets cel·lulars en la determinació de la g_m augmenta en rellevància durant l'envelliment de les fulles de l'*Arabidopsis* a causa de l'augment de la gruixa de la paret cel·lular (T_{cw}), independentment de la intensitat lumínica de creixement.

Pel que fa als diferents grups filogenètics, aquesta tesi doctoral representa el primer anàlisi exhaustiu de la g_m i les característiques anatòmiques que la determinen en tres dels grups més primitius d'embriòfits: pteridòfits, licòfits i briòfits. Aquests grups de plantes terrestres es distingeixen per una g_m baixa, generalment explicada per la baixa S_c/S i les gruixudes parets cel·lulars. Aquests resultats demostren una tendència filogenètica —ja sigui com a resultat d'una adaptació evolutiva i/o una adaptació a diferents hàbitats o formes de vida— cap a la disminució de la resistència a la difusió del CO_2 dins els òrgans fotosintètics al llarg de la diversificació de les plantes terrestres. Això és possible principalment gràcies a l'augment de S_c/S i la disminució de la T_{cw}.

Per tal de comprendre més profundament les estratègies estructurals que permeten assolir majors S_c/S a les fulles i que, per tant, disminueixen la resistència total a la difusió del CO_2 en el mesòfil, s'ha investigat el caràcter excepcional de *Thuja plicata*. Aquesta espècie demostra la capacitat d'aconseguir la S_c/S més elevada que s'ha reportat mai gràcies al desenvolupament de fulles gruixudes i cèl·lules del mesòfil de gran mida, el que identifica una nova estratègia biològicament viable per manipular l'estructura de les fulles i així augmentar la capacitat fotosintètica.

Finalment, l'estudi dels característiques fisiològiques i de les propietats de la paret cel·lular a set coníferes demostra que, almenys en espècies amb parets cel·lulars gruixudes, les propietats químiques de la paret cel·lular determinen de forma important la g_m. Específicament, la fracció de pectines sembla tenir un rol crucial en la regulació de g_m.

Resumen

La conductancia del mesófilo (interna) al CO_2 (g_m) es un rasgo fotosintético clave. La g_m, a pesar de haber sido considerada tradicionalmente como infinita, limita la difusión del CO_2 desde la cavidad subestomática hasta los sitios de carboxilación en el cloroplasto i, además, varía en respuesta a factores ambientales, tanto a corto (es decir, de segundos a minutos) cómo a largo termino, durante la ontogenia foliar, y entre genotipos y grupos filogenéticos. Sin embargo, pese a que se han identificado diversos determinantes estructurales y bioquímicos que regulan la g_m, las bases mecanicistas de la variabilidad de la g_m no son completamente comprendidas. Entre estas bases, se desconocen los mecanismos que explican os cambios inmediatos de la g_m a variaciones ambientales. Además, el alcance del efecto de estas variaciones sobre la g_m se reduce a unas pocas especies, principalmente a cultivos y especies de plantas modelo, de tal manera que es muy escasa la información disponible sobre la g_m y sus determinantes anatómicos en grupos importantes de plantas terrestres (cómo los pteridófitos, los licófitos o los briófitos). Determinar estas bases mecanicistas y las diferentes estrategias anatómicas que existen en los órganos fotosintéticos es crucial para mejorar los modelos fotosintéticos y para identificar las dianas para rediseñar la estructura de las hojas y mejorar la capacidad fotosintética de los cultivos.

Los objetivos de esta tesis son (1) proporcionar más información sobre cómo el ambiente modula la relación entre la anatomía de las hojas y la conductancia del mesófilo al CO_2, y (2) determinar los principales rasgos anatómicos foliares que influencian la conductancia del mesófilo al CO_2 a lo largo de la filogenia de las plantas terrestres.

Los resultados muestran que los cambios típicamente observados en g_m en respuesta a variaciones a corto término de las concentraciones ambientales de CO_2 o de la intensidad lumínica no se explican por mecanismos anatómicos en el tabaco. En cambio, los mecanismos anatómicos explican en gran medida la aclimatación de la g_m a diferentes condiciones lumínicas de crecimientos en el caso de la *Arabidopsis*. Las hojas desarrolladas bajo irradiaciones superiores presentan hojas más gruesas, hecho que permite más espacio para células del

mesófilo y aumenta el área de superficie del mesófilo y cloroplástica expuesta a los espacios aéreos intercelulares por unidad de área foliar (S_m/S y S_c/S, respectivamente). En consecuencia, esto afecta positivamente a la g_m. El papel de las paredes celulares en la determinación de la g_m aumenta en relevancia durante el envejecimiento de las hojas de la *Arabidopsis* a causa del aumento del grosor de la pared celular (T_{cw}), independientemente de la intensidad lumínica de crecimiento.

Por lo que se refiere a los diferentes grupos filogenéticos, esta tesis doctoral representa el primer análisis exhaustivo de la g_m y las características anatómicas que la determinan en tres de los grupos de embriófitos más primitivos: pteridofitos, licófitos y briófitos. Estos grupos de plantas terrestres se distinguen por una g_m baja, generalmente explicada por la baja S_c/S y las gruesas paredes celulares. Estos resultados demuestran una tendencia filogenética —ya sea cómo resultado de una adaptación evolutiva y/o una adaptación a diferentes hábitats o formas de vida— hacia la disminución de la resistencia a la difusión del CO_2 dentro de los órganos fotosintéticos a lo largo de la diversificación de las plantas terrestres. Esto es posible principalmente gracias al aumento de S_c/S y la disminución del T_{cw}.

Para comprender más profundamente las estrategias estructurales que permiten alcanzar mayores S_c/S a las hojas y que, por tanto, disminuyen la resistencia total a la difusión del CO_2 en el mesófilo, se ha investigado el carácter excepcional de *Thuja plicata*. Esta especie demuestra la capacidad de conseguir la S_c/S más elevada que se ha reportado nunca gracias al desarrollo de hojas gruesas y células del mesófilo de gran tamaño, lo que identifica una nueva estrategia biológicamente viable para manipular la estructura de las hojas y así aumentar la capacidad fotosintética.

Finalmente, el estudio de las características fisiológicas y de las propiedades de la pared celular en siete coníferas demuestra que, al menos en especies con paredes celulares gruesas, las propiedades químicas de la pared celular determinan de forma importante la g_m. Específicamente, la fracción de pectinas parece tener un rol crucial en la regulación de g_m.

Introduction

Mesophyll conductance: a key photosynthetic trait

Practically all life on Earth ultimately depends on photosynthetic energy capture and conversion to energy-rich organic molecules. In plants, this process is performed in beautifully specialized organs designed to maximize the use of light and CO_2 for photosynthesis. Most plants species fix CO_2 molecules into a 3-carbon (C_3) acid by the enzyme Ribulose-1,5-bisphosphate carboxylase/oxygenase (Rubisco) in the chloroplast. This process depends on the capacity to diffuse from the atmosphere to the carboxylation sites in the chloroplast stroma, as well as on the carboxylation capacity of Rubisco (Gaastra 1959, Farquhar et al. 1980). Early studies dedicated to the photosynthetic diffusional limitations included the identification of both stomatal and mesophyll diffusion (Gaastra 1959).

With the spread of gas exchange analysis as the most useful tool for in vivo assessment of photosynthesis, models and assumptions were developed. Although these allowed quantitative separation of stomatal diffusion from 'other' limitations to photosynthesis, they were not designed to separate mesophyll diffusion conductance from other 'conductances' related to the biochemical capacity of photosynthesis (Sestak et al. 1971). Consequently, CO_2 diffusion inside photosynthetic tissues was included in an integrative term (referred to as 'internal conductance') that pooled diffusional and biochemical components, or alternatively and most frequently – specially after the most commonly used leaf photosynthesis model was published (Farquhar et al. 1980) – neglected. Neglecting potential limitations imposed by CO_2 diffusion implies assuming infinite mesophyll conductance, which in turn implies the assumption that the sub-stomatal CO_2 concentration (C_i) equals the concentration in the chloroplast stroma (C_c).

Thus, photosynthesis in plants has been considered for decades to be limited only by two factors: the velocity of diffusion of CO_2 through stomata and the capacity of photosynthetic machinery to convert light energy to biochemical energy and fix CO_2 into sugars. However, once it was demonstrated and accepted by most of the scientific community that mesophyll conductance to CO_2 (g_m) is finite, and possibly dynamically regulated, it became important to quantify

how much mesophyll diffusion limits photosynthesis. Nowadays CO_2 diffusion conductance through the mesophyll from the substomatal cavities to the chloroplast stroma (i.e. g_m), is recognized as one of the main drivers of the net assimilation rate (A_N; Flexas et al 2008, 2018a; Warren 2008a). The different steps CO_2 goes through until reaching Rubisco account for various components in which g_m can be disclosed. g_m comprises both gaseous, represented by the intercellular air spaces of the leaf mesophyll, and aqueous phases, accounting for the diffusion of CO_2 across cells, (i.e. cell walls, lipid membranes, cytosol and chloroplast stroma; Evans et al 2009). The aqueous phase usually drives the overall g_m, as cell walls -primarily its thickness (T_{cw})- and the chloroplast surface area exposed to intercellular airspaces per unit of leaf surface area (S_c/S) have been widely described to be the main g_m anatomical drivers (Terashima et al 2011; Tomàs et al 2013; Onoda et al 2017; Flexas et al 2018a; Ren et al. 2019). These characteristics partially explain the variability of photosynthesis, being low g_m values usually associated to thick cell walls and lower chloroplast exposure (Tosens et al 2016; Veromann-Jürgenson et al 2017).

The CO_2 diffusion pathway inside photosynthetic organs

Before entering into the leaf from the surrounding atmosphere, CO_2 molecules must pass through a boundary layer where impaired air turbulence exert the first resistance to diffusion. From there, because the cuticle and the epidermal cells are largely impermeable to CO_2 diffusion, most molecules diffuse across the stomatal pore —in the leaves where stomata are present—, following the gradient from higher to lower CO_2 concentrations, to reach the substomatal cavities and entering into the mesophyll. From the substomatal cavity, CO_2 continues diffusing thanks to the strong diffusional gradient created by the carbon fixation by the enzyme ribulose-1,5-bisphosphate carboxylase-oxygenase (Rubisco). This subsequent diffusion is characterized by a conductance globally known as mesophyll conductance. This is a complex diffusion pathway starting by a gas phase —in the photosynthetic organs with a proper mesophyll— and then CO_2 dissolves and moves through a liquid phase until it reaches the carboxylation site in the chloroplast stroma (Fig. 1). Each of the components of

these gas and liquid phases impose a particular resistance to CO_2 diffusion, by physical barriers and/or biochemical components. The sum of the series of resistances to CO_2 diffusion defines the total efficiency of CO_2 diffusion through the photosynthetic organ (i.e. CO_2 diffusion conductance inside photosynthetic organs, generally referred as g_m).

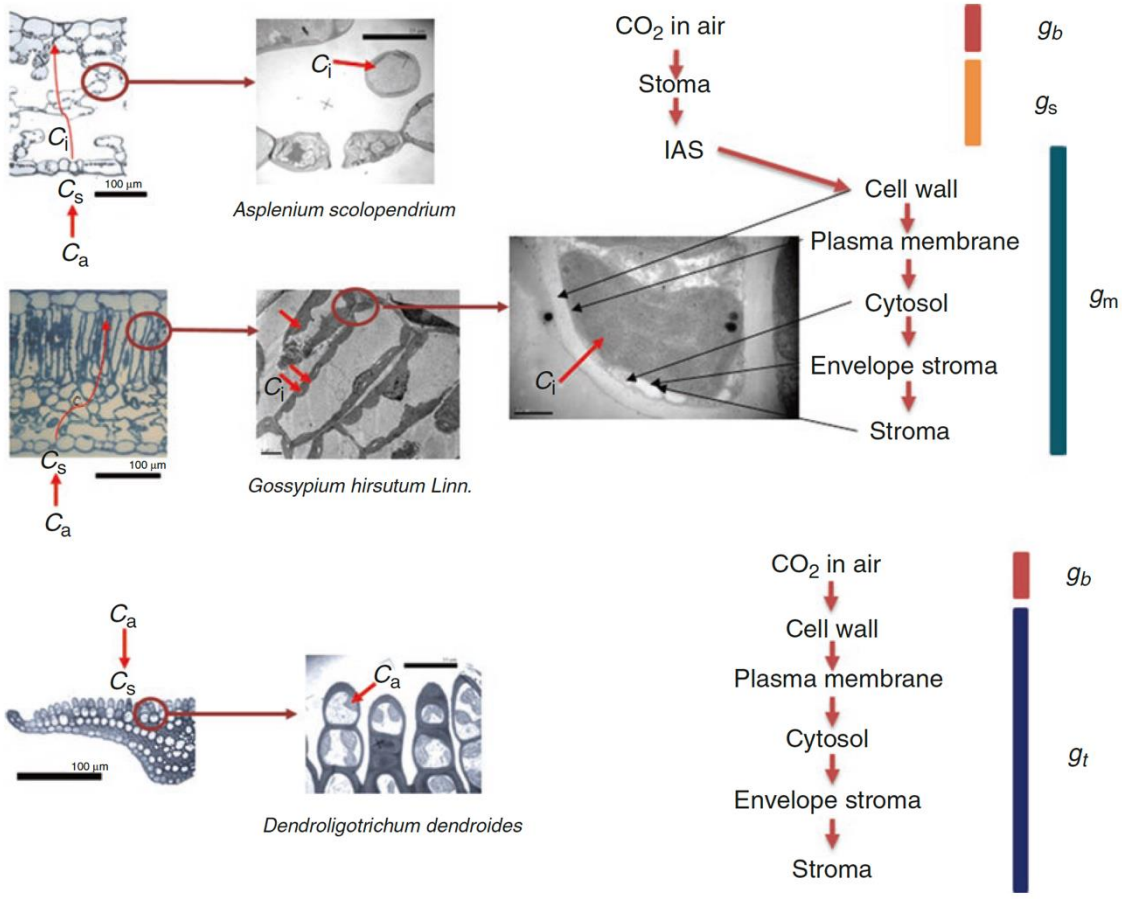

Figure 1. CO_2 pathway from atmosphere to the sites of carboxylation in photosynthetic organs with stomata (upper graph, including boundary layer, stomatal and mesophyll CO_2 conductances, g_b, g_s and g_m, respectively) and photosynthetic tissues lacking stomata (lower graph, boundary layer and total CO_2 conductances g_b and g_t, respectively). *ias* intercellular airspace. From Flexas et al. (2018).

The gas phase of the mesophyll CO_2 pathway comprises the diffusion through the intercellular airspaces from the substomatal cavity to the outer surface of mesophyll cell walls. Resistance in the gas phase is mainly defined by the leaf thickness (T_{leaf}) and the effective porosity of the mesophyll (f_{ias}), two morphological traits that in turn influence the tortuosity, the intercellular airspace connectivity and the lateral conductance. Compared to liquid, CO_2 diffusivity in

the gas phase is four orders of magnitude larger, thus is generally considered to be the component that causes a lower resistance to the CO_2 diffusion, being even neglected in many studies (Evans et al. 2009, Tholen et al. 2012, Earles et al. 2018, Ellsworth et al. 2018). However, recent 3D approaches embracing for the complex mesophyll structure revealed that gas phase limitations to g_m can be significantly high in thick leaves with especially dense mesophylls (Earles et al. 2018, 2019).

After crossing the gas phase, CO_2 dissolves into the apoplastic water at the surface of the cell wall, starting liquid phase. As CO_2 diffusion rate is significantly low in the liquid phase, the main CO_2 stream from the outer surface of cell wall to chloroplast stroma occurs through the shortest and most effective pathway. Consequently, the chloroplast surface area exposed to intercellular airspaces per unit of leaf area (S_c/S) is proportional to g_m and one of the main anatomical traits determining maximum mesophyll conductance (Tholen et al. 2008, Terashima et al. 2011, Tomás et al. 2013, 2014, Tosens et al. 2016, Peguero-Pina et al. 2017).

Once in the liquid phase, CO_2 molecules have to cross an intricate polysaccharide-rich primary cell wall. Resistance to CO_2 diffusion here depends on cell wall thickness (T_{cw}), porosity and tortuosity. T_{cw} is very variable (ranging from 0.10 to 1.15 μm within angiosperm species; Ouyang et al. 2017, Wang et al. 2018) and is considered to be, together with S_c/S, a major driver of mesophyll resistance (Evans et al. 2009, Terashima et al. 2011, Tomás et al. 2013, Ren et al. 2019). In contrast, the resistance imposed by cell wall effective porosity (tortuosity/porosity) has been scarcely studied. Although there are no direct measurements of the effective porosity for CO_2 diffusion for cell walls of land plants, it has been suggested that effective porosity might be inversely proportional to T_{cw} (Terashima et al. 2016, Tosens et al. 2012a, Tomás et al. 2013). Recently, although indirect, some first evidences of the key role of cell wall composition on cell wall conductance have been reported (Gago et al. 2016, Ellsworth et al. 2018).

The next component of the pathway in which CO_2 molecules must diffuse according to the CO_2 gradient is the plasma membrane. Early studies suggested

that due to the lipid nature of this membrane the diffusivity of lipophilic gases like CO_2 should be high (Meyer 1899, Overton 1901). However, the large proportion of proteins as well as the presence of other molecules, like sterols, might importantly increase the difussion resistance of this component (Tremmel et al. 2003, Engelman 2005, Itel et al. 2012). Aquaporins, a family of transmembrane proteins, function as facilitators of the diffusion small molecules, like H_2O, and in some subfamilies, also for CO_2, thus improving g_m (Terashima and Ono 2002, Hanba et al. 2004, Otto et al. 2010, Abascal et al. 2014, Yaneff et al. 2015).

The cytosol layer comprised between plasma membrane and chloroplast envelope constitutes the third component of the liquid-phase pathway. As chloroplasts are generally lined with cell walls, the pathway in this media tends to be short (Evans et al. 2009, Flexas et al. 2018), but there are some evidences of decreased g_m due to the removal of the chloroplasts from the cell wall (e.g. Sharkey et al. 1991, Tomás et al. 2013, Lu et al. 2018).

Chloroplast constitutes the last and major resistance for CO_2 diffusion, which comprises two components, the chloroplast envelope membrane and the stroma. Regarding to the membrane, due to its similarity with plasma membrane and the presence of aquaporins both are considered to be of the same order of relevance for the CO_2 diffusivity (Uehlein et al. 2008). In contrast, the stroma is considered, together with T_{cw} and S_c/S, a key anatomical determinant of mesophyll resistance (Evans et al. 2009, Terashima et al. 2011, Tosens et al. 2012, Tomás et al. 2013, Han et al. 2018). In the chloroplast stroma and the cytosol carbonic anhydrases may mediate CO_2 diffusion by hydrating CO_2 molecules to bicarbonate (Flexas et al. 2008). However, the role of carbonic anhydrases is still unclear, as some studies did not find a relationship between g_m and carbonic anhydrase activity (Price et al. 1994, Williams et al. 1996, Han et al. 2016), but others did (Momayyezi and Guy 2017). Once CO_2 molecules reach the chloroplast stroma, carbon fixation is finally possible and carried out by the enzyme ribulose-1,5-bisphosphate carboxylase-oxygenase (Rubisco), but also in a small percentage by other carboxylases, such as bicarbonate by phosphoenolpyruvate carboxylases (PEPC) (Weissbach et al. 1956, O'Leary 1982, Melzer and O'Leary 1987).

Methods to estimate mesophyll (internal) CO_2 diffusion conductance

Mesophyll or internal conductance to CO_2 (here, only g_m is used for simplicity) is a photosynthetic trait comparable to a black box. It cannot be measured, thus requires from complex methods based on theoretical considerations and assumptions as well as combining different techniques to estimate or to model it. g_m represents the efficiency of CO_2 diffusion from intercellular airspaces to the carboxylation site in the chloroplast stroma in leaves, and its determination requires to know the substomatal and chloroplastic CO_2 concentrations (C_i and C_c, respectively), as well as the net photosynthesis (A_N). In the case of photosynthetic organs other than leaves lacking stomata and proper mesophyll (e.g. bryophytes), ambient CO_2 concentration (C_a) instead of C_i is considered. A_N can be measured with gas exchange equipment, and stomatal conductance (g_s) and C_i easily estimated from transpiration measurements (von Caemmerer and Farquhar 1981). However, there are no direct methods to calculate C_c. In this section, a brief relation of the fundamentals, key questionable assumptions, as well as potential errors and advantages for the most accepted methods to either estimate or model g_m are presented. A more detailed revision has been recently performed in Flexas et al. (2018).

I. Variable *J* method

This method, developed by Di Marco et al. (1990) and Harley et al. (1992) has been and is the most widely used to estimate g_m. It is based on the fundamental that there is a balance in C_3 plants between Rubisco carboxylation and oxygenation that depends on (1) Rubisco kinetic properties and (2) CO_2 availability in chloroplasts. The first assumption of this method requires that O_2, due to its large concentration in the atmosphere at this era, is never limiting. Considering this, chlorophyll fluorescence (i.e. electron transport rate, ETR or *J*) can be used as a proxy for 'gross photosynthesis', while A_N obtained from gas exchange reflects the net balance between photosynthesis (i.e. carboxylation), photorespiration and day mitochondrial respiration (R_d). Therefore, knowing or

assuming Rubisco kinetics and applying the basic equations and photo/electron stoichiometries for both processes, C_c can be estimated and, from it and gas exchange-based C_i, g_m.

The strength of this method depends on the fulfillment of several questionable assumptions (Pons et al. 2009, Flexas et al. 2018): (1) that chlorophyll fluorescence and gas exchange arise from the same cell pool, while in fact the former arises from the top cell layer while the latter reflects an integration of the whole leaf; (2) that alternative electron sinks besides Rubisco carboxylation and oxygenation (e.g. nitrite reduction or the Mehler reaction) are negligible; (3) that ETR is accurately calculated —in the absence of adequate leaf absorptance and photosystem partitioning estimates it is essential to apply a calibration under low O_2 conditions as proposed by Valentini et al. (1995)—; (4) that R_d is properly estimated —given the problems indicated for all the existing methods (e.g. Kok (1948), Laisk (1977), Yin et al. (2009), etc), applying a sensitivity analysis is the optimum solution for this.

Important potential errors associated this method are (1) the type II errors (Gu and Sun 2014), the recycling of (photo)respired CO_2 (Tholen and Zhu 2011, Ubierna et al. 2019), and (3) the apparent g_m variation due to intra-leaf light profiles when measuring under no full light saturation (Théroux-Rancourt et al. 2017).

Despite the several somewhat risky assumptions and potential errors, this method has the advantages of being the most portable method (together with the curve-fitting; see below), being easy to use in any sort of species and/or in the field, and being the most robust method at low g_m values (Pons et al. 2009).

II. Curve-fitting method

This method is based on the photosynthesis model of Farquhar et al. (1980), where the part limited by the activity of Rubisco is described as:

$$A_N = V_{cmax} \frac{C_i - \Gamma^*}{C_i + K_c + (1 + O/K_o)}$$

where V_{cmax} is the carboxylation capacity, Γ^* the CO_2 compensation point in absence of mitochondrial respiration, and K_c and K_o the catalytic constants for the carboxylation and oxygenation reactions of Rubisco, respectively. Then, by substituting C_i in Farquhar's equation by $A_N/(g_m + C_c)$ it is possible to simultaneously solve for $V_{c,max}$, g_m and —if no independent estimate is available— R_d, which is achieved by curve-fitting (e.g. least-square differences) of the model to actual data obtained by running A_N-C_i response curves.

Although there are no key questionable assumptions for this method, it has several potential errors/limitations: (1) the degrees of freedom and accuracy when solving up to three unknowns with a single equation are low (Pons et al. 2009); (2) because of this, many different versions of the model exist (Ethier and Livingston 2004, Dubois et al. 2007, Sharkey et al. 2007, Bellasio et al. 2016…) that, in fact, are simply small variations in the equations and/or in the way of obtaining either the empirical data or some of the necessary model inputs (i.e. they do not really improve the overall low accuracy of the method). Finally, the greatest advantage of this method is that only gas exchange measurements are needed (Pons et al. 2009).

III. Isotopic method

This method is based on the fundamental that ^{13}C isotope discrimination occurs during CO_2 diffusion in the boundary layer, stomata and mesophyll, as well as during carboxylation by Rubisco and/or PEP carboxylase. As all the discrimination factors except g_m are known (stomata diffusion is represented by gas-exchange-estimated C_i/C_a ratio), it is possible to estimate a 'theoretical discrimination' for a given condition, and to compare it with the actual discrimination measured by a mass spectrometer, a tunable laser diode or a cavity ring spectroscope. The differences between theoretical and actual discriminations are ascribed to a finite and variable g_m (Evans 1989, Lloyd et al. 1992).

Key questionable assumptions of this method are (1) the validity of the assumed constant values for discrimination, and (2) the assumed percentage of

carboxylation via PEP carboxylase versus Rubisco. Regarding to the potential errors, the most noteworthy are (1) the leakage between the two connected instruments (^{13}C one and the infra-red gas analyzer), and (2) that current ^{13}C instruments have low accuracy, so g_m estimates are only accurate when g_m is particularly high (Pons et al. 2009).

IV. Anatomical 1-D model

The relevant characteristic of this method is that is the only one that can provide completely independent estimates of the other three methods, which are all based totally or partially on gas exchange measurements. Among the available analytical models, the 1D model of Niinemets and Reichstein (2003), later improved by Tosens et al. (2012b) and Tomás et al. (2013), is the most widely used. This model uses as main inputs anatomical features —T_{leaf}, f_{ias}, S_c/S, T_{cw}, cytoplasm thickness and chloroplast thickness and length— estimated from light microscopy and transmission electron microscopy images combined with the assumption of parameters such as wall porosity, membrane permeability, diffusion viscosity, and effective path length of CO_2 diffusion, models the resistance imposed by the different gas-phase and liquid-phase components of the CO_2 pathway to provide a value for the optimal g_m.

Its key questionable assumptions or potential errors are (1) the elevated number of biophysical diffusion properties that are assumed as constants or obviated (which have been substantially reduced in recent models, e.g. Ho et al. 2016, Xiao and Zhu 2017), (2) the simplification of the complex nature of the different liquid- and lipid-phase components as ‘pure water’ or ‘pure lipid’, and (3) the simplification of the complexity of a 3D photosynthetic organ to the information obtained from simple leaf cross-sections (Théroux-Rancourt et al. 2016, Earles et al. 2018, 2019).

Short-term, medium-term and long-term responses of mesophyll conductance

Once the nature, mechanistic basis and the most accepted estimation methods of g_m have been introduced, this section presents the evidence of the g_m variability and response to environmental factors. Despite the potential problems or artifacts or calculations of the current methods to estimate mesophyll conductance (as introduced in the previous section), g_m remains recognized as a major factor that explains responses of photosynthesis to environmental factors from the short- (i.e. from the seconds to minutes), mid- (days to years; acclimation), and long-term (evolutionary adaptations).

I. Short-term responses of mesophyll conductance to abiotic environmental variables

Photosynthesis is extremely sensitive to short-term fluctuations in environmental stimuli (i.e. light, CO_2 and temperature). It is widely accepted that the regulation of stomata aperture in response to short-term environmental variations, favoring or limiting the CO_2 entry in the substomatal cavities, or the fast and regulated adjustments in the photochemical and biochemical activities, are major causes explaining the responses of A_N to most of these changes at least in angiosperms (Adams and Terashima 2018). However, while g_m has also been suggested to respond in the short term, the mechanistic basis of its regulation are not fully understood.

The short-term responses of g_m have been assessed in several studies using the two classic methods to estimate instantaneous g_m, the variable J, based on leaf chlorophyll fluorescence, and the stable isotope ^{13}C discrimination method (Harley et al. 1992, Evans 1989, Lloyd et al. 1992). In particular, studies have focused mostly on the short-term g_m responses to temperature, CO_2 and light, which can be easily assessed with commercial gas-exchange systems which incorporate automatable software tools to perform response curves (i.e. A_N-PAR, A_N-C_i or A_N-T, respectively).

The temperature response of mesophyll conductance, for instance appears to be species-specific. In general, g_m responds strongly to leaf temperature, increasing from low to high temperatures, but with different slopes and/or different behaviors above a given maximum threshold temperature (Bernacchi et al. 2002, Warren and Dreyer 2006, Yamori et al. 2006, Scafaro et al. 2011, Evans and von Cammerer 2013, von Caemmerer and Evans 2015, Xiong et al. 2015, Shrestna et al. 2018).

In spinach and *Brassica*, the optimum temperature for g_m was shown to be dependent on the growth temperature. In spinach it was 25ºC and 20ºC for plants grown at 25-30ºC and 10-15ºC (Yamori et al. 2006), and in *Brassica* the effects were even more dramatic between plants grown at 20-25ºC and 5ºC (Flexas et al. 2008). In tobacco, according to Bernacchi et al. (2002) g_m increases exponentially following an increase in temperature from 10 to 35ºC, but decreases thereafter. The Q_{10} of g_m was approximately 2.2, which is comparable to the 1.8-2.0 found by Yamori et al. (2006). Because the Q_{10} of CO_2 diffusion in water is about 1.25, larger Q_{10} values described for g_m suggest that this is regulated by a protein facilitated process. On the other hand, in *Eperua grandiflora*, g_m decreased slightly with increasing temperature from 28ºC to 38ºC (Pons and Welschen 2003). The reasons for these different responses of g_m to temperature are unclear. To address this, Evans and von Caemmerer (2013) and von Caemmerer and Evans (2015) used the carbon isotope method to investigate the temperature dependency of g_m in nine different plant species. A variety of responses was observed; for example, g_m varied about three-fold from 15 to 40ºC in tobacco, while almost no changes occurred in *Lophostemon confertus* and *Triticum aestivum* over the same range. Therefore, the responses of g_m to temperature seem to be species-dependent, but more research efforts are required to clarify its effects (Flexas et al. 2018).

In the case of fluctuations of the CO_2 concentration surrounding the leaf, many studies, using both variable *J* and stable isotope discrimination methods, have reported a sensitive response of g_m. Increases in the atmospheric [CO_2] causing increases in C_i provoked concomitant decreases in g_m. A decrease in g_m with an increase in CO_2 was reported for many species using different measuring techniques (Flexas et al. 2007a, b, Vrabl et al. 2009, Douthe et al. 2011, Tazoe

et al. 2011, Xiong et al. 2015). However, in wheat, g_m hardly decreased in response to an increase in CO_2, even when g_s decreased as usually observed in many species (Tazoe et al. 2009). Some of the observed rapid responses could be methodological artefacts (Gu and Sun 2014). Nevertheless, it seems likely that g_m in wheat is much less responsive to environmental clues, not only CO_2 but also e.g. temperature, as compared to other species (Tazoe et al. 2009, von Caemmerer and Evans 2015). Using a three-dimensional reaction model, Tholen and Zhu (2011) suggested that leakage of HCO_3 through the chloroplast envelopes may be a possible explanation for the decrease in g_m at high CO_2. As with temperature, more research efforts are required to start understanding the responses of g_m to CO_2.

Concerning short-term fluctuations in light intensity, the number of reports is sensibly lower than for temperature or CO_2. However, an apparent decrease in g_m has been shown when measured under reduced light intensity in tobacco (Flexas et al. 2007b) and rice (Xiong et al. 2015), using the fluorescence technique. On the other hand, Tazoe et al. (2009), using the isotope discrimination technique, showed that g_m was independent of variation in light intensity. The latter authors carefully took into account the effects of fractionation associated with photorespiration and day-respiration in calculating g_m. Nevertheless, using the very same techniques and considerations, Douthe et al. (2011, 2012) found significant light-induced short term changes of g_m in *Eucalyptus* seedlings. Recently, Gu and Sun (2014) suggested some methodological artifacts that may be responsible for the dependence of g_m on light intensity. Théroux-Rancourt et al. (2017) re-evaluated the response of g_m to light intensity considering a light gradient within a leaf. Altogether, the responses of g_m to short-term light intensity changes require some re-evaluation. Some reports have also reported differences in g_m in response to different light qualities (Tholen et al. 2008, Loreto et al. 2009).

However, the responses of g_m to some environmental factors may have important problems in terms or artifacts or calculation (e.g. not accounting for the relative position of mitochondria and chloroplasts in the situations where photorespiration might be specially relevant, the existence of light gradients

inside the mesophyll, etc.; Tholen and Zhu 2011, Gu and Sun 2014, Théroux-Rancourt et al. 2017, Ubierna et al. 2019).

The main limitation to determine if the estimated short-term g_m variations are real, and therefore they reflect a physiological process or, on the contrary, they are partially or totally apparent or artefactual, is that the mechanistic basis that would explain this modulation is unknown. As stated before, several anatomical and biochemical determinants of g_m have been identified. Despite there are no direct evidences linking the immediate variations in g_m with the adjustment of anatomical and/or biochemical determinants, several possibilities have been suggested.

Regarding to the anatomical traits, most of them are thought to be constant and anatomically determined (Nobel 1999, Evans et al. 2009, Terashima et al. 2011). However, a potential role of the two main anatomical determinants of g_m, S_c/S and T_{cw} has been suggested. Tholen et al. (2008) found that short-term variations of g_m in response to changes in the light quality were correlated with changes in the chloroplast arrangement. As a result of chloroplast movements, S_c/S and therefore the diffusion pathway were modified. Although scarce changes has been observed in other studies in response to chloroplast movement (Gorton et al. 2003, Loreto et al. 2009), some authors have hypothesized that a potential change in S_c/S could also explain the short-term responses of g_m to light intensity, also provoked by chloroplast movements (Ho et al. 2016, Théroux-Rancourt et al. 2017), as well as the decrease of g_m at high temperatures, provoked by chloroplast movements and/or cell shrinkages (von Caemmerer and Evans 2015, Flexas and Díaz-Espejo 2015). Regarding to cell walls, although their structure or thickness are unlikely to change in the immediate term (Scafaro et al. 2011), changes in the nature of the chemical interactions between cell wall components and CO_2 molecules due to variations in the environmental conditions surrounding the leaves have been suggested (Flexas and Díaz-Espejo 2015).

Biochemically, the potential role of aquaporins and carbonic anhydrase, which would allow the dynamic control of g_m in response to the environment at the short-term, has been hypothesized (Terashima and Ono 2002; Hanba et al.

2004; Flexas et al. 2006, Tholen and Zhu 2011, Perez-Martin et al. 2014, Ho et al. 2016). Specifically in the case of temperature, the species-specific response of g_m has been suggested to be at least partially explained by the membrane activation energy, which would control the conductance of the cell membranes to CO_2 diffusion (von Caemmerer and Evans 2015). Finally, ABA-mediated processes have also been proposed to at least partially explain these g_m responses (Qiu et al. 2017).

In summary, there is now wide evidence for the rapid (i.e. seconds to minutes) g_m variation in response to short-term changes in environmental factors. However, due to (1) the existence of studies, although few, reporting no immediate g_m variation; (2) the growing number of plausible mathematical artefacts and over-simplifications of the models used to estimate g_m short-term responses; and (3), the fact that the implication of anatomical and biochemical traits in the regulation of such changes has not been empirically demonstrated; the evidences of the rapid g_m variation cannot be considered sufficiently convincing yet.

II. Acclimation responses of mesophyll conductance and anatomy

The capacity of species to cope with the mid-term variation (i.e. from days to years) of environmental factors is one of the key determinants of their growth form, distribution and range limits. Species are adapted to the specific environmental conditions of origin, but also exhibit the capacity to adjust to temporal variations in their environment —a process known as acclimatization or acclimation (Adams and Terashima 2018). This acclimation capacity determines the physiological performance of the species to the new growth conditions. Therefore, the photosynthetic capacity will be adjusted by the modulation of its three limiting factors: stomatal conductance, mesophyll conductance and the biochemical capacity. Having an exhaustive knowledge about the mechanisms that determine these stomatal, mesophyll and biochemical responses is especially important in order to be able to fate of plants in a changing climate (Kumarathunge et al. 2019). In this section a relation of the current knowledge about the acclimation responses of g_m to several abiotic environmental factors is

presented. Special attention is payed to the g_m responses to the environmental variables which vary substantially during the life of all terrestrial plants, regardless of their habitat or life form, i.e. the temperature (which changes over a broad range both over the diurnal and the seasonal courses) and light intensity (which changes strongly specially along the diurnal course), and to the internal factors of leaf development and ageing, which are also inherent to any plant species.

a. Effects of temperature acclimation on mesophyll conductance

Photosynthesis is one of the most sensitive plant processes to temperature variations (Berry and Björkman 1980, Quinn and Williams 1985. Yamori et al. 2014). The typical response of A_N to temperature can be generally described by a optimality curve, with low A_N at both cool and high temperatures, and a maximum rate at optimal intermediate temperatures (Berry and Björkman 1980, Fitter and Hay 2002). Hence, acclimation to new temperature conditions does not necessarily imply similar or higher A_N (Way and Yamori 2014). The shape of this acclimation response curve differs among species with different photosynthetic pathway (C_3, C_4 and CAM) and is determined by respiratory, biochemical and diffusive processes (Sage and Kubien 2007, Yamori et al. 2014). Respiration exponentially increases with temperature, varying the response of this process to temperature acclimation depending on the species thermal origin and even within species depending on growth and measurement temperatures (Atkin et al. 2005, Wright et al. 2006). With respect to biochemistry, temperature increases tend stimulate photorespiration by decreasing the specificity of Rubisco for carboxylation over oxygenation (Ogren 1984, Brooks and Farquhar 1985) and to damage the photosynthetic apparatus (e.g. affecting the photosystem II and inactivating Rubisco; Weis 1981, Kobza and Edwards 1987), reducing therefore the photosynthetic efficiency. CO_2 diffusive processes (i.e. stomatal control and CO_2 diffusivity and solubilization and membrane permeability) are also temperature-dependent (Sage and Kubien 2007). Thus, at warmer temperatures the sensitivity of A_N to g_s generally increases, so stomatal limitations to photosynthesis tend to be higher with increasing growth temperature, regardless of the stomatal response (Hendrickson et al. 2004, Sage and Kubien 2007). In comparison to g_s, g_m has been traditionally considered a minor determinant of the A_N responses to temperature acclimation.

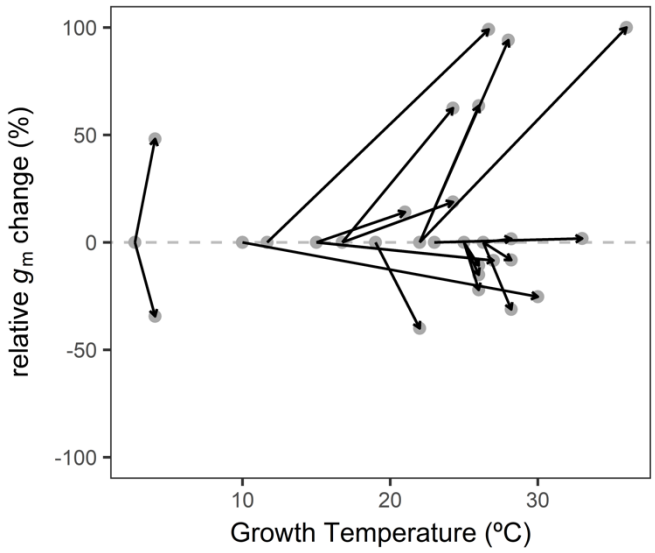

Figure 2. Response of mesophyll conductance to CO_2 (g_m) to the temperature acclimatization. Relative g_m change in each species/condition/study is represented with vectors, being the g_m value at the lowest temperature considered as the reference value. Data compiled from Yamori et al. (2006), Bunce (2008), Silim (2010), Fares et al. (2011), Crous et al. (2013), Lewis et al. (2015), Xue et al. (2016), Cai et al. (2018) and Sáez et al. (2018a). From Nadal, Carriquí and Flexas (submitted).

However, there is now sufficient evidence that mesophyll conductance varies in response to the acclimation to a new growth temperature. Nonetheless, the studies evaluating this process are few, very recent and the results between studies appear to be contradictory (Fig. 2). The first reports are from 2006, when Yamori et al. (2006) observed that in spinach plants grown at 15ºC showed a decreased g_m compared with plants grown at 30ºC when both measured at 25-35ºC, but differences disappeared when both plants where measured at 10-20ºC. Thus, Yamori et al. (2006) advertised of the potential key role of g_m in limiting photosynthesis at warmer temperatures in plants acclimated to cold temperatures. From then on, several studies reported either 50 to 100% increases, no response or even 25 to 50% decreases of g_m when acclimated to warmer temperatures (Bunce 2008, Silim 2010, Fares et al. 2011, Crous et al. 2013, Lewis et al. 2015, Xue et al. 2016, Cait et al. 2018, Sáez et al. 2018a; Fig. 2). The most dramatic response in g_m acclimation to temperature has been reported in Flexas et al. (2008), where *Brassica oleracea* plants grown at 5ºC had a 300% lower g_m than plants grown at 20ºC. Differences in the g_m response have been found even within the same genus. Thereby, both A_N and g_m strongly

decreased in *Populus x americana* plants acclimated at 35ºC compared to plants acclimated at 25ºC (Fares et al. 2011), in accordance with Yamori et al. (2006) findings, but g_m limitations were higher in *Populus balsamifera* plants grown at 15ºC in comparison to plants grown at 25ºC (Silim et al. 2010).

The mechanistic basis of g_m response to temperature acclimation has been scarcely determined. There are only three published reports which unfortunately are precisely dedicated to species that inhabit very particular and extreme environments, and are therefore not sufficiently representative of the C_3 plants. Two of these studies were performed in the only two vascular species that inhabit maritime Antarctica, first under field conditions and mild temperature acclimation treatments (i.e. + 2 ºC; Sáez et al. 2018a), and then under laboratory conditions and moderate acclimation treatments (i.e. + 12 ºC; Sáez et al. 2018b). Both studies demonstrated that the mesophyll anatomical traits helped to explain the non-significant g_m response of *Deschampsia antarctica* and the g_m increase in *Colobanthus quitensis* —mainly mediated by adjustments of the chloroplast arrangement and S_m/S— in response to plant acclimation to warmer temperatures. The other study is dedicated to the thermophilic tree *Ziziphus spina-christi* (Zait et al. 2018), where the reported hyperbolical g_m decrease with decreasing acclimation temperatures was partially explained by decreased LMA and T_{leaf} but increased f_{las}. However, the evidence reported for these three species adapted to extreme environments do not allow to explaining the high diversity of g_m responses to the acclimation to this environmental variable found in temperate species. Therefore, no general pattern can be extracted, raising the need of further studies on the g_m and its regulating traits acclimation response to temperature in different species.

b. Effects of light intensity acclimation on mesophyll conductance

Light availability for plants varies in time and space (Björkman 1981), being the gradient along the canopy up to > 50-fold in closed and as large as 10 to 20-fold in open canopies (Hirose et al. 1988, Joffre et al. 2007, Koike et al. 2001, Rambal 2001, Valladares et al. 2003, Niinemets and Anten 2009, Niinemets et

al. 2015). Leaf acclimation to light intensity is associated to countless responses associated to the photosynthetic process. These responses range from the subcellular and cellular levels (e.g. determining the characteristics of the light-harvesting complexes), the leaf level (e.g. leaf structure) to the whole-plant level (e.g. biomass allocation), including what is known as leaf plasticity (Valladares et al. 2007, Nicotra et al. 2010, Poorter et al. 2019). As recently confirmed in a meta-analysis of the plant responses to light intensity for 70 traits (Poorter et al. 2019), changes in the leaf due to light acclimation have major implications for g_m and the overall leaf photosynthetic performance (Terashima et al. 2011). Higher light intensity during growth ensures a deeper light penetration within the leaf, allowing plants to possess a higher area-based photosynthetic capacity and g_m by developing thicker and denser leaves (i.e. with higher LMA) with high light (Poorter et al. 2019). Across species, leaves grown at higher light conditions generally achieve greater thickness through an increase in mesophyll palisade cell layers and the enlargement of mesophyll cells (Terashima et al. 2001, Ivanova et al. 2006, Tosens et al. 2012a), which in turn results in a higher mesophyll surface area exposed to intercellular airspace per leaf area (S_m/S) and S_c/S (Hanba et al. 2002, Oguchi et al. 2005, Tosens et al. 2012, Morales et al. 2014, Fini et al. 2016, Ellsworth et al. 2018). Cell wall thickness, a key trait determining mesophyll CO_2 diffusion resistance (i.e. the inverse of g_m) also might play a role in the leaf light acclimation. However, the relationship of T_{cw} with light growth conditions is not that clear, since it has been reported to increase (Fini et al. 2016), remain constant (Hanba et al. 2002, Tosens et al. 2012, Fini et al. 2016, Ellsworth et al. 2018) or decrease with increasing growth light conditions (Hanba et al. 2002). Changes are generally strongest in low light, and minimum at high light (Poorter et al. 2019). However, the effect of growth light intensity on leaf structure and both A_N and g_m depend on the species adaptation to light-demand (Hanba et al. 2002). Thus, light-demanding species present higher plasticity than shade-tolerant species (Valladares et al. 2000, Portsmuth and Niinemets 2007, Chmura et al. 2017), the former presenting higher g_m values when measured under saturating light conditions. However, little is known about the relationship between leaf anatomy and g_m in species other than few trees, and specially on how this relationship changes when leaves mature and/or age (Niinemets et al. 2012, Tosens et al. 2012a, Poorter et al. 2019).

In the particular case of acclimation to light, the other limiting traits of photosynthesis might be considered to play a rather secondary role with respect to g_m and leaf anatomy. Both g_s and stomatal density increase with the daily light integral, but tend to stabilize with high light and their increases are not large enough to keep up with the photosynthetic increased demand for CO_2 (Poorter et al. 2019). Regarding biochemistry, a strong increase —similar or a bit higher than in S_m/S— in the amount of Rubisco and V_{cmax} per unit of leaf area can be found with increasing light intensity. Finally, little is known about the respiration effect on A_N under light-saturated conditions, although it is estimated to comprise from 30 to 70% of gross carbon gain at the whole-plant level (Raich et al. 2014).

c. Effects of leaf development and ageing on mesophyll conductance

Leaf development and ageing comprise an important fraction of the leaf lifespan. During these two leaf ontogenic stages a myriad of changes in the physiological and structural characteristics determining A_N occur in the leaves.

During the leaf development the formation of the internal leaf structure, the expansion of leaf surface area and the rapid growth in the chloroplast number concur with the synthesis of chlorophyll, pigment-binding complexes and photosynthetic enzymes. Thus, A_N, but also g_m, steeply increase until reaching their peak value in fully expanded leaves (Miyazawa and Terashima 2001, Miyazawa et al. 2003, Eichelmann et al. 2004, Parida et al. 2004, Flexas et al. 2007a, Marchi et al. 2008, Tosens et al. 2012). The rate of development of the photosynthetic processes widely differ between plant species and can be affected by environmental factors, typically ranging from 10 to 80 days the required time from leaf unfolding to full leaf development (Nitta and Ohsawa 1997, Miyazawa et al. 1998, 2003, Miyazawa and Terashima 2001, Wright et al. 2004, Niinemets et al. 2012). Despite the diverse processes that occur during leaf development, there are evidences linking the modifications in the leaf architecture with the increases on g_m during leaf growth. These comprise a gradual increase of f_{ias} and in S_m/S and S_c/S, but also of LMA and T_{leaf}, which align with the low CO_2 diffusion

resistance exerted by the thin walls of young cells (Miyazawa and Terashima 2001, Miyazawa et al. 2003, Tosens et al. 2012a).

Once fully expanded leaves achieve maximum g_m, this photosynthetic trait tends to decrease with leaf age (Loreto et al. 1994, Niinemets et al. 2012). Anatomically, observations from Miyazawa and Terashima (2001), Miyazawa et al. 2003 and Tosens et al. (2012) pointing towards steep decreases in g_m are potentially mainly associated to the accumulation of cell wall material which result in thicker cell walls. Moreover, Niinemets et al. (2012) suggested a possible reduction of cell-wall effective porosity with leaf ageing. However, the number of studies investigating how the leaf internal architecture modulates g_m during leaf development and ageing is still scarce. Moreover, most studies have been performed in evergreen and deciduous woody species, therefore, how the fast modifications of anatomical traits modulate g_m in short-lived leaves is unknown.

d. Effects of acclimation to other abiotic environmental variables on mesophyll conductance: CO_2, drought stress, ozone, salinity and nutrients

The acclimation to temperature and light, as well as the leaf development and ageing effects on mesophyll conductance and its regulating traits have been the most studied factors. Here, a concise relation is presented about the impacts on g_m of the acclimation to other distinct abiotic environmental factors for which there is sufficient evidence is provided below.

Numerous studies dedicated to the C_3 plants acclimation to increased [CO_2] (i.e. grown between 500 and 700 ppm of CO_2) have reported significant A_N increases —ranging from 5 to 50% depending on the functional type— as well as reported significant changes on the stomatal and biochemical characteristics related to A_N (Saxe et al. 1998, Long et al. 2004, Ainsworth and Rogers 2007). However, g_m has been ignored in most studies intending to investigate the basis of the response of A_N to elevated [CO_2] acclimation.

From up to 20 studies dedicated to 18 species —mainly herbaceous crops— in which the response of g_m has been investigated a species-dependent

response has been found, reporting either a trend towards decreased g_m (up to 75%) or no significant g_m variation under high [CO_2] (Singsaas et al. 2004, Bernacchi et al. 2005, Possell and Hewitt 2009, Velikova et al. 2009, Zhu et al. 2012, Crous et al. 2013, Singh et al. 2013, Chen et al. 2014, Aranjuelo et al. 2015, Kitao et al. 2015, Lewis et al. 2015, DaMatta et al. 2016, Singh and Reddy 2016, 2018, Xu et al. 2016, Ruiz-Vera et al. 2017, Cai et al. 2018, Mizokami et al. 2018, Zait et al. 2018). Only in the case of sun-adapted leaves of a single species, the tree *Liquidambar styraciflua*, a significant positive response of g_m has been reported (Singsaas et al. 2003). Nevertheless, the recent work of Mizokami et al. (2018) suggests that, as in some species the g_m decrease is of the same order at both mid- and short-term, g_m might not acclimate to elevated [CO_2].

The evidence for anatomical adjustments driving the g_m acclimation to elevated [CO_2] is still scarce and not conclusive. Among the different main potential anatomical properties that might be driving this species-specific g_m response, T_{cw} and chloroplast dimensions —their increase— could be playing a key role (Robertson and Leech 1995, Uprety et al. 2001, Oksanen et al. 2005, Teng et al. 2006, Zhu et al. 2012). Although some studies have pointed to S_c/S alterations, evidence show that this trait remains unaffected or is incremented, not explaining neither one nor the other possibility the general g_m downregulation (Kitao et al. 2015, Mizokami et al. 2018).

Regarding acclimation to water stress, several studies have reported a concomitant g_s and g_m decrease (Grassi and Magnani 2005, Díaz-Espejo et al. 2007, Galmés et al. 2007, Flexas et al. 2009, Galle et al. 2009, Tosens et al. 2012a, Cano et al. 2013). The ratio g_m/g_s is positively related to water use efficiency (Flexas et al. 2013) and a key to simultaneously improve photosynthesis and water use efficiency in drought-prone agriculture (Flexas et al. 2015), for which understanding the mechanisms for concomitant drought-regulation of g_s and g_m would be crucial, but they are still largely unknown. The potential anatomical adjustments potentially explaining the lower g_m under water stress seems to be species-dependent and vary depending on the intensity of the drought stress treatment (Galle et al. 2011). Some generalized anatomical responses to water stress include a reduction in chloroplast size and in f_{ias} and an increase in T_{cw} (Niinemets et al. 2009, Poorter et al. 2009, Li et al. 2012,

Galmés et al. 2013). However, in Tomás et al. (2014) anatomy did not explain the g_m decrease reported in *Vitis vinifera* cultivars acclimated to water stress once leaves were already fully-expanded. In this sense, Miyazawa et al. (2008) suggested that drought-induced g_m reductions could be mainly associated to an aquaporin deactivation.

Tropospheric ozone (O_3) is a phototoxic air pollutant causing physiological oxidative stress and reductions of plant growth (Ainsworth et al. 2012, Feng et al. 2015, McGrath et al. 2015, Li et al. 2017). However, no clear consensus has been achieved on whether observed A_N downregulation due to elevated [O_3] acclimation is primarily related to g_s, g_m or to the biochemical capacity (Calatayud et al. 2007, Feng et al. 2016, Gao et al. 2016). The few available studies focusing on the g_m response to high [O_3] acclimation have reported a downregulation of this photosynthetic trait in all studied species except in *Fagus sylvatica*, where g_m remained constant (Eichelmann et al 2004, Velikova et al 2005, Flowers et al 2007, Warren et al 2007, Watanabe et al 2018, Xu et al 2019). While no report is available on the anatomical adjustments explaining this decrease, studies on leaf anatomy alone suggest that increased [O_3] alters T_{cw} and chloroplast size and arrangement (Paoletti et al. 2009, Gao et al. 2016), i.e. some key anatomical traits in setting g_m.

Finally, leaf nutrient content strongly determines leaf photosynthesis (Wright et al. 2004), and there are some recent works evidencing a great response of g_m to nutrient content, especially nitrogen and potassium. Thus, nitrogen content, apart from improving the photosynthetic performance by determining the protein and chlorophyll content, also influences mesophyll conductance, probably mainly affecting the regulation of chloroplast number and/or size, therefore modifying S_c/S (Onoda et al. 2017). Regarding to potassium, its deficiency negatively affects both A_N and g_m, and several mechanistic bases have been recently identified to explain the increase in mesophyll resistance, including reduced f_{ias} and S_c/S, and increased T_{cyt} (Battie-Laclau et al. 2014, Lu et al. 2016, 2019, Singh and Reddy 2018).

The reported results on g_m acclimation summarized in this section provide large evidence for the variability in the response of this key photosynthetic trait to

the mid-term (from days to years) variation of several abiotic environmental factors. However, in many cases the g_m response to specific variables appears to be species-specific. Therefore, more studies are needed to extend the knowledge on the variation of g_m and its anatomical and biochemical adjustments due to plant acclimation to the different plant functional types. Moreover, studies focusing on the combined acclimation effect of two or more variables and/or along leaf development and ageing in g_m are also specially needed.

III. Adaptation aspects of mesophyll conductance

The acquisition of plant independence from water and subsequent colonization of terrestrial ecosystems supposed a great transformation of the Earth. With terrestrialization, plants experienced the challenge of capturing CO_2 while losing to much water. Early land plants were restricted to grow close to the soil, where high humidity allowed to photosynthesize with minimal desiccation (Kenrick and Crane 1997, Renzaglia et al. 1997). Major increases in the photosynthetic capacity were associated with the apparition of features allowing to maintain hydrated and functional the photosynthetic tissues in the dry atmosphere. Mainly, these features are thought to be related to the development of water conducting tissues and the regulation of the water use efficiency through the appearance of cuticles, stomata —and subsequent gradual increase of the morphological complexity of the stomata apparatus and more efficient regulation of stomatal conductance— and the development of leaves (i.e. the appearance of mesophyll) (Raven 1997, Franks and Farquhar 2007, Brodribb et al. 2009, Brodribb and McAdam 2011, Flexas and Keeley 2012, Ducket and Pressel 2018). Moreover, this decisive evolution of photosynthesis for plant colonization of terrestrial ecosystems also implied a myriad of adaptations to the strongly different atmospheric conditions under which the different terrestrial plant groups appeared, remarkably under an atmosphere with much larger CO_2 concentrations (Niklas et al. 1983, Berner 2006). Thus, different mechanisms of CO_2 internal diffusion and fixation resulted from the different selection pressures under which each plant group originated and evolved —atmospheric CO_2 concentration steeply declined during the Phanerozoic, so that, for example,

ferns emerged under 10-fold but angiosperms under two- to threefold higher [CO_2] atmospheric concentrations than present (Haworth et al. 2011)— (e.g. the development of planate leaves coincided with periods of 'low' atmospheric [CO_2]; Woodward 1998, Beerling et al. 2001, Franks and Beerling 2009).

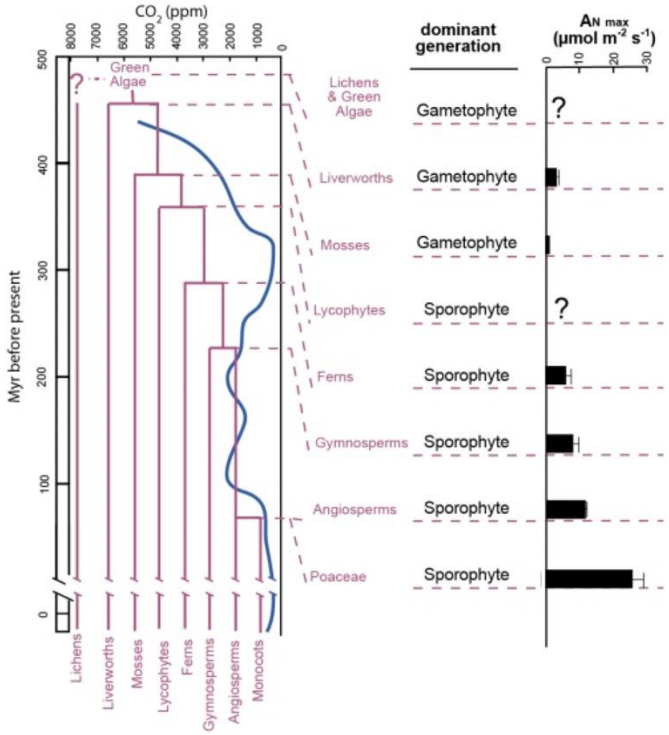

Figure 3. Photosynthetic evolutionary trend in land plants. The figure shows the concomitant changes in the maximum net photosynthesis (A_N) with the progressive reduction of atmospheric [CO_2] over Phanerozoic time (expressed in million years; myr) and the time at which each evolutionary group emerge. Blue line in the left panel indicates the estimated [CO_2] over time. Data are compiled from Niklas et al. (1983), Berner (2006) and Flexas et al. (2012).

As a result of this evolutionary adaptation, a clear increasing tendency emerges for the photosynthetic capacity (and, thus, potential growth rate) from early, non-vascular plants to the most modern plant lineage —i.e. angiosperms, the current dominant plant group, which accounts for 96% of the total diversity of vascular plants (Schuettpelz and Pryer 2009)—, with intermediate values in lycophytes, ferns and gymnosperms (Fig. 3; Flexas et al. 2012, Flexas and Keeley 2012). The underlying reasons of this increased photosynthetic capacity among land plants related to stomatal conductance are quite well established due to the substantial knowledge compiled for the evolution of stomata (Brodribb et al. 2009, Franks and Farquhar 2007, Brodribb and McAdam 2011). Instead, data

available for mesophyll conductance and Rubisco for the different land plant groups are still too scarce and spread to reach any strong conclusion, although some degree of co-evolution in photosynthetic functioning has been observed for stomatal and mesophyll conductance, as well as for Rubisco catalytic properties (Flexas et al. 2012, Flexas and Keeley 2012).

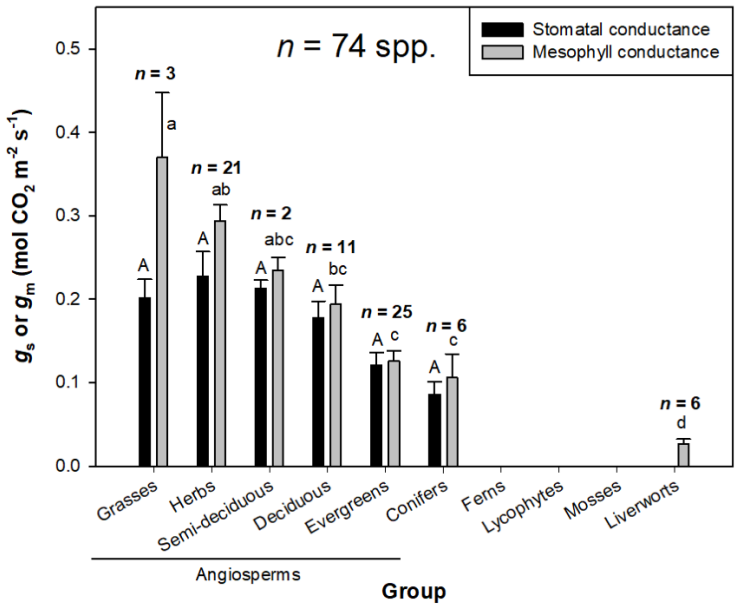

Figure 4. Phylogenetic trend towards higher mesophyll conductance. Average ± SE values for g_s and g_m for the different plant groups from Meyer et al. (2008) and Niinemets et al. (2009). Capital letters indicate differences between means for g_s and lower-case letters for g_m (Tukey test, $P < 0.05$). Modified after Flexas et al. (2012).

Mesophyll or internal conductance to CO_2 studies have been traditionally mostly restricted to crops and model plants. However, the steeply increase in the number of species in which g_m was being characterized allowed Flexas et al. (2012) to preliminary explore for phylogenetic or adaptive patterns within land plant groups, similarly to what has been in the case of the photosynthetic capacity phylogenetic trend. Based on an available dataset of g_m values composed of only angiosperms, gymnosperms and a few liverworts (Meyer et al. 2008, Niinemets et al. 2009a), significant differences were found in the average g_m between the taxonomic groups, with mean maximum values (i.e. in the absence of stress conditions) ranging from up to 0.63 mol CO_2 m^{-2} s^{-1} in highly productive crops to values close to zero in liverworts (Fig. 4). Angiosperms presented the highest

mean g_m estimated values (0.19 mol m^{-2} s^{-1}), meanwhile reported values for conifers where intermediate significantly lower (0.11 mol m^{-2} s^{-1}, averaging the values for the six species considered in Flexas et al. 2012), and lowest values were for liverworts, the unique non-vascular lineage for which estimates of the internal conductance to CO_2 diffusion were available (around 0.02 mol m^{-2} s^{-1}). Significant differences are found also between the different extant functional groups of angiosperms. Grasses and herbs have the highest estimated values of g_m, which are followed by semi-deciduous and deciduous woody plants with an average g_m close to 0.20 mol m^{-2} s^{-1}. And finally, the lowest g_m estimated values within angiosperms are for evergreen woody species. This allowed Flexas et al. (2012) to suggest, on the one side, the existence of a phylogenetic trend towards higher g_m similar to the one reported for A_N—although with a wide variation in the A_N-g_m relationship as, for instance, for a A_N value of 10 μmol CO_2 m^{-2} s^{-1} g_m can range from 0.6 to 0.31 mol CO_2 m^{-2} s^{-1}— and clearer than in the case of g_s (Fig. 4). On the other side, the high variability in maximum g_m within functional groups inside angiosperms may reflect also the particular adaptation to different habitats or life forms. Common garden experiments have revealed the existence of an important variability within genus, for example in the cases of *Solanum*, ranging from 0.15 to 0.25 mol m^{-2} s^{-1}, *Limonium*, ranging from 0.14 to 0.35 mol m^{-2} s^{-1}, or *Quercus*, ranging from 0.03 to 0.09 mol m^{-2} s^{-1}, or (Muir et al. 2014, Galmés et al. 2017, Peguero-Pina et al. 2017, respectively), and even within a single species, as reported in *Oryza sativa*, ranging from 0.19 to 0.58 mol m^{-2} s^{-1}, or *Vitis vinifera*, ranging from 0.14 to 0.22 mol m^{-2} s^{-1} (Xiong et al. 2017 and Tomás et al. 2014, respectively). However, due to the lack of estimated g_m values on several land plant groups, mainly ferns, lycophytes and mosses, do not allow to extract precluding conclusions.

As with g_m, it is also unknown whether the main anatomical and biochemical determinants of this photosynthetic trait in angiosperms and gymnosperms also account for the internal conductance of the early land plant groups. In the case that they were, there are some anatomical evidences that would make expect g_m to be significantly lower than that of the Spermatophytes. An obvious case would be in the case of mosses. As recently shown by Waite and Sack (2010), mosses, apart from low A_N, present extremely thick cell walls

(an order of magnitude higher than the average T_{cw} of Spermatophytes). Moreover, photosynthetic organs in many moss species are unistratose (i.e. conformed by a single layer of cells), so the chloroplast surface area exposed to ambient per unit of area (S_c/S, the other main anatomical determinant of g_m, together with T_{cw}, in Spermatophytes; Evans et al. 2009, Terashima et al. 2011) would be expected to be minimum.

Summarizing, despite the steeply increasing number of species in which g_m has been characterized, there is a major gap in the maximum g_m or non-stomatal diffusion conductance (g_{nsd}) and its variability within the extant representatives of the major groups of early land plants. In consequence, the apparent general phylogenetic trend towards higher mesophyll conductance to CO_2 cannot be demonstrated yet. Moreover, it is unknown whether the main anatomical determinants of g_m reported for Spermatophytes are of equal or even greater importance for these more primitive groups. In this same sense, other potential determinants of g_m (e.g. cell wall effective porosity, the arrangement of mitochondria in relation to chloroplasts or the plasma- and chloroplast-membrane conductivity) that have not yet been investigated in depth in any group of plants might have a key role in setting maximum g_m in land plants have been reported (Popper et al. 2011) yet it is unknown how these could affect g_m. This knowledge will help to understand the evolution of g_m and the mechanisms involved it its regulation.

Objectives and outline

Objectives

The general objectives of the present work were: (1) to provide further insights on how the environment modulates the relationship between leaf anatomy and mesophyll conductance to CO_2, and (2) to determine the main leaf anatomy traits influencing mesophyll conductance to CO_2 across the land plant phylogeny.

These general aims were divided into six specific objectives:

1. To discern whether fast (seconds to minutes) mesophyll conductance responses to changes in light and CO_2 concentration are caused by leaf anatomical changes.
2. To describe how anatomical traits modulate the acclimation of mesophyll conductance to growing light and during leaf age.
3. To determine the mesophyll conductance in ferns and fern allies and its determining anatomical traits.
4. To determine the mesophyll conductance and the determining anatomical traits in a large number of bryophytes.
5. To study the exceptional nature of *Thuja plicata* in relation to its anatomical characteristics.
6. To analyze the effects of the cell wall chemical composition on the relationship mesophyll conductance—leaf anatomy.

Outline of the Thesis

The Thesis is organized in a general **Introduction** followed by **5 chapters** that constitute the body of the Thesis, and a **General discussion** linking the results of the different chapters and, finally a **Conclusions** section highlighting the main contributions of the research, followed by the general **References** used. Across the chapters, the anatomical mechanistic basis underlying the CO_2 diffusion process in the mesophyll and its variation from the really short-term (i.e. seconds to minutes), the leaf acclimation to environmental variables and to the evolutionary adaptation level.

Introduction

This section provides a background of existing research and sets the context for the present Thesis. It establishes the state-of-the-art of knowledge on mesophyll (internal) CO_2 diffusion conductance, target of study of the Thesis, including its importance for the photosynthetic process, methods to estimate it, the CO_2 diffusion pathway from the substomatal cavity to the carboxylation site, its main structural and biochemical determinants, and its short to long term responses to environmental factors.

Chapter 1. Mechanistic basis of mesophyll conductance short-term variations

This chapter investigates the leaf anatomical adjustments to rapid changes (i.e. seconds to minutes) in environmental conditions surrounding the leaf that could explain the mechanistic basis of the short-term response of mesophyll conductance. Potential short-term regulation of biochemical determinants of mesophyll conductance, as well as possible artifacts in mesophyll conductance estimation are also discussed.

Specific objective 1 is addressed in this chapter.

Chapter 2. Anatomical adjustments determining mesophyll conductance acclimatization to light growth conditions

This chapter describes the effects of light growth conditions and leaf age, as well as its combined effect, on photosynthetic capacity, mesophyll conductance of the model plant species *Arabidopsis thaliana*, exploring how the observed differences are related to key leaf anatomical traits.

Specific objective 2 is addressed in this chapter.

Chapter 3. Mesophyll conductance and its main anatomical determinants along land plant's phylogeny

This chapter provides the first extensive report of photosynthetic relative limitations and mesophyll conductance to CO_2 diffusion values in the primitive land plant groups of liverworts, mosses, lycophytes and ferns. In the case of ferns, the results are compared with angiosperms grown under common garden conditions. Leaf structural and anatomical traits involved in setting total CO_2 diffusion resistance were also assessed.

Specific objectives 3 and 4 are addressed in this chapter.

Chapter 4. Chloroplast surface area-based strategies to optimize mesophyll conductance

This chapter presents the photosynthetic and anatomical characteristics of *Thuja plicata* that convert this species into an outlier in comparisons with other species, including other gymnosperms. It also assesses the extent to which the particular anatomy of *T. plicata* optimizes its photosynthesis. The implications of presenting the extremely large chloroplast surface area exposed to intercellular air spaces per projected leaf area displayed by *T. plicata* on photosynthesis and mesophyll conductance in other species are also modelled.

Specific objective 5 is addressed in this chapter.

Chapter 5. Cell wall properties impact on CO_2 diffusion resistance

This chapter focuses on how the cell wall celluloses, hemicelluloses and pectins affect the effective cell wall porosity and mesophyll conductance and photosynthesis in a survey of gymnosperm species.

Specific objective 6 is addressed in this chapter.

General discussion

This section contains an overview of the contributions of the thesis, discusses its limitations and suggests some areas for further work.

Conclusions

This section presents a list of the main conclusions derived from the present thesis in relation to the general and specific proposed objectives.

Chapter 1. Mechanistic basis of mesophyll conductance short-term variations

Leaf anatomy does not explain apparent short-term responses of mesophyll

Physiologia Plantarum

An International Journal for Plant Biology

Physiologia Plantarum 165: 604–618. 2019

Leaf anatomy does not explain apparent short-term responses of mesophyll conductance to light and CO_2 in tobacco

Marc Carriquí[a*,†], Cyril Douthe[a,†], Arántzazu Molins[b] and Jaume Flexas[a]

[a]Research Group on Plant Biology Under Mediterranean Conditions, Departament de Biologia, Universitat de les Illes Balears – Instituto de investigaciones Agroambientales y de la Economía del Agua (INAGEA), Palma 07122, Spain

[b]Departament de Botànica, ICBIBE & Jardí Botànic, Facultat de Ciències Biològiques, Universitat de València, Valencia 46100, Spain

Correspondence

*Corresponding author,

e-mail: m.carriqui@uib.cat

Received 6 March 2018;

revised 3 May 2018

doi:10.1111/ppl.12755

Mesophyll conductance to CO_2 (g_m), a key photosynthetic trait, is strongly constrained by leaf anatomy. Leaf anatomical parameters such as cell wall thickness and chloroplast area exposed to the mesophyll intercellular airspace have been demonstrated to determine g_m in species with diverging phylogeny, leaf structure and ontogeny. However, the potential implication of leaf anatomy, especially chloroplast movement, on the short-term response of g_m to rapid changes (i.e. seconds to minutes) under different environmental conditions (CO_2, light or temperature) has not been examined. The aim of this study was to determine whether the observed rapid variations of g_m in response to variations of light and CO_2 could be explained by changes in any leaf anatomical arrangements. When compared to high light and ambient CO_2, the values of g_m estimated by chlorophyll fluorescence decreased under high CO_2 and increased at low CO_2, while it decreased with decreasing light. Nevertheless, no changes in anatomical parameters, including chloroplast distribution, were found. Hence, the g_m estimated by analytical models based on anatomical parameters was constant under varying light and CO_2. Considering this discrepancy between anatomy and chlorophyll fluorescence estimates, it is concluded that apparent fast g_m variations should be due to artefacts in its estimation and/or to changes in the biochemical components acting on diffusional properties of the leaf (e.g. aquaporins and carbonic anhydrase).

Abbreviations – A, net photosynthesis; CA, carbonic anhydrases; C_c, chloroplast CO_2 concentration; C_i, substomatal CO_2 concentration; ETR, electron transport rate; f_{ias}, fraction of intercellular airspaces; g_m, mesophyll conductance; $g_{m,anat}$, mesophyll conductance inferred by anatomy measurements; g_s, stomatal conductance; IRGA, infrared gas analyser; J_{max}, maximum electron transport rate; L_{chl}, chloroplast length; l_{ias}, gas phase limitations to photosynthesis; l_i, liquid phase limitations to photosynthesis; LMA, leaf mass area; PPFD, photosynthetic photon flux density; p_{cw}, cell wall porosity; R_d, non-photorespiratory CO_2 release -respiration- in the light; S_c/S, chloroplast surface area exposed to intercellular airspaces per unit of leaf area; S_m/S, mesophyll surface area exposed to intercellular airspaces per unit of leaf area; T_{chl}, chloroplast thickness; T_{cw}, cell wall thickness; T_{cyt}, cytoplasm thickness; TEM, transmission electron microscopy; T_{leaf}, leaf thickness; T_{mes}, mesophyll thickness; $V_{c,max}$, maximum velocity of carboxylation.

[†]These authors equally contributed to this work.

Introduction

The rates of photosynthesis in vascular plants depend on the stomatal conductance (g_s), the mesophyll conductance to CO_2 (g_m) and the biochemical capacity to fix carbon. Mesophyll conductance has been widely estimated for hundreds of species, and its response to environmental changes (i.e. light, CO_2, temperature) has been reported. Two methods are the most widely recognised and used to assess g_m variations, the stable isotope method based on the discrimination of ^{13}C during photosynthesis (Evans 1989, Lloyd et al. 1992), and the variable J method based on leaf chlorophyll fluorescence (Harley et al. 1992). Both methods have revealed that g_m is finite and largely varying in response to environmental conditions, both in the short and long term, depending on the species and conditions (Flexas et al. 2012, Griffiths and Helliker 2013). However, the basics of g_m and its regulation are not fully understood, arising a continuous scientific debate. One of the major current controversies on g_m is whether the dynamic response of g_m to fast environmental changes (i.e. during a typical A-PAR or A-C_i curve) is real, apparent or even artefactual. On the one hand, g_m has been found to vary rapidly (within minutes) with changes in [CO_2] (Flexas et al. 2007b, Hassiotou et al. 2009, Yin et al. 2009, Douthe et al. 2011, 2012, Xiong et al. 2015), light (Hassiotou et al. 2009, Douthe et al. 2011, 2012, Xiong et al. 2015), or temperature (Yamori et al. 2006, von Caemmerer and Evans 2015). On the other hand, some studies did not found those rapid changes under light or CO_2 (Tazoe et al. 2009).

Assuming the observed fast changes of g_m are real, they should reflect a physiological process, which could be explained by at least two mechanisms. The first mechanism would imply that at least one of the anatomical resistances change, in seconds or minutes, significantly enough to modify g_m. The path for CO_2 starts from air-diffusion from the sub-stomatal cavity to the mesophyll cells, where it dissolves and continues by aqueous diffusion through the cell wall, plasma membrane, cytosol and chloroplast envelope. The two main anatomical determinants of g_m are the cell wall thickness (T_{cw}) and the chloroplast surface area exposed to the intercellular airspaces (S_c/S) (Evans et al. 2009, Tomás et al. 2013, Tosens et al. 2016). The estimation of anatomical parameters allowed the establishment of a simplified 1-D anatomical model of diffusion (a steady-state model) that gave estimations of g_m very close to those estimation from gas exchange (Peguero-Pina et al. 2017, Tomás et al. 2013, Tosens et al. 2012, 2016, Veromann-Jürgenson et al. 2017, Xiao and Zhu 2017), but potential rapid changes in anatomical arrangements in response to light or CO_2 have not been experimentally tested. The second mechanism implies that biochemical factors change resistances in the CO_2 pathway through the mesophyll. Such mechanism could be related with the diffusion facilitation provided by aquaporins across the plasma membrane and possibly chloroplast membrane (Uehlein et al. 2008, Heinen et al. 2009, Perez-Martin et al. 2014, Flexas and Diaz-Espejo 2015) and by carbonic anhydrase in the cytosol (Tholen and Zhu 2011, Ho et al. 2016, Momayyezi and Guy 2017).

Focusing on the first potential mechanism, most of the anatomical limitations are considered invariable in the short-term (Evans et al. 2009, Terashima et al. 2011). Indeed, it is difficult to imagine large enough changes in the cell wall composition in minutes to cause the observed changes in g_m. Thus, the main candidate to explain the observed rapid g_m changes from an anatomical point of view would be the movement of chloroplasts, which could induce changes in S_c/S (Oguchi et al. 2005, Tholen et al. 2008). Tholen et al. (2008) observed in *Arabidopsis thaliana* that a short-term increase of blue light intensities produced a reduction of S_c/S to avoid photodamage, which resulted in changes of g_m as measured by the online ^{13}C method. Similarly, transferring sun plants from low to high growth irradiance, Oguchi et al. (2005) described that, in leaves of deciduous species, an increase of S_c/S provoked by the movement of the chloroplast towards intercellular airspaces was linked with an increase of photosynthesis. Species-dependent behaviour can be the cause of such apparent discrepancies, highlighting the need of further studies in this topic (Higa and Wada 2016, Ho et al. 2016, Théroux-Rancourt and Gilbert 2017). Moreover, to date there is no direct measurement of the potential change of chloroplast surface area exposed to intercellular airspace during an A-PAR or A-Ci curve, which would help to elucidate this debate.

If anatomy cannot explain apparent the fast variations of g_m, there are two options remaining: (1) either biochemical factors modifying g_m without any anatomical changes, or (2) apparent g_m variations do not reflect a 'true' biological process. The latter may be originated by a 'mathematical artefact' and/or by an 'over-simplification' of the model used. Mathematical dependencies of the output (here g_m) on the values of other variables (mainly A and C_i) used to compute it, can provoke 'artefactuals' estimates (Gu and Sun 2014). Indeed, the shape of the equations used (Harley et al. 1992, Lloyd et al. 1992) can produce a systematic relationship between A or C_i and g_m (and any other variable that can vary with them, including light), producing erroneous g_m estimates. The use of wrong values of Γ^* and/or R_d can also produce such

artefact (an obligatory relationship between g_m and C_i, for example). Secondly, wrong estimates can be obtained by 'over-simplification', i.e. when the hypothesis of the model behind is wrong, or are too simplified when compared to 'reality'. For example, Tholen and Zhu (2011) claimed that the possibility of CO_2 recycling during photosynthesis, especially under low light/CO_2, would affect apparent g_m estimates and should be taken into account, as well as the importance of the resistance of the chloroplast membrane. In this case, 3D modelling could help to take into account position and number of mitochondria and the subsequent CO_2 fluxes between chloroplast and mitochondria (Xiao and Zhu 2017). Later, Yin and Struik (2017) proposed a generalised model including/improving the claims of Tholen and Zhu (2011), adding new parameters to the model to reflect the mitochondrial positioning in respect to the chloroplast membrane. The light gradient through the leaf profile has also been identified as a key parameter that strongly influences photosynthesis efficiency (Terashima and Saeki 1985, Vogelmann et al. 1989, Evans and Vogelmann 2003). Those light gradients through the leaf profile are also likely to produce distinct contributions of each layer to the mesophyll, producing apparent (i.e. not reflecting the 'true' biological) variations of g_m at different measuring lights (Evans 2009, Théroux-Rancourt and Gilbert 2017). Several recent studies also focused on light gradients or integrate the influence of photorespired CO_2 in a generalised model for g_m. Nevertheless, up to present, the proposed models are either based on a theoretical approach alone, or they contain numerous parameters that are difficult to estimate.

The aim of this study is to experimentally test whether the observed fast changes of g_m in a typical A-PAR or A-C_i curve could be totally or partially due to anatomical changes. Furthermore, the relationship between g_m values estimated by either the fluorescence or by two analytical models based on anatomical parameters was also investigated.

Materials and methods

Seeds of tobacco (*Nicotiana tabacum* L.) were sowed and germinated in a tray with horticultural substrate and placed in a growth chamber with a 12/12 h light/dark regime and temperature fixed at 25/20°C day/night. Seedlings were watered every 2 days. After 2 weeks, seedlings were transferred in 4-l pots containing organic soil and perlite (75:25 v:v). Plants were grown under low to moderate light intensity at plant height for this species (Flexas et al. 2006, Galmés et al. 2006, Galle et al. 2009), 300 µmol m^{-2} s^{-1} photosynthetic photon flux density (PPFD 1000 W HPS lamps, OSRAM), and maintained under optimal water conditions, watered with 25% Hoagland's solution twice a week. Growing light intensity was chosen, on the one hand, to avoid a possible loss of functionality of the chloroplast avoidance movement, as observed by Higa and Wada (2016) in leaves of climbing plants grown under strong light. On the other hand, the objective was to obtain a leaf mass per area (LMA) in the lower range of reported values in bibliography for this species (Flexas et al. 2006). Lower LMA implies lower leaf thickness and simpler mesophyll structure (Poorter et al. 2009), minimising the potential bias between chlorophyll fluorescence with gas exchange caused by contrasting photosynthetic contribution of different cell layers (Evans 2009, Théroux-Rancourt and Gilbert 2017) and/or by blue light absorption close to the illuminated surface (Evans and Vogelmann 2003, Brodersen and Vogelmann 2010). Measuring light intensities (200, 600 and 1500 µmol m^{-2} s^{-1}) were chosen to respond to two constraints: we could not use too extreme low light, because it could produce unreliable values of g_m, while the high light treatment should be far enough to induce chloroplast movements if these were a response to varying CO_2. Measurements were performed on 40–50 days old plants. All measurements were performed on the first or second youngest fully expanded leaf to ensure mature leaf anatomy and to avoid age variations between the plants.

Gas exchange and chlorophyll fluorescence measurement

Leaf gas exchange parameters were measured using a portable photosynthesis system (Li-6400; Li-Cor, Inc., Lincoln, NE) with an infrared gas analyser (IRGA) coupled with a 2 cm^2 leaf fluorescence chamber (Li −6400-40 leaf chamber fluorometer; Li-Cor, Inc.) All measurements were carried out between 09:00 and 19:00 h (Central European summer time). Block temperature was fixed at 25°C, air flow rate at 300 µmol min^{-1} and VPD kept around 1.5 kPa for all measurements.

Leaves from randomly selected plants were fully characterised. Leaf steady-state conditions were induced at 400 µmol CO_2 mol^{-1} air and saturating PPFD (1500 µmol m^{-2} s^{-1}, 90:10 red:blue light). Once steady state conditions were achieved, always after 15–20 min, complete light and CO_2 response curves at 21 and 2% O_2 were performed in a random order. Light response curves were measured at 400 µmol CO_2 mol^{-1} air at PPFD of 2000, 1500, 1000, 800, 600, 400, 200, 150, 100, 50 and 0 µmol m^{-2} s^{-1}. CO_2 response curves were measured at PPFD 1500 µmol m^{-2} s^{-1} at cuvette CO_2 concentration (C_a) of 400, 300, 200, 150, 100, 50, 0, 400, 400, 600, 800, 1000, 1200, 1500 and

Table 1. Light and CO_2 conditions in the photosynthesis chamber of the Li-6400 for each treatment applied

Treatment	[CO_2] entering the chamber (µmol mol^{-1})	PPFD (µmol photons m^{-2} s^{-1})
LCO_2	100	1500
MCO_2/HL	400	1500
HCO_2	1500	1500
LL	400	200
ML	400	600

2000 µmol mol^{-1}. Four to five curves were performed per response curve type. The order in which curves were performed did not affect the responses (data not shown). Non-photorespiratory respiration during the day (R_d) was estimated by dividing by 2 the respiration rate measured after 2 h of darkness (Niinemets et al. 2005, Martins et al. 2013, Veromann-Jürgenson et al. 2017). Any measurement performed at a non-ambient [CO_2] was corrected for leaks following Flexas et al. (2007a).

Once homogeneous responses among plants at the same conditions were verified with both light and CO_2 response curves, leaves from randomly selected plants were short-term acclimated (10–15 min) to a specific light and CO_2 treatment. Five treatments were applied, consisting of three light intensities (low, moderated and saturating), ambient C_a, and low and high C_a at saturating light (see Table 1 for each conditions applied). After the acclimation period, five logs were recorded at approximately 1 min interval. Directly after measurements, the exact portion of leaf that was inside the Li-6400-40 chamber was sampled and instantaneously (below 30 s) cut into small pieces after immersion under fixator for subsequent anatomical measurements. This procedure was repeated on 6–8 different plants per treatment.

Values of A and steady-state fluorescence (F_s) were registered just after the steady-state conditions for gas exchange were achieved. Then a saturating white light flash around 8000 µmol m^{-2} s^{-1} was applied to determine the maximum fluorescence (F_m'). Multiphase flash methodology for chlorophyll fluorescence measurements was followed, as suggested by Loriaux et al. (2013), to avoid potential maximum yield underestimation error. The electron transports rate (ETR) was estimated from Genty et al. (1989) as ETR = PPFD × ΦPSII × α × β, being ΦPSII the efficiency of photo-system II, α the leaf absorbance and β the electrons partitioning between photo-systems I and II. ΦPSII was estimated as ΦPSII = (F_m'-F_s)/F_m' (Genty et al. 1989). The $\alpha \cdot \beta$ parameter was estimated following (Valentini et al. 1995). CO_2 response curves under non-photorespiratory conditions in a low O_2 atmosphere (<2%) were performed in order to establish the relationship between ΦPSII and ΦCO_2 under non-photorespiratory conditions (with $\Phi CO_2 = (A + R_d)/PPFD$), then considering $\alpha \times \beta = 4/b$ where b is the slope of the ΦPSII to ΦCO_2 relationship. We obtained $\alpha \times \beta = 0.44$. Then, g_m was estimated following Harley et al. (1992), as:

$$g_m = \frac{A}{\frac{\Gamma^*(ETR+p2(A+R_d))}{(ETR+p1(A+R_d))}} \quad (1)$$

where A is the net assimilation rate, Γ^* is CO_2 compensation point in absence of R_d, and C_i the CO_2 concentration in intercellular air spaces. Γ^* was assumed to be 40 µmol mol^{-1} in *N. tabacum* as in Walker et al. (2013). Values of p1 and p2 depend on the limited steps of RuBP regeneration. In this study we assumed that RuBP regeneration is limited by NADPH, so $p_1 = 4$ and $p_2 = 8$, but another two combinations were used in a sensitivity analysis ($p_1 = 4$ and $p_2 = 9.33$ and $p_1 = 4.5$ and $p_2 = 10.5$) for ATP limited regeneration (Gu and Sun 2014). After calculation, g_m data were filtered following the reliability criterion established by Harley et al. (1992), in which only data with values of dC_c/dA_N between 10 and 50 can be considered as reliable. Moreover, in order to try to get an improved estimate of g_m, the method proposed by Yin et al. (2009) was tested, as:

$$A = 0.5\left\{\frac{J}{4} - R_d + g_m(C_i + 2\Gamma_*) - \sqrt{\left[\frac{J}{4} - R_d + g_m(C_i + 2\Gamma_*)\right]^2 - 4g_m\left[(C_i - \Gamma_*)\frac{J}{4} - R_d(C_i + 2\Gamma_*)\right]}\right\} \quad (2)$$

and

$$A = \frac{C_i - \frac{A}{g_m} - \Gamma_*}{4\left(C_i - \frac{A}{g_m} + 2\Gamma_*\right)} - R_d \quad (3)$$

In both cases of Eqns. 2 and 3, g_m was solved with a solver in order to match the predicted A from Eqns. 2 and 3 with the measured A.

Leaf mass per unit area

Leaf discs of known area were taken from measured leaves and placed in an oven at 60°C until constant dry weight was reached to calculate the dry leaf mass per unit leaf area (LMA).

Anatomical measurements

Immediately after gas-exchange measurements, small leaf pieces (3 × 1 mm) of the area enclosed in the leaf chamber were cut off between the main veins per sample and immersed under the fixing solution. In order

to prevent any anatomical change that may occur during cuts, when this process took more than 30 s the sample was discarded. Samples were quickly fixed with glutaraldehyde 4% and paraformaldehyde 2% in a 0.1 M phosphate buffer (pH 7.4) under vacuum pressure. Between 4 and 6 samples were taken per treatment. Afterwards, samples were post-fixed in 2% buffered osmium tetroxide for 2 h, and dehydrated in a graded series of ethanol. Dehydrated samples were embedded in resin (LRwhite, London Resin Company, London, UK) and solidified in an oven at 60°C for 48 h.

Semi-thin cross-sections of 0.8 µm and ultrathin cross-sections of 90 nm for transmission electron microscopy (TEM) were cut with an ultramicrotome (Leica UC6, Vienna, Austria). Semi-thin sections were dyed with 1% toluidine blue and observed at 200× magnifications under an Olympus BX60 (Olympus, Tokyo, Japan) light microscopy and photographed with a Moticam 3 (Motic Electric Group Co., Xiamen, China). The ultrathin sections were contrasted with uranyl acetate and lead citrate and viewed at 1200× and 30 000× magnifications with a transmission electron microscopy (TEM H600; Hitachi, Tokyo, Japan). All images were analysed using ImageJ software (Schneider et al. 2012). From light microscopy images leaf thickness (T_{leaf}), mesophyll thickness (T_{mes}), number of palisade layers and fraction of the mesophyll occupied by intercellular airspaces (f_{ias}) were measured. From TEM microscopy images cell wall thickness (T_{cw}), cytoplasm thickness (T_{cyt}), chloroplast length (L_{chl}), chloroplast thickness (T_{chl}) and mesophyll and chloroplast surface area exposed to intercellular airspace (S_m/S and S_c/S) were measured and calculated following Tomás et al. (2013). Cell curvature correction factor was calculated according to Thain (1983). Factors between 1.18 and 1.38 were applied to cell surface area estimates, depending on whether the measurement was performed in palisade (prolate spheroids) or spongy (oblate spheroids) mesophyll tissue. Four to six randomly selected different fields of view were considered per plant replicate to measure each anatomical characteristic. For each type of mesophyll tissue (spongy and palisade), 10 measurements were made for T_{leaf}, T_{mes}, f_{ias}, T_{cw}, S_m/S and S_c/S, and 15 measurements per mesophyll type were made for L_{chl} and T_{chl}. Then, weighted averages based on tissue volume fractions were calculated.

Estimation of mesophyll conductance modelled from anatomical characteristics

Analytical models for mesophyll conductance modelling of Niinemets and Reichstein (2003) and Xiao and Zhu (2017) were applied. The one-dimensional within-leaf gas diffusion model of Niinemets and Reichstein (2003) modified by Tomás et al. (2013) was applied. Mesophyll diffusion conductance as a composite conductance for within-leaf gas, liquid and lipid components is given as:

$$g_m = \frac{1}{\frac{1}{g_{ias}} + \frac{RT_k}{H \cdot g_{liq}}} \quad (4)$$

where H is the Henry's law constant ($m^3\ mol^{-1}\ K^{-1}$), R is the gas constant ($Pa\ m^3\ K^{-1}\ mol^{-1}$) and T_k is the absolute temperature (K). $H/(RT_k)$ is the dimensionless form of Henry's law constant needed to convert a liquid and lipid phase conductance (g_{liq} and g_{lip}) into a gas-phase equivalent conductance (Niinemets and Reichstein 2003). Gas-phase diffusion depends on the fraction of mesophyll volume occupied by intercellular airspaces (f_{ias}, $m^3\ m^{-3}$,) and the effective diffusion path length in the gas-phase (ΔL_{ias}) (Syvertsen et al. 1995, Terashima et al. 2011):

$$g_{ias} = \frac{D_a \cdot f_{ias}}{\Delta L_{ias} \cdot \varsigma} \quad (5)$$

where ς is the diffusion path tortuosity ($m\ m^{-1}$) and D_a ($m^2\ s^{-1}$) is the diffusion coefficient for CO_2 in the gas-phase ($1.51 \cdot 10^{-5}\ m^2\ s^{-1}$ at 22°C). ΔL_{ias} was approximated by mesophyll thickness divided by two (Niinemets and Reichstein 2003). An estimate of ς was used as a default value of $1.57\ m\ m^{-1}$ (Syvertsen et al. 1995, Niinemets and Reichstein 2003). The total liquid phase conductance is provided by the sum of the inverse of serial conductances:

$$\frac{1}{g_{liq}} = \left(\frac{1}{g_{cw}} + \frac{1}{g_{pl}} + \frac{1}{g_{ct}} + \frac{1}{g_{en}} + \frac{1}{g_{st}} \right) \cdot S_c/S \quad (6)$$

where partial conductances are for cell wall (g_{cw}), plasmalemma (g_{pl}), cytosol (g_{ct}), chloroplast envelope (g_{en}), and chloroplast stroma (g_{st}). The cell wall, cytosol and stromal conductances are given by a general equation:

$$g_i = \frac{r_{f,i} \cdot D_w \cdot p_i}{\Delta L_i} \quad (7)$$

where g_i ($m\ s^{-1}$) is either g_{cw}, g_{ct} or g_{st}, ΔL_i (m) is the diffusion path length and p_i ($m^3\ m^{-3}$) is the effective porosity in the given part of the diffusion pathway, D_w is the aqueous phase diffusion coefficient for CO_2 ($1.90 \cdot 10^{-9}\ m^2\ s^{-1}$ at 22 °C) and the dimensionless factor $r_{f,i}$ accounts for the decrease of diffusion conductance compared to free diffusion in water (Weisiger 1998). For cell walls where the aqueous-phase diffusion has been shown to approximate free water, $r_{f,i} = 1$ (Rondeau-Mouro et al. 2008). The value of r_f was set at 0.3 for g_{ct} and g_{st} to account for the reduction of diffusion conductance due to high concentrations of high

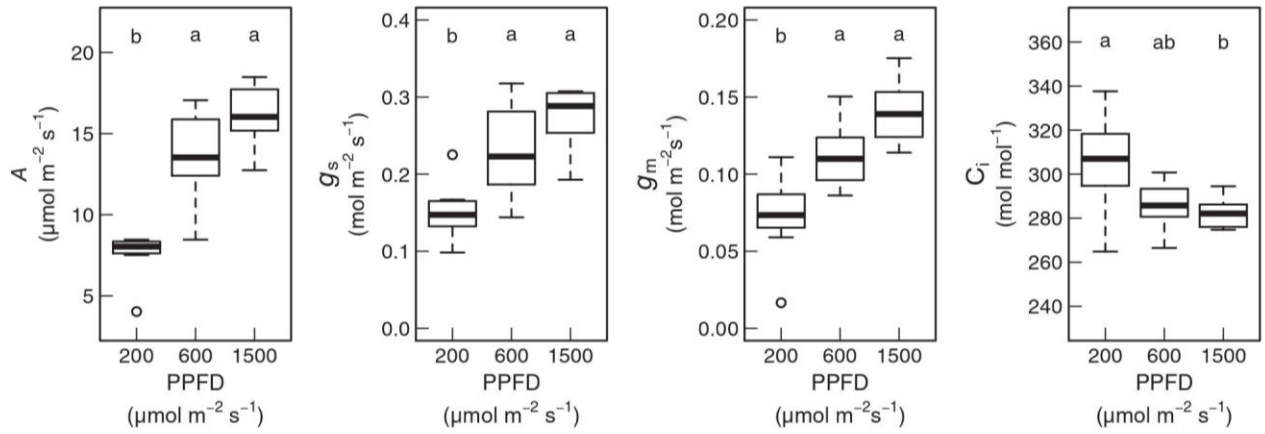

Fig. 1. Box plots of net CO_2 assimilation rate (A), stomatal conductance (g_s) and mesophyll conductance (g_m) for each low light (LL; 200 μmol photons m^{-2} s^{-1}), medium light (ML; 600 μmol photons m^{-2} s^{-1}) and high light (HL; 1500 μmol photons m^{-2} s^{-1}) treatment. The two extreme lines of the boxplot (*whiskers*) show the 10 and 90% percentiles, the two bounds of the box the 25 and 75% percentiles, and the centre thick line the median. Dots represent data out of the shown percentiles. Leaf inside the Li-6400 photosynthesis chamber was kept at least 15 min in the given environmental condition. Letters indicate significant differences following Tukey's post-hoc test, at $P < 0.05$. n = 6–7.

molecular solutes and intracellular (cytoskeleton) and intraorganellal (thylakoids) heterogeneities (Niinemets and Reichstein 2003). Effective porosity, p_i, was taken as 1 for g_{ct} and g_{st}. Cell wall porosity (p_{cw}) was taken as 0.1, as applied in (Tomás et al. 2014). Conductance in units of m s^{-1} can be converted into molar units considering that

$$g\left[\mathrm{mol\,m^{-2}\,s^{-1}}\right] = g\left[\mathrm{m\,s^{-1}}\right] 44.6 \cdot [273.16/(273.16 + T_L)]\,(P/101.325)$$

where T_L is the leaf temperature (°C) and P (Pa) is the air pressure.Due to the difficulty to measure the thickness of the plasma membrane, the chloroplast envelope and the limited information about the permeability of the lipid phase membranes, g_{pl} and g_{env} were assumed as constant values (0.0035 m s^{-1}) as previously suggested in other studies (Evans et al. 1994, Peguero-Pina et al. 2012, Tosens et al. 2012a, 2012b, Tomás et al. 2013).The analytical model of Xiao and Zhu (2017) is based on the Niinemets and Reichstein (2003) model, considering besides the effect of CO_2 diffusion the process of hydration, biochemical parameters describing carbonic anhydrases (CA) and the environmental variables A, Ci, HCO_3^- leakage across the chloroplast envelope, the mitochondrial respiration and photorespiration rate and the relative position between chloroplasts and mitochondria. Assumed biophysical parameters for the diffusion properties of CO_2 in each subcellular resistance considered in the first analytical model were maintained when applying the Xiao and Zhu (2017) model. Other assumptions needed for the Xiao and Zhu (2017) model were used as in the cited paper. Unit conversions needed for fluxes conversion were applied as described in Methods S1. The relative position between mitochondria and chloroplasts could not be measured from ultrathin cross-section images, so a sensitivity analysis changing the fractionation factor for CO_2 (photo)respiration recycling from 0 to 1 was performed.

Statistical analysis

Independent one-way ANOVA was performed to check differences between treatments, for both light and CO_2 treatments. Differences between means were detected by Tukey's honest significant difference tests (with accepted $P < 0.05$). Pearson correlation matrices were determined for each group of treatments to determine the correlations between the different parameters. All analyses were performed with the R software (R Core Team 2016). Tukey's post hoc tests were performed using the R 'agricolae' package (Mendiburu 2015).

Results

Variation in photosynthetic parameters

Under ambient conditions (C_a 400 μmol CO_2 mol^{-1} air and PPFD 1500 μmol m^{-2} s^{-1}), plants showed net assimilation rate (A) of 16.7 μmol m^{-2} s^{-1}, stomatal conductance for water (g_s) of 0.28 mol m^{-2} s^{-1} and mesophyll conductance (g_m) of 0.14 mol m^{-2} s^{-1} (Fig. 1). A, g_s and g_m all decreased with decreasing light. This induced a slight decrease of C_i between low and high light treatments. In all cases, no differences were found between 1500 and 600 μmol m^{-2} s^{-1}

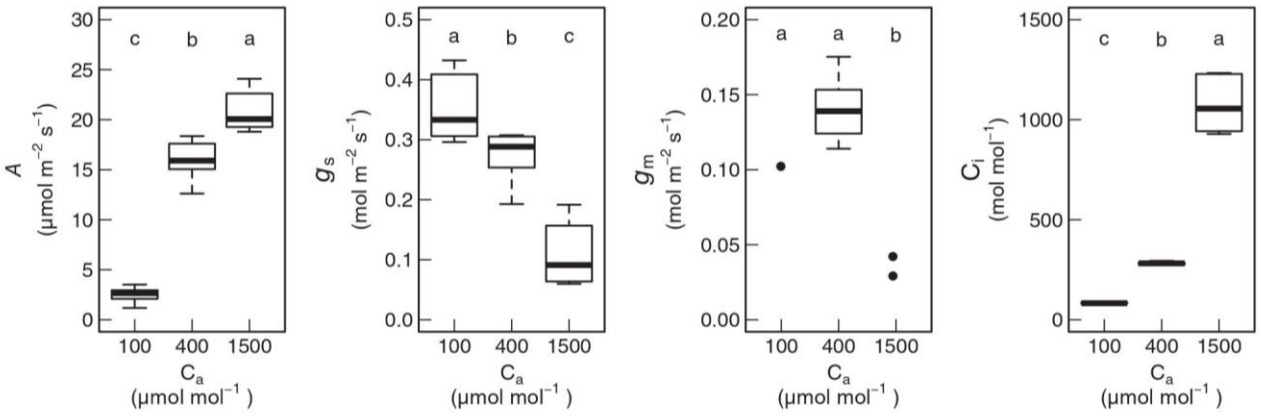

Fig. 2. Box plots of net CO_2 assimilation rate (A), stomatal conductance (g_s) and mesophyll conductance (g_m) for each low CO_2 (LCO_2; 100 ppm CO_2), medium CO_2 (MCO_2; 400 ppm CO_2) and high CO_2 (HCO_2; 1500 ppm) treatment. The two extreme lines of the boxplot (*whiskers*) show the 10 and 90% percentiles, the two bounds of the box the 25 and 75% percentiles, and the centre thick line the median. Dots represent data out of the shown percentiles. Leaf inside the Li-6400 photosynthesis chamber was kept at least 15 min in the given environmental condition. Letters indicate significant differences following Tukey's post-hoc test, at $P < 0.05$. n = 6–8, except for g_m under 100 ppm (n = 1) and 1500 ppm (n = 2) after filtering for Harley's criteria. All the g_m data (not filtered for Harley's criteria) are presented in Fig. S1.

PPFD, but differences were significant between 600 and 200 μmol m^{-2} s^{-1} PPFD (Fig. 1). When C_a was increased from ambient to 1500 μmol CO_2 mol^{-1} air, A significantly increased from 16.7 to 20.6 μmol m^{-2} s^{-1}, and both g_s and g_m decreased to 0.07 and 0.03 mol m^{-2} s^{-1}, respectively (Fig. 2). Statistical differences between the treatment at 100 μmol CO_2 mol^{-1} and the other two concentrations could not be proved, as only 1 data point for the low CO_2 passed the filtering of the Harley's criterion. Nevertheless, we observed that g_m data for 100 μmol CO_2 mol^{-1} were of the same range as at ambient CO_2, or even higher (Fig. S2). Statistical differences between g_m averages obtained for the different CO_2 and light treatments were corroborated by a sensitivity analysis performed for each variable needed for g_m estimation (Fig. S3). We also found the same range of values of g_m when estimated with the Yin et al. (2009) method (Fig. S4).

Variation in leaf anatomy and chloroplast arrangement

In order to identify any hypothetical change in the CO_2 pathway length from the substomatal cavity to the carboxylation site inside the chloroplast, a complete structural and ultrastructural analysis was performed of the photosynthetic organs in each short-term CO_2 and light variation. Little variability was observed in structural and ultrastructural parameters in response to CO_2 or light changes (Fig. S5 and Tables 1 and 2, respectively). LMA, which was not expected to change in the short-term range, was of 22 ± 2 g m^{-2}. Non-significant changes for most leaf anatomical parameters were found among CO_2 treatments (T_{leaf}, T_{mes}, number of palisade layers, f_{ias}, S_m/S, S_c/S, S_c/S_m, T_{cw}, T_{cyt} and L_{chl}; Table 2 and Fig. S5) except for chloroplast thickness (T_{chl}), which ranged from 2.81 ± 0.06 μm at 100 μmol CO_2 mol^{-1} air CO_2 to 3.44 ± 0.10 μm at 400 μmol CO_2 mol^{-1} air CO_2. Regarding to light treatments (Table 3 and Fig. S5), non-significant changes were observed in leaf anatomy except for chloroplast length (L_{chl}), which increased significantly from low light treatment (5.60 ± 0.22 μm) to high light treatments (and 6.28 ± 0.13 μm, respectively), although no significant differences were found between moderate light (5.70 ± 0.12 μm) and either low or high light treatments. No significant differences were found between light and CO_2 treatments for g_m as modelled from anatomy following Tomás et al. (Tomás et al. 2013; Tables 2 and 3). Consequently, no relationship was found between g_m modelled following Tomás et al. (2013) and g_m estimated following Harley et al. (Harley et al. 1992; Figs. 3A, 4). Considering S_c as the main determinant for g_m short-term variation, a theoretical fitting model revealed that S_c should vary between 0 and 12 m^2 m^{-2} in order to explain the observed short-term variation of g_m as estimated following Harley et al. (Harley et al. 1992; Fig. 3A, B). If potential changes in plasma membrane conductance (g_{pl}) were considered as the main determinant of g_m short-term variation, g_{pl} should have varied between 0.00 and 0.14 mol m^{-2} s^{-1} (Fig. 3C, D). We can note that only the lower values of g_m were very close to the 1:1 relationship, the highest values were impossible to fit with Harley's method. Marginally significant correlation ($P < 0.1$) was obtained between g_m modelled following Xiao and Zhu (2017) and that estimated following Harley et al. (Harley et al. 1992; Fig. 4). However,

Table 2. Leaf thickness (T_{leaf}), total mesophyll thickness (T_{mes}), number of palisade layers, fraction of the mesophyll occupied by the intercellular airspaces (f_{ias}), mesophyll surface area exposed to intercellular airspace (S_m/S), chloroplast surface area exposed to intercellular airspace (S_c/S), the ratio S_c/S_m, mesophyll cell wall thickness (T_{cw}), cytoplasm thickness (T_{cyt}), chloroplast length (L_{chl}), chloroplast thickness (T_{chl}) and mesophyll conductance to CO_2 modelled by anatomy (g_m anatomy) in tobacco leaves subjected to a short-term 100 ppm (LCO_2), 400 ppm (MCO_2) and 1500 ppm (HCO_2) CO_2 treatment. Data are mean ± SE (n = 4–6). Different letters indicate statistically significant differences ($P < 0.05$) between treatments. In bold the only significant change observed between treatments

Parameters	LCO_2	MCO_2	HCO_2
T_{leaf} (µm)	211 ± 8^a	205 ± 8^a	206 ± 12^a
T_{mes} (µm)	172 ± 7^a	170 ± 6^a	170 ± 9^a
Number of palisade layers	1.25	1.05	1.10
f_{ias}	0.41 ± 0.01^a	0.43 ± 0.01^a	0.43 ± 0.01^a
S_m/S (m^2 m^{-2})	10.4 ± 0.5^a	10.1 ± 0.8^a	11.4 ± 0.2^a
S_c/S (m^2 m^{-2})	7.7 ± 0.3^a	8.0 ± 0.7^a	9.1 ± 0.1^a
S_c/S_m	0.74 ± 0.03^a	0.81 ± 0.05^a	0.80 ± 0.00^a
T_{cw} (µm)	0.122 ± 0.012^a	0.128 ± 0.007^a	0.122 ± 0.003^a
T_{cyt} (µm)	0.28 ± 0.003^a	0.30 ± 0.02^a	0.38 ± 0.04^a
L_{chl} (µm)	5.05 ± 0.19^a	5.60 ± 0.22^a	5.26 ± 0.13^a
T_{chl} (µm)	**2.81 ± 0.06^a**	**3.44 ± 0.10^b**	**3.08 ± 0.17^{ab}**
g_m Anatomy (mol m^{-2} s^{-1})	0.086 ± 0.005^a	0.078 ± 0.005^a	0.093 ± 0.005^a

Table 3. Leaf thickness (T_{leaf}), total mesophyll thickness (T_{mes}), number of palisade layers, fraction of the mesophyll occupied by the intercellular airspaces (f_{ias}), mesophyll surface area exposed to intercellular airspace (S_m/S), chloroplast surface area exposed to intercellular airspace (S_c/S), the ratio S_c/S_m, mesophyll cell wall thickness (T_{cw}), cytoplasm thickness (T_{cyt}), chloroplast length (L_{chl}), chloroplast thickness (T_{chl}) and mesophyll conductance to CO_2 modelled by anatomy (g_m anatomy) in tobacco leaves subjected to a short-term light treatment of 200 (LL), 600 (ML) or 1500 µmol m^{-2} s^{-1} (HL) light treatment. Data are mean ± SE (n = 4–6). Different letters indicate statistically significant differences ($P < 0.05$) between treatments. In bold the only significant change observed between treatments

Parameters	LL	ML	HL
T_{leaf} (µm)	195 ± 6^a	200 ± 11^a	205 ± 8^a
T_{mes} (µm)	164 ± 6^a	165 ± 10^a	170 ± 6^a
Number of palisade layers	1.12	1.13	1.05
f_{ias}	0.42 ± 0.02^a	0.43 ± 0.02^a	0.43 ± 0.01^a
S_m/S (m^2 m^{-2})	11.0 ± 0.4^a	10.4 ± 0.5^a	10.1 ± 0.8^a
S_c/S (m^2 m^{-2})	8.3 ± 0.3^a	7.6 ± 0.6^a	8.0 ± 0.7^a
S_c/S_m	0.77 ± 0.03^a	0.73 ± 0.04^a	0.81 ± 0.05^a
T_{cw} (µm)	0.119 ± 0.008^a	0.108 ± 0.006^a	0.128 ± 0.007^a
T_{cyt} (µm)	0.27 ± 0.005^a	0.25 ± 0.02^a	0.30 ± 0.02^a
L_{chl} (µm)	**6.28 ± 0.13^b**	**5.70 ± 0.12^{ab}**	**5.60 ± 0.22^a**
T_{chl} (µm)	3.35 ± 0.08^a	3.28 ± 0.12^a	3.44 ± 0.10^a
g_m Anatomy (mol m^{-2} s^{-1})	0.084 ± 0.005^a	0.081 ± 0.006^a	0.078 ± 0.005^a

any weak correlation disappeared when partial or total CO_2 recycling from (photo)respiration was being considered (Fig. S7).

Discussion

Photosynthetic parameters and their response to CO_2 and light variations

Values of net assimilation rate and other photosynthetic traits were within the ranges usually described in the literature (Flexas et al. 2006, 2007b, Galle et al. 2009). The response of g_m observed in *Nicotiana tabacum* (Fig. S1) was the same as typically found in the literature for both CO_2 and light changes, with an expected curvilinear decrease with increasing C_i and an increase with increasing light (Figs 1 and 2). This fits well with the responses already described for different species, using either the Harley method or the isotope discrimination method (Flexas et al. 2008, Hassiotou et al. 2009, Yin et al. 2009, Douthe et al. 2011, 2012, Xiong et al. 2015). Usually, the apparent g_m response to light describes a curvilinear response, with a saturation plateau at high PPFD (Yin et al. 2009, Douthe et al. 2011). This could explain why no significant differences were found for g_m between 600 and 1500 µmol m^{-2} s^{-1}. When Harley et al. (1992) developed their model, they warned about g_m values measured at low or high [CO_2] and the possibility that they may not be reliable, providing a mathematical criterion to discern the reliability of the data.

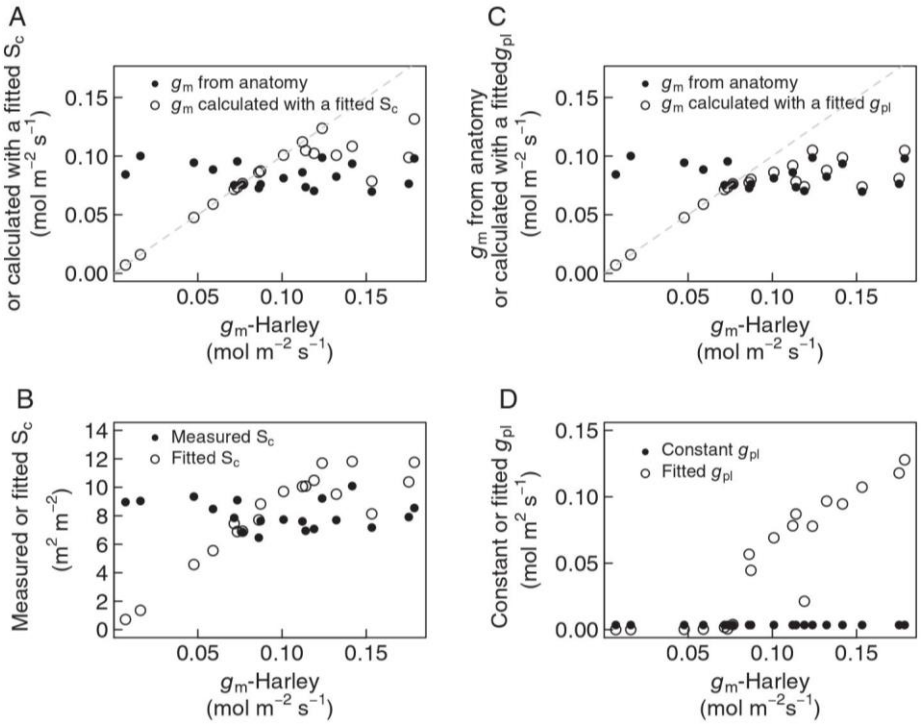

Fig. 3. Comparison of g_m calculated based on Harley et al. (1992) with g_m modelled from anatomy estimated according to the diffusion model from Tosens et al. (2012, Tosens et al. 2016). In (A) closed circles represent the estimated g_m from anatomy, while open circles are simulated g_m anatomy using a variable fitted chloroplast surface area exposed to intercellular airspaces (S_c/S); in (B) the observed S_c/S (closed circles) and the required S_c/S to match g_m anatomy to g_m Harley (open circles) are represented; in (C) closed circles represent the estimated g_m from anatomy, while open circles are simulated g_m anatomy using a variable fitted plasma membrane conductance (g_{pl}); in (D) the assumed g_{pl} (closed circles) and the required g_{pl} to match g_m anatomy to g_m Harley (open circles) are represented. Each point corresponds to an individual replicated plant for the five combinations of CO_2 and light treatments.

The application of this criterion to our data caused the removal of the vast majority of data measured at low C_i and some at high C_i. Nevertheless, it could be observed that those values were respecting the common pattern usually observed: g_m tends to increase at low C_i and is strongly decreased at $C_i > 1000$ µmol mol^{-1}. Altogether, the results confirm that a typical apparent [CO_2] and light g_m response described thus far was obtained.

Leaf anatomical parameters and the absence of response to CO_2 and light variations

No previous work has shown a detailed quantitative anatomical analysis in *N. tabacum*, although most of the parameters determined in the present study are within the expected range for non-sclerophyll, thin leaves (Tomás et al. 2013). Tobacco leaves, even after being subjected to short-term acclimation to different CO_2 and light treatments to induce fast changes in g_m, did not experienced significant changes in most anatomical parameters (Tables 2 and 3). Indeed, most of them have been suggested to be invariable in the short-term (Evans et al. 2009, Terashima et al. 2011). The only significant change was observed in the chloroplast shape. Chloroplasts had lower thickness at low light and higher length at high CO_2 (Table 2). This could be associated to changes in chloroplast from face to profile position, as a chloroplast avoidance effect (Trojan and Gabrys 1996, Kasahara et al. 2002). Even so, it would be possible that during the time elapsed between taking the sample from the IRGA chamber and the fixation (below 30 s), any additional anatomical differences having possibly occurred could have been reversed. Despite these small changes in chloroplast arrangement between different treatments, chloroplast surface area exposed to intercellular airspaces per unit of leaf area (S_c) did not significantly change among light or CO_2 treatments.

Being S_c/S one of the major anatomical determinants of g_m (Evans et al. 2009, Terashima et al. 2011, Tomás et al. 2013, Tosens et al. 2016, Peguero-Pina et al. 2017), the extent of S_c/S variation that would independently explain the variation of g_m estimated via the Harley's

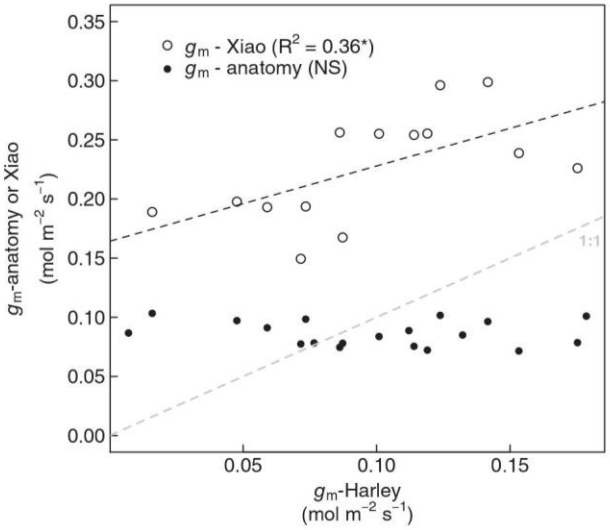

Fig. 4. Comparison of mesophyll conductance calculated from analytical models of Xiao and Zhu (2017; open circles) and Tomás et al. (2013; closed circles) in relation to mesophyll conductance calculated based on Harley et al. (1992). Grey dashed line represents 1:1 correlation.

method (Fig. 3A, B) was analysed. The measured S_c/S was 6–8 m^2 m^{-2}, while it should have varied between 0 and 12 m^2 m^{-2} in order to obtain a modelled $g_{m,anatomy}$ similar to the variable g_m observed by the variable J method (Harley et al. 1992; Fig. 3A, B). A similar simulation was performed for plasma membrane conductance (g_{pl}), as plasma membrane aquaporins could potentially affect the g_m short-term variations by modifying g_{pl}. While for the $g_{m,anatomy}$ modelling, a constant value of 0.0035 m s^{-1} was assumed, g_{pl} should have varied between 0.00 and 0.14 m s^{-1} in order to bring closer anatomical and Harley's g_m (Fig. 3C, D). Even under these circumstances, the highest g_m values were still impossible to be fitted. In both cases, the huge range of variations needed for S_c/S and g_{pl} to fit Harley g_m seems unreliable in the short-term. These results, based on measurements and simulations, tend to invalidate the possibility that fast changes of Harley's g_m observed in a typical A-PAR or A-C_i curve could be primarily associated to anatomical and/or aquaporin CO_2 diffusion changes in the CO_2 diffusion pathway through the mesophyll. Considering one of the recently published analytical models (Xiao and Zhu 2017), which incorporates to the 1-D diffusion model of Niinemets and Reichstein (2003) for g_m modelling additional variables such as measured gas exchange fluxes, (photo)respiration rates, carbonic anhydrase activities and HCO_3^- leakage, only a slight improvement was found when correlated with Harley et al. (1992). Marginal correlation ($R^2 = 0.36$) and far from the 1:1 relationship was obtained when considering both CO_2 and light treatments together but no (photo)respiration fractionation effect (Fig. 4). Considering partial or total fractionation of recycled CO_2 (e.g. considering different relative positions of mitochondria to chloroplasts) resulted in no correlation between both g_m estimates, suggesting that CO_2 recycling had minimal effect on g_m dynamic response in tobacco (Fig. S7).

Apparent discrepancy between gas exchange and leaf anatomy

Strong discrepancy between g_m estimated via the Harley's method and the estimations based on anatomy was observed (Fig. 4). These results contrast with the good agreement previously observed when comparing the two estimates among different species with contrasting leaf structure (Tomás et al. 2013, Tosens et al. 2016, Peguero-Pina et al. 2017, Veromann-Jürgenson et al. 2017) or comparing different leaf ontogenetic states within a species (Tosens et al. 2012). Apparently, this correlation falls down when applied to short-term variations, as observed in Tomás et al. (2014) when comparing well-watered and drought-stressed grapevine cultivars. Our results discard the influence of main leaf anatomical determinants of CO_2 diffusion on fast changes of g_m. Discarding the anatomy as a source for short-term g_m variation, this variation should reflect model weaknesses in the g_m estimation and/or the influence of biochemical factors like aquaporins and carbonic anhydrase.

In recent years, several reports have debated model weaknesses on g_m estimates. Gu and Sun (2014) proposed that a source of error comes from wrong parameterization of the chlorophyll fluorescence model. This source of error can be roughly solved by taking certain precautions. Specially, they suggest the use of an in-vitro based estimate of Γ* (Walker et al. 2013) instead of using the Laisk method (Laisk et al. 1984), in addition to get reliable R_d values as input (Niinemets et al. 2005, Galmés et al. 2011, Tosens et al. 2016). Gu and Sun (2014) also exposed that a source of error comes from the obligatory relationship between input parameters and g_m. This is very difficult to avoid, but a sensitivity analysis was performed to show that in most cases the observed responses of g_m were maintained even when using different parameterizations for R_d, Γ*, A, C_i, ETR or (p1, p2). Light variations were the most sensitive to parameter variations (not significant in 5 out of 12 cases), with the most influent being ETR, C_i and p1, p2. CO_2 variations (especially high CO_2 effect) were the most robust, conserved 11 out of 12 times (Fig. S3). Recently, Xiong et al. (2015) also performed a careful sensitivity

analysis of their data, showing a strong conservation of the patterns for the response to C_i. In this sense, although it is not possible to definitively discard the possibility of an artefact during g_m calculation, at least the apparent g_m response may not be due to a mathematical artefact from the fluorescence method only.

In addition to arising from mathematical artefacts, fluorescence and stable isotope models weaknesses have been suggested to be related with wrong modelling of the decarboxylation fluxes and their possible recycling (Tholen and Zhu 2011, Xiao and Zhu 2017) and from ignoring light gradients through the leaf mesophyll, both aspects potentially causing underestimation of the real g_m values (Evans et al. 2009, Théroux-Rancourt and Gilbert 2017). Both arguments describe problems that occur when the model used is too simplified, particularly with regard to: the recycling of CO_2, the balance between carboxylation and decarboxylation, and the positioning of chloroplasts and mitochondria, first pointed-out by Tholen and Zhu (2011) and further deeply described by Yin and Struik (2017) and Xiao and Zhu (2017). Parameters like the importance of chloroplast membrane conductance in respect to the total mesophyll conductance and mitochondria positioning are needed in order to estimate the importance of the recycling, and then be able to built-up a model representative of the true g_m (Xiao and Zhu 2017, Yin and Struik 2017). Also, Théroux-Rancourt and Gilbert (2017) have identified the light absorption across the leaf profile as a parameter ignored when measuring gas exchange (and leaf chlorophyll fluorescence). They conclude that highly saturating light conditions are needed to get a relatively equal contribution of all mesophyll cell layers to the total leaf apparent g_m allowing the determination of g_m variations. The only way to deal with g_m model limitations may be the use of complex modelling (3D structure, leaf ray tracing model, etc.) that needs not easy-to-measure parameters such as positioning of mitochondria, 'real' resistance of the chloroplast envelop, or leakage of CA at the chloroplast envelop (Xiao and Zhu 2017, Yin and Struik 2017). The fact that a constant g_m can be modelled and can fit with observed data of assimilation rate cannot certify that g_m is truly constant. The real nature of g_m will be revealed by a combination of strong modelling and direct measurements that fit/support the different models used, but a purely theoretical approach may not be sufficient.

Even considering the above-mentioned arguments, it can still be hypothesised that at least a part of the variations found by gas exchange are reflecting a true or partially true biological process. Thus, if leaf anatomy does not vary with $[CO_2]$ nor light, this would mean that other factors are influencing leaf CO_2 diffusion properties in the short-term. Aquaporins as trans-membrane proteins are likely to partially assume this role. Terashima and Ono (2002) and Uehlein et al. (2003) were pioneers in the idea that aquaporins, at that time already known to be involved in water transport in plants, could have the same role for trans-membrane CO_2 transport. Experiments using oocytes, transgenic plants with different expression of aquaporins and/or aquaporin inhibitors reinforced this hypothesis (Terashima and Ono 2002, Uehlein et al. 2003, Flexas et al. 2006, Maurel et al. 2008). Moreover, aquaporins seem to have some gating properties, the opening and closing of the pore (Maurel et al. 2008), that would change their diffusion capacity in the short-term. Cochard et al. (2007) nicely showed how aquaporins in walnut tree are very likely to modulate the measured leaf hydraulic conductance at the minute scale. Because such mechanisms are apparently acting on water fluxes, the equivalent effects on CO_2 diffusion are highly probable too. Nevertheless, they would not be able to explain short-term g_m variations alone, as revealed by the model fitting (Fig. 3C, D). Other proteins probably involved in the facilitation of CO_2 diffusion inside the leaf has been identified, like carbonic anhydrase (Terashima et al. 2011, Momayyezi and Guy 2017). Their role consists to catalyse the CO_2/HCO_3^- conversion in the cytosol. Indeed, carbon diffuses much faster in liquid phase when it is in the HCO_3^- form. This finally improves CO_2 diffusion in the liquid phase (Terashima et al. 2011). Nevertheless, carbonic anhydrase is thought to be at sufficient concentration in the stroma, thus not being a limiting or varying factor in the short-term. Recent studies estimating g_m from anatomical factors choose not to incorporate this factor in the anatomical model (Peguero-Pina et al. 2017, Tosens et al. 2012).

Conclusions

The present study shows that the apparent mesophyll conductance estimated from gas exchange coupled to leaf chlorophyll fluorescence varied with C_i and light, as previously described in the literature. Different simulations considering varying model inputs were performed to check whether differences were maintained, and g_m changes under C_i variations appeared to be more conserved than those induced by light variations. While g_m does vary in the short-term in tobacco as determined with the chlorophyll fluorescence method, no change in any anatomical parameter was observed. This causes the absence of significant correlation between g_m values obtained by both fluorescence and two analytical models based on anatomical parameters. Moreover, theoretical modelling suggests not significant effect of aquaporins

and (photo)respired CO_2 recycling due to the relative position of mitochondria and chloroplast on the dynamic response of g_m. Although more precise models and/or faster direct measurement methods are needed to refuse it, this work reinforces the idea that short-term variations of g_m at least partially reflect some artefactual rather than a biological effect.

Author contributions

M. C., C. D. and J. F. designed the study; M. C., C. D. and A. M. conducted the experiments; M. C., C. D. and J. F. performed the analysis and wrote the manuscript.

Acknowledgements – This work was supported by the Conselleria d'Educació, Cultura i Universitats (Govern de les Illes Balears) and European Social Fund, predoctoral fellowship FPI/1700/2014, awarded to MC. The authors are grateful to Miquel Ribas-Carbó for correction of the written English in the manuscript, to Javier Cano, for his helpful comments, to Miquel Truyols for his support to our experiment, and to Mª Teresa Mínguez, Universitat de València (Secció Microscòpia Electrònica, SCSIE), and Dr Ferran Hierro, Universitat de les Illes Balears (Serveis Cientificotècnics), for technical support during microscopic analyses. This work was supported by the project CTM2014-53902-C2-1-P from the Ministerio de Economía y Competitividad (MINECO, Spain) and the ERDF (FEDER).

References

Brodersen CR, Vogelmann TC (2010) Do changes in light direction affect absorption profiles in leaves? Funct Plant Biol 37: 403–412

von Caemmerer S, Evans JR (2015) Temperature responses of mesophyll conductance differ greatly between species. Plant Cell Environ 38: 629–637

Cochard H, Venisse J-S, Barigah TS, Brunel N, Herbette S, Guilliot A, Tyree MT, Sakr S (2007) Putative role of aquaporins in variable hydraulic conductance of leaves in response to light. Plant Physiol 143: 122–133

Douthe C, Dreyer E, Epron D, Warren CR (2011) Mesophyll conductance to CO_2, assessed from online TDL-AS records of $^{13}CO_2$ discrimination, displays small but significant short-term responses to CO_2 and irradiance in *Eucalyptus* seedlings. J Exp Bot 62: 5335–5346

Douthe C, Dreyer E, Brendel O, Warren CR (2012) Is mesophyll conductance to CO_2 in leaves of three Eucalyptus species sensitive to short-term changes of irradiance under ambient as well as low O_2? Funct Plant Biol 39: 435–448

Evans JR (1989) Photosynthesis and nitrogen relationship in leaves of C_3 plants. Oecologia 78: 9–19

Evans JR (2009) Potential errors in electron transport rates calculated from chlorophyll fluorescence as revealed by a multilayer leaf model. Plant Cell Physiol 50: 698–706

Evans JR, Vogelmann TC (2003) Profiles of ^{14}C fixation through spinach leaves in relation to light absorption and photosynthetic capacity. Plant Cell Environ 26: 547–560

Evans J, Caemmerer S, Setchell B, Hudson G (1994) The relationship between CO_2 transfer conductance and leaf anatomy in transgenic tobacco with a reduced content of Rubisco. Aust J Plant Physiol 21: 475–495

Evans JR, Kaldenhoff R, Genty B, Terashima I (2009) Resistances along the CO_2 diffusion pathway inside leaves. J Exp Bot 60: 2235–2248

Flexas J, Diaz-Espejo A (2015) Interspecific differences in temperature response of mesophyll conductance: food for thought on its regulation. Plant Cell Environ 38: 625–628

Flexas J, Ribas-Carbó M, Hanson DT, Bota J, Otto B, Cifre J, McDowell N, Medrano H, Kaldenhoff R (2006) Tobacco aquaporin NtAQP1 is involved in mesophyll conductance to CO_2 in vivo. Plant J 48: 427–439

Flexas J, Díaz-Espejo A, Berry JA, Cifre J, Galmés J, Kaldenhoff R, Medrano H, Ribas-Carbó M (2007a) Analysis of leakage in IRGA's leaf chambers of open gas exchange systems: quantification and its effects in photosynthesis parameterization. J Exp Bot 58: 1533–1543

Flexas J, Diaz-Espejo A, Galmés J, Kaldenhoff R, Medrano H, Ribas-Carbo M (2007b) Rapid variations of mesophyll conductance in response to changes in CO_2 concentration around leaves. Plant Cell Environ 30: 1284–1298

Flexas J, Ribas-Carbó M, Diaz-Espejo A, Galmés J, Medrano H (2008) Mesophyll conductance to CO_2: current knowledge and future prospects. Plant Cell Environ 31: 602–621

Flexas J, Barbour MM, Brendel O, Cabrera HM, Carriquí M, Díaz-Espejo A, Douthe C, Dreyer E, Ferrio JP, Gago J, Gallé A, Galmés J, Kodama N, Medrano H, Niinemets Ü, Peguero-Pina JJ, Pou A, Ribas-Carbó M, Tomás M, Tosens T, Warren CR (2012) Mesophyll diffusion conductance to CO_2: an unappreciated central player in photosynthesis. Plant Sci 193–194: 70–84

Galle A, Florez-Sarasa I, Tomas M, Pou A, Medrano H, Ribas-Carbo M, Flexas J (2009) The role of mesophyll conductance during water stress and recovery in tobacco (*Nicotiana sylvestris*): acclimation or limitation? J Exp Bot 60: 2379–2390

Galmés J, Medrano H, Flexas J (2006) Acclimation of Rubisco specificity factor to drought in tobacco: discrepancies between in vitro and in vivo estimations. J Exp Bot 57: 3659–3667

Galmés J, Conesa MÀ, Ochogavía JM, Perdomo JA, Francis DM, Ribas-Carbó M, Savé R, Flexas J, Medrano H, Cifre J (2011) Physiological and morphological adaptations in relation to water use efficiency in Mediterranean accessions of *Solanum lycopersicum*. Plant Cell Environ 34: 245–260

Genty B, Briantais J-M, Baker NR (1989) The relationship between the quantum yield of photosynthetic electron transport and quenching of chlorophyll fluorescence. Biochim Biophys Acta – Gen Subj 990: 87–92

Griffiths H, Helliker BR (2013) Mesophyll conductance: internal insights of leaf carbon exchange. Plant Cell Environ 36: 733–735

Gu L, Sun Y (2014) Artefactual responses of mesophyll conductance to CO_2 and irradiance estimated with the variable *J* and online isotope discrimination methods. Plant Cell Environ 37: 1231–1249

Harley PC, Loreto F, Di Marco G, Sharkey TD (1992) Theoretical considerations when estimating the mesophyll conductance to CO_2 flux by analysis of the response of photosynthesis to CO_2. Plant Physiol 98: 1429–1436

Hassiotou F, Ludwig M, Renton M, Veneklaas EJ, Evans JR (2009) Influence of leaf dry mass per area, CO_2, and irradiance on mesophyll conductance in sclerophylls. J Exp Bot 60: 2303–2314

Heinen RB, Ye Q, Chaumont F (2009) Role of aquaporins in leaf physiology. J Exp Bot 60: 2971–2985

Higa T, Wada M (2016) Chloroplast avoidance movement is not functional in plants grown under strong sunlight. Plant Cell Environ 39: 871–882

Ho QT, Berghuijs HNC, Watté R, Verboven P, Herremans E, Yin X, Retta MA, Aernouts B, Saeys W, Helfen L, Farquhar GD, Struik PC, Nicolaï BM (2016) Three-dimensional microscale modelling of CO_2 transport and light propagation in tomato leaves enlightens photosynthesis. Plant Cell Environ 39: 50–61

Kasahara M, Kagawa T, Oikawa K, Suetsugu N, Miyao M, Wada M (2002) Chloroplast avoidance movement reduces photodamage in plants. Nature 420: 829–832

Laisk A, Kiirats O, Oja V (1984) Assimilatory power (postillumination CO_2 uptake) in leaves: measurement, environmental dependencies, and kinetic properties. Plant Physiol 76: 723–729

Lloyd J, Syvertsen JP, Kriedemann PE, Farquhar GD (1992) Low conductances for CO_2 diffusion from stomata to the sites of carboxylation in leaves of woody species. Plant Cell Environ 15: 873–899

Loriaux SD, Avenson TJ, Welles JM, Mcdermitt DK, Eckles RD, Riensche B, Gnety B (2013) Closing in on maximum yield of chlorophyll fluorescence using a single multiphase flash of sub-saturating intensity. Plant, Cell & Environment 36, 1755–1770

Martins SCV, Galmés J, Molins A, DaMatta FM (2013) Improving the estimation of mesophyll conductance to CO2: on the role of electron transport rate correction and respiration. J Exp Bot 64: 3285–3298

Maurel C, Verdoucq L, Luu D-T, Santoni V (2008) Plant aquaporins: membrane channels with multiple integrated functions. Annu Rev Plant Biol 59: 595–624

Mendiburu F (2015). agricolae: Statistical Procedures for Agricultural Research. R package version 1:2-3. Available at https://CRAN.R-project.org/package=agricolae

Momayyezi M, Guy RD (2017) Substantial role for carbonic anhydrase in latitudinal variation in mesophyll conductance of *Populus trichocarpa* Torr. & Gray. Plant Cell Environ 40: 138–149

Niinemets Ü, Reichstein M (2003) Controls on the emission of plant volatiles through stomata: differential sensitivity of emission rates to stomatal closure explained. J Geophys Res 108: 4208

Niinemets Ü, Cescatti A, Rodeghiero M, Tosens T (2005) Leaf internal diffusion conductance limits photosynthesis more strongly in older leaves of Mediterranean evergreen broad-leaved species. Plant Cell Environ 28: 1552–1566

Oguchi R, Hikosaka K, Hirose T (2005) Leaf anatomy as a constraint for photosynthetic acclimation: differential responses in leaf anatomy to increasing growth irradiance among three deciduous trees. Plant Cell Environ 28: 916–927

Peguero-Pina JJ, Flexas J, Galmés J, Niinemets U, Sancho-Knapik D, Barredo G, Villarroya D, Gil-Pelegrín E (2012) Leaf anatomical properties in relation to differences in mesophyll conductance to CO_2 and photosynthesis in two related Mediterranean *Abies* species. Plant Cell Environ 35: 2121–2129

Peguero-Pina JJ, Sisó S, Flexas J, Galmés J, García-Nogales A, Niinemets Ü, Sancho-Knapik D, Saz MÁ, Gil-Pelegrín E (2017) Cell-level anatomical characteristics explain high mesophyll conductance and photosynthetic capacity in sclerophyllous Mediterranean oaks. New Phytol 214: 585–596

Perez-Martin A, Michelazzo C, Torres-Ruiz JM, Flexas J, Fernandez JE, Sebastiani L, Diaz-Espejo A (2014) Regulation of photosynthesis and stomatal and mesophyll conductance under water stress and recovery in olive trees: correlation with gene expression of carbonic anhydrase and aquaporins. J Exp Bot 65: 3143–3156

Poorter H, Niinemets Ü, Poorter L, Wright IJ, Villar R, Niinemets U, Poorter L, Wright IJ, Villar R (2009) Causes and consequences of variation in leaf mass per area (LMA):a meta-analysis. New Phytol 182: 565–588

R Core Team (2016). R: a language and environment for statistical computing. R Foundation for Statistical

Computing, Vienna, Austria. Available at https://www.R-project.org/
Rondeau-Mouro C, Defer D, Leboeuf E, Lahaye M (2008) Assessment of cell wall porosity in *Arabidopsis thaliana* by NMR spectroscopy. Int J Biol Macromol 42: 83–92
Schneider CA, Rasband WS, Eliceiri KW (2012) NIH image to ImageJ: 25 years of image analysis. Nat Methods 9: 671–675
Syvertsen JP, Lloyd J, McConchie C, Kriedemann PE, Farquhar GD (1995) On the relationship between leaf anatomy and CO_2 diffusion through the mesophyll of hypostomatous leaves. Plant Cell Environ 18: 149–157
Tazoe Y, Von Caemmerer S, Badger MR, Evans JR (2009) Light and CO_2 do not affect the mesophyll conductance to CO_2 diffusion in wheat leaves. J Exp Bot 60: 2291–2301
Terashima I, Ono K (2002) Effects of $HgCl_2$ on CO_2 dependence of leaf photosynthesis: evidence indicating involvement of aquaporins in CO_2 diffusion across the plasma membrane. Plant Cell Physiol 43: 70–78
Terashima I, Saeki T (1985) A new model for leaf photosynthesis incorporating the gradients of light environment and of photosynthetic properties of chloroplasts within a leaf. Ann Bot 56: 489–499
Terashima I, Hanba YT, Tholen D, Niinemets Ü (2011) Leaf functional anatomy in relation to photosynthesis. Plant Physiol 155: 108–116
Thain JF (1983) Curvature correlation factors in the measurements of cell surface areas in plant tissues. J Exp Bot 34: 87–94
Théroux-Rancourt G, Gilbert ME (2017) The light response of mesophyll conductance is controlled by structure across leaf profiles. Plant Cell Environ 40: 726–740
Tholen D, Zhu X-G (2011) The mechanistic basis of internal conductance: a theoretical analysis of mesophyll cell photosynthesis and CO_2 diffusion. Plant Physiol 156: 90–105
Tholen D, Boom C, Noguchi K, Ueda S, Katase T, Terashima I (2008) The chloroplast avoidance response decreases internal conductance to CO_2 diffusion in *Arabidopsis thaliana* leaves. Plant Cell Environ 31: 1688–1700
Tomás M, Flexas J, Copolovici L, Galmés J, Hallik L, Medrano H, Ribas-Carbó M, Tosens T, Vislap V, Niinemets Ü (2013) Importance of leaf anatomy in determining mesophyll diffusion conductance to CO_2 across species: quantitative limitations and scaling up by models. J Exp Bot 64: 2269–2281
Tomás M, Medrano H, Brugnoli E, Escalona JM, Martorell S, Pou A, Ribas-Carbó M, Flexas J (2014) Variability of mesophyll conductance in grapevine cultivars under water stress conditions in relation to leaf anatomy and water use efficiency. Aust J Grape Wine Res 20: 272–280
Tosens T, Niinemets Ü, Westoby M, Wright IJ (2012) Anatomical basis of variation in mesophyll resistance in eastern Australian sclerophylls: news of a long and winding path. Journal of Experimental Botany 63, 5105–5119
Tosens T, Niinemets U, Vislap V, Eichelmann H, Castro Díez P (2012a) Developmental changes in mesophyll diffusion conductance and photosynthetic capacity under different light and water availabilities in *Populus tremula*: how structure constrains function. Plant Cell Environ 35: 839–856
Tosens T, Niinemets Ü, Westoby M, Wright IJ (2012b) Anatomical basis of variation in mesophyll resistance in eastern Australian sclerophylls: news of a long and winding path. J Exp Bot 63: 5105–5119
Tosens T, Nishida K, Gago J, Coopman RE, Cabrera HM, Carriquí M, Laanisto L, Morales L, Nadal M, Rojas R, Talts E, Tomas M, Hanba Y, Niinemets Ü, Flexas J (2016) The photosynthetic capacity in 35 ferns and fern allies: mesophyll CO_2 diffusion as a key trait. New Phytol 209: 1576–1590
Trojan A, Gabrys H (1996) Chloroplast distribution in *Arabidopsis thaliana* (L.) depends on light conditions during growth. Plant Physiol 111: 419–425
Uehlein N, Lovisolo C, Siefritz F, Kaldenhoff R (2003) The tobacco aquaporin NtAQP1 is a membrane CO_2 pore with physiological functions. Nature 425: 734–737
Uehlein N, Otto B, Hanson DT, Fischer M, McDowell N, Kaldenhoff R (2008) Function of *Nicotiana tabacum* aquaporins as chloroplast gas pores challenges the concept of membrane CO_2 permeability. Plant Cell 20: 648–657
Valentini R, Epron D, Deangelis P, Matteucci G, Dreyer E (1995) In-situ estimation of net CO_2 assimilation, photosynthetic electron flow and photorespiration in Turkey oak (*Q.cerris* L.) leaves: diurnal cycles under different levels of water supply. Plant Cell Environ 18: 631–640
Veromann-Jürgenson L-L, Tosens T, Laanisto L, Niinemets Ü (2017) Extremely thick cell walls and low mesophyll conductance: welcome to the world of ancient living! J Exp Bot 68: 1639–1653
Vogelmann TC, Bornman JF, Josserand S (1989) Photosynthetic light gradients and spectral regime within leaves of *Medicago sativa*. Philos Trans R Soc B Biol Sci 323: 411–421
Walker B, Ariza LS, Kaines S, Badger MR, Cousins AB (2013) Temperature response of in vivo Rubisco kinetics and mesophyll conductance in Arabidopsis thaliana: comparisons to *Nicotiana tabacum*. Plant Cell Environ 36: 2108–2119

Weisiger R (1998) Impact of extracellular and intracellular diffusion barriers on transport. In: Bassingthwaighte J, Goresky C, Linehan J (eds) Whole Organ Approach to Cell. Metab Springer-Verlag, New York, NY, pp 389.423

Xiao Y, Zhu X-G (2017) Components of mesophyll resistance and their environmental responses a theoretical modeling analysis. Plant Cell Environ 40: 2729–2742. https://doi.org/10.1111/pce.13040

Xiong D, Liu X, Liu L, Douthe C, Li Y, Peng S, Huang J (2015) Rapid responses of mesophyll conductance to changes of CO_2 concentration, temperature and irradiance are affected by N supplements in rice. Plant Cell Environ 38: 2541–2550

Yamori W, Noguchi K, Hanba YT, Terashima I (2006) Effects of internal conductance on the temperature dependence of the photosynthetic rate in spinach leaves from contrasting growth temperatures. Plant Cell Physiol 47: 1069–1080

Yin X, Struik PC (2017) Simple generalisation of a mesophyll resistance model for various intracellular arrangements of chloroplasts and mitochondria in C_3 leaves. Photosynth Res 132: 211–220

Yin X, Struik PC, Romero P, Harbinson J, Evers JB, Van Der Putten PEL, Vos J (2009) Using combined measurements of gas exchange and chlorophyll fluorescence to estimate parameters of a biochemical C_3 photosynthesis model: a critical appraisal and a new integrated approach applied to leaves in a wheat (*Triticum aestivum*) canopy. Plant Cell Environ 32: 448–464

Supporting Information

Additional supporting information may be found online in the Supporting Information section at the end of the article.

Fig. S1. g_m under CO_2 variation not filtered for the Harley's criteria.

Fig. S2. Light response curves and CO_2 response curves for net assimilation rate and g_m.

Fig. S3. Sensitivity analysis of the g_m estimates presented in this study.

Fig. S4. Comparison of g_m calculations between Harley's method (Harley et al. 1992) and Yin and Stuik (2009) method.

Fig. S5. Representative semi-thin and ultra-thin cross-section photographs for each CO_2 and light treatment.

Fig. S6. Bootstrap performed on the chloroplast length and thickness.

Fig. S7. Sensitivity analysis of the effect of the fraction of CO_2 from respiration and photorespiration.

Methods S1. Calculation of variables used for unit conversion using the model Xiao and Zhu (2017).

Edited by A. Krieger-Liszkay

Supporting information

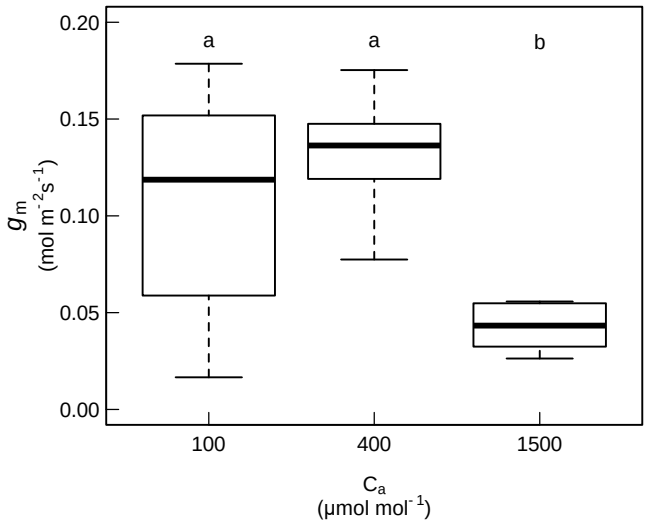

Figure S1. g_m under CO_2 variation not filtered for the Harley's criteria.

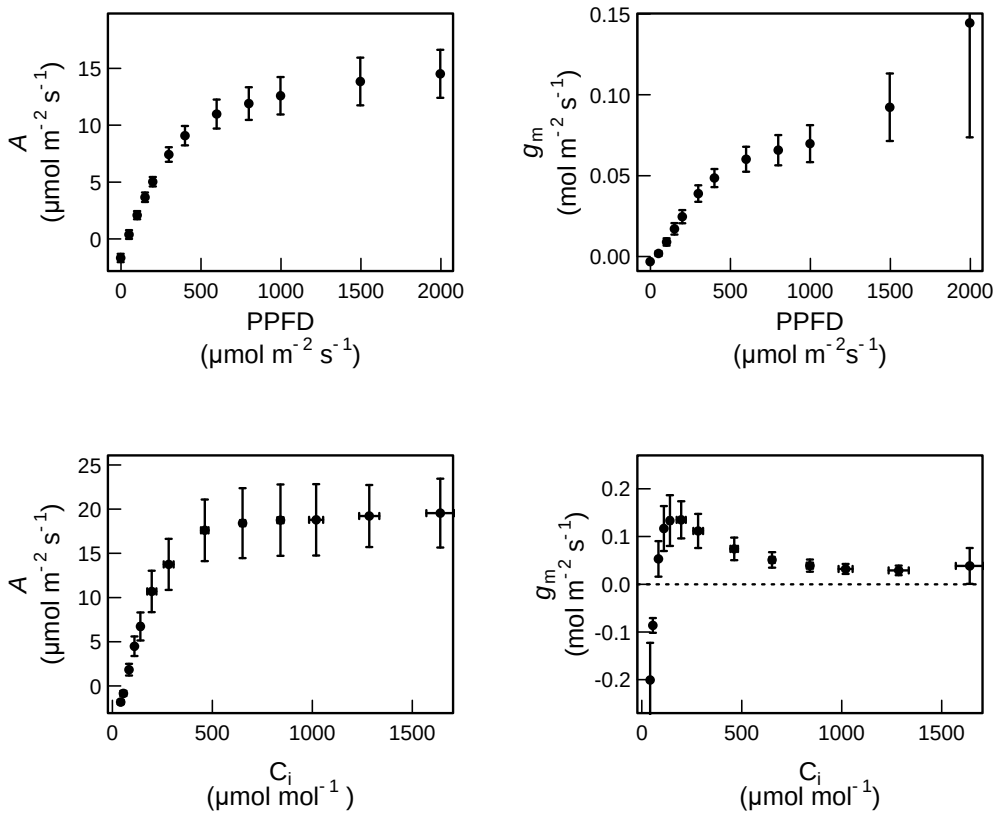

Figure S2. Light response curves (upper panels) and CO_2 response curves (lower panels, C_a = [CO_2] surrounding the leaf) for net assimilation rate (*A*; left panels) and g_m estimated by Harley's method (right panels) of respectively 4 and 5 random plants used in the experiment.

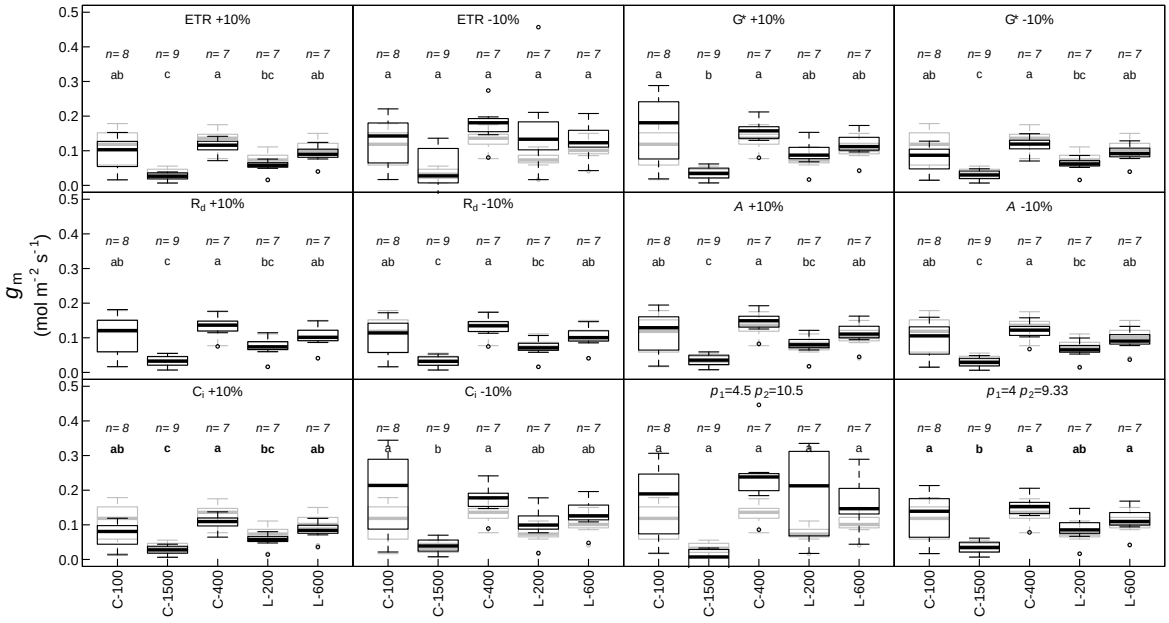

Figure S3. Sensitivity analysis of the g_m estimates presented in this study. For ETR, R_d, Γ*, A, C_i p_1 and p_2, we recalculated the g_m using +10% or -10% variations for each parameter. For each simulation, a boxplot is shown with the original calculations (grey) and the recalculated data (black), this for each treatment. Different letters denote significant (at p<0.05) difference between treatments following a HSD Tukey Post-Hoc test applied on the recalculated g_m.

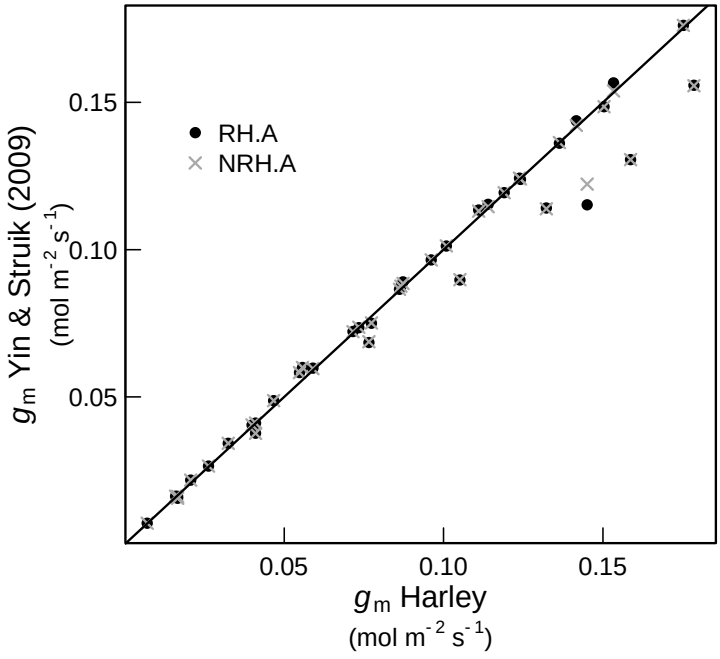

Figure S4. Comparison of g_m calculations between Harley's method (Harley et al., 1992) and Yin and Stuik (2009) method. "RH.A" and "NRH.A" correspond to the two different equations proposed by Yin and Struik (respectively Eq. 6 and 7 from their study). Both of them consist in using chlorophyll fluorescence for ETR estimates, but g_m is estimated based on Farquhar et al., (1982) equations, and replaced by C_i -A/g_m. g_m is then solved by matching measured and computed A (see M&M section).

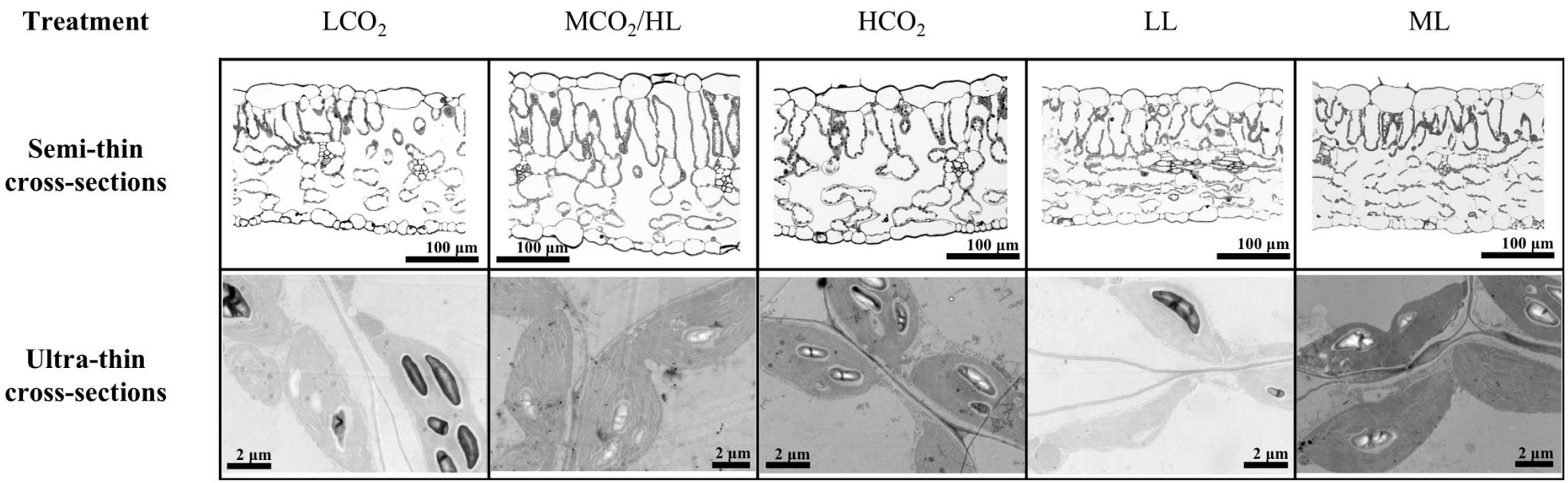

Figure S5. Representative semi-thin and ultra-thin cross-section photographs (first and second row, respectively) for each CO_2 and light treatment. Treatment codes are the same as detailed in Table 1. Complete leaf cross-section can be observed in the semi-thin cross-section photographs, meanwhile chloroplasts and cell wall can be observed in ultra-thin cross-sections.

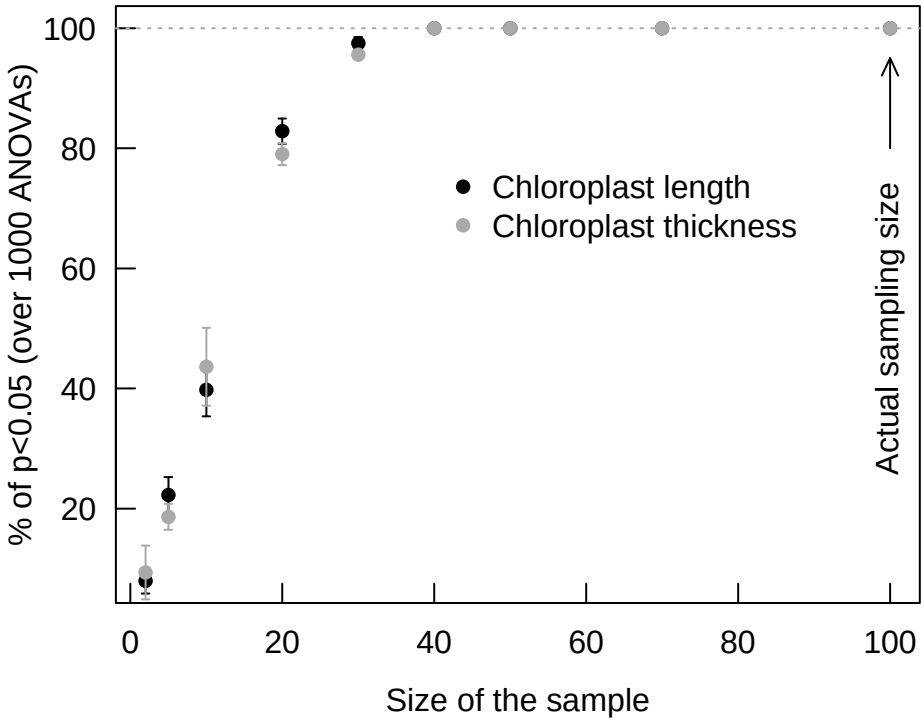

Figure S6. Bootstrap performed on the chloroplast length (black circles) and thickness (grey circles). The sample size of this study is 106-120, depending of the treatment. Here, we randomly sampled 2, 5, 10, 20, 40, 50, 70 or 100 within each treatment, and performed an ANOVA to check differences between treatments (and this, for each variable presented in the graph). This procedure was repeated 1000 times for each sample size. The percentage of significative treatment effect ($p<0.05$) among the 1000 ANOVAs is shown for each sample size. The grey discontinuous line represents the 100% of significative ANOVAs.

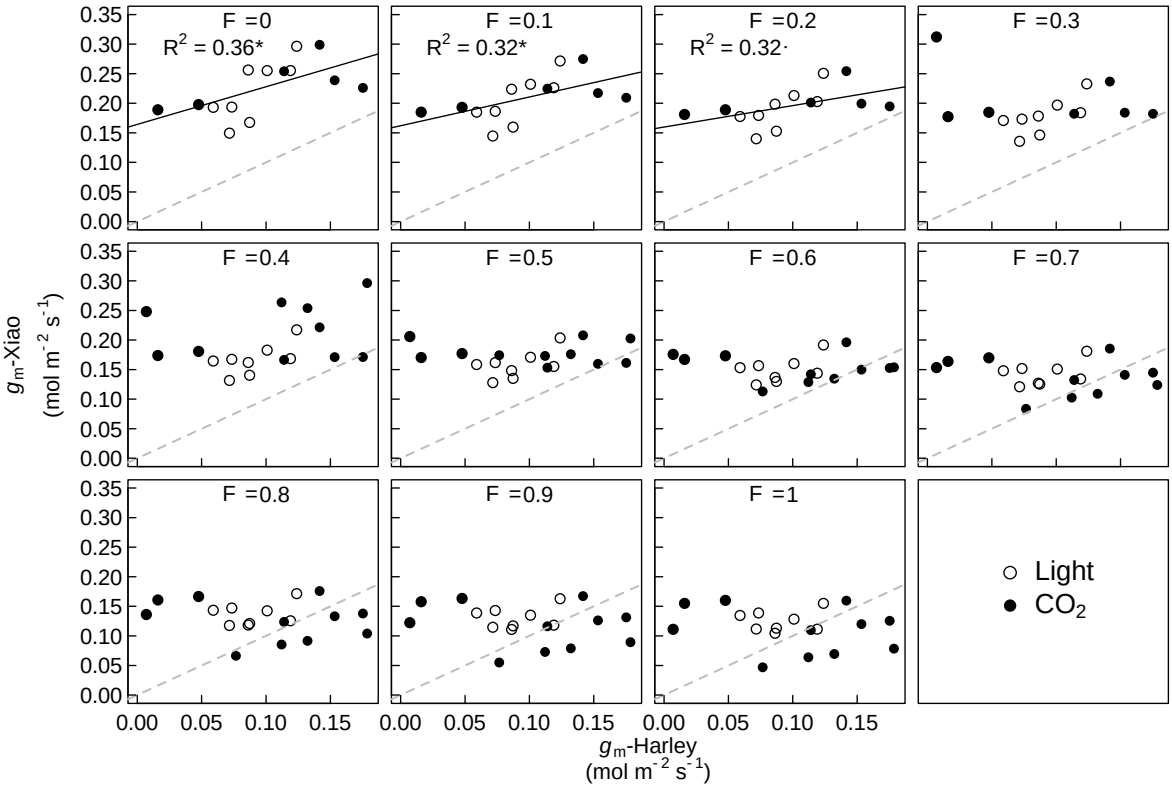

Figure S7. Sensitivity analysis of the effect of the fraction of CO_2 from respiration and photorespiration from the mitochondria that would be recycled depending on the mitochondrial positioning in relation to the chloroplast membrane (Φ) in modelled g_m following Xiao et al. (2017) in relation to g_m estimated following Harley et al. (1992) for both light and CO_2 treatments. Dashed lines represent 1:1 relationship.

Methods S1 – Calculation of variables used for unit conversion using the model of Xiao and Zhu (2017)

Mesophyll surface area for one cell (A_{mes_ave}) was calculated for palisade and spongy mesophyll cells, considering them as prolate and oblate spheroids, respectively. Surface areas where corrected by Thain (1983) and then a weighted average was calculated. A_{mes_ave} for prolate spheroids was calculated as

$$A_{mes\_ave\_prol} = 2\pi a^2 \left(1 + \left(\frac{c}{ae}\right) sin^{-1} e\right)$$

where a is the equatorial radius of the spheroid, c is the distance from centre to pole along the symmetry axis and e is the eccentricity of the oval, calculated as $e=(1-(a^2/c^2))^{1/2}$.

A_{mes_ave} for oblate spheroids was calculated as

$$A_{mes\_ave\_obl} = 2\pi a^2 \left(1 + \left(1 + \frac{1-e^2}{e}\right) tan^{-1} e\right)$$

where e was calculated as $e=(1-(c^2/a^2))^{1/2}$. Surface area of outer boundary of chloroplast cell for one cell (A_{se_o}) was calculated as for A_{mes_ave} but subtracting cell wall and chloroplast thickness to a and c. In the case of surface area of inner boundary of chloroplast for one cell (A_{se_i}) chloroplast thickness was also subtracted to a and c.

Volume of chloroplasts per leaf area (V_{chlo}) was calculated as

$$V_{chlo} = S_c/S\ T_{chl}$$

where S_c/S is the chloroplast surface area exposed to intercellular air spaces per unit of leaf area and T_{chl} is the chloroplast thickness.

Chapter 2. Anatomical adjustments determining mesophyll conductance acclimatization to light growth conditions

Acclimation of mesophyll anatomy and photosynthesis to light during leaf ageing in *Arabidopsis thaliana*

Title and running head

Title: Acclimation of mesophyll anatomy and photosynthesis to light during leaf ageing in *Arabidopsis thaliana*

Running head: Light and age effects on *Arabidopsis*' leaf physiology

Corresponding authors

M. Carriquí, Research Group in Plant Biology under Mediterranean Conditions, Universitat de les Illes Balears, Palma 07122, Illes Balears, Spain. Tel +34-971-25-95-56, Fax +34-971-17-31-84, mcarriqui@gmail.com

J. Flexas, Research Group in Plant Biology under Mediterranean Conditions, Universitat de les Illes Balears, Palma 07122, Illes Balears, Spain. Tel +34-971-17-23-65, Fax 971-17-31-84, jaume.flexas@uib.es

Subject areas

(5) photosynthesis, respiration and bioenergetics

(6) structure and function of cells

Number of black and white figures, colour figures, tables and type and number of supplementary materials

Black and white figures, 6; colour figures, 1; tables, 1; supplementary materials, 2

Title: Acclimation of mesophyll anatomy and photosynthesis to light during leaf ageing in *Arabidopsis thaliana*

Running head: Light and age effects on *Arabidopsis*' physiology and anatomy

Authors by line

Marc Carriquí[1*], Miquel Nadal[1], Jaume Flexas[1*]

Authors' addresses

[1]Research Group in Plant Biology under Mediterranean Conditions, Universitat de les Illes Balears, Palma 07122, Illes Balears, Spain.

Corresponding authors (*)

M. Carriquí, mcarriqui@gmail.com; J. Flexas, jaume.flexas@uib.es

Abstract

Maximum mesophyll conductance (g_m) appears to be driven by foliage leaf anatomy, which has been found to be determined by several environmental and leaf ontogenic factors. If applicable in *Arabidopsis thaliana*, the most broadly used model species in plant physiology investigations, it would at least partially explain the important variability in the photosynthetic capacity and its related features within control treatments -without a unified criterion of how to grow them- for the same genotypes between studies. To test this, we studied the variation in the anatomical and photosynthetic characteristics in *A. thaliana* Col-0 plants acclimated at three contrasting light intensities in leaves of two different ages. Leaf acclimation to increasing growth light conditions was mainly associated with increases in leaf dry mass per unit area, thickness, number of palisade cell layers, mesophyll and chloroplast surface area exposed to intercellular airspace per leaf area (S_m/S and S_c/S, respectively). However, although photosynthesis and g_m accordingly increased from low to moderate growth light conditions, they did not change from moderate to high light, leading to a mismatch between measured and modelled g_m. Leaf ageing was associated with increases in cell wall thickness in all light treatments and in increases in leaf thickness in low and moderate light treatments. However, g_m did not appear to be affected by our leaf age treatments, and photosynthesis only decreased with leaf age in moderate and high light treatments, suggesting a compensatory effect decreasing chloroplast thickness and/or other anatomical traits and changes in biochemical traits such as cell wall porosity. These results emphasize the need of a standardised protocol for *A. thaliana*'s growth and measurement conditions in order to avoid anatomical adjustments leading to differences in their g_m and photosynthetic performance.

Keywords

Arabidopsis thaliana, leaf age, light growth intensity, photosynthesis, mesophyll conductance, leaf anatomy

Introduction

Arabidopsis thaliana is the standard model species for studies on plant biology. From the very first works on the variation in physiological traits among its accessions (Laibach 1943), the number of physiological, biochemical, molecular biology and genetic studies on *Arabidopsis* has grown exponentially, standing alone as the most exhaustively studied species (Koornneef and Meinke 2010). However, as Lake (2004) first pointed out, an important variation in the photosynthetic performance -one of the most widely used approaches to evaluate the plant physiological status-, even between measurements performed on single leaves instead of the whole plant, has been reported among reference genotypes used as control treatments. For instance, in the commonly used Col-0 genotype net photosynthesis (A_N) has been reported to vary under 'control' conditions from at least 4 to 24 μmol m^{-2} s^{-1} (e.g. Bunce 2008, Weraduwage et al. 2016). The same applies for the photosynthetic-related traits stomatal conductance to CO_2 (g_s), mesophyll conductance (g_m) and maximum velocity of carboxylation ($V_{c,max}$), with reported variations ranging at least 0.09 to 0.42 mol m^{-2} s^{-1}, from 0.05 to 0.65 mol m^{-2} s^{-1}, and from 25 to 190 μmol m^{-2} s^{-1}, respectively (Bunce 2008, Jin et al. 2011, Sade et al. 2014, Xiong et al. 2017, Mizokami et al. 2018). Consequently, the opportunities for cross-study comparisons are greatly reduced.

Lake (2004) suggested differences in the gas exchange procedures and equipment, potential genetic drift and growth conditions, as the main causes of such variation. In the case of g_m, although part of the variation observed may be caused by the method used (e.g. the values estimated with the isotopic method are generally higher than those estimated with the variable *J* method; Pons et al. 2009, Mizokami et al. 2016), since the publication of the 'ice-cream cone-like' trick by Flexas et al. (2007a) most researchers perform single-leaf measurements with commercial gas exchange cuvettes, but the enormous variation in photosynthetic capacity and related traits between studies remains. Environmental conditions during both growth and measurements have never been unified, so that each laboratory is actually acclimating its *Arabidopsis* plants to different environmental conditions.

Among the environmental variables that could be responsible for the aforementioned variability, light growth conditions stand out: 'standard' light growth conditions for *Arabidopsis* vary from 75 to up to 900 μmol m^{-2} s^{-1} (e.g. Tian et al. 2015 and Bunce 2008, respectively), although in most studies *Arabidopsis* are grown between 100 and 400 μmol m^{-2} s^{-1} (e.g. Teng et al. 2006, Watanabe et al. 2014, Weise et al. 2015, Weraduwage et al. 2016, Xiong et al. 2017, Boyd et al. 2019). There are countless long-term responses of plants to light growth conditions -the set of which defines the plant plasticity-, which occur from the subcellular and cellular levels (e.g. determining the characteristics of the light-harvesting complexes), the leaf level (e.g. leaf structure) or the whole-plant level (e.g. biomass allocation; Valladares et al. 2007, Nicotra et al. 2010, Poorter et al. 2019). Leaf structure is specially important for the light acclimation of the leaf. Higher light intensity during growth conditions ensures a deeper light penetration within the leaf, allowing plants to possess a higher area-based photosynthetic capacity and g_m by developing thicker and denser leaves with high light (Poorter et al. 2019). Across species, leaves grown at higher light conditions generally achieve greater thickness through an increase in mesophyll palisade cell layers and the enlargement of mesophyll cells (Terashima et al. 2001, Ivanova et al. 2006, Tosens et al. 2012), which in turn results in a higher mesophyll surface area exposed to intercellular airspace per leaf area (S_m/S) and S_c/S (Hanba et al. 2002, Oguchi et al. 2005, Tosens et al. 2012, Morales et al. 2014, Fini et al. 2016, Ellsworth et al. 2018). Cell wall thickness, a key trait determining mesophyll CO_2 diffusion resistance (i.e. the inverse of g_m) also might play a role in the leaf light acclimation. However, the relationship of T_{cw} with light growth conditions is not that clear, since it has been reported to increase (Fini et al. 2016), remain constant (Hanba et al. 2002, Tosens et al. 2012, Fini et al. 2016, Ellsworth et al. 2018) or decrease with increasing growth light conditions (Hanba et al. 2002). Changes are generally strongest in low light, and minimum at high light (Poorter et al. 2019). However, the effect of growth light intensity on leaf structure and both A_N and g_m depend on the species adaptation to light-demand (Hanba et al. 2002). Thus, light-demanding species present higher plasticity than shade-tolerant species (Valladares et al. 2000, Portsmuth and Niinemets 2007, Chmura et al. 2017). As a light-demanding species (Poorter et al. 2019), *Arabidopsis* leaf anatomical plasticity in response to light growth conditions is expected to be high.

However, despite the large variability in the key anatomical traits determining g_m, and therefore A_N, observed in *Arabidopsis* between studies (Teng et al. 2006, Tholen et al. 2008, Jin et al. 2011, Weraduwage et al. 2016, Xiong et al. 2017, Mizokami et al. 2018), no study has directly addressed its relationship with light growth conditions. The implication of other environmental variables on the anatomical determinants of g_m in *Arabidopsis* seems to be, although the fundamentals are not completely clear, less important. For example, no (Bunce 2008, Walker et al. 2013, von Caemmerer and Evans 2015) or minor (Jin et al. 2011) differences in A_N and g_m were reported in *Arabidopsis* plants acclimated to different temperatures. Regarding to CO_2 growth conditions, only small differences in g_m and no differences in key anatomical traits but T_{cw} have been reported (Teng et al. 2006, Mizokami et al. 2018).

Anatomical adjustments associated with leaf ageing might be another important source of variation of the photosynthetic performance reported in *Arabidopsis*. Flexas et al. (2007a) reported that *Arabidopsis* fully expanded leaves achieve and keep maximum photosynthetic capacity between 28 and 34 days after germination, moment from which leaf senescence started and both net photosynthesis and g_m importantly decreased with leaf ageing. However, most studies still consider plant instead of leaf age when evaluating the leaf physiological status of this species. Although the several processes that occur during leaf development and ageing (see Niinemets et al. 2012 for a review), there are several studies providing correlative evidence of the impact of leaf architecture modifications on g_m. Particularly, modifications in f_{ias} and S_c/S during leaf development and cell-wall thickening during leaf ageing appear to be the main causes of the variation of g_m. However, the effect of those anatomical adjustments during leaf ageing on g_m has been studied only in few species -most of them woody species-(Hanba et al. 2001, Miyazawa and Terashima 2001, Marchi et al. 2008, Tosens et al. 2012), and the speed of foliar development and ageing can be affected by many environmental factors (Niinemets et al. 2012), so not firm conclusions can be drawn yet. Due to its especially short life cycle and leaf longevity (Meinke et al. 1998) it would be expected that in *Arabidopsis* anatomical adjustments occur fast, making then crucial to define the time interval

in which measurements of photosynthesis and related characteristics should be performed. However, no study has investigated this in depth yet.

The aim of this study is to contribute to a better knowledge of the combined light acclimation and leaf age effects on the leaf anatomical traits determining g_m and photosynthesis in *Arabidopsis*. In relation to leaf age, this study specially aims to investigate the potential anatomical subjacent changes during the time range in which the leaf has its maximum g_m. Thus, the importance of standardizing these two variables to allow cross comparison between studies dedicated to *Arabidopsis* will be further highlighted. This is explored by analysing the foliage anatomy, net photosynthesis, mesophyll conductance, and diffusion limitations of photosynthesis in leaves of *A*. *thaliana* Col-0 plants grown at three contrasting light intensities in leaves of two different leaf ages. Moreover, we quantified the relative contribution of the various anatomical components involved in the mesophyll CO_2 diffusion. We hypothesized that acclimating to increased light growth conditions will lead to increases on both g_m and photosynthesis, which will be mainly determined by increases in leaf thickness and S_c/S, while increasing leaf age will have a negative effect on both g_m and photosynthesis mainly due to increases in cell wall thickness.

Materials and methods

Growth conditions and leaf age determination

Arabidopsis thaliana L. (Heyhn) ecotype Col 0 seeds were sown in pre-wetted pots filled with substrate containing peat, perlite and vermiculite (2:1:1 v/v) forming an 'ice-cream cone-like' shape to facilitate later gas-exchange measurements, as suggested by Flexas et al. (2007a). Pots were placed in plastic trays with 4 cm of deionized water and kept in dark conditions for 48 h at 4 ºC to stratify the culture. Then, trays with pots were placed in a growth chamber with controlled environmental conditions: 23:20 ºC day:night temperature, 69.8 ± 0.8 % relative humidity and 12:12 h photoperiod. Light was provided by LED panels adjusted to provide three light intensity treatments, 76 ± 4 µmol m^{-2} s^{-1}, 242 ± 10 µmol m^{-2} s^{-1} and 490 ± 15 µmol m^{-2} s^{-1} at pot level, which corresponded to low-

light (LL), moderate-light (NL) and high-light (HL) treatments, respectively. To ensure that light growth conditions were uniform among plants of the same light treatment, the position between pots under the LED panels was changed every two days. One week after stratification, the most uniform plants were selected and the rest removed, remaining one plant per pot. At day 10, deionized water was removed from the plastic trays to let the soil dry. From day 14, plants were watered every two days with half-strength Hoagland solution (Epstein, 1972). At day 14, leaves from the third pair of the rosette were labelled. Measurements were performed with the labelled leaves at two different leaf ages: 11-13 days after labelling (24-26 days after germination) and 19-21 days after labelling (32-34 days after germination). These two ages were selected to represent the peak of leaf photosynthesis. Flexas et al. (2007) showed maximum and constant photosynthesis rates in *Arabidopsis* leaves 24-35 days after germination and strong decreases after that (70% reduction by 42 days after germination). Therefore, here we aim describing any incipient physiological and/or anatomical changes preceding the age-related decline of photosynthesis.

Gas exchange and chlorophyll fluorescence measurement

Gas exchange and chlorophyll fluorescence measurements were simultaneously performed using a portable photosynthesis system equipped with an integrated 2 cm^2 leaf fluorescence chamber (LI-COR, Inc., Lincoln, NE, USA). In all measurements, block temperature was fixed at 25ºC and vapor pressure deficit (VPD) kept around 1.5 kPa. To ensure the reliability of the photosynthetic rates, air flow rate was regulated from 100 to 300 µmol s^{-1} in order to achieve >4 µmol mol^{-1} CO_2 delta between sample and reference infrared gas analysers. First, light response curves to determine saturating photosynthetic photon flux density (PPFD) were performed by varying PPFD between 0 and 2000 µmol m^{-2} s^{-1} (90:10 % red:blue light) at 400 µmol CO_2 mol^{-1} of ambient CO_2 concentration (C_a). Then, complete CO_2 response curves were performed after achieving maximum steady state conditions, always after 25-30 minutes at 400 µmol CO_2 mol^{-1} and 1500 µmol m^{-2} s^{-1} PPFD, by varying C_a between 50 and 1200 µmol mol^{-1}. CO_2 response curves were repeated under non-photorespiratory conditions (< 2%

O_2). After equilibration to a steady state, gas exchange parameters, steady-state fluorescence (F_s) and maximal fluorescence (F_m') were registered with a white light saturating flash of around 8000 µmol m^{-2} s^{-1}. The efficiency of the photosystem II (ΦPSII) was estimated as ΦPSII = (F_m'-F_s) / F_m' (Genty et al. 1989). Electron transport rate (ETR) was estimated as ETR = PPFD × ΦPSII × α × β, being α the leaf absorbance and β the electron partitioning between photosystems I and II (Genty et al. 1989). CO_2 response curves under non-photorespiratory conditions were used to establish the relationship between ΦPSII and ΦCO_2 (with ΦCO_2 = (A + R_d) / PPFD), then considering α × β = 4 × b^{-1} where b is the slope of the ΦPSII ~ ΦCO_2 relationship (Valentini et al. 1995). Non-photorespiratory respiration during the day (R_d) was estimated by dividing by 2 the respiration rate measured in at least 1 h dark-adapted plants at a C_a of 400 µmol CO_2 mol^{-1} (Martins et al. 2013; Niinemets et al. 2005; Veromann-Jürgenson et al. 2017). In the cases where the leaves did not cover completely the 2 cm^2 of the cuvette, a digital image of the leaf enclosed in the chamber was taken in order to determine the real area and therefore recalculate gas-exchange data. Any measurement performed at a non-ambient CO_2 concentration was corrected for leaks following Flexas et al. (2007b). Then, mesophyll conductance (g_{m_FLU}) was estimated following Harley et al. (1992), as:

$$g_{m\_FLU} = \frac{A_N}{C_i - \frac{\Gamma^* (ETR + 8 (A_N + R_d))}{(ETR - 4(A_N + R_d))}} \quad (1)$$

where A_N is the net assimilation rate, Γ^* is CO_2 compensation point in absence of R_d, and C_i the CO_2 concentration in intercellular air-spaces. Γ^* was taken as 42.9 µmol mol^{-1} at 25ºC (Bernacchi et al. 2001). g_{m_FLU} values were used to transform A_N-C_i to A_N-C_c curves, being C_c the chloroplastic CO_2 concentration. Maximum velocity of carboxylation ($V_{c,max}$) and maximum electron transport rate on a C_c basis (J_{max}) were calculated from A_N-C_c following Farquhar et al. (1980).

Anatomical measurements and modelled mesophyll conductance

After the gas-exchange measurements, small cross-sections (approx. 3 × 2 mm) of the leaf area enclosed in the leaf chamber were cut off with a razor

blade and immediately fixed in paraformaldehyde (2%) and glutaraldehyde (4%) in 0.1 M phosphate buffer solution (pH 7.4) under vacuum pressure. Five leaves were sampled per each light and age treatment. Samples were afterwards post-fixed for 2 h in 2% osmium tetroxide, dehydrated in a graded series of ethanol, embedded in resin (LR-White, London Resin Company, London, UK) and solidified in an oven at 60ºC for 48h.

Semi-thin (0.8 µm) and ultrathin transverse sections (90 nm), for light and transmission electron microscopy (TEM), respectively, were cut with an ultramicrotome (Leica UC6, Vienna, Austria). Semi-thin sections were dyed with toluidine blue (1 %) photographed with a Moticam 3 (Motic Electric Group Co., Xiamen, China) coupled to an Olympus BX60 (Olympus, Tokyo, Japan) light microscope. Ultrathin sections were contrasted with uranyl acetate and lead citrate and observed with a transmission electron microscopy (TEM H600; Hitachi, Tokyo, Japan). Between four to six fields of view per sample were photographed and analysed using IMAGEJ software (Schneider et al. 2012). Light microscopy images were used to determine leaf thickness (T_{leaf}), mesophyll thickness (T_{mes}), number of palisade layers, fraction of the mesophyll occupied by intercellular airspaces (f_{ias}) and cell dimensions. Transmission electron microscope images were used to determine mesophyll cell wall thickness (T_{cw}), cytoplasm thickness (T_{cyt}), chloroplast dimensions, length (L_{chl}) and thickness (T_{chl}), and mesophyll and chloroplast surface area exposed to intercellular airspace per leaf area (S_m/S and S_c/S, respectively). Cell curvature correction factor was calculated according to Thain (1983). Measurements were performed following Tomás et al. (2013). Due to differences in cell dimensional ratio between treatments, applied correction factors to cell surface area estimates varied between 1.16 and 1.25 for the spongy mesophyll tissue and between 1.33 and 1.42 for the palisade mesophyll tissue. At least ten measurements per mesophyll tissue (spongy and palisade) were performed per anatomical trait and replicate. Then, weighted averages based on tissue volume fractions were calculated.

Mesophyll conductance modelled from anatomical parameters (g_{m_ANAT}) was estimated according to the one-dimensional within-leaf gas diffusion model of Niinemets and Reichstein (2003) as modified by Tomás et al. (2013) and Earles et al. (2018). Mesophyll diffusion conductance, as a composite

conductance for within-leaf gas, liquid and lipid components (g_{m_ANAT}), is given as:

$$g_{m\_ANAT} = \frac{1}{\frac{1}{g_{ias}} + \frac{RT_k}{H \cdot g_{liq}}} \quad (2)$$

where R is the gas constant (Pa m^3 K^{-1} mol^{-1}), T_k is the absolute temperature (K) and H is the Henry's law constant (m^3 mol^{-1} K^{-1}). $H/(RT_k)$ is the dimensionless form of Henry's law constant needed to convert a liquid phase conductance (g_{liq}) into a gas-phase equivalent conductance (Niinemets and Reichstein 2003). Gas-phase diffusion depends on f_{ias} (m^3 m^{-3}) and the effective diffusion path length in the gas-phase (ΔL_{ias}) (Syvertsen et al. 1995; Terashima et al. 2011), given as formulated by Earles et al. (2018):

$$g_{ias} = \frac{D_a \cdot f_{ias}}{\lambda \cdot \Delta L_{ias} \cdot \varsigma} \quad (3)$$

where D_a (m^2 s^{-1}) is the diffusion coefficient for CO_2 in the gas-phase ($1.51 \cdot 10^{-5}$ m^2 s^{-1} at 25°C), λ is the lateral path lengthening (m m^{-1}) and ς is the diffusion path tortuosity (m m^{-1}). ΔL_{ias} was approximated by mesophyll thickness divided by two (Niinemets and Reichstein 2003). λ and ς where assumed to be $f_{ias}^{-0.5}$ (Earles et al. 2018). The total liquid phase conductance is provided by the sum of the inverse of serial conductances:

$$g_{liq} = \left(\frac{1}{\sum \frac{1}{g_i}}\right) \cdot S_c/S \quad (4)$$

where g_i (m s^{-1}) is the partial conductance of cell wall (g_{cw}), plasmalemma (g_{pl}), cytosol (g_{ct}), chloroplast envelope (g_{env}), or chloroplast stroma (g_{st}). The conductance of a given component of the diffusion pathway is given by the general equation:

$$g_i = \frac{r_{f,i} \cdot D_w \cdot p_i}{\Delta L_i} \quad (5)$$

where $r_{f,i}$ is a dimensionless factor that accounts for the decrease of diffusion conductance compared to free diffusion in water (Weisiger 1998), D_w is the aqueous phase diffusion coefficient for CO_2 ($1.79 \cdot 10^{-9}$ m^2 s^{-1} at 25°C), p_i (m^3 m^{-3}) is the effective porosity in the given part of the diffusion pathway and ΔL_i (m) is

the diffusion path length. For cell walls where the aqueous-phase diffusion has been shown to approximate free water, $r_{f,i}$ = 1 (Rondeau-Mouro et al. 2008). The value of $r_{f,i}$ was set at 0.3 for g_{ct} and g_{st} to account for the reduction of diffusion conductance due to high concentrations of high molecular solutes and intracellular (cytoskeleton) and intraorganellal (thylakoids) heterogeneities (Niinemets and Reichstein 2003). Effective porosity, p_i, was taken as 1 for g_{ct} and g_{st}. Cell wall porosity (p_{cw}) was taken as 0.3 (Nobel 1999). Due to the difficulty to measure the thickness of the plasma membrane, the chloroplast envelope and the limited information about the permeability of the lipid phase membranes, g_{pl} and g_{env} were assumed as constant values (0.0035 m s^{-1}) as previously suggested in other studies (Tomás et al. 2013).

Conductance in units of m s^{-1} can be converted into molar units considering that

g[mol m^{-2} s^{-1}] = g[m s^{-1}]44.6·[273.16/(273.16 + T_L)(P/101.325),

where T_L is the leaf temperature (ºC) and P (Pa) is the air pressure.

Quantitative limitation analysis of photosynthesis and mesophyll conductance

The relative photosynthetic limitations including stomatal (l_s), mesophyll (l_m) and biochemical (l_b) relative limitations (l_s + l_m + l_b = 1) were calculated following Grassi and Magnani (2005):

$$l_s = \frac{g_{tot}/g_s \cdot \partial A_N/\partial C_c}{g_{tot}+\partial A_N/\partial C_c} \quad (6)$$

$$l_m = \frac{g_{tot}/g_m \cdot \partial A_N/\partial C_c}{g_{tot}+\partial A_N/\partial C_c} \quad (7)$$

$$l_b = \frac{g_{tot}}{g_{tot}+\partial A_N/\partial C_c} \quad (8)$$

where g_{tot} is the total CO_2 diffusion conductance (calculated as g_{tot} = 1/(1/g_s + 1/g_{m_FLU})). $\partial A_N/\partial$Cc was calculated as the slope of A_N-C_c response curves over a C_c range of 50-100 μmol mol $^{-1}$.

The anatomical determinants of g_{m_ANAT} were quantified following Tomás et al. (2013) by considering the component parts of the diffusion pathway. The gas-phase limitation of mesophyll conductance (l_{ias}) was calculated as:

$$l_{ias} = \frac{g_{\mathrm{m\_ANAT}}}{g_{\mathrm{ias}}} \quad (9)$$

The share of g_{m_ANAT} by different components of the cellular phase conductances (l_i) was estimated as:

$$l_i = \frac{g_{\mathrm{m\_ANAT}}}{g_{\mathrm{i}} \cdot S_c/S} \quad (10)$$

where l_i is the limitation by the cell wall, the plasmalemma, cytosol, chloroplast envelope and stroma.

Statistical analysis

Independent two-way analysis of variance (ANOVA) was performed to check differences between treatments and for both light and leaf age treatments. Differences between means were detected by Tukey's honest significant difference tests (with accepted $P < 0.05$). Model was re-assessed for Tukey's HSD (honestly significant difference) test when interaction was not significant. Then, the two resultant models were chosen using the Aikake Information Criterion (AIC). Pearson correlation matrices were determined for each group of treatments to determine the correlations between the different parameters. The statistical relationships between different traits within treatments were explored by linear and non-linear regression analyses and considered significant at $P < 0.05$. All analyses were performed with the R software (R Core Team 2016). Tukey's Post-Hoc tests were performed using the R "agricolae" package (Mendiburu 2015).

Results

In order to investigate the effects of light growth conditions and leaf age on the *Arabidopsis thaliana* leaf's physiology and anatomy, the photosynthetic

characteristics and the main structural traits involved in constraining the CO_2 diffusion were analysed in leaves at two different leaf age stages from plants grown under three different light treatments. Both treatments had significant effects on the leaf photosynthetic characteristics, apart from the visual phenotypic differences within plants of the same age (see Fig. 1 for plant rosettes 40 days after germination). Light and age treatments had significant effects on net photosynthesis (A_N) across the supplied CO_2 concentrations for a given chloroplastic CO_2 concentration (C_c), although light saturation point was similar for all light and age treatments (Fig. 2A-C, Table S1), and was lower in leaves grown under low light (LL) than in moderate and high light (ML and HL, respectively); Fig. 2B, C; Table S1).

A_N was significantly lower in young leaves grown under low light (LL) compared to leaves grown under moderate and high light conditions (ML and HL, respectively). Instead, only significant differences between ages in A_N were found in HL, where A_N decreased by more than 35 % from age 1 to 2 (Fig. 3A). Non-photorespiratory respiration during the day (R_d) presented strong significant differences between light treatments, being higher in HL (0.55 ± 0.04 μmol m^{-2} s^{-1}) than in LL and ML (0.36 ± 0.03 and 0.22 ± 0.02 μmol m^{-2} s^{-1}, respectively; Table S1). Stomatal conductance to CO_2 (g_s) was highly variable within each treatment, and only a leaf age effect was reported with a tendency to decrease (Fig. 3B). On the contrary, only a light treatment significance was found in mesophyll conductance to CO_2, although the effect of diverging light growth conditions was different depending on the g_m estimation method. Whereas the fluorescence method yielded the largest g_{m_FLU} values in ML (Fig. 3C), according to the analytical model based on anatomical traits g_{m_ANAT} linearly increased with the increasing photosynthetic photon flux density (PPFD) at which plants grew (Fig. 3D). Regarding the leaf biochemical capacity, a highly significant interaction was found between light and age, following both maximum carboxylation rate ($V_{c,max}$) and electron transport rate (J_{max}) the same pattern: both parameters linearly increased with light growth condition in younger leaves, but an important decrease was reported in older as compared to younger leaves in HL (Fig. 3E, F). The quantitative limitation analysis showed that meanwhile *relative* mesophyll conductance limitation (l_m) remained similar between light and age treatments

(ranged from 31 to 38 %), a light treatment effect was found for stomatal (l_s) and biochemical limitations (l_b), increasing the first and decreasing the second with increasing light growth conditions (Fig. 4).

Most of the studied leaf morphoanatomical traits presented significant differences between treatments, although no general pattern was found for light and age treatments (Fig. 5; Table 3, S2). Dry leaf mass per area (LMA) and the number of palisade layers significantly increased with light growth conditions, but no differences were found between leaf ages (Fig. 6A, C). Similarly, leaf thickness (T_{leaf}) increased with growth light conditions in younger leaves, but differences disappeared between ML and HL at age 2 (Fig. 6B). The fraction of the mesophyll occupied by the intercellular air spaces (f_{ias}) was kept constant between light and age treatments, except in LL young leaves, which was significantly higher (25.8 ± 2.0 %), to later equal the others in age 2 (17.7 ± 1.4 %; Fig. 6D). Mesophyll and chloroplast surface area exposed to intercellular airspace per leaf area (S_m/S and S_c/S, respectively) increased as LMA and number of palisade layers increased with light growth intensities and, similarly to those two last parameters, no changes were found between leaf ages (Fig. 6E, F). Thus, the ratio S_c/S_m increased with light growth intensity, but differences in the increase percentage between S_m/S and S_c/S lead to significant differences between leaf ages, being the S_c/S_m ratio lower at older leaf age (Fig. 6G). In this sense, as the leaf aged, chloroplasts significantly decreased their thickness, increasing the distance between chloroplasts, but chloroplast did not change their length (Table 1). Significant differences were found in mesophyll cell wall thickness between light and age treatments, although no light × age interaction was found (Fig. 6H). Based on the quantitative structural limitation analysis, the estimated gas phase limitation inside the leaf significantly increased with growth light conditions from 1.55 to 17.27 %, and no differences were found between leaf ages (Fig. 7A). Among all the components of liquid phase limitations, the stroma (l_{st}) represented about two-thirds of the diffusion resistance to CO_2 (ranging from 59.5 % in HL-age 2 to 70.6 % in ML-age 1), followed by the cytoplasm (l_{ct}; which ranged from 6.07 % in LL-age 1 to 18.87 % in HL-age 2). Cell walls (l_{cw}) and membranes (l_{pl} and l_{en}) played a minor role (Fig. 7B). Significant differences were found for each

cellular phase among light and age treatments, but the light × age interaction was significant only for l_{ct} and l_{st} (Fig. 7B).

Discussion

In this study, we have shown that light acclimation in *Arabidopsis thaliana* causes significant changes in most physiological characteristics and structural traits (Figs. 1-3 and 5). Differences in A_N and its related physiological traits (except for g_s CO_2) were much more important between LL and ML than between ML and HL (Fig. 3, Table S1). Due to the fact that most studies grow *Arabidopsis* under light intensities in the range comprised between LL and ML (e.g. Teng et al. 2006, Watanabe et al. 2014, Weise et al. 2015, Weraduwage et al. 2016, Xiong et al. 2017, Boyd et al. 2019), the results of the present study confirm the low comparability among studies suggested by Lake (2004). Significant differences in g_m found between light treatments can be attributed to the great phenotypic response found in leaf morphological and anatomical traits, as previously reported by several studies (Hanba et al. 2002, Oguchi et al. 2005, Tosens et al. 2012, Morales et al. 2014, Fini et al. 2016, Peguero-Pina et al. 2016, Ellsworth et al. 2018). The anatomical traits followed different patterns with increasing growth light conditions. LMA, the most integrative morphological trait integrating leaf structure complexity (Niinemets et al. 2009, Onoda et al. 2017), the number of palisade layers and both mesophyll and chloroplast surface area exposed to intercellular airspaces per leaf area (S_m/S and S_c/S) steeply increased with increasing growth light without showing signs of saturation at high light, as recently reviewed by Poorter et al. (2019) (Fig. 6A, C, E-F). Other traits like leaf thickness (T_{leaf}), the ratio S_c/S_m and cell wall thickness (T_{cw}), instead, mostly increased from LL to ML treatments, and showed signals of saturation between ML and HL (Fig. 6B, G-H). This is in agreement with observations in other species where T_{cw} remains constant with increasing light (Hanba et al. 2002; Tosens et al. 2012; Ellsworth et al. 2018), although it has also been reported to increase in some species (Fini et al. 2016). When compared with higher light growth conditions, the young leaves of *A. thaliana* grown in LL showed a higher fraction of the mesophyll occupied by intercellular air spaces (f_{ias}) (Fig. 6D), which is a

common response of plants grown under low light conditions (Terashima et al. 2011). Higher f_{ias} and thinner leaves supposed a lower gas-phase partial limitation on g_m (Fig. 7A), as already shown by Galmés et al. (2013), Tomás et al. (2013) and Peguero-Pina et al. (2016), among others. The fact that the anatomy-based modelled values of g_m (Tosens et al. 2012) closely resemble the estimates made by gas exchange and chlorophyll fluorescence measurements (Harley et al. 1992) strongly suggests that there must be at least a partial causality between changes in anatomy and changes in g_m. The changes reported in this study in terms of mesophyll anatomical traits and their implications in g_m constitute a new insight into the functional acclimation to environmental variables in the model species *Arabidopsis thaliana*.

There may still be additional factors that further complicate the comparison. In Flexas et al. (2007a), *Arabidopsis* leaf photosynthetic capacity was similar between 28 and 34 days after germination. However, after day 34 g_m started to importantly decrease, being up to 70% lower between 42–46 days after germination. In this study, we used the same the Col-0 ecotype and followed the same protocol to grow the plants, in order to investigate the subjacent anatomic changes that are expected to occur during the time range in which the peak g_m is achieved. As in Flexas et al. (2007), g_m did not significantly differ between ages 1 and 2 (24–26 and 32–34 days after germination, respectively; Fig. 3C). Based on this, it could be argued that studies performed on 24- or 34-days-old leaves are comparable. However, this might not be the case as shown by the next results.

The scarce studies investigating how the leaf internal architecture modulates g_m during leaf development and ageing demonstrate that g_m can be a significant constraint to photosynthesis during leaf life span (Hanba et al. 2001, Miyazawa and Terashima 2001, Miyazawa et al. 2003, Marchi et al. 2008, Tosens et al. 2012, Niinemets et al. 2012). Once fully expanded leaves achieve maximum g_m, this photosynthetic trait tends to decrease with leaf age (Loreto et al. 1994, Niinemets et al. 2012), being suggested by Miyazawa and Terashima (2001), Miyazawa et al. 2003 and Tosens et al. (2012) to be mainly due to the accumulation of cell wall material which result in thicker cell walls. Moreover, Niinemets et al. (2012) suggested a possible reduction of cell-wall effective

porosity with leaf ageing. Therefore, we investigated whether foliar anatomy changed with leaf age despite the constancy of g_m between leaf ages 1 and 2.

Anatomically, the maximum modelled g_m for the leaves (g_{m_ANAT}; Tomás et al. 2013) was similar between the two leaf ages, irrespective of growth light intensity, supporting the reliability of the reported values of g_m estimated from chlorophyll fluorescence (g_{m_FLU}; Harley et al. 1992; Fig. 3C-D). However, as first hypothesized, and in accordance with Miyazawa and Terashima (2001), Miyazawa et al. (2003) and Tosens et al. (2012), older leaves presented thicker cell walls, also irrespective of growth light conditions (Fig. 6H). Thicker cell walls, as well as increased leaf thickness (T_{leaf}) without consequent increases in S_c/S in LL and ML (Figs. 3B, 5), increased distance between chloroplasts lined with cell walls (L_{betchl}) in all light treatments, and increased cytoplasm thickness between chloroplasts and cell walls (T_{cyt}) in ML and HL (Table 1), are all age-related changes that suppose a lengthening of the CO_2 pathway across the mesophyll, and usually would involve a higher total mesophyll resistance to CO_2 diffusion (Evans et al. 2009, Terashima et al. 2011, Tosens et al. 2012, Tomás et al. 2013, Carriquí et al. 2019). However, the partial limitation analysis on g_m revealed that neither cell wall, plasma membrane nor cytoplasm cell components imposed separately >20% of total liquid-phase limitations to g_m (Fig.7B). In the case of the cell wall, the variability in its thickness with leaf age although significant ($P < 0.001$, Fig. 6H) was small compared to the T_{cw} range reported for angiosperms (from 0.10 in *Triticum aestivum* to 1.15 in *Paphiopedilum* spp.; Ouyang et al. 2017, Yang et al. 2018). Thus, changes in cell wall effective porosity, although possible (Niinemets et al. 2012) due to constant cell wall remodeling and reconstruction during leaf ontogeny (Sarkar et al. 2009), would be expected to be small —in this study a constant cell wall effective porosity of 0.3 $m^3\ m^{-3}$, the value suggested by Nobel (1999) for a species with thin cell walls, was assumed for g_m modelisation in *Arabidopsis*—. The reason by which g_m did not decrease in the older leaves seems to lie in the chloroplast stroma, the principal component limiting g_m in *Arabidopsis* in this study (accounting for 57 to 71% of the liquid-phase conductance, depending on the light and age treatment; Fig. 7B) and in Xiong et al. (2017), as well as in other species with thin-walled mesophyll (Tosens et al. 2012, Han et al. 2018). In this study, chloroplast thickness was significantly

reduced during ageing in all three light treatments (Table 1). Thus, reducing the liquid-phase CO_2 pathway and compensating for the negative effect of increased T_{cw}, T_{leaf}, L_{betchl} and T_{cyt}. Finally, the fact that no remarkable changes in LMA, f_{ias} and S_m/S were found between leaf ages, in disagreement with age-dependent modifications reported by previous studies (Miyazawa and Terashima 2001, Hanba et al. 2002, Marchi et al. 2008, Tosens et al. 2012), although major age-dependent changes in LMA are not likely to occur in short-lived herbaceous species (Niinemets 2016). While we did not performed measurements beyond age 32-34 days, however, if the observed tendencies for T_{cw}, T_{leaf}, L_{betchl} and T_{cyt} continued from day 32-34 to day 42-44, then g_{m_anat} would decrease by 25-35%, i.e. in agreement with the observations of Flexas et al. (2007).

In conclusion, *Arabidopsis thaliana* presented significant modifications of the leaf architecture depending on the light intensity to which it has acclimated and during leaf ageing (Figs. 5, 6). These modifications, which were especially important between LL and ML treatments, had important consequences on both g_m and A_N (Fig. 3). As most studies using *Arabidopsis* grow their plants in the range of light intensities comprised between LL and ML, our findings reveal that at least a significant fraction of the variability reported across studies in both physiological characteristics and anatomical properties for control *Arabidopsis* plants is due to growth light conditions. Nevertheless, the significant light x age interactions in some parameters (Table 1, Figs. 3E-F, 6D) demonstrates that measuring leaves expressing the optimal physiological peak depends not only on the light intensity employed for growing plants, but also on the leaf age. Therefore, the results from this study confirm the low comparability between *Arabidopsis* studies early stated by Lake (2004) and highlight the relevance of standardizing both growth and measuring conditions in *Arabidopsis* to enable cross-study comparisons.

Funding

This work was supported by the Conselleria d'Educació, Cultura i Universitats (Govern de les Illes Balears) and European Social Fund [FPI/1700/2014 to M.C.];

and the Ministerio de Economía y Competitividad (MINECO, Spain) and the ERDF (FEDER) [CTM2014-53902-C2-1-P].

Disclosures

The authors have no conflicts of interest.

Acknowledgments

We thank Miquel Ribas-Carbó and Cyril Douthe for their dedication to the maintenance of the infrared gas analysers.

References

Bernacchi C.J., Singsaas E.L., Pimentel C., Portis A.R. Jr., Long, S.P. (2001) Improved temperature response functions for models of Rubisco-limited photosynthesis. *Plant, Cell and Environment* 24, 253–259.

Boyd R.A., Cavanagh A.P., Kubien D.S, Cousins A.B. (2019) Temperature response of Rubisco kinetics in *Arabidopsis thaliana*: thermal breakpoints and implications for reaction mechanisms. *Journal of Experimental Botany* 70, 231–242.

Bunce J.A. (2008) Acclimation of photosynthesis to temperature in *Arabidopsis thaliana* and *Brassica oleracea*. Photosynth 46, 517–524.

von Caemmerer S., Evans J.R. (2015) Temperature responses of mesophyll conductance differ greatly between species. *Plant, Cell and Environment* 38, 629–637.

Chmura D.J., Modrzynski J., Chmielarz P., Tjoelker M.G. (2017) Plasticity in seedling morphology, biomass allocation and physiology among ten temperature tree species in response to shade is related to shade tolerance and not leaf habit. *Plant Biology* 19, 172–182.

Earles J.M., Théroux-Rancourt G., Roddy A.B., Gilbert M.E., McElrone A.J., Brodersen C.R. (2018) Beyond porosity: 3D leaf intercellular airspace traits that impact mesophyll conductance. *Plant Physiology* doi: 10.1104/pp.1800550.

Ellsworth P.V., Ellsworth P.Z., Koteyeva N.K., Cousins A.B. (2018) Cell wall properties in *Oryza sativa*. New Phytologist 19, 66–76.

Epstein E. (1972) *Mineral nutrition of plants: principles and perspectives*. John Wiley and Sons, New York. Pp. 39.

Farquhar G.D., von Caemmerer S., Berry J.A. (1980) A biochemical model of photosynthetic CO_2 assimilation in leaves of C_3 species. *Planta* 149, 78–90.

Fini A., Loreto F., Tattini M., Giordano C., Ferrini F., Brunetti C., Centritto M.

(2016) Mesophyll conductance plays a central role in leaf functioning of Oleaceae species exposed to contrasting sunlight irradiance. *Physiologia Plantarum* 157, 54–68.

Flexas J., Ortuño M.F.M., Ribas-Carbo M., Diaz-Espejo A., Flórez-Sarasa I.D., Medrano H. (2007a) Mesophyll conductance to CO_2 in *Arabidopsis thaliana*. *New Phytologist* 175 501–511.

Flexas J., Díaz-Espejo A., Berry J.A., Galmés J., Cifre J., Kaldenhoff R., Medrano H., Ribas-Carbó M. (2007b) Leakage in leaf chambers in open gas exchange systems: quantification and its effects in photosynthesis parameterization. *Journal of Experimental Botany* 58, 1533–1543.

Galmés J., Ochogavía J.M., Gago J., Roldán E.J., Cifre J., Conesa M.À. (2013) Leaf responses to drought stress in Mediterranean accessions of *Solanum lycopersicum*: anatomical adaptations in relation to gas exchange parameters. *Plant, Cell and Environment* 36, 920–935.

Genty B., Briantais J.M., Baker N.R. (1989) The relationship between the quantum yield of photosynthetic electron-transport and quenching of chlorophyll fluorescence*. Biochimica et Biophysica* Acta 990, 87–92.

Grassi G., Magnani F. (2005) Stomatal, mesophyll conductance and biochemical limitations to photosynthesis as affected by drought and leaf ontogeny in ash and oak trees. *Plant, Cell and Environment* 28, 834–849.

Hanba Y.T., Miyazawa S.-I., Kogami H., Terashima I. (2001) Effects of leaf age on internal CO_2 transfer conductance and photosynthesis in tree species having different types of shoot phenology. *Australian Journal of Plant Physiology* 28, 1075–1084.

Hanba Y.T., Kogami H., Terashima I. (2002) The effect of growth irradiance on leaf anatomy and photosynthesis in *Acer* species differing in light demand. *Plant, Cell and Environment* 25, 1021–1030.

Harley P.C., Loreto F., Dimarco G., Sharkey T.D. (1992) Theoretical considerations when estimating the mesophyll conductance to CO_2 flux by

analysis of the response of photosynthesis to CO_2. *Plant Physiology* 98: 1429–1436.

Ivanova L.A., Petrov M.S., Kadushnikov R.M. (2006) Determination of mesophyll diffusion resistance in *Chamaerion angustifolium* by the method of three-dimensional reconstruction of the leaf cell packing. *Russian Journal of Plant Physiology* 53, 316–322.

Jin B., Wang L., Wang J., Jiang K.-Z., Wang Y., Jiang X.-X., Ni C.-Y., Wang Y.-L., Teng N.-J. (2011) The effect of experimental warming on leaf functional traits, leaf structure and leaf biochemistry in *Arabidopsis thaliana*. *BMC Plant Biol* 11 35.

Koornneef M., Meinke D. (2010) The development of *Arabidopsis* as a model plant. Plant J 61, 909–921.

Laibach, F. (1943) *Arabidopsis thaliana* (L.) Heynh. Als Objekt für genetische und entwicklungsphysiologische Untersuchungen. Bot Arch 44, 439–455.

Lake J.A. (2004) Gas Exchange: new challenges with *Arabidopsis. New Phytologist* 162, 1–3.

Loreto F., Dimarco G., Tricoli D., Sharkey T.D. (1994) Measurement of mesophyll conductance, photosynthetic electron transport and alternative electron sinks of field grown wheat leaves. *Photosynthesis Research* 98, 1437–1443.

Marchi S., Tognetti R., Minnocci A., Borghi M., Sebastiani, L. (2008) Variation in mesophyll anatomy and photosynthetic capacity during leaf development in a deciduous mesophyte fruit tree (*Prunus persica*) and an evergreen sclerophyllous Mediterranean shrub (*Olea europaea*). *Trees* 22: 559–571.

Martins S.C.V., Galmés J., Molins A., DaMatta, F.M. (2013) Improving the estimation of mesophyll conductance to CO_2: on the role of electron transport rate correction and respiration. *Journal of Experimental Botany* 64 3285–3298.

Meinke D.W., Cherry J.M., Dean C., Rounsley S.D., Koornneef M. (1998) *Arabidopsis thaliana*: A model plant for genome analysis. *Science* 282, 662–682.

Miyazawa S.-I., Terashima I. (2001) Slow development of leaf photosynthesis in an evergreen broad-leaved tree, *Castanopsis sieboldii*: relationships between leaf anatomical characteristics and photosynthetic rate. *Plant, Cell and Environment* 24, 279–291.

Miyazawa S.I., Makino A., Terashima, I. (2003) Changes in mesophyll anatomy and sink-source relationships during leaf development in *Quercus glauca*, an evergreen tree showing delayed leaf greening. *Plant, Cell and Environment* 26, 745–755.

Mizokami Y., Terashima I. (2016) Cross-point of water and carbon in the leaf -CO_2 diffusion conductance-. *The Ecological Society of Japan* 66, 477–487.

Mizokami Y., Noguchi K., Kojima M., Sakakibara H., Terashima I. (2018) Effects of instantaneous and growth CO_2 levels, and ABA on stomatal and mesophyll conductances. *Plant, Cell and Environment* 42, 1257–1269.

Morales L.V., Coopman R.E., Rojas R., Escandón A.B., Flexas J., Galmés J., García-Plazaola J.I., Gago J., Cabrera H.M., Corcuera L.J. (2014) Acclimation of leaf cohorts expanded under light and water stresses: an adaptive mechanism of *Eucryphia cordifolia* to face changes in climatic conditions? *Tree Physiology* 34, 1305–1320.

Nicotra A.B., Atkin O.K., Bonser S.P., Davidson A.M., Finnegan E.J., Mathesius U., Poot P., Purugganan M.D., Richards C.L., Valladares F., van Kleunen M. (2010) Plant phenotypic plasticity in a changing climate. *Trends Plant Science* 15, 684–692.

Niinemets Ü. (2016) Leaf age dependent changes in within-canopy variation in leaf functional traits: a meta-analysis. *Journal of Plant Research* 129, 313–338.

Niinemets Ü., Reichstein M. (2003) Controls on the emission of plant volatiles through stomata: a sensitivity analysis. *Journal of Geophysical Research* 108, 4211.

Niinemets Ü., Cescatti A., Rodeghiero M., Tosens T. (2005) Leaf internal diffusion conductance limits photosynthesis more strongly in older leaves of Mediterranean evergreen broad-leaved species. *Plant, Cell and Environment* 28, 1552–1566.

Niinemets Ü., Wright I.J., Evans J.R. (2009) Leaf mesophyll diffusion conductance in 35 Australian sclerophylls covering a broad range of foliage structural and physiological variation. *Journal of Experimental Botany* 60, 2433–2449.

Niinemets Ü., García-Plazaola J.I., Tosens T. (2012) Photosynthesis during leaf development and ageing. In: Flexas J., Loreto F., Medrano H. (eds) Terrestrial photosynthesis in a changing environment. The molecular, physiological and ecological bases of photosynthesis driving its response to the environmental changes. Cambridge University Press, Cambridge, pp 357–376.

Nobel P.S. (1999) Physicochemical and environmental plant physiology. San Diego: Academic Press, Inc.

Oguchi R., Hikosaka K., Hirose T. (2005) Leaf anatomy as a constraint for photosynthetic acclimation: differential responses in leaf anatomy to increasing growth irradiance among three deciduous trees. *Plant, Cell and Environment* 28, 916–927.

Onoda Y., Wright I.J., Evans J.R., Hikosaka K., Kitajima K., Niinemets Ü., Poorter H., Tosens T., Westoby M. (2017) Physiological and structural tradeoffs underlying the leaf economics spectrum. *New Phytologist* 214: 1447–1463.

Ouyang W., Struik P.C., Yin X., Yang J. (2017) Stomatal conductance, mesophyll conductance, and transpiration efficiency in relation to leaf anatomy in rice and wheat genotypes under drought. *Journal of Experimental Botany* 68, 5191–5205.

Peguero-Pina J.J., Sancho-Knapik D., Flexas J., Galmés J., Niinemets Ü., Gil-Pelegrín E. (2016) Light acclimation of photosynthesis in two closely related firs (*Abies pinsapo* Boiss. and *Abies alba* Mill.): the role of leaf anatomy and mesophyll conductance to CO_2. *Tree Physiology* 36, 300–310.

Pons T.L., Flexas J., von Caemmerer S., Evans J.R., Genty B., Ribas-Carbó M., Brugnoli E. (2009) Estimating mesophyll conductance to CO_2: methodology, potential errors, and recommendations. *Journal of Experimental Botany* 60, 2217–2234.

Poorter H., Niinemets Ü., Ntagkas N., Siebenkäs A., Mäenpää M., Matusbara S., Pons T.L. (2019) A meta-analysis of plant responses to light intensity for 70 traits ranging from molecules to whole plant performance. *New Phytologist* doi: 10.1111/nph.15754.

Portsmuth A., Niinemets Ü. (2007) Structural and physiological plasticity in response to light and nutrients in five temperate deciduous woody species of contrasting shade tolerance. *Functional Ecology* 21, 61–77.

R Core Team. (2016) R: a language and environment for statistical computing. R Foundation for Statistical Computing, Vienna, Austria. Available at: https://www.R-project.org/.

Rondeau-Mouro C., Defer D., Leboeuf E., Lahaye, M. (2008) Assessment of cell wall porosity in *Arabidopsis thaliana* by NMR spectroscopy. *International Journal of Biological Macromolecules* 42, 83–92.

Sade N., Galle A., Flexas J., Lerner S., Peleg G., Yaaran A., Moshelion M. (2014) Differential tissue-specific expression of NtAQP1 in *Arabidopsis thaliana* reveals a role for this protein in stomatal and mesophyll conductance of CO_2 under standard and salt-stress conditions. *Planta* 239, 357–366.

Sarkar P., Bosneaga E., Auer, M. (2009) Plant cell walls throughout evolution: towards a molecular understanding of their design principles. *Journal of Experimental Botany* 60, 3615–3635.

Schneider C.A., Rashband W.S., Eliceiri K.W. (2012) “NIH Image to ImageJ: 25 years of image analysis”. *Nature methods* 9, 671–675.

Syvertsen J.P., Lloyd J., McConchie C., Kriedemann P.E., Farquhar G.D. (1995) On the relationship between leaf anatomy and CO_2 diffusion through the mesophyll of hypostomatous leaves. *Plant, Cell and Environment* 18, 149–157.

Teng N., Wang J., Chen T., Wu X., Wang Y., Lin J. (2006) Elevated CO_2 induces physiological, biochemical and structural changes in leaves of *Arabidopsis thaliana*. *New Phytologist* 172, 92–103.

Terashima I., Miyazawa S.-I., Hanba Y.T. (2001) Why are sun leaves thicker than shade leaves? – Consideration based on analyses of CO_2 diffusion in the leaf. *Journal of Plant Research* 114, 93–105.

Terashima I., Hanba Y.T., Tholen D., Niinemets, Ü. (2011) Leaf functional anatomy in relation to photosynthesis. *Plant Physiology* 155, 108–116.

Thain J.F. (1983) Curvature correlation factors in the measurements of cell surface areas in plant tissues. *Journal of Experimental Botany* 34, 87–94.

Tholen D., Boom C., Noguchi K., Ueda S., Katase T., Terashima, I. (2008) The chloroplast avoidance response decreases internal conductance to CO_2 diffusion in *Arabidopsis thaliana* leaves. *Plant, Cell and Environment* 31, 1688–1700.

Tian W., Hou C., Ren Z., Pan Y., Jia J., Zhang H., Bai F., Zhang,P., Zhu H., He Y., Luo S., Li L., Luan, S. (2015) A molecular pathway for CO_2 response in *Arabidopsis* guard cells. *Nature communications* 6, 6057.

Tomás M., Flexas J., Copolovici L., Galmés J., Hallik L., Medrano H., Tosens T., Vislap V., Niinemets, Ü. (2013) Importance of leaf anatomy in determining mesophyll diffusion conductance to CO_2 across species: quantitative limitations and scaling up by models. *Journal of Experimental Botany* 64, 2269–2281.

Tosens T., Niinemets Ü., Vislap V., Eichelmann H., Castro Díez P. (2012) Developmental changes in mesophyll diffusion conductance and photosynthetic capacity under different light and water availabilities in *Populus tremula*: how structure constrains function. *Plant, Cell and*

Environment 35, 839–856.

Valentini R., Epron D., Angelis P.D.E., Matteucci G., Dreyer E. (1995) In situ estimation of net CO_2 assimilation, photosynthetic electron flow and photorespiration in Turkey oak (*Q. cerris* L.) leaves: diurnal cycles under different levels of water supply*. Plant, Cell and Environment* 38, 2462–2474.

Valladares F., Wright S.J., Lasso E., Kitajima K., Pearcy R.W. (2000) Plastic phenotypic response to light of 16 congeneric shrubs from a Panamanian rainforest. *Ecology* 91, 1925–1936.

Valladares F., Gianoli E., Gómez J.M. (2007) Ecological limits to plant phenotypic plasticity. *New Phytologist* 176, 749–763.

Veromann-Jürgenson L.-L., Tosens T., Laanisto L., Niinemets Ü. (2017) Extremely thick cell walls and low mesophyll conductance: welcome to the world of ancient living! Journal of Experimental Botany 68, 1639–1653.

Walker B., Ariza L.S., Kaines S., Badger M.R., Cousins A.B. (2013) Temperature response of in vivo Rubisco kinetics and mesophyll conductance in *Arabidopsis thaliana*: comparisons to *Nicotiana tabacum*. Plant, Cell and Environment 36, 2108–2119.

Watanabe C.K., Sato S., Yanagisawa S., Uesono Y., Terashima I., Noguchi, K. (2014) Effects of elevated CO_2 on levels of primary metabolites and transcripts of genes encoding respiratory enzymes and their diurnal patterns in *Arabidopsis thaliana*: possible relationships with respiratory rates. *Plant and Cell Physiology* 55, 341-357.

Weise S.E., Carr D.J., Bourke A.M., Hanson D.T., Swarthout D., Sharkey T.D. (2015) The arc mutants of *Arabidopsis* with fewer large chloroplasts have a lower mesophyll conductance*. Photosynthesis Research* 124, 117–126.

Weisiger R. (1998) Impact of extracellular and intracellular diffusion barriers on transport. In: Bassingthwaighte, J.B., Goresky, C.A., Linehan, J.H. (eds) *Whole Organ Approach to Cellular Metabolism. Springer Verlag*, New York, pp, 389–423.

Weraduwage S.M., Kim S.-J., Renna L., Anozie F.C., Sharkey T.D., Brandizzi F. (2016) Pectin methylesterification impacts the relationship between photosynthesis and plant growth. *Plant Physiology* 171, 833–848.

Xiong D., Huang J., Peng S., Li Y. (2017) A few enlarged chloroplasts are less efficient in photosynthesis than a large population of small chloroplasts in *Arabidopsis thaliana*. *Scientific Reports* UK 7, 5782.

Yang Z.-H., Huang,W., Yang Q.-Y., Chang,W., Zhang S.-B. (2018) Anatomical and diffusional determinants inside leaves explain the difference in photosynthetic capacity between *Cypripedium* and *Paphiopedilum*, Orchidaceae. *Photosynthesis Research* 136, 315–328.

Tables

Table 1. Chloroplast thickness (T_{chl}), chloroplast length (L_{chl}), length between chloroplasts (L_{betchl}) and cytoplasm thickness (T_{cyt}) for *Arabidopsis thaliana* grown under low, moderate and high light intensities at two different leaf ages. Values are average ± SE (n = 5).

Growth light intensity	Age	T_{chl} (µm)	L_{chl} (µm)	L_{betchl} (µm)	T_{cyt} (µm)
Low light	1	3.47 ± 0.15^{abc}	6.33 ± 0.17	0.69 ± 0.08^{bc}	0.31 ± 0.04^{bc}
	2	3.15 ± 0.07^{bc}	6.58 ± 0.29	1.38 ± 0.31^{ab}	0.14 ± 0.04^{c}
Moderate light	1	4.03 ± 0.23^{a}	7.22 ± 0.39	0.51 ± 0.08^{c}	0.30 ± 0.03^{bc}
	2	2.84 ± 0.34^{c}	6.34 ± 0.20	2.08 ± 0.22^{a}	0.44 ± 0.06^{ab}
High light	1	3.93 ± 0.10^{ab}	6.73 ± 0.44	0.55 ± 0.12^{c}	0.35 ± 0.01^{ab}
	2	3.26 ± 0.18^{abc}	6.50 ± 0.25	1.07 ± 0.12^{bc}	0.52 ± 0.06^{a}
Two-way ANOVA[1]	L	0.376	0.600	0.037	0.0001
	A	0.0002	0.273	< 0.0001	0.197
	L x A	0.112	-	0.015	0.001

[1] A two-way ANOVA was performed with growth light condition (L) and leaf age (A) to test the significance. *P* values obtained using Tukey's honest significant difference (HSD) test when L, A or L x A interaction was significant are displayed. Model was reassessed for HSD test when interaction was not significant, and the two resultant models were chosen following the Aikake Information Criterium (AIC) test. Values with the same superscript letters are not significantly different.

Legends to figures

Fig. 1. Representative phenotypes of plant rosettes grown at three different light intensities- low light (76 ± 5 µmol m^{-2} s^{-1}), moderate light (242 ± 10 µmol m^{-2} s^{-1}) and high light (489 ± 25 µmol m^{-2} s^{-1})-, 40 days after germination.

Fig. 2. Response of net assimilation (A_N) to (A) photosynthetic photon flux density (PPFD), (B) sub-stomatal CO_2 concentration (C_i), and (C) chloroplastic CO_2 concentration (C_c) of leaves of plants grown at low light (LL), moderate light (ML) and high light (HL) intensities measured at two different ages. Values are average ± SE of four to six replicates per response curve.

Fig. 3. Variations in (A) net photosynthesis (A_N), (B) stomatal conductance to CO_2 (g_s), (C) mesophyll conductance estimated from chlorophyll fluorescence (g_{m_FLU}), (D) mesophyll conductance modelled from anatomical traits (g_{m_ANAT}), (E) maximum carboxylation rate ($V_{c,max}$), and (F) electron transport rate (J_{max}) in leaves grown under three different light intensities and measured at two different leaf ages. Data are average ± SE (n = 4-6). Significance in light growth intensity (L), leaf age (A) and L x A interaction is symbolized by: *, $P < 0.05$; **, $P < 0.01$; ***, $P < 0.001$; ^{ns}, not significant.

Fig. 4. *Relative* stomatal (l_s), mesophyll conductance (l_m) and biochemical (l_b) photosynthesis limitations for *Arabidopsis thaliana* leaves at two different leaf ages from plants grown at low, moderate and high light intensities.

Fig. 5. Leaf cross-sections of Arabidopsis thaliana at two different leaf ages and grown under low (A, B), moderate (C, D) and high (E, F) light intensities.

Fig. 6. Variations in (A) dry leaf mass per area (LMA), (B) leaf thickness (T_{leaf}), (C) number of palisade layers, (D) fraction of the mesophyll occupied by the intercellular air spaces (f_{ias}), (E and F) mesophyll and chloroplast surface area exposed to intercellular airspace per leaf area (S_m/S and S_c/S, respectively), (G) the ratio S_c/S_m, and (H) mesophyll cell wall thickness (T_{cw}) in leaves grown under three different light intensities and measured at two different leaf ages. Data are average ± SE (n = 5). Significance in light growth intensity (L), leaf age (A) and L x A interaction is symbolized by: *, $P < 0.05$; **, $P < 0.01$; ***, $P < 0.001$; ^{ns}, not significant.

Fig. 7. Limitation of mesophyll conductance due to anatomical constraints. (A) Share of the overall g_{m_ANAT} limitation by the gas (l_{ias}) and liquid phase (l_{liquid}), and (B) the liquid-phase limitation among its components: cell wall (l_{cw}), plasma membrane (l_{pl}), cytoplasm (l_{ct}), chloroplast envelope (l_{en}) and chloroplast stroma (l_{st}).

Supplementary data

Table S1. Photosynthetic characteristics for each leaf age and growth light condition treatment.

Table S2. Morphoanatomical characteristics for each leaf age and growth light condition treatment.

Figures

Figure 1

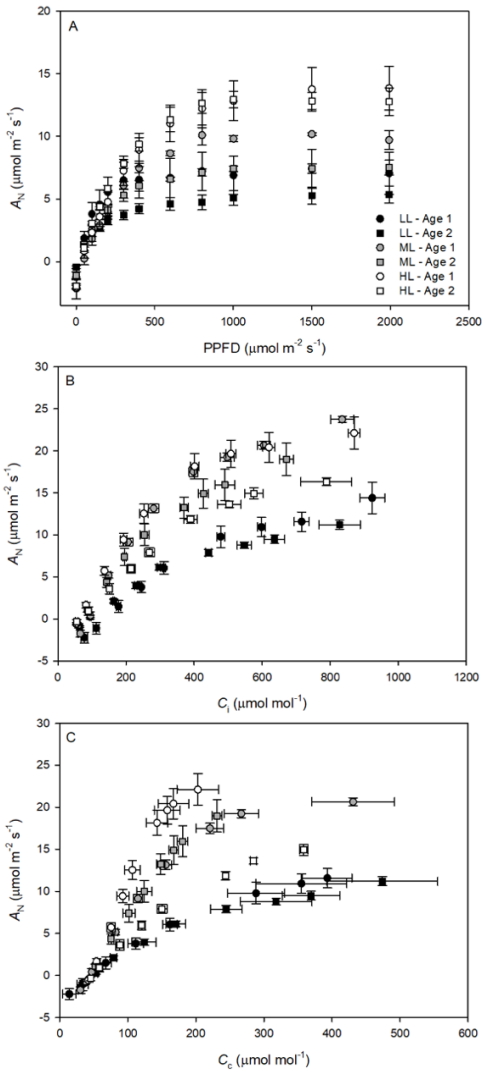

Figure 2

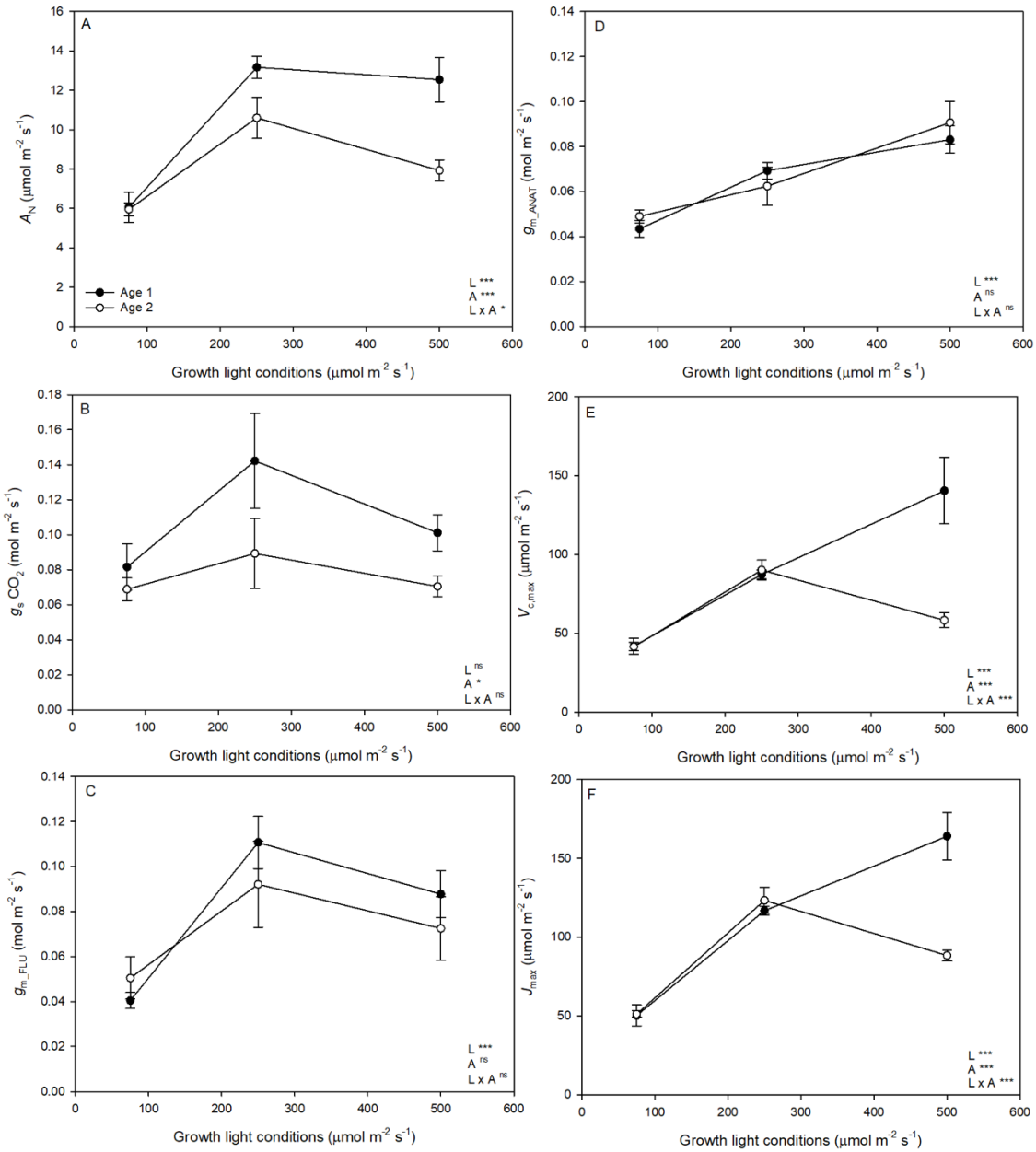
A
A_N (µmol m^{-2} s^{-1})
Age 1
Age 2
L ***
A ***
L x A *
Growth light conditions (µmol m^{-2} s^{-1})
D
g_{m_ANAT} (mol m^{-2} s^{-1})
L ***
A ns
L x A ns
Growth light conditions (µmol m^{-2} s^{-1})
B
g_s CO_2 (mol m^{-2} s^{-1})
L ns
A *
L x A ns
Growth light conditions (µmol m^{-2} s^{-1})
E
$V_{c,max}$ (µmol m^{-2} s^{-1})
L ***
A ***
L x A ***
Growth light conditions (µmol m^{-2} s^{-1})
C
g_{m_FLU} (mol m^{-2} s^{-1})
L ***
A ns
L x A ns
Growth light conditions (µmol m^{-2} s^{-1})
F
J_{max} (µmol m^{-2} s^{-1})
L ***
A ***
L x A ***
Growth light conditions (µmol m^{-2} s^{-1})

Figure 3

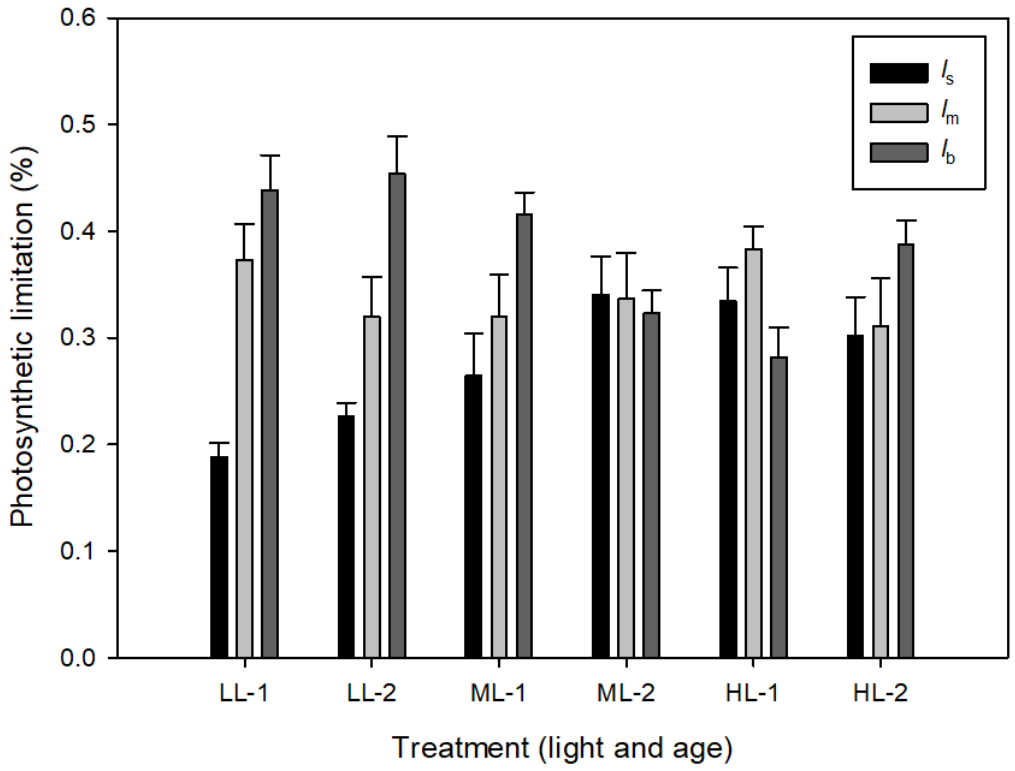

Figure 4

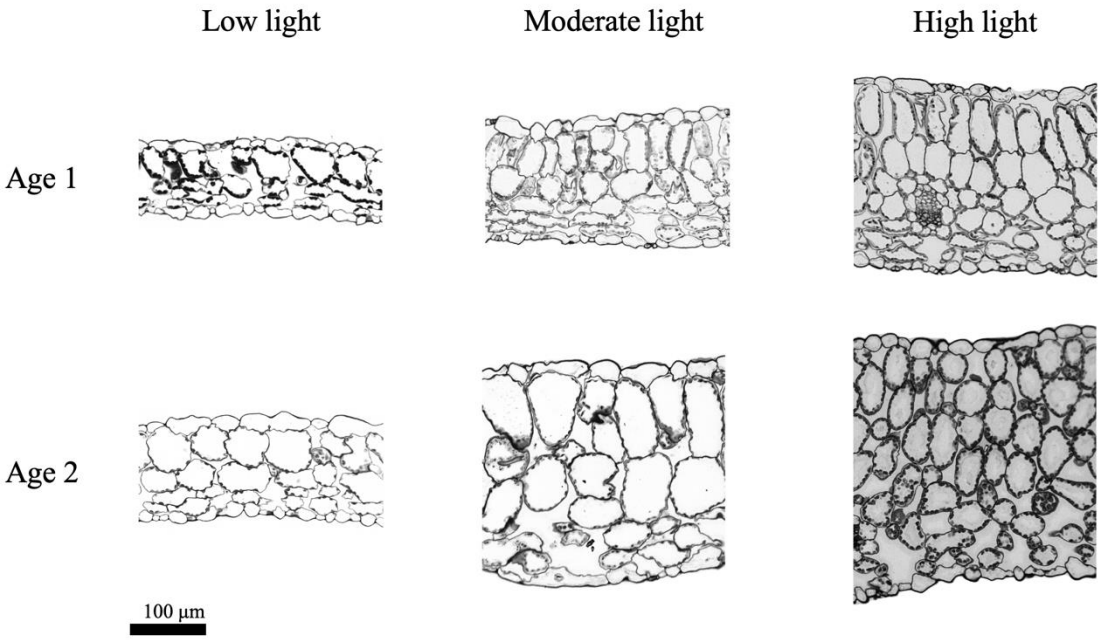

Figure 5

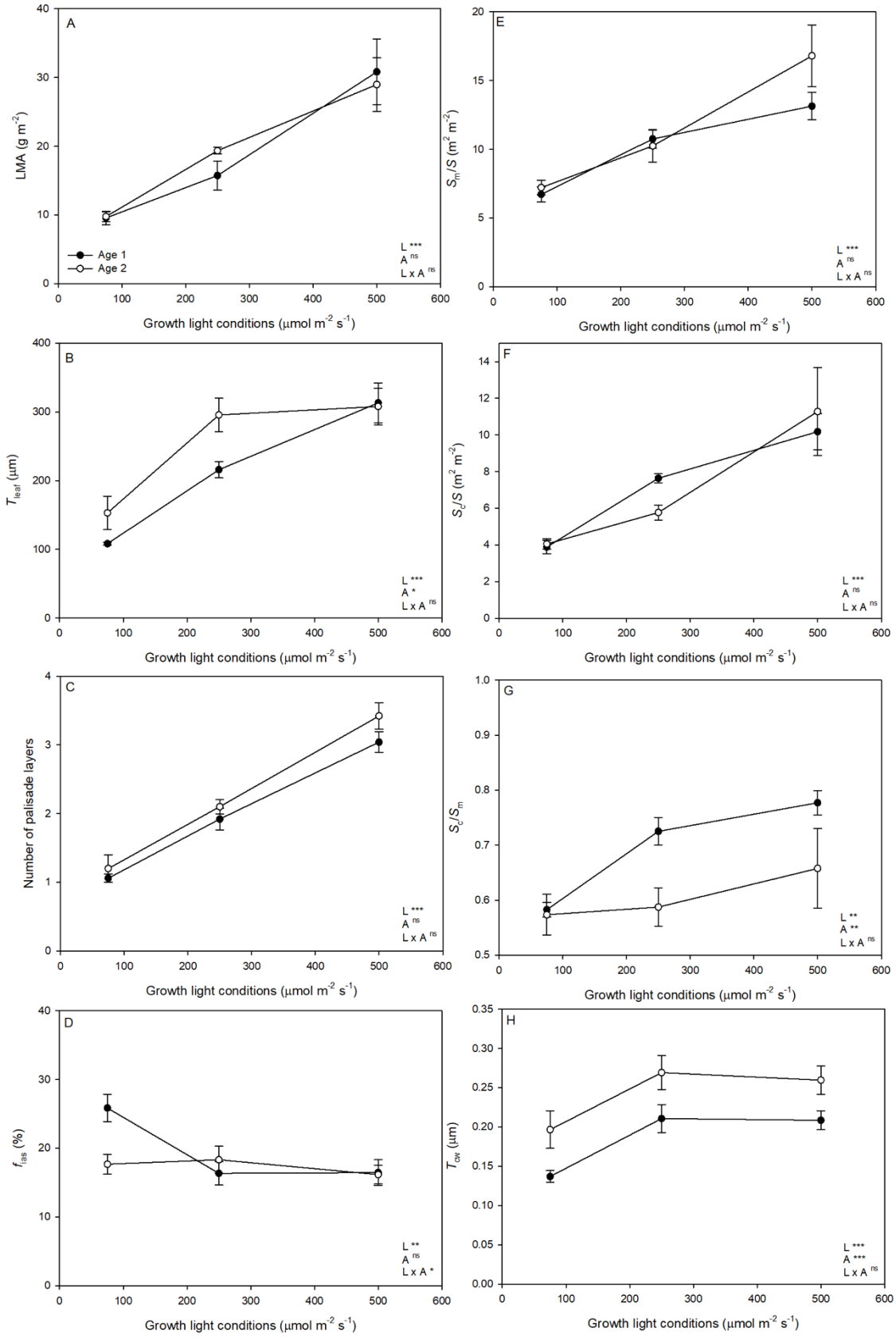
A
LMA (g m-2)
Age 1
Age 2
L ***
A ns
L x A ns
Growth light conditions (µmol m-2 s-1)
E
Sm/S (m2 m-2)
L ***
A ns
L x A ns
Growth light conditions (µmol m-2 s-1)
B
Tleaf (µm)
L ***
A *
L x A ns
Growth light conditions (µmol m-2 s-1)
F
Sc/S (m2 m-2)
L ***
A ns
L x A ns
Growth light conditions (µmol m-2 s-1)
C
Number of palisade layers
L ***
A ns
L x A ns
Growth light conditions (µmol m-2 s-1)
G
Sc/Sm
L **
A **
L x A ns
Growth light conditions (µmol m-2 s-1)
D
fdss (%)
L **
A ns
L x A *
Growth light conditions (µmol m-2 s-1)
H
Tcw (µm)
L ***
A ***
L x A ns
Growth light conditions (µmol m-2 s-1)

Figure 6

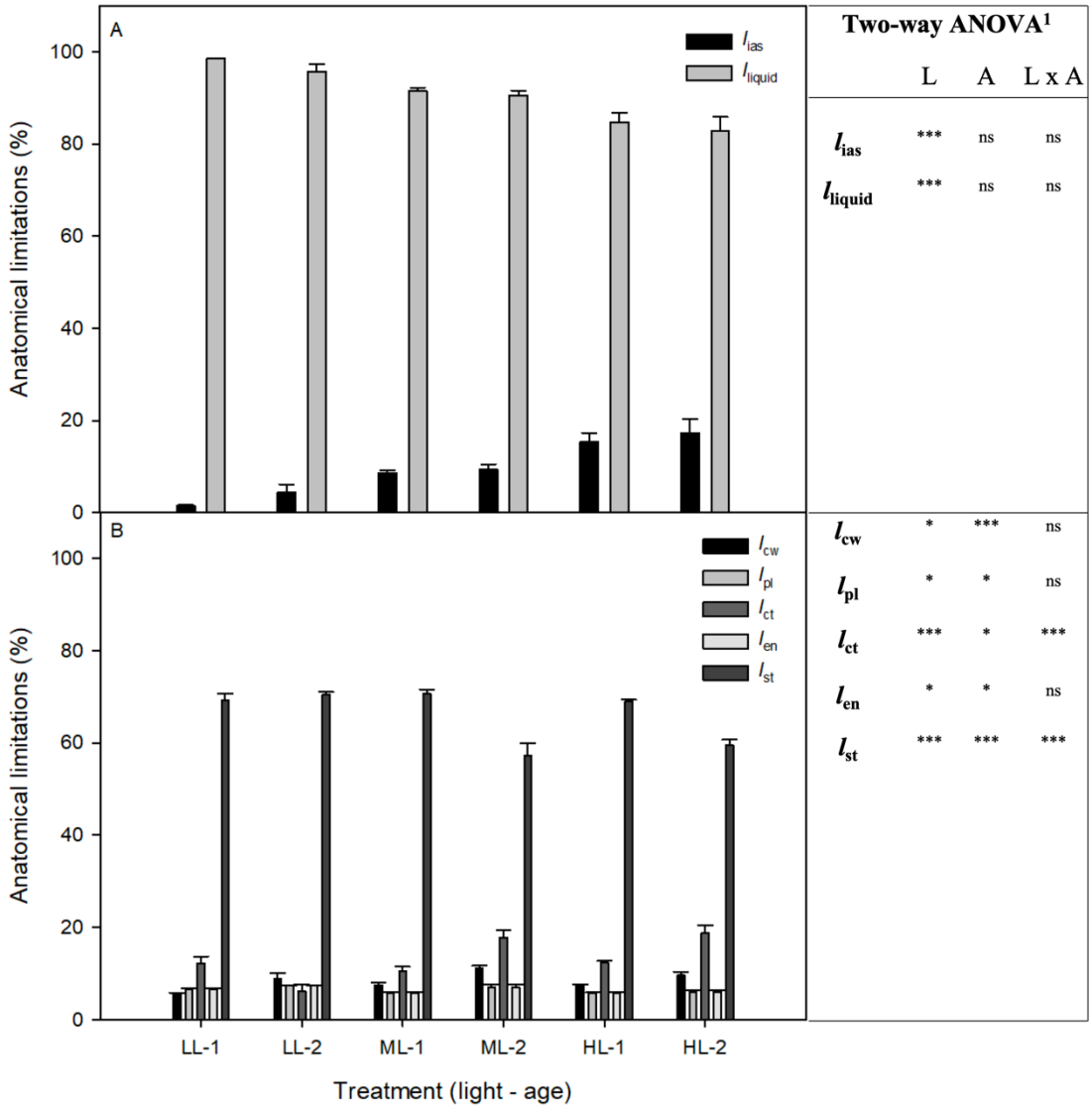
A
B
Anatomical limitations (%)
Anatomical limitations (%)
Treatment (light - age)
LL-1
LL-2
ML-1
ML-2
HL-1
HL-2
Two-way ANOVA[1]
L
A
L x A
l_{ias} *** ns ns
l_{liquid} *** ns ns
l_{cw} * *** ns
l_{pl} * * ns
l_{ct} *** * ***
l_{en} * * ns
l_{st} *** *** ***

Figure 7

Supplementary data

Table S1. Net assimilation rate (A_N), stomatal conductance (g_s), mesophyll conductance estimated from chlorophyll fluorescence and modelled from anatomical characteristics (g_{m_FLU} and g_{m_ANAT}, respectively) substomatal CO_2 concentration, chloroplastic CO_2 concentration (C_c), non-photorespiratory respiration during the day (R_d), maximum carboxylation rate ($V_{c,max}$) and electron transport rate (J_{max}) for *Arabidopsis thaliana* grown under low, moderate and high light intensities at two different leaf ages. Values are average ± SE (n = 4-6). Dashes account for non-available data.

Growth light intensity	Age	A_N (µmol m^{-2} s^{-1})	g_s CO_2 (mol m^{-2} s^{-1})	g_{m_FLU} (mol m^{-2} s^{-1})	g_{m_ANAT} (mol m^{-2} s^{-1})	C_i (µmol mol^{-1})	C_c (µmol mol^{-1})	R_d (µmol m^{-2} s^{-1})	$V_{c,max}$ (µmol m^{-2} s^{-1})	J_{max} (µmol m^{-2} s^{-1})
Low light	1	6.1 ± 0.8^{c}	0.082^{ab}	0.040 ± 0.004^{b}	0.043 ± 0.004^{c}	312 ± 4^{a}	162 ± 11	-	41.9 ± 4.9^{c}	50.3 ± 6.7^{c}
	2	6.0 ± 0.3^{c}	0.070^{b}	0.050 ± 0.009^{b}	0.049 ± 0.003^{c}	298 ± 6^{ab}	167 ± 17	0.36 ± 0.03^{b}	41.5 ± 2.7^{c}	51.2 ± 2.0^{c}
Moderate light	1	13.2 ± 0.6^{a}	0.142^{a}	0.111 ± 0.012^{a}	0.069 ± 0.004^{abc}	281 ± 16^{ab}	156 ± 9	-	87.3 ± 2.9^{b}	116.7 ± 2.7^{b}
	2	10.6 ± 1.0^{ab}	0.089^{ab}	0.092 ± 0.019^{ab}	0.062 ± 0.008^{bc}	255 ± 13^{b}	128 ± 8	0.22 ± 0.02^{a}	90.1 ± 6.3^{b}	123.3 ± 8.2^{b}
High light	1	12.5 ± 1.1^{a}	0.101^{ab}	0.088 ± 0.010^{ab}	0.083 ± 0.006^{ab}	252 ± 13^{b}	107 ± 11	-	140.5 ± 21.1^{a}	164.0 ± 15.0^{a}
	2	7.9 ± 0.5^{bc}	0.071^{ab}	0.072 ± 0.014^{ab}	0.091 ± 0.009^{a}	269 ± 15^{ab}	150 ± 7	0.55 ± 0.04^{c}	58.3 ± 4.7^{bc}	88.3 ± 3.5^{b}
Two-way ANOVA[1]	L	< 0.0001	0.055	0.0008	< 0.0001	0.002	0.006	< 0.0001	< 0.0001	< 0.0001
	A	0.0002	0.015	0.279	0.685	0.682	0.240	-	0.0007	0.0001
	L x A	0.024	-	-	-	0.199	0.016	-	0.0003	< 0.0001

[1] A two-way ANOVA was performed with growth light condition (L) and leaf age (A) to test the significance. *P* values obtained using Tukey's honest significant difference (HSD) test when L, A or L x A interaction was significant are displayed. Model was reassessed for HSD test when interaction was not significant, and the two resultant models were chosen following the Aikake Information Criterium (AIC) test. Values with the same superscript letters are not significantly different.

Table S2. Dry leaf mass per leaf area (LMA), leaf density (D_{leaf}), leaf thickness (T_{leaf}), mesophyll thickness (T_{mes}), number of palisade layers, fraction of the mesophyll occupied by the intercellular air spaces (f_{ias}), mesophyll and chloroplast surface area exposed to intercellular airspace per leaf area (S_m/S and S_c/S, respectively) and mesophyll cell wall thickness (T_{cw}) for *Arabidopsis thaliana* grown under low, moderate and high light intensities at two different leaf ages. Values are average ± SE (n = 5).

Growth light intensity	Age	LMA ($g\ m^{-2}$)	D_{leaf} ($g\ cm^{-3}$)	T_{leaf} (µm)	T_{mes} (µm)	Number of palisade layers	f_{ias} (%)	S_m/S ($m^2\ m^{-2}$)	S_c/S ($m^2\ m^{-2}$)	S_c/S_m	T_{cw} (µm)
Low light	1	9.6 ± 1.0^{b}	0.088 ± 0.009	108 ± 2^{d}	88 ± 2^{c}	1.06 ± 0.06^{c}	25.8 ± 2.0^{a}	6.72 ± 0.54^{c}	3.89 ± 0.37^{b}	0.58 ± 0.01^{b}	0.137 ± 0.007^{b}
	2	9.8 ± 0.7^{b}	0.068 ± 0.009	153 ± 24^{cd}	127 ± 24^{bc}	1.20 ± 0.20^{c}	17.7 ± 1.4^{b}	7.21 ± 0.53^{c}	4.05 ± 0.29^{b}	0.57 ± 0.04^{b}	0.197 ± 0.024^{ab}
Moderate light	1	15.7 ± 2.1^{b}	0.073 ± 0.010	216 ± 12^{bc}	188 ± 15^{ab}	1.92 ± 0.16^{b}	16.3 ± 1.7^{b}	10.75 ± 0.67^{bc}	7.63 ± 0.24^{ab}	0.73 ± 0.03^{ab}	0.211 ± 0.018^{ab}
	2	19.3 ± 0.5^{ab}	0.067 ± 0.005	296 ± 24^{ab}	262 ± 20^{a}	2.10 ± 0.10^{b}	18.3 ± 2.0^{ab}	10.24 ± 1.17^{bc}	5.77 ± 0.42^{b}	0.59 ± 0.03^{b}	0.269 ± 0.022^{a}
High light	1	30.8 ± 4.8^{a}	0.104 ± 0.023	313 ± 29^{a}	278 ± 32^{a}	3.04 ± 0.15^{a}	16.5 ± 1.9^{b}	13.14 ± 0.99^{ab}	10.18 ± 0.98^{a}	0.78 ± 0.02^{a}	0.208 ± 0.012^{ab}
	2	29.0 ± 3.9^{a}	0.093 ± 0.005	308 ± 27^{ab}	278 ± 26^{a}	3.42 ± 0.19^{a}	16.2 ± 1.4^{b}	16.80 ± 2.23^{a}	11.28 ± 2.41^{a}	0.66 ± 0.07^{ab}	0.260 ± 0.018^{a}
Two-way ANOVA	L	< 0.0001	0.052	< 0.0001	< 0.0001	< 0.0001	0.010	< 0.0001	< 0.0001	0.003	0.0003
	A	0.764	0.181	0.036	0.049	0.064	0.141	0.352	0.521	0.004	0.0004
	L x A	-	-	0.171	-	-	0.019	0.161	-	0.164	-

[1] A two-way ANOVA was performed with growth light condition (L) and leaf age (A) to test the significance. *P* values obtained using Tukey's honest significant difference (HSD) test when L, A or L x A interaction was significant are displayed. Model was reassessed for HSD test when interaction was not significant, and the two resultant models were chosen following the Aikake Information Criterium (AIC) test. Values with the same superscript letters are not significantly different.

Chapter 3. Mesophyll conductance and its main anatomical determinants along land plant's phylogeny

Note: The study of ferns and fern allies was extended and complemented with the following paper (not included in the present Thesis):

Tosens T., Nishida K., Gago J., Coopman R.E., Cabrera H.M., **Carriquí M.**, Laanisto L., Morales L., Nadal M., Rojas R., Talts E., Tomas M., Hanba Y., Niinemets Ü., Flexas J. (2016) The photosynthetic capacity in 35 ferns and fern allies: mesophyll CO_2 diffusion as a key trait. New Phytologist 209, 1576–1590.

Diffusional limitations explain the lower photosynthetic capacity of ferns as compared with angiosperms in a common garden study

Plant, Cell & Environment

Plant, Cell and Environment (2015) **38**, 448–460 doi: 10.1111/pce.12402

Original Article

Diffusional limitations explain the lower photosynthetic capacity of ferns as compared with angiosperms in a common garden study

M. Carriquí[1], H. M. Cabrera[2], M. À. Conesa[1], R. E. Coopman[3], C. Douthe[1], J. Gago[4], A. Gallé[5], J. Galmés[1], M. Ribas-Carbo[1], M. Tomás[1] & J. Flexas[1]

[1]*Research Group on Plant Biology under Mediterranean Conditions, Departament de Biologia, Universitat de les Illes Balears, Palma de Mallorca Illes Balears 07122, Spain,* [2]*Centro de Ecología Aplicada Ltda, Avenida Príncipe de Gales 6465, Santiago, Chile,* [3]*Laboratorio de Ecofisiología para la Conservación de Bosques, Instituto de Conservación, Biodiversidad y Territorio, Facultad de Ciencias Forestales y Recursos Naturales, Universidad Austral de Chile, Valdivia 567, Chile,* [4]*Applied Plant and Soil Biology, Faculty of Biology, University of Vigo, Vigo 36310, Spain and* [5]*Bayer CropScience NV Innovation Center Trait, Zwijnaarde B9052, Belgium*

ABSTRACT

Ferns are thought to have lower photosynthetic rates than angiosperms and they lack fine stomatal regulation. However, no study has directly compared photosynthesis in plants of both groups grown under optimal conditions in a common environment. We present a common garden comparison of seven angiosperms and seven ferns paired by habitat preference, with the aims of (1) confirming that ferns do have lower photosynthesis capacity than angiosperms and quantifying these differences; (2) determining the importance of diffusional versus biochemical limitations; and (3) analysing the potential implication of leaf anatomical traits in setting the photosynthesis capacity in both groups.

On average, the photosynthetic rate of ferns was about half that of angiosperms, and they exhibited lower stomatal and mesophyll conductance to CO_2 (g_m), maximum velocity of carboxylation and electron transport rate. A quantitative limitation analysis revealed that stomatal and mesophyll conductances were co-responsible for the lower photosynthesis of ferns as compared with angiosperms. However, g_m alone was the most constraining factor for photosynthesis in ferns. Consistently, leaf anatomy showed important differences between angiosperms and ferns, especially in cell wall thickness and the surface of chloroplasts exposed to intercellular air spaces.

Key-words: leaf anatomy; photosynthesis; pteridophytes.

INTRODUCTION

Ferns appeared nearly 420 million years ago (Myr) in the Devonian, having their colonization splendour during the Mesozoic, followed by appearance of the angiosperms, about 200 Myr ago, attaining their major colonization of the terrestrial surface by the end of the Cretaceous period, between 100 and 65 Myr (Kenrick & Crane 1997). Ferns are a key group in the phenomenon of radiation of land plants (approximately 11 000 species reaching 80% of vascular plants without flowers) being the group phylogenetically closest to spermatophytes (Kenrick & Crane 1997; Smith *et al.* 2006). However, the current dominant plant group is the angiosperms, accounting for 96% of the total diversity of vascular plants (Schuettpelz & Pryer 2009).

The reason of the higher success of angiosperms than ferns could be related with the different atmospheric conditions prevailing when each group appeared (Brodribb *et al.* 2009; Flexas & Keeley 2012). Ferns emerged under 10-fold higher than present atmospheric CO_2 concentration and slightly lower oxygen (18–20%). Meanwhile, angiosperms emerged under atmospheric CO_2 concentration only two- to threefold higher than the present, and the concentration of oxygen was 23–25% (Haworth *et al.* 2011). These large differences in atmospheric conditions imply that, originally, both plant groups evolved under different selection pressures, which may have resulted in different mechanisms of CO_2 diffusion and fixation, which perhaps are still partially reflected in extant plants of both groups.

Globally, photosynthetic capacity in ferns typically is lower than 10 μmol CO_2 m^{-2} s^{-1}, with highest values approximately 15 μmol CO_2 m^{-2} s^{-1}. In contrast, angiosperms have averages higher than 10 μmol CO_2 m^{-2} s^{-1}, with some species reaching values above 50 μmol CO_2 m^{-2} s^{-1} (Wright *et al.* 2004, 2005; Volkova *et al.* 2009, 2011; Gago *et al.* 2013). Even normalizing the comparison between ferns and angiosperms by mass and nitrogen bases, ferns still present a significantly lower photosynthetic capacity (Wright *et al.* 2004, 2005), but the number of fern species in which their photosynthetic metabolism has been characterized up to date is very low. Assuming that ferns have indeed a lower photosynthetic capacity, the physiological reasons remain unclear. Commonly smaller photosynthetic capacity is exerted by lower

Correspondence: J. Flexas. Fax: +34 971 173184; e-mail: jaume.flexas@uib.es

nitrogen investment in Rubisco (ribulose 1·5-bisphosphate carboxylase/oxygenase) or electron transport components, and/or lower carboxylation efficiency of Rubisco (Yeoh *et al.* 1981). However, it has been shown that photosynthetic capacity scales with nitrogen content similarly in ferns and angiosperms (Karst & Lechowicz 2007), suggesting that in the photosynthetic apparatus the carbon/nitrogen allocation patterns in relation to photosynthetic capacities are similar in both groups. In addition, Rubisco constant kinetics, although studied in relatively few fern species, show similar values to those described for angiosperms (Yeoh *et al.* 1981; Bird *et al.* 1982; Jordan & Ogren 1983; Gago *et al.* 2013), suggesting that the efficiency of photosynthesis should be similar as well.

Most likely, and linked with the hypothesis of different CO_2/O_2 selection pressures at the origin of both groups, diffusional CO_2 limitations could help explain the lower photosynthetic capacity of ferns. Among CO_2 diffusional limitations, we can distinguish stomatal and mesophyll conductance. A lower stomatal conductance to CO_2 in ferns would be expected based on their described stomata characteristics especially the absence of well-defined stomatal guard cells, presenting a low sensitivity to changes in the cell turgor, so that opening and closing is much less regulated compared with angiosperms (Franks & Farquhar 2007). In addition, recent studies have shown fern stomata not responding to abscisic acid (ABA), CO_2 or blue light (Doi & Shimazaki 2008; Brodribb & McAdam 2011; McAdam & Brodribb 2012), but this is controversial yet (Ruszala *et al.* 2011; Haworth *et al.* 2013). In this sense, ferns could be considered as water spender species. Gago *et al.* (2013) showed in three phylogenetically distant fern species that stomatal limitation indeed may not be the main cause for their low photosynthetic rates. Another is that the case of mesophyll conductance (g_m) limitations could be strongly related with the low photosynthesis rates observed in ferns (Flexas & Keeley 2012; Flexas *et al.* 2012). To the best of our knowledge, only four values of g_m have been published for fern species (Volkova *et al.* 2009; Gago *et al.* 2013), and all of them are in the lower range of published values for higher plants, that is, similar to those displayed by some conifers and CAM succulent plants (Flexas & Keeley 2012; Flexas *et al.* 2012). Hence, mesophyll conductance limitations seem to be a good candidate to understand the low photosynthetic capacity in ferns, and interestingly there is no insight for the causes of low g_m in ferns.

In angiosperms, leaf anatomical characteristics have an important role driving the photosynthesis and the potential g_m (Evans *et al.* 2009; Hassiotou *et al.* 2009; Scafaro *et al.* 2011; Peguero-Pina *et al.* 2012; Tosens *et al.* 2012a,b; Tomás *et al.* 2013). In particular, CO_2 diffusion through the mesophyll tissues is significantly limited by the cell wall thickness and the chloroplast envelope. Furthermore, parameters related with reducing or neglecting the traffic of CO_2 in the liquid phase through cytoplasm have been proposed as major determinants of differences in g_m between species (e.g. the chloroplast surface area exposed to intercellular air spaces per leaf area; Terashima *et al.* 2011; Tomás *et al.* 2013). How these parameters affect g_m and photosynthesis in ferns is unknown. No previous studies simultaneously compared the photosynthetic functioning of fern and angiosperm species growing in a common garden under optimal conditions. This comparison is necessary to corroborate the lower photosynthetic capacity of ferns than angiosperms and their physiological basis. Here we present a photosynthetic comparison among seven ferns and seven angiosperms, paired by sharing similar ecological niches. The aims of the study are (1) to quantify how much lower is the photosynthetic capacity of ferns as compared with angiosperms; (2) to assess the physiological determinants for such lower capacity; and (3) to analyse the potential implication of leaf anatomical traits in setting maximum photosynthesis in the two groups.

MATERIALS AND METHODS

Studied plants and growth conditions

Fourteen native species to the Balearic Islands were selected. They belong to two phylogenetically distinct groups, ferns and angiosperms (Supporting Information Fig. S1 and Table 1). The seven fern species were: *Adiantum capillus-veneris* L., *Asplenium scolopendrium* L., *Asplenium trichomanes* L., *Dryopteris tyrrhena* F.-J. & Reichst., *Equisetum telmateia* Ehrh., *Pteridium aquilinum* (L.) Kuhn, and *Pteris vittata* L.; and the seven angiosperms were: *Alisma plantago-aquatica* L., *Digitalis minor* L. var. *palaui* (G. Font) Hinz & Rosselló, *Lysimachia minoricensis* J.J. Rodr., *Pastinaca lucida* L., *Phlomis italica* L., *Vinca difformis* Pourr., and *Viola jaubertiana* Marès et Vigineix. The species were selected to include fern-angiosperm pairs based on a wide generalization of their habitat preference in their native niches (Table 1), to avoid biases in the comparison of the two groups. Nevertheless, to further avoid any effect of the site or stress conditions, all the species were evaluated in a common garden at the Sóller Botanic Garden (Mallorca, 39°45′51.58″N, 2°42′33.75″E, 47 m of elevation) under optimal growing conditions for all the species. Therefore, and because all the measured species were developed in the garden, species similarities and differences responded to genetic adaptations to their native habitats, discarding traits related to acclimation to a particular sampling location. In the garden, the average annual rainfall was approximately 740 mm and mean temperature was 17.3 °C. The study was realized under typical Mediterranean conditions from the end of April to mid of May 2012, the average temperature was 16.5 °C and the total accumulated rainfall was 190.1 mm in the previous 3 months (Sa Vinyassa meteorological station, Spanish Ministry of Agriculture, Food and Environment). All species were grown at full sunlight, with maximum values at midday of 1500 μmol m^{-2} s^{-1} extended for at least 3 h. At some times of the day, some species were momentarily shaded, but such periods were avoided during measurements. Irrigation was provided in dry periods, in the amount and frequency, to avoid any water stress during growing season.

Gas exchange and fluorescence measurement

Fully expanded fronds/leaves were selected for the simultaneous measurement of gas exchange and chlorophyll *a*

Table 1. List of fern (F) and angiosperm (A) species pairs based on the similarity in their native habitat. Habitats were generalized and unified based on Bolòs *et al.* (2005)/HVMO (2007). Family, lifestyle and evolutionary history were extracted from Bolòs *et al.* (2005)

Species	Group	Generalized habitat	Family	Lifestyle	Evolutionary history
Adiantum capillus-veneris	F	Wet understory/shady places	Pteridaceae	Hemicryptophyte	Not endemic
Vinca difformis	A		Apocynaceae	Chamaephyte	Not endemic
Asplenium scolopendrium	F	Wet, shady rocky places	Aspleniaceae	Hemicryptophyte	Not endemic
Lysimachia minoricensis	A		Primulaceae	Hemicryptophyte	Endemic
Asplenium trichomanes	F	Rock crevices and walls, frequently vertical habitat	Aspleniaceae	Hemicryptophyte	Not endemic
Viola jaubertiana	A		Violaceae	Hemicryptophyte	Endemic
Dryopteris tyrrhena	F	Rock crevices/cliff basis in shady and humid places	Dryopteridaceae	Hemicryptophyte	Endemic (microareal)
Digitalis minor var. *palaui*	A		Schrophulariaceae	Hemicryptophyte	Endemic
Equisetum telmateia	F	Torrents, ponds and wetlands	Equisetaceae	Geophyte	Not endemic
Alisma plantago-aquatica	A		Alismataceae	Hydrophyte	Not endemic
Pteridium aquilinum	F	Forest borders and sunny places with some degree of drought (summer)	Dennstaedtiaceae	Geophyte	Not endemic
Phlomis italica	A		Lamiaceae	Chamaephyte	Endemic
Pteris vittata	F	Mountain plant in stony places and path sidewalks. Areas with low shrub cover.	Pteridaceae	Geophyte	Not endemic
Pastinaca lucida	A		Apiaceae	Hemicryptophyte	Endemic

fluorescence using an infrared gas analyser (IRGA) LI-6400XTR coupled with the fluorometer (Li-6400-40; Li-Cor Inc., Lincoln, NE, USA). The leaves/fronds (hereafter 'leaves') were clamped into a 2 cm^2 cuvette. For all measurements, block temperature was fixed to 25 °C and the vapour pressure deficit (VPD) was kept around 1.5 kPa. No significant differences in the average leaf temperature were found between angiosperms and ferns (25.9 ± 0.3 and 26.1 ± 0.3 °C, respectively), the maximum value for a single species being 27.1 (found in the angiosperm *D. minor* and in the fern *A. capillus-veneris*). Leaf steady-state conditions were induced at saturating photosynthetic photon flux density (PPFD 1500 μmol m^{-2} s^{-1}, 90–10% red-blue light) and 400 μmol CO_2 mol^{-1} air. The flow rate within the chamber was regulated from 100 to 300 mmol air min^{-1} depending on photosynthesis rates in the different species, in order to ensure CO_2 delta values >4 μmol CO_2 mol^{-1} air between sample and reference IRGAs, allowing for reliable estimates of photosynthesis rates. Once steady-state conditions were achieved, usually after 15–20 min, A_N-C_i response curves were performed in the CO_2-limited range to estimate the maximum velocity of carboxylation ($V_{c,max}$), considering eight atmospheric CO_2 concentration (C_a) steps of 50 μmol CO_2 mol^{-1} air, decreasing from 400 to 50 μmol CO_2 mol^{-1}. According to previous studies (Gago *et al.* 2013), at ambient CO_2 fern photosynthesis is mostly limited by $V_{c,max}$, we preferred to keep the sampling period to a minimum to ensure that the 14 species were completely sampled before the beginning of the dry season rather than to perform complete A_N-C_i curves doubling the total sampling time. Three plants per species were measured. Because some fern fronds did not completely cover the area of the cuvette, a digital picture of the frond fraction inside the chamber's foam gasket was taken to re-calculate the area with image analysis software (ImageJ; Wayne Rasband/NIH, Bethesda, MD, USA).

In all cases, the measurements of the values of A_N and steady-state fluorescence (F_s) were registered just after the stabilization of the gas exchange rates in a given C_a. Then a saturating white light flash around 8000 μmol m^{-2} s^{-1} was applied to determine the maximum fluorescence (F_m'). From these values, the real quantum efficiency of photosystem II (Φ_{PSII}) was calculated as

$$\Phi_{PSII} = \frac{(F_m' - F_s)}{F_m'} \quad (1)$$

and the electron transport rate (ETR) through PSII was calculated as

$$ETR = \Phi_{PSII} \cdot PAR \cdot \alpha \cdot \beta \quad (2)$$

where the PAR value corresponded to the saturated quantum flux density stated above, α was the absorbance of the leaf determined according to Schultz (1996) using a spectroradiometer (HR2000CG-UV-NIR; Ocean Optics Inc., Dunedin, FL, USA), and β is the theoretical partition of absorbed PAR between PSII, which was assumed to be 0.5. The respiration rate in the dark (R_d) was considered as the half of the dark-adapted mitochondrial respiration (R_n; measured after darkening the leaves for 30 min, following Niinemets *et al.* 2005 and Gallé *et al.* 2011). Cuvette CO_2 leakage curves were used to correct A_N-C_i curves, following Flexas *et al.* (2007).

For all species, the following estimations were performed: chloroplastic CO_2 concentration (C_c), g_m according to Harley *et al.* (1992) and Ethier & Livingston (2004), and the maximum velocity of carboxylation ($V_{c,max}$) according to

Farquhar *et al.* (1980). The method of Harley *et al.* (1992) is based in the comparison of ETR as a measure of gross photosynthesis with A_N to estimate the photorespiration rate using the known value of the specificity factor of Rubisco for ferns ($S_{C/O}$; Gago *et al.* 2013) or the CO_2 compensation point (Γ^*), allowing the calculation of C_c, with the following equation:

$$g_m = \frac{A_N}{C_i - \frac{\Gamma^*(ETR + 8(A_N + R_d)}{ETR - 4(A_N + R_d)}} \quad (3)$$

These values were used to transform the A_N-C_i response curves into A_N-C_c curves using the equation

$$g_m = \frac{A_N}{C_i - C_c} \quad (4)$$

The method of Ethier & Livingston (2004), instead, uses only gas exchange measurements, adjusting the non-linear model of Farquhar *et al.* (1980) to extract, in conjunction with $V_{c,max}$ and the g_m. Probably because of the reduced number of points in the curves, the curve-fitting method (Ethier & Livingston 2004) did not reach satisfactory results in some of the replicates. For this reason, although a good correlation was obtained between the two estimates of g_m considering all the data averaged per species (Fig. 1), we use the values obtained by the method of Harley *et al.* (1992) to compare with other parameters through the manuscript. However, in the case of *E. telmateia*, the method of Ethier & Livingston (2004) showed less dispersion among replicates than the Harley method, which indeed provided some unreliable estimates. The reason is that the large leaf thickness and the cylindrical shape of these leaves could provoke heterogeneous PSII saturations at different depths in the mesophyll. This situation decouples gas exchange and ETR, so the basic requirement of the method of Harley *et al.* (1992) was not accomplished. For this cause, and just for this species, the considered g_m was the one obtained with the Ethier & Livingston (2004) method.

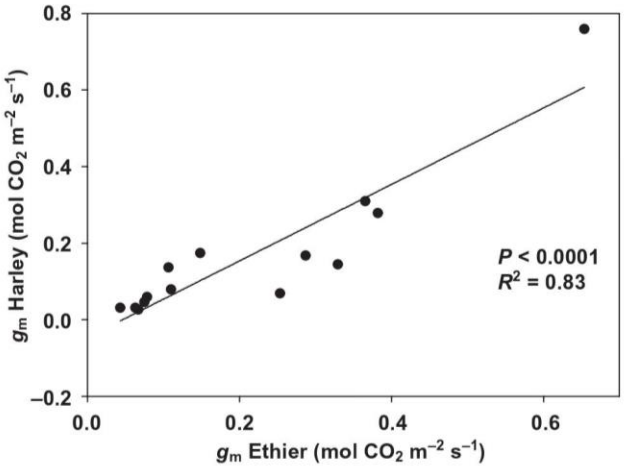

Figure 1. Correlation estimates of mesophyll conductance (g_m) for all species measured following the methods of Harley *et al.* (1992) and Ethier & Livingston (2004). Values represent the mean of three replicates for each species.

The CO_2 compensation point (Γ^*) required by the method of Harley *et al.* (1992) was derived from published values of Rubisco specific factor ($S_{C/O}$) from the equation

$$\Gamma^* = \frac{0.5 \cdot [O_2]}{S_{C/O}} \quad (5)$$

The values for *D. minor* var. *palaui*, *L. minoricensis* and *P. italica* were obtained from Galmés *et al.* (2005) and *P. lucida* from Delgado *et al.* (1995). For the rest of angiosperms, due to the absence of values for the species studied, an average for the same functional group was taken according to Galmés *et al.* (2005). With regard to the ferns, only one study (Gago *et al.* 2013) showed values of $S_{C/O}$ for three species, all of them remaining approximately 100 mol mol^{-1}. Therefore, this value was used for all the ferns studied.

Quantitative limitation analysis of A_N

Following Grassi & Magnani (2005), photosynthetic limitations were assessed for all species. This approach requires knowledge of A_N, g_s, g_m and the maximum velocity of carboxylation or ETR. Because a good agreement was found between $V_{c,max}$ and ETR (see Table 4), and ETR values showed generally less intraspecific dispersion, we used ETR following Gallé *et al.* (2011) and Varone *et al.* (2012). Using this method, stomatal (l_s), mesophyll conductance (l_{mc}) and biochemical (l_b) relative limitations are calculated for each species, which represent a measure of the relative importance of stomatal diffusion, mesophyll diffusion and photosynthetic biochemistry in setting the observed value of A_N. Relative photosynthetic limitations were calculated as follows:

$$l_s = \frac{g_{tot}/g_{sc} \cdot \partial A_N/\partial C_c}{g_{tot} + \partial A_N/\partial C_c}$$

$$l_{mc} = \frac{g_{tot}/g_m \cdot \partial A_N/\partial C_c}{g_{tot} + \partial A_N/\partial C_c}$$

$$l_b = \frac{g_{tot}}{g_{tot} + \partial A_N/\partial C_c}$$

where g_{tot} is the total conductance to CO_2 between the leaf surface and carboxylation sites (Grassi & Magnani 2005).

Leaf mass per unit area and leaf density

Leaf area was determined from images of scanned leaves with the software ImageJ (Wayne Rasband/NIH). After this, they were placed in an oven at 60 °C until they reached constant dry weight to calculate the dry leaf mass per unit leaf area (LMA). Using leaf thickness from anatomical measurements, leaf density (D_L) was calculated as the LMA per leaf thickness (Niinemets 1999).

Anatomical measurements

A partial anatomic analysis was performed to assess the four structural traits most likely affecting g_m according to the literature (Terashima *et al.* 2011; Tosens *et al.* 2012a,b; Tomás

et al. 2013): the fraction of mesophyll occupied by intercellular air spaces (f_{ias}), the surface of mesophyll cells (S_m/S) and chloroplasts intercellular air spaces per leaf area (S_c/S), and cell wall thickness (T_{cw}). For this, 1 × 1 mm pieces were cut off between the main veins of the leaves for anatomical measurements. The samples were quickly fixed under vacuum pressure with glutaraldehyde 4% and paraformaldehyde 2% in a 0.1 M phosphate buffer (pH 7.4). Subsequently, the samples were fixed in 2% osmium tetroxide for 2 h, and dehydrated in a graded series of ethanol. Dehydrated segments were embedded in LR-White resin and solidified in an oven at 60 °C for 48 h. Semi-fine (0.8 μm) and ultra-fine (90 nm) cross sections were cut with an ultramicrotome (Leica UC6). Semi-fine sections were dyed with 1% toluidine blue and observed under the Olympus BX60 optic microscope. The photographs were taken at 200× magnifications with a digital camera (U-TVO.5XC; Olympus, Tokyo, Japan, see Supporting Information Fig. S2a). The ultra-fine sections for transmission electron microscopy (TEM H600; Hitachi, Tokyo, Japan) were contrasted with uranyl acetate and lead citrate. The electron micrographs were taken at 2 000× magnification (Supporting Information Fig. S2b). All images were analysed using ImageJ (Wayne Rasband/NIH) and AutoCAD (AutoCAD 2011 Mac; Autodesk, San Rafael, CA, USA), and the parameters were estimated as described in detail in Tomás *et al.* (2013). The curvature cell correction factor was measured and calculated for each species according to Thain (1983), making an average length-width ratio of 3–5 cells in 2–4 different fields of view for each tissue fraction. All parameters were analysed in four to six fields of view in three different sections. For S_m/S and S_c/S, weighted averages were calculated from the volume fractions of tissue. The mesophyll cell wall thickness was measured at 30 000× magnification (Supporting Information Fig. S2c) in 4–6 different fields of view and 3 different sections per species. The micrographs were randomly selected in each section and the cell wall thickness was measured for 2–3 cells per micrograph.

Statistics and modelling

Two independent one-way analyses of variance (ANOVAS) were performed to reveal differences between species within types, and between ferns and angiosperms. The differences between means were detected by Tukey's honest significant difference tests ($P < 0.05$). Pearson correlation matrices were determined for all species and for each type to determine the correlated structure of the different parameters; for a conservative evaluation of the correlation parameters, these were only considered to be significant when $P < 0.05$ and $P < 0.01$. These analyses were performed with the software package IBM SPSS 19.0 (SPSS, Chicago, IL, USA).

RESULTS

Photosynthetic comparison between ferns and angiosperms

At ambient CO_2, the photosynthetic traits were generally higher for angiosperms than ferns (Table 2). The net CO_2 assimilation rate (A_N) and the stomatal conductance (g_s) were about 2.5-fold higher in angiosperms than in ferns. As a consequence of covariation of A_N and g_s in all species, the intrinsic water use efficiency (A_N/g_s) was similar in both plant groups. Among the studied angiosperms, the lowest value of A_N was 9.1 μmol CO_2 m^{-2} s^{-1}, obtained for *V. difformis*, and the highest value was 32.0 μmol CO_2 m^{-2} s^{-1}, obtained for *P. lucida*. In contrast, the largest value for a fern, *E. telmateia*, was 13.7 μmol CO_2 m^{-2} s^{-1}, that is, only slightly higher than the minimum for angiosperms, and the minimum in *A. scolopendrium* as low as 3.9 μmol CO_2 m^{-2} s^{-1} (Table 2). Even larger differences between groups were observed for the mesophyll conductance to CO_2 (g_m), which was up to fourfold in angiosperms than in ferns, with an average of 0.287 and 0.074 mol CO_2 m^{-2} s^{-1}, respectively (Table 2). As a consequence of covariation of A_N and g_s, no significant difference was observed between the two groups for C_i, but the chloroplast CO_2 concentration (C_c) was 1.5-fold higher in angiosperms than in ferns. Comparing the response of A_N to C_i and C_c in ferns and angiosperms, the slope of the A_N-C_i curve was significantly slower in ferns, while the differences were unclear for the A_N-C_c curve due to large variability and range overlapping among the two groups (Fig. 2). Other parameters showed differences between the two groups, although these were less marked than those shown for diffusive parameters. Hence, the respiration rate in the dark (R_d) was 40, significantly higher in angiosperms than ferns. Similarly, the characters driving the photo- and biochemical capacity for photosynthesis in plants, that is, the maximum velocity of carboxylation ($V_{c,max}$) and the ETR, were 43 and 52% larger in angiosperms than in ferns (Table 2).

Because we analyse many different species belonging to different families and having quite different habitat preferences (Table 1), in addition to average values it may be important to look at the intra-group variability. We therefore compare the values analysed as medians, 25 and 75% percentiles, extreme values and outliers (Fig. 3). It can be observed that, while the dispersion of data in absolute values was larger for angiosperms than for ferns, when compared relative to the median for each group the dispersion of the data was similar. Therefore, the average and median values for all the photosynthetic parameters were lower in ferns than in angiosperms and with similar intra-group variability.

Anatomical comparison between ferns and angiosperms

For the case of anatomical traits – such as cell wall thickness (T_{cw}), the chloroplast surface area exposed to intercellular air spaces per leaf area (S_c/S), the mesophyll tissue occupied by the intercellular air spaces (f_{ias}), and the leaf mass per area (LMA) – significant differences were observed between species and groups in some parameters but not in others. LMA presented no major differences between groups, although these were remarkable between species, with a maximum value of 90.4 g m^{-2} for *E. telmateia* and a minimum of 31.4 g m^{-2} for *L. minoricensis* (Table 3). Non-significant differences in leaf thickness were observed between ferns

Table 2. Photosynthetic characteristics for each studied species and averages for ferns and angiosperms. Average values ± SE are shown for net assimilation (A_N), stomatal conductance (g_s), mesophyll conductance (g_m) – according to the Ethier & Livingston (2004) method for *Equisetum* and to the Harley *et al.* (1992) method for the other species – maximum carboxylation rate on a C_c basis ($V_{c,max}$), sub-stomatal CO_2 concentration (C_i), chloroplastic CO_2 concentration (C_c), electron transport rate (*ETR*) and dark respiration rate (R_d)

Species	A_N (μmol CO_2 m^{-2} s^{-1})	g_s (mol CO_2 m^{-2} s^{-1})	A_N/g_s (μmol mol^{-1})	g_m (mol CO_2 m^{-2} s^{-1})	$V_{c,max}$ (μmol CO_2 m^{-2} s^{-1})	C_i (μmol mol^{-1})	C_c (μmol mol^{-1})	*ETR* (μmol m^{-2} s^{-1})	R_d (μmol m^{-2} s^{-1})
Ferns									
Equisetum telmateia	13.7 ± 0.7^{cd}	0.143 ± 0.010^{abcd}	59.3 ± 6.3^{ab}	0.253 ± 0.074^{a}	68.1 ± 1.90^{ab}	284 ± 9^{bc}	216 ± 17^{ef}	193.1 ± 4.3^{ef}	–0.8 ± 0.1
Pteridium aquilinum	10.6 ± 2.1^{bc}	0.085 ± 0.021^{abc}	79.6 ± 5.0^{ab}	0.073 ± 0.007^{a}	127.5 ± 35.9^{abcd}	256 ± 7^{abc}	113 ± 14^{abc}	125.0 ± 30.8^{bcd}	–1.3 ± 0.2
Adiantum capillus-veneris	5.9 ± 0.9^{ab}	0.059 ± 0.007^{abc}	61.8 ± 7.4^{ab}	0.031 ± 0.006^{a}	100.0 ± 5.8^{abcd}	287 ± 11^{c}	88 ± 7^{ab}	80.6 ± 7.5^{abc}	–0.5 ± 0.0
Pteris vittata	9.1 ± 1.1^{abc}	0.062 ± 0.011^{abc}	92.2 ± 8.6^{ab}	0.059 ± 0.009^{a}	160.3 ± 8.2^{cdef}	236 ± 13^{abc}	81 ± 2^{a}	131.5 ± 15.7^{cd}	–0.4 ± 0.1
Asplenium trichomanes	5.9 ± 0.7^{ab}	0.053 ± 0.009^{ab}	70.9 ± 3.6^{ab}	0.031 ± 0.003^{a}	120.8 ± 7.7^{abcd}	273 ± 6^{abc}	85 ± 3^{a}	93.9 ± 8.0^{abcd}	–1.2 ± 0.2
Asplenium scolopendrium	3.9 ± 0.5^{a}	0.032 ± 0.005^{a}	77.0 ± 4.6^{ab}	0.026 ± 0.003^{a}	46.5 ± 5.0^{a}	265 ± 7^{abc}	115 ± 5^{abc}	46.8 ± 5.8^{a}	–0.9 ± 0.1
Dryopteris tyrrhena	6.8 ± 0.4^{ab}	0.063 ± 0.004^{abc}	67.2 ± 2.8^{ab}	0.046 ± 0.004^{a}	75.1 ± 12.0^{ab}	280 ± 5^{abc}	130 ± 9^{abc}	70.6 ± 4.4^{ab}	–1.2 ± 0.1
Average	**8.0 ± 0.8^{a}**	**0.071 ± 0.008^{a}**	**72.6 ± 2.99^{a}**	**0.074 ± 0.019^{a}**	**99.7 ± 9.5^{a}**	**269 ± 5^{a}**	**118 ± 10^{a}**	**105.9 ± 11.0^{a}**	**–0.9 ± 0.1^{a}**
Angiosperms									
Alisma plantago-aquatica	17.0 ± 0.6^{de}	0.169 ± 0.024^{cd}	63.0 ± 6.6^{ab}	0.144 ± 0.015^{a}	135.9 ± 16.4^{bcde}	278 ± 11^{abc}	159 ± 17^{bcde}	150.4 ± 5.8^{de}	–1.6 ± 0.2
Digitalis minor var. *palaui*	21.9 ± 0.8^{ef}	0.138 ± 0.017^{abcd}	99.3 ± 8.5^{b}	0.278 ± 0.008^{a}	221.5 ± 31.7^{f}	219 ± 13^{a}	140 ± 13^{abcd}	199.9 ± 6.3^{ef}	–1.2 ± 0.2
Lysimachia minoricensis	17.7 ± 0.9^{de}	0.163 ± 0.019^{bcd}	67.4 ± 5.4^{ab}	0.310 ± 0.049^{a}	102.3 ± 2.3^{abcd}	268 ± 6^{abc}	209 ± 7^{def}	130.9 ± 4.4^{cd}	–1.5 ± 0.1
Pastinaca lucida	32.0 ± 1.3^{g}	0.363 ± 0.058^{e}	54.4 ± 7.4^{a}	0.760 ± 0.209^{b}	167.1 ± 6.9^{def}	282 ± 12^{bc}	234 ± 19^{f}	237.2 ± 5.3^{f}	–2.7 ± 0.2
Vinca difformis	9.1 ± 0.4^{abc}	0.061 ± 0.006^{abc}	95.8 ± 15.3^{b}	0.174 ± 0.019^{a}	76.7 ± 19.6^{ab}	224 ± 22^{ab}	169 ± 30^{cdef}	83.8 ± 14.9^{abc}	–1.1 ± 0.0
Phlomis italica	24.0 ± 1.1^{f}	0.240 ± 0.019^{d}	60.5 ± 2.5^{ab}	0.168 ± 0.014^{a}	214.8 ± 12.9^{ef}	277 ± 3^{abc}	133 ± 7^{abc}	218.9 ± 2.3^{f}	–1.3 ± 0.2
Viola jaubertiana	13.4 ± 1.9^{cd}	0.107 ± 0.028^{abc}	84.6 ± 14.3^{ab}	0.174 ± 0.010^{a}	82.9 ± 5.2^{abc}	248 ± 22^{abc}	171 ± 15^{cdef}	109.9 ± 9.1^{bcd}	–1.1 ± 0.1
Average	**19.3 ± 1.6^{b}**	**0.177 ± 0.022^{b}**	**75.0 ± 4.81^{a}**	**0.287 ± 0.052^{b}**	**143.0 ± 13.5^{b}**	**257 ± 7^{a}**	**174 ± 9^{b}**	**161.6 ± 12.3^{b}**	**–1.5 ± 0.1^{b}**

Superscript letters indicate significant difference ($P < 0.05$) between different species and groups based on Tukey's multiple comparison test for each of the features.

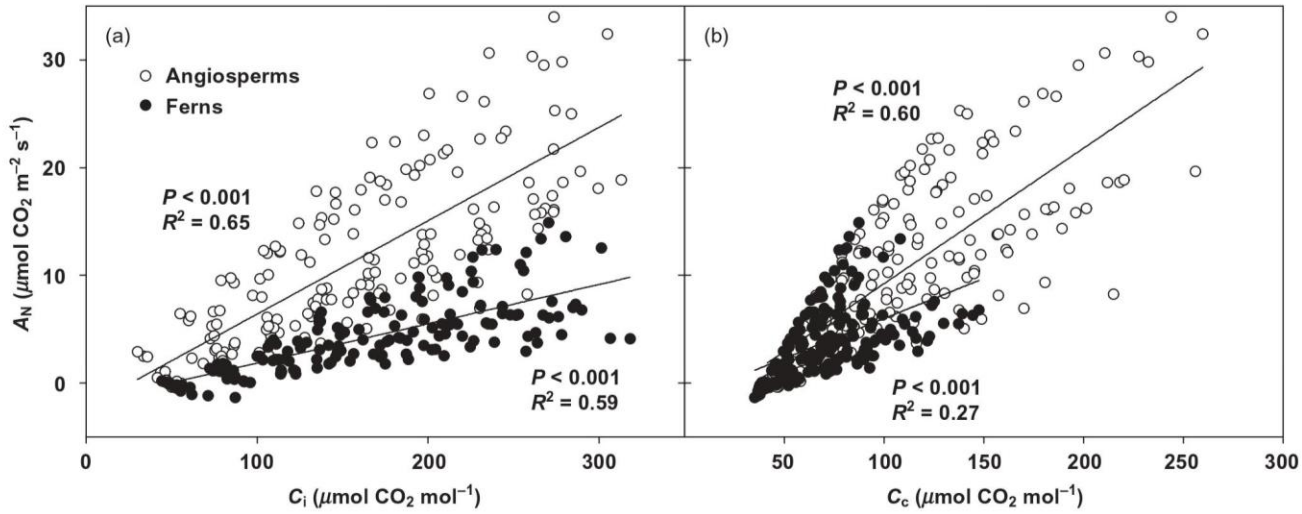

Figure 2. Net CO_2 assimilation response (A_N) (at 25 °C and 1500 μmol photons m^{-2} s^{-1}) to variations in (A) sub-stomatal CO_2 concentration (C_i) and (B) chloroplastic CO_2 concentration (C_c) in all studied species. Values represent the three replicates for each angiosperm specie (white dots) and fern (black dots). *, ** and *** denote significant relationships at $P < 0.05$, $P < 0.01$ and $P < 0.001$, respectively.

and seed plants (mean ± SE: 254 ± 74 and 219 ± 37 μm, respectively), as LMA and leaf thickness did not vary among ferns and angiosperms either (data not shown). Ferns did not differ from angiosperms either in f_{ias}, which averaged 30% among all species, with the exception of *A. scolopendrium*, which showed a significantly higher f_{ias} of 68%. The largest anatomical differences between the two phylogenetically differentiated groups were observed in T_{cw}, S_m/S and S_c/S (Table 3). Thus, ferns presented on average 30% thicker cell walls than angiosperms (0.359 and 0.251 μm, respectively). Furthermore, mean values of S_m/S and S_c/S were 1.4-fold lower in ferns than in angiosperms (12.2 and 7.6 for ferns, and 17.1 and 10.3 for angiosperms, respectively). In contrast, no significant difference was observed for the ratio S_c/S_m (Table 3).

Regarding the intra-group variability for anatomical traits, and contrary to physiological characters, ferns showed higher variability than angiosperms, with the exception of leaf mass per unit leaf area (Fig. 4). Therefore, although differences in average and median values between the two groups for several anatomical traits were consistent with the observed differences in photosynthetic traits, the intra-group variability of the former was larger for ferns, while the variability of the latter was larger in angiosperms (absolute values) or similar (relative to median) in both groups.

Correlation between characters

A Pearson correlation matrix was made for all the analysed parameters combining the 14 species studied in this work (Table 4). The largest correlations were found, in general, between photosynthetic characters. For instance, A_N correlated positively with the CO_2 diffusive parameters g_m, and g_s ($r = 0.80$ and 0.90, respectively). A_N also correlated positively with the two characters that define the photosynthetic capacity – photo and biochemistry –, that is, $V_{c,max}$ ($r = 0.57$) and ETR ($r = 0.90$). These high correlations were strengthened when plotting the data, as some correlations were revealed as non-linear. Positive polynomial trends were observed between A_N and g_m (Fig. 5a) or g_s (Fig. 5b). For ETR (Fig. 5d) and, to a lesser extent, $V_{c,max}$ (Fig. 5c), two different linear relationships were revealed for angiosperms and ferns. The fact that for any given ETR net photosynthesis is lower in ferns could reflect a greater proportion of alternative electron sinks that were present in ferns. If so, because the Harley *et al.* (1992) method for the estimation of g_m assumes that alternative electron sinks other than photorespiration are negligible, Eqn 3 would need to be calibrated to factor out this excess ETR allocated to photochemistry to avoid an underestimation of g_m. However, in some of the species, we checked the relationship between ETR and A_N under low O_2 and did not find differences between ferns and angiosperms (data not shown). In addition, the similar values of g_m obtained by the approaches of Ethier and Livingston and Harley *et al.* – considering that the former method should not be affected by alternative electron sinks – are certainly the best indication for a low influence if any of the potentially greater proportion of alternative electron sinks in ferns (Fig. 1). The anatomical traits were less correlated among each other and with photosynthetic characteristics. Still, significant correlations between net photosynthesis and g_m were found with T_{cw}, S_m/S and S_c/S (Table 4).

Photosynthetic limitations

The quantitative limitation analysis (Fig. 6) revealed that, in angiosperms the biochemical limitation (l_b) was the largest (0.41), followed by mesophyll conductance (l_{mc}, 0.31) and stomatal (l_s, 0.28) limitations. Instead, in ferns, the mesophyll conductance (l_{mc}) was by far the most important (0.57), while

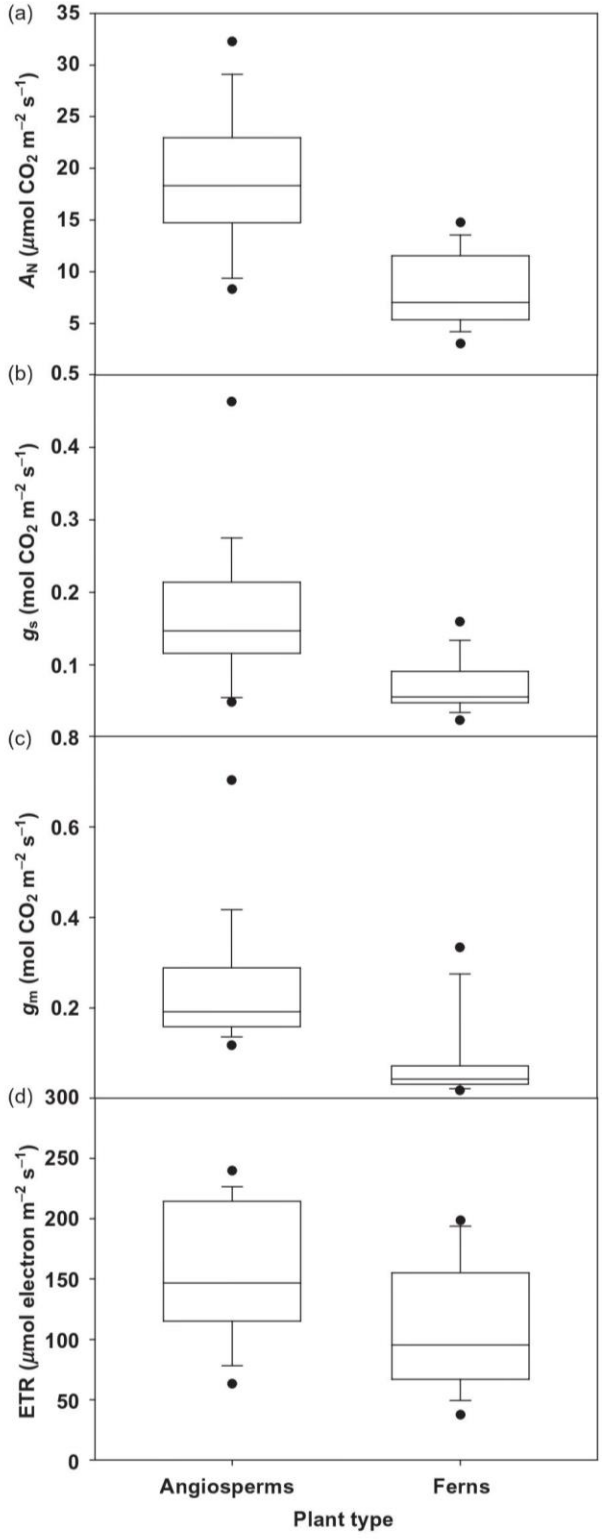

Figure 3. Box plots of (a) net CO_2 assimilation rate (A_N), (b) stomatal conductance (g_s), (c) mesophyll conductance (g_m), and (d) the electron transport rate (ETR) for angiosperm and fern species with $n = 14$ for each group. The two extreme lines of the boxplot (*whiskers*) show the 10 and 90% percentiles, the two bounds of the box the 25 and 75% percentiles, and the center thick line the median. Dots represent data out of the shown percentiles.

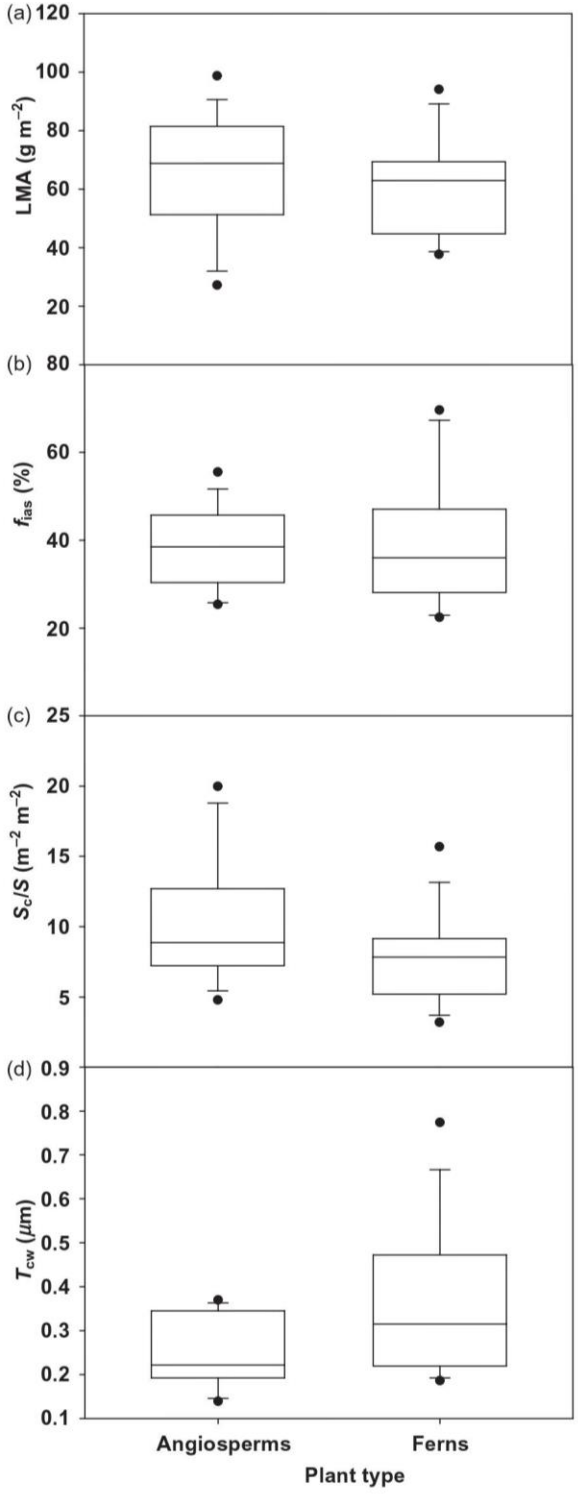

Figure 4. Box plots of (a) leaf mass per unit leaf area (LMA), (b) the mesophyll tissue occupied by the intercellular air spaces (f_{ias}), (c) chloroplast surface area exposed to intercellular air spaces per leaf area (S_c/S), and (d) cell wall thickness (T_{cw}) for angiosperm and fern species with $n = 14$ for each group. The two extreme lines of the boxplot (*whiskers*) show the 10 and 90% percentiles, the two bounds of the box the 25 and 75% percentiles, and the center thick line the median. Dots represent data out of the shown percentiles.

Table 3. Anatomical characteristics for each studied species and averages for ferns and angiosperms. Average values ± SE are shown for the dried leaf mass per unit area (LMA), fraction of the mesophyll tissue occupied by intercellular air spaces (f_{ias}), cell wall thickness (T_{cw}), mesophyll surface area exposed to intercellular air spaces per leaf area (S_m/S), chloroplast surface area exposed to intercellular air spaces per leaf area (S_c/S) and the ratio S_c/S_m

Species	LMA (g m^{-2})	f_{ias} (%)	T_{cw} (μm)	S_m/S (m^2 m^{-2})	S_c/S (m^2 m^{-2})	S_c/S_m
Ferns						
Equisetum telmateia	90.4 ± 2.2^{h}	24.8 ± 1.9^{a}	0.232 ± 0.021^{abcd}	15.5 ± 1.6^{abc}	13.5 ± 1.4^{de}	0.86 ± 0.00^{fg}
Pteridium aquilinum	62.2 ± 1.1^{bcdef}	37.7 ± 2.4^{abcd}	0.194 ± 0.006^{ab}	9.7 ± 0.1^{ab}	8.8 ± 0.2^{abcd}	0.90 ± 0.01^{g}
Adiantum capillus-veneris	47.1 ± 5.3^{abc}	39.3 ± 6.2^{abcd}	0.238 ± 0.010^{abcd}	8.3 ± 1.0^{a}	4.6 ± 0.3^{a}	0.56 ± 0.03^{bcd}
Pteris vittata	67.9 ± 2.0^{cdefg}	33.0 ± 1.2^{abc}	0.313 ± 0.013^{bcdef}	15.0 ± 0.7^{abc}	9.3 ± 0.4^{abcd}	0.62 ± 0.01^{cde}
Asplenium trichomanes	70.2 ± 6.2^{defgh}	28.8 ± 3.9^{ab}	0.421 ± 0.045^{ef}	11.0 ± 1.2^{ab}	7.3 ± 0.7^{abc}	0.67 ± 0.01^{de}
Asplenium scolopendrium	44.6 ± 4.3^{ab}	67.5 ± 1.4^{e}	0.687 ± 0.055^{g}	13.9 ± 1.1^{abc}	4.2 ± 0.8^{a}	0.30 ± 0.03^{a}
Dryopteris tyrrhena	43.5 ± 1.3^{ab}	51.8 ± 6.5^{de}	0.428 ± 0.060^{f}	12.3 ± 0.7^{abc}	5.9 ± 0.3^{ab}	0.48 ± 0.03^{bc}
Average	**60.8 ± 3.7^{a}**	**40.4 ± 3.3^{a}**	**0.359 ± 0.037^{a}**	**12.2 ± 0.6^{a}**	**7.6 ± 0.7^{a}**	**0.63 ± 0.04^{a}**
Angiosperms						
Alisma plantago-aquatica	53.6 ± 2.7^{abcd}	44.1 ± 4.6^{bcd}	0.279 ± 0.027^{abcde}	15.3 ± 1.4^{abc}	7.4 ± 0.4^{abc}	0.49 ± 0.02^{bc}
Digitalis minor var. *palaui*	88.2 ± 7.2^{gh}	27.6 ± 1.8^{ab}	0.199 ± 0.013^{ab}	16.6 ± 3.2^{bc}	12.7 ± 2.4^{cde}	0.77 ± 0.03^{efg}
Lysimachia minoricensis	31.4 ± 2.7^{a}	44.4 ± 1.1^{bcd}	0.213 ± 0.009^{abc}	17.4 ± 2.0^{bc}	8.9 ± 1.0^{abcd}	0.51 ± 0.01^{bc}
Pastinaca lucida	78.6 ± 2.9^{efgh}	27.8 ± 1.5^{ab}	0.207 ± 0.012^{abc}	26.2 ± 2.5^{d}	17.6 ± 2.0^{e}	0.67 ± 0.02^{de}
Vinca difformis	58.2 ± 5.6^{bcde}	33.5 ± 2.6^{abc}	0.364 ± 0.003^{def}	12.5 ± 0.2^{abc}	5.5 ± 0.5^{ab}	0.43 ± 0.04^{ab}
Phlomis italica	67.5 ± 6.7^{cdefg}	49.6 ± 3.1^{cd}	0.149 ± 0.008^{a}	12.3 ± 0.6^{abc}	9.0 ± 0.2^{abcd}	0.73 ± 0.05^{ef}
Viola jaubertiana	83.8 ± 3.9^{fgh}	41.7 ± 3.4^{abcd}	0.348 ± 0.013^{cdef}	19.5 ± 1.7^{cd}	10.8 ± 1.7^{bcd}	0.55 ± 0.05^{bcd}
Average	**65.9 ± 4.4^{a}**	**38.4 ± 2.0^{a}**	**0.251 ± 0.017^{b}**	**17.1 ± 1.2^{b}**	**10.3 ± 0.9^{b}**	**0.59 ± 0.03^{a}**

Superscript different letters indicate significant difference ($P < 0.05$) between different species and groups based on Tukey's multiple comparison test for each of the features.

stomatal (0.24) and biochemical (0.19) limitations were much less important.

DISCUSSION

While many previous studies have reported photosynthetic rates in ferns (e.g. Wright *et al.* 2004, 2005; Karst & Lechowicz 2007; Volkova *et al.* 2009, 2011; Gago *et al.* 2013), to the best of our knowledge this is the first study that specifically compares an equal number of angiosperms and ferns, paired by habitat preferences, and growing under optimal conditions in a common garden. The obtained values of net CO_2 assimilation (A_N) were within the range of values previously documented for each group (e.g. Wright *et al.* 2004). Average A_N was approximately double in angiosperms than ferns (Table 2). As the differences in leaf respiration were not so large, it turns out that ferns do have a much lower carbon balance at the leaf level. It is therefore confirmed that, even when analysed under conditions favouring maximum photosynthesis rates, the photosynthetic capacity of ferns is generally much lower than that of most angiosperms.

Table 4. Pearson correlation matrix of the anatomical and physiological parameters measured for the 14 species. Values in italics and bold indicate significant ($P < 0.05$) and highly significant ($P < 0.01$) correlation coefficients, respectively. Parameter abbreviations as in Tables 2 and 3

	A_N	g_s	A_N/g_s	g_m	C_i	C_c	$V_{c,max}$	ETR	R_d	LMA	f_{ias}	S_m/S	S_c/S	S_c/S_m	T_{cw}
A_N		***0.903***	–0.26	***0.80***	–0.06	***0.66***	***0.57***	***0.90***	***–0.73***	*0.38*	–0.28	***0.64***	***0.73***	*0.36*	***–0.63***
g_s			***–0.52***	***0.78***	0.19	***0.67***	***0.46***	***0.80***	***–0.75***	0.27	–0.19	***0.66***	***0.71***	0.30	***–0.53***
A_N/g_s				–0.18	***–0.78***	–0.24	–0.05	–0.20	0.30	0.11	–0.15	–0.17	–0.19	–0.06	0.18
g_m					0.04	***0.77***	0.21	***0.59***	***–0.78***	0.23	–0.26	***0.64***	***0.56***	0.08	*–0.36*
C_i						0.09	–0.17	–0.10	–0.16	–0.17	0.12	0.13	0.11	–0.02	0.07
C_c							–0.18	0.28	***–0.77***	–0.05	0.09	***0.68***	***0.41***	–0.21	–0.23
$V_{c,max}$								***0.86***	–0.11	***0.55***	***–0.54***	0.14	***0.56***	***0.73***	***–0.59***
ETR									***–0.50***	***0.54***	***–0.46***	***0.46***	***0.74***	***0.62***	***–0.69***
R_d										–0.09	0.12	***–0.60***	***–0.52***	–0.08	0.25
LMA											***–0.56***	*0.33*	***0.62***	***0.57***	*–0.31*
f_{ias}												–0.15	***–0.47***	***–0.55***	***0.47***
S_m/S													***0.81***	–0.01	–0.12
S_c/S														***0.57***	***–0.48***
S_c/S_m															***–0.66***
T_{cw}															

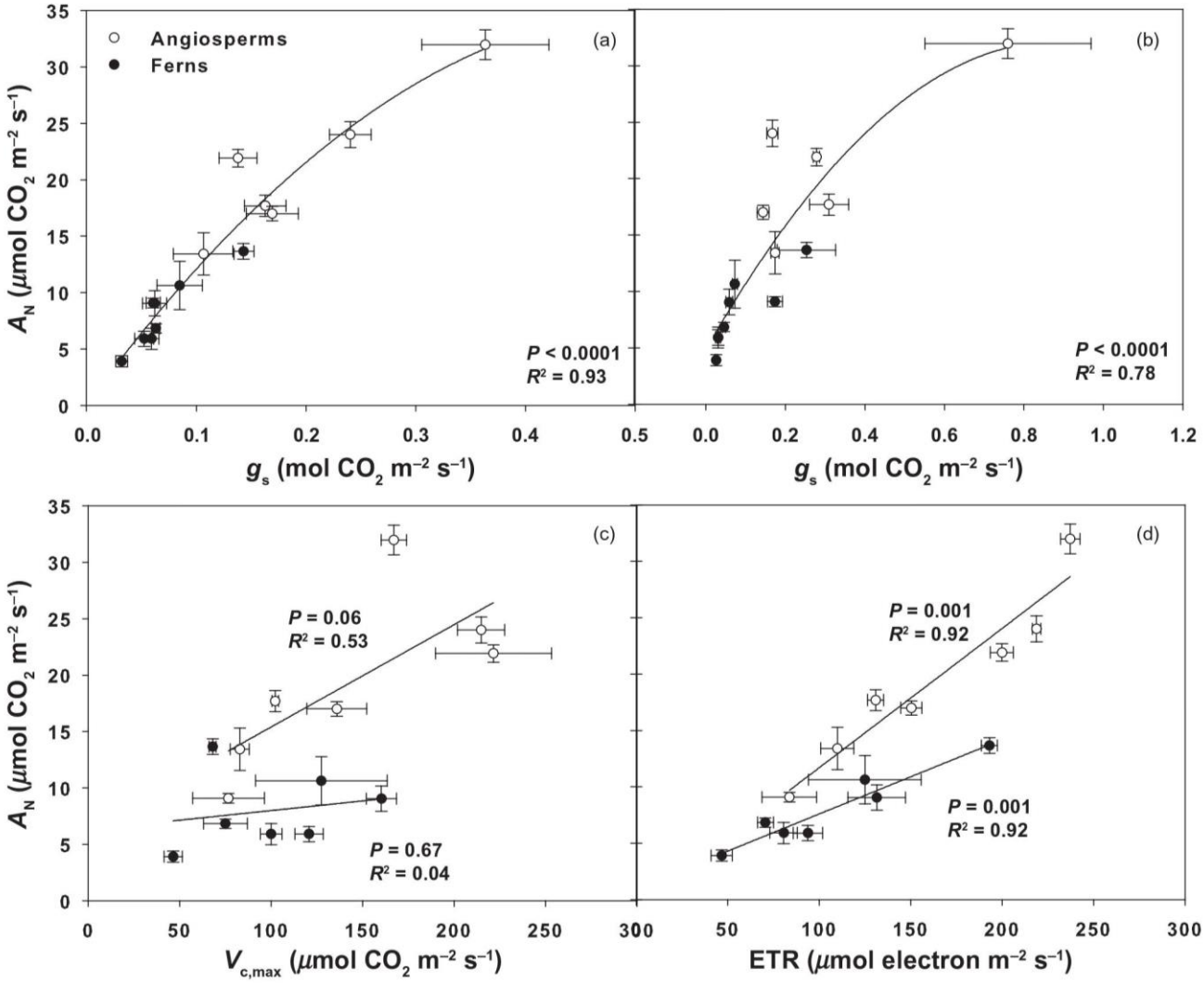

Figure 5. Correlation between net CO_2 assimilation (A_N) and (a) stomatal conductance (g_s), (b) mesophyll conductance (g_m), (c) maximum velocity of carboxylation ($V_{c,max}$) and (d) electron transport rate (ETR). Values are means ± SE of three replicates per species in angiosperms (white dots) and ferns (black dots).

A second central aim of this work was to determine the physiological causes for the lower photosynthetic capacity exhibited by ferns, which could be diffusive limitations – either at the level of stomata regulated by stomatal conductance (g_s), or the mesophyll regulated by stomatal conductance (g_m) – or biochemical limitations – due to the functioning of Rubisco, which regulates the velocity of carboxylation ($V_{c,max}$) and/or the functioning of the photochemical and the Calvin cycle, which regulates the maximum electron transport capacity (ETR). All these parameters (g_s, g_m, $V_{c,max}$ and ETR) were lower in ferns than angiosperms, although to different extents. For instance, the average value of 0.071 mol CO_2 m^{-2} s^{-1} for g_s was much lower than that found in angiosperms, although it was slightly higher than that measured in other fern species in previous studies (Gago *et al.* 2013). Regarding the mesophyll conductance, until the present study, values had been only documented for four fern species: *Dicksonia antarctica* showing a value of 0.15 mol CO_2 m^{-2} s^{-1} (Volkova *et al.*

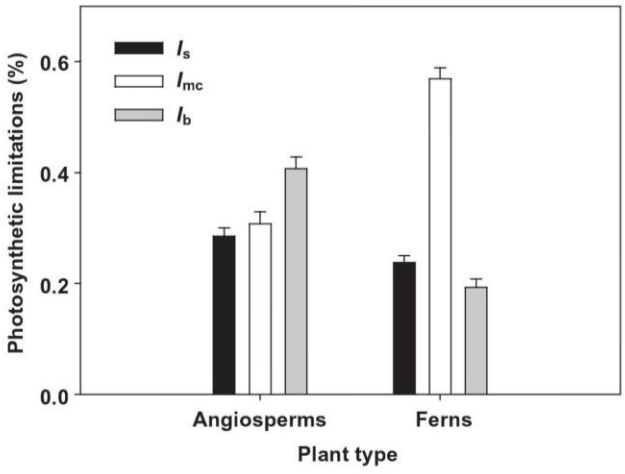

Figure 6. Relative stomatal (l_s), mesophyll conductance (l_{mc}) and biochemical (l_b) photosynthesis limitations in angiosperms and ferns.

2009), and *Osmunda regalis*, *Blechnum gibbum* and *Nephrolepis exaltata* showing values of 0.073, 0.05 and 0.03 mol CO_2 m^{-2} s^{-1}, respectively (Gago *et al.* 2013). Combining these values with those obtained for the seven ferns in this study yields an average of 0.075 mol CO_2 m^{-2} s^{-1}, which is almost identical to the average obtained when only the new seven species measured are considered, and much lower (74%) than the average for angiosperm. This value is below the approximate 0.1 mol CO_2 m^{-2} s^{1} averaged for conifers, and higher than the few values available for liverworts and hornworts (Flexas & Keeley 2012; Flexas *et al.* 2012), which somehow positions the ferns in a phylogenetic coherence between these two groups, supporting the hypothesis that an evolutionary trend exists towards a higher g_m along the process of diversification of embryophytes. Finally, concerning the biochemical parameters, although they were also lower in ferns than in angiosperms, the difference was lower to that observed for the diffusive parameters. Summarizing, g_m was the trait showing the largest difference between ferns and angiosperms, followed by g_s, with much lower reductions displayed by the bio/photochemical characters. In addition, for a given value of $V_{c,max}$ or ETR, A_N was larger in angiosperms than in ferns (Fig. 5). All together, these results suggest that, although the biochemical capacity of the ferns may contribute to their lower photosynthetic capacity, diffusional limitations exert a greater control, which was already suggested by Gago *et al.* (2013). Among the two conductances, g_s was lower in ferns in a similar proportion to A_N, so that the ratio between A_N and g_s (i.e. the intrinsic water use efficiency) was identical in ferns and in angiosperms, also suggesting that the photosynthetic limitation imposed by stomatal closure may be similar in both groups. In contrast, the limitation imposed by g_m could be much larger in ferns, which was confirmed applying the photosynthesis limitation analysis following Grassi & Magnani (2005). This showed that, contrary to angiosperms, in which the three limitations are of similar magnitude, although biochemistry plays the major role in establishing their maximum photosynthesis, in ferns the low mesophyll conductance exhibited by ferns – which positions them between liverworts/mosses and conifers, in accordance to their relative phylogenetic position – was the largely the main cause for their limited photosynthetic capacity as compared with angiosperms. These results suggest that the evolution of g_m may have been crucial to support the evolution towards larger photosynthetic rates along the terrestrial plant phylogeny (Flexas & Keeley 2012; Flexas *et al.* 2012).

The central role of g_m in setting a much limited photosynthetic capacity of ferns as compared with angiosperms leads to the question of which are the intrinsic causes for these marked differences. In seed plants, evidence has accumulated in the recent years that leaf anatomical parameters determining the length and nature of the CO_2 pathway exert a major control over the maximum g_m that a given species can display (Terashima *et al.* 2011; Peguero-Pina *et al.* 2012; Tosens *et al.* 2012a,b; Tomás *et al.* 2013). To preliminarily address this issue, we chose measuring those anatomical traits that had been revealed as the most important for g_m in seed plants, that is, LMA and, especially, f_{ias}, S_c/S and T_{cw} (Tomás *et al.* 2013). The obtained values of LMA were well within the range documented for both ferns (Brach *et al.* 1993; Durand & Goldstein 2001; Gago *et al.* 2013) and angiosperms (Wright *et al.* 2004), and did not differ significantly between the two groups. Similarly, f_{ias} did not differ between ferns and angiosperms either for which, contrary to what was previously suggested (Evans *et al.* 2009), this parameter may not exert a significant effect in setting the differences in g_m between species or the two phylogenetic groups. Instead, important and significant differences between the two groups were observed for S_c/S and T_{cw}, the former being lower and the latter higher in ferns than angiosperms. A significant positive correlation was obtained between S_c/S and both A_N and g_m, corroborating the results of several comparative studies performed only within angiosperms (Terashima *et al.* 2006; Tosens *et al.* 2012a,b; Tomás *et al.* 2013), and suggesting that this character may contribute strongly to the observed differences. Nevertheless, a closer inspection of the data reveals that establishing this correlation separately for the two groups instead of pooling all data together improves the correlation (data not shown), that is, ferns and angiosperms show similar correlations but with different slopes, suggesting that there must be at least some additional factor contributing to explaining the differences in g_m among groups.

A likely additional candidate is T_{cw}, which also showed significant differences among groups. Comparing the results obtained here for T_{cw}, with those for angiosperms from this and other studies (Peguero-Pina *et al.* 2012; Tosens *et al.* 2012a,b; Tomás *et al.* 2013), as well as with few values published for mosses (Waite & Sack 2010), a phylogenetic trend emerges consisting of a reduction of the cell wall thickness from bryophytes (values ranging between 1 and 5 μm) to angiosperms (0.1 and 0.5 μm), with ferns occupying an intermediate position (0.2 and 0.8 μm), in agreement with their intermediate position in terms of g_m. These results suggest that the cell wall thickness, which was essential for the plant colonization of the terrestrial environment – as it allows them to maintain the tissue turgor and to preserve the structure of the cells under desiccation conditions (Proctor & Tuba 2002) – has undergone an evolutionary trend towards reduced thickness, probably being crucial to allow plants to achieve larger photosynthetic rates. In fact, not only the thickness but also the chemical composition of the walls has been shown to be different between ferns and angiosperms (Popper & Fry 2004). Cell wall properties may not affect g_m and photosynthesis only, but they have been related with desiccation tolerance as well (Proctor & Tuba 2002). We hypothesize that the multiple variations in cell wall properties among distant phylogenetic groups – from thickness to composition, likely having implications in pore complexity, flexibility, etc. – may operate towards optimizing photosynthesis on one hand and favouring desiccation tolerance on the other, hence establishing a trade-off between these two plant characteristics. In this sense, ferns may represent a transition group between bryophytes – desiccation-tolerant plants but with low photosynthetic capacity due to their thick cell wall – and angiosperms – desiccation intolerant plants but with high photosynthetic capacity due to their thinner cell wall. As

desiccation tolerance becomes less frequent in the most modern plant lineages, stomata regulating mechanisms to avoid desiccation develop larger complexities (Brodribb & McAdam 2011; McAdam & Brodribb 2012). While this explanation may be attractive, the correlation between cell wall thickness and g_m and A_N was less significant than that obtained with S_c/S. Hence, although the implication of cell wall thickness is likely, there may be additional factors involved in constraining g_m in ferns. As already indicated, S_c/S is also playing a central role. Differences in S_c/S do not seem to be due to increasing S_c/S_m (which was similar in both plant groups), but instead through an increase in mesophyll surface, despite the fact that the intercellular air space fraction (f_{ias}) was similar in both groups. Clearly, a more detailed anatomical analysis is deserved to fully understand the reasons for a larger mesophyll limitation to photosynthesis in ferns than angiosperms.

CONCLUSIONS

We performed a specific comparative study of photosynthesis in ferns and angiosperms under optimal conditions in a common garden. The comparison confirms that ferns have on average about half the photosynthetic capacity of angiosperms. This is mostly due to CO_2 diffusion limitations, with mesophyll conductance playing the most relevant role. Structural differences between angiosperm leaves and fern fronds explain partially the lower mesophyll conductance attained by the latter. In particular, the chloroplast surface exposed to the intercellular air spaces and cell wall thickness appear to exert an important role, but additional factors may also be involved. Additional studies are required including a larger number of species and a more complete set of anatomical characters to improve our understanding of the factors involved in the low g_m observed in ferns.

ACKNOWLEDGMENTS

This work was supported by the Spanish Ministry of Education and Science, project BFU2011-23294, awarded to J.F. and by the Chilean Ministry of Education, postdoctoral fellowship 2 2010 Nº 74100061, awarded to H.M.C. The authors are grateful to the *Jardí Botànic de Sóller* and, especially, to Magdalena Vicens for allowing them to run the experiment in his living plant collection, and to Ma Teresa Mínguez, Universitat de València (Secció Microscòpia Electrònica, SCSIE), and Dr Ferran Hierro, Universitat de les Illes Balears (Serveis Cientificotècnics), for technical support during microscopic analyses. We also thank Benjamón for help in field measurements.

REFERENCES

Bird I.F., Cornelius M.J. & Keys A.J. (1982) Affinity of RuBP carboxylases for carbon dioxide inhibition of the enzymes by oxygen. *Journal of Experimental Botany* **33,** 1004–1013.

Bolòs O., Vigo J., Massalles R. & Ninot J.M. (2005) *Flora Manual dels Països Catalans*, 3rd edn, Pòrtic Editorial, Barcelona.

Brach A.R., McNaughton S.J. & Raynal D.J. (1993) Photosynthetic adaptability of two fern species of a Northern Hardwood Forest. *American Fern Journal* **83,** 47–53.

Brodribb T.J. & McAdam S.A.M. (2011) Passive origins of stomatal control in vascular plants. *Science* **331,** 582–585.

Brodribb T.J., McAdam S.A.M., Jordan G.J. & Feild T.S. (2009) Evolution of stomatal responsiveness to CO_2 and optimization of water-use efficiency among land plants. *The New Phytologist* **183,** 839–847.

Delgado E., Medrano H., Keys A.J. & Parry M.A.J. (1995) Species variation in Rubisco Specificity Factor. *Journal of Experimental Botany* **46,** 1775–1777.

Doi M. & Shimazaki K. (2008) The stomata of the fern *Adiantum capillus-veneris* do not respond to CO_2 in the dark and open by photosynthesis in guard cells. *Plant Physiology* **47,** 748–755.

Durand Z.E. & Goldstein G. (2001) Photosynthesis, photoinhibition, and nitrogen use efficiency in native and invasive tree ferns in Hawaii. *Oecologia* **126,** 345–354.

Ethier G.H. & Livingston N.J. (2004) On the need to incorporate sensitivity to CO_2 transfer conductance into the Farquhar-von Caemmerer-Berry leaf photosynthesis model. *Plant, Cell & Environment* **27,** 137–153.

Evans J.R., Kaldenhoff R., Genty B. & Terashima I. (2009) Resistances along the CO_2 diffusion pathway inside leaves. *Journal of Experimental Botany* **60,** 2235–2248.

Farquhar G.D., von Caemmerer S. & Berry J.A. (1980) A biochemical model of photosynthetic CO_2 assimilation in leaves of C_3 species. *Planta* **149,** 78–90.

Flexas J. & Keeley J.E. (2012) Evolution of photosynthesis I. Basic leaf morphological traits and diffusion and photosynthetic structures. In *Terrestrial Photosynthesis in a Changing Environment: A Molecular, Physiological, and Ecological Approach* (eds J. Flexas, F. Loreto & H. Medrano), pp. 373–385. Cambridge University Press, Cambridge, UK.

Flexas J., Díaz-Espejo A., Berry J.A., Galmés J., Cifre J., Kaldenhoff R., ... Ribas-Carbó M. (2007) Leakage in leaf chambers in open gas exchange systems: quantification and its effects in photosynthesis parameterization. *Journal of Experimental Botany* **58,** 1533–1543.

Flexas J., Barbour M., Brendel O., Cabrera H.M., Carriquí M., Díaz-Espejo A., ... Warren R.C. (2012) Mesophyll diffusion conductance to CO_2: an unappreciated central player in photosynthesis. *Plant Science* **193–194,** 70–84.

Franks P.J. & Farquhar G.D. (2007) The mechanical diversity of stomata and its significance in gas-exchange control. *Plant Physiology* **143,** 78–87.

Gago J., Coopman R.E., Cabrera H.M., Hermida C., Molins A., Conesa M.A., ... Flexas J. (2013) Photosynthesis limitations in three fern species. *Physiologia Plantarum* **149,** 599–611.

Gallé A., Flórez-Sarasa I., El Aououad H. & Flexas J. (2011) The Mediterranean evergreen *Quercus ilex* and the semi-deciduous *Cistus albidus* differ in their leaf gas exchange regulation and acclimation to repeated drought and re-watering cycles. *Journal of Experimental Botany* **62,** 5207–5216.

Galmés J., Flexas J., Keys A.J., Cifre J., Mitchell R.A.C., Madgwick P.J., ... Parry M.A.J. (2005) Rubisco specificity factor tends to be larger in plant species from drier habitats and in species with persistent leaves. *Plant, Cell & Environment* **28,** 571–579.

Grassi G. & Magnani F. (2005) Stomatal, mesophyll conductance and biochemical limitations to photosynthesis as affected by drought and leaf ontogeny in ash and oak trees. *Plant, Cell & Environment* **28,** 834–849.

Harley P.C., Loreto F., Di Marco G. & Sharkey T.D. (1992) Theoretical considerations when estimating the mesophyll conductance to CO_2 flux by the analysis of the response of photosynthesis to CO_2. *Plant Physiology* **98,** 1429–1436.

Hassiotou F., Ludwig M., Renton M., Veneklaas E.J. & Evans J.R. (2009) Influence of leaf dry mass per area, CO_2, and irradiance on mesophyll conductance in sclerophylls. *Journal of Experimental Botany* **60,** 2303–2314.

Haworth M., Kingston C. & McElwain J.C. (2011) Stomatal control as a driver of plant evolution. *Journal of Experimental Botany* **62,** 2419–2423.

Haworth M., Elliot-Kingston C. & McElwain J.C. (2013) Co-ordination of physiological and morphological responses of stomata to elevated [CO_2] in vascular plants. *Oecologia* **171,** 71–82.

HVMO (2007). *Herbari Virtual del Mediterrani Occidental*. Recovered on 21th May 2013 from http://herbarivirtual.uib.es.

Jordan D.B. & Ogren W.L. (1983) Species variation in kinetic properties of ribulose 1,5-bisphosphate carboxylase oxygenase. *Archives of Biochemistry and Biophysics* **227,** 425–433.

Karst A.L. & Lechowicz M.J. (2007) Are correlations among foliar traits in ferns consistent with those in seed plants? *The New Phytologist* **173,** 306–312.

Kenrick P. & Crane P.R. (1997) The origin and early evolution of plants on land. *Nature* **389,** 33–39.

McAdam S.A.M. & Brodribb T.J. (2012) Fern and lycophyte guard cells do not respond to endogenous abscisic acid. *The Plant Cell* **24,** 1510–1521.

Niinemets U., Cescatti A., Rodeghiero M. & Tosens T. (2005) Leaf internal diffusion conductance limits photosynthesis more strongly in older leaves of Mediterranean evergreen broad-leaved species. *Plant, Cell & Environment* **28,** 1552–1566.

Niinemets Ü. (1999) Components of leaf dry mass per area – thickness and density – alter leaf photosynthetic capacity in reverse directions in woody plants. *The New Phytologist* **144,** 35–47.

Peguero-Pina J.J., Flexas J., Galmés J., Niinemets Ü., Sancho-Knapik D., Barredo G. & Gil-Pelegrín E. (2012) Leaf anatomical properties in relation to differences in mesophyll conductance to CO_2 and photosynthesis in two related Mediterranean *Abies* species. *Plant, Cell & Environment* **35,** 2121–2129.

Popper Z.A. & Fry S.C. (2004) Primary cell wall composition of pteridophytes and spermatophytes. *The New Phytologist* **164,** 165–174.

Proctor M.C.F. & Tuba Z. (2002) Poikilohydry and homoihydry: antithesis or spectrum of possibilities? *The New Phytologist* **156,** 327–349.

Ruszala E.M., Beerling D.J., Franks P.J., Chater C., Casson S.A., Gray J.E. & Hetherington A.M. (2011) Land plants acquired active stomatal control early in their evolutionary history. *Current Biology* **21,** 1030–1035.

Scafaro A.P., von Caemmerer S., Evans J.R. & Atwell B.J. (2011) Temperature response of mesophyll conductance in cultivated and wild *Oryza* species with contrasting mesophyll cell wall thickness. *Plant, Cell & Environment* **34,** 1999–2008.

Schuettpelz E. & Pryer K.M. (2009) Evidence for a Cenozoic radiation of ferns in an angiosperm-dominated canopy. *Proceedings of the National Academy of Sciences* **106,** 11200–11205.

Schultz H.R. (1996) Leaf absorptance of visible radiation in *Vitis vinifera* L.: estimates of age and shade effects with a simple field method. *Scientia Horticulturae* **66,** 93–102.

Smith A.R., Pryer K.M., Schuettpelz E., Jorall P., Schneider H. & Wolf P.G. (2006) A classification for extant ferns. *Taxon* **55,** 705–731.

Terashima I., Hanba Y.T., Tazoe Y., Vyas P. & Yano S. (2006) Irradiance and phenotype: comparative eco-development of sun and shade leaves in relation to photosynthetic CO_2 diffusion. *Journal of Experimental Botany* **57,** 343–354.

Terashima I., Hanba Y.T., Tholen D. & Niinemets Ü. (2011) Leaf functional anatomy in relation to photosynthesis. *Plant Physiology* **155,** 108–116.

Thain J.F. (1983) Curvature correlation factors in the measurements of cell surface areas in plant tissues. *Journal of Experimental Botany* **34,** 87–94.

Tomás M., Flexas J., Copolovici L., Galmés J., Hallik L., Medrano H., ... Niinemets Ü. (2013) Importance of leaf anatomy in determining mesophyll diffusion conductance to CO_2 across species: quantitative limitations and scaling up by models. *Journal of Experimental Botany* **64,** 2269–2281.

Tosens T., Niinemets Ü., Vislap V., Eichelmann H. & Castro-Díez P. (2012a) Developmental changes in mesophyll diffusion conductance and photosynthetic capacity under different light and water availabilities in *Populus tremula*: how structure constrains function. *Plant, Cell & Environment* **35,** 839–856.

Tosens T., Niinemets U., Westoby M. & Wright I.J. (2012b) Anatomical basis of variation in mesophyll resistance in eastern Australian sclerophylls: news of a long and winding path. *Journal of Experimental Botany* **63,** 5105–5119.

Varone L., Ribas-Carbo M., Cardona C., Gallé A., Medrano H., Gratani L. & Flexas J. (2012) Stomatal and non-stomatal limitations to photosynthesis in seedlings and saplings of Mediterranean species pre-conditioned and aged in nurseries: different response to water stress. *Environmental and Experimental Botany* **75,** 235–247.

Volkova L., Bennett L.T. & Tausz M. (2009) Effects of sudden exposure to high light levels on two tree fern species *Dicksonia antarctica* (Dicksoniaceae) and *Cyathea australis* (Cyatheaceae) acclimated to different light intensities. *Australian Journal of Botany* **57,** 562–571.

Volkova L., Bennett L.T. & Tausz M. (2011) Diurnal and seasonal variations in photosynthetic and morphological traits of the tree ferns *Dicksonia antarctica* (Dicksoniaceae) and *Cyathea australis* (Cyatheaceae) in wet sclerophyll forests of Australia. *Environmental and Experimental Botany* **70,** 11–19.

Waite M. & Sack L. (2010) How does moss photosynthesis relate to leaf and canopy structure? Trait relationships for 10 Hawaiian species contrasting light habitats. *The New Phytologist* **185,** 156–172.

Wright I.J., Reich P.B., Westoby M., Ackerly D.D., Baruch Z., Bongers F., ... Villar R. (2004) The world-wide leaf economics spectrum. *Nature* **428,** 821–827.

Wright I.J., Reich P.B., Cornelissen J.H.C., Falster D.S., Garnier E., Hikosaka K. & Westoby M. (2005) Assessing the generality of global leaf trait relationships. *The New Phytologist* **166,** 485–496.

Yeoh H.-H., Badger M.R. & Watson L. (1981) Variations in kinetic properties of ribulose-1,5-bisphosphate carboxylases among plants. *Plant Physiology* **67,** 1151–1155.

Received 13 May 2014; received in revised form 25 June 2014; accepted for publication 27 June 2014

SUPPORTING INFORMATION

Additional Supporting Information may be found in the online version of this article at the publisher's web-site:

Figure S1. Pictures of the different species studied in this work. In the left box are ferns: (A) *Pteris vittata*; (B) *Pteridium aquilinum*; (C) *Adiantum capillus-veneris*; (D) *Asplenium scolopendrium*; (E) *Dryopteris tyrrhena*; (F) *Equisetum telmateia*; (G) *Asplenium trichomanes*; and in the right box there are angiosperms: (H) *Phlomis italica*; (I) *Viola jaubertiana*; (J) *Pastinaca lucida*; (K) *Digitalis minor* var. *palaui*; (L) *Vinca difformis*; (M) *Lysimachia minoricensis*; (N) *Alisma plantago-aquatica*.

Figure S2. Selection of photographs of semi-fine cross sections at 200× magnification (A) and ultrafine cross sections at 2000× (B) and at 30 000× magnification (C) of leaves of some of the studied species. It can be observed that there is a leaf cross section in the first row, different size and shape cells in the second row, and the large variation of cell wall thickness in the third row.

SUPPORTING INFORMATION

Supporting Figure 1. Pictures of the different species studied in this work. In the left box are ferns: **A**, *Pteris vittata*; **B**, *Pteridium aquilinum*; **C**, *Adiantum capillus-veneris*; **D**, *Asplenium scolopendrium*; **E**, *Dryopteris tyrrhena*; **F**, *Equisetum telmateia*; **G**, *Asplenium trichomanes*; and in the right box there are angiosperms: **H**, *Phlomis italica*; **I**, *Viola jaubertiana*; **J**, *Pastinaca lucida*; **K**, *Digitalis minor* var. *palauii*; **L**, *Vinca difformis*; **M**, *Lysimachia minoricensis*; **N**, *Alisma plantago-aquatica*.

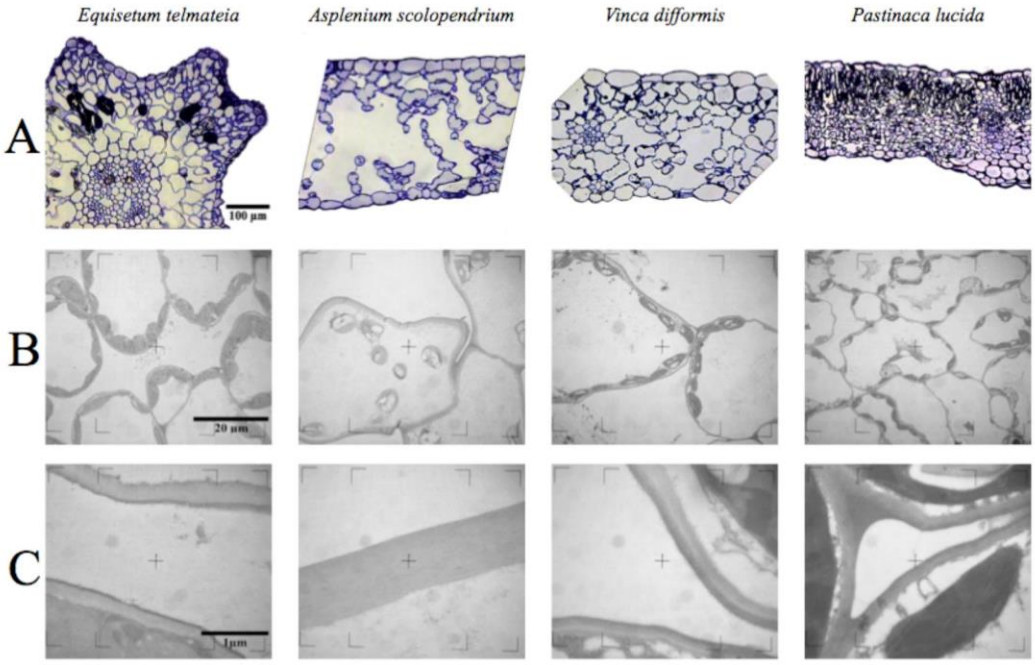

Supporting Figure 2. Selection of photographs of semi-fines cross sections at 200x magnification (**A**) and ultrafine cross sections at 2000x (**B**) and at 30000x magnification (**C**) of leaves of some of the studied species. It can be observed a leaf cross-section in the first row, different size and shape cells in the second row and the large variation of cell wall thickness in the third row.

Anatomical constraints to nonstomatal diffusion conductance and photosynthesis in lycophytes and bryophytes

Research

New Phytologist

Anatomical constraints to nonstomatal diffusion conductance and photosynthesis in lycophytes and bryophytes

Marc Carriquí[1], Margalida Roig-Oliver[1], Timothy J. Brodribb[2], Rafael Coopman[3], Warwick Gill[4], Kristiina Mark[5], Ülo Niinemets[5,6], Alicia V. Perera-Castro[1], Miquel Ribas-Carbó[1], Lawren Sack[7], Tiina Tosens[5], Mashuri Waite[8] and Jaume Flexas[1]

[1]Research Group on Plant Biology under Mediterranean Conditions, Universitat de les Illes Balears (UIB) – Instituto de Investigaciones Agroambientales y de Economía del Agua (INAGEA), Carretera de Valldemossa Km 7.5, 07122 Palma, Illes Balears, Spain; [2]School of Biological Sciences, University of Tasmania, Hobart, TAS 7001, Australia; [3]Ecophysiology Laboratory for Forest Conservation, Instituto de Conservación, Biodiversidad y Territorio, Facultad de Ciencias Forestales y Recursos Naturales, Universidad Austral de Chile, Campus Isla Teja, Casilla 567, Valdivia, Chile; [4]Tasmanian Institute of Agriculture, University of Tasmania, Hobart, TAS 7001, Australia; [5]Institute of Agricultural and Environmental Sciences, Estonian University of Life Sciences, Kreutzwaldi 1, Tartu 51006, Estonia; [6]Estonian Academy of Sciences, Kohte 6, 10130 Tallinn, Estonia; [7]Department of Ecology and Evolutionary Biology, University of California Los Angeles, 621 Charles E. Young Drive South, Los Angeles, CA 90095, USA; [8]Center for Regional System Analysis, Planning, and Development, Bogor Agricultural University, Bogor 16153, Indonesia

Author for correspondence:
Marc Carriquí
Tel: +34 971 25 95 56
Email: m.carriqui@uib.cat

Received: *31 July 2018*
Accepted: *22 December 2018*

New Phytologist (2019) **222:** 1256–1270
doi: 10.1111/nph.15675

Key words: bryophytes, cell wall, chloroplast, CO_2 diffusion, lycophytes, nonstomatal diffusion conductance.

Summary

- Photosynthesis in bryophytes and lycophytes has received less attention than terrestrial plant groups. In particular, few studies have addressed the nonstomatal diffusion conductance to CO_2 g_{nsd} of these plant groups.
- Their lower photosynthetic rate per leaf mass area at any given nitrogen concentration compared with vascular plants suggested a stronger limitation by CO_2 diffusion. We hypothesized that bryophyte and lycophyte photosynthesis is largely limited by low g_{nsd}. Here, we studied CO_2 diffusion inside the photosynthetic tissues and its relationships with photosynthesis and anatomical parameters in bryophyte and lycophyte species in Antarctica, Australia, Estonia, Hawaii and Spain.
- On average, lycophytes and, specially, bryophytes had the lowest photosynthetic rates and nonstomatal diffusion conductance reported for terrestrial plants. These low values are related to their very thick cell walls and their low exposure of chloroplasts to cell perimeter.
- We conclude that the reason why bryophytes lie at the lower end of the leaf economics spectrum is their strong nonstomatal diffusion conductance limitation to photosynthesis, which is driven by their specific anatomical characteristics.

Introduction

Bryophytes (the broad plant group that integrates Anthocerotophyta, Marchantiophyta and Bryophyta *sensu stricto*, i.e. hornworts, liverworts and mosses, respectively) and lycophytes (Lycopodiopsida) are land plants with simple organization that evolved in the Late Silurian (Edwards *et al.*, 1998; Graham & Gray, 2001). Bryophytes are represented by 13 000 extant species, making them the second most diverse group of land plants, surpassed only by angiosperms (Hedderson *et al.*, 1996; Goffinet *et al.*, 2001; Shaw & Renzaglia, 2004). Despite the modern prevalence of spermatophytes, the nonvascular community contributes substantially to primary productivity in high-latitude and high-altitude ecosystems, where vascular plants are largely constrained (Sjögersten *et al.*, 2006; Arndal *et al.*, 2009; Turetsky *et al.*, 2010, 2012; Porada *et al.*, 2013). Moreover, bryophytes coexist in spermatophyte-dominated habitats, but thanks to their poikilohydry they also co-dominate with lichens in niches where vascular plants are excluded by a lack of soil and/or nutrients, very low air temperatures and irregular or unpredictable water availability (Proctor *et al.*, 2007). Despite their importance, the number of studies centered on their comparative physiological performance is much smaller than those on tracheophytes.

Bryophytes are dominated by the gametophyte stage, which often lacks a differentiated vascular system, and never possess stomata. In addition, bryophytes lack a significant degree of foliage cuticularization (Edwards *et al.*, 1998; Renzaglia *et al.*, 2004, 2007; Shaw & Renzaglia, 2004), thus preventing control of leaf surface evaporation rates (Glime, 2007). Their poikilohydry imposes a high dependence on their photosynthetic rates on water availability, with limitations caused under conditions of both water deficit and excess (Proctor, 2001). The presence of surface water filling the pore space among neighboring foliage elements is also an important limitation, since the diffusion coefficient for CO_2 in water is 10^4 times lower than in air (Rice &

Giles, 1996; Proctor, 2001; Green *et al.*, 2011). Consequently, bryophytes can only attain maximum photosynthesis capacity at intermediate ranges of water content that might be species specific (Silvola & Aaltonen, 1984; Titus & Wagner, 1984; Maseyk *et al.*, 1999; Wagner *et al.*, 2013; Wang & Bader, 2018). However, even within this range of optimal hydration, the photosynthetic capacity per unit dry mass is much lower in bryophytes than in tracheophytes (Proctor, 2001; Brodribb *et al.*, 2007; Meyer *et al.*, 2008; Waite & Sack, 2010; Wang *et al.*, 2016). The mechanistic reasons for this have not been determined. In contrast to bryophytes, lycophytes are vascular plants that possess stomata on their microphylls, but like mosses they also show low photosynthetic capacity (Ruszala *et al.*, 2011; Brodribb *et al.*, 2017), which could be due to a poorly developed hydraulic system (Boyce, 2010) and diffusive limitations in the mesophyll (Tosens *et al.*, 2016; Veromann-Jürgenson *et al.*, 2017).

The leaf economics spectrum (LES) is a general set of interspecific trait relationships that reflects the cost and benefits of leaf investment, such that species with high leaf mass per area (LMA) tend to have longer lived photosynthetic organs with lower nitrogen (N) per dry mass and lower light-saturated photosynthetic rates. These trends have been shown for spermatophytes (Reich *et al.*, 1997; Wright *et al.*, 2004; Zhang *et al.*, 2015) and ferns (Tosens *et al.*, 2016). In bryophytes, LES relationships have been recently tested in moss species from tropical (Waite & Sack, 2010) and temperate climates (Wang *et al.*, 2017), and these relationships have been supported when considering projected canopy mass per area (CMA) instead of LMA, with CMA being considered as analogous to tracheophyte LMA (Proctor, 2000; Waite & Sack, 2010). Both studies observed that mosses followed the same relationships as tracheophytes, but with very different slopes and/or intercepts. Indeed, mosses had a much lower mass-based photosynthetic rate than tracheophytes for a given mass-based N concentration (Waite & Sack, 2010; Wang *et al.*, 2017), suggesting a diffusional limitation of their photosynthetic capacity or much greater investment in nonphotosynthetic biomass within foliage, including investment in cell walls (Onoda *et al.*, 2017). Furthermore, thick cell walls are directly associated with low mesophyll conductance due to the slow diffusion in the liquid phase (Niinemets *et al.*, 2009; Tosens *et al.*, 2012a,b; Tomás *et al.*, 2013; Onoda *et al.*, 2017; Veromann-Jürgenson *et al.*, 2017).

Photosynthetic limitations in tracheophytes can be divided among limitations imposed by stomatal conductance g_s, mesophyll conductance g_m (which we rename nonstomatal diffusion conductance g_{nsd} to account for plants lacking a true mesophyll, like those studied here), and leaf biochemistry/photochemistry. The relative importance of each limitation in bryophytes remained unexamined to our knowledge, and it has only been reported in three species of lycophytes (two Lycopodiales and one Selaginalles; Tosens *et al.*, 2016; Veromann-Jürgenson *et al.*, 2017). The existence of a phylogenetic trend towards increasing photosynthesis has been already suggested by Brodribb *et al.* (2007), and Flexas *et al.* (2012) noticed that this was linked to a trend towards increasing both g_s and g_m (or g_{nsd}) based on data for spermatophytes and a few hornwort and liverwort species. This hypothesis was further supported with recent data for ferns and fern allies (Gago *et al.*, 2013; Carriquí *et al.*, 2015; Tosens *et al.*, 2016). Whereas g_{nsd} data are available for a few hornwort and liverwort species (Meyer *et al.*, 2008), for mosses a value is available for only a single species (Hanson *et al.*, 2014), representing a significant gap of knowledge.

We hypothesized that, under optimum hydration, bryophytes would be mainly limited by diffusive resistance – that is, by the CO_2 diffusion through the tissues (hereinafter termed thallus for all nonleafy gametophytes and phyllidium for leaves of mosses and leafy liverworts) – rather than by biochemistry. Bryophytes are thought to have evolved mainly under selection pressure to support biomechanical stress associated with desiccation (Hanson *et al.*, 2014). These pressures have led, among other traits, to thick cell walls (Waite & Sack, 2010), which we hypothesize could result in a constitutively low g_{nsd}. Mesophyll conductance in a typical angiosperm leaf is the sum of gas- and liquid-phase pathways that CO_2 molecules have to pass in their pathway from the substomatal cavities to the carboxylation site in the chloroplast stroma. This gas-phase pathway is absent for unistratose mosses (i.e. with one cell layer thick phyllidium), theoretically enhancing CO_2 diffusion from the atmosphere to the cell surface, but present in Polytrichaceae species, which possess an air-filled 'pseudomesophyll' formed by lamellae columns (Clayton-Greene *et al.*, 1985). However, the main limitations to CO_2 diffusion are in the liquid phase, determined by the length and chemical characteristics of cell wall, plasmamembrane, cytoplasm and chloroplast envelope stroma. Also important are the mesophyll (or photosynthetic tissue in plants lacking mesophyll) and chloroplast surface areas exposed to cell perimeter – either intercellular (in multistratose photosynthetic organs) or ambient (in unistratose photosynthetic organs), S_m/S and S_c/S, respectively (Evans *et al.*, 2009; Terashima *et al.*, 2011). Our hypothesis of a low g_{nsd} in bryophytes rests on the following evidence: (1) mosses have the thickest cell walls reported for photosynthetic cells of land plants (Waite & Sack, 2010), a trait that negatively correlates with g_m in tracheophytes (Terashima *et al.*, 2011; Tosens *et al.*, 2016; Veromann-Jürgenson *et al.*, 2017); (2) their simple body structure could result in a lower S_m/S and S_c/S, negatively affecting g_m.

To test our hypothesis that the combination of thick cell walls and low S_c/S in bryophytes and lycophytes result in low g_{nsd}, we conducted a detailed analysis of gas exchange, anatomy and N content in a diversity of species. These measurements were designed, first, to assess the physiological and anatomical limitations on photosynthesis, second, to link morphoanatomical traits with variations in g_{nsd} and, third, to assess differences in the LES relationships for bryophytes compared with tracheophytes.

Materials and Methods

Experimental sites and growth conditions

Three lycophytes, 26 mosses and seven liverwort species (Table 1), adapted to different climates and microhabitats (Supporting

Information Table S1) from Antarctica, Australia, Estonia, Hawaii and Spain, were studied (Fig. 1; Methods S1). Moreover, the moss *Polytrichum juniperinum* and the liverwort *Marchantia polymorpha* were measured at two different sites, in Spain and Tasmania and in Estonia and Tasmania, respectively. Plants of all 36 species were measured at the time of the year when their growth conditions were most favorable (i.e. with least environmental stress). All plants (except for *M. polymorpha*, *Selaginella martensii* and *Selaginella uncinate*, which were grown in pots in a glasshouse) were collected in the field with the underlying substrate (i.e. soil or bark) and placed in plastic bags. Plants were watered as frequently as necessary to maintain hydration from collection to measurement (i.e. days to weeks depending on the species). Environmental conditions – including watering, fertilization and substrate – where plants were collected or kept until measurements were performed are specified in Table S2. Owing to logistic difficulties, all the traits could only be measured in a subset of species. Thus, species were divided into four categories depending on the completeness of the measurements (Table S3). Data for the Hawaiian species were already partially published (Waite & Sack, 2010), and new measurements were made from existing micrographs.

Photosynthesis measurements and estimation of nonstomatal diffusion conductance

For Hawaiian species, photosynthesis measurements were performed using an acrylic custom cuvette attached to an LI-6400 gas-exchange system (Li-Cor Inc., Lincoln, NE, USA), as detailed in Waite & Sack (2010). For all other species, simultaneous gas-exchange and fluorescence measurements were performed in young fully expanded microphylls (in lycophytes) and in healthy shoot or thalli (in mosses and liverworts) using either the gas-exchange system LI-6400XT coupled with a 2 cm^2 fluorimeter chamber (Li-6400-40) for Antarctic and five out of 14 Spanish species (changing the 2 cm^2 chamber to a 6 cm^2 chamber for respiration measurements) or the GFS-3000 gas-exchange system (Walz, Effeltrich, Germany) equipped with a leaf chamber fluorimeter with an 8 cm^2 cuvette for Australian,

Table 1 Phylogenetic classification following Kenrick & Crane (1996) for the 36 liverwort, moss and lycophyte species included in this study.

Phylum	Class	Order	Family	Species
Marchantiophyta (liverworts)	Jungermanniospida	Fossombroniales	Pelliaceae	*Pellia endiviifolia*
		Jungermanniales	Saccogynaceae	*Saccogyna viticulosa*
		Porellales	Porellaceae	*Porella canariensis*
	Marchantiopsida	Lunulariales	Lunuriaceae	*Lunularia cruciata*
		Marchantiales	Conocephalaceae	*Conocephalum conicum*
			Dumortieraceae	*Dumortiera hirsuta*
			Marchantiaceae	*Marchantia polymorpha*
Bryophyta (mosses)	Bryopsida	Polytrichales	Polytrichaceae	*Polytrichum formosum*
				Polytrichum juniperinum
		Fissidentales	Fissidentaceae	*Fissidens pacificus*
				Fissidens serrulatus
		Dicranales	Dicranaceae	*Dicranum polysetum*
				Dicranum scoparium
			Ditrichaceae	*Ceratodon purpureus*
				Campylopus hawaiicus
				Holomitrium seticalycinum
				Leucobryum seemannii
		Orthotrichales	Orthotrichaceae	*Macromitrium microstomum*
				Macromitrium piliferum
		Bryales	Mniaceae	*Plagiomnium elatum*
				Plagiomnium undulatum
			Briaceae	*Bryum pseudotriquetrum*
			Rhizogoniaceae	*Pyrrhobryum pungens*
		Hookeriales	Hookeriaceae	*Distichophyllum freycinetii*
				Hookeria acutifolia
		Hypnales	Thuidiaceae	*Thuidium tamariscinum*
			Entodontaceae	*Pseudoscleropodium purum*
			Hylocomiaceae	*Hylocomium splendens*
				Pleurozium schreberi
			Hypnaceae	*Ctenidium molluscum*
				Hypnum cupressiforme
			Amblystegiaceae	*Sanionia uncinata*
			Sematophyllaceae	*Acroporium fuscoflavum*
Tracheophyta	Lycopodiopsida (lycophytes)	Selaginalles	Selaginaceae	*Selaginella denticulata*
				Selaginella martensii
				Selaginella uncinata

Common names used throughout the paper for plant groups are described in parentheses after the scientific name.

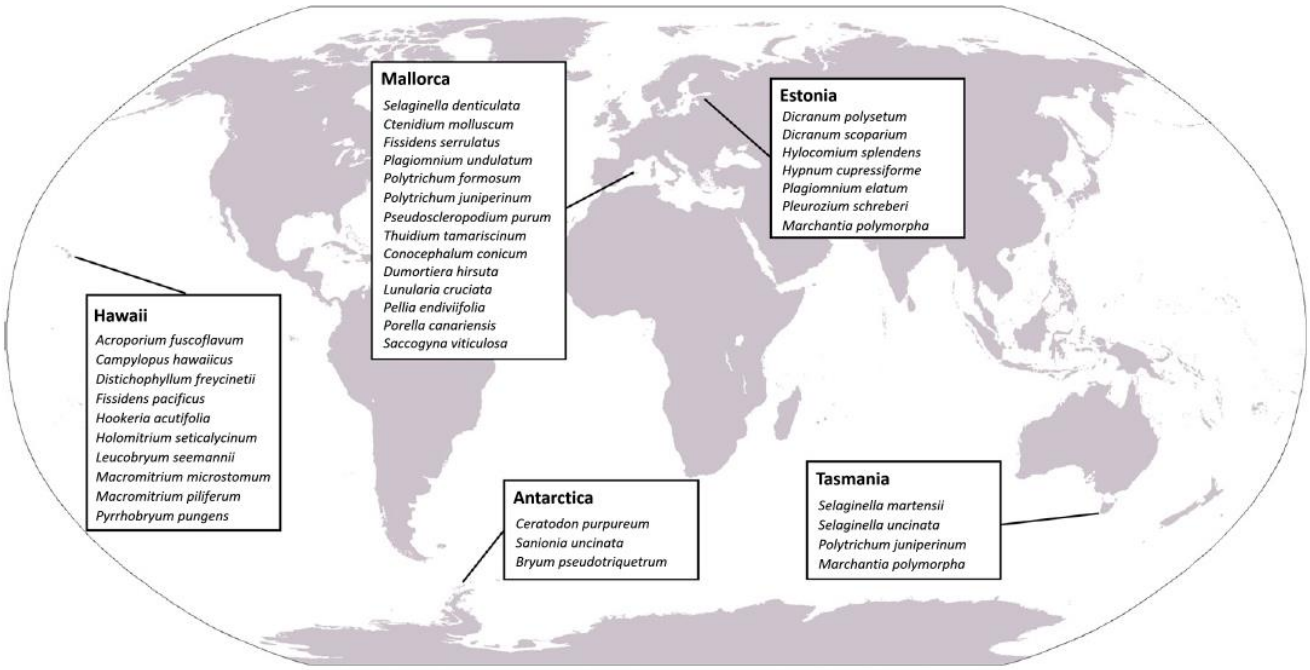

Fig. 1 Study sites of the species included in this study.

Estonian and nine out of 14 Spanish species. Details on how the measurements were performed, and the precautions taken, are given in Methods S1. Methods S1 also explains how the different photosynthetic parameters were estimated. Here, we just want to make explicit that the parameter defined as nonstomatal diffusion conductance g_{nsd} is analogous to the so-called mesophyll conductance g_m in higher plants, except that, first, most bryophytes do not show a true mesophyll, many of them consisting of a single layer of photosynthetic cells with no intercellular air spaces; and second, because of the approach used for its estimation, unavoidably g_{nsd} includes any potential residual component of diffusion through water film external to the photosynthetic tissue and/or cuticle, in addition to diffusion through the photosynthetic tissue itself.

LMA and CMA and N concentration

Shoots and thalli were dissected and an orthogonal photograph was taken, and dry mass was determined after oven drying at 70°C for 48 h. Total area was determined from photographs with ImageJ software (Schneider *et al.*, 2012) and LMA was calculated by dividing by dry mass. In mosses, CMA (see Notes S1 for a full list of trait abbreviations) was calculated by dividing the gametophyte dry mass by projected area. When testing the LES in mosses, CMA was used for mosses instead of LMA, except for *Polytrichum* species, as they have relatively large phillidia with an air-filled 'pseudomesophyll' (Clayton-Greene *et al.*, 1985) that resemble true leaves.

Total N concentration of oven-dried samples from Antarctica, Australia, Estonia and 9 out of 14 Spanish species was quantified with an elemental analyser (Truspec CN628; Leco Corp., St Joseph, MI, USA), and whole-sample average N concentration was estimated as the mass-weighted average. Total N concentration of 5 out of 14 Spanish species was quantified with an elemental analyzer (Thermo Flash EA 1112 Series; ThermoFisher Scientific, Bremen, Germany) at Universitat de les Illes Balears. Total N concentration of samples from Hawaii was determined by Kjeldahl digestion (Hue *et al.*, 2000; University Hawaii at Manoa Agricultural Diagnostic Center).

Anatomical measurements and modeling of nonstomatal diffusion conductance

Small pieces of microphylls, phyllidia or thalli from three to six individuals per species were taken after the gas exchange measurements. Samples were quickly fixed and prepared for light and transmission electron microscopy observation as detailed in Methods S1. All samples were photographed at ×100–×1000 magnification with a digital camera (U-TVO.5XC; Olympus, Tokyo, Japan; or DS-Fi1; Nikon Corp., Kyoto, Japan). Ultrathin sections for transmission electron microscopy (TEM H600; Hitachi, Tokyo, Japan) were contrasted with uranyl acetate and lead citrate. The electron micrographs were taken between ×1500 and ×30 000 magnification (see later Fig. 4). All images were analysed using ImageJ (Schneider *et al.*, 2012). Anatomical traits were estimated as described in detail in Tosens *et al.* (2016), considering the anatomical particularities of these phylogenetic groups, as detailed in Video S1. The curvature cell correction factor was measured and calculated for each species according to Thain (1983), using the average length/width ratio of three to five cells in two to four different fields of view for each tissue fraction. All traits were analysed in four to six fields of view in three

to six different sections. The micrographs were randomly selected in each section.

The fraction of photosynthetic tissue occupied by intercellular air space f_{ias} and photosynthetic tissue and chloroplast surface area exposed to air, either intercellular (in multistratose photosynthetic organs) or ambient (in unistratose photosynthetic organs) per unit of leaf area (S_m/S and S_c/S) were measured and calculated from light and transmission electron microscopy micrographs following Syvertsen *et al.* (1995) and Tosens *et al.* (2012a,b, 2016). Cell wall thickness T_{cw}, cytoplasm thickness T_{cyt} and chloroplast length L_{chl} and thickness T_{chl} were measured either from light or transmission electron microscopy micrographs, as deemed necessary for each species. These characteristics were measured for at least 10 cells per sampled individual per species.

The one-dimensional gas diffusion model of Niinemets & Reichstein (2003) was applied as modified by Tomás *et al.* (2013), with some particularities depending on the different foliar anatomies, some of which are very different compared with a typical angiosperm leaf (see later Fig. 4). The model allows estimation of the theoretical nonstomatal diffusion conductance supported by the given set of foliage anatomical characteristics (g_{nsd_ANAT}; see details in Methods S1).

Quantitative limitation analysis of A_N and partial limitations of g_{nsd}

Relative limitations on net assimilation per unit area A_{area} for lycophytes were calculated following Grassi & Magnani (2005) as described in Tomás *et al.* (2013). This analysis quantifies the relative importance of stomatal, nonstomatal diffusion conductance and biochemical limitations – the latter integrating light and carbon reactions, which co-limit photosynthesis; see Gallé *et al.* (2009) and Varone *et al.* (2012) for further explanation. In the bryophytes, the limitation was assumed to be only due to nonstomatal diffusion conductance and biochemistry (see Methods S1). Moreover, the partial limitation of the different anatomical traits to nonstomatal diffusion CO_2 conductance were calculated following the quantitative analysis described in Tomás *et al.* (2013). See Methods S1 for further details.

Statistical analyses

At least three individual plants were measured for each species for all measurements. Relationships among physiological and structural traits were explored by SPSS (SPSS Inc., Chicago, IL, USA) and all statistical tests were considered significant at $P < 0.05$. We used standardized major axis estimation and tested for a common slope among mosses and other plant groups using the likelihood ratio and then compared with a χ^2 distribution; if the mosses and other plant groups shared a common slope, we tested for a difference in intercepts by calculating the Wald statistic and comparing the χ^2 distribution between plant groups. These analyses were performed by means of the R library SMATR (Warton *et al.*, 2006, 2012).

Results

Photosynthesis, nonstomatal diffusion conductance and photosynthetic limitations

Net assimilation per unit area A_{area}, considering total area for lycophytes, *Polytrichum* and liverwort species and shoot projected area for all other moss species, varied 17.5-fold across species, from 0.43 ± 0.09 μmol CO_2 m^{-2} s^{-1} in *Fissidens serrulatus* to 7.55 ± 0.90 μmol CO_2 m^{-2} s^{-1} in *P. juniperinum*. If A_{area} based on total area is considered for mosses without intercellular airspace (i.e. except *Polytrichum*), A_{area} ranged between 0.044 ± 0.006 μmol CO_2 m^{-2} s^{-1} in *Leucobryum seemannii* to 0.774 ± 0.028 μmol CO_2 m^{-2} s^{-1} in *Plagiomnium undulatum* (Table S4). Nonstomatal diffusion conductance to CO_2 estimated from Chl fluorescence (g_{nsd_FLU}) varied 12-fold, from 1.86 ± 0.261 mmol CO_2 m^{-2} s^{-1} in *Pleurozium schreberi* to 23.8 ± 8.074 mmol CO_2 m^{-2} s^{-1} in *Selaginella denticulata* (Table S4). Maximum velocity of carboxylation $V_{c,max}$, chloroplastic CO_2 concentration C_c and electron transport rate ETR also varied strongly across species, but non-photorespiratory day respiration (R_d) varied only narrowly (Table S4). Despite potential uncertainties in the calculation of $V_{c,max}$, a strong correlation was found between ETR measured at 400 μmol CO_2 mol^{-1} air and $V_{c,max}$ (Fig. S1; $r^2 = 0.95$, $P < 0.0001$). Moreover, $V_{c,max}$ values remained within the same range when they were obtained with fast A_{area}–C_a (ambient CO_2 concentration) curves (e.g. without rehydrating the moss during the 10–15 min of the curve) or slow A–C_a curves (e.g. removing the moss from the cuvette and rehydrating it between each C_a point; Table S5). In mosses, A_{area} was strongly correlated with g_{nsd_FLU} (Fig. 2a; $r^2 = 0.93$, $P < 0.0001$) and with ETR (Fig. 2b; $r^2 = 0.83$, $P = 0.0006$), and not with $V_{c,max}$ (Fig. 2c). To discern the relative impact of stomatal limitation l_s (only in lycophytes), nonstomatal diffusion conductance limitation l_{nsd} and biochemical limitation l_b on A_{area} for each species, a quantitative limitation analysis was performed. For all bryophytes in which limitation analysis could be performed (one liverwort and nine mosses), l_m was the most important limitation of A_{area}. In lycophytes, the major limitations of photosynthesis were shared between l_{nsd} and l_b, and stomata had only a minor role in constraining A_{area} in the conditions in which they were measured (Fig. 3).

Leaf anatomy

Foliage of bryophytes presents structural features that make it vastly different from typical angiosperm leaves (Fig. 4), exhibiting a lack of stomata, presence of pores and/or a uni- or reduced multilayered cell structure. To resolve how these distinctive features influence nonstomatal diffusional limitations to photosynthesis, a structural and ultrastructural analysis of the photosynthetic organs was performed for each species. Groups and species varied strongly in their macroscopic and structural and ultrastructural characteristics (Video S1; Tables S5, S6). Dry LMA and CMA varied 12.4-fold and 6.5-fold, respectively, among species: from 6.4 ± 0.4 g m^{-2} in *Distichophyllum freycinetti* to 79.3 ± 4.7 g m^{-2} in *Polytrichum*

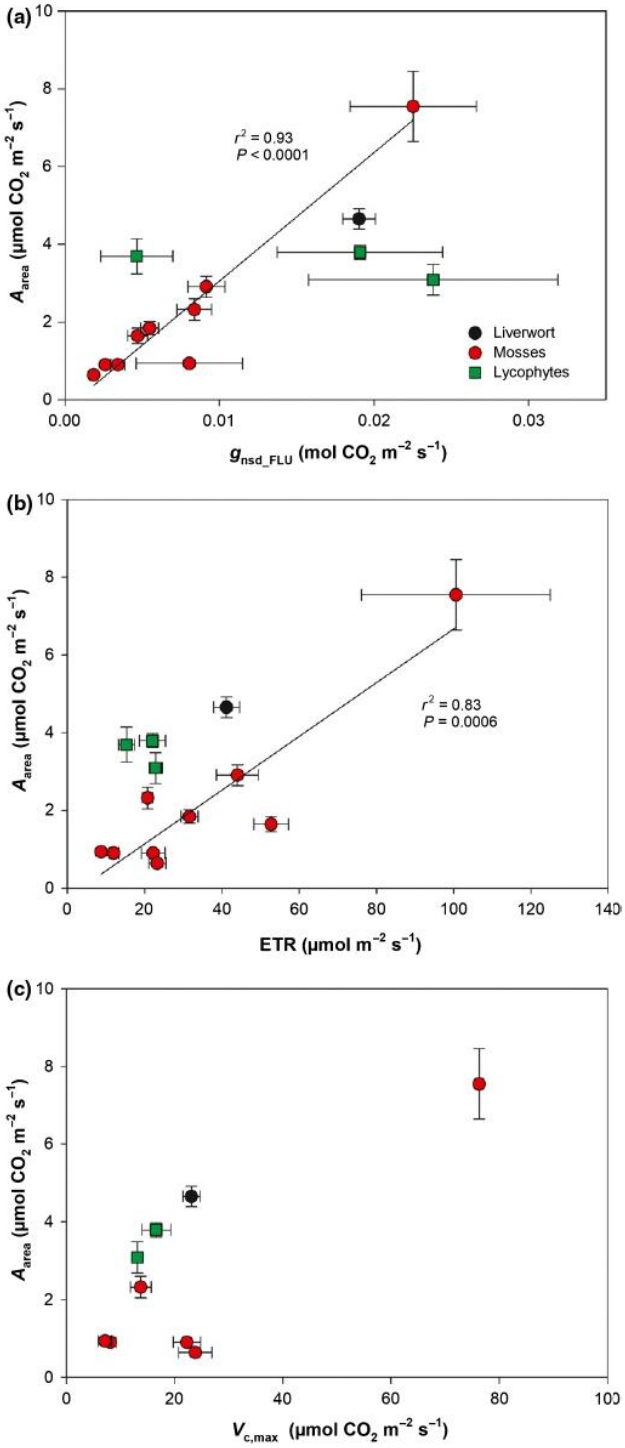

Fig. 2 Area-based net assimilation rate A_{area} in relation to (a) area-based nonstomatal diffusion conductance g_{nsd_FLU}, (b) electron transport rate ETR and (c) maximum velocity of carboxylation $V_{c,max}$. Values are means ± SE of 4–12 replicates per species. Data for moss species were fitted by linear regressions.

formosum for LMA, and from 48.1 ± 3.0 g m^{-2} in *P. schreberi* to 317 ± 49.3 g m^{-2} in *Hylocomium splendens*. Leaf density D_{leaf} and leaf thickness T_{leaf} varied 53.4-fold and 61.2-fold, respectively. f_{ias} varied from 51 ± 4% in *Selaginella uncinata* to zero in mosses with a single layer of cells (Table S6). Photosynthetic tissue and chloroplast surface area exposed to air, either intercellular (in multistratose photosynthetic organs) – S_m/S and S_c/S, respectively – varied 5.4-fold and 8.6-fold, respectively: from 2.34 ± 0.02 m^2 m^{-2} in *Plagiomnium elatum* to 13.04 ± 0.58 m^2 m^{-2} in *P. juniperinum* for S_m/S, and from 0.59 ± 0.01 m^2 m^{-2} in *Pseudoscleropodium purum* to 5.18 ± 0.18 m^2 m^{-2} in *P. juniperinum*. T_{cw} varied 12.6-fold: from 0.270 ± 0.031 μm in *S. denticulata* to 3.40 ± 0.74 μm in *Distichophyllum freycinetii*. T_{chl}, L_{chl} and T_{cyt} varied 6.2-fold, 4.9-fold and 36.2-fold, respectively (Table S7). As a result of the extensive variation in anatomical characteristics, g_{nsd_ANAT} varied 45-fold: from 1.36 ± 0.26 mmol CO_2 m^{-2} s^{-1} in the moss *L. seemannii* to 45.09 ± 6.10 mmol CO_2 m^{-2} s^{-1} in the lycophyte *S. denticulata* when a cell wall porosity p_{cw} of 0.028 was considered (Table S8; see Methods S1). When scenarios were tested with a range of p_{cw} values, g_{nsd_ANAT} remained very low relative to the published values for vascular plants (Fig. S1; Table S8).

When pooling all species together, LMA (for lycophytes, *Polytrichum* and liverwort species) CMA (for the rest of moss species) did not correlate with either D_{leaf} or T_{leaf} (Fig. 5a,b). For the same LMA or CMA, bryophytes and lycophytes invested more dry mass to produce thicker cell walls compared with the spermatophyte dataset compiled by Onoda *et al.* (2017) (Fig. 5c), which comprises from herbs to evergreen angiosperms and a few gymnosperm species. Conversely, bryophytes and lycophytes had significantly lower S_c/S values for the same LMA or CMA range compared with the rest of embryophytes (Fig. 5d).

Anatomical determinants of nonstomatal diffusion conductance

A_{mass} was not correlated with T_{leaf} and D_{leaf} (Fig. 6a,b), but both A_{area} and A_{mass} were negatively correlated with T_{cw} (Fig. 6c,d), and positively with S_c/S in mosses (Fig. 6e,f). Comparing the estimates of g_{nsd_FLU} and g_{nsd_ANAT}, a highly significant positive correlation close to the 1 : 1 line was found when p_{cw} was considered as 0.028 ($r^2 = 0.73$, $P < 0.001$). When p_{cw} was considered as 0.1 or variable assuming a negative linear relationship (Fig. S2), positive relationships were still found, but the data shifted from the 1 : 1 line (Fig. S3).

To quantify the influence of subcellular liquid–phase limitations (gas-phase limitations in most mosses were zero due to the lack of intercellular airspace) in determining g_{nsd_ANAT}, a quantitative limitation analysis of liquid-phase limitations was also performed. Cell walls constituted the major component limiting CO_2 transfer into the chloroplast in the liverwort, mosses and lycophytes (Fig. 7). Inside each group, the different species presented similar values for each liquid-phase limitation (Fig. S4).

LES

The N content per area and mass (N_{mass} and N_{area}, respectively) varied 13.4-fold and 16.3-fold, respectively: from 0.24 ± 0.05%

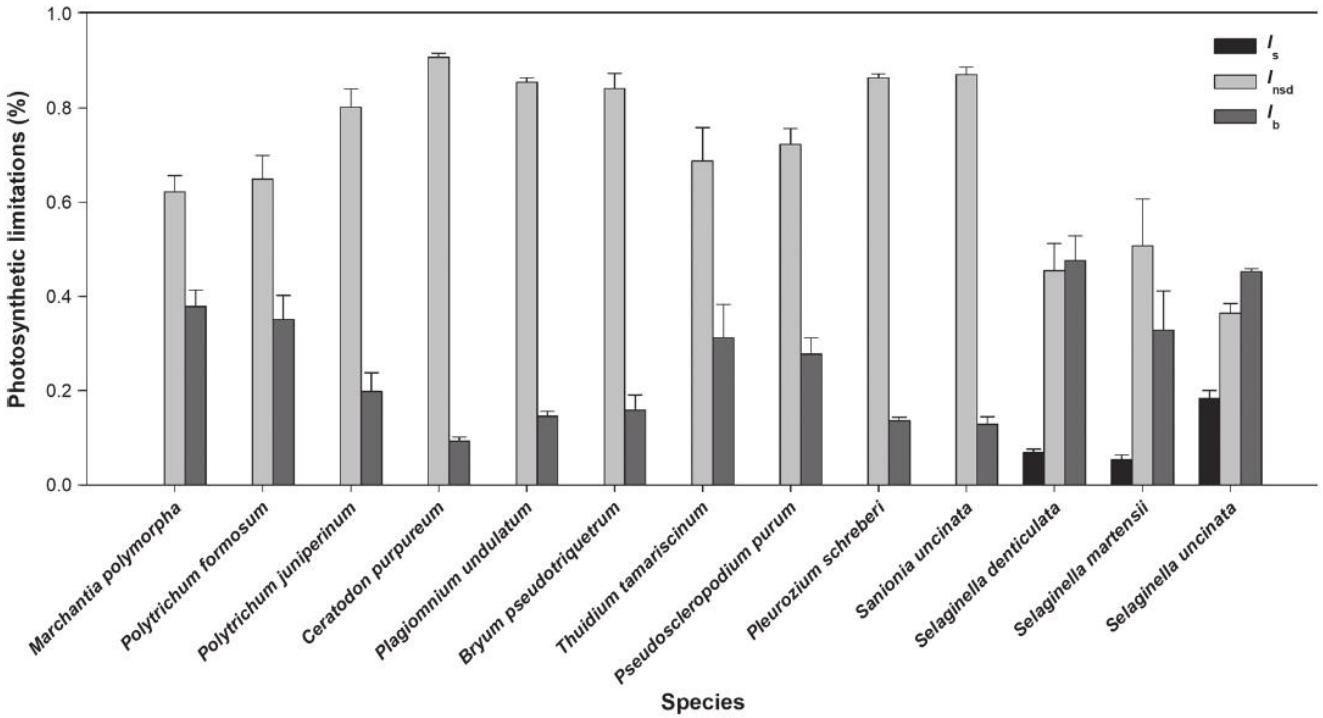

Fig. 3 The percentage of net assimilation limited by stomatal conductance l_s, nonstomatal diffusion conductance l_{nsd} and biochemistry l_b in the liverwort, mosses and lycophytes studied. Values are means ± SE of 3–10 replicates per species.

in *L. seemannii* to 3.22 ± 0.06% in *Ctenidium molluscum* for N_{mass}, and from 0.25 ± 0.01 g m^{-2} in *Pellia endiviifolia* to 4.09 ± 0.39 g m^{-2} in *Dicranum scoparium* for N_{area} (Table S9). The N_{mass} of the bryophytes and lycophytes studied was located at the low end of the spermatophyte range reported by Wright *et al.* (2004), ranging from 0.25% to 6.36%. To investigate potential differences in the LES relationships for bryophytes and lycophytes relative to angiosperms, gymnosperms and ferns, we compared trends with those described by Wright *et al.* (2004) for angiosperms, by Zhang *et al.* (2015) and Veromann-Jürgenson *et al.* (2017) for gymnosperms and by Tosens *et al.* (2016) for ferns. The low values of moss and liverwort species (with the exception of *Polytrichum* species) for A_{mass} for a given value of CMA (Fig. 8a), LMA (Fig. 8b) or – only in the case of mosses – N_{mass} (Fig. 8c) separated them from the rest of land plant groups. Although no significant differences were found between plant groups' slopes using a likelihood ratio test ($P = 0.19$ in Fig. 6a; $P = 0.51$ in Fig. 8c), intercepts between mosses and the other plant groups were different with a significance of $P > 0.0001$ in Fig. 8(a,c). Instead, lycophytes, a group in which no trendline was drawn due to the limited data available, were located in between the other groups of vascular plants.

Discussion

This study shows, from a survey of species from contrasting climates, that bryophytes constitute a unique trait space in the LES. Moreover, this study is the first to provide a comprehensive analysis of the photosynthesis-related and anatomical traits in bryophytes. They are revealed as the land plant group with the lowest nonstomatal diffusion conductance g_{nsd} values (confirmed by two independent techniques: the Chl fluorescence and the anatomical models), followed by lycophytes, thus confirming the hypothesis of a phylogenetic trend towards progressively increasing g_{nsd} from bryophytes to angiosperms. Whereas photosynthesis in mosses was mostly limited by g_{nsd} and in lycophytes co-limited by both g_{nsd} and biochemistry, g_{nsd} and photosynthesis in both primitive land plant groups were strongly determined by large cell wall thickness T_{cw} and low chloroplast surface area exposed to air per leaf area (S_c/S).

Low photosynthetic rates in bryophytes and lycophytes

Low values for maximum A_{area} (i.e. under optimum water content with no external water restricting CO_2 diffusion) were recorded for liverwort, mosses and lycophytes, and these were linked to low nonstomatal diffusion conductance estimated from Chl fluorescence (g_{nsd_FLU}). In fact, average g_{nsd_FLU} values for the mosses and the liverworts were the lowest within the land plant groups (Flexas *et al.*, 2012; Tosens *et al.*, 2016), followed by lycophytes. These data – within the rage of values previously reported for a few species of bryophytes (Meyer *et al.*, 2008; Hanson *et al.*, 2014) and lycophytes (Veromann-Jürgenson *et al.*, 2017) – support the suggested phylogenetic trend of g_{nsd}: bryophytes < lycophytes < pteridophytes < spermatophytes (Flexas *et al.*, 2012; Carriquí *et al.*, 2015).

The absolute values for both A_{area} and g_{nsd} must be taken with some caution. Even after taking all the precautions during

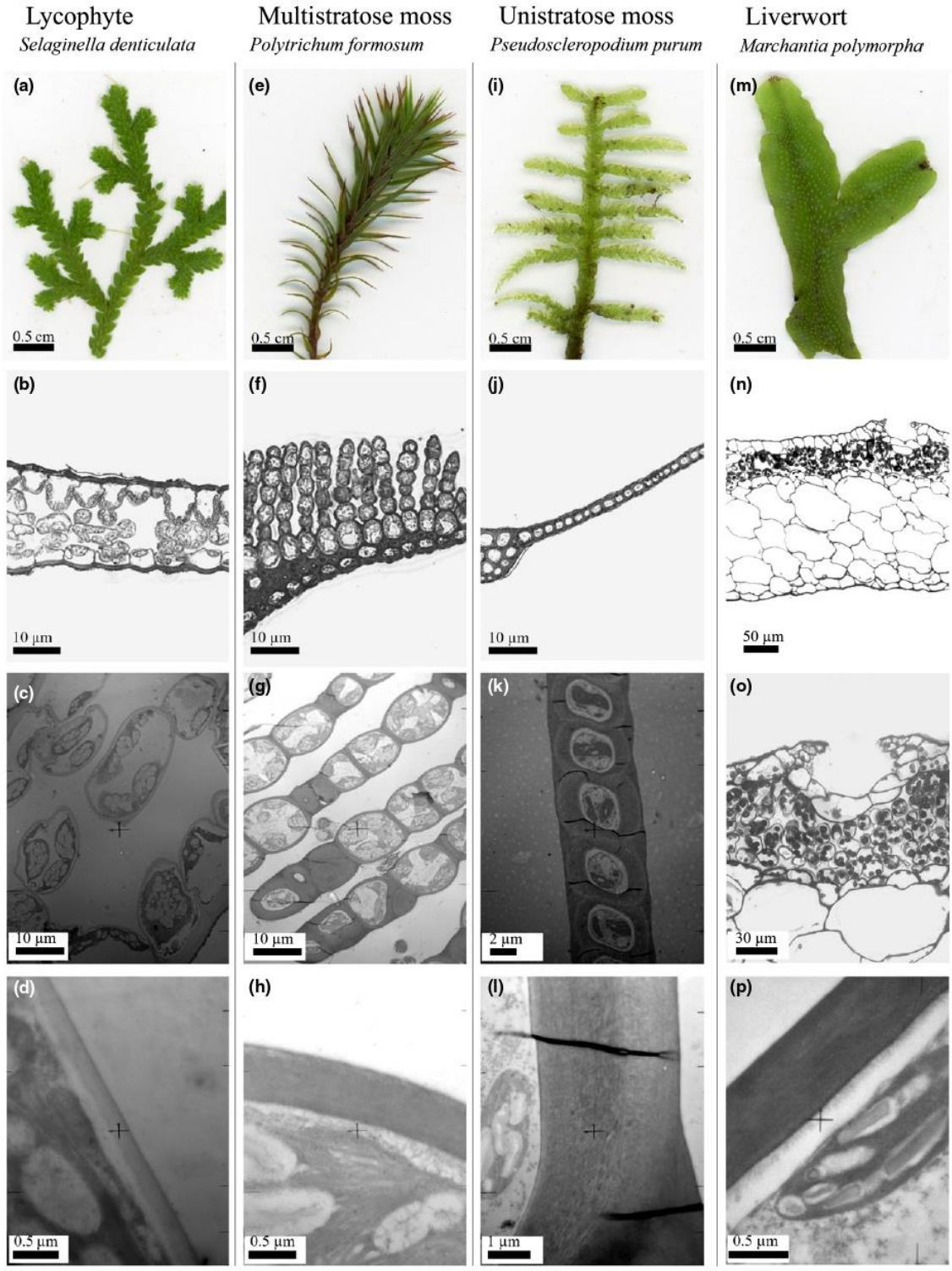

Fig. 4 Photographs and images of semithin and ultrathin microscopy cross-sections showing four representative morphologies of microphylls, phillidia and thalli of the species included in this study: (a–d) a lycophyte microphyll of *Selaginella denticulata*, (e–h) a phyllidium with multiple cell layers of the moss *Polytrichum formosum*, (i–l) a phyllidium with one layer of cells of the moss *Pseudoscleropodium purum* and (m–p) thallus of the liverwort *Marchantia polymorpha*.

measurements described in the Materials and Methods section, several issues can lead to misinterpretation of photosynthesis rates. For instance, we assume that the resistance to diffusion between CO_2 in the bulk air C_a and the leaf surface C_s is zero, which implies that there is no still air at the surface of the photosynthetic cells, which is unclear given the canopy and shoot

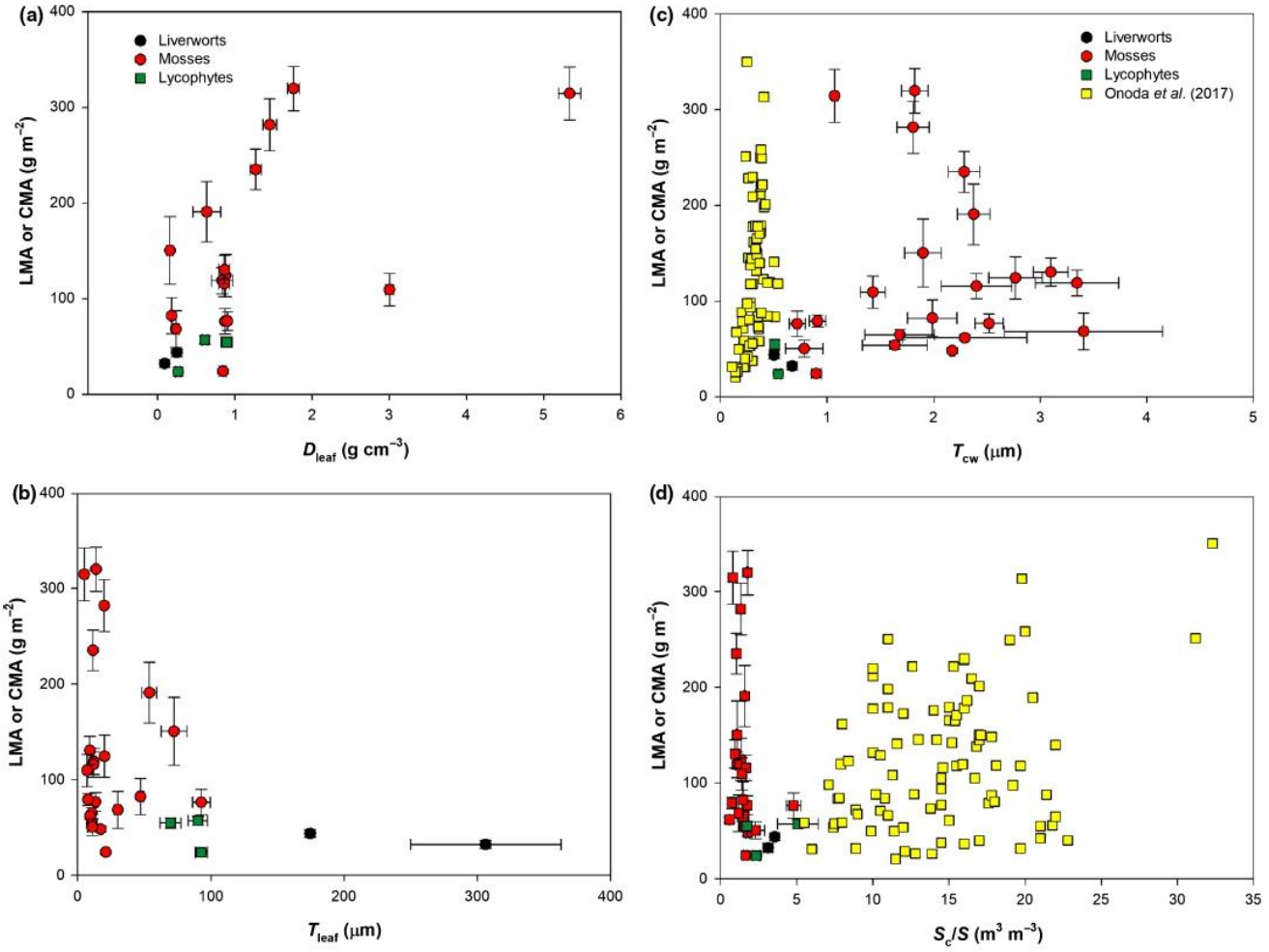

Fig. 5 Leaf or canopy dry mass per unit area (LMA or CMA, in lycophytes and bryophytes, respectively) in relation to (a) leaf density D_{leaf}, (b) leaf thickness T_{leaf}, (c) cell wall thickness T_{cw}, and (d) chloroplast surface area exposed to air S_c/S. Values are means ± SE of two to six replicates per species. Data from Onoda *et al.* (2017) for angiosperms and gymnosperms are presented for the available traits to allow a better comparison between groups.

complexity of mosses (Rice *et al.*, 2005; Rice & Cornelissen, 2014). Moreover, although we loosened the canopies and tried to place shoots next one another to avoid overlapping tissue (i.e. simulating a 'normal leaf'), some overlapping could have unavoidably occurred, thus leading to some underestimation of the actual photosynthetic area in the gas exchange cuvette, which would also be affected if there was some contribution of stem fractions (not considered to estimate the area) to total photosynthesis inside the cuvette. And, finally, the need for keeping humidity in the high range when measuring mosses creates a constant and large difference in water content between reference and sample air, and the equations to correct for direct water interference with the CO_2 signal are sensitive to errors in these conditions, which could result in biased estimates of A_{area}. There are even more concerns when estimating g_{nsd}. Besides the general limitations of the method for any species (Gu *et al.*, 2010; Gu & Sun, 2014), the potential uncoupling between gas exchange and Chl measurements due to the arrangements inside the cuvette, the use of hypothetical CO_2 compensation point without R_d (Γ*) values from angiosperms (due to the absence of published Γ* and Rubisco kinetics values for bryophytes; Griffiths *et al.*, 2004) and some potential influence of microbiome CO_2 methanogenic synthesis (Kostka *et al.*, 2016) add more uncertainties to g_{nsd} values. Despite all of these concerns, and recognizing that the absolute values presented should be taken with precaution, several lines of evidence suggest that the real values for A_{area} and g_{nsd} in bryophytes are at least in the range of the estimated ones. These include: (1) two parameters reflecting photosynthetic activity, acquired using two completely independent instruments and principles (ETR with a fluorometer and A_{area} with the infrared gas analyzer), showed a ratio ETR/A_{area} ≥ 7 in all species but one (*S. uncinata*, 5.8); that is, the values expected for C_3 species (Flexas *et al.*, 2002); (2) a sensitivity analysis reveals that even assuming large errors in, for example, ETR, Γ*, or R_d, the estimated g_{nsd} values remain in the low range (Table S10); (3) despite all of the uncertainties related to the use of Chl fluorescence, the values obtained for bryophytes are well in the same range of those previously obtained using the isotopic method

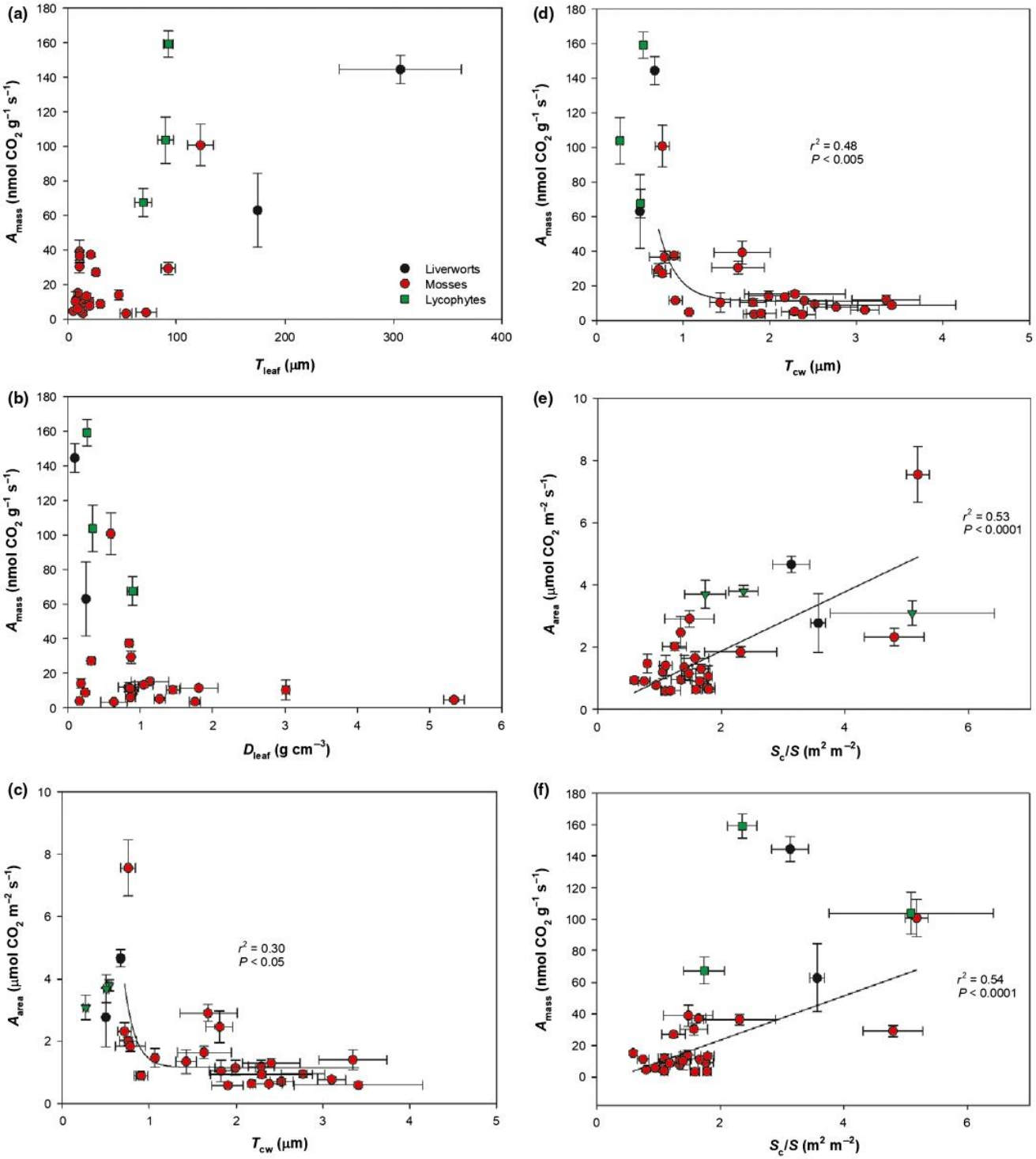

Fig. 6 Mass-based net assimilation rate A_{mass} in relation to (a) leaf thickness T_{leaf} and (b) leaf density D_{leaf}. (c) Area-based net assimilation rate A_{area} and (d) A_{mass} in relation to cell wall thickness T_{cw}. (e) A_{area} and (f) A_{mass} in relation to chloroplast surface area exposed to air S_c/S. Values are means ± SE of 3–12 replicates per species.

(Meyer *et al.*, 2008; Hanson *et al.*, 2014); and (4) using an absolutely independent method (i.e. anatomical modelling) similar values of g_{nsd} are obtained (see next section). In view of all this evidence, we consider that A_{area} and g_{nsd} in bryophytes (and lycophytes) are indeed as low as estimated, even if the precise absolute value for each species is subject to some limitations.

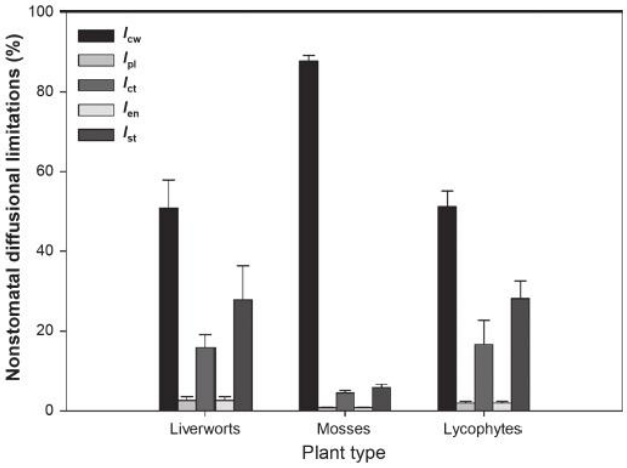

Fig. 7 The percentage of nonstomatal diffusion conductance per area limited by liquid-phase components in mosses, lycophytes and liverwort *Marchantia polymorpha*: cell wall l_{cw}, plasma membrane l_{pl}, cytoplasm l_{ct}, chloroplast envelope l_{en} and stroma l_{st}. Values are means ± SE per plant group.

The quantitative limitation analysis (Grassi & Magnani, 2005) revealed that bryophytes were mostly limited by g_{nsd} – from *c.* 60% to up to 90%, depending on the species – whereas biochemical limitations were of minor importance (Fig. 3). This confirms our hypothesis, based on the particularities of bryophytes' LES, of strong g_{nsd} limitation to photosynthesis. The phylogenetic explanation for this high g_{nsd} limitation to photosynthesis could be associated with different factors: first, that CO_2 transfer was relatively nonlimiting for photosynthesis under the elevated atmospheric CO_2 concentrations prevailing when bryophytes emerged on land (Graham & Gray, 2001; Berner, 2006); second, their adaptation to grow close to the soil, where CO_2 concentration can be high due to soil respiration (Hanson *et al.*, 2014); and/or third, their cell wall mechanical selection pressure to support desiccation rather than to maximize CO_2 diffusion (Hanson *et al.*, 2014). Conversely, lycophytes were mainly photosynthetically co-limited by both g_{nsd} and biochemistry (Fig. 3), in coincidence with what Veromann-Jürgenson *et al.* (2017) found in *S. uncinata*.

Anatomical determinants of CO_2 diffusion in bryophytes and lycophytes

With g_{nsd} being the most limiting factor for A_{area} in bryophytes, we aimed to determine whether this was related to anatomical traits being widely reported to constrain CO_2 diffusion in tracheophytes (Evans *et al.*, 2009; Terashima *et al.*, 2011). We found that cell wall thickness T_{cw} and chloroplast surface area exposed to the air, either intercellular (in multistratose photosynthetic organs) or ambient (in unistratose photosynthetic organs) per unit of leaf area (S_c/S), had extreme values in mosses. Although T_{cw} in lycophytes was similar to that of ferns (Tosens *et al.*, 2016), mosses had the largest T_{cw} reported for land plants. Hence, T_{cw} ranges from 0.170 to 0.81 µm in ferns (Tosens *et al.*, 2016), from 0.236 µm (Peguero-Pina *et al.*, 2016) to 1.22 µm in

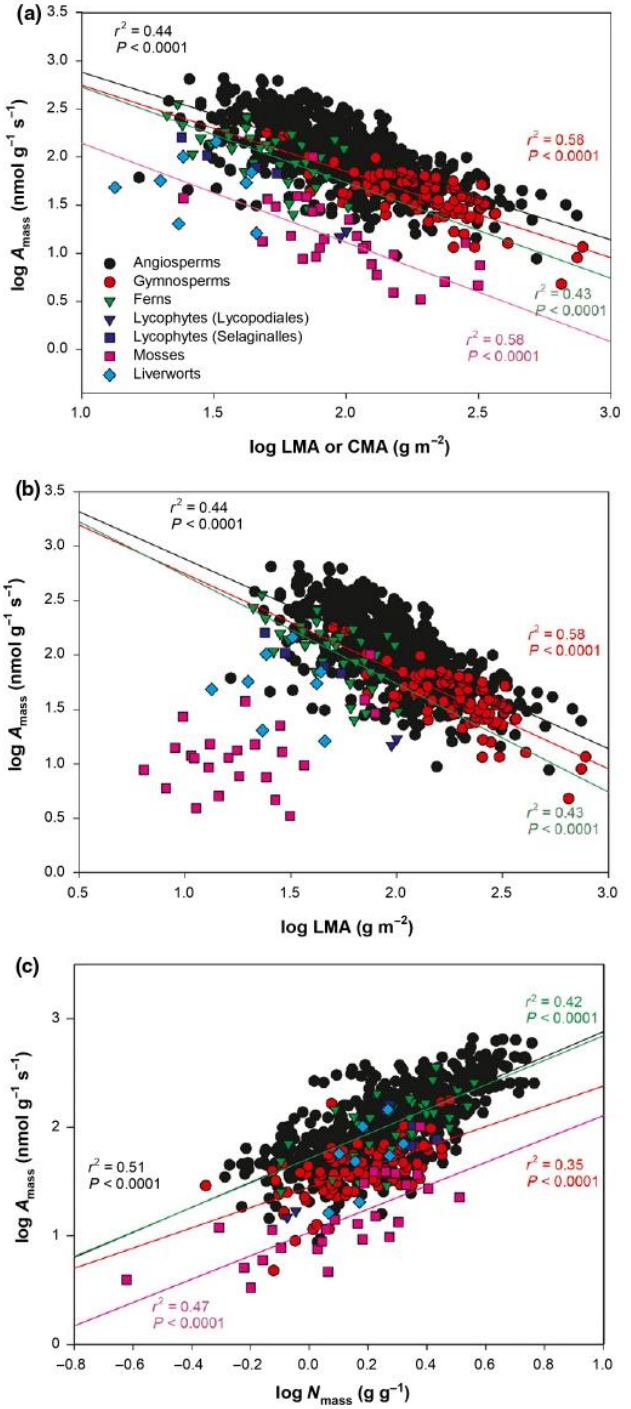

Fig. 8 Mass-based net photosynthesis as a function of (a) leaf dry mass per unit area (LMA), (b) canopy dry mass per unit area (CMA) for mosses and LMA for all other groups and (c), nitrogen content per mass N_{mass}. The axes are $\log_{10}$ scaled, and the data for each plant type were separately fitted by standardized major axis estimation. Common slopes across groups were tested using a likelihood ratio test ((a) $P = 0.19$; (c) $P = 0.51$); intercepts were compared between mosses and other plant groups by calculating the Wald statistic for (a) and (c); see the Materials and Methods section). The intercepts were different with a significance of $P < 0.0001$. Data for plant groups other than lycophytes, mosses and liverwort come from Wright *et al.* (2004), Zhang *et al.* (2015), Tosens *et al.* (2016) and Veromann-Jürgenson *et al.* (2017).

gymnosperms (Veromann-Jürgenson *et al.*, 2017), and from 0.096 μm (Han *et al.*, 2016) to 0.540 μm in angiosperms (Tomás *et al.*, 2013), whereas most mosses had a $T_{cw} > 1$ μm, the highest value being 3.4 μm in *D. freycinetti* (Table S6). Moreover, the values of S_c/S in mosses were among the lowest reported for ferns and spermatophytes (Onoda *et al.*, 2017). These two anatomical traits were strongly correlated with both area- and mass-based net photosynthesis (Fig. 6a,b and c,d, respectively), suggesting that these two traits explain a large part of variability of observed g_{nsd}. In addition, the other anatomical traits of these plant groups with particularly diverse photosynthetic organs (Fig. 4) also pointed to a high CO_2 diffusive resistance. Photosynthetic organs were especially thin in unistratose species, but within the pool of leaf thicknesses reported for tracheophytes in the species with multiple cell layers (Tosens *et al.*, 2012a,b, 2016; Tomás *et al.*, 2013; Xiong *et al.*, 2017; Veromann-Jürgenson *et al.*, 2017; Carriquí *et al.*, 2018; Table S6). The fraction of photosynthetic tissue occupied by intercellular air space f_{ias}, existing only in *M. polymorpha*, lycophytes and in the 'pseudomesophyll' of *Polytrichum* species, also ranged within the values reported for tracheophytes (Tosens *et al.*, 2012a,b, 2016; Tomás *et al.*, 2013). Moreover, all the species studied had a low S_c/S_m ratio (< 0.7), which suggests that many CO_2 molecules do not cross the cell wall specifically where there is a close chloroplast, implying that their CO_2 pathway (and resistance) would be larger. Neither leaf density D_{leaf}, T_{leaf}, T_{cw} nor S_c/S correlated with LMA (for lycophytes, liverworts and *Polytrichum* species) and CMA (for other moss species) (Fig. 5a–d).

Nonstomatal diffusion conductance modelled from anatomical traits g_{nsd_ANAT} was also very low in bryophytes and lycophytes, confirming with a fully independent method the estimations made from Chl fluorescence, g_{nsd_FLU} (Table S8; Fig. S4). The g_{nsd_ANAT} in these plants was low no matter which value was assumed for the cell wall porosity p_{cw}; see Methods S1.

Finally, a g_{nsd_ANAT} limitation analysis was performed to test the relative importance of each liquid-phase limitation. Whereas both cell wall and chloroplast thickness were the major components limiting g_{nsd_ANAT} in the single liverwort species, cell walls imposed on average more than the 65% of g_{nsd_ANAT} limitations in mosses, being three times greater than the limitation imposed by the chloroplast (Fig. 7). In the case of lycophytes, despite their gigantic chloroplasts (Table S7), g_{nsd_ANAT} was also limited mainly by cell walls (Fig. 7). Thus, bryophytes and lycophytes are revealed as the groups presenting the highest CO_2 diffusive resistance, which is mainly driven by extremely high T_{cw} and low S_c/S.

Impacts of anatomically reduced CO_2 diffusion on the LES in bryophytes and lycophytes

The LES is a set of relationships that reflect the physical influence of leaf structure and N content on net photosynthesis (Wright *et al.*, 2004). By characterizing climate-diverse species from around the world and with a wide range of morphologies, we demonstrate that mosses' LES diverges from all major vascular plant groups (Fig. 8). Mosses, as already reported for tropical (Waite & Sack, 2010) and temperate species (Wang *et al.*, 2014, 2017), possess a lower mass-based net assimilation rate A_{mass} for a given structural complexity, either considering the CMA or dry LMA than ferns (Karst & Lechowicz, 2007; Tosens *et al.*, 2016), gymnosperms (Wright *et al.*, 2004; Zhang *et al.*, 2015; Veromann-Jürgenson *et al.*, 2017) and angiosperms (Wright *et al.*, 2004; Fig. 8a, b). Despite sharing slopes ($P = 0.19$), differences within intercepts were highly significant ($P < 0.0001$), supporting the hypothesis for a strong anatomically determined g_{nsd} limitation to photosynthesis in mosses. Moreover, the stronger agreement of moss CMA, instead of LMA, with the other plant groups reinforces the analogous function of the moss canopy with the spermatophyte's leaf first suggested by Proctor (2000) and reported by Waite & Sack (2010). Liverworts had a behavior similar to mosses in the A_{mass}–LMA or –CMA relationship (Fig. 8a) but were aligned with tracheophytes (in the same way as lycophytes) in its A_{area} for a given N concentration (Fig. 8c). Even so, more data from these last two groups are needed to verify this. Similar to Wang *et al.* (2017), for the relationship between A_{mass} and the N concentration per mass N_{mass}, mosses had a lower photosynthesis than the rest of plant groups for the same content of N_{mass}, presenting the same slope ($P = 0.45$) but different intercept ($P < 0.0001$; Fig. 8c). This strongly suggests that biochemical limitation is not the main constraint to A_{mass} and/or that bryophytes allocate comparatively more N than tracheophytes to compounds other than Rubisco, but this is yet to be tested empirically.

Concluding remarks

In summary, this work confirms, using a large number of species, previous evidence that the net CO_2 assimilation capacity of bryophytes and lycophytes is low compared with that of ferns, gymnosperms and angiosperms. Although the absolute values might be viewed with caution due to limitations in the precision of measurements and estimations at these very low rates, several independent lines of evidence suggest that the low photosynthetic capacity exhibited by these species is largely due to low CO_2 diffusion conductance of their tissues, which in turn is largely explained by their anatomy, especially the very thick cell walls and low chloroplast exposure to intercellular air spaces. These characteristics have an effect in the trait relationships of bryophytes (i.e. the LES), so that bryophytes present a lower photosynthetic use efficiency of their leaf and canopy mass areas and N content.

Acknowledgements

The research leading to these results has been supported by the project CTM2014-53902-C2-1-P from the Ministerio de Economía y Competitividad (MINECO, Spain) and the ERDF (FEDER), the project FONDECYT-1171640 from the Fondo Nacional de Desarrollo Científico y Tecnológico (FONDECYT, Chile), by the predoctoral fellowship FPI/1700/2014, awarded to MC, from the Conselleria d'Educació, Cultura i Universitats (Govern de les Illes Balears) and the European Social Fund, and the European Regional Development Fund (Centre of Excellence

EcolChange) and the Estonian Ministry of Science and Education (institutional grants IUT-8-3 and PUT1473).

We are grateful to Dr Javier Martínez-Abaigar and Dr Ana Losada for identifying the Spanish mosses, to Roke Rojas, Dr Shelley Urquhart, Mª Teresa Mínguez, Universitat de València (Secció Microscòpia Electrònica, SCSIE), and Dr Ferran Hierro, Universitat de les Illes Balears (Serveis Cientificotècnics), for technical support during microscopic analyses, to Mateu Fullana-Pericàs and Marcel Font for providing us N content values for the Spanish species, and to Miquel Nadal for his help in the analyses. We wish to thank Comité Polar Español (CPE), CSIC's Unidad de Tecnología Marina (UTM), and the personnel at Base Juan Carlos I and on the vessels *Sarmiento de Gamboa* and *Hespérides* for their help during the Antarctic campaign. Dr Javier Gulías and Dr María J. Clemente are also acknowledged for helping during measurements in Antarctica.

Author contribution

MC, MR-O, MR-C and JF designed the study; MC, MR-O, TJB, WG, RC, KM, AVP-C, LS, MW and JF conducted the experiments; MC, ÜN, TT and JF performed the analysis and MC and JF wrote the first version of manuscript; all authors contributed to the following versions of the manuscript to produce the final version.

ORCID

Timothy J. Brodribb https://orcid.org/0000-0002-4964-6107
Marc Carriquí https://orcid.org/0000-0002-0153-2602
Rafael Coopman https://orcid.org/0000-0001-5646-1875
Jaume Flexas https://orcid.org/0000-0002-3069-175X
Kristiina Mark https://orcid.org/0000-0002-3229-3122
Ülo Niinemets https://orcid.org/0000-0002-3078-2192
Miquel Ribas-Carbó https://orcid.org/0000-0002-7337-2089
Margalida Roig-Oliver https://orcid.org/0000-0002-8727-2564
Lawren Sack https://orcid.org/0000-0002-7009-7202
Tiina Tosens https://orcid.org/0000-0003-3802-2478

References

Arndal MF, Illeris L, Michelsen A, Albert K, Tamstorf M, Hansen BU. 2009. Seasonal variation in gross ecosystem production, plant biomass, and carbon and nitrogen pools in five high arctic vegetation types. *Arctic, Antarctic, and Alpine Research* **41**: 164–173.

Berner RA. 2006. GEOCARBSULF: a combined model for Phanerozoic atmospheric O_2 and CO_2. *Geochimica et Cosmochimica Acta* **70**: 5653–5664.

Boyce CK. 2010. The evolution of plant development in a paleontological context. *Current Opinion in Plant Biology* **13**: 102–107.

Brodribb TJ, Feild TS, Jordan GJ. 2007. Leaf maximum photosynthetic rate and venation are linked by hydraulics. *Plant Physiology* **144**: 1890–1898.

Brodribb TJ, McAdam SAM, Carins Murphy MR. 2017. Xylem and stomata, coordinated through time and space. *Plant, Cell & Environment.* **40**: 872–880.

Carriquí M, Cabrera HM, Conesa MÀ, Coopman RE, Douthe C, Gago J, Gallé A, Galmés J, Ribas-Carbó M, Tomás M *et al.* 2015. Diffusional limitations explain the lower photosynthetic capacity of ferns as compared with angiosperms in a common garden study. *Plant, Cell & Environment* **38**: 448–460.

Carriquí M, Douthe C, Molins A, Flexas J. 2018. Leaf anatomy does not explain apparent short-term responses of mesophyll conductance to light and CO_2 in tobacco. *Physiologia Plantarum.* doi: 10.1111/ppl.12755

Clayton-Greene KA, Collins NJ, Green TGA, Proctor MCF. 1985. Surface wax, structure and function in leaves of Polytrichaceae. *Journal of Bryology* **13**: 549–562.

Edwards D, Wellman CH, Axe L. 1998. Interrelationships between primitive embryophytes and the fossil record of early land plants: too little and too late? In: Bates JW, Ashton NW, Duckett JG, eds. *Bryology for the twenty-first century.* Leeds, UK: British Bryological Society, 15–43.

Evans JR, Kaldenhoff R, Genty B, Terashima I. 2009. Resistances along the CO_2 diffusion pathway inside leaves. *Journal of Experimental Botany* **60**: 2235–2248.

Flexas J, Barbour MM, Brendel O, Cabrera HM, Carriquí M, Díaz-Espejo A, Douthe C, Dreyer E, Ferrio JP, Gago J *et al.* 2012. Mesophyll conductance to CO_2: an unappreciated central player in photosynthesis. *Plant Science* **193–194**: 70–84.

Flexas J, Escalona JM, Evain S, Gulías J, Moya I, Osmond CB, Medrano H. 2002. Steady-state chlorophyll fluorescence (F_s) measurements as a tool to follow variations of net CO_2 assimilation and stomatal conductance during water-stress in C_3 plants. *Physiologia Plantarum* **114**: 231–240.

Gago J, Coopman RE, Cabrera HM, Hermida C, Molins A, Conesa MÀ, Galmés J, Ribas-Carbó M, Flexas J. 2013. Photosynthesis limitations in three fern species. *Physiologia Plantarum* **149**: 599–611.

Gallé A, Florez-Sarasa I, Tomas M, Pou A, Medrano H, Ribas-Carbó M, Flexas J. 2009. The role of mesophyll conductance during water stress and recovery in tobacco (*Nicotiana sylvestris*): acclimation or limitation? *Journal of Experimental Botany* **60**: 2379–2390.

Glime JM. 2007. *Bryophyte ecology. Volume 1: physiological ecology.* Ebook sponsored by Michigan Technological University and the International Association of Bryologists. [WWW document] URL http://www.bryoecol.mtuy.edu/ [accessed 29 November 2017].

Goffinet B, Cox CJ, Shaw K, Hedderson TA. 2001. The Bryophyta (mosses): systematic and evolutionary inferences from an *rps4* gene (cpDNA) phylogeny. *Annals of Botany* **87**: 191–208.

Graham LE, Gray J. 2001. The origin, morphology, and ecophysiology of early embryophytes: neontological and paleontological perspectives. In: Gensel PG, Edwards D, eds. *Plants invade the land: evolutionary and environmental perspectives.* New York, NY, USA: Columbia University Press, 140–158.

Grassi G, Magnani F. 2005. Stomatal, mesophyll conductance and biochemical limitations to photosynthesis as affected by drought and leaf ontogeny in ash and oak trees. *Plant, Cell & Environment* **28**: 834–849.

Green TGA, Sancho LG, Pintado A. 2011. Ecophysiology of desiccation/rehydration cycles in mosses and lichens. In: Lüttge U, Beck E, Bartels D, eds. *Plant desiccation tolerance.* Berlin, Germany: Springer, 89–120.

Griffiths H, Maxwell K, Richardson D, Robe W. 2004. Turning the land green: inferring photosynthetic physiology and diffusive limitations in early bryophytes. In: Hemsley AR, Poole I, eds. *The evolution of plant physiology.* Amsterdam, Netherlands: Elsevier Academic Press, 3–16.

Gu L, Pallardy SG, Tu K, Law BE, Wullschleger SD. 2010. Reliable estimation of biochemical parameters from C_3 leaf photosynthesis–intercellular carbon dioxide response curves. *Plant, Cell & Environment* **33**: 1852–1874.

Gu L, Sun Y. 2014. Artefactual responses of mesophyll conductance to CO_2 and irradiance estimated with the variable *J* and online isotope discrimination method. *Plant, Cell & Environment* **37**: 1231–1249.

Han J-M, Meng H-F, Wang S-Y, Jiang C-D, Liu F, Zhang W-F, Zhang Y-L. 2016. Variability of mesophyll conductance and its relationships with water use efficiency in cotton leaves under drought pretreatment. *Journal of Plant Physiology* **194**: 61–71.

Hanson DT, Renzaglia K, Villarreal JC. 2014. Diffusional limitations to CO_2 concentrating mechanisms in bryophytes. In: Hanson DT, Rice SK, eds. *Photosynthesis in bryophytes and early land plants.* Berlin, Germany: Springer, 95–111.

Hedderson TAJ, Chapman RL, Rootes WL. 1996. Phylogenetic relationships of bryophytes inferred from nuclear-encoded rRNA gene sequences. *Plant Systematics and Evolution* **200**: 213–224.

Hue NV, Uchida R, Ho MC. 2000. Sampling and analysis of soils and plant tissues. In: Silva JA, Uchida RS, eds. *Plant nutrient management in Hawaii's soils: approaches for tropical and subtropical agriculture*. Honolulu, HI, USA: University of Hawaii, 23–30.

Karst AL, Lechowicz MJ. 2007. Are correlations among foliar traits in ferns consistent with those in the seed plants? *New Phytologist* **173**: 306–312.

Kenrick P, Crane C. 1996. *Embryophytes. Land plants. Version 01 January 1996.* http://tolweb.org/Embryophytes/20582/1996.01.01 in The Tree of Life Web Project, http://tolweb.org/ [accessed 23 November 2017].

Kostka JE, Weston DJ, Glass JB, Lilleskov EA, Shaw AJ, Turetsky MR. 2016. The *Sphagnum* microbiome: new insights from an ancient plant lineage. *New Phytologist* **211**: 57–64.

Maseyk KS, Green TGA, Klinac D. 1999. Photosynthetic responses of New Zealand *Sphagnum* species. *New Zealand Journal of Botany* **37**: 155–165.

Meyer M, Seibt U, Griffiths H. 2008. To concentrate or ventilate? Carbon acquisition, isotope discrimination and physiological ecology of early land plant life forms. *Philosophical Transactions of the Royal Society of London. Series B: Biological Sciences* **363**: 2767–2778.

Niinemets Ü, Díaz-Espejo A, Flexas J, Galmés J, Warren CR. 2009. Role of mesophyll conductance in constraining potential photosynthetic productivity in the field. *Journal of Experimental Botany* **60**: 2249–2270.

Niinemets Ü, Reichstein M. 2003. Controls on the emission of plant volatiles through stomata: a sensitivity analysis. *Journal of Geophysical Research* **108**: e4211.

Onoda Y, Wright IJ, Evans JR, Hikosaka K, Kitajima K, Niinemets Ü, Poorter H, Tosens T, Westoby M. 2017. Physiological and structural tradeoffs underlying the leaf economics spectrum. *New Phytologist* **214**: 1447–1463.

Peguero-Pina JJ, Sancho-Knapik D, Flexas J, Galmés J, Niinemets Ú, Gil-Pelegrín E. 2016. Light acclimation of photosynthesis in two closely related firs (*Abies pinsapo* Boiss. and *Abies alba* Mill.): the role of leaf anatomy and mesophyll conductance to CO_2. *Tree Physiology* **36**: 300–310.

Porada P, Weber B, Elbert W, Poschl U, Kleidon A. 2013. Estimating global carbon uptake by lichens and bryophytes with a process-based model. *Biogeosciences* **10**: 6989–7033.

Proctor MCF. 2000. The bryophyte paradox: tolerance of desiccation, evasion and drought. *Plant Ecology* **151**: 41–49.

Proctor MCF. 2001. Patterns of desiccation tolerance and recovery in bryophytes. *Plant Growth Regulation* **25**: 147–156.

Proctor MCF, Oliver MJ, Wood AJ, Alpert P, Stark LR, Cleavitt NL, Mishler BD. 2007. Desiccation-tolerance in bryophytes: a review. *The Bryologist* **110**: 595–621.

Reich PB, Walters MB, Ellsworth DS. 1997. From tropics to tundra: global convergence in plant functioning. *Proceedings of the National Academy of Sciences, USA* **94**: 13730–13734.

Renzaglia KS, Duff RJ, Nickrent DL, Garbary DJ. 2004. Vegetative and reproductive innovations of early land plants: implications for a unified phylogeny. *Philosophical Transactions of the Royal Society of London. Series B: Biological Sciences* **363**: 2641–2650.

Renzaglia KS, Schuette S, Duff RJ, Ligrone R, Shaw AJ, Mishler BD, Duckett JG. 2007. Bryophyte phylogeny: advancing the molecular and morphological frontiers. *The Bryologist* **110**: 179–213.

Rice SK, Cornelissen JHC. 2014. Best practices for measuring photosynthesis at multiple scales. In: Hanson DT, Rice SK, eds. *Photosynthesis in bryophytes and early land plants*. Berlin, Germany: Springer, 79–93.

Rice SK, Giles L. 1996. The influence of water content and leaf anatomy on carbon isotope discrimination and photosynthesis in *Sphagnum*. *Plant, Cell & Environment* **19**: 118–124.

Rice SK, Gutman C, Krouglicof N. 2005. Laser scanning reveals bryophyte canopy structure. *New Phytologist* **162**: 695–704.

Ruszala EM, Beerling DJ, Franks PJ, Chater C, Casson SA, Gray JE, Hetherington AM. 2011. Land plants acquired active stomatal control early in their evolutionary history. *Current Biology* **21**: 1030–1035.

Schneider CA, Rashband WS, Eliceiri KW. 2012. NIH Image to ImageJ: 25 years of image analysis. *Nature Methods* **9**: 671–675.

Shaw J, Renzaglia K. 2004. Phylogeny and diversification of bryophytes. *American Journal of Botany* **91**: 1557–1581.

Silvola J, Aaltonen H. 1984. Water content and photosynthesis in the peat mosses *Sphagnum fuscum* and *S. angustifolium*. *Annales Botanici Fennici* **21**: 1–6.

Sjögersten S, van der Wal R, Woodin SJ. 2006. Small-scale hydrological variation determines landscape CO_2 fluxes in the high Arctic. *Biogeochemistry* **80**: 205–216.

Syvertsen JP, Lloyd J, McConchie C, Kriedemann PE, Farquhar GD. 1995. On the relationship between leaf anatomy and CO_2 diffusion through the mesophyll of hypostomatous leaves. *Plant, Cell & Environment* **18**: 149–157.

Terashima I, Hanba YT, Tholen D, Niinemets Ü. 2011. Leaf functional anatomy in relation to photosynthesis. *Plant Physiology* **155**: 108–116.

Thain JF. 1983. Curvature correlation factors in the measurements of cell surface areas in plant tissues. *Journal of Experimental Botany* **34**: 87–94.

Titus JE, Wagner DJ. 1984. Carbon balance for two *Sphagnum* mosses: water balance resolves a physiological paradox. *Ecology* **65**: 1109–1115.

Tomás M, Flexas J, Copolovici L, Galmés J, Hallik L, Medrano H, Tosens T, Vislap V, Niinemets Ü. 2013. Importance of leaf anatomy in determining mesophyll diffusion conductance to CO_2 across species: quantitative limitations and scaling up by models. *Journal of Experimental Botany* **64**: 2269–2281.

Tosens T, Niinemets Ü, Vislap V, Eichelmann H, Castro-Díez P. 2012a. Developmental changes in mesophyll diffusion conductance and photosynthetic capacity under different light and water availabilities in *Populus tremula*: how structure constrains function. *Plant, Cell & Environment* **35**: 839–856.

Tosens T, Niinemets Ü, Westoby M, Wright IJ. 2012b. Anatomical basis of variation in mesophyll resistance in eastern Australian sclerophylls: news of a long and winding path. *Journal of Experimental Botany* **63**: 5105–5119.

Tosens T, Nishida K, Gago J, Coopman RE, Cabrera HM, Carriquí M, Laanisto L, Morales L, Nadal M, Rojas R *et al.* 2016. The photosynthetic capacity in 35 ferns and fern allies: mesophyll CO_2 diffusion as a key trait. *New Phytologist* **209**: 1576–1590.

Turetsky MR, Bond-Lamberty B, Euskirchen E, Talbot J, Frolking S, McGuire AD, Tuittila E-S. 2012. The resilience and functional role of moss in boreal and arctic ecosystems. *New Phytologist* **196**: 49–67.

Turetsky MR, Mack MC, Hollingsworth TN, Harden JW. 2010. The role of mosses in ecosystem succession and function in Alaska's boreal forest. *Canadian Journal of Forest Research* **40**: 1237–1264.

Varone L, Ribas-Carbo M, Cardona C, Gallé A, Medrano H, Gratani L, Flexas J. 2012. Stomatal and non-stomatal limitations to photosynthesis in seedlings and saplings of Mediterranean species pre-conditioned and aged in nurseries: Different response to water stress. *Environmental and Experimental Botany* **75**: 235–247.

Veromann-Jürgenson L-L, Tosens T, Laanisto L, Niinemets Ü. 2017. Extremely thick cell walls and low mesophyll conductance: welcome to the world of ancient living!. *Journal of Experimental Botany* **68**: 1639–1653.

Wagner S, Zotz G, Salazar AN, Bader MY. 2013. Altitudinal changes in temperature responses of net photosynthesis and dark respiration in tropical bryophytes. *Annals of Botany* **111**: 455–465.

Waite M, Sack L. 2010. How does moss photosynthesis relate to leaf and canopy structure? Trait relationships for 10 Hawaiian species of contrasting light habitats. *New Phytologist* **185**: 156–172.

Wang Z, Bader MY. 2018. Associations between shoot-level water relations and photosynthetic responses to water and light in 12 moss species. *AoB Plants* **10**: ply034.

Wang Z, Bao W, Feng D, Lin H. 2014. Functional trait scaling relationships across 13 temperate mosses growing in wintertime. *Ecological Research* **29**: 629–639.

Wang Z, Liu X, Bader MY, Feng D, Bao W. 2017. The 'plant economic spectrum' in bryophytes, a comparative study in subalpine forest. *American Journal of Botany* **104**: 261–270.

Wang Z, Liu X, Bao W. 2016. Higher photosynthetic capacity and different functional trait scaling relationships in erect bryophytes compared with prostrate species. *Oecologia* **180**: 359–369.

Warton DI, Duursma RA, Falster DS, Taskinen S. 2012. SMART 3: an R package for estimation and inference about allometric lines. *Methods in Ecology and Evolution* **3**: 257–259.

Warton DI, Wright IJ, Falster DS, Westoby M. 2006. Bivariate linefitting methods for allometry. *Biological Reviews* **81**: 259–291.

Wright IJ, Reich PB, Westoby M, Ackerly DD, Baruch Z, Bongers F, Cavender-Bares J, Chapin T, Cornelissen JHC, Diemer M *et al.* 2004. The worldwide leaf economics spectrum. *Nature* **428**: 821–827.

Xiong D, Huang J, Peng S, Li Y. 2017. A few enlarged chloroplasts are less efficient in photosynthesis than a large population of small chloroplasts in *Arabidopsis thaliana*. *Scientific Reports* **7**: e5782.

Zhang Y-J, Cao K-F, Sack L, Li N, Wei X-M, Goldstein G. 2015. Extending the generality of leaf economic design principles in the cycads, an ancient lineage. *New Phytologist* **206**: 817–829.

Supporting Information

Additional Supporting Information may be found online in the Supporting Information section at the end of the article:

Fig. S1 Maximum velocity of carboxylation ($V_{c,max}$) in relation to electron transport rate (ETR).

Fig. S2 Hypothetical relationships between cell wall porosity and thickness.

Fig. S3 Comparison of g_{nsd_FLU} estimated with the variable J method and modelled from anatomy.

Fig. S4 Limitation analysis on g_{nsd_ANAT}.

Methods S1 Detailed materials and methods.

Notes S1 List of abbreviations for traits.

Table S1 Climate, range of dispersal and microhabitat.

Table S2 Environmental conditions.

Table S3 Measured data available.

Table S4 Average values for diffusional and biochemical photosynthetic characteristics.

Table S5 Agreement between maximum velocity of carboxylation ($V_{c,max}$) obtained from fast and slow A_{area}–C_a curves.

Table S6 Average values for morphological and structural traits.

Table S7 Average values for ultrastructural characteristics.

Table S8 Average values for non-stomatal diffusion conductance modelled from anatomy.

Table S9 Average values for nitrogen content.

Table S10 Sensitivity analysis of the effects of biases in Γ^*, α, and R_d on the estimation of g_{nsd_FLU}.

Video S1 Measurement of anatomical foliage traits in two species.

Please note: Wiley Blackwell are not responsible for the content or functionality of any Supporting Information supplied by the authors. Any queries (other than missing material) should be directed to the *New Phytologist* Central Office.

New Phytologist - Supporting Information

Tables S1-S8, Figs S1-S1 and Movie S1

Article title: Anatomical constraints to non-stomatal diffusion conductance and photosynthesis in lycophytes and bryophytes

Authors: Marc Carriquí, Margalida Roig-Oliver, Timothy J. Brodribb, Warwick Gill, Rafael E. Coopman, Kristiina Mark, Ülo Niinemets, Alicia V. Perera-Castro, Miquel Ribas-Carbó, Lawren Sack, Tiina Tosens, Mashuri Waite, Jaume Flexas

Article acceptance date: 22 December 2018

The following Supporting Information is available for this article:

Methods S1 Detailed materials and methods

Notes S1 List of abbreviations

Table S1 Climate, range of dispersal and microhabitat

Table S2 Environmental conditions

Table S3 Measured data available

Table S4 Average values for diffusional and biochemical photosynthetic characteristics

Table S5 Agreement between maximum velocity of carboxylation ($V_{c,max}$) obtained from fast and slow A_{area}-C_a curves.

Table S6 Average values for morphological and structural traits

Table S7 Average values for ultrastructural characteristics

Table S8 Average values for non-stomatal diffusion conductance modelled from anatomy

Table S9 Average values for nitrogen content

Table S10 Sensitivity analysis of the effects of biases in Γ*, α, and R_d on the estimation of g_{nsd_FLU}

Fig. S1. Maximum velocity of carboxylation ($V_{c,max}$) in relation to electron transport rate (ETR).

Fig. S2 Hypothetical relationships between cell wall porosity and thickness.

Fig. S3 Comparison of g_{nsd_FLU} estimated with the variable J method and modelled from anatomy

Fig. S4 Limitation analysis on g_{nsd_ANAT}

Video S1 Measurement of anatomical foliage traits in two species

Methods S1

Experimental sites

In Antarctica, the study site was Livingston Island (South Shetland Islands; 62º39'94''S, 60º23'20''W, 12 masl, mean annual precipitation 377 mm and mean min/max annual temperatures -4.6/2.6 ºC). Measurements were performed in January, i.e. high summer (mean min/max temperatures -0.4/2.7 ºC). In Australia the study site was Hobart (Tasmania; 42º54'17''S 147º19'28''E, 57 masl, mean annual precipitation 494 mm and mean min/max annual temperatures 8.1/17.6 ºC). Measurements were performed in December (mean min/max temperatures 10.8/20.3 ºC). In Estonia, the study site was Tartu (58º49'22''N, 26º43'21''E, 72 masl, mean annual precipitation 650 mm and mean min/max annual temperatures 1.0/8.0ºC), and measurements were performed in July (mean min/max temperatures 12.5/22.7 ºC). In Hawaii, the study site was Oahu (21º20'43''N, 157º48'13''W, 591 masl, mean annual precipitation of 3329 mm and mean min/max annual temperatures 21.6/29.1 ºC), and the measurements were performed from January to March (mean min/max temperatures 19.2/26.9 ºC). In Spain, the study site was Palma (Illes Balears, 39º45'51''N, 2º42'33''E, mean annual precipitation 320.8 mm and mean min/max annual temperatures 14.4/21.8 ºC). Measurements were performed from February to April (mean min/max temperatures 8.7/16.0 ºC).

Photosynthesis measurements and estimation of non-stomatal diffusion conductance

Prior to measurements, litter, shoots from other moss species and dead tissue were carefully removed. Photosynthetic tissues were moistened with distilled water for several minutes and external water drops were removed with a tissue paper. Photosynthetic tissues were arranged side by side in the leaf chamber to avoid any overlap. During measurements, parts of the individual remaining outside the chamber were kept moist inside a plastic bag to prevent that its desiccation affected the measurements. The CO_2 fluxes in these groups of plants are especially low, and thus measurements were performed at low flow rates (100-200 μmol air s^{-1} for the 2 cm^2 cuvette and 600-800 μmol air s^{-1} for the 8 cm^2 cuvette, to ensure CO_2 delta values >4 μmol CO_2 mol^{-1} air between sample and reference IRGAs) and at low vapour pressure deficit (*ca* 0.2 - 0.9 kPa). Leaf (i.e., microphyll or thallus/shoots) temperature, measured with a thermocouple, ranged 20-22ºC- a common temperature close to the mean habitat temperature for each study

site, which was reported to be closely related to optimum temperature of net photosynthesis (Wagner *et al.*, 2013). The only exception was in Antarctica, where due to the low temperatures outdoors measurements could be performed only at 13-14°C. Leaf steady-state conditions were induced at saturating photosynthetic photon flux density (PPFD 400 to 1200 μmol m^{-2} s^{-1}, depending on the species, 90% red and 10% blue light) and 400 μmol CO_2 mol^{-1} air. Net photosynthesis was recorded when maximum assimilation was achieved (e.g. when the resistance imposed by external water was minimal), usually 5-10 min after the enclosure of photosynthetic tissue in the chamber for mosses and liverworts, and after 20-30 min for lycophytes to ensure stomatal opening. Dilution correction of water evaporation from the plant material effects on CO_2 fluxes was applied. Responses of net assimilation to ambient CO_2 concentration (C_a) were measured by varying C_a between 50 and 800 μmol CO_2 mol^{-1} for most Australian, Estonian and Spanish species (Table S3). These measurements lasted for about 15 minutes, resulting in some degree of dehydration of the plants during measurements. To check the validity of the method, in some species, additional CO_2 response curves were performed on which plants were rehydrated after each measurement at a given C_a. At each C_a, assimilation was monitored during a few minutes, and a trend was observed consisting in progressive increases of photosynthesis during the first 4-5 minutes (likely reflecting the removal of water in the moss surface restricting CO_2 diffusion), a steady-state maximum during the next 7-9 minutes, and a slow but progressive decline thereafter (likely reflecting the effects of dehydration). The data used were those at the maximum steady-state rate. Data from CO_2 response curves were corrected for cuvette leakage as in Flexas *et al.* (2007). Simultaneous to gas exchange, the steady-state fluorescence level (F) was recorded and a saturating light pulse was given by the leaf chamber fluorimeter to measure the maximum fluorescence yield (F_m') and estimate the effective photosystem II quantum yield (ΦP_{SII}) as (F_m'-F)/F_m' (Genty *et al.*, 1989).

Mitochondrial respiration rate (R_n) was measured at predawn or after dark-acclimating the photosynthetic tissue for at least 60 min (except for the Hawaiian mosses where R_n was measured without dark acclimation). Non-photorespiratory CO_2 respiration in the light (R_d) was estimated as half of R_n (Niinemets *et al.*, 2005; Gallé *et al.*, 2009). Photorespiration (P_r) was estimated by combining fluorescence and gas-exchange measurements following Valentini *et al.*, (1995). Net assimilation per unit area (A_{area}) for

all species, and g_s and intercellular CO_2 concentration (C_i) for lycophytes were calculated according to von Caemmerer & Farquhar (1981).

From A_{area}-C_a response curves chloroplastic CO_2 concentration (C_c), non-stomatal diffusion conductance (g_{nsd_FLU}) and the maximum velocity of carboxylation were estimated. Non-stomatal diffusion conductance was calculated for lycophytes according to Harley *et al.* (1992):

$$g_{nsd\_FLU} = \frac{A_{area}}{C_i - \frac{\Gamma^* J_{ETR} + 8(A_{area} + R_d)}{J_{ETR} - 4(A_{area} + R_d)}} \quad (1)$$

where A_{area} is the net assimilation rate, J_{ETR} is the rate of photosynthetic electron transport derived from chlorophyll fluorescence measurements, C_i is the CO_2 concentration in sub-stomatal cavities, R_d is the rate of non-photorespiratory respiration in the light and Γ^* is the hypothetical CO_2 compensation point without R_d. Γ^* was taken as 42.9 μmol mol^{-1} at 25ºC (Bernacchi *et al.*, 2001) as there are no published values for liverwort, moss and lycophyte species. J_{ETR} was estimated as $J_{ETR} = PPFD \times \Phi P_{SII} \times \alpha \times \beta$ (Genty *et al.* 1989), being α the leaf absorbance and β the electron partitioning between photosystems I and II. The α × β product was estimated from additional A-C_a curves performed at non-photorespiratory conditions (2% oxygen) following Valentini *et al.* (1995). In the case of liverwort and moss species, because they lack stomata, g_{nsd_FLU} was calculated considering C_a (i.e. the CO_2 concentration inside the gas exchange cuvette) instead of C_i:

$$g_{nsd\_FLU} = \frac{A_{area}}{C_a - \frac{\Gamma^* J_{ETR} + 8(A_{area} + R_d)}{J_{ETR} - 4(A_{area} + R_d)}} \quad (2)$$

Notably, this apparent g_{nsd_FLU} would in principle be influenced by the cuticular conductance, but cuticles are either absent or very thin in bryophytes (Proctor, 2010; Hanson *et al.*, 2014). $V_{c,max}$ was estimated according to Farquhar *et al.* (1980). The previous parameters were measured/estimated in three to twelve individuals per species. Photosynthesis per unit of dry mass at leaf scale was calculated by dividing A_{area} by leaf dry mass per area (LMA).

To determine the photosynthetic area enclosed in the gas exchange cuvette during measurements, once these were finished, digital pictures of the enclosed photosynthetic organs were taken. Species having photosynthetic organs resembling higher plant's

leaves, i.e. lycophytes, *Polytrichum* and liverworts, were dissected and their total photosynthetic area determined. In the other species, i.e. mosses, the entire shoot was used to determine their projected area. In the species where this was possible, shoots were also dissected and the real total photosynthetic area determined. All areas were estimated using ImageJ (Schneider *et al.*, 2012). The fact of using projected area instead of photosynthetic area in mosses is due to their particular canopy anatomy. Waite and Sack (2010) already showed that the canopy mass area (CMA) of mosses is functionally analogous to the LMA of angiosperms. Additionally, using shoot projected photosynthetic area instead of total photosynthetic area in mosses other than *Polytrichum* species resulted in ETR/A_{area} ratios closer to 8, which is the reference value for the rest of C_3 terrestrial plants (Table S4; Flexas *et al.*, 2002) and only these data fulfill the reliability criterion established by Harley *et al.* (1992) for estimates of g_{nsd} using this method (data not shown).

Sample preparation for leaf anatomy

Samples from Antarctica, Estonia and Spain were quickly fixed under vacuum with solution of glutaraldehyde (4%) and paraformaldehyde (2%) in a 0.1 M phosphate buffer (pH = 7.4). Subsequently, the samples were postfixed in 2% osmium tetroxide for 2h, and dehydrated in a graded series of ethanol. Dehydrated segments were embedded in LR-White resin and solidified in an oven at 60ºC for 48h. Semi-thin (0.8 µm) and ultra-thin (90 nm) cross sections were cut with an ultramicrotome (Leica UC6). Semi-thin sections were dyed with 1% toluidine blue and observed under an Olympus BX60 or a Nikon Eclipse E600 optical microscope. Samples from Australia were fixed under vacuum in 2.5% glutaraldehyde in 0.1M phosphate buffer (pH 7.4) and dehydrated in an acetone series and embedded in Spurr's resin. Semi-thick sections (4-5 µm) cut on a Reichert OmU2 ultramicrotome were stained with 0.1% toluidine blue in 1% borax and mounted in Euparal. For Hawaiian species, fresh samples were cross-sectioned to be 5-20 µm thick (CM1850 Cryostat; Leica Microsystems, Nussloch, Germany), mounted fresh with water and photographed at 63 to 400x.

Non-stomatal conductance modelled from anatomical characteristics

The 1-D gas diffusion model of Niinemets & Reichstein (2003) was applied as modified by Tomás et al. (2013), with some particularities depending on the different foliar anatomies, some of which are very different as compared to a *classic* leaf (Fig. 4). The model allows estimating the theoretical non-stomatal diffusion conductance (g_{nsd_ANAT}). This model considers g_{nsd_ANAT} as a composite conductance for within-leaf gas and liquid components, considered as:

$$g_{nsd\_ANAT} = \frac{1}{\frac{1}{g_{ias}} + \frac{RT_k}{H \cdot g_{liq}}} \quad (3)$$

where g_{ias} is the gas phase conductance inside the leaf from substomatal cavities to outer surface of cell walls, g_{liq} is the conductance in liquid and lipid phases from outer surface of cell walls to chloroplasts, R is the gas constant (Pa m^3 K^{-1} mol^{-1}), T_k is the absolute temperature (K), and H is the Henry's law constant for CO_2 at the given temperature (Pa m^3 mol^{-1}). g_{nsd_ANAT} is defined as a gas-phase conductance, and thus $H/(RT_k)$, the dimensionless form of Henry's law constant, is needed to convert g_{liq} to corresponding gas-phase equivalent conductance (Niinemets & Reichstein, 2003). In the model, the gas-phase conductance (and the reciprocal term, r_{ias}) is determined by average gas-phase thickness, ΔL_{ias}, and gas-phase porosity, f_{ias} (fraction of leaf air space):

$$g_{ias} = \frac{1}{r_{ias}} = \frac{D_a \cdot f_{ias}}{\Delta L_{ias} \cdot \varsigma} \quad (4)$$

where D_a (m^2 s^{-1}) is the diffusion coefficient for CO_2 in the gas phase at the given temperature and ς is the diffusion path tortuosity (m m^{-1}). ΔL_{ias} was taken as half the photosynthetic organ thickness. Except for *Polytrichum* species, g_{ias} was considered to be infinite in moss species, as they only have one layer of cells or multiple layers of cells but without intercellular airspace. The partial determinants of the liquid-phase diffusion pathway (the reciprocal term r_i, where $_i$ stands either for cell wall, cytosol, or stroma conductance) were calculated as:

$$g_i = \frac{1}{r_i} = \frac{r_{f,i} \cdot D_w \cdot p_i}{\Delta L_i} \quad (5)$$

where ΔL_i (m) is the diffusion path length in the corresponding component of the diffusion pathway, p_i (m^3 m^{-3}) is its effective porosity, and D_w is the aqueous phase

diffusion coefficient for CO_2 at the given temperature. The dimensionless factor $r_{f,i}$ accounts for the reduction of D_w compared with free diffusion in water, and was taken as 1.0 for cell walls (Rondeau-Mouro *et al.*, 2008) and 0.3 for cytosol and stroma (Niinemets & Reichstein, 2003). In addition, $r_{f,i}$ values for cytosol and stroma were taken as 0.3. p_i was set to 1.0 for cytosol and stroma. Due to the lack of direct measurements of cell wall effective porosity (p_{cw}; representing tortuosity/porosity) for land plants, three different possibilities were explored to determine their effect on the final modelled g_{nsd_ANAT}. First, a constant p_{cw} of 0.1 m^3 m^{-3} was considered following Tomás *et al.* (2014). Second, a constant p_{cw} of 0.028 m^3 m^{-3}, i.e. the minimum value of p_{cw} considered in Tomás *et al.* (2013) and Tosens *et al.* (2016), was tested. Third, a variable p_{cw} inversely correlated with T_{cw} was tested, following previous suggestions by Terashima *et al.* (2006) and Evans *et al.* (2009), and later applications by Tomás *et al.* (2013), Tosens *et al.* (2016) and Veromann-Jürgenson *et al.* (2017). However, because T_{cw} for some bryophytes in this study are one order of magnitude higher than in most tracheophytes, previously reported p_{cw}-T_{cw} regressions and slopes seemed unreliable (Fig. S2). For example, Tomás *et al.* (2013) assumed an exponential decay p_{cw}-T_{cw} regression, assigning a constant p_{cw} of 0.028 for species with $T_{cw} > 0.4$ µm. Even more unreliable is that by Tosens *et al.* (2016), who assumed a negative linear relationship resulting in negative values of p_{cw} for species with $T_{cw} > 1.0$ µm, i.e. for most species studied here. In this third case, p_{cw} was estimated assuming a linear regression from *Gossypium hirsutum*- the reported species with thinnest cell walls (Han *et al.*, 2016)-, which was assigned a p_{cw} of 0.3 m^3 m^{-3} (Nobel 1991), to *Distichophyllum freicinetii*- the reported species with thickest cell walls (the present study)-, which was assigned a p_{cw} of 0.028 m^3 m^{-3} (Fig. S2). Both three p_{cw} estimates gave a significant positive correlation between g_{nsd_ANAT} and g_{nsd_FLU}, although the highest correlation ($r^2 = 0.73$, $P < 0.001$) and the closest to the 1:1 relationship was obtained when a constant p_{cw} of 0.028 was considered (Table S8; Fig. S4). We used an estimate of 0.0035 m s^{-1} for both plasma membrane conductance (g_{pl}) and chloroplast envelope conductance (g_{env}) as previously suggested (Evans *et al.*, 1994; Tosens *et al.*, 2012a). Following Tosens *et al.* (2012a) and Tomás *et al.* (2013), we did not include the potential effect of carbonic anhydrase in our analysis.

As in previous studies (Tosens *et al.*, 2012a), total liquid-phase diffusion conductance was scaled by S_c/S ratio, defining the number of parallel diffusion pathways from outer surfaces of cell wall to chloroplasts.

$$g_{liq} = \frac{S_c}{(r_{cw} + r_{pl} + r_{cyt} + r_{en} + r_{st})\, S} \tag{6}$$

Two different pathways of CO_2 inside the cell were considered, one for cell wall parts with chloroplasts and the other for interchloroplastical areas as described by Tholen *et al.* (2012). For exposed cell wall portions lined with chloroplasts, the partial liquid phase conductance, $g_{cel,1}$, inside the cell is given as:

$$g_{cel,1} = \frac{1}{r_{cyt,1} + r_{env} + r_{st,1}} \tag{7}$$

where $r_{cyt,1}$ and $r_{st,1}$ are cytosolic resistance from the plasmalemma inner surface to the outer surface of chloroplasts and the stromal resistance in the direction perpendicular to cell wall, respectively, both calculated by Eqn 5. For $r_{cyt,1}$, the diffusion pathway length, $\Delta L_{cyt,1}$, is given as the average distance between the chloroplasts and cell wall in cell wall areas lined by chloroplasts, whilst for $r_{st,1}$, ΔL_i, was taken as half of the chloroplast thickness, $\Delta T_{chl}/2$. For the cell wall portions without chloroplasts, the partial conductance, $g_{cel,2}$, is given analogously as:

$$g_{cel,2} = \frac{1}{r_{cyt,2} + r_{env} + r_{st,2}} \tag{8}$$

Where $r_{cyt,2}$ is the cytosolic resistance from interchloroplastic cell wall portions towards the chloroplast and $r_{st,2}$ is the stromal conductance in a direction parallel with the cell wall. The diffusion path length for $r_{cyt,2}$, $\Delta L_{cyt,2}$, is driven both by the distance between the neighboring chloroplasts, chloroplast thickness, and chloroplast distance from the cell wall and was approximated as:

$$\Delta L_{cyt,2} = \sqrt{\left(\frac{\Delta T_{chl}}{2} + \Delta L_{cyt,1}\right)^2 + \left(\frac{\Delta L_{chl}}{2}\right)^2} \tag{9}$$

where ΔL_{chl} is the distance between the neighboring chloroplasts. $\Delta L_{cyt,2}$ was calculated as a harmonic average, which more correctly represents the diffusion pathway of $r_{cyt,2}$. Finally, the diffusion pathway length for $r_{st,2}$ was taken as a quarter of the chloroplast length.

Considering further that the fraction of exposed cell wall area lined with chloroplasts is given by S_c/S_m and the fraction free of chloroplasts as $1\text{-}S_c/S_m$, the total cellular conductance (sum of parallel conductances) is given as:

$$g_{cel,tot} = \frac{S_c}{S_m} g_{cel,1} + \left(1 - \frac{S_c}{S_m}\right) g_{cel,2} \quad (10)$$

Total liquid phase conductance from the outer surface of cell walls to carboxylation sites in the chloroplasts is the sum of serial conductances in the cell wall, plasmalemma, and inside the cell:

$$g_{liq} = \frac{S_m}{\left(r_{cw} + r_{pl} + r_{cel,tot}\right) S} \quad (11)$$

In the case of *Leucobryum semmannii*, a species in which only small central cells have chloroplasts, the resistance to CO_2 diffusion imposed by the external layer of cells was accounted for in the model.

Quantitative limitation analysis of A_N and partial limitations of g_{nsd}

The relative limitations on A_{area} for lycophytes were calculated following Grassi & Magnani (2005) as applied in Tomás et al. (2013). This analysis quantifies the relative importance of stomatal, non-stomatal diffusion conductance and biochemical limitations (the latter integrating both Rubisco and photochemistry/Calvin cycle, owing to the fact that photosynthesis operates at co-limitation between these two factors; see Gallé *et al.*, 2009, and Varone *et al.*, 2012, for further explanation). Fractional limitations, that is, those imposed by limited stomatal (l_s) or non-stomatal diffusion conductance (l_{nsd}), and reduced biochemical capacity (l_b), were calculated as:

$$l_s = \frac{\frac{g_{tot}}{g_s} \cdot \frac{\partial A_{area}}{\partial C_c}}{g_{tot} + \frac{\partial A_{area}}{\partial C_c}} \quad (12)$$

$$l_{nsd} = \frac{\frac{g_{tot}}{g_{nsd\_FLU}} \cdot \frac{\partial A_{area}}{\partial C_c}}{g_{tot} + \frac{\partial A_{area}}{\partial C_c}} \quad (13)$$

$$l_b = \frac{g_{tot}}{g_{tot} + \frac{\partial A_{area}}{\partial C_c}} \quad (14)$$

where g_s and g_{nsd_FLU} are the stomatal and non-stomatal diffusion conductances to CO_2 and g_{tot} is the total conductance (the sum of inversed serial conductances g_{nsd_FLU} and g_s). $\delta A_{area}/\delta C_c$ is the slope of A_{area}-C_c response curves over a C_c range of 50-100 μmol mol^{-1}. In species where A_{area}-C_c response curves was not performed, the quotient A_{area}/C_c was taken as a proxy of $\delta A_{area}/\delta C_c$.

These three values sum 100% and characterize the extent to which any of the three limitations curbs photosynthesis at the given values of the other two. In the case of moss and liverwort species, which lack stomata, l_m and l_b where calculated considering $g_{tot} = g_{nsd\_FLU}$.

The limitations derived from the different components involved in the cellular CO_2 diffusion (cell walls, plasmalemma, cytosol, chloroplast envelope and stroma) were calculated following Tomás *et al.* (2013) as:

$$l_i = \frac{g_{nsd\_ANAT}}{g_i \cdot \frac{S_c}{S}} \quad (15)$$

where l_i is the limitation in the cell wall, plasmalemma, cytosol, chloroplast envelope and stroma, and g_i refers to the diffusion conductance of each corresponding diffusion pathway. The analysis was performed from the g_{nsd_ANAT} model considering a constant effective cell wall porosity of 0.028 (see above).

References

Bernacchi CJ, Singsaas EL, Pimentel C, Portis AR Jr, Long SP. 2001. Improved temperature response functions for models of Rubisco-limited photosynthesis. *Plant, Cell and Environment* **24:** 253–259.

von Caemmerer S, Farquhar GD. 1981. Some relationships between the biochemistry of photosynthesis and the gas exchange of leaves. *Planta* **153:** 376–387.

Evans JR, von Caemmerer S, Setchell BA, Hudson GS. 1994. The relationship between CO2 transfer conductance and leaf anatomy in transgenic tobacco with a reduced content of Rubisco. *Australian Journal of Plant Physiology* **21:** 475-495.

Evans JR, Kaldenhoff R, Genty B, Terashima I. 2009. Resistances along the CO_2 diffusion pathway inside leaves. *Journal of Experimental Botany* **60:** 2235-2248.

Farquhar GH, von Caemmeter S, Berry JA. 1980. A biochemical model of photosynthetic CO_2 assimilation in leaves of C_3 species. *Planta* **149:** 78–90.

Flexas J, Escalona JM, Evain S, Gulías J, Moya I, Osmond CB, Medrano H. 2002. Steady-state chlorophyll fluorescence (F_s) measurements as a tool to follow variations of net CO_2 assimilation and stomatal conductance during water-stress in C_3 plants. *Physiologia Plantarum* **114:** 231–240.

Flexas J, Díaz-Espejo A, Berry JA, Cifre J, Galmés J, Kaldenhoff R, Medrano H, Ribas-Carbó M. 2007. Analysis of leakage in IRGA's leaf chambers of open gas exchange systems: quantification and its effects in photosynthesis parameterization. *Journal of Experimental Botany* **58:** 1533-1543.

Gallé A, Florez-Sarasa I, Tomás M, Pou A, Medrano H, Ribas-Carbó M, Flexas J. 2009. The role of mesophyll conductance during water stress and recovery in tobacco (*Nicotiana sylvestris*): acclimation or limitation? *Journal of Experimental Botany* **60:** 2379-2390.

Genty B, Briantais JM, Baker NR. 1989. The relationship between the quantum yield of photosynthetic electron-transport and quenching of chlorophyll fluorescence. *Biochimica et Biophysica Acta* **990:** 87–92.

Grassi G, Magnani F. 2005. Stomatal, mesophyll conductance and biochemical limitations to photosynthesis as affected by drought and leaf ontogeny in ash and oak trees. *Plant, Cell & Environment* **28:** 834-849.

Han J-M, Meng H-F, Wang S-Y, Jiang C-D, Liu F, Zhang W-F, Zhang Y-L. 2016. Variability of mesophyll conductance and its relationships with water use efficiency in cotton leaves under drought pretreatment. *Journal of Plant Physiology* **194:** 61–71.

Hanson DT, Renzaglia K, Villarreal JC. 2014. Diffusional limitations to CO_2 concentrating mechanisms in bryophytes. In: Hanson DT, Rice SK, eds. *Photosynthesis in Bryophytes and Early Land Plants*. Berlin, Heidelberg: Springer Berlin Heidelberd, 95–111.

Harley PC, Loreto F, Dimarco G, Sharkey TD. 1992. Theoretical considerations when estimating the mesophyll conductance to CO_2 flux by analysis of the response of photosynthesis to CO_2. *Plant Physiology* **98:** 1429–1436.

Niinemets Ü, Reichstein M. 2003. Controls on the emission of plant volatiles through stomata: a sensitivity analysis. *Journal of Geophysical Research* **108:** 4211.

Niinemets Ü, Cescatti A, Rodeghiero M, Tosens T. 2005. Leaf internal diffusion conductance limits photosynthesis more strongly in older leaves of Mediterranean evergreen broad-leaved species. *Plant, Cell and Environment* **28:** 1552–1566.

Nobel PS. 1991. *Physicochemical and environmental plant physiology*, 4th edn (Academic Press, Inc: San Diego, CA, USA).

Proctor MCF. 2010. Trait correlations in bryophytes: Exploring an alternative world. *New Phytologist* **185:** 1–3.

Rondeau-Mouro C, Defer D, Leboeuf E, Lahaye M. 2008. Assessment of cell wall porosity in *Arabidopsis thaliana* by NMR spectroscopy. *International Journal of Biological Macromolecules* **42:** 83-92.

Schneider CA, Rashband WS, Eliceiri KW. 2012. "NIH Image to ImageJ: 25 years of image analysis". *Nature methods* **9:** 671–675.

Terashima I, Hanba YT, Tazoe Y, Vyas P, Yano S. 2006. Irradiance and phenotype: comparative eco-development of sun and shade leaves in relation to photosynthetic CO_2 diffusion. *Journal of Experimental Botany* **57:** 343-354.

Tholen D, Ethier G, Genty B, Pepipn S, Zhu XG. 2012. Variable mesophyll conductance revisited: theoretical background and experimental implications. *Plant, Cell & Environment* **35:** 2087-2103.

Tomás M, Flexas J, Copolovici L, Galmés J, Hallik L, Medrano H, Tosens T, Vislap V, Niinemets Ü. 2013. Importance of leaf anatomy in determining mesophyll diffusion conductance to CO_2 across species: quantitative limitations and scaling up by models. *Journal of Experimental Botany* **64:** 2269-2281.

Tomás M, Medrano H, Brugnoli E, Escalona JM, Martorell S, Pou A, Ribas-Carbó M, Flexas J. 2014. Variability of mesophyll conductance in grapevine cultivars

under water stress conditions in relation to leaf anatomy and water use efficiency. *Australian Journal of Grape and Wine Research* **20:** 272-280.

Tosens T, Niinemets Ü, Vislap V, Eichelmann H, Castro-Díez P. 2012a. Developmental changes in mesophyll diffusion conductance and photosynthetic capacity under different light and water availabilities in *Populus tremula*: how structure constrains function. *Plant, Cell & Environment 35:* 839-856.

Tosens T, Nishida K, Gago J, Coopman RE, Cabrera HM, Carriquí M, Laanisto L, Morales L, Nadal M, Rojas R, et al. 2016. The photosynthetic capacity in 35 ferns and fern allies: mesophyll CO_2 diffusion as a key trait. *New Phytologist* **209:** 1576-1590.

Valentini R, Epron D, Deangelis P, Matteucci G, Dreyer E. 1995. In-situ estimation of net CO_2 assimilation, photosynthetic electron flow and photorespiration in Turkey oak (*Q. cerris* L.) leaves: diurnal cycles under different levels of water supply. *Plant, Cell and Environment* **18:** 631–640.

Varone L, Ribas-Carbo M, Cardona C, Gallé A, Medrano H, Gratani L, Flexas J. 2012. Stomatal and non-stomatal limitations to photosynthesis in seedlings and saplings of Mediterranean species pre-conditioned and aged in nurseries: Different response to water stress. *Environmental and Experimental Botany* **75:** 235-247.

Veromann-Jürgenson L-L, Tosens T, Laanisto L, Niinemets Ü. 2017. Extremely thick cell walls and low mesophyll conductance: welcome to the world of ancient living! *Journal of Experimental Botany* **68:** 1639-1653.

Wagner S, Zotz G, Salazar AN, Bader MY. 2013. Altitudinal changes in temperature responses of net photosynthesis and dark respiration in tropical bryophytes. *Annals of Botany* **111:** 455–465.

Waite M, Sack L. 2010. How does moss photosynthesis relate to leaf and canopy structure? Trait relationships for 10 Hawaiian species of contrasting light habitats. *New Phytologist* **185:** 156–172.

Notes S1. List of abbreviations for traits.

Abbreviation	Definition
A_{area}	Area-based net assimilation rate
A_{mass}	Mass-based net assimilation rate
C_a	Ambient CO_2 concentration
C_c	Chloroplastic CO_2 concentration
C_i	Sub-stomatal CO_2 concentration
C_s	Leaf surface CO_2 concentration
CMA	Canopy dry mass per unit area
D_{leaf}	Leaf density
ETR	Electron transport rate
f_{ias}	Fraction of photosynthetic tissue occupied by intercellular air spaces
Γ^*	Hypothetical CO_2 compensation point without non-photorespiratory CO_2 respiration in the light
g_m	Mesophyll diffusion conductance to CO_2
g_{nsd}	Non-stomatal diffusion conductance to CO_2
g_{nsd_ANAT}	Non-stomatal diffusion conductance to CO_2 calculated from anatomical data
g_{nsd_FLU}	Non-stomatal diffusion conductance to CO_2 calculated from chlorophyll fluorescence data
g_s	Stomatal diffusion conductance to CO_2
l_b	Biochemical limitations to photosynthesis
L_{chl}	Chloroplast length
l_i	Liquid phase limitations to photosynthesis
LES	Leaf economics spectrum
LMA	Leaf dry mass per unit area
l_{nsd}	Non-stomatal diffusion limitations to photosynthesis
l_s	Stomatal limitations to photosynthesis
N_{area}	Nitrogen content per area
N_{mass}	Nitrogen content per mass
p_{cw}	Cell wall effective porosity
R_d	Non-photorespiratory CO_2 respiration in the light
R_n	Mitochondrial respiration rate
S_c/S	Chloroplast surface area exposed to cell perimeter, either intercellular (in multi-stratose photosynthetic organs) or ambient (in unistratose photosynthetic organs)
S_m/S	Photosynthetic tissue surface area exposed to cell perimeter, either intercellular or ambient
T_{chl}	Chloroplast thickness
T_{cw}	Cell wall thickness
T_{cyt}	Cytoplasm thickness
T_{leaf}	Leaf thickness
T_{mes}	Mesophyll thickness
$V_{c,max}$	Maximum velocity of carboxylation

Table S1. The climate, range of dispersal and microhabitat type of the studied species.

Species	Climate	Range of dispersal	Microhabitat
Pellia endiviifolia	Boreal to mediterranean	Eurasia, North America	Ground-dwelling
Saccogyna viticulosa	Temperate to mediterranean	Europe, Azores, Canary Islands	Ground-dwelling
Porella canariensis	Temperate to subtropics	Iberian Peninsula, Azores, Canary Islands	Branch-dwelling
Lunularia cruciata	Temperate to subtropics	Worldwide	Ground-dwelling
Conocephalum conicum	Boreal to mediterranean	Eurasia, North America	Ground-dwelling
Dumortiera hirsuta	Temperate to tropics	Worldwide	Ground-dwelling
Marchantia polymorpha	Arctic to tropics	Worldwide	Ground-dwelling
Polytrichum formosum	Temperate	Europe	Ground-dwelling
Polytrichum juniperinum	Polar to subtropics	Worldwide	Ground-dwelling
Fissidens pacificus	Tropics	Hawaii	Ground-dwelling
Fissidens serrulatus	Temperate to mediterranean	Europe, Azores, Canary Islands	Ground-dwelling
Dicranum polysetum	Boreal to temperate	Eurasia, North America	Ground-dwelling
Dicranum scoparium	Polar to temperate	Eurasia, North America, Australia, New Zealand	Ground-dwelling
Ceratodon purpureus	Polar to tropics	Worldwide	Ground-dwelling
Campylopus hawaiicus	Tropics	Hawaii	Trunk-dwelling[1]
Holomitrium seticalycinum	Tropics	Hawaii	Branch-dwelling
Leucobryum seemannii	Tropics	Hawaii	Trunk-dwelling[1]
Macromitrium microstomum	Temperate to tropics	Worldwide	Branch-dwelling
Macromitrium piliferum	Tropics	Hawaii	Branch-dwelling
Plagiomnium elatum	Temperate	Europe	Ground-dwelling
Plagiomnium undulatum	Temperate to mediterranean	Eurasia	Ground-dwelling
Bryum pseudotriquetrum	Polar to mediterranean	Worldwide	Ground-dwelling
Pyrrhobryum pungens	Tropics	Hawaii	Trunk-dwelling[1]
Distichophyllum freycinetii	Tropics	Hawaii	Ground-dwelling
Hookeria acutifolia	Temperate to tropics	Hawaii, America, Asia	Ground-dwelling
Thuidium tamariscinum	Temperate	Europe	Ground-dwelling
Pseudoscleropodium purum	Temperate to mediterranean	Eurasia, North America, North Africa, New Zealand	Ground-dwelling
Hylocomium splendens	Polar to temperate	Eurasia, North America, New Zealand	Ground-dwelling
Pleurozium schreberi	Boreal to temperate	Northern hemisphere, South America	Ground-dwelling
Ctenidium molluscum	Boreal to mediterranean	Eurasia, North America	Ground-dwelling
Hypnum cupressiforme	Boreal to tropics	Worldwide	Trunk-dwelling[1]
Sanionia uncinata	Polar to temperate	Eurasia, North America, Greenland, New Zealand, Australia, Antarctica, South America	Ground-dwelling
Acroporium fuscoflavum	Tropics	Hawaii	Trunk-dwelling[1]
Selaginella denticulata	Mediterranean	Mediterranean, Atlantic	Ground-dwelling
Selaginella martensii	Subtropics to tropics	Mesoamerica	Ground-dwelling
Selaginella uncinata	Subtropics to tropics	China (native), North America (introduced)	Ground-dwelling

[1] Usually <2 m above the soil

Table S2. Environmental conditions of the different species studied in each site.

Country	Group	Species	Growth site	Watering	Fertilization	Potted/rooted in soil	Substrate
Antarctica	Moss	*Bryum pseudotriquetrum*	Outdoors (open field)	None	None	Rooted in soil	Natural soil
	Moss	*Ceratodon purpureus*	Outdoors (open field)	None	None	Rooted in soil	Natural soil
	Moss	*Sanionia uncinata*	Outdoors (open field)	None	None	Rooted in soil	Natural soil
Australia	Liverwort	*Marchantia polymorpha*	Indoors (Glasshouse)	Daily	Yes	3 l pots	Peat moss:perlite
	Lycophyte	*Selaginella martensii*	Indoors (Glasshouse)	Daily	Yes	4 l pots	Peat moss:perlite
	Lycophyte	*Selaginella uncinata*	Indoors (Glasshouse)	Daily	Yes	4 l pots	Peat moss:perlite
	Moss	*Polytrichum juniperinum*	Outdoors (open field)	Daily	None	Rooted in soil	Natural soil
Estonia	Moss	*Dicranum polysetum*	Outdoors (open field)	Daily	None	Rooted in soil	Natural soil
	Moss	*Dicranum scoparium*	Outdoors (open field)	Daily	None	Rooted in soil	Natural soil
	Moss	*Hylocomium splendens*	Outdoors (open field)	Daily	None	Rooted in soil	Natural soil
	Moss	*Hypnum cupressiforme*	Outdoors (open field)	Daily	None	Rooted in rock	Rock
	Moss	*Plagiomnium elatum*	Outdoors (open field)	Daily	None	Rooted in soil	Natural soil
	Moss	*Pleurozium schreberi*	Outdoors (open field)	Daily	None	Rooted in soil	Natural soil
	Liverwort	*Marchantia polymorpha*	Outdoors (open field)	Daily	None	Rooted in soil	Natural soil
Hawaii	Moss	*Acroporium fuscoflavum*	Outdoors (open field)	Daily	None	Rooted on tree bark	Tree bark
	Moss	*Campylopus hawaiicus*	Outdoors (open field)	Daily	None	Rooted on tree bark	Tree bark
	Moss	*Distichophyllum freycinetii*	Outdoors (open field)	Daily	None	Rooted in soil	Natural soil
	Moss	*Fissidens pacificus*	Outdoors (open field)	Daily	None	Rooted in soil	Natural soil
	Moss	*Holomitrium seticalycinum*	Outdoors (open field)	Daily	None	Rooted on tree bark	Tree bark
	Moss	*Hookeria acutifolia*	Outdoors (open field)	Daily	None	Rooted in soil	Natural soil
	Moss	*Leucobryum seemannii*	Outdoors (open field)	Daily	None	Rooted in soil	Natural soil
	Moss	*Macromitrium microstomum*	Outdoors (open field)	Daily	None	Rooted on tree bark	Tree bark
	Moss	*Macromitrium piliferum*	Outdoors (open field)	Daily	None	Rooted on tree bark	Tree bark
	Moss	*Pyrrhobryum pungens*	Outdoors (open field)	Daily	None	Rooted on tree bark	Tree bark
Spain	Lycophyte	*Selaginella denticulata*	Outdoors (open field)	Daily	None	Rooted in soil	Natural soil

Moss	*Ctenidium molluscum*	Outdoors (open field)	Daily	None	Pot	Wet tissue
Moss	*Fissidens serrulatus*	Outdoors (open field)	Daily	None	Rooted in soil	Natural soil
Moss	*Plagiomnium undulatum*	Outdoors (open field)	Daily	None	Rooted in soil	Natural soil
Moss	*Polytrichum formosum*	Outdoors (open field)	Daily	None	Rooted in soil	Natural soil
Moss	*Polytrichum juniperinum*	Outdoors (open field)	Daily	None	Pot	Compost soil
Moss	*Pseudoscleropodium purum*	Outdoors (open field)	Daily	None	Rooted in soil	Natural soil
Moss	*Thuidium tamariscinum*	Outdoors (open field)	Daily	None	Rooted in soil	Natural soil
Liverwort	*Conocephalum conicum*	Outdoors (open field)	Daily	None	Pot	Wet tissue
Liverwort	*Dumortiera hirsuta*	Outdoors (open field)	Daily	None	Pot	Compost soil
Liverwort	*Lunularia cruciata*	Outdoors (open field)	Daily	None	Pot	Compost soil
Liverwort	*Pellia endiviifolia*	Outdoors (open field)	Daily	None	Pot	Compost soil
Liverwort	*Porella canariensis*	Outdoors (open field)	Daily	None	Rooted on tree branch	Tree branch
Liverwort	*Saccogyna viticulosa*	Outdoors (open field)	Daily	None	Pot	Compost soil

Table S3. Measured data available for each studied species.

Level 0	Leaf structure parameters, nitrogen content, A_{area}
Level 1	Level 0 + leaf anatomy
Level 2	Level 1 + Variable J method (Harley et al., 1992)
Level 3	Level 2 + Complete A-C_a curves + $V_{c,max}$ estimation (Farquhar *et al.*, 1980)

Species	Level 0	Level 1	Level 2	Level 3
Pellia endiviifolia	■			
Saccogyna viticulosa	■			
Porella canariensis	■			
Lunularia cruciate	■			
Conocephalum conicum	■			
Dumortiera hirsuta	■			
Marchantia polymorpha (Estonia)	■	■		
Marchantia polymorpha (Tasmania)	■	■	■	■
Polytrichum formosum	■	■	■	■
Polytrichum juniperinum (Spain)	■			
Polytrichum juniperinum (Tasmania)	■	■	■	■
Fissidens pacificus	■	■		
Fissidens serrulatus	■			
Dicranum polysetum	■	■		
Dicranum scoparium	■	■		
Ceratodon purpureus	■	■	■	
Campylopus hawaiicus	■	■		
Holomitrium seticalycinum	■	■		
Leucobryum seemannii	■	■		
Macromitrium microstomum	■	■		
Macromitrium piliferum	■	■		
Plagiomnium elatum	■	■		
Plagiomnium undulatum	■	■	■	■
Bryum pseudotriquetrum	■	■	■	
Pyrrhobryum pungens	■	■		
Distichophyllum freycinetii	■	■		
Hookeria acutifolia	■	■		
Thuidium tamariscinum	■	■	■	■
Pseudoscleropodium purum	■	■	■	■
Hylocomium splendens	■	■		
Pleurozium schreberi	■	■	■	■
Ctenidium molluscum	■			
Hypnum cupressiforme	■	■		
Sanionia uncinata	■	■	■	
Acroporium fuscoflavum	■	■		
Selaginella denticulata	■	■	■	■
Selaginella martensii	■	■	■	
Selaginella uncinata	■	■	■	■

Table S4. Photosynthetic characteristics for each studied species. Average values ± SE are shown for net assimilation based on both projected and total area ($A_{area\_projected}$ and A_{area_total}, respectively), stomatal conductance (g_s), non-stomatal diffusion conductance estimated from chlorophyll fluorescence (g_{nsd_FLU}), maximum carboxylation rate on a C_c basis ($V_{c,max}$), sub-stomatal CO_2 concentration (C_i), chloroplastic CO_2 concentration (C_c), electron transport rate (ETR) and dark respiration rate (R_d). Dashes (-) account for non-available data.

Species	$A_{area\_projected}$ (µmol CO_2 m^{-2} s^{-1})	A_{area_total} (µmol CO_2 m^{-2} s^{-1})	g_s (mmol CO_2 m^{-2} s^{-1})	g_{nsd_FLU} (mmol CO_2 m^{-2} s^{-1})	$V_{c,max}$ (µmol CO_2 m^{-2} s^{-1})	C_i (µmol CO_2 mol^{-1})	C_c (µmol CO_2 mol^{-1})	ETR (µmol m^{-2} s^{-1})	R_d (µmol m^{-2} s^{-1})
Marchantiophyta									
Pellia endiviifolia	1.13 ± 0.14	1.126 ± 0.138							
Saccogyna viticulosa	0.85 ± 0.14	0.643 ± 0.106							
Porella canariensis	0.49 ± 0.12	0.412 ± 0.097							
Lunularia cruciata	2.27 ± 0.32	2.267 ± 0.323							
Conocephalum conicum	2.12 ± 0.14	2.116 ± 0.143							
Dumortiera hirsuta	0.72 ± 0.19	0.719 ±0.189							
Marchantia polymorpha (Estonia)	3.08 ± 0.42	3.075 ± 0.423							-0.78 ± 0.06
Marchantia polymorpha (Tasmania)	4.65 ± 0.26	4.652 ± 0.264		19.036 ± 1.063	23.1 ± 1.6		150 ± 13	41.2 ± 3.3	-0.84 ± 0.22
Bryophyta									
Polytrichum formosum	-	2.321 ± 0.279		8.374 ± 1.128	13.7 ± 1.9		174 ± 38	20.8 ± 1.4	-0.55 ± 0.07
Polytrichum juniperinum (Spain)	5.71 ± 0.25	2.874 ± 0.126							
Polytrichum juniperinum (Tasmania)	-	7.547 ± 0.902		22.530 ± 4.083	76.3 ± 0.8		78 ± 15	100.6 ± 24.4	-0.25 ± 0.04
Fissidens pacificus	0.71 ± 0.10	0.119 ± 0.017							-0.08 ± 0.02
Fissidens serrulatus	0.43 ± 0.09	0.330 ± 0.071							
Dicranum polysetum	2.26 ± 0.77	0.171 ± 0.058							-1.13 ± 0.30
Dicranum scoparium	3.07 ± 0.44	0.313 ± 0.045							-1.05 ± 0.21
Ceratodon purpureum	1.64 ± 0.20	-		4.711 ± 0.641			36 ± 3	52.8 ± 4.5	-0.15 ± 0.04
Campylopus hawaiicus	1.19 ± 0.21	0.073 ± 0.013							-0.53 ± 0.04
Holomitrium seticalycinum	0.96 ± 0.11	0.139 ± 0.015							-0.85 ± 0.19
Leucobryum seemannii	0.59 ± 0.08	0.044 ± 0.006							-0.20 ± 0.03
Macromitrium microstomum	1.41 ± 0.32	0.127 ± 0.029							-0.16 ± 0.07
Macromitrium piliferum	1.30 ± 0.14	0.124 ± 0.014							-0.10 ± 0.04
Plagiomnium undulatum	0.90 ± 0.03	0.774 ± 0.028		2.616 ± 0.074	22.2 ± 2.6		53 ± 3	22.2 ± 3.1	-0.16 ± 0.01

Plagiomnium elatum	2.01 ± 0.12	0.265 ± 0.016							-0.20 ± 0.03
Bryum pseudotriquetrum	2.91 ± 0.27	-		9.151 ± 0.001			62 ± 13	44.0 ± 5.4	-0.30 ± 0.06
Pyrrhobryum pungens	0.63 ± 0.04	0.104 ± 0.007							-0.51 ± 0.02
Distichophyllum freycinetii	0.60 ± 0.09	0.056 ± 0.009							-0.10 ± 0.06
Hookeria acutifolia	1.15 ± 0.24	0.126 ± 0.026							-0.19 ± 0.02
Thuidium tamariscinum	0.90 ± 0.06	0.168 ± 0.011		3.426 ± 0.453	8.1 ± 1.0		124 ± 28	12 ± 1.3	-0.38 ± 0.06
Pseudoscleropodium purum	0.94 ± 0.09	0.183 ± 0.020		8.045 ± 3.441	7.1 ± 1.3		192 ± 32	8.8 ± 0.4	-0.36 ± 0.04
Hylocomium splendens	3.07 ± 0.99	0.261 ± 0.084							-1.24 ± 0.38
Pleurozium schreberi	0.64 ± 0.08	0.233 ± 0.031		1.863 ± 0.261	23.8 ± 3.1		54 ± 3	23.3 ± 2.2	-0.37 ± 0.02
Ctenidium molluscum	1.26 ± 0.08	0.626 ± 0.039							
Sanionia uncinata	1.84 ± 0.17	-		5.474 ± 0.589			50 ± 6	31.6 ± 2.2	-0.20 ± 0.02
Hypnum cupressiforme	1.33 ± 0.20	0.258 ± 0.038							-0.42 ± 0.02
Acroporium fuscoflavum	0.78 ± 0.08	0.048 ± 0.005							-0.21 ± 0.04
Tracheophyta									
Selaginella denticulata	3.09 ± 0.40	3.088 ± 0.399	124 ± 13	23.823 ± 8.074	13.1 ± 0.9	350 ± 4	178 ± 19	22.9 ± 1.7	-0.50 ± 0.05
Selaginella uncinata	3.79 ± 0.18	3.792 ± 0.182	72 ± 7	19.092 ± 5.348	16.6 ± 2.6	303 ± 7	107 ± 26	22.1 ± 3.4	-0.31 ± 0.04
Selaginella martensii	3.69 ± 0.45	3.690 ± 0.453	66 ± 11	4.646 ± 2.343	-	299 ± 8	-	15.3 ± 2.1	-0.32 ± 0.04

Table S5. Agreement between maximum velocity of carboxylation ($V_{c,max}$) obtained from fast and slow area-based net assimilation (A_{area})-ambiental CO_2 concentration (C_a) curves (e.g. without rehydrating the moss during the 10-15 minutes of the curve or removing the moss from the cuvette and rehydrating it between each C_a point).

Species	$V_{c,max}$ (µmol CO_2 m^{-2} s^{-1}) **Fast A_{area}-C_a curves**	$V_{c,max}$ (µmol CO_2 m^{-2} s^{-1}) **Slow A_{area}-C_a curves**
Polytrichum formosum	13.7 ± 1.9	21.2 ± 2.1
Polytrichum juniperinum	76.3 ± 0.8	42.9 ± 5.5
Thuidium tamariscinum	8.1 ± 1.0	8.8 ± 1.8
Pseudoscleropodium purum	7.1 ± 1.3	6.3 ± 1.6

Table S6. Structural and anatomical characteristics for each studied species. Average values ± SE are shown for dry leaf mass per unit area (LMA), dry canopy mass per unit area (CMA), leaf density (D_{leaf}), leaf thickness (T_{leaf}), leaf mesophyll thickness (T_{mes}) and fraction of the photosynthetic tissue occupied by intercellular air spaces (f_{ias}). Dashes (-) account for non-available data.

Species	LMA (g m^{-2})	CMA (g m^{-2})	D_{leaf} (g cm^{-3})	T_{leaf} (μm)	T_{mes} (μm)	f_{ias} (%)
Marchantiophyta						
Pellia endiviifolia	19.8 ± 0.5	-				
Saccogyna viticulosa	13.4 ± 1.0	17.5 ± 1.1				
Porella canariensis	23.2 ± 1.3	73.6 ± 2.4				
Lunularia cruciata	24.2 ± 2.1	-				
Conocephalum conicum	41.8 ± 5.5	-				
Dumortiera hirsuta	45.7 ± 2.7	-				
Marchantia polymorpha (Estonia)	43.8 ± 4.0	-	0.25 ± 0.01	175 ± 1	151.2 ± 0.2	25 ± 1
Marchantia polymorpha (Tasmania)	32.2 ± 4.0	-	0.10 ± 0.01	306 ± 56	270.5 ± 55.0	18 ± 2
Bryophyta						
Polytrichum formosum	79.3 ± 4.7	-	0.88 ± 0.04	93 ± 7	60.8 ± 5.1	24 ± 3
Polytrichum juniperinum (Spain)	70.7 ± 3.1	183.1 ± 18.6				
Polytrichum juniperinum (Tasmania)	74.9 ± 2.3	-	0.60 ± 0.03	123 ± 12	67.5 ± 10.5	31 ± 1
Fissidens pacificus	12.9 ± 0.8	76.7 ± 9.8	0.91 ± 0.03	13 ± 1		0
Fissidens serrulatus	36.5 ± 1.3	150.8 ± 31.8				
Dicranum polysetum	24.2 ± 1.8	319.8 ± 23.8	1.76 ± 0.08	14 ± 1		0
Dicranum scoparium	28.8 ± 2.4	281.8 ± 27.1	1.45 ± 0.09	20 ± 1		0
Ceratodon purpureum	-	54.1 ± 3.9	-	11 ± 1		0
Campylopus hawaiicus	14.4 ± 0.2	235.1 ± 21.2	1.27 ± 0.07	12 ± 1		0
Holomitrium seticalycinum	18.0 ± 1.0	124.3 ± 22.1	0.88 ± 0.03	20 ± 0		0
Leucobryum seemannii	11.3 ± 1.3	150.4 ± 35.5	0.16 ± 0.04	72 ± 9	9.2 ± 0.8	0
Macromitrium microstomum	10.7 ± 1.5	118.9 ± 13.5	0.84 ± 0.14	12 ± 1		0
Macromitrium piliferum	11.0 ± 1.2	115.6 ± 13.2	0.86 ± 0.07	12 ± 1		0
Plagiomnium elatum	9.8 ± 1.1	74.3 ± 12.9	0.32 ± 0.05	26 ± 2		0
Plagiomnium undulatum	19.3 ± 2.0	24.2 ± 2.1	0.85 ± 0.05	21 ± 1		0
Bryum pseudotriquetrum	-	65.0 ± 5.6	-	11 ± 1		0
Pyrrhobryum pungens	31.4 ± 3.1	190.8 ± 31.7	0.64 ± 0.18	54 ± 5		0
Distichophyllum freycinetii	6.4 ± 0.4	68.3 ± 19.1	0.24 ± 0.04	30 ± 2		0
Hookeria acutifolia	9.0 ± 0.9	82.3 ± 19.0	0.18 ± 0.02	47 ± 2		0
Thuidium tamariscinum	16.0 ± 2.4	79.2 ± 6.2	1.81 ± 0.25	8 ± 0		0
Pseudoscleropodium purum	13.1 ± 2.3	61.7 ± 3.0	1.14 ± 0.26	9 ± 1		0
Hylocomium splendens	26.7 ± 1.9	314.5 ± 27.7	5.34 ± 0.15	5 ± 0		
Pleurozium schreberi	17.6 ± 1.6	48.1 ± 3.0	-	17 ± 0		0
Ctenidium molluscum	28.1 ± 1.0	102.2 ± 19.2				
Hypnum cupressiforme	21.4 ± 1.51	109.5 ± 16.9	3.01 ± 0.05	7 ± 0		
Sanionia uncinata	-	50.4 ± 8.6	-	11 ± 3		0
Acroporium fuscoflavum	8.1 ± 0.5	130.4 ± 14.7	0.87 ± 0.07	9 ± 0		0
Tracheophyta						

Selaginella denticulata	29.8 ± 2.5	-	0.61 ± 0.04	90 ± 7	48.3 ± 6.8	32 ± 6
Selaginella uncinata	23.8 ± 1.1	-	0.27 ± 0.03	93 ± 5	51.9 ± 3.9	51 ± 4
Selaginella martensii	54.7 ± 5.4	-	0.90 ± 0.07	70 ± 8	31.2 ± 6.3	30 ± 4

Table S7. Anatomical characteristics for each studied species. Average values ± SE are shown for the curvature correction factor (F), photosynthetic tissue and chloroplast surface area exposed to air, either intercellular (in multi-stratose leaves) or ambient (in unistratose leaves) per leaf area (S_m/S and S_c/S, respectively), the ratio S_c/S_m, cell wall thickness (T_{cw}), chloroplast thickness (T_{chl}), chloroplast length (L_{chl}) and cytoplasm thickness (T_{cyt}). Non-available data are shown by dashes (-).

Species	F	S_m/S ($m^2\ m^{-2}$)	S_c/S ($m^2\ m^{-2}$)	S_c/S_m	T_{cw} (μm)	T_{chl} (μm)	L_{chl} (μm)	T_{cyt} (μm)
Marchantiophyta								
Marchantia polymorpha (Estonia)	1.242	6.00 ± 0.11	3.57 ± 0.12	0.59 ± 0.01	0.502 ± 0.004	3.60 ± 0.08	3.42 ± 0.15	1.913 ± 0.761
Marchantia polymorpha (Tasmania)	1.266	5.36 ± 1.13	3.13 ± 0.30	0.61 ± 0.07	0.673 ± 0.011	3.99 ± 0.06	5.28 ± 0.16	0.368 ± 0.083
Bryophyta								
Polytrichum formosum	1.238	8.34 ± 0.84	4.79 ± 0.48	0.58 ± 0.02	0.719 ± 0.076	3.02 ± 0.24	4.96 ± 0.34	0.301 ± 0.030
Polytrichum juniperinum (Tasmania)	1.320	13.04 ± 0.58	5.18 ± 0.18	0.40 ± 0.03	0.762 ± 0.084	2.42 ± 0.09	3.82 ± 0.15	0.515 ± 0.025
Fissidens pacificus	1.308	2.68 ± 0.03	1.77 ± 0.12	0.66 ± 0.05	2.520 ± 0.131	2.90 ± 0.21	4.55 ± 0.20	0.640 ± 0.112
Dicranum polysetum	1.107	2.97 ± 0.03	1.79 ± 0.07	0.59 ± 0.02	1.822 ± 0.124	2.71 ± 0.12	6.66 ± 0.31	0.206 ± 0.039
Dicranum scoparium	1.333	2.83 ± 0.03	1.34 ± 0.03	0.47 ± 0.01	1.807 ± 0.150	1.24 ± 0.08	4.42 ± 0.52	0.192 ± 0.041
Ceratodon purpureum	1.345	2.36 ± 0.24	1.58 ± 0.23	0.69 ± 0.15	1.635 ± 0.304	2.29 ± 0.30	3.66 ± 0.23	0.815 ± 0.514
Campylopus hawaiicus	1.294	2.59 ± 0.04	1.06 ± 0.02	0.41 ± 0.01	2.287 ± 0.149	2.49 ± 0.20	4.64 ± 0.28	0.489 ± 0.107
Holomitrium seticalycinum	1.408	3.00 ± 0.06	1.35 ± 0.16	0.45 ± 0.05	2.767 ± 0.250	3.45 ± 0.31	4.94 ± 0.34	2.285 ± 0.364
Leucobryum seemannii	1.346	2.84 ± 0.12	1.10 ± 0.06	0.39 ± 0.01	1.900 ± 0.173	2.61 ± 0.33	4.23 ± 0.60	0.912 ± 0.066
Macromitrium microstomum	1.336	2.80 ± 0.13	1.10 ± 0.10	0.40 ± 0.05	3.345 ± 0.392	2.23 ± 0.06	3.30 ± 0.19	0.842 ± 0.004
Macromitrium piliferum	1.376	3.24 ± 0.15	1.67 ± 0.14	0.52 ± 0.06	2.400 ± 0.333	2.30 ± 0.14	3.48 ± 0.23	0.978 ± 0.133
Plagiomnium undulatum	1.215	2.42 ± 0.01	1.65 ± 0.11	0.68 ± 0.04	0.897 ± 0.047	2.67 ± 0.15	6.14 ± 0.13	0.454 ± 0.098
Plagiomnium elatum	1.158	2.34 ± 0.02	1.25 ± 0.19	0.53 ± 0.08	0.761 ± 0.098	2.60 ± 0.37	7.28 ± 0.45	0.824 ± 0.193
Bryum pseudotriquetrum	1.353	2.74 ± 0.46	1.49 ± 0.40	0.51 ± 0.08	1.682 ± 0.326	2.18 ± 0.34	4.02 ± 0.27	0.089 ± 0.032
Pyrrhobryum pungens	1.284	3.51 ± 0.10	1.59 ± 0.07	0.45 ± 0.02	2.375 ± 0.153	2.75 ± 0.10	3.97 ± 0.30	0.780 ± 0.188
Distichophyllum freycinetii	1.292	2.63 ± 0.02	1.18 ± 0.16	0.44 ± 0.06	3.407 ± 0.741	2.93 ± 0.15	4.69 ± 0.36	0.889 ± 0.378
Hookeria acutifolia	1.232	2.62 ± 0.05	1.47 ± 0.12	0.56 ± 0.05	1.988 ± 0.232	4.17 ± 0.28	6.71 ± 1.01	0.453 ± 0.105
Thuidium tamariscinum	1.233	2.55 ± 0.02	0.75 ± 0.09	0.29 ± 0.03	0.911 ± 0.078	1.55 ± 0.16	2.68 ± 0.22	0.468 ± 0.137
Pseudoscleropodium purum	1.319	2.64 ± 0.01	0.59 ± 0.01	0.22 ± 0.00	2.292 ± 0.582	0.89 ± 0.12	2.10 ± 0.07	0.323 ± 0.025
Hylocomium splendens	1.262	2.80 ± 0.00	0.81 ± 0.00	0.29 ± 0.00	1.071 ± 0.027	1.01 ± 0.09	2.05 ± 0.12	0.065 ± 0.006
Pleurozium schreberi	1.360	3.97 ± 0.08	1.80 ± 0.11	0.45 ± 0.02	2.174 ± 0.019	-	-	-
Hypnum cupressiforme	1.112	2.37 ± 0.03	1.40 ± 0.01	0.59 ± 0.01	1.430 ± 0.119	2.46 ± 0.31	3.37 ± 0.31	0.063 ± 0.013

Sanionia uncinata	1.362	3.25 ± 0.40	2.31 ± 0.58	0.69 ± 0.12	0.786 ± 0.175	1.44 ± 0.11	3.92 ± 0.83	0.401 ± 0.147
Acroporium fuscoflavum	1.290	2.65 ± 0.04	0.95 ± 0.01	0.35 ± 0.01	3.098 ± 0.161	2.20 ± 0.23	3.69 ± 0.76	0.412 ± 0.094
Tracheophyta								
Selaginella denticulata	1.220	11.22 ± 0.82	5.08 ± 1.33	0.45 ± 0.10	0.270 ± 0.031	4.31 ± 0.40	8.47 ± 0.36	0.199 ± 0.046
Selaginella uncinata	1.164	6.25 ± 0.13	2.36 ± 0.24	0.38 ± 0.05	0.541 ± 0.023	4.90 ± 0.33	9.82 ± 0.54	0.589 ± 0.135
Selaginella martensii	1.106	3.87 ± 0.73	1.74 ± 0.33	0.46 ± 0.00	0.507 ± 0.032	5.58 ± 0.03	10.35 ± 0.37	2.128 ± 0.668

Table S8. Non-stomatal diffusion conductance calculated from anatomical measurements following different models for each studied species. Average ± SE values are shown for the non-stomatal diffusion conductance calculated based on Tomás et al. (2013; g_{nsd_ANAT}) considering constant or variable cell wall porosity (p_{cw}; see Methods S1). Dashes (-) account for non-available data.

Species	g_{nsd_ANAT} (mmol CO_2 m^{-2} s^{-1}) p_{cw} = 0.028	g_{nsd_ANAT} (mmol CO_2 m^{-2} s^{-1}) variable p_{cw}
Marchantiophyta		
Marchantia polymorpha (Estonia)	16.49 ± 1.39	32.00 ± 5.23
Marchantia polymorpha (Tasmania)	25.46 ± 3.57	32.22 ± 4.05
Bryophyta		
Polytrichum formosum	22.57 ± 3.73	61.61 ± 4.85
Polytrichum juniperinum (Tasmania)	32.79 ± 1.80	89.63 ± 1.58
Fissidens pacificus	2.55 ± 0.18	7.23 ± 0.40
Dicranum polysetum	3.78 ± 0.18	13.87 ± 0.30
Dicranum scoparium	3.81 ± 0.35	15.45 ± 1.01
Ceratodon purpureum	2.41 ± 0.30	9.01 ± 1.31
Campylopus hawaiicus	2.69 ± 0.14	8.46 ± 0.30
Holomitrium seticalycinum	2.46 ± 0.17	5.41 ± 0.41
Leucobryum seemannii	1.36 ± 0.26	5.87 ± 0.72
Macromitrium microstomum	2.15 ± 0.35	2.18 ± 0.35
Macromitrium piliferum	3.40 ± 0.49	9.83 ± 1.11
Plagiomnium undulatum	5.64 ± 0.24	18.56 ± 1.38
Plagiomnium elatum	6.00 ± 0.96	16.37 ± 3.11
Bryum pseudotriquetrum	3.03 ± 0.95	11.88 ± 3.18
Pyrrhobryum pungens	3.49 ± 0.26	10.26 ± 0.6
Distichophyllum freycinetii	2.65 ± 0.41	2.63 ± 0.41
Hookeria acutifolia	3.28 ± 0.20	9.96 ± 0.47
Thuidium tamariscinum	5.95 ± 0.29	20.13 ± 0.87
Pseudoscleropodium purum	3.13 ± 0.64	10.56 ± 1.85
Hylocomium splendens	5.99 ± 0.09	25.44 ± 0.36
Pleurozium schreberi	-	-
Hypnum cupressiforme	3.86 ± 0.03	15.5 ± 0.12
Sanionia uncinata	7.43 ± 2.54	26.78 ± 6.38
Acroporium fuscoflavum	2.17 ± 0.05	3.84 ± 0.06
Tracheophyta		
Selaginella denticulata	45.09 ± 6.10	70.71 ± 9.31
Selaginella uncinata	15.83 ± 0.70	29.60 ± 1.96
Selaginella martensii	8.71 ± 1.86	14.06 ± 3.06

Table S9. Average ± SE values for mass-based and area-based nitrogen content, respectively N_{mass} and N_{area}, for each studied species. Dashes (-) account for non-available data.

Species	N_{mass} (%)	N_{area} (g m^{-2})
Marchantiophyta		
Pellia endiviifolia	1.26 ± 0.01	0.25 ± 0.01
Saccogyna viticulosa	1.42 ± 0.06	0.25 ± 0.01
Porella canariensis	1.47 ± 0.07	1.08 ± 0.05
Lunularia cruciata	1.51 ± 0.02	0.37 ± 0.01
Conocephalum conicum	1.86 ± 0.04	0.78 ±0.02
Dumortiera hirsuta	1.16 ± 0.04	0.53 ± 0.02
Marchantia polymorpha (Estonia)	2.08 ± 0.05	0.91 ± 0.02
Marchantia polymorpha (Tasmania)	1.84 ± 0.18	1.26 ± 0.19
Bryophyta		
Polytrichum formosum	2.12 ± 0.22	2.59 ± 0.33
Polytrichum juniperinum (Spain)	1.81 ± 0.05	0.67 ± 0.09
Polytrichum juniperinum (Tasmania)	2.37 ± 0.11	0.90 ± 0.09
Fissidens pacificus	1.51 ± 0.09	1.16 ± 0.07
Fissidens serrulatus	1.86 ± 0.03	0.78 ± 0.04
Dicranum polysetum	1.06 ± 0.02	3.19 ± 0.06
Dicranum scoparium	1.45 ± 0.14	4.09 ± 0.39
Ceratodon purpureum	1.53 ± 0.09	0.82 ± 0.05
Campylopus hawaiicus	0.60 ± 0.06	1.40 ± 0.14
Holomitrium seticalycinum	0.80 ± 0.10	0.99 ± 0.13
Leucobryum seemannii	0.24 ± 0.05	0.36 ± 0.07
Macromitrium microstomum	0.49 ± 0.09	0.58 ± 0.10
Macromitrium piliferum	0.74 ± 0.06	0.86 ± 0.07
Plagiomnium elatum	2.52 ± 0.06	1.88 ± 0.04
Plagiomnium undulatum	1.95 ± 0.12	0.42 ± 0.01
Bryum pseudotriquetrum	1.65 ± 0.21	1.07 ± 0.13
Pyrrhobryum pungens	0.63 ± 0.04	1.20 ± 0.08
Distichophyllum freycinetii	1.10 ± 0.09	0.75 ± 0.06
Hookeria acutifolia	1.21 ± 0.11	1.00 ± 0.09
Thuidium tamariscinum	1.13 ± 0.07	0.40 ± 0.03
Pseudoscleropodium purum	1.67 ± 0.22	0.63 ± 0.05
Hylocomium splendens	1.15 ± 0.19	3.62 ± 0.60
Pleurozium schreberi	2.00 ± 0.07	0.96 ± 0.03
Ctenidium molluscum	3.22 ± 0.06	0.72 ± 0.02
Hypnum cupressiforme	1.67 ± 0.21	1.83 ± 0.22
Sanionia uncinata	2.32 ± 0.08	1.17 ± 0.04
Acroporium fuscoflavum	0.69 ± 0.05	0.90 ± 0.07
Tracheophyta		
Selaginella denticulata	2.25 ± 0.05	0.80 ± 0.03
Selaginella uncinata	1.88 ± 0.17	0.55 ± 0.01
Selaginella martensii	2.22 ± 0.05	1.77 ± 0.03

Table S10. Sensitivity analysis of the influence of hypothetical biases in the CO_2 compensation point (Γ*), the leaf absorptance (α), and the rate of non-photorespiratory respiration in the light (R_d), on the estimation of non-stomatal diffusion conductance to CO_2 estimated from chlorophyll fluorescence (g_{nsd_FLU}).

Species	g_{nsd_FLU} mmol m^{-2} s^{-1} (original)	g_{nsd_FLU} mmol m^{-2} s^{-1} (+10% Γ*)	g_{nsd_FLU} mmol m^{-2} s^{-1} (-10% Γ*)	g_{nsd_FLU} mmol m^{-2} s^{-1} (+30% α)	g_{nsd_FLU} mmol m^{-2} s^{-1} (-30% α)	g_{nsd_FLU} mmol m^{-2} s^{-1} (x2 R_d)	g_{nsd_FLU} mmol m^{-2} s^{-1} (x0 R_d)
Marchantiophyta							
Marchantia polymorpha	19.036 ± 1.063	20.357 ± 1.268	17.891 ± 0.926	15.854 ± 0.809	29.096 ± 12.711	26.89 ± 4.951	16.586 ± 0.891
Bryophyta							
Polytrichum formosum	8.374 ± 1.128	9.044 ± 1.459	7.827 ± 0.892	6.831 ± 0.423	15.087 ± 4.777	2.248 ± 6.796	6.916 ± 0.476
Polytrichum juniperinum	22.53 ± 4.083	23.207 ± 4.387	21.898 ± 3.811	21.359 ± 3.425	27.557 ± 7.746	22.721 ± 4.175	22.35 ± 3.998
Ceratodon purpureum	4.711 ± 0.641	4.763 ± 0.653	4.659 ± 0.629	4.658 ± 0.622	4.834 ± 0.689	4.729 ± 0.645	4.693 ± 0.637
Plagiomnium undulatum	2.616 ± 0.074	2.698 ± 0.072	2.608 ± 0.072	2.599 ± 0.075	2.782 ± 0.072	2.693 ± 0.07	2.616 ± 0.074
Bryum pseudotriquetrum	9.151 ± 1.192	9.376 ± 1.278	8.94 ± 1.117	8.646 ± 0.959	0.666 ± 8.421	9.447 ± 1.349	8.932 ± 1.092
Thuidium tamariscinum	3.426 ± 0.453	3.645 ± 0.564	3.24 ± 0.369	2.943 ± 0.222	2.385 ± 1.507	0.579 ± 2.948	2.847 ± 0.203
Pseudoscleropodium purum	8.045 ± 3.441	6.035 ± 2.521	5.655 ± 1.726	3.445 ± 0.477	10.087 ± 8.463	-2.240 ± 5.915	3.401 ± 0.514
Pleurozium schreberi	1.863 ± 0.261	1.894 ± 0.268	1.833 ± 0.255	1.829 ± 0.251	1.943 ± 0.289	1.925 ± 0.275	1.814 ± 0.251
Sanionia uncinata	5.474 ± 0.589	5.566 ± 0.608	5.386 ± 0.571	5.320 ± 0.550	5.974 ± 0.752	5.547 ± 0.606	5.410 ± 0.575
Tracheophyta							
Selaginella denticulata	23.823 ± 8.074	32.784 ± 13.58	19.246 ± 5.659	12.84 ± 2.643	27.012 ± 19.544	44.886 ± 27.099	15.676 ± 4.41
Selaginella uncinata	19.092 ± 5.348	21.37 ± 6.394	17.359 ± 4.519	13.493 ± 4.234	19.876 ± 14.028	22.833 ± 6.677	16.704 ± 4.637

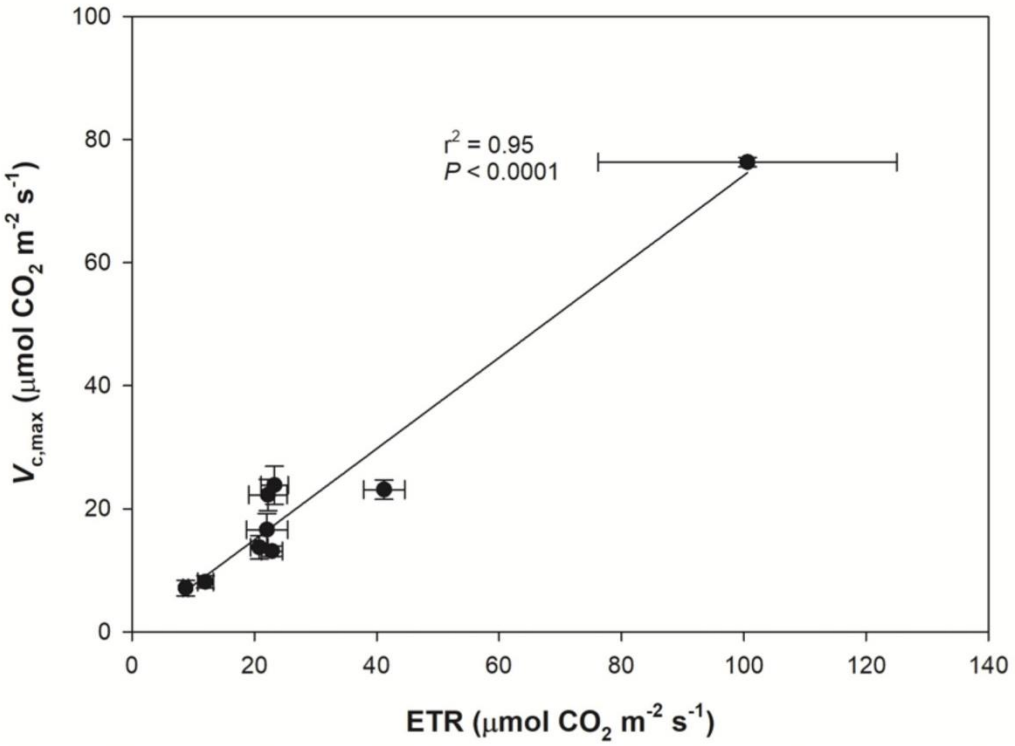

Fig. S1. Maximum velocity of carboxylation ($V_{c,max}$) in relation to electron transport rate (ETR). Even removing the species with the highest values, the correlation remains significant ($r^2 = 0.59$; $P < 0.0001$). Values are means ± SE per species.

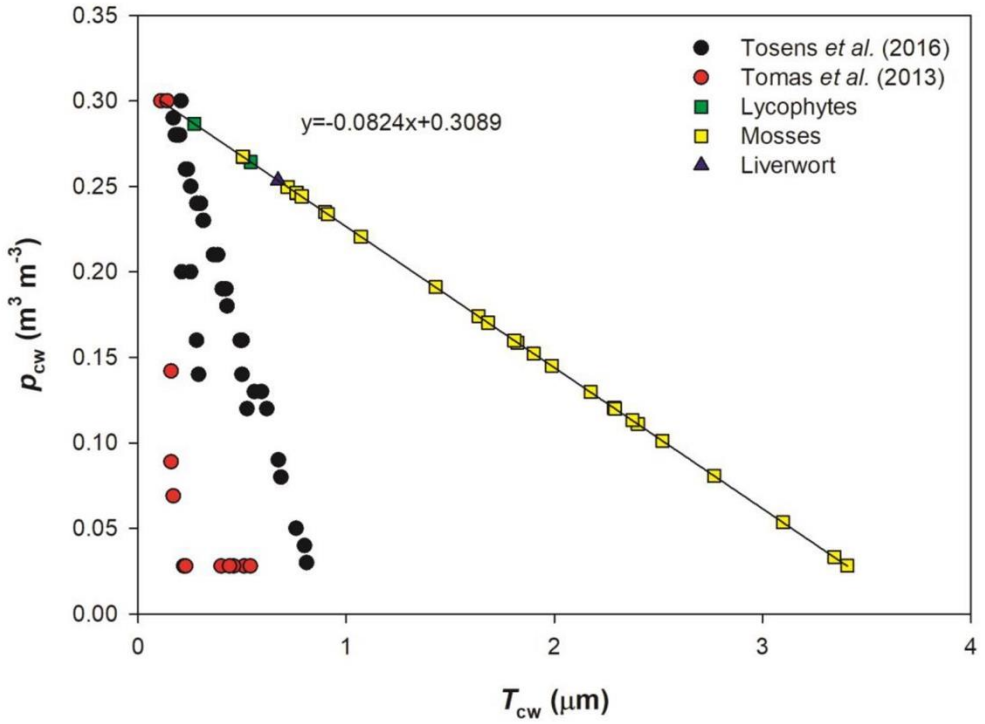

Fig. S2. Hypothetical relationship between effective porosity of the cell wall (p_{cw}) and cell wall thickness (T_{cw}) considered by Tomás *et al*. (2013), Tosens *et al*. (2016) and this study based on the negative linear relationship suggested by Terashima *et al*. (2006). The three studies assigned a maximum p_{cw} of 0.3 m^3 m^{-3} (value suggested by Nobel *et al*., 1991) to the species with thinner cell walls, and a minimum p_{cw} of 0.028 m^3 m^{-3} (value suggested by Tomás *et al*., 2013) to the species with the thickest cell walls reported at the time of study publication. Tomás et al. (2013) considered an exponential decay relationship between p_{cw} and T_{cw}, while Tosens et al. (2016) and the present study considered a linear relationship.

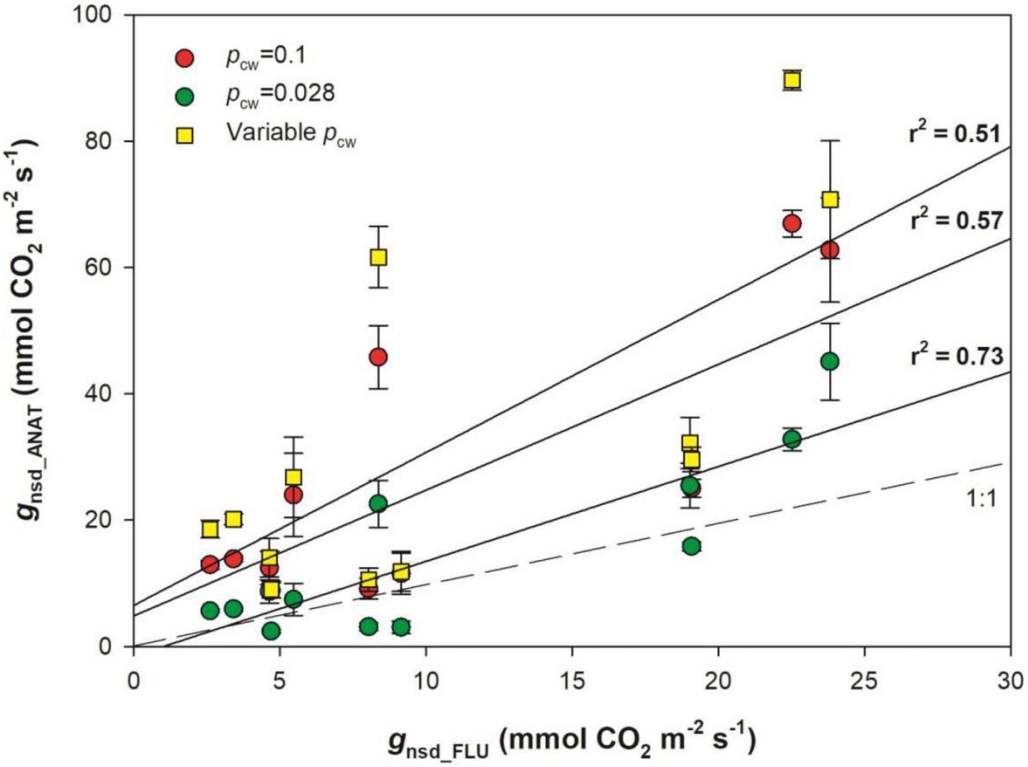

Fig. S3. Non-stomatal diffusion conductance modelled from anatomy following Tomás et al. (2013; g_{nsd_ANAT}) and considering cell wall porosities (p_{cw}) of 0.1, 0.028 or variable p_{cw} in relation to non-stomatal diffusion conductance estimated following Harley et al. (1992; g_{nsd_FLU}). The data were fitted by linear regression. Dashed line corresponds to the 1:1 relationship.

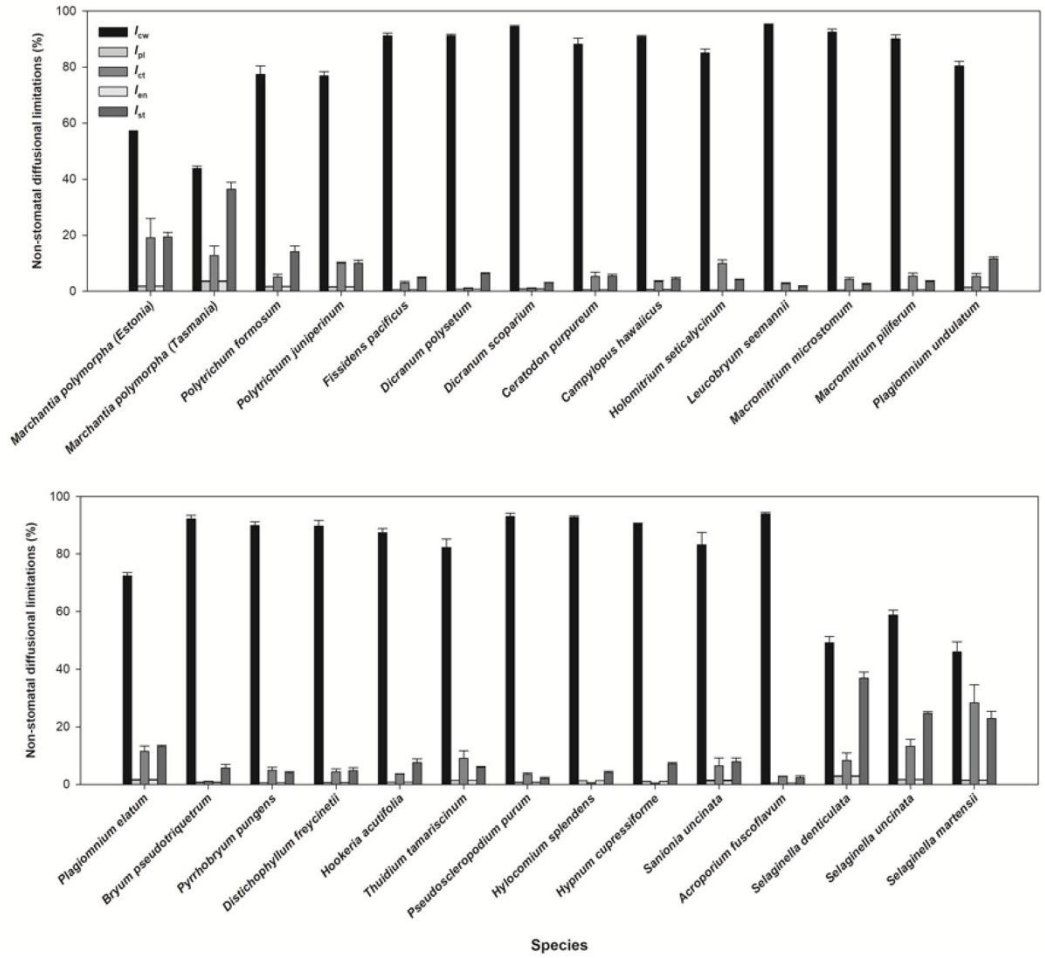

Fig. S4. The percentage of non-stomatal diffusion conductance per area limited by liquid phase components: cell wall (l_{cw}), plasma membrane (l_{pl}), cytoplasm (l_{ct}), chloroplast envelope (l_{en}) and stroma (l_{st}). Values are means ± SE per species.

Video S1. Measurement of the anatomical characteristics in two species with contrasting morphologies that are representative of this study. **(See video file as an additional Supporting Information file)**

Chapter 4. Chloroplast surface area-based strategies to optimize mesophyll conductance

Thuja plicata, a conifer species with very thick leaves and cell walls, compensates low CO_2 diffusion by extremely high exposure of chloroplasts to intercellular air spaces

Marc Carriquí[1*], Miquel Nadal[1], Jaume Flexas[1]

[1]Research Group in Plant Biology under Mediterranean Conditions, Universitat de les Illes Balears, Palma 07122, Illes Balears, Spain

*Corresponding author

Email: m.carriqui@uib.cat

Telephone number: +34 971 25 95 56

Keywords: Cell wall; chloroplast distribution; conifer; mesophyll conductance

Running head:

Extreme leaf anatomy to compensate CO_2 diffusion

Abstract

Mesophyll conductance (g_m) is mainly set by several anatomical traits that are generally inter-coordinated, and extreme values for these traits have been reported thus far in species with high or low photosynthetic capacity. However, recently published work on mesophyll conductance in gymnosperm species (with thick leaves and extreme cell walls) opened the possibility of finding within this plant group some outlier species in the general relationships widely reported for tracheophytes. Searching for outliers, we performed a screening of gymnosperm species, characterizing their main physiological and morphoanatomical traits. We found that *Thuja plicata* Donn ex D.Don, with extremely thick leaves and cell walls, also had the highest chloroplast surface area exposed to intercellular airspace per leaf projected area (S_c/S) ever reported for a land plant. Modelling revealed that this high S_c/S allows *T. plicata* reaching a reasonable g_m and compensating the negative effect of the other anatomical traits. However, if other wild species with lower cell wall thickness would have had such large S_c/S, they would express crop-like g_m values. The discovery of this outlier species empirically demonstrates that leaves with modified anatomy to increase or maintain their mesophyll conductance while increasing their stress tolerance are biologically possible.

Introduction

Mesophyll conductance (g_m) is, together with stomatal conductance and biochemistry, a main limitation to photosynthesis. Defined as the inverse of the diffusive resistance found by CO_2 molecules to move inside the leaf from the substomatal cavity to the carboxylation site in the chloroplast stroma, it is composed by several anatomical and biochemical traits. Now that g_m has been characterized in many terrestrial plant species, certain common patterns are

observed to be followed by species in order to achieve a greater g_m (Flexas et al. 2018).

In this sense, the main anatomical traits involved in constraining g_m are: leaf thickness (T_{leaf}), chloroplast surface area exposed to intercellular airspace per leaf area (S_c/S) and cell wall thickness (T_{cw}; Evans et al. 2009, Niinemets et al. 2009, Terashima et al. 2011, Tomás et al. 2013, Tosens et al. 2012, 2016, Veromann-Jürgenson et al. 2017, Ren et al. 2019). Plants with higher g_m tend to have thinner leaves and cell walls and increased leaf density, with more and smaller cells (Lehmeier et al. 2017, Ren et al. 2019), which in turn results in a higher S_c/S (Onoda et al. 2017, Ren et al. 2019). High values of S_c/S and low values of T_{cw} tend to be associated to crops and annual angiosperms, and the opposite to ferns, gymnosperms and long-lived leaves (Tosens et al. 2016, Onoda et al. 2017, Veromann-Jürgenson et al. 2017, Flexas et al. 2018). Conflicting strategies (e.g. high T_{cw} and high S_c/S, or low T_{cw} and low S_c/S) have not been reported yet in leaves of plants grown in optimal conditions. However, while a biological limit seems to impede the development of mesophyll cell walls < 0.09 micrometers thick (Tomás et al. 2013, Han et al. 2016, Ouyang et al. 2017, Carriquí et al. 2019a), no upper limit has been suggested for S_c/S (Ren et al. 2019).

We hypothesize that some perennial species with extremely high T_{leaf} and T_{cw} could have developed also extremely high S_c/S to partially compensate the low CO_2 diffusion conductance (thus improving their carbon balance). Good candidate species could be found within ferns (but none was found in a survey of > 30 species (Tosens et al. 2016) or in gymnosperms (Veromann-Jürgenson et al. 2017). In a survey of several gymnosperm species (unpublished data) we found *Thuja plicata* Donn ex D. Don, an economically important evergreen tree species of the Pacific North-west forests of North America that can grow up to 70 meters height (Harlow et al. 2005), to be an outlier to the above described tendencies. The objectives of the present work are: (1) to describe the photosynthetic and anatomical characteristics of *T. plicata* that convert this species into an outlier in comparison to other species, including other gymnosperms; (2) to assess the extent to which the particular anatomy of *T.*

plicata optimizes its photosynthesis; and (3) to model how large could be the g_m and photosynthesis rate of other species should they have the extremely large S_c/S displayed by *T. plicata*.

Material and methods

Seven 80-cm tall plant of *Thuja plicata* Donn ex. D. Don were bought from a nursery. Then, plants were transplanted into pots (15 L) containing 75:25 mixture of horticultural substrate (peat) and pearlite (granulometry A13) and were fertilised with 5 g l^{-1} of slow release NPK (4/1/2 ratio) fertilizer (Multigreen, Haifa Chemicals, Madrid, Spain). Plants were grown outdoors fully exposed to direct sunlight under Mediterranean conditions at the University of the Balearic Islands (Mallorca, Spain; 39º45'51''N, 2º42'33''E) and watered by automatic drip every three days to maintain optimum water status. Measurements were performed in April 2016 (mean max/min temperatures 20.4/9.0 ºC, mean relative humidity 67.6 % and mean photosynthetic active radiation at noon ca. 1515 μmol m^{-2} s^{-1}). All measurements were performed on young fully expanded leaves to ensure mature leaf anatomy and to limit variation among plants.

Gas exchange and chlorophyll fluorescence measurements

Leaf gas exchange parameters were measured using a LI-6400 portable photosynthesis system (LI-COR, Inc., Lincoln, NE, USA) with an infrared gas analyser (IRGA) coupled with a 2 cm^2 leaf fluorescence chamber (Li-6400-40 leaf chamber fluorometer; Li-Cor, Inc.). All measurements were carried out between 10:00 and 17:00 h (Central European summer time). Block temperature was fixed at 25ºC, vapor pressure deficit (VPD) kept between 1.5-2.0 kPa and air flow rate between 150 to 200 μmol s^{-1} for all measurements.

Leaves from randomly selected plants were fully characterized. Leaf steady-state conditions were induced at 400 μmol CO_2 mol^{-1} air and saturating photosynthetic photon flux density (PPFD 1500 μmol m^{-2} s^{-1}, 90:10 red:blue light). Once steady state conditions were achieved, typically after 35-50 minutes,

complete light and CO_2 response curves (11 and 13 steps, respectively) were performed in a random order. Then, additional CO_2 response curves were performed under non-photorespiratory conditions (O_2 < 2%). Six to seven curves were performed per response curve type. The order in which curves were performed did not affect the responses (data not shown). Values of net assimilation rate (A_N) and the efficiency of photosystem II (ΦPSII) were registered just after the steady-state conditions for gas exchange were reached. Multiphase flash methodology for chlorophyll fluorescence measurements was followed, as suggested by Loriaux *et al.* (2013). The electron transport rate (ETR) was estimated from Genty et al. (1989) as ETR = PPFD × ΦPSII × α × β, being α the leaf absorbance and β the electron partitioning between photo-systems I and II. The $\alpha \cdot \beta$ parameter was estimated following Valentini et al. (1995) from light response curves under non-photorespiratory conditions. Non-photorespiratory respiration during the day (R_d) was estimated as half the respiration rate measured after 2 h of dark-adapting the plants (Martins et al. 2013, Niinemets et al. 2005, Veromann-Jürgenson et al. 2017). As *T. plicata* leaves did not fully cover the 2 cm^2 cuvette (covered between 1.4 and 1.9 cm^2), an image of the leaf fraction placed in the chamber was taken, and the actual projected area was calculated using ImageJ software (Wayne Rasband/NIH, Bethesda, MD, USA). The corrected projected areas were used to recalculate gas-exchange data. Moreover, any measurement performed at a non-ambient CO_2 concentration was corrected for leaks following Flexas et al. (2007). Then, mesophyll conductance (g_{m_FLU}) was estimated following Harley et al. (1992), as:

$$g_{m\_FLU} = \frac{A_N}{C_i - \frac{\Gamma^* (ETR + 8 (A_N + R_d)}{(ETR - 4(A_N + R_d)}} \quad (1)$$

where A_N is the net assimilation rate, Γ^* is CO_2 compensation point in absence of R_d, and C_i the CO_2 concentration in intercellular air-spaces. Γ^* was assumed to be 42.5 µmol mol^{-1} as in Bernacchi et al. (2001) due to the lack of available data for the CO_2/O_2 specificity factors in conifer species. The g_m values were used to transform the previous CO_2 response curves to A_N-C_c curves. A_N-C_c curves were used to calculate the maximum velocity of carboxylation ($V_{c,max}$), and the maximum electron transport rate on a C_c basis (J_{max}).

Leaf mass per unit area

Leaves were sampled and photographed in an orthogonal plane to determine its projected leaf area using IMAGEJ software (Schneider et al. 2012). Afterwards, leaf portions were placed in an oven at 60ºC until constant dry weight was reached to calculate the dry leaf mass per unit leaf area (LMA).

Anatomical measurements

Immediately after gas-exchange measurements, small leaf pieces (3 × 2 mm) of the area enclosed in the leaf chamber were cut off, immersed and fixed under vacuum pressure with a glutaraldehyde 4% and paraformaldehyde 2% in a 0.1 M phosphate buffer (pH 7.4) fixing solution. 5 plants were sampled. Afterwards, samples were post-fixed in 2% buffered osmium tetroxide for 2h, and dehydrated in a graded series of ethanol. Dehydrated samples were embedded in resin (LR-White, London Resin Company, London, UK) and solidified in an oven at 60ºC for 48h.

Semi-thin cross-sections of 0.8 µm and ultrathin cross-sections of 90 nm for transmission electron microscopy (TEM) were cut with an ultramicrotome (Leica UC6, Vienna, Austria). Semi-thin sections were dyed with 1% toluidine blue and observed at 200× magnifications under an Olympus BX60 (Olympus, Tokyo, Japan) light microscopy and photographed with a Moticam 3 (Motic Electric Group Co., Xiamen, China). The ultrathin sections were contrasted with uranyl acetate and lead citrate and viewed at 1200× and 30000× magnifications with a transmission electron microscopy (TEM H600; Hitachi, Tokyo, Japan). All images were analysed using IMAGEJ software (Schneider et al. 2012). Leaf thickness from adaxial to abaxial cuticle (T_{leaf}), mesophyll thickness between the two epidermal layers but excluding vascular bundles (T_{mes}), fraction of the mesophyll occupied by intercellular airspaces (f_{ias}), mesophyll cell diameter and length in randomly selected cells and mesophyll surface area exposed to intercellular airspace per unit of projected leaf area (S_m/S) were measured from light microscopy images. Cell wall thickness (T_{cw}), cytoplasm thickness (T_{cyt}),

chloroplast length (L_{chl}), chloroplast thickness (T_{chl}) and chloroplast surface area exposed to intercellular airspace per unit of projected leaf area (S_c/S) were measured and calculated following Tomás et al. (2013) from TEM images. Cell curvature correction factor was calculated according to Thain (1983). Correction factors of 1.22 and 1.45 were applied to cell surface area estimates for the palisade and mesophyll tissue, respectively. Four to six randomly selected different fields of view were considered per plant replicate to measure each anatomical characteristic. At least 10 measurements were performed per anatomical characteristic (15 for L_{chl} and T_{chl} and 30 for cell dimensions), mesophyll tissue type (spongy and palisade) and replicate across the entire leaf cross-section. Then, weighted averages based on tissue volume fractions were calculated.

Estimation of mesophyll conductance modelled from anatomical characteristics

The one-dimensional within-leaf gas diffusion model of Niinemets & Reichstein (2003) as modified by Tomás et al. (2013) was applied. Mesophyll diffusion conductance as a composite conductance for within-leaf gas, liquid and lipid components (g_{m_ANAT}) is given as:

$$g_{m\_ANAT} = \frac{1}{\frac{1}{g_{ias}} + \frac{RT_k}{H \cdot g_{liq}}} \quad (2)$$

where H is the Henry's law constant ($m^3\ mol^{-1}\ K^{-1}$), R is the gas constant ($Pa\ m^3\ K^{-1}\ mol^{-1}$) and T_k is the absolute temperature (K). $H/(RT_k)$ is the dimensionless form of Henry's law constant needed to convert a liquid phase conductance (g_{liq}) into a gas-phase equivalent conductance (Niinemets & Reichstein 2003). Gas-phase diffusion depends on the fraction of mesophyll volume occupied by intercellular air spaces (f_{ias}, $m^3\ m^{-3}$) and the effective diffusion path length in the gas-phase (ΔL_{ias}) (Syvertsen et al. 1995, Terashima et al. 2011). Gas phase conductance (g_{ias}) was given as formulated by Earles et al. (2018):

$$g_{ias} = \frac{D_a \cdot f_{ias}}{\lambda \cdot \Delta L_{ias} \cdot \varsigma} \quad (3)$$

where D_a (m^2 s^{-1}) is the diffusion coefficient for CO_2 in the gas-phase ($1.51 \cdot 10^{-5}$ m^2 s^{-1} at 25°C), λ is the lateral path lengthening (m m^{-1}) and ς is the diffusion path tortuosity (m m^{-1}). ΔL_{ias} was approximated by mesophyll thickness divided by two (Niinemets & Reichstein 2003). λ and ς where assumed to be $f_{ias}^{-0.5}$ following Earles et al. (2018). The total liquid phase conductance is provided by the sum of the inverse of serial conductances:

$$\frac{1}{g_{liq}} = \left(\frac{1}{g_{cw}} + \frac{1}{g_{pl}} + \frac{1}{g_{ct}} + \frac{1}{g_{en}} + \frac{1}{g_{st}}\right) \cdot S_c/S \quad (4)$$

where partial conductances are for cell wall (g_{cw}), plasmalemma (g_{pl}), cytosol (g_{ct}), chloroplast envelope (g_{en}), and chloroplast stroma (g_{st}). The cell wall, cytosol and stromal conductances are given by a general equation:

$$g_i = \frac{r_{f,i} \cdot D_w \cdot p_i}{\Delta L_i} \quad (5)$$

where g_i (m s^{-1}) is either g_{cw}, g_{ct} or g_{st}, ΔL_i (m) is the diffusion path length and p_i (m^3 m^{-3}) is the effective porosity in the given part of the diffusion pathway, D_w is the aqueous phase diffusion coefficient for CO_2 ($1.79 \cdot 10^{-9}$ m^2 s^{-1} at 25°C) and the dimensionless factor $r_{f,i}$ accounts for the decrease of diffusion conductance compared to free diffusion in water (Weisiger 1998). For cell walls where the aqueous-phase diffusion has been shown to approximate free water, $r_{f,i}$ = 1 (Rondeau-Mouro et al. 2008). The value of r_f was set at 0.3 for g_{ct} and g_{st} to account for the reduction of diffusion conductance due to high concentrations of high molecular solutes and intracellular (cytoskeleton) and intraorganellal (thylakoids) heterogeneities (Niinemets & Reichstein 2003). Effective porosity, p_i, was taken as 1 for g_{ct} and g_{st}. Cell wall porosity (p_{cw}) was taken as 0.028, as applied in Tomás et al. (2013) for species with species with T_{cw}>0.4 μm. Conductance in units of m s^{-1} can be converted into molar units considering that

g[mol m^{-2} s^{-1}] = g[m s^{-1}]44.6·[273.16/(273.16 + T_L)(P/101.325)],

where T_L is the leaf temperature (ºC) and P (Pa) is the air pressure.

Due to the difficulty to measure the thickness of the plasma membrane, the chloroplast envelope and the limited information about the permeability of the lipid phase membranes, g_{pl} and g_{env} were assumed as constant values (0.0035 m s^{-1})

as previously done in other studies (Evans et al. 1994, Peguero-Pina et al. 2012, Tosens et al. 2012a, 2012b, Tomás et al. 2013).

Analysis of quantitative limitations of A_N and g_m

The relative limitations on A_N were calculated following Grassi & Magnani (2005). This analysis quantifies the relative importance of stomatal, mesophyll conductance and biochemical limitations (the latter integrating both Rubisco and photochemistry/Calvin cycle, owing to the fact that photosynthesis usually operates at co-limitation between these two factors; see Gallé et al. 2009, and Varone et al. 2012, for further explanation). *Relative* limitations, that is, those imposed by limited stomatal (l_s) or mesophyll conductance (l_m), and reduced biochemical capacity (l_b), were calculated as:

$$l_s = \frac{\frac{g_{tot}}{g_s} \cdot \frac{\delta A_N}{\delta C_c}}{g_{tot} + \frac{\delta A_N}{\delta C_c}} \quad (6)$$

$$l_m = \frac{\frac{g_{tot}}{g_m} \cdot \frac{\delta A_N}{\delta C_c}}{g_{tot} + \frac{\delta A_N}{\delta C_c}} \quad (7)$$

$$l_b = \frac{g_{tot}}{g_{tot} + \frac{\delta A_N}{\delta C_c}} \quad (8)$$

where g_s and g_{m_FLU} are the stomatal and mesophyll conductances to CO_2 and g_{tot} is the total conductance (the sum of inversed serial conductances g_{m_FLU} and g_s). $\delta A_N/\delta C_c$ is the slope of A_N-C_c response curves over a C_c range of 50-100 µmol mol^{-1}. These three values sum 100% and characterize the extent to which any of the three limitations curbs photosynthesis at the given values of the other two. The contribution of different components of cellular resistance to cellular resistance to CO_2 diffusion was estimated from the anatomical model following Tosens et al. (2016). This share of limitation (l_i) by different liquid phase components was calculated as:

$$l_i = \frac{g_{m\_ANAT}}{g_i \cdot S_c/S} \quad (9)$$

where l_i is the limitation by the cell wall, the plasmalemma, cytosol, chloroplast envelope and stroma, and g_i refers to the diffusion conductance of each

corresponding diffusion pathway. The limitation of each cellular component was scaled up with S_c/S.

This analytical model served to test the potential effect on g_{m_ANAT} of a hypothetical single anatomical trait exchange between species with contrasting leaf morphoanatomies.

Statistical analysis

Relationships among physiological and structural traits were explored by SPSS (SPSS, Chicago, IL, USA) and all statistical tests were considered significant at $P < 0.05$. Data for tracheophytes from the 44 datasets assembled by Ren et al. (2019) and Veromann-Jürgenson et al. (2017), Kuusk et al. (2018a, 2018b) and Carriquí et al. (2019b) subsequent publications were used to compare the main physiological and structural traits of *Thuja plicata* with other species of gymnosperms and other vascular plants groups. Only data for young fully-expanded leaves were used for the comparisons. Presented data for the cellular dimensions of ferns and angiosperms were measured from existing micrographs from Carriquí et al. (2015).

Results

Thuja plicata averaged a net assimilation rate (A_N) of 7.8 ± 0.6 μmol m^{-2} s^{-1} (mean ± SE), a stomatal conductance to CO_2 (g_s) of 0.058 ± 0.004 mol m^{-2} s^{-1}, and a mesophyll conductance to CO_2 estimated from fluorescence measurements (g_{m_FLU}) of 0.067 ± 0.011 mol m^{-2} s^{-1}, and a maximum carboxylation rate on a C_c basis ($V_{c,max}$) of 111 ± 9 μmol m^{-2} s^{-1} (Table 1, Fig. S1). A_N was photosynthetically co-limited by the mesophyll (l_m = 43.5 ± 3.5 %) and stomatal limitations (l_s = 38.7 ± 2.1 %), whereas biochemical limitation (l_b) accounted for only 17.7 ± 2.6 %. Its particular leaf morphoanatomy (Table 2) conferred *T. plicata* a maximum mesophyll conductance modelled from anatomical traits (g_{m_ANAT}) of 0.081 ± 0.012 mol m^{-2} s^{-1}. This g_{m_ANAT} was mainly constrained by liquid-phase limitations (79.2 %), among which the most important ones were those imposed by the cell wall (77.1 %) and chloroplast stroma (15.3

%), whereas plasma membrane, cytosol and chloroplast envelope limitations played a minor role (Fig. S2).

T. plicata presented the highest leaf thickness (T_{leaf}) values- followed by *Taxus baccata* with a T_{leaf} of 687 μm- among the reported gymnosperms (Fig. 1A). Moreover, with a chloroplast surface area exposed to intercellular airspace per unit of projected leaf area (S_c/S) of 34.0 ± 6.5 $m^2\ m^{-2}$ (Table 2), behaved as an outlier of the hyperbolic function described by gymnosperms for the relationship A_N-S_c/S (Fig. 1B; $r^2 = 0.64$, $P < 0.01$) and the linear function for the relationship g_{m_FLU}-S_c/S (Fig. 1C; $r^2 = 0.64$, $P < 0.0001$). For a given A_N and g_{m_FLU}, *T. plicata* had a significantly higher S_c/S. *T. plicata* presented a cell wall thickness (T_{cw}) with no differences between mesophyll tissue types (data not shown) and slightly higher than the average T_{cw} value for gymnosperms (0.556 ± 0.08 μm). Thus, *T. plicata* remains within the pool of gymnosperm species in the relation A_N-T_{cw} (Fig. 1D) but being outlier (together with *Picea abies*) of the exponential decay function described by gymnosperms in the g_{m_FLU}-T_{cw} relation (Fig. 1E; $r^2 = 0.55$, $P < 0.0005$). *T. plicata* was a clear outlier of the general relationship between S_c/S and T_{cw} followed by gymnosperms (Fig. 1F; $r^2 = 0.35$, $P < 0.005$). When expanding the comparison to other groups within tracheophytes (angiosperms, ferns and lycophytes), *T. plicata* was the species with the highest S_c/S, just closely followed by another gymnosperm, *Abies pinsapo* (32.3 $m^2\ m^{-2}$). Apart from these two species, only in the crop *Oryza sativa* and the evergreen angiosperm tree *Castanopsis sieboldii* $S_c/S > 25\ m^2\ m^{-2}$ values were reported (Fig. 2A-B). Again, *T. plicata* behaved as an outlier of the A_N-S_c/S and g_m-S_c/S correlations (Fig. 2A-B; $r^2 = 0.18$, $P < 0.0001$ and $r^2 = 0.23$, $P < 0.0001$, respectively), and was fitted into the exponential decay functions described in A_N-T_{cw} and g_m-T_{cw}, being within the 10% of tracheophyte species with thicker T_{cw} (Fig. 2C-D; $r^2 = 0.35$, $P < 0.0001$ and $r^2 = 0.26$, $P < 0.0001$, respectively).

When examining the relative position of *T. plicata* morphoanatomical traits in relation to other fern, gymnosperm and angiosperm species, *T. plicata* stood out for having the largest leaf thickness (T_{leaf}; Fig. 3A). Moreover, *T. plicata* had the lowest leaf density (D_{leaf}) among the species with high LMA (i.e. above 100 g

m^{-2}; Fig. 3B). *T. plicata* did not differ from the rest of tracheophytes in its fraction of mesophyll occupied by intercellular airspaces (f_{ias}) or T_{cw} (Fig. 3C-D).

When comparing LMA and S_c/S, whereas no correlation was found for gymnosperm species, a positive linear function emerged for ferns and angiosperms (Fig. 3E; $r^2 = 0.31$; $P < 0.05$). In this case, *T. plicata*, being an outlier for gymnosperms, instead tends to fit in the positive correlation found for the fern and angiosperm species for which also data on cell dimensions were available (Fig. 3E). In order to elucidate the anatomical reasons for that high S_c/S, relations between T_{leaf}, the percentage of mesophyll occupied by each mesophyll type fraction, and the cell diameter and length dimensions for both palisade and spongy mesophyll cells were evaluated in relation to other species available from literature, including gymnosperms, ferns and angiosperms. *T. plicata*, in addition to have the thickest leaves among the considered species (Fig. 4A), also showed a high percentage of mesophyll thickness occupied by spongy tissue (75.7%; Fig. 4B). Moreover, *T. plicata* had the biggest cell dimensions among the species for which S_m/S and S_c/S were also available for palisade cells (Fig. 4C), but especially for spongy cells, being spongy cells a 38% longer and a 54% wider than in *Alisma plantago-aquatica*, the second ranking species for large spongy cells (Fig. 4D).

Analytical models based on leaf anatomy revealed that exchanging a single key anatomical trait between *T. plicata* and the fern *Pteris vitatta* and the angiosperm *Phlomis italica*, the first with similar g_{m_FLU} (0.059 mol m^{-2} s^{-1}) and the second with the same S_c/S as *P. vitatta* (*ca.* 9.0-9.3 m^2 m^{-2}) but with a 2.1-fold higher g_{m_FLU} than *T. plicata*, would have strong consequences on the total mesophyll resistance. As the three species had strongly diverging leaf thickness (Fig. 5), we improved the estimation of the gas-phase limitation by accounting for the tortuosity factor and the path lengthening in the intercellular air space following the approach recommended by Earles et al. (2018). Hypothetical changes in leaf thickness had no significant effect on g_{m_ANAT} for none of the species, even considering the improvements of the analytical model suggested by Earles et al. (2018). Conversely, changes in cell wall thickness would impose a significant boost to g_{m_ANAT} in *T. plicata*, placing the species close to the position

of *Abies pinsapo* (Fig. 1A-D, 6A,B), and a significant decrease for *P. italica*'s g_{m_ANAT}, that would be reduced to only a fifth part with *Thuja*'s T_{cw} (Fig. 6C). However, the most relevant effect in g_{m_ANAT} would be the imposed by the hypothetical S_c/S of *T. plicata* in *P. vitatta*, from real 0.050 ± 0.002 mol m^{-2} s^{-1} to 0.166 ± 0.001 mol m^{-2} s^{-1} (Fig. 6D), but especially in the case of *P. italica*, from real g_{m_ANAT} of 0.143 ± 0.008 mmol m^{-2} s^{-1} to 0.495 ± 0.029 mmol m^{-2} s^{-1} (6C), close to the high-photosynthetic yield crops (Fig. 2B).

Discussion

Thuja plicata is an outlier of the previously described gas exchange-leaf anatomy relationships

Thuja plicata, a gymnosperm with very long-lived leaves (average leaf longevity of 8.9 ± 0.2 years, Harlow et al. 2005), was found to present the largest chloroplast surface area exposed to intercellular airspace per unit of projected leaf area (S_c/S) ever reported in plants. This was associated to having the largest cell dimensions for both palisade and spongy tissues among all the plants in which S_m/S and S_c/S values were also available- although still within the cell dimensions range reported for C_3 plants, and lower than in most CAM plants (Nelson et al., 2005, Earles et al., 2018). C_3 plants with higher g_m tend towards greater number of smaller cells per leaf area, since this theoretically increases the mesophyll surface area exposed to the intercellular airspace per unit of projected leaf area (S_m/S; Maxwell et al. 1997, Griffiths et al. 2008). If the chloroplast number remains similar in mesophyll cells (Terashima et al. 2006), a greater S_m/S directly implies a higher S_c/S (Ren et al. 2019). Thus, higher S_c/S increases the CO_2 fixation capacity through creating more parallel and shorter pathways for CO_2 liquid-phase diffusion (Nobel 1991). However, we found that *T. plicata* achieves the highest ever reported S_c/S using a different strategy. *T. plicata* increased its S_m/S (and therefore S_c/S) by developing thick (Fig. 3A) but not dense leaves (Fig. 3B). This resulted in the quasi-alignment of *T. plicata* with angiosperm and ferns linear function for the LMA-S_c/S relationship. (Fig. 3E). Contrarily what has been previously reported (Terashima et al. 2011, He et al. 2017 Lehmeier et al. 2017, Ren et al. 2019), *T. plicata* presented extremely high S_c/S while presenting big (instead of smaller and/or lobed) cells (Fig. 4A-D).

Specially in the case of spongy mesophyll, that represented close to 70% of total mesophyll fraction (Fig. 4B), cells were strongly higher when compared to the angiosperm and fern species for which S_m/S and S_c/S values were also available (Fig. 4D). Lehmeier et al. (2017) demonstrated in *Arabidopsis* mutants that mesophyll cell proliferation can be either promoted or repressed to modify cell density and airspace patterning. That is, affecting g_{ias} (both tortuosity, path lengthening and intercellular air spaces connectivity), as claimed by Earles et al. (2018) but also allowing for an increase in S_m/S, and therefore in S_c/S. Increasing the fraction of spongy mesophyll tissue allows *T. plicata* to build a very large (>30%) fraction of intercellular air spaces. Consequently, while quantitative limitation analysis revealed that the mesophyll gas-phase limitation to CO_2 diffusion surprisingly just accounted for less than 1% of the total limitation in gymnosperms (Veromann-Jürgenson et al. 2017), in *T. plicata* gas-phase limitations accounted for up 20.8 %. Figure 7 illustrates in a conceptual comparison how the vast majority of leaves and thick flat leaves following the strategy of *Thuja plicata* would differently achieve high S_c/S. Leaves with relatively low S_c/S often present few cell layers of a given size (Fig. 7A). Leaves reported up to now with large S_c/S essentially present a larger number of smaller cells, thus increasing S_m/S and S_c/S at the expense of reducing f_{ias} (Fig. 7B). Instead, *Thuja plicata* achieves the highest ever reported S_c/S by increasing leaf thickness as well as mesophyll cell size, which is achieved by differentially increasing the fraction of spongy tissue, thus also incrementing f_{ias} (Fig. 7C).

Besides these peculiarities, *T. plicata* still showed other anatomical traits common to gymnosperms, such as very large T_{leaf} and T_{cw} (Fig. 1A,D; Peguero-Pina et al. 2012,Veromann-Jürgenson et al. 2017, Kuusk et al. 2018a). These particular anatomical arrangements resulted in breaking the commonly-observed negative relationship between S_c/S and T_{cw} for vascular plants (Syvertsen et al. 1995, Onoda et al. 2017, Xiong et al. 2017, Ren et al. 2019; see also Fig. 1F). With its particular traits, *T. plicata* behaves as a clear outlier of the strong relationships found between physiological and anatomical traits in both gymnosperms and spermatophytes, revealing the possibility to build leaves with strong structural and defensive properties (through high T_{leaf} and T_{cw}) while maintaining or increasing mesophyll conductance (by increasing S_c/S).

Large S_c/S in Thuja plicata partially compensates low photosynthesis imposed by very large T_{leaf} and T_{cw}

Peguero-Pina et al. (2012) argued that large assimilation rates found in *Abies pinsapo* might be aided by a more densely packed mesophyll per unit leaf area (Niinemets et al. 2009). However, as shown in Fig. 1, large photosynthesis and g_m in *A. pinsapo* are perhaps more related to a high S_c/S (Fig. 1B, C) coupled with a low T_{cw} (Fig. 1D, E). This species thus follows the general rule, in which species with large S_c/S also tend to present low T_{cw}, which results in large photosynthesis. *T. plicata* had an even larger S_c/S than *A. pinsapo*, but its g_m and photosynthesis rates were lower. While very large T_{leaf} and T_{cw} may be necessary for this species to achieve its large leaf life-span (Harlow et al. 2005) as well as defence against biotic and abiotic stresses (Wright et al. 2004), they have a penalty on g_m and photosynthesis. Thus, we hypothesize that the very large S_c/S exhibited by this species is a strategy to partially compensate the negative effects of its anatomy on photosynthesis, which could compromise the plant's carbon balance.

Consistently, based on the regression shown in Fig. 1E for the other gymnosperm species, the T_{cw} displayed by *T. plicata* should have resulted in a g_m of 0.030 mol m^{-2} s^{-1}. Considering the g_s and $V_{c,max}$ displayed by this species, this would have resulted in a net CO_2 assimilation of only 5.0 μmol m^{-2} s^{-1}, instead of the actually exhibited (7.8 ± 0.6 μmol m^{-2} s^{-1}). As mesophyll conductance limitation is the largest in this species (43.5 ± 3.5 %), and S_c/S and T_{cw} are the most limiting anatomical constraints to g_m, it is expected that these two traits will have the largest influence on setting the observed values of photosynthesis. Because S_c/S positively affects g_m and photosynthesis, and T_{cw} negatively affects them, we have plotted the relationship between A_n and g_m and the ratio S_c/S / T_{cw} (Fig. 8). Positive linear relationships emerge between both parameters and this ratio, *T. plicata* falling well within them, further confirming that increased S_c/S compensates large T_{cw}, so that the same photosynthesis is achieved as in other species for a given value of their ratio.

Therefore, we conclude that the large S_c/S in *T. plicata* partially compensates for the negative effects on photosynthesis of its very large T_{leaf} and T_{cw}. This effect was recently observed in *Quercus* species, which increase g_m and off-set the constraints imposed by high LMA by increasing S_c/S, although only the 5-15 m^2 m^{-2} range (Peguero-Pina et al. 2017).

Concluding remarks

We describe for the first time a species, the conifer *Thuja plicata*, which shows simultaneously large leaf thickness, cell wall thickness, and S_c/S, the latter being the largest value ever reported for any species. In addition, high S_c/S in this species is achieved by anatomical arrangements very different to those exhibited by other species with high S_c/S, which include a large fraction of spongy tissue and very large cell dimensions. Increased S_c/S partially compensates for the negative effects of large T_{leaf} and T_{cw} on mesophyll conductance and photosynthesis, thus probably allowing *T. plicata* to present a large leaf life-span while keeping a positive leaf carbon balance. These results imply that it may be possible to break the often-observed negative relationship between S_c/S and T_{cw}, which could open a way to improve photosynthesis and/or to develop plants with simultaneous investments in leaf supporting, defensive structures and photosynthesis. Modelling shows that inducing S_c/S values as large as those of *T. plicata* could result in very large g_m and photosynthesis in other species.

Funding

Ministerio de Economía y Competitividad (MINECO, Spain) and the ERDF (FEDER, CTM2014-53902-C2-1-P); Conselleria d'Educació, Cultura i Universitats (Govern de les Illes Balears) and European Social Fund (FPI/1700/2014 to M.C.); Ministerio de Economía y Competitividad (MINECO, Spain) and European Social Fund (BES-2015-072578 to MN).

Acknowledgments

The authors are grateful to Miquel Truyols (Camp experimental, UIB) for taking care of the plants, and to Mª Teresa Mínguez, Universitat de València (Secció Microscòpia Electrònica, SCSIE), and to Dr Ferran Hierro, Universitat de les Illes Balears (Serveis Cientificotècnics), for technical support during microscopy analyses. We thank Guillaume Théroux-Rancourt for his helpful comments on the manuscript.

References

Adachi S., Nakae T., Uchida M., Soda K., Takai T., Oi T., Yamamoto T., Ookawa T., Miyake H., Yano M., Hirasawa T. (2013) The mesophyll anatomy enhancing CO_2 diffusion is a key trait for improving rice photosynthesis. *Journal of Experimental Botany* 64, 1061–1072.

Bernacchi C.J., Singsaas E.L., Pimentel C., Portis A.R. Jr., Long S.P. (2001) Improved temperature response functions for models of Rubisco-limited photosynthesis. *Plant, Cell and Environment* 24, 253–259.

Carriquí M., Cabrera H.M., Conesa M.À., Coopman R.E., Douthe C., Gago J., Gallé A., Galmés J., Ribas-Carbó M., Tomás M., Flexas J. (2015) Diffusional limitations explain the lower photosynthetic capacity of ferns as compared with angiosperms in a common garden study. *Plant, Cell and Environment* 38, 448–460.

Carriquí M., Douthe C., Molins A., Flexas J. (2019a) Leaf anatomy does not explain apparent short-term responses of mesophyll conductance to light and CO_2 in tobacco. *Plant Physiology* 165, 604–618.

Carriquí M., Roig-Oliver M., Brodribb T.J., Coopman R., Gill W., Mark K., Niinemets Ü., Perera-Castro A.V., Ribas-Carbó M., Sack L., Tosens T., Waite M., Flexas J. (2019b) Anatomical constraints to nonstomatal diffusion conductance and photosynthesis in lycophytes and bryophytes. *New Phytologist* 222, 1256–1270.

Earles J.M., Théroux-Rancourt G., Roddy A.B., Gilbert M.E., McElrone A.J., Brodersen C.R. (2018) Beyond porosity: 3D leaf intercellular airspace traits that impact mesophyll conductance. *Plant Physiology* doi: https://doi.org/10.1104/pp.18.00550.

Evans J.R., von Caemmerer S., Setchell B.A., Hudson G.S. (1994) The relationship between CO_2 transfer conductance and leaf anatomy in transgenic tobacco with a reduced content of Rubisco. *Australian Journal of Plant Physiology* 21, 475–495.

Evans J.R., Kaldenhoff R., Genty B., Terashima I. (2009) Resistances along the CO_2 diffusion pathway inside leaves. *Journal of Experimental Botany* 60, 2235–2248.

Flexas J., Díaz-Espejo A., Berry J.A., Galmés J., Cifre J., Kaldenhoff R., Medrano H., Ribas-Carbó M. (2007) Leakage in leaf chambers in open gas exchange systems: quantification and its effects in photosynthesis parameterization. *Journal of Experimental Botany* 58, 1533–1543.

Flexas J., Cano F.J., Carriquí M., Coopman R.E., Mizokami Y., Tholen D., Xiong D. (2018) CO_2 diffusion inside photosynthetic organs. In: Adams W.W., Terashima I. (eds) *The Leaf: A platform for performing photosynthesis, Advances in Photosynthesis and Respiration (including bioenergy and related processes)*, Vol. 44. Springer, Cham, pp. 163–208.

Gallé A., Florez-Sarasa I., Tomas M., Pou A., Medrano H., Ribas-Carbó M., Flexas J. (2009) The role of mesophyll conductance during water stress and recovery in tobacco (*Nicotiana sylvestris*): acclimation or limitation? *Journal of Experimental Botany* 60, 2379–2390.

Genty B., Briantais J.M., Baker N.R. (1989) The relationship between the quantum yield of photosynthetic electron-transport and quenching of chlorophyll fluorescence. *Biochimica et Biophysica Acta* 990, 87–92.

Grassi G., Magnani F. (2005) Stomatal, mesophyll conductance and biochemical limitations to photosynthesis as affected by drought and leaf ontogeny in ash and oak trees. *Plant, Cell and Environment* 28, 834–849.

Griffiths H., Robe W.E., Girnus J., Maxwell K. (2008) Leaf succulence determines the interplay between carboxylase systems and light use during Crassulacean acid metabolism in *Kalanchoë* species*. Journal of Experimental Botany* 59, 1851–1861.

Han J.-M., Meng H.-F., Wang S.-Y., Jiang C.-D., Liu F., Zhang W.-F., Zhang Y.-L. (2016) Variability of mesophyll conductance and its relationship with water use efficiency in cotton leaves under drought pretreatment. *Journal of Plant Physiology* 194, 61–71.

Harley P.C., Loreto F., Dimarco G., Sharkey T.D. (1992) Theoretical considerations when estimating the mesophyll conductance to CO_2 flux by analysis of the response of photosynthesis to CO_2. *Plant Physiology* 98, 1429–1436.

Harlow B.A., Duursma R.A., Marshall J.D. (2005) Leaf longevity of western red cedar (*Thuja plicata*) increases with depth in the canopy. *Tree Physiology* 25, 557–562.

He W., Adachi S., Sage R.F., Ookawa T., Hirasawa T. (2017) Leaf photosynthetic rate and mesophyll cell anatomy changes during ontogenesis in backcrossed *indicaxjaponica* rice inbred lines. *Photosynthesis Research* 134, 27–38.

Kuusk V., Niinemets Ü., Valladares F. (2018a) A major trade-off between structural and photosynthetic investments operative across plant and needle ages in three Mediterranean pines. *Tree Physiology* 38, 543–557.

Kuusk V., Niinemets Ü., Valladares F. (2018b) Structural controls on photosynthetic capacity through juvenile-to-adult transition and needle aging in Mediterranean pines. *Functional Ecology* doi, 10.1111/1365-2435.13087.

Lehmeier C., Pajor R., Lundgren M.R., Mathers A., Sloan J., Bauch M., Mitchell A., Bellasio C., Green A., Bouyer D., Schnittger A., Sturrock C., Osborne C.P., Rolfe S., Mooney S., Fleming A.J. (2017) Cell density and airspace patterning in the leaf can be manipulated to increase leaf photosynthetic capacity. *The Plant Journal* 92, 981–994.

Loriaux S.D., Avenson T.J., Welles J.M., McDermitt D.K., Eckles R.D., Riensche B., Genty B. (2013) Closing in on maximum yield of chlorophyll fluorescence using a single multiphase flash of sub-saturating intensity. *Plant, Cell and Environment* 36, 1755–1770.

Martins S.C.V., Galmés J., Molins A., DaMatta F.M. (2013) Improving the estimation of mesophyll conductance to CO_2: on the role of electron

transport rate correction and respiration. *Journal of Experimental Botany* 64, 3285–3298.

Maxwell K., von Caemmerer S., Evans J.R. (1997) Is low internal conductance to CO_2 a consequence of succulence in plants with Crassulacean acid metabolism? *Australian Journal of Plant Physiology* 24, 777–786.

Nelson E.A., Sage T.L., Sage R.F. (2005) Functional leaf anatomy of plants with Crassulacean acid metabolism. *Functional Plant Biology* 32, 409–419.

Niinemets Ü., Reichstein M. (2003) Controls on the emission of plant volatiles through stomata: a sensitivity analysis. *Journal of Geophysical Research* 108, 4211.

Niinemets Ü., Cescatti A., Rodeghiero M., Tosens T. (2005) Leaf internal diffusion conductance limits photosynthesis more strongly in older leaves of Mediterranean evergreen broad-leaved species. *Plant, Cell, and Environment* 28, 1552–1566.

Niinemets Ü., Díaz-Espejo A., Flexas J., Galmés J., Warren C. (2009) Role of mesophyll diffusion conductance in constraining potential photosynthetic productivity in the field. *Journal of Experimental Botany* 60, 2249–2270.

Nobel P.S. (1999) Physicochemical and environmental plant physiology. San Diego: Academic Press, Inc.

Onoda Y., Wright I.J., Evans J.R., Hikosaka K., Kitajima K., Niinemets Ü., Poorter H., Tosens T., Westoby M. (2017) Physiological and structural tradeoffs underlying the leaf economics spectrum. *New Phytologist* 214, 1447–1463.

Ouyang W., Struik P.C., Yin X., Yang J. (2017) Stomatal conductance, mesophyll conductance, and transpiration efficiency in relation to leaf anatomy in rice and wheat genotypes under drought. *Journal of Experimental Botany* 68, 5191–5205.

Peguero-Pina J.J., Flexas J., Galmés J., Sancho-Knapik D., Barredo G., Villarroya D., Gil-Pelegrín E. (2012) Leaf anatomical properties in relation

to differences in mesophyll conductance to CO_2 and photosynthesis in two related Mediterranean *Abies* species. *Plant, Cell and Environment* 35, 2121–2129.

Peguero-Pina J.J., Sancho-Knapik D., Flexas J., Galmés J., Niinemets Ü., Gil-Pelegrín E. (2016) Light acclimation of photosynthesis in two closely related firs (*Abies pinsapo* Boiss. and *Abies alba* Mill.): the role of leaf anatomy and mesophyll conductance to CO_2. *Tree Physiology* 36, 300–310.

Peguero-Pina J.J., Sisó S., Flexas J., Galmés J., García-Nogales A., Niinemets Ü., Sancho-Knapik D., Saz M.A., Gil-Pelegrín E. (2017) Cell-level anatomical characteristics explain high mesophyll conductance and photosynthetic capacity in sclerophyllous Mediterranean oaks. *New Phytologist* 214, 585–596.

Ren T., Weraduwage S.M., Sharkey T.D. (2019) Prospects for enhancing leaf photosynthetic capacity by manipulating mesophyll cell morphology. *Journal of Experimental Botany* 70, 1153–1165.

Rondeau-Mouro C., Defer D., Leboeuf E., Lahaye M. (2008) Assessment of cell wall porosity in *Arabidopsis thaliana* by NMR spectroscopy. *International Journal of Biological Macromolecules* 42, 83–92.

Schneider C.A., Rashband W.S., Eliceiri K.W. (2012) “NIH Image to ImageJ: 25 years of image analysis”. *Nature methods* 9, 671–675.

Syvertsen J.P., Lloyd J., McConchie C., Kriedemann P.E., Farquhar G.D. (1995) On the relationship between leaf anatomy and CO_2 diffusion through the mesophyll of hypostomatous leaves. *Plant, Cell and Environment* 18, 149–157.

Terashima I., Hanba Y.T., Tazoe Y., Vyas P., Yano S. (2006) Irradiance and phenotype: comparative eco-development of sun and shade leaves in relation to photosynthetic CO_2 diffusion. *Journal of Experimental Botany* 57, 343–354.

Terashima I., Hanba Y.T., Tholen D., Niinemets Ü. (2011) Leaf functional anatomy in relation to photosynthesis. *Plant Physiology* 155, 108–116.

Thain J.F. (1983) Curvature correlation factors in the measurements of cell surface areas in plant tissues. *Journal of Experimental Botany* 34, 87–94.

Tomás M., Flexas J., Copolovici L., Galmés J., Hallik L., Medrano H., Tosens T., Vislap V., Niinemets Ü. (2013) Importance of leaf anatomy in determining mesophyll diffusion conductance to CO_2 across species: quantitative limitations and scaling up by models. *Journal of Experimental Botany* 64, 2269–2281.

Tosens T., Niinemets Ü., Vislap V., Eichelmann H., Castro-Díez P. (2012a) Developmental changes in mesophyll diffusion conductance and photosynthetic capacity under different light and water availabilities in *Populus tremula*: how structure constrains function. *Plant, Cell and Environment* 35, 839–856.

Tosens T., Niinemets Ü., Westoby M., Wright I.J. (2012b) Anatomical basis of variation in mesophyll resistance in eastern Australian sclerophylls: news of a long and winding path. *Journal of Experimental Botany* 63, 5105–5119.

Tosens T., Nishida K., Gago J., Coopman R.E., Cabrera H.M., Carriquí M., Laanisto L., Morales L., Nadal M., Rojas R., Talts E., Tomas M., Hanba Y., Niinemets T., Flexas J. (2016). The photosynthetic capacity in 35 ferns and fern allies: mesophyll CO_2 diffusion as a key trait. *New Phytologist* 209, 1576–1590.

Valentini R., Epron D., Angelis P.D.E., Matteucci G., Dreyer E. (1995) In situ estimation of net CO_2 assimilation, photosynthetic electron flow and photorespiration in Turkey oak (*Q. cerris* L.) leaves: diurnal cycles under different levels of water supply. *Plant, Cell and Environment* 38, 2462–2474.

Varone L., Ribas-Carbó M., Cardona C., Gallé A., Medrano H., Gratani L., Flexas J. (2012) Stomatal and non-stomatal limitations to photosynthesis in

seedlings and saplings of Mediterranean species pre-conditioned and aged in nurseries: different response to water stress. *Environmental and Experimental Botany* 75, 235–247.

Veromann-Jürgenson L.-L., Tosens T., Laanisto L., Niinemets Ü. (2017) Extremely thick cell walls and low mesophyll conductance: welcome to the world of ancient living! *Journal of Experimental Botany* 68, 1639–1653.

Weisiger R. (1998) Impact of extracellular and intracellular diffusion barriers on transport. In: Bassingthwaighte J.B., Goresky C.A., Linehan J.H. (eds) Whole Organ Approach to Cellular Metabolism. Springer Verlag, New York, pp, 389–423.

Wright I.J., Reich P.B., Westoby M., et al. (2004) The world-wide leaf economics spectrum. *Nature* 428, 821–827.

Xiong D., Yu T., Zhang T., Li Y., Peng S., Huang J. (2015) Leaf hydraulic conductance is coordinated with leaf morpho-anatomical traits and nitrogen status in the genus *Oryza*. *Journal of Experimental Botany* 66, 741–748.

Xiong D., Flexas J., Yu T., Peng S., Huang J. (2017). Leaf anatomy mediates coordination of leaf hydraulic conductance and mesophyll conductance to CO_2 in *Oryza*. *New Phytologist* 213, 572–583.

Tables

Table 1. Photosynthetic characteristics for *Thuja plicata*. Average value ± SE of seven replicates are shown for net assimilation (A_N), stomatal (g_s) and mesophyll conductance to CO_2 (g_m), sub-stomatal CO_2 concentration (C_i), chloroplastic CO_2 concentration (C_c), maximum carboxylation rate on a C_c basis ($V_{c,max}$), electron transport rate (J_{max}) and dark respiration rate (R_d).

Table 2. Morphoanatomical characteristics for *Thuja plicata*. Average value ± SE of five replicates are shown for dry leaf mass per unit area (LMA), leaf density (D_{leaf}), leaf thickness (T_{leaf}), mesophyll thickness (T_{mes}), fraction of the mesophyll tissue occupied by intercellular air spaces (f_{ias}), mesophyll surface area exposed to intercellular air spaces per unit of projected leaf area (S_m/S), chloroplast surface area exposed to intercellular air spaces per unit of projected leaf area (S_c/S), the ratio S_c/S_m, chloroplast thickness (T_{chl}), chloroplast length (L_{chl}), mesophyll cell wall thickness (T_{cw}), cytoplasm thickness (T_{cyt}), and mesophyll conductance modelled from anatomical characteristics (g_{m_anat}).

Figure legends

Figure 1. *Thuja plicata*'s position in relation to the other gymnosperm species for the main physiology-leaf anatomy correlations. (A) The influence of leaf thickness (T_{leaf}) on net assimilation (A_N). The influence of chloroplast surface area exposed to intercellular airspaces per unit of projected leaf area (S_c/S) on (B) A_N, and (C) mesophyll conductance (g_m). The influence of cell wall thickness (T_{cw}) on (D) A_N and (E) g_m. (F) S_c/S in relation to T_{cw} (axes are Log_{10}-scaled). Data are average values from this study and from Peguero-Pina et al. (2012, 2016), Veromann-Jürgenson et al. (2017) and young fully-expanded needles of *Pinus* spp. from Kuusk et al. (2018a, 2018b). Open circles: *Thuja plicata*. Closed circles: other gymnosperms.

Figure 2. *Thuja plicata*'s position in relation to the other vascular plant species for the main physiology-leaf anatomy correlations. The influence of chloroplast surface area exposed to intercellular airspaces per unit of projected leaf area (S_c/S) on (A) net assimilation (A_N) and (B) mesophyll conductance (g_m). The influence of cell wall thickness (T_{cw}) on (C) A_N and (D) g_m. Data are average values from this study and from Veromann-Jürgenson et al. (2017), young fully-expanded needles of *Pinus* spp. from Kuusk et al. (2018a, 2018b), Carriquí et al. (2019b) and Ren et al. (2019).

Figure 3. Leaf dry mass per area (LMA) in relation to (A) leaf thickness (T_{leaf}), (B) leaf density (D_{leaf}), (C) fraction of mesophyll occupied by intercellular air spaces (f_{ias}), (D) cell wall thickness (T_{cw}), and (E) chloroplast surface area exposed to intercellular air spaces per unit of projected leaf area (S_c/S) for different lycophyte, fern, gymnosperm and angiosperm species. Data are average values from this study and from Tosens et al. (2012b), Peguero-Pina et al. (2012, 2016), Carriquí et al. (2015), Veromann-Jürgenson et al. (2017) and young fully-expanded needles of *Pinus* spp. from Kuusk et al. (2018a).

Figure 4. Leaf thickness (T_{leaf}) in relation to (A) chloroplast surface area exposed to intercellular air spaces per unit of projected leaf area (S_c/S), and (B) fraction of the mesophyll thickness occupied by spongy mesophyll tissue (T_{spo}/T_{mes}). Cell diameter in relation to cell length for (C) palisade and (D) spongy mesophyll cells.

Data are average values from this study and from Carriquí et al. (2015), Veromann-Jürgenson et al. (2017) and young fully-expanded needles of *Pinus* spp. from Kuusk et al. (2018a).

Figure 5. Representative micrographs of leaf cross-sections and mesophyll cell walls of *Phlomis italica*, *Thuja plicata* and *Pteris vitatta*. Micrographs of *P. italica* and *P. vitatta* are from the study reported in Carriquí et al. (2015).

Figure 6. Mesophyll conductance modelled from anatomical traits (g_{m_anat}) for (A, B) the gymnosperm *Thuja plicata* considering own and *Phlomis italica*'s and *Pteris vitatta*'s traits, respectively, and (C, D) the angiosperm *Phlomis italica* and the fern *Pteris vitatta*, considering the traits of their own species and *T.plicata*'s traits. In each case, dot plots combined with box plots are shown for g_{m_ANAT} modelled considering (1) the own traits from the species, or considering either (2) cell wall thickness (T_{cw}), (3) chloroplast surface area exposed to intercellular air space per unit of projected leaf area (S_c/S) or (4) leaf thickness (T_{leaf}) from another species.

Figure 7. Schematic representation of the different leaf structures leading to high chloroplast exposure. From a 'regular' leaf with average S_c/S (A), an increase of S_m/S keeping a constant chloroplast number per cell leads to high S_c/S, with more packed cells and low f_{ias} (B). On the other hand, *Thuja plicata* (C) is able to achieve extremely high S_c/S through increased leaf thickness and cell size, thus disposing a high number of chloroplasts through the leaf profile.

Figure 8. The influence of the ratio chloroplast surface area exposed to intercellular air spaces per unit of projected leaf area (S_c/S) – cell wall thickness (T_{cw}) on (A) net assimilation (A_N), and (B) mesophyll conductance (g_m). Data are average values from this study and from Veromann-Jürgenson et al. (2017), young fully-expanded needles of *Pinus* spp. from Kuusk et al. (2018a, 2018b), Carriquí et al. (2019b) and Ren et al. (2019).

Table 1

	Thuja plicata
A_N (µmol m^{-2} s^{-1})	7.83 ± 0.59
g_s (mol m^{-2} s^{-1})	0.058 ± 0.004
g_{m_flu} (mol m^{-2} s^{-1})	0.067 ± 0.011
C_i (µmol mol^{-1} air)	246 ± 9
C_c (µmol mol^{-1} air)	112 ± 8
$V_{c,max}$ (µmol m^{-2} s^{-1})	111 ± 9
J_{max} (µmol m^{-2} s^{-1})	172 ± 8
R_d (µmol m^{-2} s^{-1})	-1.76 ± 0.24

Table 2

	Thuja plicata
LMA (g m^{-2})	201 ± 4
D_{leaf} (g cm^{-3})	0.272 ± 0.030
T_{leaf} (µm)	767 ± 72
T_{mes} (µm)	685 ± 75
f_{ias} (%)	30.7 ± 1.8
S_m/S (m^2 m^{-2})	48.5 ± 9.3
S_c/S (m^2 m^{-2})	34.0 ± 6.5
S_c/S_m	0.70 ± 0.03
T_{chl} (µm)	2.53 ± 0.12
L_{chl} (µm)	5.17 ± 0.24
T_{cw} (µm)	0.602 ± 0.048
T_{cyt} (µm)	0.311 ± 0.016
g_{m_anat} (mol m^{-2} s^{-1})	0.078 ± 0.011

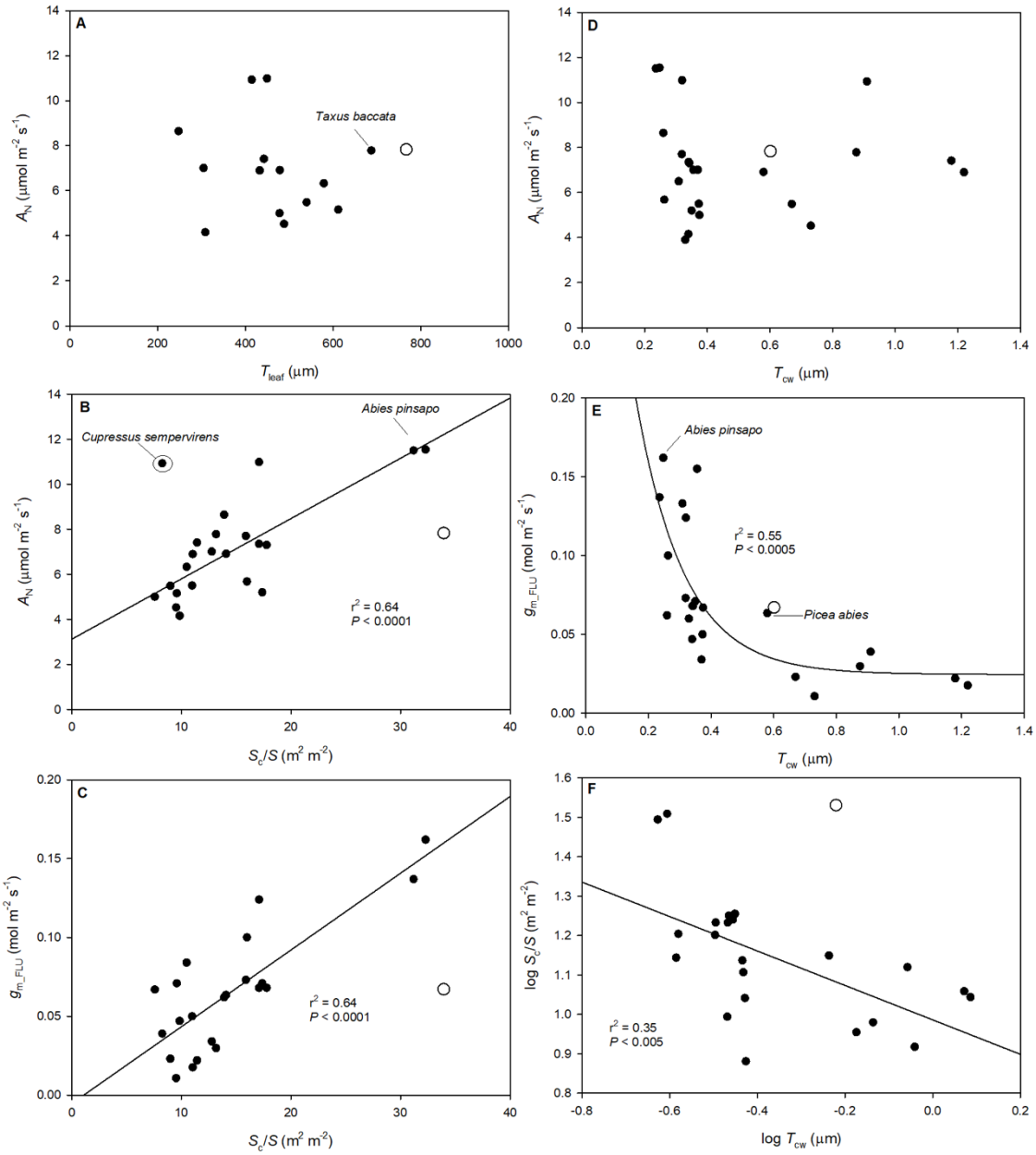
A
Taxus baccata
A_N (µmol m^{-2} s^{-1})
T_{leaf} (µm)
D
T_{cw} (µm)
B
Abies pinsapo
Cupressus sempervirens
r^2 = 0.64
P < 0.0001
S_c/S (m^2 m^{-2})
E
Abies pinsapo
Picea abies
r^2 = 0.55
P < 0.0005
g_{m_FLU} (mol m^{-2} s^{-1})
C
r^2 = 0.64
P < 0.0001
F
r^2 = 0.35
P < 0.005
log S_c/S (m^2 m^{-2})
log T_{cw} (µm)

Figure 1

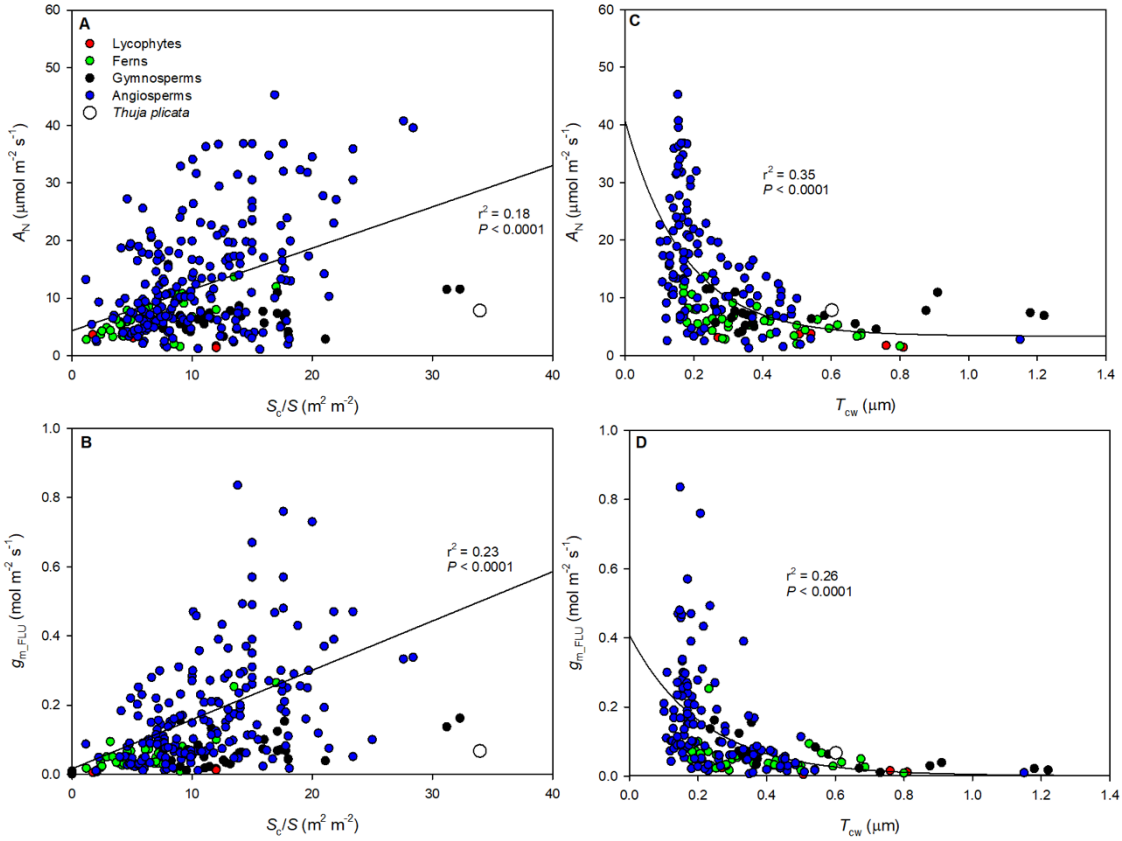
A
Lycophytes
Ferns
Gymnosperms
Angiosperms
Thuja plicata
r^2 = 0.18
P < 0.0001
A_N (µmol m^{-2} s^{-1})
S_c/S (m^2 m^{-2})
C
r^2 = 0.35
P < 0.0001
T_{cw} (µm)
B
r^2 = 0.23
P < 0.0001
g_{m_FLU} (mol m^{-2} s^{-1})
D
r^2 = 0.26
P < 0.0001

Figure 2

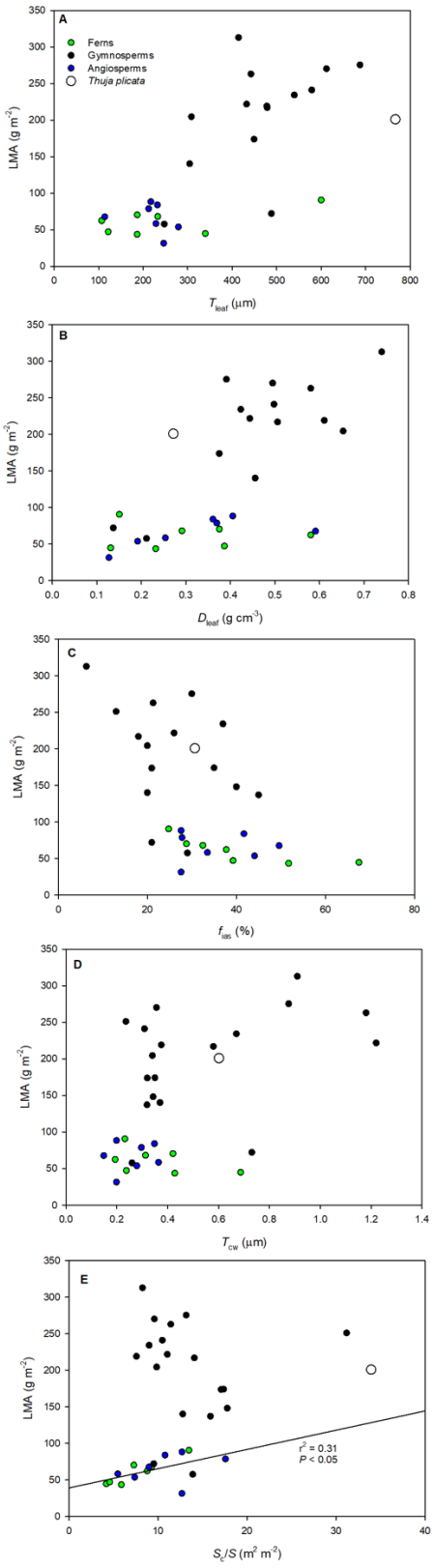
A
Ferns
Gymnosperms
Angiosperms
Thuja plicata
LMA (g m-2)
Tleaf (µm)
B
LMA (g m-2)
Dleaf (g cm-3)
C
LMA (g m-2)
flas (%)
D
LMA (g m-2)
Tcw (µm)
E
LMA (g m-2)
r2 = 0.31
P < 0.05
Sc/S (m2 m-2)

Figure 3

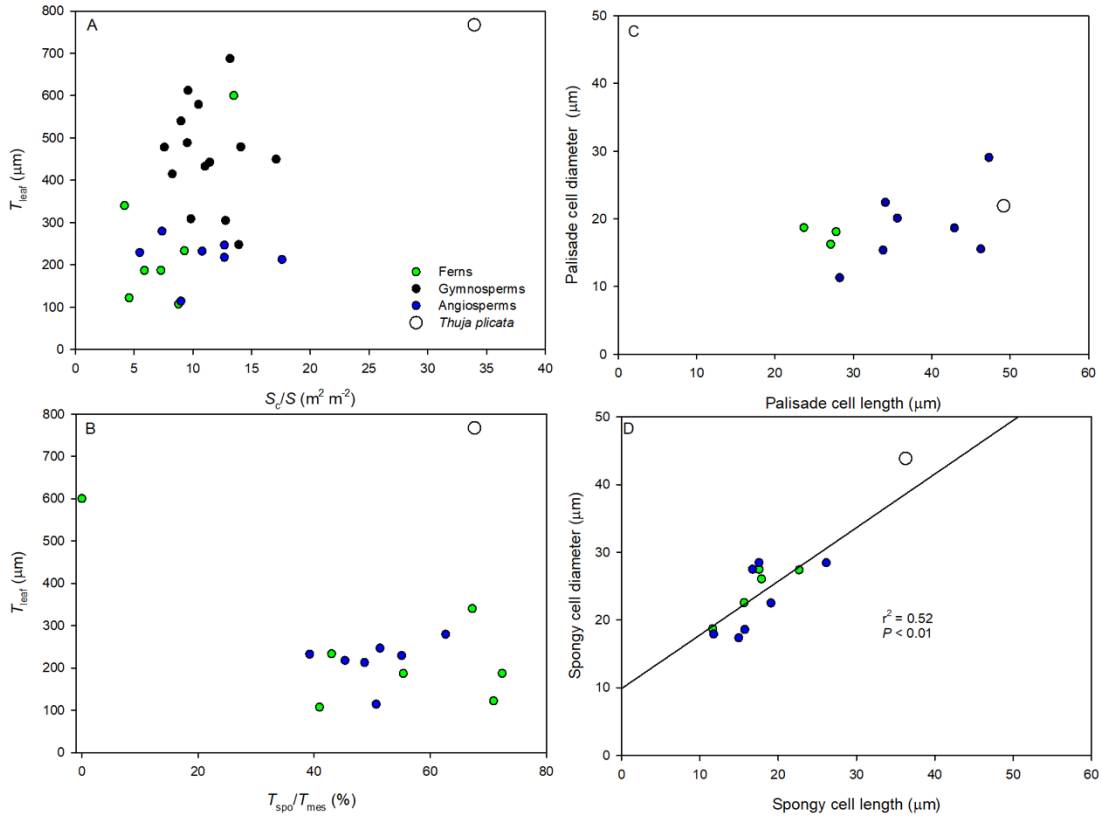
A
B
C
D
Ferns
Gymnosperms
Angiosperms
Thuja plicata
T_{leaf} (µm)
S_c/S (m^2 m^{-2})
T_{spo}/T_{mes} (%)
Palisade cell diameter (µm)
Palisade cell length (µm)
Spongy cell diameter (µm)
Spongy cell length (µm)
r^2 = 0.52
P < 0.01

Figure 4

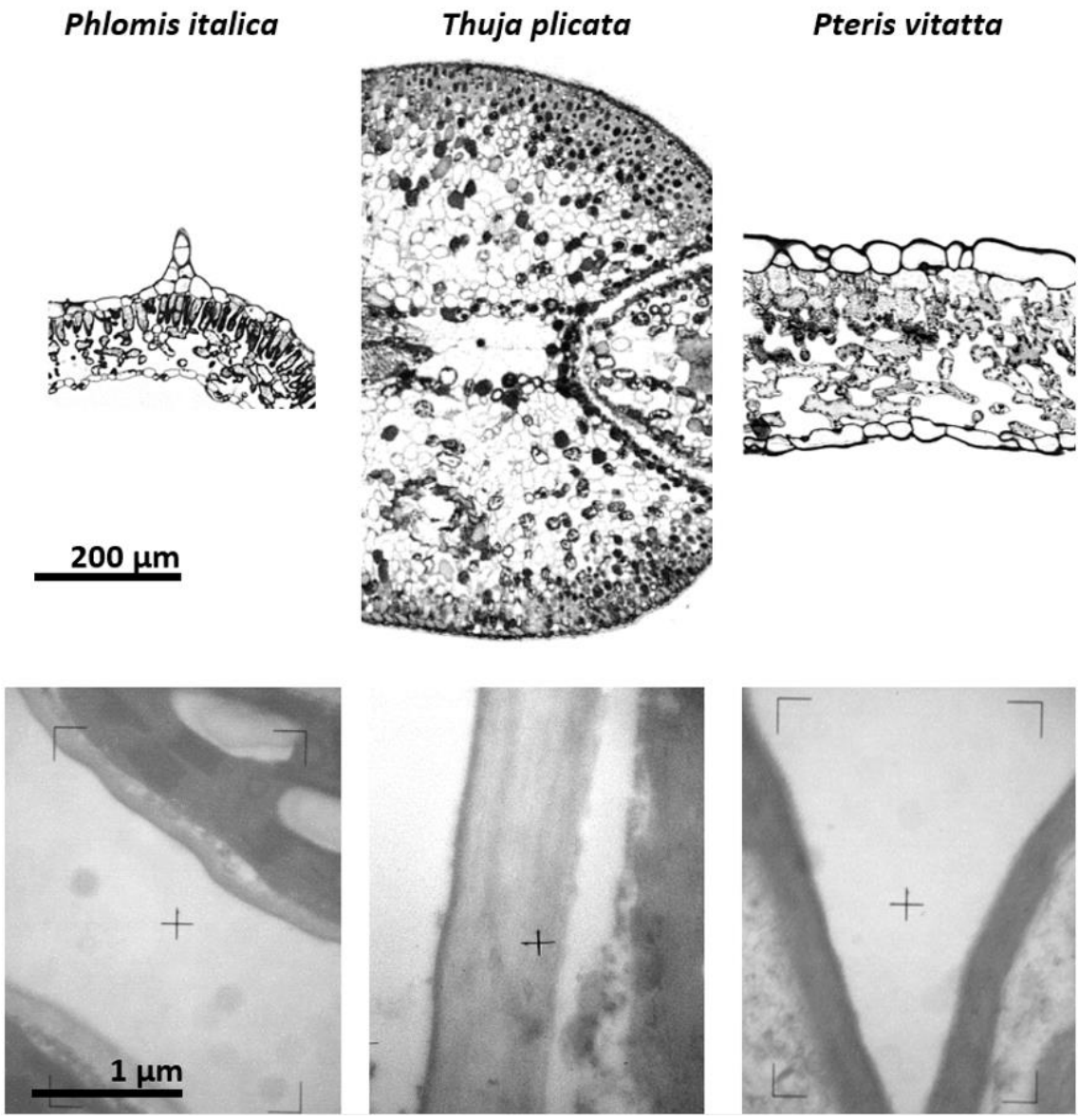

Figure 5

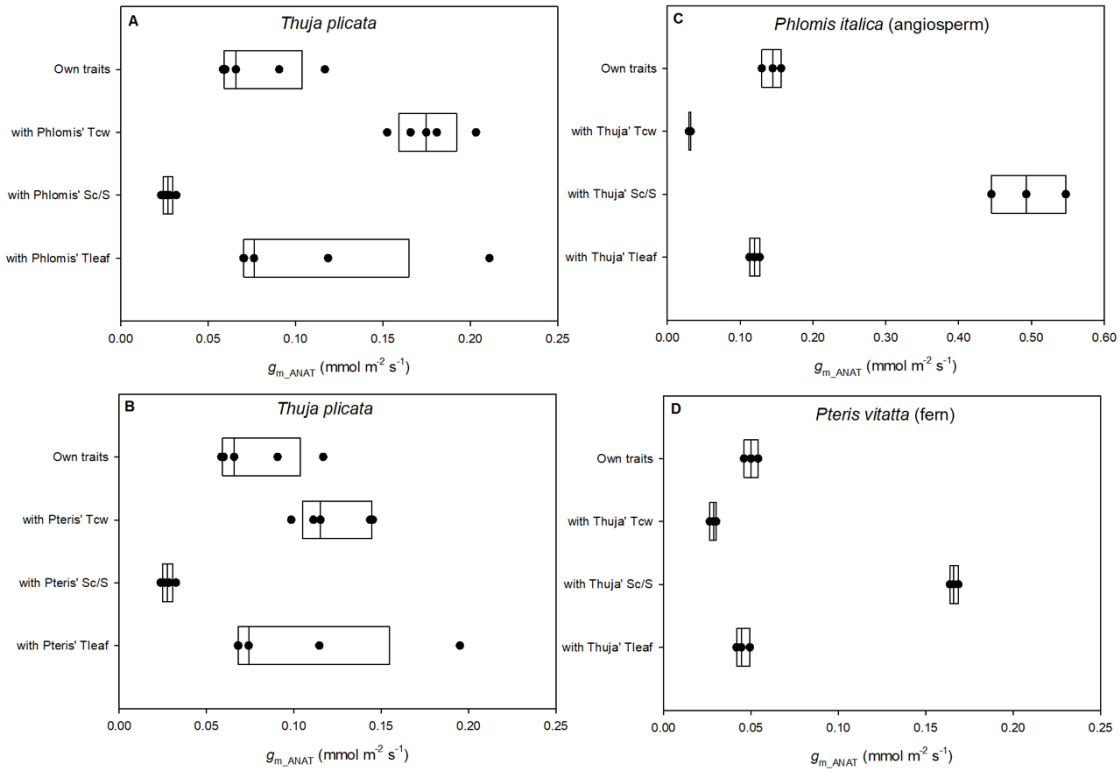
A
Thuja plicata
Own traits
with Phlomis' Tcw
with Phlomis' Sc/S
with Phlomis' Tleaf
0.00
0.05
0.10
0.15
0.20
0.25
gm_ANAT (mmol m-2 s-1)
C
Phlomis italica (angiosperm)
Own traits
with Thuja' Tcw
with Thuja' Sc/S
with Thuja' Tleaf
0.00
0.10
0.20
0.30
0.40
0.50
0.60
gm_ANAT (mmol m-2 s-1)
B
Thuja plicata
Own traits
with Pteris' Tcw
with Pteris' Sc/S
with Pteris' Tleaf
0.00
0.05
0.10
0.15
0.20
0.25
gm_ANAT (mmol m-2 s-1)
D
Pteris vitatta (fern)
Own traits
with Thuja' Tcw
with Thuja' Sc/S
with Thuja' Tleaf
0.00
0.05
0.10
0.15
0.20
0.25
gm_ANAT (mmol m-2 s-1)

Figure 6

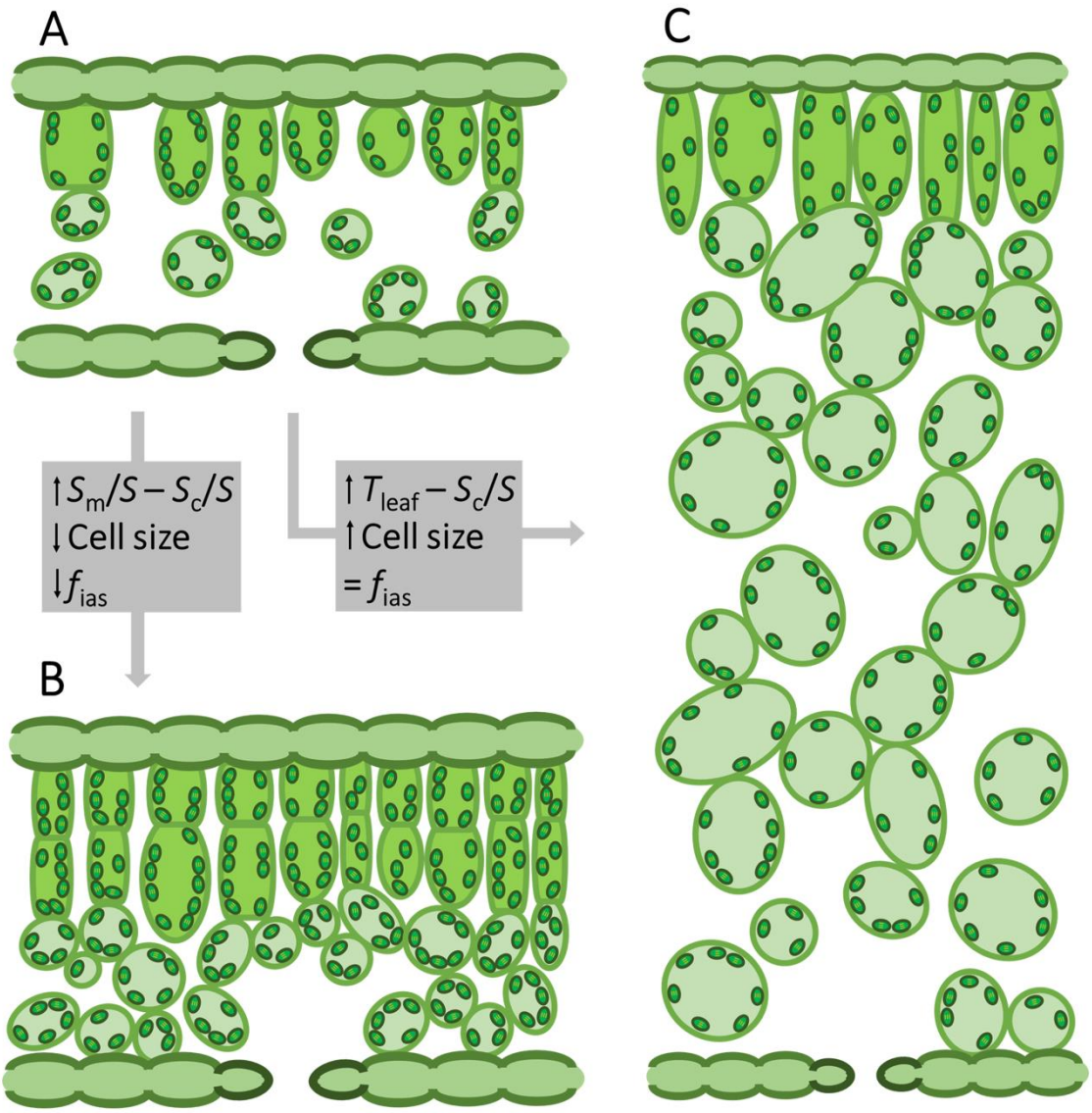

Figure 7

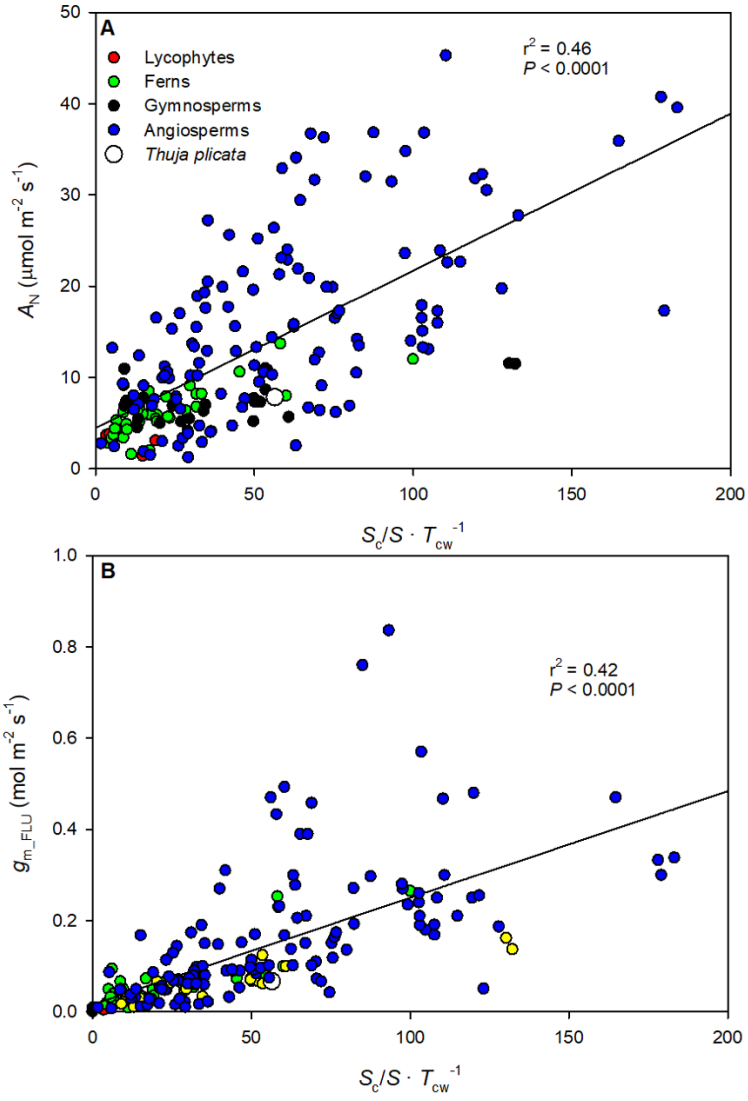
A
Lycophytes
Ferns
Gymnosperms
Angiosperms
Thuja plicata
r² = 0.46
P < 0.0001
A_N (µmol m⁻² s⁻¹)
S_c/S · T_cw⁻¹
B
r² = 0.42
P < 0.0001
g_m_FLU (mol m⁻² s⁻¹)
S_c/S · T_cw⁻¹

Figure 8

Supporting information

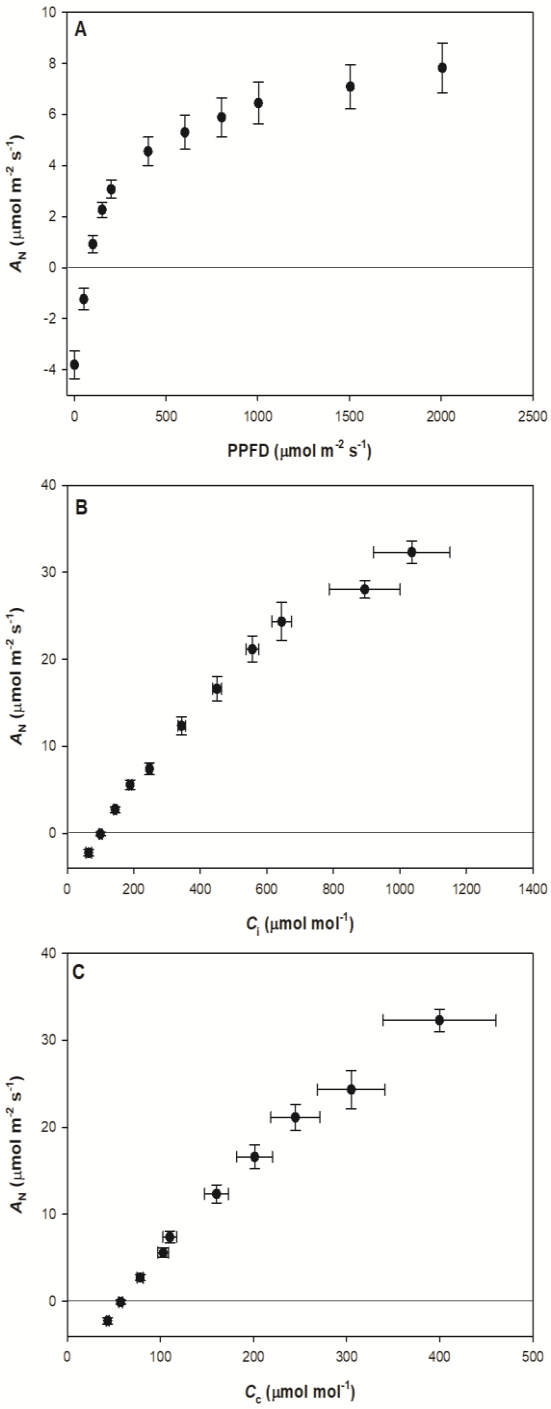

Figure S1. Response of net assimilation (A_N) to (A) photosynthetic photon flux density (PPFD), (B) sub-stomatal CO_2 concentration (C_i), and (c) chloroplastic CO_2 concentration (C_c). Values are averages ± SE of six replicates for PPFD response curves and of seven replicates for C_i and C_c response curves.

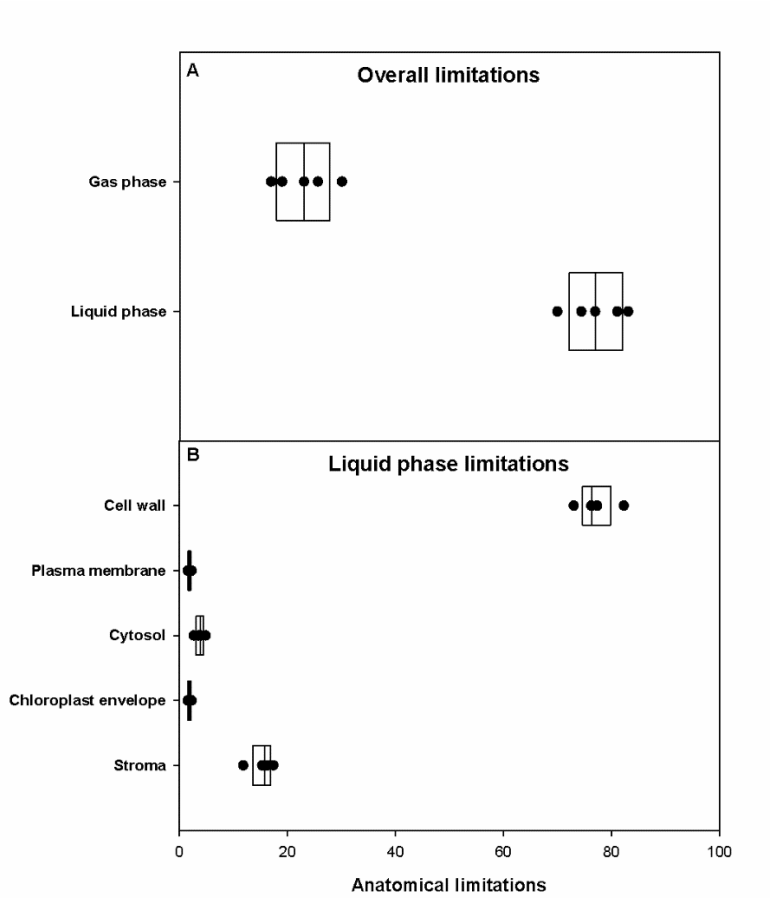

Figure S2. Limitation of mesophyll conductance (g_m) due to anatomical constraints in *Thuja plicata*. (A) Share of the overall g_m limitation by gas and liquid phase and (B) the liquid-phase limitation among its components: cell wall, plasma membrane, cytosol, chloroplast envelope and stroma. Data are average values ± SE for five replicates.

Chapter 5. Cell wall properties impact on CO_2 diffusion resistance

Cell wall composition is a key determinant of mesophyll conductance in conifers

Marc Carriquí[1*#], Miquel Nadal[1*], María José Clemente-Moreno[1], Jorge Gago [1], Eva Miedes[2,3], Antonio Molina[2,3], Jaume Flexas[1]

[1]Research Group in Plant Biology under Mediterranean Conditions, Universitat de les Illes Balears (UIB) - Agro-Environmental and Water Economics Institute (INAGEA), Palma 07122, Illes Balears, Spain.

[2] Centro de Biotecnología y Genómica de Plantas, Universidad Politécnica de Madrid (UPM)–Instituto Nacional de Investigación y Tecnología Agraria y Alimentaria (INIA), Campus Montegancedo UPM, 28223 Pozuelo de Alarcón, Madrid, Spain.

[3]Departamento de Biotecnología-Biología Vegetal, Escuela Técnica Superior de Ingeniería Agronómica, Alimentaria y de Biosistemas, 28040, Madrid, Spain.

*Both authors have equally contributed to this work.

Corresponding author:

Marc Carriquí

E-mail: m.carriqui@uib.cat

Phone: 0034 971 25 95 56

Author email addresses:

m.carriqui@uib.cat; miquel.nadal@uib.cat; esojariam2@gmail.com; xurxogago@gmail.com; eva.miedes@upm.es; antonio.molina@upm.es; jaume.flexas@uib.es

Running head: cell wall composition regulates mesophyll conductance in conifers

Keywords: Cell wall composition, cell wall thickness, mesophyll conductance, photosynthesis, leaf anatomy, cellulose, hemicellulose, pectin

Summary

Cell wall thickness is widely recognized as one of the main determinants of mesophyll conductance to CO_2 (g_m). However, little is known about the components that regulate cell wall effective porosity to CO_2 diffusion (i.e. the ratio between tortuosity and actual porosity, the other two cell wall biophysical diffusion properties). The aim of this study was to gain further insight into the potential relationships between cell wall composition and cell wall thickness (T_{cw}) and g_m. Because they present the thickest but strongly variable cell walls within spermatophytes, gymnosperms constitute an interesting group to deepen on these relationships. We characterized the foliar gas exchange, the main morphoanatomical traits related with g_m, the leaf fraction constituted by cell walls and three main components of cell walls (hemicelluloses, cellulose and pectins) in seven conifer species. We found that, although the relatively low g_m of conifers was mainly determined by their elevated T_{cw}, their fine-scale g_m determination was mainly driven by cell wall composition, which presumably sets the final effective porosity to CO_2 diffusion. However, this had no direct effect on photosynthesis rate, since it was not limited by g_m in the studied species. The data presented here demonstrate: (a) a positive impact of the fraction of pectin on g_m and (b) there might be no direct relationship between cell wall thickness and effective porosity.

Significance statement

Cell walls impose a relevant and increasing resistance to CO_2 diffusion, constraining photosynthetic capacity, with increasing wall thickness. However, the effect of cell wall composition on mesophyll conductance is poorly understood. This study reveals strong effect of the relative cell wall content in cellulose, hemicelluloses and pectins on mesophyll conductance, extending the knowledge of the mechanistic basics of internal CO_2 diffusion resistance.

Introduction

Mesophyll conductance (g_m), one of the three main limitations (together with stomatal conductance and the biochemical capacity to fix CO_2 into sugars) to net assimilation (A_N), drives the decrease in CO_2 concentration from the substomatal cavity (C_i) to the chloroplast (C_c). CO_2 molecules must diffuse through a gas-phase resistance, the intercellular air space path from the substomatal cavity to the cell wall surface, and several liquid-phase resistances, composed by the different cellular structures that separate the cell wall surface from the carboxylation site into the stroma (e.g. cell wall, plasma membrane, cytoplasm, chloroplast envelope and stroma; Evans et al. 2009, Terashima et al. 2011). The relevance of each resistance depends on structural (path lengths and surface areas of different traits) and biochemical determinants - mainly ascribed to aquaporins in cell membranes and carbonic anhydrases in the cytosol and chloroplasts. The structural determinants, which set a maximum g_m, can be adjusted in response to specific environmental conditions (Tholen et al. 2008, Morales et al. 2014, Momayyezi et al. 2017, among others) or during leaf ontogeny (Miyazawa & Terashima 2001, Tosens et al. 2012a), although not in the seconds to minutes range (Carriquí et al. 2019a), opposite to the biochemical determinants (Bernacchi et al. 2001, Yamori et al. 2014). In addition, anatomical and biochemical determinants can present a wide range of variation, partially explaining the differences in the photosynthetic capacity between species or even genotypes (Carriquí et al. 2015, Tosens et al. 2016, Muir et al. 2014, Veromann-Jürgenson et al. 2017, Peguero-Pina et al. 2017, Carriquí et al. 2019b). However, there are still big uncertainties regarding the biophysical diffusion properties of the different components of the diffusion pathway. Such uncertainties especially affect mesophyll cell walls, a key component of the CO_2 pathway determining g_m in many species (Terashima et al. 2011, Tosens et al. 2016, Veromann-Jürgenson et al. 2017, Ellsworth et al. 2018, Carriquí et al. 2019b).

Cell wall resistance to CO_2 diffusion depends on three wall properties: thickness, tortuosity and porosity. Cell wall thickness can be easily measured using transmission electron microscope images. For this reason, it has been determined, together with g_m, in more than 130 species across all land plant

groups under optimum growth conditions (Veromann-Jürgenson et al. 2017, Carriquí et al. 2019b, Ren et al. 2019), revealing the existence of a strong exponential decay of g_m as T_{cw} increases (Onoda et al. 2017, Ren et al. 2019). Below 0.4 μm thick cell walls g_m ranges from 0.03 to 0.76 mol m^{-2} s^{-1}. Instead, when T_{cw} > 0.4 μm none of the reported correspondent g_m values exceeded 0.12 mol m^{-2} s^{-1} (Carriquí et al. submitted). Thus, while in the 0.1-0.4 μm range a small increase in T_{cw} has a significant negative effect on g_m, above 0.4 μm thick cell walls g_m values are always low, but not necessarily increasingly lower as the T_{cw} increases. This suggests that spermatophyte species with thicker mesophyll cell walls would have to modify alternative anatomical traits, including their effective porosity (=tortuosity/porosity) for a given T_{cw}, in comparison to species with thinner cell walls (but still >0.4 μm) to reach similar g_m values. However, due to methodological limitations, there is little information available on the effective porosity of cell walls in land plants. Although there are no direct measurements of the cell wall effective porosity to CO_2 diffusion, several authors have tried to calculate what its approximate value would be. Nobel (1999) first postulated, based only on physicochemical estimations, that effective porosity would be around 0.3 m^3 m^{-3}, which implies that cell wall conductance is large enough to do not constrain A_N. Then, Terashima et al. (2006), based on the variability of g_m between species for a given S_c/S, proposed that the cell wall effective porosity value is around 0.1 or lower, implying that cell wall conductance would be a key determinant of g_m. Terashima et al. (2006) also noted, based on previous studies of water cell wall permeabilities on algae species with >10 μm thick cell walls, that effective porosity might be inversely proportional to the thickness of the cell walls. Later, Evans et al. (2009) suggested that effective porosity value could be 0.07 μm thick based on a simple model on the CO_2 pathway through pores from onion cell wall images from McCann et al. (1990). From then on, due to lack of accurate measurements of wall resistance to CO_2 diffusion, several authors have been using these published effective porosity values in analytical models based on anatomical traits to estimate g_m. While some authors considered a constant effective porosity, some others adjusted it to be correlated with cell wall thickness following either a linear or an exponential decay function (Tosens et al. 2012a,b, 2016, Tomás et al. 2013, 2014, Peguero-Pina et al. 2012, Carriquí et al. 2015,

Xiao & Zhu 2017, Veromann-Jürgenson et al. 2017). Nevertheless, such approaches based solely on assumptions can easily lead to an under- or overestimation of the cell wall role on A_N.

Cell wall composition remains an almost unexplored factor that could affect g_m through its effects on porosity and tortuosity. Primary plant cell walls are composed of a relatively small number of basic components: microfibrils of cellulose and a matrix of hemicelluloses, pectins and structural proteins (Cosgrove 2005; Sarkar et al. 2009, Cosgrove and Jarvis 2012). The structure, organization and interactions of microfibrils with the glycan matrix form a tangled web resulting in nanometric and micrometric pores that regulate the exchange of macromolecules, water and gas (Carpita et al. 1979, Evans et al. 2009). This cell wall assembly is regulated during cell elongation and differentiation (Rondeau-Mouro et al. 2008, Cosgrove 2016) and is constantly remodelled and reconstructed (Sarkar et al. 2009). The result is an intricate pathway of greater or lesser difficulty according the size to that of the pore of each component. CO_2 molecules can cross cell walls because they are several times smaller than pore breadth (Carpita et al. 1979, Read and Bacic 1996, Evans et al. 2009). Although cell wall porosity in high plants is known to be regulated by cell wall composition, especially by pectins in the primary cell walls (Baron-Epel et al. 1988, Fleischer et al. 1999, Rondeau-Mouro et al. 2008), little information is available for its direct effect on CO_2 diffusion. Recently, Weraduwage et al. (2016) reported that the manipulation of the pectin methylesterification level, which modulates cell wall plasticity and plant growth, affected the relationship between photosynthesis and plant growth. However, while this effect could be explained potentially by changes in the cell wall properties affecting CO_2 diffusion, g_m and T_{cw} were not determined in this study. Another indirect evidence may be found in Gago et al. (2016), where a significant correlation was found between some soluble sugars (mainly Gal, arabinose and raffinose) and g_m. Gago et al. (2016) suggested that this correlation was given by the use of these sugars to the synthesis and maintenance of cell walls. Moreover, Ellsworth et al. (2018) deduced that cell wall effective porosity has a relevant effect on g_m from the differences in physiology and leaf anatomy observed in rice mutants lacking mixed-linkage glucan. Based on these indirect evidences, we hypothesize that cell wall composition and the

ratios between the main cell wall components, particularly the pectin relative content, could have a significant role on wall conductance to CO_2. To test this hypothesis, we selected a group of gymnosperm species only, because most of them have T_{cw} > 0.4 μm and present high interspecific T_{cw} variability (Peguero-Pina et al. 2012, Veromann-Jürgenson et al. 2017, Kuusk et al. 2018), and to avoid extra difficulties in the results interpretation due to differences in the cell wall components observed between more distant plant groups (Sarkar et al. 2009).

In this study we present a photosynthetic, morphoanatomical and cell wall composition characterization for seven gymnosperm species. The aims of the study are: (1) to demonstrate the important role of CO_2 diffusion in the photosynthesis limitation in gymnosperms; (2) to confirm that cell wall thickness and chloroplast surface area exposed to the intercellular air spaces are the strongest sources of mesophyll conductance limitation in gymnosperms; and (3) to analyse the implication of cell wall composition in setting the cell wall thickness and effective porosity, photosynthetic capacity and mesophyll conductance within the studied species.

Results

Photosynthetic capacity and its physiological constraints

Conifers sampled here exhibited a narrow range of variation in their physiological performance (Table S1). Net assimilation (A_N) ranged 2-fold from 4.3 ± 0.3 μmol m^{-2} s^{-1} in *Chamaecyparis obtusa* to 9.2 ± 0.4 μmol m^{-2} s^{-1} in *Taxus baccata*, meanwhile stomatal and mesophyll conductance estimated from chlorophyll fluorescence (g_s and g_{m_FLU}, respectively) varied only about 2- and 3-fold, respectively. g_s ranged from 0.033 ± 0.004 in *C. obtusa* to 0.095 ± 0.013 mol m^{-2} s^{-1} in *Sequoiadendron giganteum*, whereas g_{m_FLU} varied from 0.047 ± 0.015 in *Juniperus oxycedrus* to 0.104 ± 0.025 mol m^{-2} s^{-1} in *T. baccata*. A_N was linearly correlated with g_s (r^2 = 0.69, P < 0.0001) and g_{m_FLU} (r^2 = 0.28, P < 0.05) across all species, considering also the gymnosperm species reported by Veromann-Jürgenson et al. (2017; Fig. 1A,B). The quantitative limitation analysis revealed

that none of the three limitations (stomatal, mesophyll conductance and biochemistry) was found to be significantly higher than the other two when pooling all species together (Fig. 2). However, diffusive limitations (the sum of stomatal and mesophyll conductance limitation) were the main factors constraining A_N (from 56 to 68%).

Morphoanatomical determinants of mesophyll conductance

Leaf morphological and anatomical traits potentially involved in setting A_N and g_m were found to be diverse in our species sample (Table S2 and S3) but generally within the previously reported range for gymnosperms (Fig. S1). High leaf dry mass per unit area (LMA) but also high leaf thickness (T_{leaf}) values lead to a leaf density (D_{leaf}) ranging only from 0.26 to 0.46 g cm^{-3} (Fig. S1A,B). LMA was not related to variation in cell wall thickness (T_{cw}; Fig. 1C) nor mesophyll and chloroplast surface area exposed to intercellular air space per leaf area (S_m/S and S_c/S, respectively), either considering species from this study only, nor considering also species from Veromann-Jürgenson et al. (2017; Fig. 1D).

Contrarily to LMA, significant correlations were found between g_{m_FLU} and the anatomical traits S_c/S and T_{cw} (Fig. 3). A significant positive logarithmic correlation (r^2 = 0.31, P < 0.05) was found between g_{m_FLU} and S_c/S when considering both species from this study and species measured in Veromann-Jürgenson et al. (2017; Fig. 3A), being S_c/S average values from this study generally higher than those of Veromann-Jürgenson et al. (2017) species. Regarding to the relationship between g_{m_FLU} and T_{cw} (Fig. 3B), no correlation was found when considering all conifer species, which were located in the horizontal region of the significant exponential decay regression obtained when considering data from all spermatophyte species compiled by Onoda et al. (2017; Fig. 3B inset). Instead, a significant positive linear regression (r^2 = 0.59, P < 0.05) was found for species from the current study and, conversely, a significant negative linear regression (r^2 = 0.38, P < 0.05) was found for species studied in Veromann-Jürgenson et al. (2017). Based on the structural limitation analysis of g_m, the estimated gas phase limitation in the mesophyll was between 8.0 and

20.5%, being conifer's g_m mainly limited by liquid-phase components (Fig. 4A). Among the different liquid-phase limitations, cell wall limitation (l_{cw}) was the predominant g_m constraint for all species (ranging from 65.9 to 80.9 %) except for *T. baccata*, whose l_{cw} was of 31.9 ± 6.9 %. Chloroplast stroma limitation (l_{st}) was the second limitation in importance (except in *T. baccata*, being of 47.1 ± 4.6 %), meanwhile plasma membrane, cytoplasm and chloroplast envelope played a minor role (Fig. 4B).

In order to model g_m from anatomical characteristics (g_{m_ANAT}), due to the lack of knowledge of the species-specific cell wall porosity, two scenarios were considered. On one side, a constant cell wall porosity of 0.028 m^3 m^{-3} was considered as in Tomás et al. (2013) for all species with T_{cw} > 0.4 μm. On the other side, a variable cell wall porosity was considered, estimated as the porosity allowing g_{m_ANAT} to match g_{m_FLU} in each species. Those p_{cw} values ranged between 0.017 and 0.293 m^3 m^{-3}, and where not correlated with T_{cw} (Figs. 5A, B). As a result, obviously a 1:1 relationship was forced between g_{m_ANAT} and g_{m_FLU} as compared to the scattered relationship obtained when using a constant p_{cw} = 0.028 for all species (Fig. 6).

Cell wall composition in relation to leaf morphoanatomy and physiology

Cell wall weight per total leaf dry weight, considered as alcohol insoluble residues (AIR), as well as the AIR's weight fraction of hemicelluloses (H), celluloses (C) and pectins (P), were determined for the seven conifer species (Table S4). AIR ranged from 0.425 ± 0.026 g g^{-1} in *T. baccata* to 0.870 ± 0.042 g g^{-1} in *J. oxycedrus*. Their hemicelluloses content ranged from 180 ± 7 mg g^{-1} AIR in *T. cuspidata* to 357 ± 35 mg g^{-1} AIR in *P. glauca*, meanwhile cellulose content ranged from 98 ± 9 mg g^{-1} AIR in *T. baccata* to 341 ± 9 mg g^{-1} AIR in *J. oxycedrus*, and pectins content ranged only from 48 ± 3 mg g^{-1} AIR in *T. cuspidata* to 65 ± 5 mg g^{-1} AIR in *S. giganteum*.

Neither AIR nor main cell wall components (considering them separately, the sum of the three, or the ratio (H+C)/P) were correlated with LMA (not shown). Instead, for T_{cw}, no correlation was found between AIR and T_{cw} (Fig. 7A). Non- or

marginally-significant ($P < 0.1$) relationships were found between hemicellulose, cellulose and pectin weight fraction of AIR with T_{cw} (Fig. 7B), although when those fractions were expressed on a leaf area basis highly significant negative linear correlations between hemicelluloses and pectins and T_{cw} were found ($r^2 = 0.69$, $P < 0.05$; $r^2 = 0.65$, $P < 0.05$; Fig. 7C). Then, potential relationships between cell wall content and composition and A_N and g_{m_FLU} were investigated. Neither AIR nor main cell wall components content, expressed on a mass or leaf area basis, were correlated with net photosynthesis (Figs. 8A-C). Conversely, AIR was negatively correlated with g_{m_FLU} ($r^2 = 0.76$, $P < 0.01$; Fig. 8D), as well as mass-based hemicellulose ($r^2 = 0.61$, $P < 0.05$) and cellulose fraction ($r^2 = 0.75$, $P < 0.05$; Fig. 8E), and area-based hemicellulose ($r^2 =0.90$, $P < 0.005$) and cellulose fraction ($r^2 = 0.68$, $P < 0.05$; Fig. 8F). No correlation in the $P < 0.05$ range between pectins weight fraction and g_{m_FLU} was found (Figs. 8E, F). The most significant correlation between g_{m_FLU} and main cell wall components was obtained when the ratio (H+C)/P was considered ($r^2 = 0.91$, $P < 0.01$; Fig. 9).

Discussion

The present work provides the first correlative evidence for the relationship between leaf cell wall composition and mesophyll conductance to CO_2 diffusion (g_m). This comprehensive analysis in seven conifers revealed that cell wall composition, and more specifically the pectin relative content, have an influence on the mesophyll cell wall thickness and effective porosity (tortuosity/porosity), the two biophysical properties setting CO_2 diffusion through the cell wall.

Cell wall thickness (T_{cw}) is widely recognized as a key structural determinant of A_N that correlates negatively with g_m (Evans et al. 2009, Onoda et al. 2017, Ren et al. 2019). However, until recently, the shape of the relationship between A_N or g_m and T_{cw} resembled more a negative linear regression than the exponential decay regression that is now established. The reason is that the vast majority of studies including the determination of both physiological characteristics and mesophyll ultrastructural traits were performed in angiosperms, and more specifically in model plants and crops (Flexas et al. 2012,

2018). These species are characterized by possessing high photosynthetic capacity, which coincides with their low T_{cw}. With the emergence of comprehensive similar studies focused on other groups of terrestrial plants, such as gymnosperms (Peguero-Pina et al. 2012, Veromann-Jürgenson et al. 2017, Kuusk et al. 2018, Carriquí et al. submitted), ferns and fern allies (Carriquí et al. 2015, Tosens et al. 2016) and bryophytes (Carriquí et al. 2019b) the range of mesophyll T_{cw} reported for terrestrial plants was considerably extended. The new shape for these relations confirms that although high T_{cw} sets a low limit for g_m and thus A_N, at a narrower rage higher T_{cw} does not necessarily implies lower A_N and g_m (Carriquí et al. 2019b, submitted). The present study represents a clear example of these new paradigm. The interspecific variation of T_{cw} in the seven conifers -which covered 60 % of the T_{cw} variation range reported for spermatophytes (from 0.372 to 1.033 μm; Fig. 5A, Table S3; Veromann-Jürgenson et al. 2017, Carriquí et al. 2019b, Ren et al. 2019)- correlated positively with g_m (r^2=0.59, P < 0.05), instead of the often reported negative correlation (Fig. 3B). These results might be explained by at least one of the following two possibilities: (a) the key participation of another g_m determinant (structural or biochemical) in conifers which might compensate part of the extra resistance to CO_2 diffusion imposed by having thicker T_{cw}, or (b) the existence of significant interspecific variability in the cell wall effective porosity to CO_2 diffusion -the great unknown among the biophysical diffusion properties of the different components of the CO_2 diffusion pathway-, which also might have this compensatory effect.

In addition to its high T_{cw}, conifers are characterized for possessing extreme values for several structural and anatomical characteristics determining g_m. In accordance with the finding of Veromann-Jürgenson et al. (2017), conifers presented elevated LMA values (ranging from 148 to 245 g m^{-2}; Table S2) more related to leaf density (D_{leaf}) than to their (also elevated) leaf thickness (T_{leaf}; Fig. S1A,B). High values for these characteristics allow conifer leaves to accommodate more and/or larger cells, which has two opposing effects on the CO_2 diffusion resistance. On the one hand, it implies lengthening the average distance that a CO_2 molecule has to travel from the substomatal cavity to the cell wall surface. Intercellular airspace conductance (g_{ias}) has been generally

considered to be high. However, a recent study by Earles et al. (2018) demonstrated, by evaluating the 3D leaf intercellular airspace traits -tortuosity, lateral path lengthening and intercellular airspace connectivity-, that g_{ias} was significantly lower in the thick leaves with small mesophyll porosity (f_{ias}) of CAM species. In the present work we have considered the g_{ias} equation as reevaluated by Earles et al. (2018) in order to account for the different intercellular airspace traits in the thicked leaves of our seven conifers. Thus, the gas-phase limitation on g_m (l_{ias}) ranged between 8.5 and 20.6% (Fig. 4A), being significantly higher than the <1% reported for gymnosperm species with the previous formulation (Veromann-Jürgenson et al. 2017). On the other hand, possessing more and/or bigger cells per projected leaf area directly implies a higher mesophyll surface area exposed to intercellular airspaces per projected leaf area (S_m/S) and, if the proportion of chloroplasts lined with cell walls remains proportional, also a higher chloroplast surface area exposed to intercellular airspaces per projected leaf area (S_c/S; Ren et al. 2019). Although it would be possible for conifers with thicker cell walls to achieve larger, instead of reduced g_m than species with thinner T_{cw}, thanks to the compensatory effect of g_{ias} and S_c/S, the two other key anatomical characteristics (Fig. 4B), this is not fully supported by the data (Fig. 3, Table S2, S3) with the already reported exception of *Thuja* (Carriquí et al. submitted). No tight agreement was found between g_m modelled from anatomical traits (g_{m_ANAT}) and g_m estimated from chlorophyll fluorescence (g_{m_FLU}) when constant cell wall effective porosity (p_{cw}) was considered for g_{m_ANAT} modelling, the two *Taxus* species being particularly outliers (Fig. 6). In order to fit g_{m_ANAT} and g_{m_FLU} p_{cw} should be variable between species and not proportionately higher the thickest T_{cw}, against what previously hypothesized. Thus, it seems that the other biophysical diffusion properties of the cell wall, tortuosity and porosity, might play an important role in fine-scale determination of g_m in conifers.

Cell wall properties are determined by the cell wall composition, the assembly, orientation and cross-linkage between wall components. Genetic systems induce alterations in these cell walls determinants in response to developmental and environmental signals, which has direct implications on leaf architecture (see Weraduwage et al. 2018 for a review) and in some cases even in the CO_2 diffusion through the leaf mesophyll (Weraduwage et al. 2016, 2018,

Ellsworth et al. 2018). However, none of these studies have focused on determining the potential mechanisms regulating cell wall effective porosity (i.e. tortuosity/porosity) to CO_2 diffusion. Here, we aimed to provide novel insight in the mechanistic basis of g_m by the determination of cell wall composition in seven conifer species with a g_m severely limited by mesophyll cell walls. Specifically, we analyzed the total leaf cell wall content and the relative proportion of the three major constituents of the plant cell wall: cellulose, hemicelluloses and pectins. Each of these components generally constitutes about 20-40% of the wall weight in angiosperms (Buchanan et al. 2000, Cosgrove 2005, Caffall and Mohnen 2009, Ochoa-Villareal et al. 2012, Tenhaken 2015), although this can vary significantly between species -while pectin is the single largest constituent of the cell wall in *Arabidopsis* (Zablackis et al. 1995), it is only about 2-10% in grasses (Ochoa-Villarreal et al. 2012). Lignins are the major cell wall component missing from the present analysis; they can account for 30-40% of AIR in conifers (Renault and Zwiazek 1997, Mediavilla et al. 2008); however, they are mostly present in secondary walls of structural tissue (Poorter et al. 2009, Zhong et al. 2019) which are not directly involved in photosynthesis (Kuusk et al. 2018). In the case of the conifers studied here, an important interspecific variability in the relative content of the measured cell wall constituents was found. The relative content in cellulose microfibrils and hemicellulose polymers was significantly higher than the relative content for pectins (18.0-35.7%, 9.8-34.1% and 4.8-6.5%, respectively; Table S4), contrasting with the around of 22% proportion of each cell wall component previously reported by Renault and Zwiazek (1997) in *Picea glauca*. Leaf cell wall content, expressed as alcohol insoluble residues (AIR), did not correlate with the structural parameters LMA, D_{leaf} (not shown) or T_{cw} (Fig. 7A); and the different components of the cell wall negatively correlated with T_{cw} when expressed on an area basis (7C), but not on their relative content (Fig. 7B). Net photosynthesis (A_N) did not correlate with any cell wall component (Fig. 8A-C). Instead, tight correlations were found between leaf cell wall content and the different cell wall components -except for pectins-, and g_m, both expressed as their relative content or concentration on an area basis (Fig. 8 D-F). Conifers with lower content of both cellulose and hemicelluloses presented higher g_m and, as the pectin content remained relatively invariable, we found that a higher proportion of pectins in

respect to both cellulose and hemicelluloses lead to higher g_m values (Fig. 9). These results express an unequivocal relationship between the cell wall composition and both g_m and T_{cw}, but not with A_N, likely because g_m was not the dominant limiting factor of the photosynthetic capacity across the seven conifers (Figs. 1 and 2). Nonetheless, the mechanisms that explain the observed correlations are not so straightforward. There are at least two possible explanations.

First, the cell wall content and composition results presented here represent the bulk composition of the leaf. As the mesophyll was not isolated from the rest of leaf tissues for the analyses, differences in the proportion of leaf tissues other than mesophyll (i.e. cuticle, epidermis, vessels or resin ducts) could be driving the main observed changes. Wall component molecules are combined in different ways in different cell types, resulting in contrasting mechanical properties within leaf tissues (Kitajima et al. 2012, Onoda et al. 2015). Thus, leaves with a smaller mesophyll proportion could present more cellulose due to a higher presence of support tissues and, in contrast, leaves with a bigger fraction of mesophyll could present a higher proportion of pectins, which are related to the cell wall porosity (Baron-Epel et al. 1988, Fleischer et al. 1999, Rondeau-Mouro et al. 2008). Despite being an intriguing possibility, there are no clear studies reporting the differentiation of cell wall composition by leaf tissue (and, in addition, most cell wall composition studies in plants focus in organs other than leaves). Neither LMA, which partially scales with the fraction of support tissues in conifers (Kuusk et al. 2018), nor mesophyll thickness did correlate with the cellulose and hemicelluloses content (both *Taxus* species, those with the highest pectin content, presented intermediate LMA and mesophyll thickness values; Table S2, S3). The lack of correlation observed between T_{cw} and AIR (Fig. 7A) could be due to the presence of other cell wall components, such as fibers, which are strongly related with LMA (Onoda et al. 2012) or lignins, associated with secondary cell walls of the vascular tissue (Kitajima et al. 2016), potentially not affecting significantly the leaf content in hemicelluloses, cellulose and pectins.

The other possibility implies the (cellulose+hemicellulose)/pectin ratio as a driver of cell wall effective porosity, being the g_m greater as the lower this ratio is.

This possibility needs the not-so-straightforward assumption that cell wall composition is highly conserved across leaf tissues. Making this assumption, this makes a very intriguing possibility strongly supported by previous observations on the role of the biophysical macromolecule diffusion properties of the cell wall. Pectins have been reported to determine cell wall thickness, pore size, structure and consequent diffusion of macromolecules across the cell wall in dicots in a much more relevant way than the celluloses (Baron-Epel et al. 1988, Read and Bacic 1996, Fleischer et al. 1999), and there are more recent indirect evidences that support this hypothesis. For instance, Yang et al. (2010) suggested that observed reductions in the pectin relative content of roots apices during osmotic stress could be associated with cell wall changes reducing its porosity. In a similar way, McKenna et al. (2010) hypothesized that the reductions in hydraulic conductivity they observed after treating plants with metals was a result of conformational changes of the pectin relative content in the cell walls, which would be increasing the total cell wall tortuosity by modifying pore size. Direct evidences suggest that pectins regulate cell wall porosity and macromolecule diffusion by forming hydrated gels that push cellulose microfibrils, decreasing the distance between microfibrils entanglements due to a decrease in the pectin relative content (Whitney et al. 1999, Cosgrove 2005). These evidences support our hypothesis that under similar relative pectin content, higher relative cellulose content results in lower g_m (i.e. microfibrils would be more tightly packed). Another indirect evidence suggesting that this could be valid in other plant groups is the fact that the relative pectin content is the highest in angiosperms (Buchanan et al. 2000, Cosgrove 2005, Caffall and Mohnen 2009, Ochoa-Villareal et al. 2012, Tenhaken 2015), the terrestrial plant group with the highest average g_m (Flexas et al. 2018; Nadal and Flexas 2019), but the lowest in bryophytes (unpublished data), which represent the group with smaller g_m (Carriquí et al. 2019b). Nevertheless, the regression between p_{cw} fitted from the discrepancies between g_{m_ANAT} and g_{m_FLU} and the (hemicellulose+cellulose)/pectin ratio is not fully clear and therefore the observed effects might be a combined effect of converging factors related to changes in cell wall composition. Moreover, similar studies in groups other than conifers are needed to confirm this hypothesis, as there are important differences in the main cell wall components between land plant groups

(Sarkar et al. 2009, Popper et al. 2011), and grass species, while presenting reduced pectin content (Ochoa-Villarreal et al. 2012), they do present the highest g_m values (Flexas et al. 2018).

Conclusions

The present study is the first to show correlative evidences for the effect of cell wall composition on mesophyll CO_2 diffusion resistance. Due to their thick cell walls gymnosperms are in the low end of the mesophyll conductance range reported for spermatophytes, but differences in cell wall composition correlated with differences in g_m within this range, likely reflecting an effect of composition on the cell wall's effective porosity. Leaf cell wall content of cellulose, hemicelluloses and pectins significantly decreased, although with different slopes for each component, as the cell walls became thicker and the mesophyll conductance larger across this range of species. The ratio (hemicelluloses + cellulose)/pectins was negatively correlated with g_m, suggesting an active but complex role of pectin relative content on the regulation of cell wall effective porosity. However, as photosynthesis was not mainly limited by g_m, no correlations were found between cell wall components and ratios and A_N. Finally, our findings challenge, at least for species with thick cell walls (>0.4 μm), the common assumption of an inverse relationship between cell wall thickness and effective porosity. More studies are needed on the relationship between cell wall composition and high plants to: 1) specifically perform the cell wall components determination analysis on mesophyll tissue, in order to avoid the interference of cuticle, epidermal and vascular tissue; and 2) perform the analysis on different plant groups to confirm the existence of a general role of pectin proportion in setting cell wall effective porosity.

Experimental procedures

Plant material

Seven 40- to 60-cm tall plants of seven conifer species were bought from a nursery. Plants were transplanted into pots (15 L, 30 cm pot diameter) containing 75:25 mixture of horticultural substrate (peat) and pearlite (granulometry A13) and fertilised with 5 g l^{-1} of slow release fertilizer (Multigreen, Haifa Chemicals, Madrid, Spain). Plants were grown outdoors fully exposed to direct sunlight at the University of the Balearic Islands (Mallorca, Spain) and watered by automatic drip every three days to maintain optimum water status and vigour. Measurements were performed in April 2016, being environmental conditions of 9.0 ºC to 20.4 ºC mean min/max temperatures, 67.6 % mean relative humidity and 1515 μmol m^{-2} s^{-1} mean daily photosynthetic active radiation (PAR) at noon. All measurements were performed on young fully expanded leaves to ensure mature leaf anatomy and to minimise variation between replicates.

Gas exchange and chlorophyll fluorescence measurement

Leaf gas exchange parameters were measured using a portable photosynthesis system (Li-6400; Li-Cor, Inc., Nebraska, USA) with an infrared gas analyser (IRGA) coupled with a 2 cm^2 leaf fluorescence chamber (Li -6400-40 leaf chamber fluorometer; Li-Cor, Inc.) All measurements were carried out between 10:00 and 17:00 h (Central European summer time). Block temperature was fixed at 25ºC, air flow rate between 150 to 200 μmol min^{-1} to ensure the reliability of the measurements and VPD kept between 1.5-2.0 kPa for all measurements.

Leaves from randomly selected plants were fully characterized. Leaf steady-state conditions were induced at 400 μmol CO_2 mol^{-1} air and saturating photosynthetic photon flux density (PPFD 1500 μmol m^{-2} s^{-1}, 90:10 red:blue light). Once steady state conditions were achieved, typically after 30-40 minutes, complete light and CO_2 response curves at 21% O_2 and CO_2 response curves at 2% O_2 were performed in a random order. Light response curves were measured at 400 μmol CO_2 mol^{-1} air at PPFD of 2000, 1500, 1000, 800, 600, 400, 200, 150, 100, 50 and 0 μmol m^{-2} s^{-1}. CO_2 response curves were measured at PPFD 1500 μmol m^{-2} s^{-1} at cuvette CO_2 concentration (C_a) of 400, 50, 100, 200, 300, 400, 600, 800, 1000, 1200, 1500, 2000 and 400 μmol mol^{-1}. Six to seven curves were performed per response curve type and per species on different individuals. The

order in which curves were performed did not affect the responses (data not shown). Values of assimilation (A) and steady-state fluorescence (F_s) were registered immediately after the steady-state conditions for gas exchange were achieved and then a saturating white light flash around 8000 µmol m^{-2} s^{-1} was applied to determine the maximum fluorescence (F_m'). Multiphase flash methodology for chlorophyll fluorescence measurements was followed, as suggested by Loriaux et al. (2013), to avoid potential maximum yield underestimation error. The electron transports rate (ETR) was estimated from Genty et al. (1989) as ETR = PPFD × ΦPSII × α × β, being ΦPSII the efficiency of photo-system II, α the leaf absorbance and β the electrons partitioning between photo-systems I and II. ΦPSII was estimated as ΦPSII = (F_m'-F_s)/F_m' (Genty et al. 1989). The $\alpha \cdot \beta$ parameter was estimated following (Valentini et al. 1995). Light response curves under non-photorespiratory conditions in a low O_2 atmosphere (< 2%) were used to establish the relationship between ΦPSII and ΦCO_2 under non-photorespiratory conditions (with ΦCO_2 = (A + R_d)/PPFD), then considering $\alpha \times \beta = 4/b$ where b is the slope of the ΦPSII ~ ΦCO_2 relationship. Non-photorespiratory respiration during the day (R_d) was estimated as half the respiration rate measured after 2 h of darkness (Martins et al. 2013, Niinemets et al. 2005, Veromann-Jürgenson et al. 2017). As conifer leaves did not fully cover the 2 cm^2 cuvette, an image of the leaf fraction placed in the chamber was taken, and the actual area was calculated using ImageJ software (Wayne Rasband/NIH, Bethesda, MD, USA). The corrected areas were used to recalculate gas-exchange data. Moreover, any measurement performed at a non-ambient [CO_2] was corrected for leaks following Flexas et al. (2007). Then, g_m was estimated following Harley et al. (1992), as:

$$(1)\ g_{m\_FLU} = \frac{A_N}{C_i - \frac{\Gamma^* (ETR + p_2 (A_N + R_d))}{(ETR - p_1 (A_N + R_d))}}$$

where A is the net assimilation rate, Γ^* is CO_2 compensation point in absence of R_d, and C_i the CO_2 concentration in intercellular air-spaces. Γ^* was assumed to be 42.5 µmol mol^{-1} as in Bernacchi et al. (2001) due to the absence of Γ^* values for conifer species. Values of p_1 and p_2, which depend on the limited steps of RuBP regeneration, where assumed to be 4 and 8, respectively.

Leaf mass per unit area

Leaf portions similar to the measured leaves were taken and photographed to determine leaf area. Afterwards, leaf portions were placed in an oven at 60ºC until constant dry weight was reached to calculate the dry leaf mass per unit leaf area (LMA).

Anatomical measurements

Immediately after gas-exchange measurements, small leaf pieces (3 × 2 mm) of the area enclosed in the leaf chamber were cut off, immersed and fixed under vacuum pressure with a glutaraldehyde 4% and paraformaldehyde 2% in a 0.1 M phosphate buffer (pH 7.4) fixing solution. 5 plants per species were sampled. Afterwards, samples were post-fixed in 2% buffered osmium tetroxide for 2h, and dehydrated in a graded series of ethanol. Dehydrated samples were embedded in resin (LR-White, London Resin Company, London, UK) and solidified in an oven at 60ºC for 48h.

Semi-thin cross-sections of 0.8 µm and ultrathin cross-sections of 90 nm for transmission electron microscopy (TEM) were cut with an ultramicrotome (Leica UC6, Vienna, Austria). Semi-thin sections were dyed with 1% toluidine blue and observed at 200× magnifications under an Olympus BX60 (Olympus, Tokyo, Japan) light microscopy and photographed with a Moticam 3 (Motic Electric Group Co., Xiamen, China). The ultrathin sections were contrasted with uranyl acetate and lead citrate and viewed at 1200× and 30000× magnifications with a transmission electron microscopy (TEM H600; Hitachi, Tokyo, Japan). All images were analysed using IMAGEJ software (Schneider et al. 2012). From light microscopy images leaf thickness (T_{leaf}), mesophyll thickness (T_{mes}), number of palisade layers, fraction of the mesophyll occupied by intercellular airspaces (f_{ias}) and mesophyll surface area exposed to intercellular airspace (S_m/S) were measured. From TEM microscopy images cell wall thickness (T_{cw}), cytoplasm thickness (T_{cyt}), chloroplast length (L_{chl}), chloroplast thickness (T_{chl}) and chloroplast surface area exposed to intercellular airspace (S_c/S) were measured and calculated following Tomás et al. (2013). Cell curvature correction factor was calculated according to Thain (1983). Factors between 1.18 and 1.26 and between 1.37 and 1.48 were applied to cell surface area estimates for mesophyll

spongy (oblate spheroids) and palisade cells (prolate spheroids), respectively. Four to six randomly selected different fields of view were considered per plant replicate to measure each anatomical characteristic. For each type of mesophyll tissue (spongy and palisade), ten measurements were made for T_{leaf}, T_{mes}, f_{ias}, T_{cw}, S_m/S and S_c/S, and 15 measurements per mesophyll type were made for L_{chl} and T_{chl}. Then, weighted averages based on tissue volume fractions were calculated.

Estimation of mesophyll conductance modelled from anatomical characteristics

The one-dimensional within-leaf gas diffusion model of Niinemets and Reichstein (2003) modified by Tomás et al. (2013) was applied. Mesophyll diffusion conductance as a composite conductance for within-leaf gas, liquid and lipid components is given as:

(2) $$g_{m\_ANAT} = \frac{1}{\frac{1}{g_{ias}} + \frac{RT_k}{H \cdot g_{liq}}}$$

where H is the Henry's law constant (m^3 mol^{-1} K^{-1}), R is the gas constant (Pa m^3 K^{-1} mol^{-1}) and T_k is the absolute temperature (K). $H/(RT_k)$ is the dimensionless form of Henry's law constant needed to convert a liquid and lipid phase conductance (g_{liq} and g_{lip}) into a gas-phase equivalent conductance (Niinemets and Reichstein 2003). Gas-phase diffusion depends on the fraction of mesophyll volume occupied by intercellular air spaces (f_{ias}, m^3 m^{-3},) and the effective diffusion path length in the gas-phase (ΔL_{ias}) (Syvertsen et al. 1995, Terashima et al. 2011):

(3) $$g_{ias} = \frac{D_a \cdot f_{ias}}{\Delta L_{ias} \cdot \varsigma}$$

where ς is the diffusion path tortuosity (m m^{-1}) and D_a (m^2 s^{-1}) is the diffusion coefficient for CO_2 in the gas-phase ($1.51 \cdot 10^{-5}$ m^2 s^{-1} at 22 °C). ΔL_{ias} was approximated by mesophyll thickness divided by two (Niinemets and Reichstein 2003). An estimate of ς was used as a default value of 1.57 m m^{-1} (Niinemets and Reichstein 2003, Syvertsen et al. 1995). The total liquid phase conductance is provided by the sum of the inverse of serial conductances:

(4) $\frac{1}{g_{\mathrm{liq}}} = \left(\frac{1}{g_{\mathrm{cw}}} + \frac{1}{g_{\mathrm{pl}}} + \frac{1}{g_{\mathrm{ct}}} + \frac{1}{g_{\mathrm{en}}} + \frac{1}{g_{\mathrm{st}}}\right) \cdot S_c/S$

where partial conductances account for cell wall (g_{cw}), plasmalemma (g_{pl}), cytosol (g_{ct}), chloroplast envelope (g_{en}), and chloroplast stroma (g_{st}). The cell wall, cytosol and stromal conductances are given by a general equation:

(5) $g_i = \frac{r_{f,i} \cdot D_w \cdot p_i}{\Delta L_i}$

where g_i (m s^{-1}) is either g_{cw}, g_{ct} or g_{st}, ΔL_i (m) is the diffusion path length and p_i (m^3 m^{-3}) is the effective porosity in the given part of the diffusion pathway, D_w is the aqueous phase diffusion coefficient for CO_2 ($1.79 \cdot 10^{-9}$ m^2 s^{-1} at 25 °C) and the dimensionless factor $r_{f,i}$ accounts for the decrease of diffusion conductance compared to free diffusion in water (Weisiger 1998). For cell walls where the aqueous-phase diffusion has been shown to approximate free water, $r_{f,i}$ = 1 (Rondeau-Mouro et al. 2008). The value of r_f was set at 0.3 for g_{ct} and g_{st} to account for the reduction of diffusion conductance due to high concentrations of high molecular solutes and intracellular (cytoskeleton) and intraorganellar (thylakoids) heterogeneities (Niinemets and Reichstein 2003). Effective porosity, p_i, was taken as 1 for g_{ct} and g_{st}. Cell wall porosity (p_{cw}) was taken as 0.028, as applied in Tomás et al. (2013) for species with species with T_{cw}>0.4 μm, but was also fitted in order to know what its value would have to be so that g_{m_ANAT} = g_{m_FLU}. Conductance in units of m s^{-1} can be converted into molar units considering that

g[mol m^{-2} s^{-1}] = g[m s^{-1}]44.6·[273.16/(273.16 + T_L)(P/101.325),

where T_L is the leaf temperature (ºC) and P (Pa) is the air pressure. Due to the difficulty to measure the thickness of the plasma membrane, the chloroplast envelope and the limited information about the permeability of the lipid phase membranes, g_{pl} and g_{env} were assumed as constant values (0.0035 m s^{-1}) as previously suggested in other studies (Evans et al. 1994, Peguero-Pina et al. 2012, Tomás et al. 2013, Tosens et al. 2012a, 2012b).

Analysis of quantitative limitations of A_N and g_m

The relative limitations on A_N for conifers were calculated following Grassi & Magnani (2005). This analysis quantifies the relative importance of stomatal, mesophyll conductance and biochemical limitations (the latter integrating both Rubisco and photochemistry/Calvin cycle, owing to the fact that photosynthesis operates at co-limitation between these two factors; see Gallé et al. 2009, and Varone et al., 2012, for further explanation). Fractional limitations, that is, those imposed by limited stomatal (l_s) or mesophyll conductance (l_{mc}), and reduced biochemical capacity (l_b), were calculated as:

(6) $$l_s = \frac{\frac{g_{tot}}{g_s} \cdot \frac{\delta A_N}{\delta C_c}}{g_{tot} + \frac{\delta A_N}{\delta C_c}}$$

(7) $$l_m = \frac{\frac{g_{tot}}{g_m} \cdot \frac{\delta A_N}{\delta C_c}}{g_{tot} + \frac{\delta A_N}{\delta C_c}}$$

(8) $$l_b = \frac{g_{tot}}{g_{tot} + \frac{\delta A_N}{\delta C_c}}$$

where g_s and g_{m_FLU} are the stomatal and mesophyll conductances to CO_2 and g_{tot} is the total conductance (the sum of inversed serial conductances g_{m_FLU} and g_s). $\delta A_N/\delta C_c$ is the slope of A_N-C_c response curves -estimated from 21% O_2 A/C_i curves following Harley et al. (1992)- over a C_c range of 75-150 µmol mol^{-1}. These three values sum 100% and characterize the extent to which any of the three limitations curbs photosynthesis at the given values of the other two. The contribution of the gas-phase and the liquid-phase resistances, and then only of the different components of cellular resistance, to mesophyll resistance to CO_2 diffusion was estimated from the anatomical model following Tosens et al. (2016). This share of limitation (l_i) by different liquid phase components was calculated as:

(9) $$l_i = \frac{g_{m\_ANAT}}{g_i \cdot S_c/S}$$

where l_i is the limitation by the cell wall, the plasmalemma, cytosol, chloroplast envelope and stroma, and g_i refers to the diffusion conductance of each corresponding diffusion pathway. The limitation of each cellular component was scaled up with S_c/S.

Cell wall composition determination

Leaves of four plants per species were sampled (ca. 1 g) for cell wall analysis. In order to minimize the leaf starch content, sampling was performed early in the morning. Samples were boiled in absolute ethanol until bleached. Afterwards, in order to eliminate any alcohol soluble compound, samples were cleaned in acetone shaking for 30 min twice. Then, samples were air-dried and homogenized by dry milling. The resulting alcohol insoluble residue (AIR), which represents the cell wall crude material, was subjected to a treatment with α-amylase (Sigma) overnight to remove the starch retained in the sample, and then used for the polysaccharides and bound phenolic compounds analysis. For each sample, 3 mg of AIR were hydrolysed with 2 M trifluoroacetic acid (TFA) for 1 h a 121 ºC and then centrifuged at 13 000 *g* for 10 min. Supernatant (non-cellulosic cell wall components, mainly hemicellulose and pectins) was separated and kept at 4 ºC, while precipitated (cellulosic cell wall components) was cleaned once in distilled water, twice in acetone, and then air-dried. The dry fraction was hydrolysed with 200 µl sulfuric acid (72 %) for 1 h at room temperature, diluted with distilled water to 6 mL (0.5 M sulfuric acid) and heated to 121 ºC for 2 h to obtain the total sugar corresponding to the cellulose fraction. Total sugars from both AIR fractions (hemicelluloses and celluloses from the soluble and insoluble 2 M TFA fraction, respectively) were separately determined with the phenol sulfuric colorimetric method (Dubois et al. 1956) by considering glucose equivalents as standard in a Varioskan Lux (Thermo Scientific). Uronic acids (pectins) were quantified from the soluble 2 M TFA fraction by colorimetry (Blumenkratz and Asboe-Hansen 1973) using 2 hydroxydiphenyl as reagent and galacturonic acid as standard in a Varioskan Lux.

Statistical analysis

Pearson correlation matrices were determined to reveal the relationships between traits. Significances were distinguished at the $P < 0.05$, $P < 0.01$ and $P < 0.0001$ levels. These analyses were performed with the software package IBM SPSS 11.0 (SPSS, Chicago, IL, USA).

Acknowledgments

This work was supported by the project CTM2014-53902-C2-1-P from the Ministerio de Economía y Competitividad (MINECO, Spain) and the ERDF (FEDER). MC acknowledges the predoctoral fellowship FPI/1700/2014 by Conselleria d'Educació, Cultura i Universitats (Govern de les Illes Balears) and European Social Fund, and MN acknowledges predoctoral fellowship BES-2015-072578 by Ministerio de Economía y Competitividad (MINECO, Spain) and European Social Fund. The authors are grateful to Miquel Truyols (Camp experimental, UIB) for his support to our experiment, to Mª Teresa Mínguez, Universitat de València (Secció Microscòpia Electrònica, SCSIE), and to Dr Ferran Hierro, Universitat de les Illes Balears (Serveis Cientificotècnics), for technical support during microscopic analyses.

Conflicts of interest

The authors declare no conflicts of interest.

Short supporting legends

Table S1. Photosynthetic characteristics.

Table S2. Morphological and anatomical structural traits.

Table S3. Ultrastructural anatomic traits.

Table S4. Cell wall content and composition.

Figure S1. LMA in relation to morphoanatomical traits.

Figure S2. Relationship between fitted cell wall porosity and cell wall composition.

Figure S3. Relationship between fitted cell wall porosity and the (hemicelluloses+cellulose)/pectins ratio.

References

Baron-Epel O., Gharyal P.K., Schlinder M. (1988) Pectins as mediators of wall porosity in soybean cells. *Planta* 175, 389–395.

Bernacchi C.J., Singsaas E.L., Pimentel C., Portis J.R. A.R., Long S.P. (2001) Improved temperature response functions for models of Rubisco-limited photosynthesis. *Plant, Cell and Environment* 24, 253–259.

Blumenkrantz N., Asboe-Hansen G. (1973) New method for quantitative determination of uronic acids. *Analytical Biochemistry* 54, 484–489.

Caffall K.H., Mohnen D. (2009) The structure, function, and biosynthesis of plant cell wall pectic polysaccharides. *Carbohydrate Research* 344, 1879–1900.

Carpita N.C., Sabularse D., Montezinos D., Delmer D.P. (1979) Determination of the pore size of cell walls of living plant cells. *Science 205,* 1144–1147.

Carriquí M., Cabrera H.M., Conesa M.À., Coopman R.E., Douthe C., Gago J., Gallé A., Galmés J., Ribas-Carbo M., Tomás M., Flexas J. (2015) Diffusional limitations explain the lower photosynthetic capacity of ferns as compared with angiosperms in a common garden study. *Plant, Cell and Environment* 38, 448–460.

Carriquí M., Douthe C., Molins A., Flexas J. (2019a) Leaf anatomy does not explain apparent short-term responses of mesophyll conductance to light and CO_2 in tobacco. *Physiologia Plantarum* 165, 604–618.

Carriquí M., Roig-Oliver M., Brodribb T.J., Coopman R., Gill W., Mark K., Niinemets Ü., Perera-Castro A.V., Ribas-Carbó M., Sack L., Tosens T., Waite M., Flexas J. (2019b) Anatomical constraints to mesophyll conductance and photosynthesis in lycophytes and bryophytes from arctics to tropics. *New Phytologist* 222, 1256–1270.

Carriquí M., Nadal M., Flexas J. *Thuja Plicata*, a species with very thick leaves and cell walls compensates low CO_2 diffusion by extremely high S_c/S. *Tree Physiology* (submitted).

Cosgrove DJ (2005) Growth of the plant cell wall. *Nature Reviews* 6, 850–861.

Cosgrove D.J., Jarvis M.C. (2012) Comparative structure and biomechanics of plant primary and secondary cell walls. *Frontiers in Plant Science* 3, 1–6.

Cosgrove D.J. (2016) Plant cell wall extensibility: connecting plant cell growth with cell wall structure, mechanics, and the action of wall modifying enzymes. *Journal of Experimental Botany* 67, 463–476.

Dubois M., Gilles K.A., Hamilton J.K., Rebers P.A., Smith F. (1956) Colorimetric mehotd for determination of sugars and related substances. *Analytical Chemistry* 28, 350–356.

Earles J.M., Théroux-Rancourt G., Roddy A.B., Gilbert M.E., McElrone A.J., Brodersen C.R. (2018). Beyond porosity: 3D leaf intercellular airspace traits that impact mesophyll conductance. *Plant Physiology* 178, 148–162.

Ellsworth P.V., Ellsworth P.Z., Koteyeva N.K., Cousins A.B. (2018) Cell wall properties in *Oryza sativa* influence mesophyll CO_2 conductance. *New Phytologist* 219, 66–76.

Evans J., Caemmerer S., Setchell B., Hudson G. (1994) The relationship between CO_2 transfer conductance and leaf anatomy in transgenic tobacco with a reduced content of Rubisco. *Australian Journal of Plant Physiology* 21, 475–495.

Fleischer A., O'Neill M.A., Ehwald R. (1999) The pore size of non-graminaceous plant cell walls is rapidly decreased by borate ester cross-linking of the pectic polysaccharide rhamnogalacturonan II. *Plant Physiology* 121, 829–838.

Flexas J., Díaz-Espejo A., Berry J.A., Galmés J., Cifre J., Kaldenhoff R., Medrano H. Ribas-Carbó M. (2007) Leakage in leaf chambers in open gas exchange systems: quantification and its effects in photosynthesis parameterization. *Journal of Experimental Botany* 58, 1533–1543.

Flexas J., Barbour M.M., Brendel O., Cabrera H.M., Carriquí M., Díaz-Espejo A., Douthe C., Dreyer E., Ferrio J.P., Gago J., Gallé A., Galmés J., Kodama N., Medrano H., Niinemets Ü., Peguero-Pina J.J., Pou A., Ribas-Carbó M., Tomás M., Tosens T., Warren C.R. (2012) Mesophyll conductance to CO_2:

An unappreciated central player in photosynthesis. *Plant Science* 193-194, 70–84.

Flexas J., Cano F.J., Carriquí M., Coopman R.E., Mizokami Y., Tholen D., Xiong D. (2018). CO_2 diffusion inside photosynthetic organs. In *The Leaf: A platform for performing photosynthesis*, Advances in Photosynthesis and Respiration (including bioenergy and related processes) (eds WW Adams and I Terashima), Vol. 44 pp .163–208. Springer, Cham.

Gago J., Daloso D.d.M., Figueroa C.M., Flexas J., Fernie A.R. (2016) Relationships of leaf net photosynthesis, stomatal conductance, and mesophyll conductance to primary metabolism: a multispecies meta-analysis approach. *Plant Physiology* 171, 265–279.

Galle A., Florez-Sarasa I., Tomas M., Pou A., Medrano H., Ribas-Carbo M., Flexas J. (2009) The role of mesophyll conductance during water stress and recovery in tobacco (*Nicotiana sylvestris*): acclimation or limitation? *Journal of Experimental Botany* 60, 2379–90.

Genty B., Briantais J.-M., Baker N.R. (1989) The relationship between the quantum yield of photosynthetic electron transport and quenching of chlorophyll fluorescence. *Biochimica et Biophysica Acta - General Subjects* 990, 87–92.

Grassi G., Magnani F. (2005) Stomatal, mesophyll conductance and biochemical limitations to photosynthesis as affected by drought and leaf ontogeny in ash and oak trees. *Plant, Cell and Environment* 28, 834–849.

Harley P.C., Loreto F., Di Marco G., Sharkey T.D. (1992) Theoretical considerations when estimating the mesophyll conductance to CO_2 flux by analysis of the response of photosynthesis to CO_2. *Plant Physiology* 98, 1429–36.

Kitajima K., Llorens A.-M., Stefanescu C., Timchenko M.V., Lucas P.W., Wright S.J. (2012) How cellulose-based leaf thoughness and lamina density contribute to long leaf lifespans of shade-tolerant species. *New Phytologist* 195, 640–652.

Kitajima K., Wright S.J., Westbrook J.W. (2016) Leaf cellulose density as the key determinant of inter- and intra-specific variation in leaf fracture toughness in a species-rich tropical forest. *Interface Focus* 6, 20150100.

Kuusk V., Niinemets Ü., Valladares F. (2018) A major trade-off between structural and photosynthetic investments operative across plant and needle ages in three Mediterranean pines. *Tree Physiology* 38, 543–557.

Loriaux S.D., Avenson T.J., Welles J.M., McDermitt D.K., Eckles R.D., Riensche B., Genty B. (2013) Closing in on a maximum yield of chlorophyll fluorescence using a single multiphase flash of sub-saturating intensity. *Plant, Cell and Environment* 36, 1755–1770.

Martins S.C.V., Galmés J., Molins A., DaMatta F.M. (2013) Improving the estimation of mesophyll conductance to CO_2: on the role of electron transport rate correction and respiration. *Journal of Experimental Botany* 64, 3285–3298.

McCann M.C., Wells B., Roberts K. (1990) Direct visualization of cross-links in the primary cell wall. *Journal of Cell Science* 96, 323–334.

McKenna B.A., Kopittke P.M., Wehr J.B., Blamey F.P.C., Menzies N.W. (2010) Metal ion effects on hydraulic conductivity of bacterial cellulose-pectin composites used as plant cell wall analogs. *Physiologia Plantarum* 138, 205–214.

Mediavila S., Garcia-Ciudad A., Garcia-Criado B., Escudero A. (2008) Testing the correlations between leaf life span and leaf structural reinforcement in 13 species of European Mediterranean woody plants. *Functional Ecology* 22, 787–793.

Miyazawa S.-I., Terashima I. (2001) Slow development of leaf photosynthesis in an evergreen broad-leaved tree, *Castanopsis sieboldii*: relationships between leaf anatomical characteristics and photosynthetic rate. *Plant, Cell and Environment* 24, 279–291.

Momayyezi M., Guy R.D. (2017) Substantial role for carbonic anhydrase in

latitudinal variation in mesophyll conductance of *Populus trichocarpa* Torr. & Gray. *Plant, Cell and Environment* 40, 138–149.

Morales L.V., Coopman R.E., Rojas R., Escandón A.B., Flexas J., Galmés J., García-Plazaola J.I., Gago J., Cabrera H.M., Corcuera L.J. (2014) Acclimation of leaf cohorts expanded under light and water stresses: an adaptive mechanism of *Eucryphia cordifolia* to face changes in climatic conditions? *Tree Physiology* 34,. 1305–1320.

Muir C.D., Hangarter R.P., Moule L.C., Davis P.A. (2014) Morphological and anatomical determinants of mesophyll conductance in wild relatives of tomato (*Solanum* sect. *Lycopersicon*, sect. *Lycopersicoides*; Solanaceae). *Plant, Cell and Environment* 37, 1415–1426.

Nadal M., Flexas J. (2019) Variation in photosynthetic characteristics with growth form in a water-limited scenario: Implications for assimilation rates and water use efficiency in crops. *Agricultural Water Management* 216, 457–472.

Niinemets Ü., Cescatti A., Rodeghiero M., Tosens T. (2005) Leaf internal diffusion conductance limits photosynthesis more strongly in older leaves of Mediterranean evergreen broad-leaved species. *Plant, Cell and Environment* 28, 1552–1566.

Niinemets Ü., Reichstein M. (2003) Controls on the emission of plant volatiles through stomata: Differential sensitivity of emission rates to stomatal closure explained. *Journal of Geophysical Research* 108, 4208.

Nobel P.S. (1999) Physicochemical and environmental plant physiology. *Academic Press*.

Ochoa-Villareal M., Aispuro-Hernández E., Vargas-Arispuro I., Martínez-Téllez M.Á. (2012) Plant cell wall polymers: function, structure and biological activity of their derivatives. In: De Souza Gomes A (ed) Polymerization. InTech, Rijeka.

Onoda Y., Schieving F., Anten N.P.R. (2015) A novel method of measuring leaf epidermis and mesophyll stiffness shows the ubiquitous nature of the

sandwich structure of leaf laminas in broad-leaved angiosperm species. *Journal of Experimental Botany* 66, 2487–2499.

Onoda Y., Wright I.J., Evans J.R., Hikosaka K., Kitajima K., Niinemets Ü., Poorter H., Tosens T., Westoby M. (2017) Physiological and structural tradeoffs underlying the leaf economics spectrum. *New Phytologist* 214, 1447–1463.

Peguero-Pina J.J., Flexas J., Galmés J., Niinemets Ü,, Sancho-Knapik D., Barredo G., Villarroya D., Gil-Pelegrín E. (2012) Leaf anatomical properties in relation to differences in mesophyll conductance to CO_2 and photosynthesis in two related Mediterranean *Abies* species. *Plant Cell and Environment* 35, 2121–2129.

Peguero-Pina J.J., Sisó S., Flexas J., Galmés J., García-Nogales A., Niinemets Ü., Sancho-Knapik D., Saz M.A., Gil-Pelegrín E. (2017) Cell-level anatomical characteristics explain high mesophyll conductance and photosynthetic capacity in sclerophyllous Mediterranean oaks. *New Phytologist* 214, 585–596.

Popper Z.A., Michel G., Hervé C., Domozych D.S., Willats W.G.T., Tuohy M.G., Kloareg B., Stengel D. (2011) Evolution of plant cell walls: from algae to flowering plants. *Annual Revision of Plant Biology* 62, 567–590.

Poorter H., Niinemets Ü., Poorter L., Wright I.J., Villar R. (2009) Causes and consequences of variation in leaf mass per area (LMA): a meta-analysis. *New Phytologist* 182, 565–588.

Read S.M., Bacic A. (1996) Cell wall porosity and its determination. In: *Plant Cell Wall Analysis* pp. 63–80. Springer.

Ren T., Weraduwage S., Sharkey T.D. (2019) Prospects for enhancing leaf photosynthetic capacity by manipulating mesophyll cell morphology. *Journal of Experimental Botany* 70, 1153–1165.

Renault S., Zwiazek J.J. (1997) Cell wall composition and elasticity of dormant and growing white spruce (*Picea glauca*) seedlings. *Physiologia Plantarum* 101, 323–327.

Rondeau-Mouro C., Defer D., Leboeuf E., Lahaye M. (2008) Assessment of cell wall porosity in *Arabidopsis thaliana* by NMR spectroscopy. *International Journal of Biological Macromolecules* 42, 83–92.

Sarkar P., Bosneaga E., Auer M. (2009) Plant cell walls throughout evolution: towards a molecular understanding of their design principles. *Journal of Experimental Botany* 60, 3615–3635.

Schneider C.A., Rasband W.S., Eliceiri K.W. (2012) NIH Image to ImageJ: 25 years of image analysis. *Nature Methods* 9, 671–675.

Syvertsen J.P., Lloyd J., McConchie C., Kriedemann P.E., Farquhar G.D. (1995) On the relationship between leaf anatomy and CO_2 diffusion through the mesophyll of hypostomatous leaves. *Plant, Cell and Environment* 18, 149–157.

Tenhaken R. (2015) Cell wall remodeling under abiotic stress. *Frontiers in Plant Science* 5, 771.

Terashima I., Hanba Y.T., Tazoe Y., Vyas P., Yano S. (2006) Irradiance and phenotype: comparative eco-development of sun and shade leaves in relation to photosynthetic CO_2 diffusion. *Journal of Experimental Botany* 57, 343–354.

Terashima I., Hanba Y.T., Tholen D., Niinemets Ü. (2011) Leaf functional anatomy in relation to photosynthesis. *Plant Physiology* 155, 108–116.

Thain J.F. (1983) Curvature correlation factors in the measurements of cell surface areas in plant tissues. *Journal of Experimental Botany* 34, 87–94.

Tholen D., Boom C., Noguchi K.O., Ueda S., Katase T., Terashima I. (2008) The chloroplast avoidance response decreases internal conductance to CO_2 diffusion in *Arabidopsis thaliana* leaves. *Plant, Cell and Environment* 31, 1688–1700.

Tomás M., Flexas J., Copolovici L., Galmés J., Hallik L., Medrano H., Ribas-Carbó M., Tosens T., Vislap V., Niinemets Ü. (2013) Importance of leaf anatomy in determining mesophyll diffusion conductance to CO_2 across

species: quantitative limitations and scaling up by models. *Journal of Experimental Botany* 64 2269–2281.

Tomás M., Medrano H., Brugnoli E., Escalona J.M., Martorell S., Pou A., Ribas-Carbó M., Flexas J. (2014) Variability of mesophyll conductance in grapevine cultivars under water stress conditions in relation to leaf anatomy and water use efficiency. *Australian Journal of Grape and Wine Research* 20, 272–280.

Tosens T., Niinemets U., Vislap V., Eichelmann H., Castro Díez P. (2012a) Developmental changes in mesophyll diffusion conductance and photosynthetic capacity under different light and water availabilities in *Populus tremula*: how structure constrains function. *Plant, Cell and Environment* 35, 839–56.

Tosens T., Niinemets Ü., Westoby M., Wright I.J. (2012b) Anatomical basis of variation in mesophyll resistance in eastern Australian sclerophylls: news of a long and winding path. *Journal of Experimental Botany* 63, 5105–5119.

Tosens T., Nishida K., Gago J., Coopman R.E., Cabrera H.M., Carriquí M., Laanisto L., Morales L., Nadal M., Rojas R., Talts E., Tomas M., Hanba Y., Niinemets Ü., Flexas J. (2016) The photosynthetic capacity in 35 ferns and fern allies: mesophyll CO_2 diffusion as a key trait. *New Phytologist* 209, 1576–1590.

Valentini R., Epron D., De Angelis P., Matteucci G., Dreyer E. (1995) *In situ* estimation of net CO_2 assimilation, photosynthetic electron flow and photorespiration in Turkey oak (*Quercus cerris* L.) leaves: diurnal cycles under different levels of water supply. *Plant, Cell and Environment* 18, 631–640.

Varone L., Ribas-Carbo M., Cardona C., Gallé A., Medrano H., Gratani L., Flexas J. (2012) Stomatal and non-stomatal limitations to photosynthesis in seedlings and saplings of Mediterranean species pre-conditioned and aged in nurseries: Different response to water stress. *Environmental and Experimental Botany* 75, 235–247.

Veromann-Jürgenson L.-L., Tosens T., Laanisto L., Niinemets Ü. (2017)

Extremely thick cell walls and low mesophyll conductance: welcome to the world of ancient living! *Journal of Experimental Botany* 68, 1639–1653.

Weisiger R. (1998) Impact of extracellular and intracellular diffusion barriers on transport. In J Bassingthwaighte, C Goresky, J Linehan, eds, Whole organ approach to Cell. Metab, pp. 389–423. Springer-Verlag, New York, NY, US.

Weraduwage S.M., Kim S.-J., Renna L., Anozie F.C., Sharkey T.D., Brandizzi F. (2016) Pectin methylesterification impacts the relationship between photosynthesis and plant growth. Plant Physiology 171, 833–848.

Weraduwage S.M., Campos M.L., Yoshida Y., Major I.T., Kim Y.-S., Kim S.-J., Renna L., Anozie F.C. (2018) Molecular mechanismes affecting cell wall properties and leaf architecture. In *The Leaf: A platform for performing photosynthesis*, Advances in Photosynthesis and Respiration (including bioenergy and related processes) (eds W.W. Adams and I. Terashima), Vol 44 pp 209–253. Springer, Cham.

Whitney S.E.C., Gothard M.G.E., Mitchell J.T., Gidley M.J. (1999) Roles of cellulose and xyloglucan in determining the mechanical properties of primary plant cell walls. *Plant Physiology* 121, 657–663.

Xiao Y., Zhu X.-G. (2017) Components of mesophyll resistance and their environmental responses: A theoretical modelling analysis. *Plant, Cell and Environment* 40, 2729–2742.

Yamori W., Hikosaka K., Way D.A. (2014) Temperature response of photosynthesis in C3, C4 and CAM plants: temperature acclimation and temperature adaptation. *Photosynthesis Research* 119, 101–117.

Yang Z.B., Eticha D., Rao I.M., Horst W.J. (2010) Alteration of cell-wall porosity is involved in osmotic stress-induced enhancement of aluminium resistance in common bean (*Phaseolus vulgaris* L.). *Journal of Experimental Botany* 61, 3245–3258.

Zablackis E., Huang J., Müller B., Darvill A., Albersheim P. (1995) Characterization of the cell-wall polysaccharides of *Arabidopsis thaliana*

leaves. *Plant Physiology* 107, 1129–1138.

Zhong R., Cui D., Ye Z.H. (2019) Secondary cell wall biosynthesis. *New Phytologist* 221, 1703–1723.

Figure legends

Figure 1. Net photosynthesis (A_N) in relation to (A) stomatal conductance to CO_2 (g_s) and (B) mesophyll conductance estimated by chlorophyll fluorescence (g_{m_FLU}). Each point corresponds to one species (n = 3-7). Species from this study are marked as closed circles, while gymnosperm species from Veromann-Jürgenson et al. (2017) are marked as open circles. Closed circles with error bars display average ± SE values for the seven species considered in the present study. Data were fitted by linear regression (significance at $P < 0.05$).

Figure 2. *Relative* stomatal (l_s), mesophyll conductance (l_m) and biochemical (l_b) photosynthesis limitations per species. Error bars represent standard errors (n= 3-7).

Figure 3. Mesophyll conductance estimated by chlorophyll fluorescence (g_{m_FLU}) in relation to (A) chloroplast surface area exposed to intercellular airspaces per projected leaf area (S_c/S), and (B) cell wall thickness (T_{cw}). Inset in (B) shows the general relationship observed between g_{m_FLU} and T_{cw} for vascular plants, with the relative position of gymnosperm species highlighted with an ellipse. Species from this study are marked as closed circles, gymnosperm species from Veromann-Jürgenson et al. (2017) are marked as open circles and data from spermatophytes species compiled by Onoda et al. (2017) are marked as orange triangles. Closed circles with error bars display average ± SE values for the seven species considered in the present study. Data were fitted in (A) by a logarithmic regression in considering all species, while data from each study was separately fitted by linear regression in (B).

Figure 4. (A) Relative gas- and liquid-phase mesophyll conductance limitations (l_{ias} and l_{liq}, respectively) per species. (B) Relative limitation of liquid-phase components- cell wall (l_{cw}), plasma membrane (l_{pl}), cytoplasm (l_{ct}), chloroplast envelope (l_{en}) and stroma (l_{st})- on mesophyll conductance in each species. Error bars represent standard errors (n= 3-7).

Figure 5. (A) Average ± SE mesophyll cell wall thickness (T_{cw}) for each species. (B) Average ± SE adjusted cell wall porosity (p_{cw}) required to fit mesophyll

conductance modelled from anatomy (g_{m_ANAT}) with mesophyll conductance estimated by chlorophyll fluorescence (g_{m_FLU}).

Figure 6. Comparison of mesophyll conductance values modelled according to the diffusion model from Tosens et al. (2016; g_{m_ANAT}) considering both constant or fitted cell wall porosity (p_{cw}) and estimated according to the variable *J* method (Harley et al. (1992; g_{m_FLU}).

Figure 7. The relationship between cell wall thickness (T_{cw}) and (A) the mass of cell walls prepared as alcohol insoluble residues per leaf dry weight (AIR), (B) the mass of each cell wall component per AIR mass, and (C) cell wall component mass per leaf area. Data are means ± SE (n = 4) for each species. Linear regressions were fitted to the data.

Figure 8. The relationship between net photosynthesis (A_N) and (A) the mass of cell walls prepared as alcohol insoluble residues per leaf dry weight (AIR), (B) the mass of each cell wall component per AIR mass, and (C) cell wall component mass per leaf area. The relationship between mesophyll conductance estimated by chlorophyll fluorescence (g_{m_FLU}) and (D) AIR, (E) the proportion of each cell wall component, and (F) cell wall component mass per leaf area. Data are means ± SE of four replicate measurements for each species. Linear regressions were fitted to the data.

Figure 9. The relationship between mesophyll conductance estimated by chlorophyll fluorescence (g_{m_FLU}) and the ratio (hemicelluloses + celluloses) / pectins. Exponential decay regression was fitted to the data.

Figures

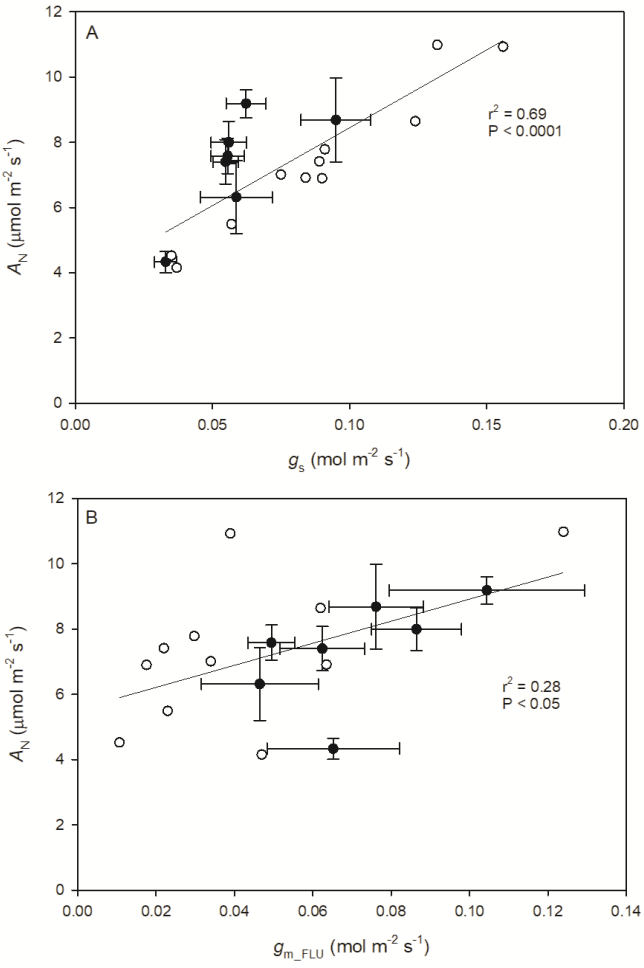

Figure 1

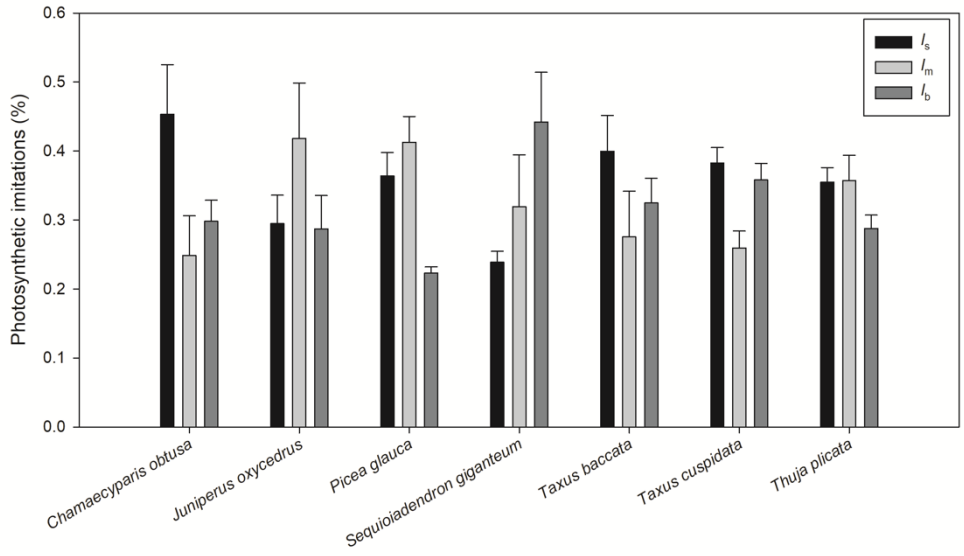
Photosynthetic imitations (%)
0.0
0.1
0.2
0.3
0.4
0.5
0.6
I_s
I_m
I_b
Chamaecyparis obtusa
Juniperus oxycedrus
Picea glauca
Sequioiadendron giganteum
Taxus baccata
Taxus cuspidata
Thuja plicata

Figure 2

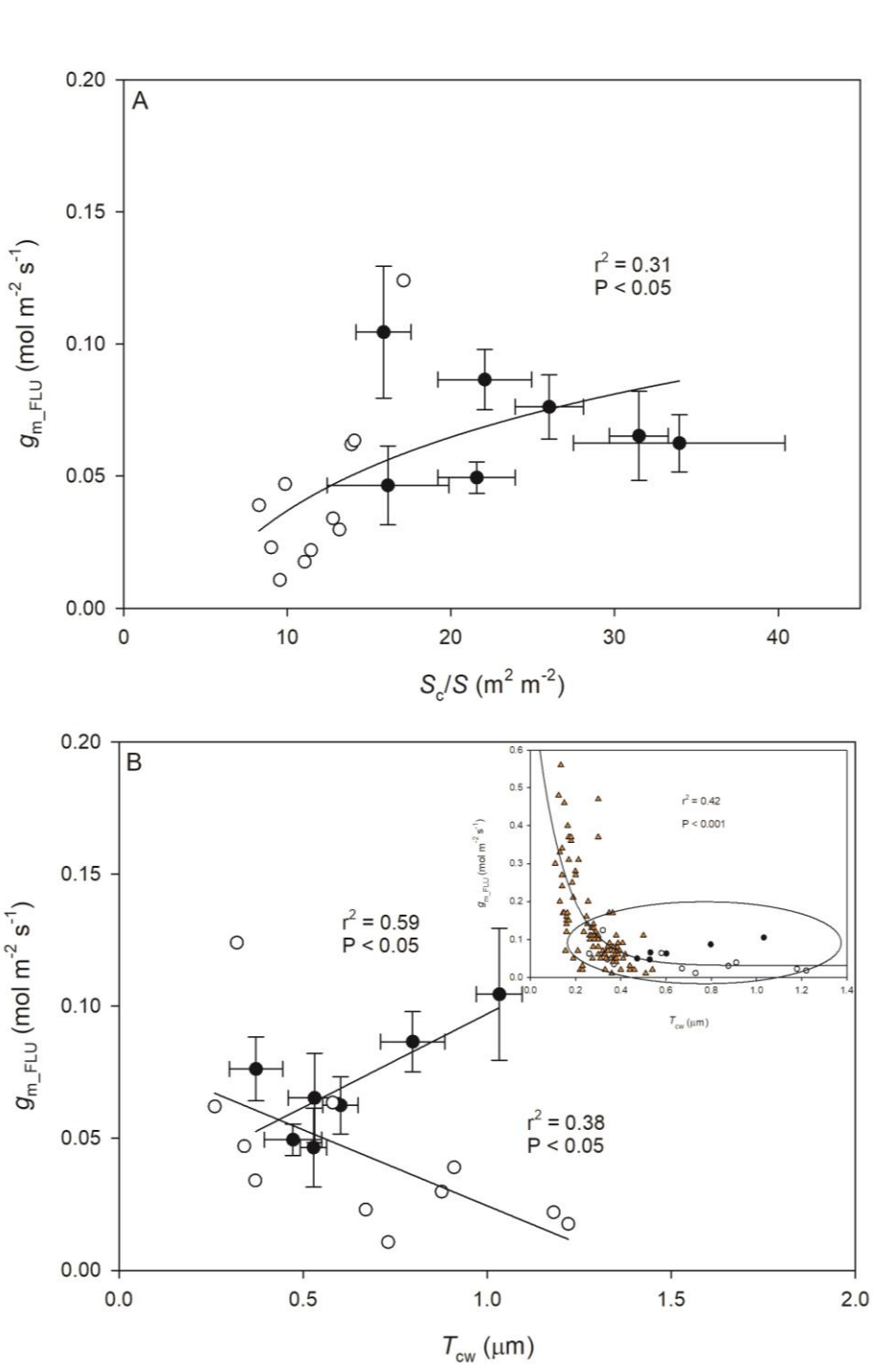
A
r^2 = 0.31
P < 0.05
g_{m_FLU} (mol m^{-2} s^{-1})
S_c/S (m^2 m^{-2})
B
r^2 = 0.59
P < 0.05
r^2 = 0.38
P < 0.05
r^2 = 0.42
P < 0.001
T_{cw} (µm)

Figure 3

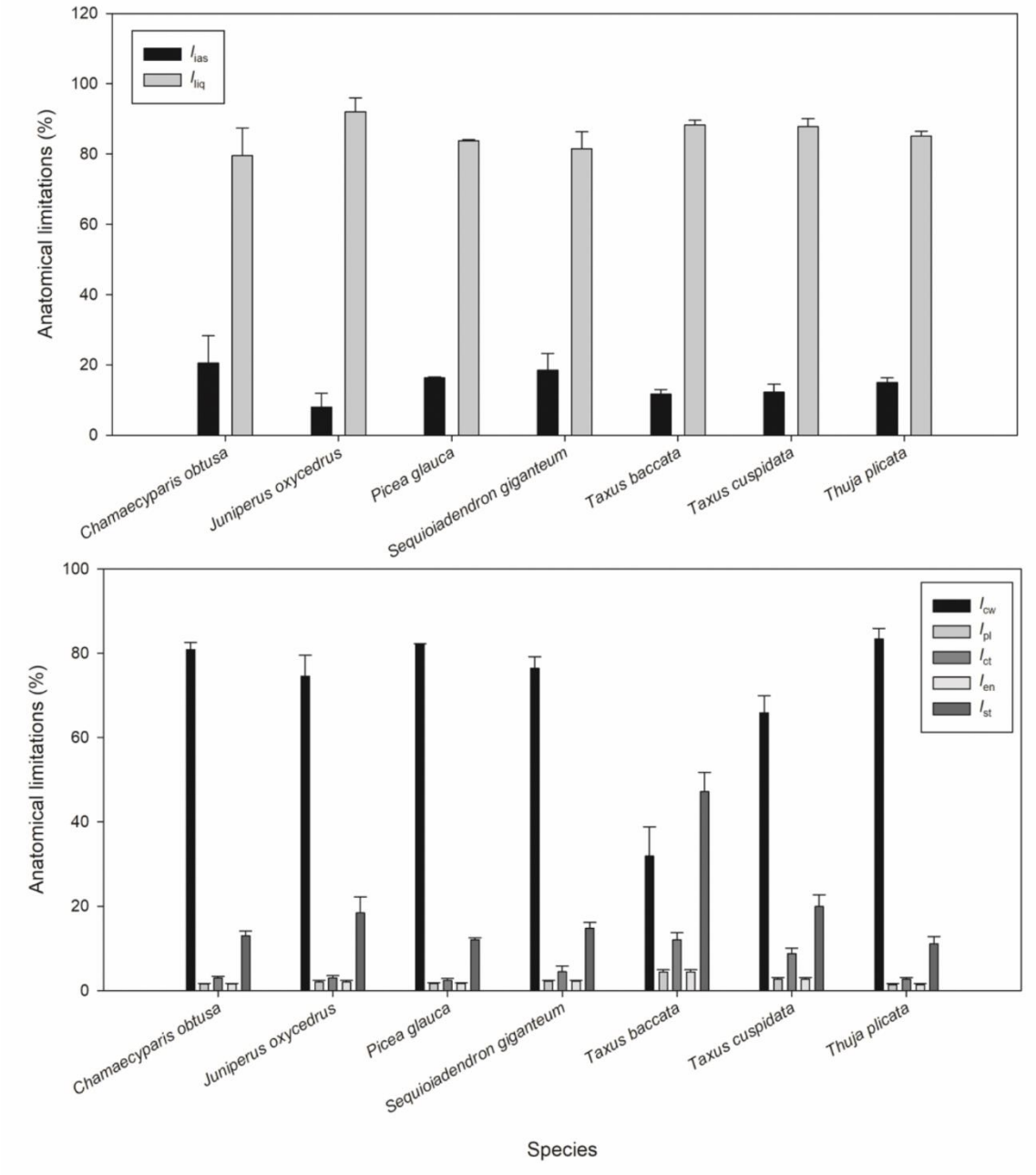
120
100
80
60
40
20
0
Anatomical limitations (%)
l_{ias}
l_{liq}
Chamaecyparis obtusa
Juniperus oxycedrus
Picea glauca
Sequioiadendron giganteum
Taxus baccata
Taxus cuspidata
Thuja plicata
100
80
60
40
20
0
Anatomical limitations (%)
l_{cw}
l_{pl}
l_{ct}
l_{en}
l_{st}
Chamaecyparis obtusa
Juniperus oxycedrus
Picea glauca
Sequioiadendron giganteum
Taxus baccata
Taxus cuspidata
Thuja plicata
Species

Figure 4

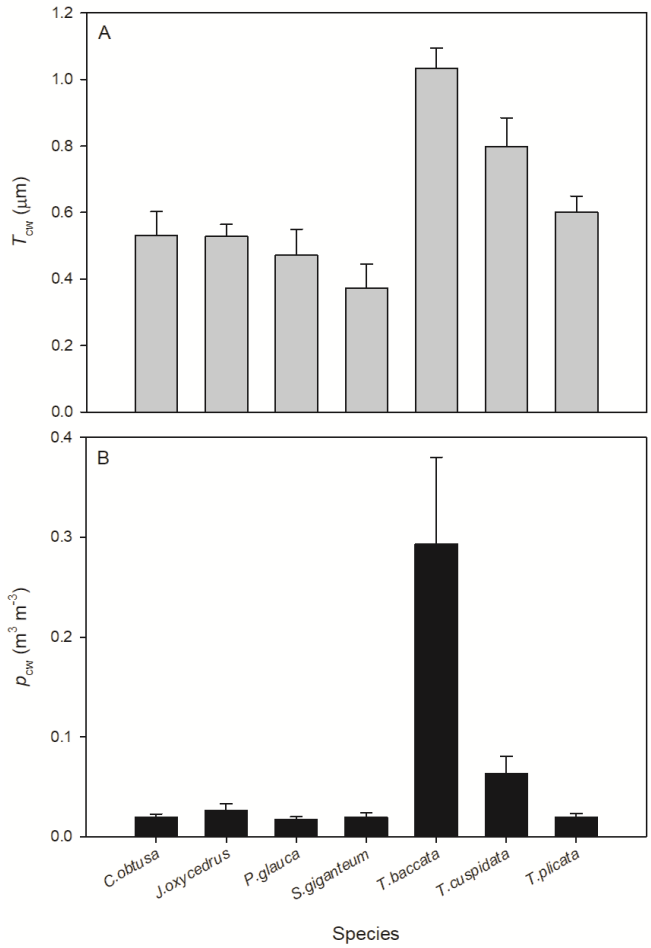
A
B
T_{cw} (µm)
p_{cw} (m^3 m^{-3})
1.2
1.0
0.8
0.6
0.4
0.2
0.0
0.4
0.3
0.2
0.1
0.0
C.obtusa
J.oxycedrus
P.glauca
S.giganteum
T.baccata
T.cuspidata
T.plicata
Species

Figure 5

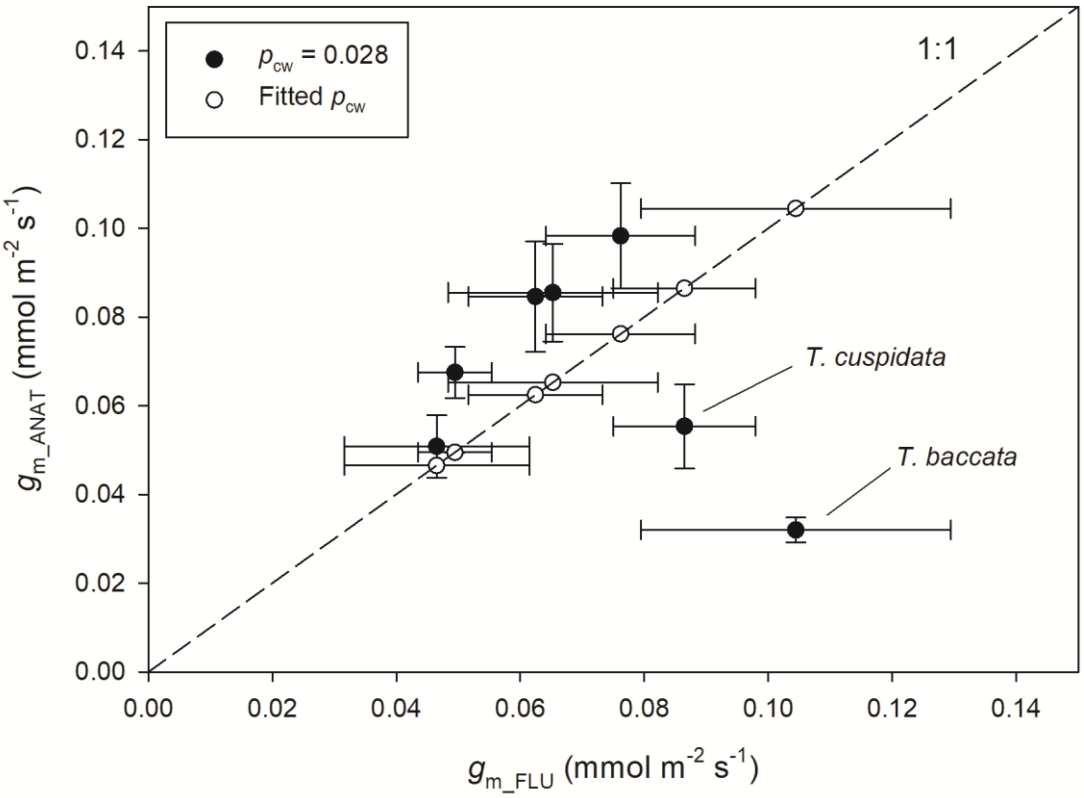
p_{cw} = 0.028
Fitted p_{cw}
1:1
T. cuspidata
T. baccata
g_{m_ANAT} (mmol m^{-2} s^{-1})
g_{m_FLU} (mmol m^{-2} s^{-1})
0.00
0.02
0.04
0.06
0.08
0.10
0.12
0.14

Figure 6

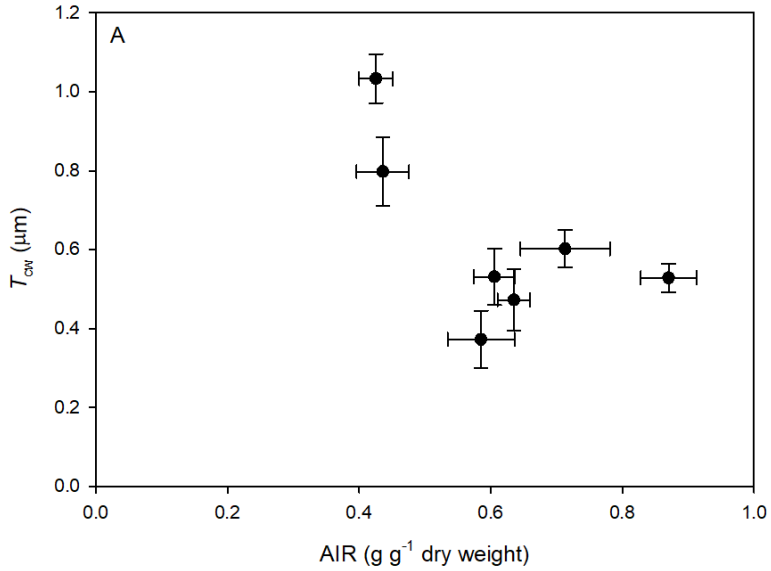
A
T_{CW} (µm)
AIR (g g^{-1} dry weight)

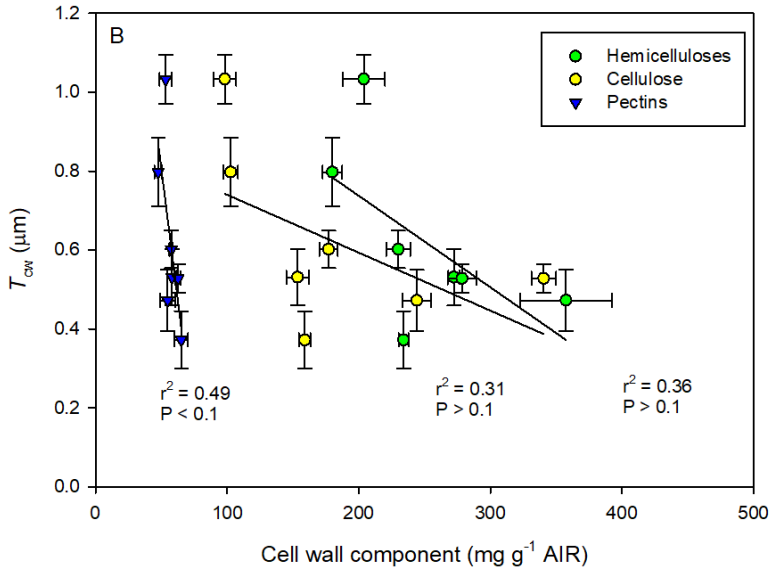
B
Hemicelluloses
Cellulose
Pectins
r^2 = 0.49
P < 0.1
r^2 = 0.31
P > 0.1
r^2 = 0.36
P > 0.1
T_{CW} (µm)
Cell wall component (mg g^{-1} AIR)

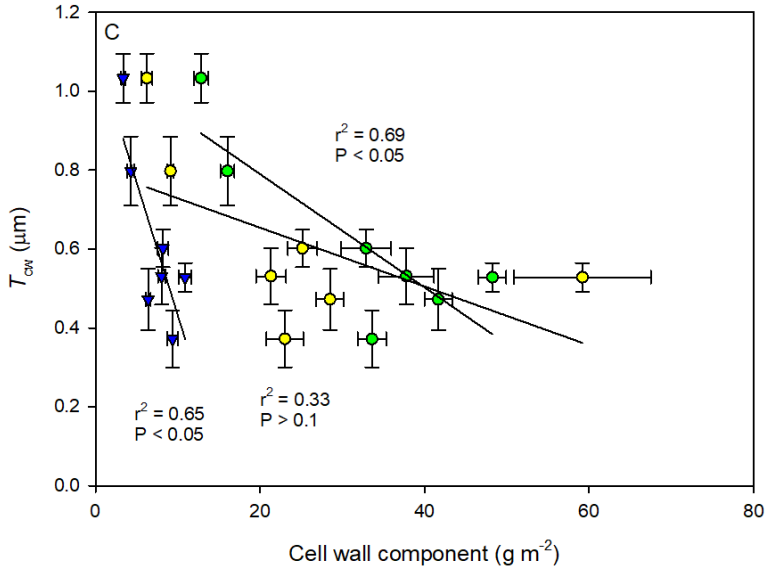
C
r^2 = 0.69
P < 0.05
r^2 = 0.65
P < 0.05
r^2 = 0.33
P > 0.1
T_{CW} (µm)
Cell wall component (g m^{-2})

Figure 7

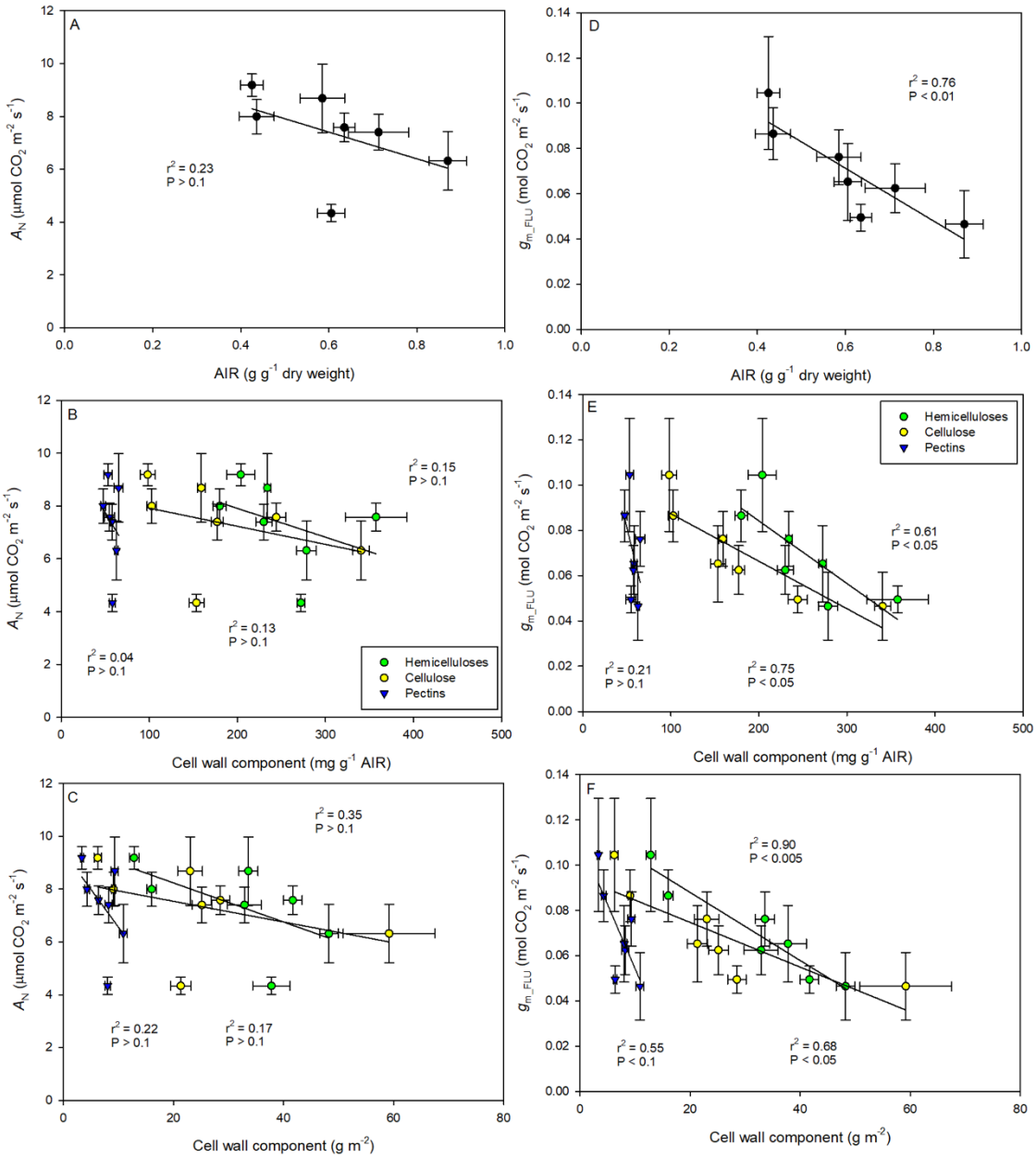
A
r^2 = 0.23
P > 0.1
A_N (µmol CO_2 m^{-2} s^{-1})
AIR (g g^{-1} dry weight)
D
r^2 = 0.76
P < 0.01
g_{m_FLU} (mol CO_2 m^{-2} s^{-1})
AIR (g g^{-1} dry weight)
B
r^2 = 0.15
P > 0.1
r^2 = 0.13
P > 0.1
r^2 = 0.04
P > 0.1
Hemicelluloses
Cellulose
Pectins
A_N (µmol CO_2 m^{-2} s^{-1})
Cell wall component (mg g^{-1} AIR)
E
Hemicelluloses
Cellulose
Pectins
r^2 = 0.61
P < 0.05
r^2 = 0.21
P > 0.1
r^2 = 0.75
P < 0.05
g_{m_FLU} (mol CO_2 m^{-2} s^{-1})
Cell wall component (mg g^{-1} AIR)
C
r^2 = 0.35
P > 0.1
r^2 = 0.22
P > 0.1
r^2 = 0.17
P > 0.1
A_N (µmol CO_2 m^{-2} s^{-1})
Cell wall component (g m^{-2})
F
r^2 = 0.90
P < 0.005
r^2 = 0.55
P < 0.1
r^2 = 0.68
P < 0.05
g_{m_FLU} (mol CO_2 m^{-2} s^{-1})
Cell wall component (g m^{-2})

Figure 8

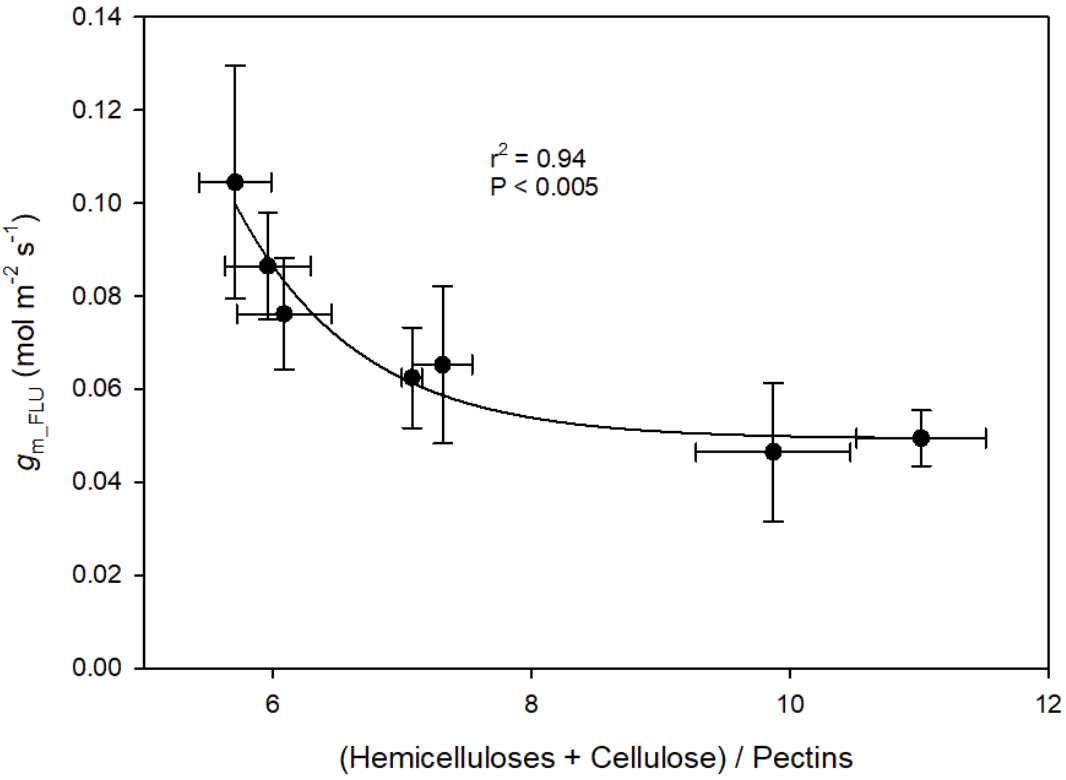
0.14
0.12
0.10
0.08
0.06
0.04
0.02
0.00
g_{m_FLU} (mol m^{-2} s^{-1})
r^2 = 0.94
P < 0.005
6
8
10
12
(Hemicelluloses + Cellulose) / Pectins

Figure 9

Supporting information

Supplemental Table 1. Photosynthetic characteristics for the gymnosperm species. Average values ± SE (n = 3-7) are shown for net assimilation (A_N), stomatal conductance to CO_2 (g_s), mesophyll conductance calculated with the variable J method (g_{m_flu}), sub-stomatal CO_2 concentration (C_i), chloroplastic CO_2 concentration (C_c) and dark respiration rate (R_d).

Species	A_N (µmol m^{-2} s^{-1})	g_s (mol m^{-2} s^{-1})	g_{m_flu} (mol m^{-2} s^{-1})	C_i (µmol mol^{-1} air)	C_c (µmol mol^{-1} air)	R_d (µmol m^{-2} s^{-1})
Chamaecyparis obtusa	4.3 ± 0.3	0.033 ± 0.004	0.065 ± 0.017	211 ± 27	115 ± 12	0.8 ± 0.1
Juniperus oxycedrus	6.3 ± 1.1	0.059 ± 0.013	0.047 ± 0.015	272 ± 16	111 ± 19	1.3 ± 0.3
Picea glauca	7.6 ± 0.5	0.056 ± 0.006	0.049 ± 0.006	245 ± 13	86 ± 3	1.6 ± 0.3
Sequoiadendron giganteum	8.7 ± 1.3	0.095 ± 0.013	0.076 ± 0.012	292 ± 6	169 ± 27	1.6 ± 0.3
Taxus baccata	9.2 ± 0.4	0.062 ± 0.007	0.104 ± 0.025	231 ± 20	125 ± 13	0.7 ± 0.1
Taxus cuspidata	8.0 ± 0.6	0.056 ± 0.006	0.086 ± 0.011	236 ± 9	137 ± 9	0.9 ± 0.0
Thuja plicata	7.4 ± 0.7	0.055 ± 0.005	0.062 ± 0.011	247 ± 8	110 ± 7	1.8 ± 0.2

Supplemental Table 2. Morphological and structural anatomic characteristics for the gymnosperm species. Average value ± SE (n = 3-7) are shown for dried leaf mass per unit area (LMA), leaf density (D_{leaf}), leaf thickness (T_{leaf}), mesophyll thickness (T_{mes}), fraction of the mesophyll occupied by intercellular air spaces (f_{ias}), mesophyll surface area exposed to intercellular air spaces per projected leaf area (S_m/S), chloroplast surface area exposed to intercellular air spaces per projected leaf area (S_c/S), and the ratio S_c/S_m.

Species	LMA (g m^{-2})	D_{leaf} (g cm^{-3})	T_{leaf} (µm)	T_{mes} (µm)	f_{ias} (%)	S_m/S (m^2 m^{-2})	S_c/S (m^2 m^{-2})	S_c/S_m
Chamaecyparis obtusa	228 ± 11	0.32	716 ± 47	578 ± 100	23.1 ± 4.2	45.8 ± 4.8	31.5 ± 1.8	0.70 ± 0.04
Juniperus oxycedrus	197 ± 5	0.46	425 ± 34	320 ± 53	27.5 ± 8.0	24.5 ± 5.6	16.1 ± 3.7	0.66 ± 0.00
Picea glauca	184 ± 6	0.32	567 ± 58	528 ± 63	17.2 ± 1.9	32.8 ± 3.6	21.6 ± 2.4	0.66 ± 0.01
Sequoiadendron giganteum	245 ± 28	0.44	554 ± 36	486 ± 45	24.1 ± 5.9	41.2 ± 2.6	26.0 ± 2.1	0.63 ± 0.01
Taxus baccata	148 ± 9	0.32	469 ± 52	434 ± 50	41.2 ± 2.9	22.9 ± 2.0	15.9 ± 1.7	0.69 ± 0.01
Taxus cuspidata	207 ± 3	0.32	647 ± 26	472 ± 75	36.0 ± 1.6	35.3 ± 2.4	22.1 ± 2.9	0.62 ± 0.04
Thuja plicata	201 ± 4	0.26	767 ± 72	685 ± 75	30.7 ± 1.8	48.5 ± 9.3	34.0 ± 6.5	0.70 ± 0.03

Supplemental Table 3. Ultrastructural anatomic characteristics and modelled mesophyll conductance for the gymnosperm species. Average value ± SE (n = 3-7) are shown for chloroplast thickness (T_{chl}), chloroplast length (L_{chl}), mesophyll cell wall thickness (T_{cw}), cytoplasm thickness (T_{cyt}).

Species	T_{chl} (µm)	L_{chl} (µm)	T_{cw} (µm)	T_{cyt} (µm)
Chamaecyparis obtusa	2.67 ± 0.03	4.12 ± 0.23	0.531 ± 0.072	0.306 ± 0.019
Juniperus oxycedrus	3.00 ± 0.27	4.38 ± 0.45	0.528 ± 0.036	0.248 ± 0.020
Picea glauca	2.44 ± 0.30	4.30 ± 0.25	0.472 ± 0.078	0.251 ± 0.059
Sequoiadendron giganteum	2.21 ± 0.05	3.35 ± 0.12	0.372 ± 0.072	0.339 ± 0.082
Taxus baccata	3.47 ± 0.27	5.72 ± 0.37	1.033 ± 0.062	0.443 ± 0.055
Taxus cuspidata	2.43 ± 0.27	3.90 ± 0.29	0.798 ± 0.087	0.526 ± 0.034
Thuja plicata	2.53 ± 0.12	5.17 ± 0.24	0.602 ± 0.048	0.311 ± 0.016

Supplemental Table 4. Mass-based leaf cell wall fraction considered as alcohol insoluble residues (AIR), and mass-based hemicellulose, cellulose and pectin fractions of AIR. Average value ± SE (*n* = 4) are shown for AIR and for each cell wall component.

Species	AIR (g g^{-1} dry weight)	Hemicelluloses (mg g^{-1} AIR)	Cellulose (mg g^{-1} AIR)	Pectins (mg g^{-1} AIR)
Chamaecyparis obtusa	0.606 ± 0.031	272 ± 4	154 ± 9	58 ± 3
Juniperus oxycedrus	0.870 ± 0.042	278 ± 11	341 ± 9	63 ± 2
Picea glauca	0.635 ± 0.024	357 ± 35	244 ± 11	55 ± 6
Sequoiadendron giganteum	0.585 ± 0.051	234 ± 4	159 ± 4	65 ± 5
Taxus baccata	0.425 ± 0.026	204 ± 16	98 ± 9	53 ± 5
Taxus cuspidata	0.436 ± 0.040	180 ± 7	103 ± 5	48 ± 3
Thuja plicata	0.713 ± 0.068	230 ± 9	177 ± 7	58 ± 1

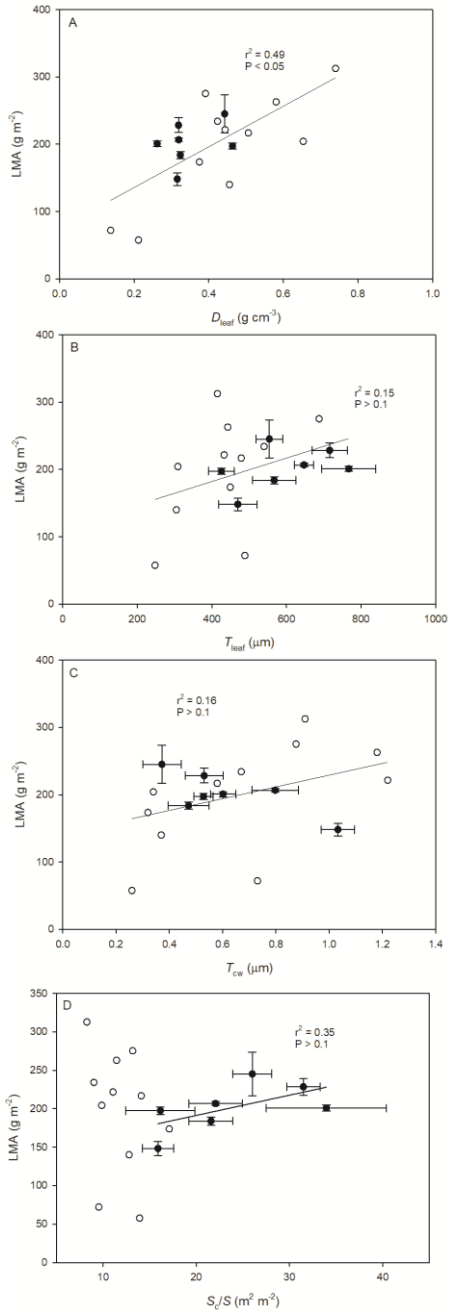

Supplemental Figure 1. Leaf dry mass per area (LMA) in relation to (A) leaf density (D_{leaf}), (B) leaf thickness (T_{leaf}), (C) mesophyll cell wall thickness (T_{cw}), and (D) chloroplast surface area exposed to intercellular airspaces (S_c/S). Species from this study are marked as closed circles, while gymnosperm species from Veromann-Jürgenson et al. (2017) are marked as open circles. Closed circles with error bars display average ± SE values for the seven species considered in the present study. Data were fitted by linear regression

(significance at P<0.05) considering all species except in (D), where only species from this study were considered in the regression.

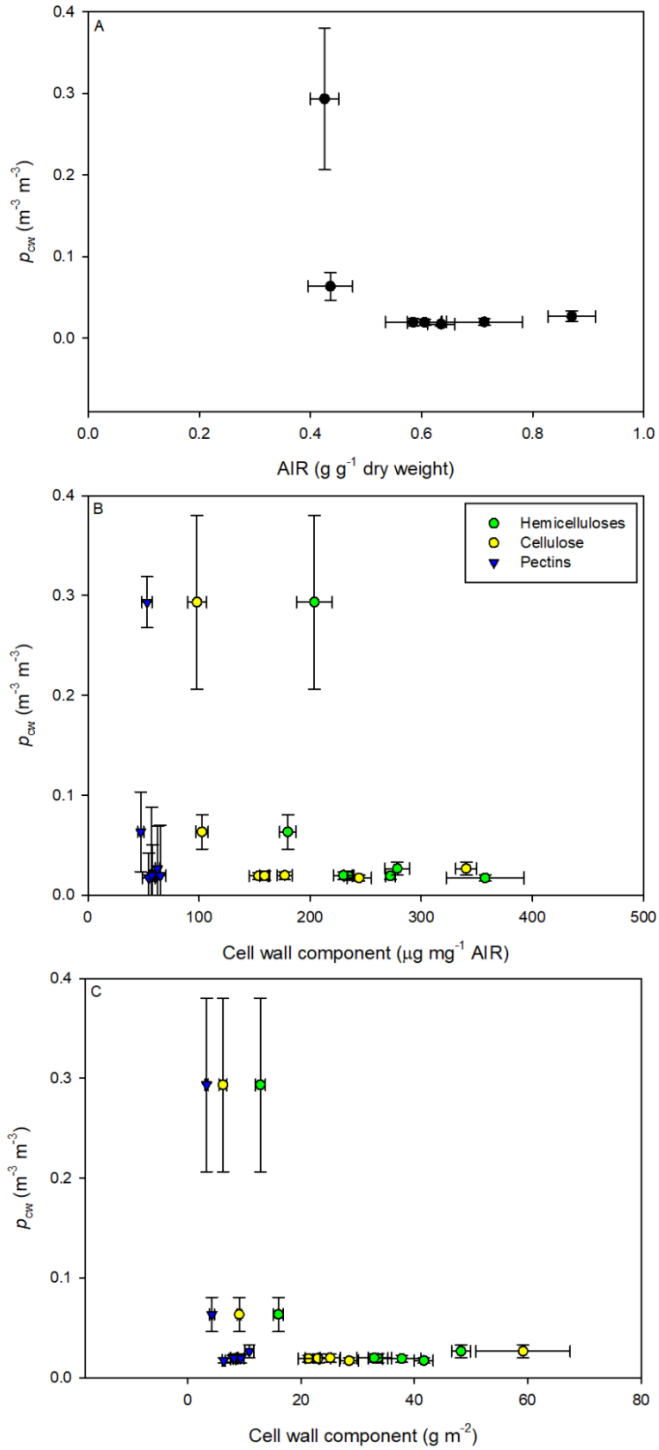

Figure S2. The relationship between fitted cell wall porosity (p_{CW}) and (A) percentage of cell walls prepared as alcohol insoluble residues per leaf weight (AIR), (B) main cell wall components weight per cell wall weight (hemicelluloses,

celluloses and pectins), and (C) main cell wall components weight per leaf area. Data are means ± SE of four to six replicate measurements for each species.

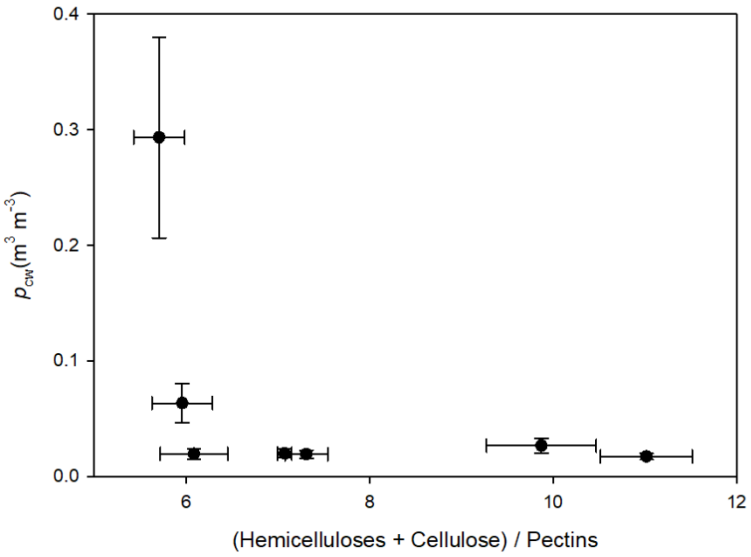

Figure S3. The relationship between fitted cell wall porosity (p_{cw}) and the ratio (hemicelluloses+cellulose)/pectins. Data are means ± SE of four to six replicate measurements for each species.

General discussion

The results of this Thesis have been structured in five chapters which include six publications. As the different chapters provide a profuse discussion of the relevance of each finding addressing the different general and specific objectives of the present Thesis, this chapter aims to provide a brief integrated view about the contributions of the present work to the available scientific knowledge on the anatomical bases that modulate mesophyll conductance to CO_2 at three terms: short (i.e. seconds to minutes), medium (i.e. acclimation/ acclimatization), and long (i.e. adaptation) (Fig. 1).

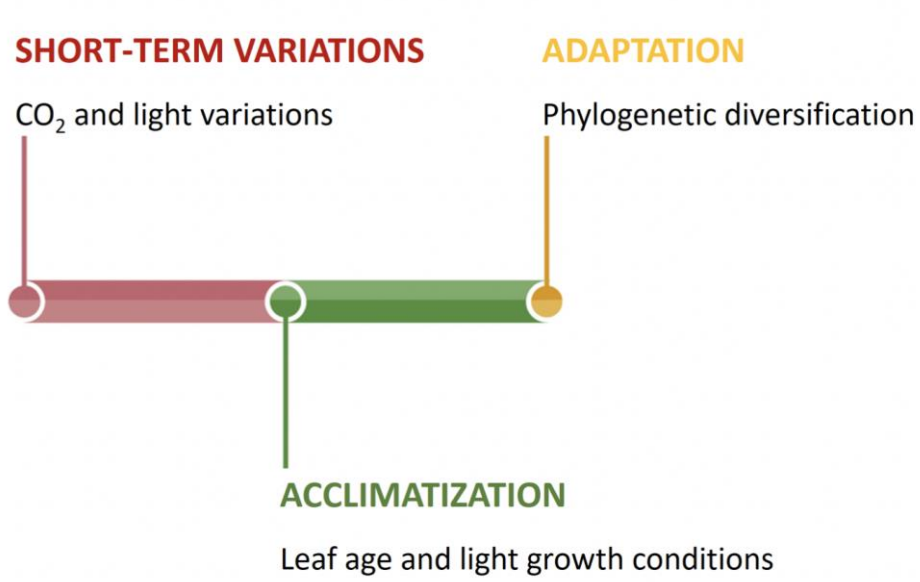

Figure 1. Schematic diagram of the three terms in which the anatomical adjustments determining mesophyll conductance to CO_2 have been investigated in this Thesis.

First, the predictability of mesophyll conductance by anatomical models as well as the new knowledge and questions derived from the present Thesis are presented. Second, the implication of the mesophyll anatomical traits in the regulation of mesophyll conductance to CO_2 (g_m) with changing environmental conditions from the short-term to acclimatization is discussed. Finally, the involvement of the main anatomical traits determining g_m as a possible result of evolutionary adaptation to the terrestrial environment is evaluated.

General overview: agreement between leaf anatomy and g_m and new evidence on key anatomical determinants of g_m

Globally, the results from the present Thesis significantly strengthen the current knowledge on the role of mesophyll anatomical traits in determining mesophyll conductance. Although the anatomical mechanistic bases seem not involved in the regulation of g_m in the immediate term (Chapter 1), the anatomical adjustments that occur as a result of leaf's acclimation or adaptation to specific environmental conditions, habitats or life forms strongly determine leaf's maximum g_m (Chapters 2-5). The close relationship between leaf anatomy and g_m is very important for several reasons. On the one hand, it allows to totally independently validate the estimates of g_m obtained with the most used methods, all of them based at least on the same gas exchange technique (Pons et al. 2009, Flexas et al. 2018), and being them all currently strongly questioned by their numerous assumptions, methodological weaknesses and simplifications of their underlying models (Tholen and Zhu 2011, Loriaux et al. 2013, Gu and Sun 2014, but see Mizokami et al. 2016 for a revision). On the other hand, the predictability of g_m from cellular traits allows adding g_m to models of photosynthesis (Niinemets et al. 2009, Flexas et al. 2018) and reveals the large potential of redesigning leaf anatomy to improve plants' photosynthetic capacity (Tholen et al. 2012, Ort et al. 2015, Lehmeier et al. 2017, Ren et al. 2019).

Due to the lack of common methods allowing to directly determine the chloroplastic CO_2 concentration (C_c), it is rather difficult to estimate g_m (Pons et al. 2009, Mizokami et al. 2016, Flexas et al. 2018). Thus, in order to override potential misestimations produced by the weaknesses of the different methods, the precise estimate of g_m requires the use of two or more methods. Among them, the strength of the analytical models of g_m based on anatomical traits lies in that they are the only ones that can provide completely independent estimates of the others, which are all based totally or partially on gas exchange measurements.

Among the available analytical models, the 1D model of Niinemets and Reichstein (2003), later improved by Tosens et al. (2012b) and Tomás et al.

(2013), is the most widely used and has been validated in more than 160 species including all major land plant groups (except hornworts). Modelled g_m values obtained with the 1D model, which uses as main inputs several anatomical features estimated from light microscopy and transmission electron microscopy images, tightly correlated with measured g_m values with the variable *J* method of Harley et al. (1992), and the obtained correlation is close to the 1:1 line, (r^2 = 0.78, $P < 0.0001$; Fig. 2).

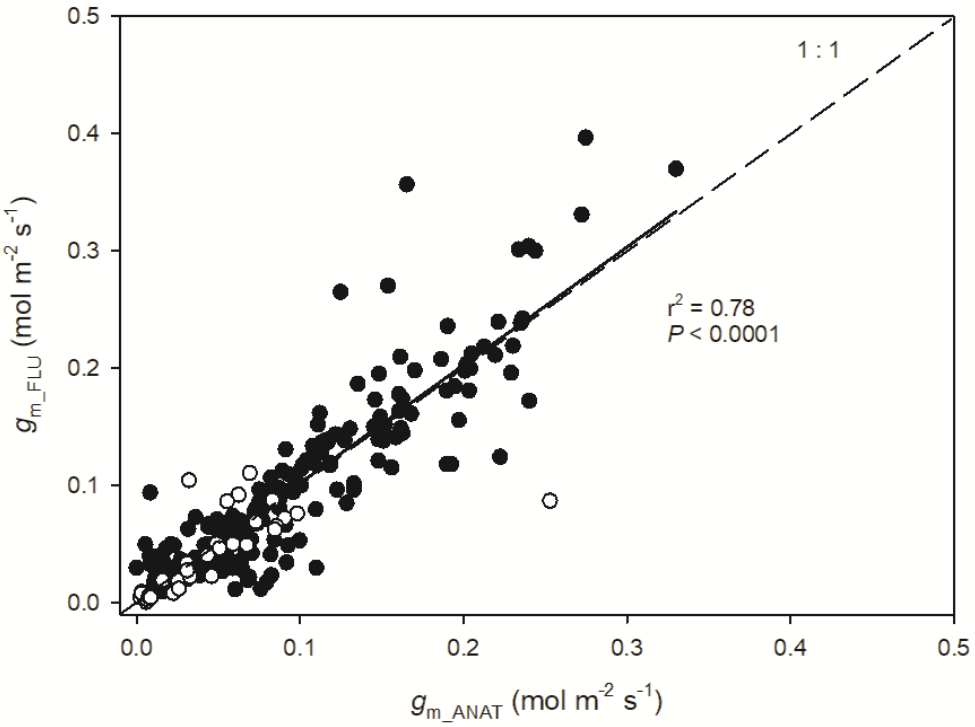

Figure 2. Agreement between chlorophyll fluorescence and anatomical methods to estimate mesophyll conductance. Correlation between mesophyll conductance estimated from chlorophyll fluorescence (g_{m_FLU}) following Harley et al. (1992) and mesophyll conductance modelled from anatomical traits (g_{m_ANAT}) following Niinemets & Reichstein (2003) measured in the same leaves grown under optimal conditions. Closed circle are average data from the following studies: Peguero-Pina et al. (2012; 2016; 2017a,b), Tosens et al. (2012a,b; 2016), Tomás et al. (2013, 2014), Lu et al. (2016), Fini et al. (2016), Veromann-Jürgenson et al. (2017), Xiong et al. (2017), and Han et al. (2018), while open circles are average data from Chapters 1 (*Nicotiana tabacum*), 2 (*Arabidopsis thaliana*), 3 (bryophytes, lycophytes and pteridophytes) and 4 and 5 (gymnosperms).

Despite the tight agreement between both g_m independent estimation methods, several weaknesses still beset the 1D analytical method. On average, a 42% discrepancy was found between modelled and estimated g_m, showing that the complex nature of resistance to CO_2 diffusion in the mesophyll cannot be

totally assessed from 2D cross-sections, and that the different biophysical diffusion properties that are assumed as constants or obviated by the model can have an important role in setting maximum g_m in some species. Recent studies comparing the reliability and accuracy of 1D and 2D models from 3D approaches have demonstrated a bias in the estimation of 3D traits such as f_{ias} and S_m/S *and* S_c/S from cross-sections and ascertained that 2D images cannot embrace the complex cell geometries (Tholen and Zhu 2012, Théroux-Rancourt et al. 2017, Earles et al. 2018, 2019). Apart from methodological limitations, suggested causes of the discrepancy include the simplification of the role of the biochemical determinants of g_m, the not-so-straightforward assumption that there is no recycling of (photo)respired mitochondrial CO_2 (Tholen and Zhu 2012, Xiao and Zhu 2017, Yin and Struik 2017, Ubierna et al. 2019) as well as the still important knowledge gaps on the anatomical mechanistic bases of g_m regulation: mesophyll cell wall effective porosity, membrane permeability, diffusion viscosity and effective path length of CO_2 diffusion (Xiao and Zhu 2017, Tosens and Laanisto 2018).

Among the currently poorly understood fundamental structural factors affecting g_m, this Thesis has provided particularly novel suggestions on the impact of cell wall effective porosity to CO_2 diffusion on g_m (Chapter 5). Cell wall effective porosity, determined by the relation between cell wall tortuosity and porosity, has never been experimentally determined in mesophyll cells of land plants. First thought to be large enough to do not constrain A_N (Nobel 1991), cell wall effective porosity was later proposed as a key determinant of g_m based on the noisy relationship between g_m and key anatomical traits such as S_c/S (Terashima et al. 2006) and on a simple model of the CO_2 pathway through pores from onion cell wall images (Evans et al. 2009), and it was suggested to be linearly variable with T_{cw} (Terashima et al. 2006, Tosens and Laanisto 2018). However, recent reports of leaf anatomy and g_m in species with thick cell walls (Chapter 3, Tosens et al. 2016, Veromann-Jürgenson et al. 2017) described an exponential decay-, instead of a negative lineal-relationship between g_m and T_{cw}, suggesting that these species compensated the negative effects on CO_2 diffusion of possessing extremely elevated T_{cw} with the regulation of their cell wall effective porosity. The results from Chapter 5 in seven conifer species support this

hypothesis, providing the first direct correlative evidence of the effect of cell wall composition. Specifically, the results showed that both cell wall relative fraction in cellulose and hemicellulose decreased but pectin relative fraction remained constant with increasing T_{cw} in conifers, so g_m increased as the ratio (hemicelluloses+celluloses)/pectins decreased. This evidence confirms, in agreement with previous recent studies reporting the effect of alteration of specific cell wall components on plant growth and CO_2 diffusion resistance (Weraduwage et al. 2016, 2018, Ellsworth et al. 2018) and correlation between primary metabolites on g_m from a meta-analysis approach (Gago et al. 2016), the key role of cell wall composition on g_m.

In summary, although 2-D and, especially, 3-D models should better represent mesophyll conductance and its properties (Earles et al. 2019), the 1-D models are the only currently readily available for practical purposes. The use of two 1-D models (anatomical vs gas exchange and chlorophyll fluorescence) in the present Thesis has confirmed the agreement among them, regardless of the fact that they are completely independent each other both in their assumptions and in the input parameters used to parameterize them. Therefore, the estimated values may reflect to a large extent the magnitude of this physical variable, and can then be used to compare the effects of short-to-mid-term variations in environmental conditions as well as differences among species and phylogenetic groups, which is the aim of the next two sections.

New insights into the anatomical mechanisms regulating the response of mesophyll conductance to abiotic environmental variables

The two most used methods to estimate g_m, i.e. the variable *J* method based on the combination of gas exchange and chlorophyll fluorescence (Harley et al. 1992) and the isotope method based on the ^{13}C discrimination during photosynthesis (Evans 1989, Lloyd et al. 1992), have revealed g_m to be finite and variable, responding to abiotic environmental changes from the very short (i.e. from seconds to minutes) to the long terms (Flexas et al. 2018). g_m is determined

by a series of physical barriers and biochemical components that impose a resistance to the diffusion of CO_2 molecules from the substomatal cavity to the site of carboxylation inside the chloroplast stroma (Evans et al. 2009, Terashima et al. 2011). However, the mechanistic basics of g_m and its regulation are not fully understood, complicating the predictability of g_m and the possibility of considering it in models estimating large-scale carbon gain and global change (Niinemets et al. 2009). Thus, an objective of the present Thesis was to gain further insights on the determinants -focusing particularly on the structural ones- of g_m response to abiotic environmental variables.

The dynamic response of g_m to rapid environmental variation is undoubtedly one of the current controversies about this photosynthetic trait. First, because reports of fast g_m regulation are contradictory. While some studies have reported rapid variations (i.e. within minutes) of g_m in response to changes in light (Hassiotou et al. 2009, Douthe et al. 2011, 2012, Xiong et al. 2015), substomatal CO_2 concentration (C_i; Flexas et al. 2007b, Hassiotou et al. 2009, Yin et al. 2009, Douthe et al. 2011, 2012, Xiong et al. 2015, Mizokami et al. 2019), or temperature (Yamori et al. 2006, von Caemmerer and Evans 2015, Shrestha et al. 2019), some other studies have reported g_m to be unaffected by light and/or C_i fast variations (Tazoe et al. 2009). Second, because the mechanistic basis that could allow explaining these variations remain elusive. Most of the anatomical determinants are assumed to be invariable in the short term (Evans et al. 2009, Terashima et al. 2011) and the main determinant of this variation have been hypothesized to be linked to chloroplast movements and redistribution along the cell wall, varying the chloroplast surface area exposed to intercellular airspace per leaf area (S_c/S, Oguchi et al. 2005, Tholen et al. 2008), the main anatomical determinant —together with cell wall thickness, T_{cw}— of maximum g_m (Evans et al. 2009, Tomás et al. 2013, Tosens et al. 2016). However, no direct measurements of the potential changes in the structural traits during a light or CO_2 photosynthetic response curve have been reported previous to this Thesis. Moreover, the implication of biochemical determinants, although likely, has not been tested (Cochard et al. 2007, Maurel et al. 2008, Terashima et al. 2011). And third, several ‘mathematical artefacts’ and/or ‘over-simplifications’ of the models to estimate g_m have been targeted (Pons et al. 2009, Tholen and Zhu 2011, Gu

and Sun 2014, Théroux-Rancourt et al. 2017). Thus, the controversy is such that the current scientific debate discusses whether these observed g_m variations are real (i.e. are regulated by anatomical and/or biochemical determinants), apparent (i.e. are the result from averaging fluxes and concentrations across the mesophyll) or even artifactual (i.e. are the result of a biased estimate of parameters and/or mathematical artefacts). In the present Thesis the potential involvement of anatomical mesophyll traits in the short-term regulation of g_m due to CO_2 and light rapid variations was experimentally tested in tobacco (Chapter 1). Tobacco leaves, even after being subjected to different light and CO_2 treatments in the short-term to produce rapid variations in g_m, did not experienced significant changes in most anatomical parameters. The only observable change was in the chloroplast shape, perhaps due to a chloroplast avoidance effect (Trojan and Gabrys 1996, Kasahara et al. 2002), which was insufficient to significantly modify S_c/S. This led to a discrepancy between the g_m values obtained by fluorescence (Harley et al. 1992) and those obtained using two analytical models based on anatomical parameters (Tosens et al. 2012a, Xiao and Zhu 2017), discarding the influence of main leaf anatomical determinants of CO_2 diffusion on fast changes of g_m. These findings have been recently extended to short-term g_m variations in response temperature in different species and genotypes (Shrestha et al. 2019). Shrestha et al. (2019) also did not find differences in S_c/S in response to temperature changes, dismantling the hypothesis by Flexas and Díaz-Espejo (2015) of a progressive decrease of S_c/S due to chloroplast movement or cell shrinkage at elevated temperature that could explain g_m variations. Moreover, theoretical modelling discarded the potential role of aquaporins and (photo)respiration as the unique sources for short-term g_m response in response to light and CO_2 variations. Thus, being the implication of anatomy discarded, the observed short-term g_m variation might be apparent and should also reflect model weaknesses.

The aforementioned uncertainties could also bias the interpretation of g_m responses to longer exposures to one or several combined abiotic environmental variables. g_m acclimation has been studied in response to environmental variables such as temperature (Yamori et al. 2006, Bunce 2008, Silim et al. 2010, Fares et al. 2011, Crous et al. 2013, Lewis et al. 2015, Xue et al. 2016, Cai et al.

2018, Sáez et al. 2018), light intensity (Lloyd et al. 1992, Syversten et al. 1995, Piel et al. 2002, Hanba et al. 2002, Singsaas et al. 2004, Laisk et al. 2005, Niinemets et al. 2006, Warren et al. 2007, Montpied et al. 2009, Cano et al. 2011, Tosens et al. 2012a, Cano et al. 2013), drought stress (Grassi and Magnani 2005, Flexas et al. 2006, 2009, Díaz-Espejo et al. 2007, Galmés et al. 2007, Miyazawa et al. 2008, Bunce 2009, Gallé et al. 2009, Warren et al. 2011, Aranda et al. 2012, Ferrio et al. 2012, Tosens et al. 2012a, Brilli et al. 2013, Cano et al. 2013, 2014, Perez-Martin et al. 2014, Théroux-Rancourt et al. 2014, 2015, Mizokami et al. 2015, Silva et al. 2015, Zhou et al. 2015, Olsovska et al. 2016, Shrestha et al. 2018, Zait et al. 2018), CO_2 concentration (Singsaas et al. 2004, Bernacchi et al. 2005, Possell and Hewitt 2009, Velikova et al. 2009, Zhu et al. 2012, Crous et al. 2013, Singh et al. 2013, Chen et al. 2014, Aranjuelo et al. 2015, Kitao et al. 2015, Lewis et al. 2015, DaMatta et al. 2016, Singh and Reddy 2016, 2018, Xu et al. 2016, Ruiz-Vera et al. 2017, Cai et al. 2018, Mizokami et al. 2018, Zait et al. 2018), ozone concentration (Eichelmann et al. 2004, Velikova et al. 2005, Flowers et al. 2007, Warren et al. 2007, Watanabe et al. 2018, Xu et al. 2019), salinity (Sade et al. 2014, Zait et al. 2018) or nutrient availability (Singh et al. 2013, Kitao et al. 2015, Xiong et al. 2015, Barbour and Kaiser 2016, Singh and Reddy 2016, 2018, Ruiz-Vera et al. 2017, Shrestha et al. 2018). The studies characterizing the acclimation of g_m to these environmental variables have been performed almost in their totality in standard 'youngest fully-expanded' leaves.

Despite the relatively extensive number of species in which the g_m acclimation to different abiotic environmental variables has been described, the relationship between leaf anatomy and g_m resulting from these acclimations has been evaluated in a much more reduced number of species variables. In the case of temperature, the only three published studies were dedicated to species that are not sufficiently representative of the C_3 plants and do not allow to explain the high diversity of g_m responses to the acclimation to this environmental variable reported for different species. Two of these studies were performed in the two Antarctic vascular species, first under field conditions and mild temperature acclimation treatments (i.e. + 2 ºC; Sáez et al. 2018a), and then under laboratory conditions and moderate acclimation treatments (i.e. + 12 ºC; Sáez et al. 2018b). Both studies demonstrated that the mesophyll anatomical traits helped to explain

the non-significant g_m response of *Deschampsia antarctica* and the g_m increase in *Colobanthus quitensis* —mainly mediated by adjustments of the chloroplast arrangement and S_m/S— in response to plant acclimation to warmer temperatures. And the other study is dedicated to the thermophilic tree *Ziziphus spina-christi* (Zait et al. 2018), where the reported hyperbolical g_m decrease with decreasing acclimation temperatures was partially explained by decreased LMA and T_{leaf} but increased f_{ias}.

Regarding to light acclimation, although most studies have been performed in tree species, most of the observed g_m variability relied on the species-specific leaf anatomical plasticity (Hanba et al. 2002, Oguchi et al. 2005, Tosens et al. 2012, Morales et al. 2014, Fini et al. 2016, Peguero-Pina et al. 2016, Ellsworth et al. 2018, Poorter et al. 2019), being higher in species adapted to grow in the open sky (Valladares et al. 2000, Portsmuth and Niinemets 2007, Chmura et al. 2017). In general terms, the main anatomical adjustments determining g_m response to acclimation to higher growth light conditions were an increase in T_{leaf}, the number of palisade layers, S_m/S and S_c/S. T_{cw}, despite its importance in determining g_m across species (Tosens et al. 2012, 2016, Tomás et al. 2013, Peguero-Pina et al. 2017), either increased, remained constant or decreased with light growth conditions depending on the species (Hanba et al. 2002, Tosens et al. 2012, Fini et al. 2016, Ellsworth et al. 2018), being its role in light acclimation not that clear.

In relation to drought stress acclimation, the type and importance of anatomical adjustments potentially explaining the lower g_m values related to acclimation to water stress seems to be dependent on the species and on the drought stress treatment (Galle et al. 2011). The general anatomical responses to this acclimation seem to be a reduction in chloroplast size and in f_{ias} and an increase in T_{cw} (Niinemets et al. 2009, Poorter et al. 2009, Li et al. 2012, Galmés et al. 2013). However, Tomás et al. (2014) could not explain by anatomical variability the g_m decrease reported in *Vitis vinifera* cultivars acclimated to water stress once leaves were already fully-expanded. In this sense, Miyazawa et al. (2008) suggested that drought-induced g_m reductions could be mainly associated to an aquaporin deactivation.

As for the acclimation of g_m to varying CO_2 concentration, there is little and non-conclusive information on the subjacent anatomical adjustments that would help to explain the reported general but species-specific decrease of g_m at higher [CO_2]. The major role for this g_m decrease might be partially related to T_{cw} and chloroplast size increases (Robertson and Leech 1995, Uprety et al. 2001, Oksanen et al. 2005, Teng et al. 2006, Zhu et al. 2012), meanwhile S_c/S has been reported to be unaffected or incremented with increased [CO_2] (Kitao et al. 2015, Mizokami et al. 2018).

Acclimation to high [O_3] reduced g_m in all studies species except *Fagus sylvatica*, where g_m remained unaffected (Eichelmann et al. 2004, Velikova et al. 2005, Flowers et al. 2007, Warren et al. 2007, Watanabe et al. 2018, Xu et al. 2019). Although there are still no direct reports on the anatomical adjustments explaining this decrease, from studies based on leaf anatomy only it may appear that increased [O_3] affects T_{cw} and chloroplast size and arrangement (Paoletti et al. 2009, Gao et al. 2016), all of them key anatomical traits in setting g_m.

With regard to leaf age, the changes in the leaf internal structural properties constrain g_m are different between the development and ageing processes (Niinemets et al. 2012). During leaf development, as cell walls tend to be thin, the major anatomical changes determining initial g_m increases are associated to be the increase in T_{leaf}, f_{ias}, S_m/S and S_c/S. Instead, during leaf ageing, g_m decreases with leaf ageing that happen after reaching the peak value have been mainly associated to changes in the cell wall properties. However, as well as in light acclimation studies, the scarce studies examining the relationship between anatomy and g_m during leaf development and ageing were mainly dedicated to tree species (Hanba et al. 2001, Miyazawa and Terashima 2001, Miyazawa et al. 2003, Marchi et al. 2008, Tosens et al. 2012, Niinemets et al. 2012), so that the changes in this relationship in leaves with especially short life-span (e.g. in the model species *Arabidopsis thaliana*), despite being expected to be fast, have not been analyzed in depth.

The results from the present Thesis provide further insight on the relationship between leaf anatomy and g_m in the acclimation of *Arabidopsis* plants to contrasting light intensities at two different leaf ages (Chapter 2). Across growth

light conditions, anatomy-based modelled values of g_m (following Tosens et al. 2012) closely resembled the estimates of g_m obtained from gas exchange and chlorophyll fluorescence measurements (following Harley et al. 1992), strongly suggesting an important causality between changes in the mesophyll anatomical properties and changes in g_m. Among the main morphoanatomical changes, LMA, the most integrative morphological trait integrating leaf structure complexity (Niinemets et al. 2009, Onoda et al. 2017), the number of palisade layers and both mesophyll and chloroplast surface area exposed to intercellular airspaces per leaf area (S_m/S and S_c/S) steeply increased with increasing growth light without showing signs of saturation at high light, as recently reviewed by Poorter et al. (2019). Instead, in this light-demanding species T_{cw} only increased from low- to moderate-light growth conditions, in agreement with previous observations. Regarding to leaf age, the data demonstrated that incipient anatomical changes preceding the age-related decline of photosynthesis compensated each other in order to keep the peak of g_m for a longer period. Specifically, ageing generally supposed a reduction in the intercellular airspace, cell wall and cytoplasm partial conductances to CO_2 diffusion, but total mesophyll resistance did not decrease due to the compensatory effect of an increased chloroplast stroma conductance, the main component limiting g_m in *Arabidopsis.*

Summarizing, the implication of the anatomical adjustments on the modulation of mesophyll conductance to CO_2 responses to abiotic environmental variations vary between the short-and mid-term. On the one hand, main mesophyll anatomical traits remain constant when leaves are exposed to short-term variations in light, CO_2 and temperature, not determining, therefore, the observed apparent g_m fast responses (i.e. from seconds to minutes) to these environmental stimuli. On the other hand, the data presented here demonstrate a major role of mesophyll anatomy in, at least partially, determining the g_m response to acclimation and leaf ontogeny. Nevertheless, in order to be able to generalize the existence of this relationship in terms of g_m acclimation, significant efforts are necessary to test the implication of leaf internal structure in the g_m response to mid-term (i.e. plant growth and development) temperature variations, among other environmental variables.

Anatomical parameters determining mesophyll conductance in the main groups of terrestrial plants

Another main objective of this Thesis focused on the mesophyll conductance to CO_2 diffusion in the groups of terrestrial land plants in which it had not been determined yet, in order to provide an in-depth global picture of the g_m variation across phylogeny and to reveal the main anatomical traits regulating it.

Net photosynthesis (A_N) presents an impressive 36-fold variation across C_3 vascular species (Wright et al. 2004, Onoda et al. 2017), becoming even one order of magnitude greater when considering the very small A_N of bryophytes (Hanson et al. 2014, Wang et al. 2017). Determining what determines this enormous range of variation is of great importance, and to do so it is necessary to investigate the different photosynthetic characteristics that limit A_N: stomatal conductance (g_s; when present), g_m and the photochemical/biochemical potential. However, physiological studies involving mesophyll conductance initially have been mainly focused on a few species of Spermatophytes (gymnosperms and angiosperms) due to their interest as crops or model plants. Over time, this number kept increasing to over the half hundred species when Flexas et al. (2012) first suggested the existence of some evolutionary or phylogenetic pattern in g_m, but any conclusion on an evolutionary trend towards g_m optimization along the land plant phylogeny was precluded by a gap in available g_m data for key land plant groups (Fig. 3A). At that time, the species in which g_m had been determined only included angiosperms, gymnosperms and a few liverworts, being unknown the range of g_m values for ferns, fern allies and mosses. This knowledge gaps have been largely fulfilled by the results obtained in Chapter 3. Specifically, g_m estimates are provided for one liverwort, which adds to Meyer et al. (2008) estimates, mosses -23 with the anatomical method (Tomás et al. 2013) and 9 with the chlorophyll fluorescence one (Harley et al. 1992)-, which adds to the only one previous estimate for this plant group (Hanson et al. 2014), 3 fern allies and 7 ferns, that are integrated together with the 3 ferns studied by Gago et al. (2013) in a wider study comprising 35 ferns and fern allies

(Tosens et al. 2016). In addition, new g_m data are provided for 7 gymnosperms (Chapters 4 and 5).

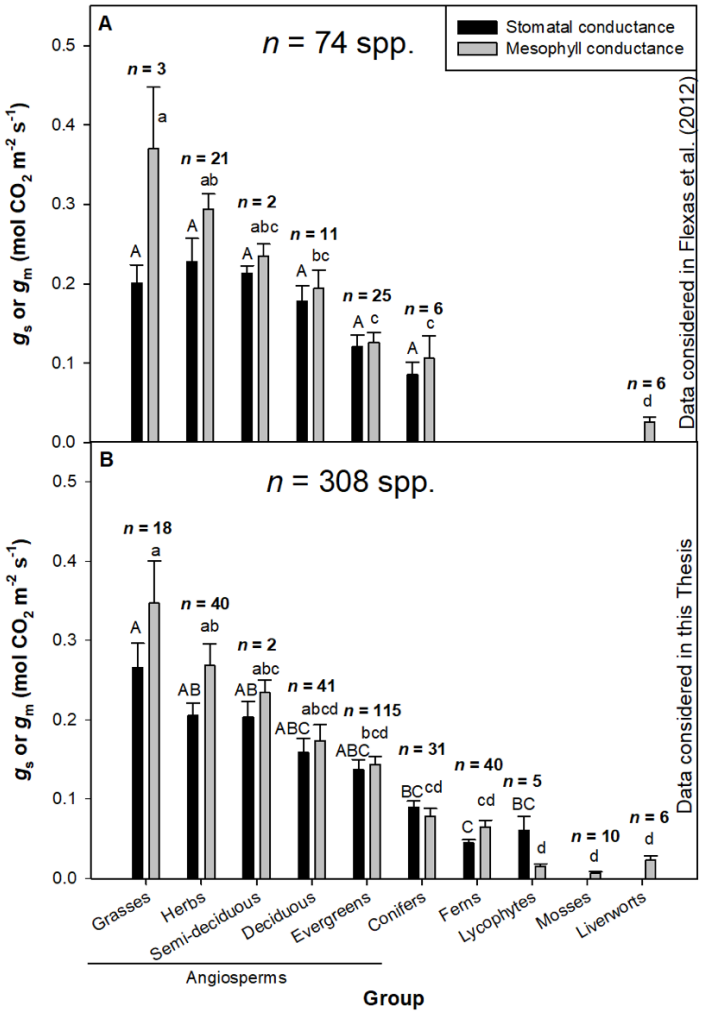

Figure 3. Phylogenetic trend towards higher mesophyll conductance. Average ± SE values for g_s and g_m for the different plant groups. (A) Data considered in Flexas et al. (2012). (B) Data considering Flexas et al. (2012) dataset, from the present Thesis and from Bahar et al. (2018), Barbour et al. (2010), Bazihizina et al. (2015), Benomar et al. (2015), Brito et al. (2014), Cai et al. (2015), Cano et al. (2013), von Caemmerer & Evans (2015), Dong et al. (2016), Douthe et al. (2011), Duan et al. (2009), Egea et al. (2011), Fini et al. (2016), Gago et al. (2013), Gallé et al. (2009, 2011), Galmés et al. (2017), Han (2011), Hassiotou et al. (2009), Hommel et al. (2014), Hu et al. (2010), Huang et al. (2016), Jaikumar et al. (2016), Jin et al. (2011), Kitao et al. (2015), Li et al. (2009), Lima Nieto et al. (2015), Lu et al. (2016), Martins et al. (2013, 2014), Medeiros et al. (2016), Mizokami et al. (2015), Monti et al. (2009), Nadal et al. (2018), Peguero-Pina et al. (2012, 2017a,b), Pérez-Martín et al. (2009), Resco et al. (2008), Scafaro et al. (2011), Shi et al. (2015), Soolanayakanahally et al. (2009), Théroux-Rancourt et al. (2014), Tomás et al. (2013, 2014), Tosens et al. (2012a,b, 2016), Varone et al. (2012), Velikova et al. (2009), Veromann-Jürgenson et al. (2017), Warren et al. (2006, 2011), Warren (2008), Xiong et al. (2015, 2017a,b, 2018), Xu and Zhou (2011), Yang et al. (2018), and from the present thesis. Capital letters indicate differences between means for g_s and lower-case letters for g_m (Tukey test, $P < 0.05$).

Currently, and counting on the species reported in this Thesis, g_m has been determined in more than 300 species (Fig. 3B). These data confirm the existence of the phylogenetic trend in g_m initially suggested by Flexas et al. (2012) and similar to that observed for A_N. Angiosperms present the highest g_m values, especially grasses and herbs, followed by conifers and ferns, and in the lowest end are located lycophytes, mosses, liverworts, without significant differences between them. Nevertheless, this evolutionary or phylogenetic trend might be importantly biased by the adaptation of the species to particular habitats or life forms. The clearest evidence is the important variation in g_m found within the angiosperm groups (Fig. 3B), or even within a single genus (e.g. within *Limonium*, *Quercus* or *Solanum* species; Galmés et al. 2017, Muir et al. 2014, Peguero-Pina et al. 2017, respectively) or species (e.g. within *Vitis vinifera* or *Oryza sativa* genotypes; Tomás et al. 2014, Xiong et al. 2017, respectively). This marked phylogenetic trend for g_m, together with the not so clear trend for g_s (in the groups that possess stomata in their photosynthetic tissue) has important implications for the *relative* photosynthetic limitations for the different plant groups (Fig. 4): g_m prevails as the higher source of A_N limitation in bryophytes and lycophytes, but co-limits with g_s in ferns and gymnosperms and equals in importance to g_s and the biochemical capacity in angiosperms.

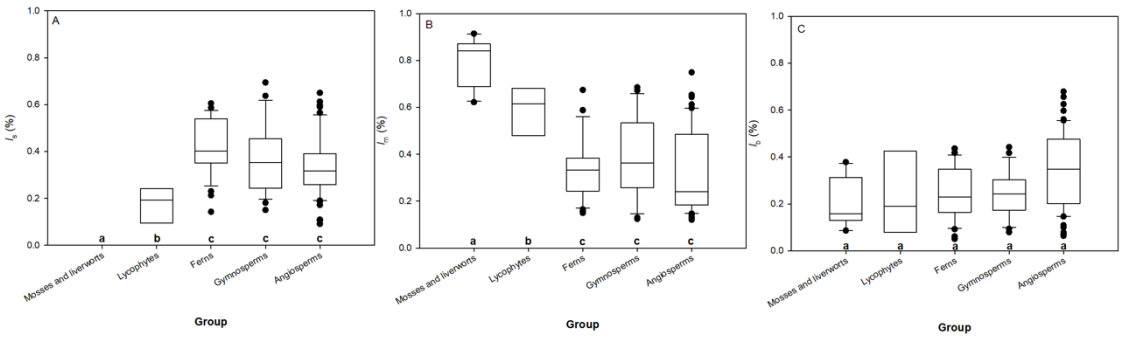

Figure 4. A phylogenetic trend towards balanced co-limitation is observed for the photosynthetic limitations. Relative (A) stomatal (l_s), (B) mesophyll conductance (l_m), and (C) biochemical (l_b) limitations to photosynthesis for the main land plant groups. Average ± SE values for the different plant groups from species measured in Tomás et al. (2013), Martins et al. (2014), Medeiros et al. (2016), Huang et al. (2016), Tosens et al. (2016), Galmés et al. (2017), Peguero-Pina et al. (2017), Veromann-Jürgenson et al. (2017), Xiong et al. (2017, 2018), Bahar et al. (2018), Nadal et al. (2018), Yang et al. (2018), and from the present Thesis. Different letters indicate significant differences (Tukey test, $P < 0.05$).

Once the range of g_m variation inside the different groups of terrestrial plants has been established, in addition to having determined the existence of significant differences between groups, it is now possible to establish the general anatomical mechanistic bases that allow this great variability in g_m along C_3 plant phylogeny. As stated in the previous section, several mesophyll anatomical traits have been identified to influence g_m (Evans et al. 2009, Terashima et al. 2011, Tholen and Zhu 2011) in both air and liquid phases, again only in angiosperms and in a few gymnosperms (Flexas et al. 2012). It is currently established that gas phase conductance is mainly influenced by mesophyll thickness (T_{mes}) and porosity (f_{ias}) -although recent 3D models have raised that tortuosity, lateral path lengthening and intercellular airspace connectivity can be relevant in thick dense leaves (Earles et al. 2018)-, and liquid phase conductance is anatomically mainly set by cell wall thickness (T_{cw}), the mesophyll and chloroplast surface area exposed to intercellular airspaces per leaf area (S_m/S and S_c/S, respectively), and the chloroplast shape and size and tuned by biochemical determinants, mainly aquaporins and carbonic anhydrases (Evans et al. 2009, Terashima et al. 2011, Tholen and Zhu 2011). The knowledge about the range of variation in these anatomical traits across plant phylogeny and the relative importance of them in early land plant groups has been significantly expanded with the present Thesis, in which the anatomy of widely diverse photosynthetic organs of ferns, fern allies, mosses and liverworts has been studied (Fig. 5).

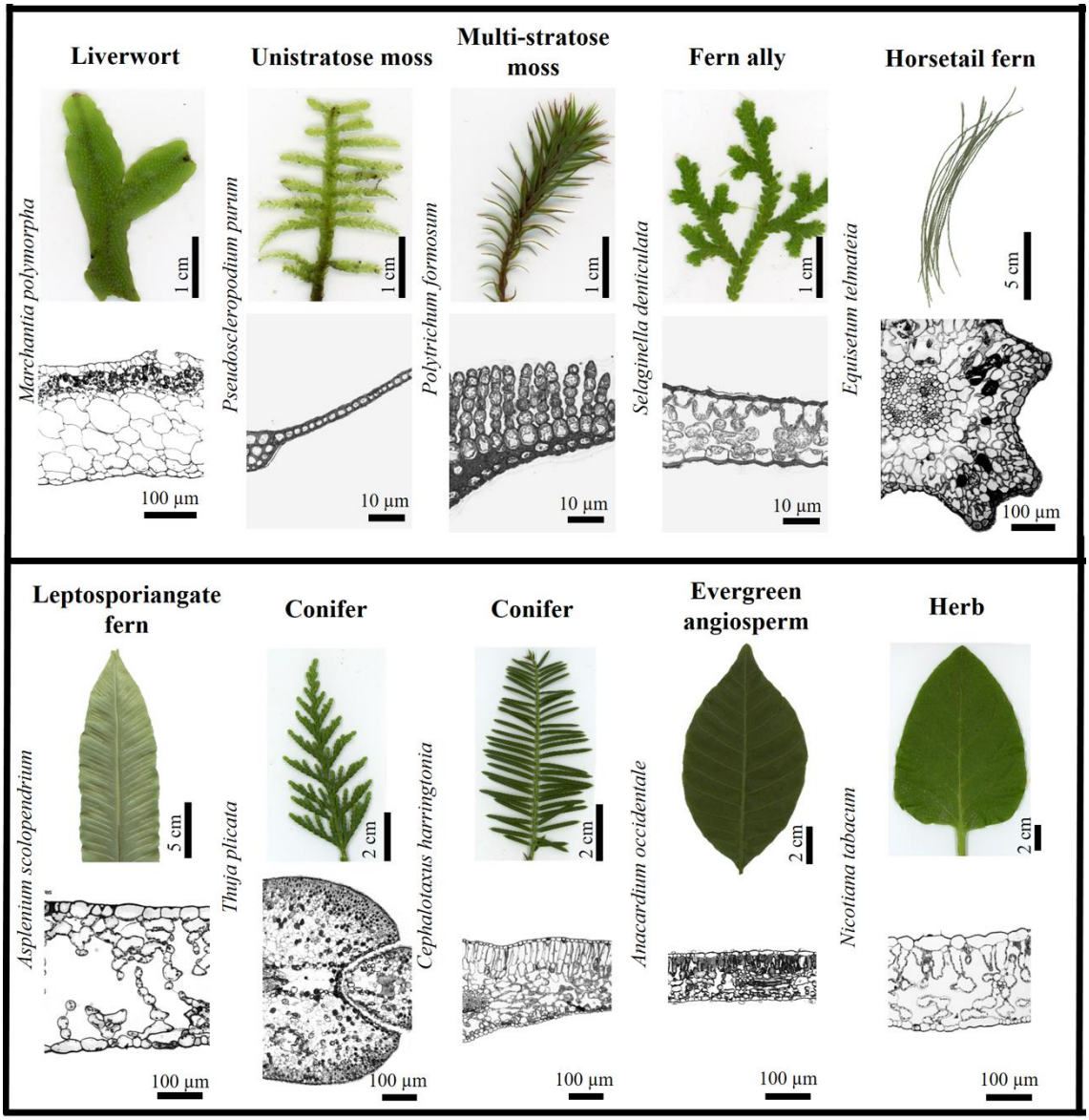

Figure 5. Representative pictures and light micrographs of the large variability in leaf laminas and leaf cross-sections, respectively, evaluated in this Thesis, covering species of the main groups of terrestrial plants.

The main anatomical traits determining g_m in photosynthetic organs across the land plant's phylogeny are S_c/S and T_{cw}. These two traits, apparently independently regulated, are negatively related to each other along the phylogeny (Fig. 6), supporting the evidence for a phylogenetic trend towards higher g_m previously shown (Fig. 3). While the first trait is linearly and positively correlated with A_N and g_m (Fig. 6A,B), the second forces an exponential decay of both A_N and g_m with increasing T_{cw} (Fig. 6C,D). Extreme average values for these two traits are found in mosses, liverworts and angiosperms. While mosses and liverworts, located at the lower end of A_N and g_m, present the lowest S_c/S values

(especially in the case of unistratose mosses) as well as the thickest cell walls reported for land plants (Waite and Sack, 2010), angiosperms, the group with the highest average A_N and g_m values (Flexas et al. 2018), are characterized by their average and extreme highest S_c/S and low T_{cw} values (Fig. 6A-D). At the center of the range, the average values of S_c/S increase stepwise in lycophytes, ferns and gymnosperms, while for T_{cw} these intermediate groups present values within the same range. In addition, T_{leaf}, f_{ias} (in the species with proper mesophyll) and chloroplast dimensions are also important to establish the total mesophyll resistance to CO_2 diffusion in all terrestrial plant groups. However, there is no clear tendency in any of these parameters considered separately, unlike S_c/S and T_{cw}, which allow explaining the phylogenetic trend previously stated for g_m. For example, the thinnest leaves are mainly found in mosses and grasses such as *Oryza* spp. (around 5-55 μm for unistratose mosses and 50-100 μm for *Oryza* spp.), which have the most extreme values reported for g_m (Scaffaro et al. 2011, Giuliani et al. 2013, Ellsworth et al. 2018, Ren et al. 2019). This is because T_{leaf}, similar to LMA, is a rather complex structural parameter (Niinemets et al. 2009, Onoda et al. 2017). Possessing thicker leaves not only involves a lengthening of the CO_2 pathway across the mesophyll (Niinemets and Reichstein 2003, Evans et al. 2009, Tosens et al. 2012b, Earles et al. 2018) but also allows increasing the mesophyll volume on an area basis, either for intercellular airspaces (i.e. a greater f_{ias}), increased cell density by means of more and/or enlarged cells, which allows for a greater S_m/S and S_c/S, and/or supporting and/or vascular tissue (Terashima et al. 2011, Kuusk et al. 2018). The same happens with the chloroplast dimensions, as thicker chloroplasts allow on one side to allocate a higher content of Rubisco in the stroma per S_c/S, but on the other side it supposes a lengthening of the liquid-phase CO_2 pathway (Terashima et al. 2011). Among the species in which both g_m and leaf anatomy have been determined, the larger chloroplast dimensions have been found in lycophytes, followed closely only by a few ferns (Chapter 3, Tosens et al. 2016, Veromann-Jürgenson et al. 2017) and angiosperms and gymnosperms (Sáez et al. 2017, Kuusk et al. 2018), while the smaller chloroplasts have been found in a few mosses and woody angiosperm species (Tosens et al. 2012a, Tomás et al. 2013, Peguero-Pina et al. 2017).

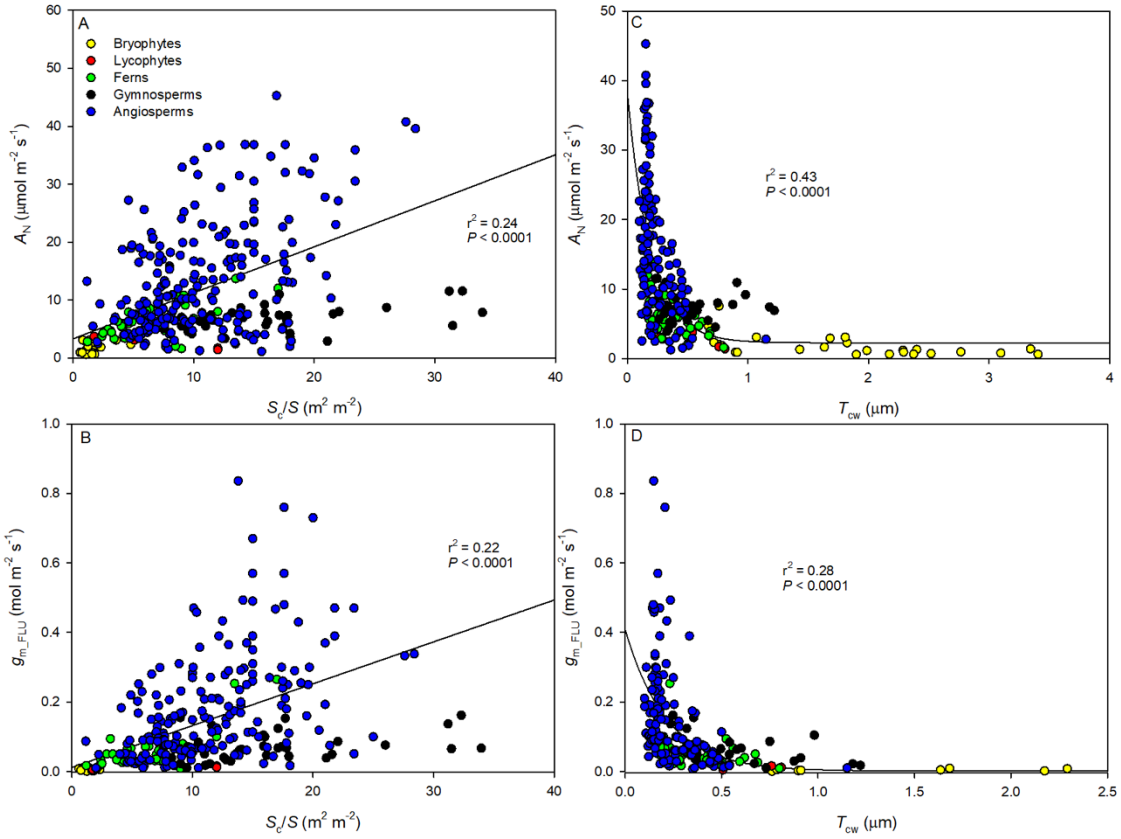

Figure 6. Photosynthesis and mesophyll conductance are tightly constrained by two key anatomical traits along plant phylogeny. (A) Net photosynthesis (A_N) in relation to chloroplast surface area exposed to intercellular air space per leaf area (S_c/S), (B) mesophyll conductance estimated from chlorophyll fluorescence (g_{m_FLU}) in relation to S_c/S, (C) A_N in relation to cell wall thickness (T_{cw}), and (D) g_{m_FLU} in relation to T_{cw}. Data corresponds to published values from Veromann-Jürgenson et al. (2017), Kuusk et al. (2018a, 2018b), the 44 datasets compiled by Ren et al. (2019), and from this thesis.

Once the main anatomical determinants of g_m have been revealed in pteridophytes, lycophytes and bryophytes, studies are urged to determine the role of g_m's biochemical determinants —as well as the short-to-long term anatomical adjustments determining g_m to environmental changes— in these primitive land plant groups.

Conclusions

A series of conclusions have been achieved, in relation to the main and specific objectives.

(1) To provide further insights on how the environment modulates the relationship between leaf anatomy and mesophyll conductance to CO_2 (g_m).

1. The leaf anatomical traits remained invariable during g_m changes induced by short-term (seconds to minutes) changes in atmospheric CO_2 and/or light intensity in tobacco. This result suggests that short-term variations of g_m could at least partially reflect some artefactual effect and/or are induced by non-anatomical components.
2. Instead, acclimation of g_m to increasing growing light intensity was mainly explained by anatomical traits in *Arabidopsis thaliana*. Increases in leaf thickness, although resulting in a longer gas-phase diffusion pathway within the leaf, allowed for significant increases in mesophyll and chloroplast surface area exposed to intercellular airspace per leaf area (S_m/S and S_c/S, respectively), directly implying more parallel pathways for CO_2 liquid-phase diffusion and, thus, larger g_m.
3. Photosynthesis and g_m variations along leaf ageing in *Arabidopsis thaliana* were strongly associated with developmental changes in the thickness of cell walls and in an impairment between S_m/S and S_c/S, which resulted in a decrease in the S_c/S_m ratio in older leaves.

(2) To determine the main leaf anatomy traits influencing mesophyll conductance to CO_2 across the land plant phylogeny.

4. Ferns, when compared to angiosperms growing in a common garden, exhibited lower photosynthetic rates, stomatal and mesophyll conductance and biochemical capacity for photosynthesis. Large mesophyll conductance limitations to photosynthesis were mainly determined by thicker cell walls and lower S_c/S.

5. Lycophyte photosynthesis, a former group of fern allies, was mainly determined by mesophyll conductance and biochemical limitations to photosynthesis. Thick cell walls and extremely big chloroplasts, presumably setting a low Rubisco content per unit chloroplast surface area, largely explained their low g_m values.
6. Bryophytes presented the lowest light saturated photosynthesis rates and g_m among terrestrial plants, which was mostly due to strong mesophyll conductance limitation driven by their specific anatomical characteristics: the largest cell wall thicknesses and lowest exposure of chloroplasts to cell perimeter per leaf area ever reported in land plants.
7. The conifer *Thuja plicata* compensated the large resistances to CO_2 diffusion imposed by extremely thick leaves and cell walls by presenting the highest S_c/S ever reported for a land plant. *T. plicata* represents a clear outlier in the widely reported relationships between leaf anatomy and net photosynthesis, demonstrating that leaves with modified anatomy to increase or maintain their mesophyll conductance while increasing their stress tolerance are biologically possible.
8. Cell wall composition was strongly correlated with both cell wall thickness and g_m in conifers. Species with thicker cell walls presented a larger proportion of pectins in respect to both cellulose and hemicelluloses, which presumably led to an increased cell wall effective porosity to CO_2 diffusion, and therefore to a higher g_m. The common assumption of an inverse relationship between cell wall thickness and effective porosity is discarded, at least in conifer species.
9. A phylogenetic trend towards increased g_m is reported for land plants: bryophytes<lycophytes<pteridophytes<spermatophytes. The relationship between specific leaf anatomical trait relationships and g_m is conserved throughout land plant phylogeny, with a predominant role of cell wall thickness and chloroplast surface area exposed either to intercellular or ambient air per leaf area.

Reference list

Abascal F., Irisarri I., Zardoya R. (2014) Diversity and evolution of membrane intrinsic proteins. Biochimica et Biophysica Acta 1840, 1468–1481.

Adams W.W., Terashima I. (2018) *The leaf: A platform for performing photosynthesis. Advances in Photosynthesis and Respiration (including bioenergy and related processes)*, Vol. 44. Springer, Cham.

Ainsworth E.A., Rogers A. (2007) The response of photosynthesis and stomatal conductance to rising [CO_2]: mechanisms and environmental interactions. *Plant, Cell and Environment* 30, 258-270.

Ainsworth E.A., Yendrek C.R., Sitch S., Collins W.J., Emberson L.D. (2012) The effects of tropospheric ozone on net primary productivity and implications for climate change. *Annual Review of Plant Biology* 63, 637–661.

Aranda I., Rodriguez-Calcerrada J., Robson T.M., Cano F.J., Alté L., Sanchez-Gomez D. (2012) Stomatal and non-stomatal limitations on leaf carbon assimilation in beech (*Fagus sylvatica* L.) seedlings under natural conditions. *Forest Systems* 21, 405–417.

Aranjuelo I., Tcherkez G., Jauregui I., Gilard F., Ancin M., Fernández San Millán A., Larraya L., Veramendi J., Farrán I. (2015) Alteration by thioredoxin f over-expression of primary carbon metabolism and its response to elevated CO_2 in tobacco (*Nicotiana tabacum* L.). *Environmental and Experimental Botany* 118, 40–48.

Atkin O.K., Bruhn D., Hurry V.M., Tjoelker M.G. (2005) The hot and the cold: unravelling the variable response of plant respiration to temperature. *Functional Plant Biology* 32, 87–105.

Bahar N.H.A., Hayes L., Scafaro A.P., Atkin O.K., Evans J.R. (2018) Mesophyll conductance does not contribute to greater photosynthetic rate per unit nitrogen in temperate compared with tropical evergreen wet-forest tree leaves. *New Phytologist* 218, 492–505.

Barbour M.M., Warren C., Farquhar G., Forrester G., Brown H. (2010) Variability in mesophyll conductance between barley genotypes, and effects on

transpiration efficiency and carbon isotope discrimination. *Plant, Cell and Environment* 33, 1176–1185.

Barbour M.M., Kaiser B.N. (2016) The response of mesophyll conductance to nitrogen and water availability differs between wheat genotypes. *Plant Science* 251, 119–127.

Battie-Laclau P., Laclau J.-P., Beri C., Mietton L., Muniz M.R.A., Arenque B.C., Nouvellon Y. (2014) Photosynthetic and anatomical responses of *Eucalyptus grandis* leaves to potassium and sodium supply in a field experiment. *Plant, Cell and Environment* 37, 70–81.

Bazihina N., Colzi I., Giorni E., Mancuso S., Gonnelli C. (2015) Photosynthesizing in metal excess: copper differently induced changes in various photosynthetic parameters in copper tolerant and sensitive *Silene paradoxa* L. populations. *Plant Science* 232, 67–76.

Beerling D.J., Osborne C.P., Chaloner W.G. (2001) Evolution of leaf-form in land plants linked to atmospheric CO_2 decline in the late Paleozoic era. *Nature* 410, 352–354.

Bellasio C., Beerling D.J., Griffiths H. (2016) An Excel tool for deriving key photosynthetic parameters from combined gas exchange and chlorophyll fluorescence: theory and practice. *Plant, Cell and Environment* 39, 1180–1197.

Benomar L., Lamhamedi M.S., Villeneuve I., Rainville A., Beaulieu J., Bousquet J., Margolis H.A. (2015) Fine-scale geographic variation in photosynthetic-related traits of *Picea glauca* seedlings indicates local adaptation to climate. *Tree Physiology* 35, 864–878.

Bernacchi C.J., Portis A.R., Nakano H., von Caemmerer S., Long S.P. (2002) Temperature response of mesophyll conductance. Implications for the determination of Rubisco enzyme kinetics and for limitations to photosynthesis in vivo. *Plant Physiology* 130, 1992–1998.

Bernacchi C., Morgan P., Ort D., Long S. (2005) The growth of soybean under free air [CO_2] enrichment (FACE) stimulates photosynthesis while decreasing *in vivo* Rubisco capacity. *Planta* 220, 434–446.

Berner R.A. (2006) GEOCARBSULF: A combined model for Phanerozoic atmospheric O_2 and CO_2. *Geochimica et Cosmochimica Acta* 70, 5653–5664.

Berry J.A., Björkman O. (1980) Photosynthetic Response and Adaptation to Temperature in Higher Plants. *Annual Review of Plant Physiology* 31(1), 491–543.

Björkman O. (1981) Responses to different quantum flux densities. In: O.L. Lange, P.S. Nobel, C.B. Osmond, H. Ziegler (eds.) *Encyclopedia of Plant Physiology, New Series, Vol. 12A: Physiological Plant Ecology. I: Responses to Physical Environment*, pp. 57–107. Springer, New York, NY, USA.

Brilli F., Tsonev T., Mahmood T., Velikova V., Loreto F., Centritto M. (2013) Ultradian variation of isoprene emission, photosynthesis, mesophyll conductance, and optimum temperature sensitivity for isoprene emission in water-stressed *Eucalyptus citridora* saplings. *Journal of Experimental Botany* 64, 519–528.

Brito C.E., Bown H.E., Fuentes J.P., Franck N., Perez-Quezada J.F. (2014) Mesophyll conductance constrains photosynthesis in three common sclerophyllous species in Central Chile. *Revista Chilena de Historia Natural* 87, 8.

Brodribb T.J., McAdam S.A.M. (2011) Passive origins of stomatal control in vascular plants. *Science* 331, 582–585.

Brodribb T.J., McAdam S.A.M., Jordan G.J., Feild T.S. (2009) Evolution of stomatal responsiveness to CO_2 and optimization of water-use efficiency among land plants. *New Phytologist* 183, 839–847.

Bunce J.A. (2008) Acclimation of photosynthesis to temperature in *Arabidopsis thaliana* and *Brassica oleracea*. *Photosynthetica* 46, 517–524.

Bunce J.A. (2009) Use of the response of photosynthesis to oxygen to estimate mesophyll conductance to carbon dioxide in water-stressed soybean leaves. *Plant, Cell and Environment* 32, 875–881.

von Caemmerer S., Evans J.R. (1991) Determination of the average partial pressure of CO_2 in chloroplasts from leaves of several C_3 plants. *Australian Journal of Plant Physiology* 18, 287–305.

von Caemmerer S., Evans J.R. (2015) Temperature responses of mesophyll conductance differ greatly between species. *Plant, Cell and Environment* 38, 629–637.

Cai Y., Wang J., Li S., Zhang L., Peng L., Xie W., Liu F. (2015) Photosynthetic response of an alpine plant, *Rhododendron delavayi* Franch, to water stress and recovery: the role of mesophyll conductance. *Frontiers in Plant Science* 6, 1089.

Cai C., Li G., Yang H., Yang J., Liu H., Struik P.C., Luo W., Yin X., Di L., Guo X., Jiang W., Si C., Pan G., Zhu J. (2018) Do all leaf photosynthesis parameters or rice acclimate to elevated CO_2, elevated temperature, and their combination, in FACE environments? *Global Change Biology* 24, 1685–1707.

Calatayud V., Cerveró J., Sanz M.J. (2007) Foliar, physiological and growth responses of four maple species exposed to ozone. *Water, Air and Soil Pollution*. 185, 239–254.

Cano F.J., Sánchez-Gómez D., Gascó A., Rodríguez-Calcerrada J., Gil L., Warren C., Aranda I. (2011) Light acclimation at the end of the growing season in two broadleaved oak species. *Photosynthetica* 49, 581–592.

Cano F.J., Sánchez-Gómez D., Rodríguez-Calcerrada J., Warren C.R., Gil L. and Aranda I. (2013) Effects of drought on mesophyll conductance and

photosynthetic limitations at different tree canopy layers. *Plant, Cell and Environment* 36, 1961–1980.

Cano F.J., López R., Warren C.R. (2014) Implications of the mesophyll conductance to CO_2 for photosynthesis and water-use efficiency during long-term water stress and recovery in two contrasting *Eucalyptus* species. *Plant, Cell and Environment* 37, 2470–2490.

Chmura, D.J., Modrzynski, J., Chmielarz, P., Tjoelker ,M.G. (2017) Plasticity in seedling morphology, biomass allocation and physiology among ten temperature tree species in response to shade is related to shade tolerance and not leaf habit. *Plant Biology* 19, 172–182.

Cochard H., Venisse J.S., Barigah T.S., Brunel N., Herbette S., Guilliot A., Tyree M.T., Sakr S. (2007) Putative role of aquaporins in variable hydraulic conductance of leaves in response to light. *Plant Physiology* 143, 122–133.

Crous K., Quentin A., Lin Y., Medlyn B., Williams D., Barton C., Ellsworth D. (2013) Photosynthesis of temperate *Eucalyptus globulus* trees outside their native range has limited adjustment to elevated CO_2 and climate warming. *Global Change Biology* 19, 3790–3807.

DaMatta F.M., Godoy A.G., Menezes-Silva P.E., Martins S.C.V., Sanglard L.M.V.P, Morais L.E., Torre-Nieto A., Ghini R. (2016) Sustained enhancement of photosynthesis in coffee trees grown under free-air CO_2 enrichment conditions: disentangling the contributions of stomatal, mesophyll, and biochemical limitations. *Journal of Experimental Botany* 67, 341–352.

Di Marco G., Manes F., Tricoli D., Vitale E. (1990) Fluorescence parameters measured concurrently with net photosynthesis to investigate chloroplastic CO_2 concentration in leaves of *Quercus ilex* L. *Journal of Plant Physiology* 136, 538–543.

Díaz-Espejo A., Nicolas E., Fernandez J.E. (2007) Seasonal evolution of diffusional limitations and photosynthetic capacity in olive under drought. *Plant, Cell and Environment* 30, 922–933.

Dong T., Zhang Y., Zhang Y., Zhang S. (2016) Continuous planting under a high density enhances the competition for nutrients among young *Cunninghamia lanceolata* saplings. *Annals of Forest Science* 73, 331–339.

Douthe C., Dreyer E., Epron D., Warren C.R. (2011) Mesophyll conductance to CO_2, assessed from online TDL-AS records of $^{13}CO_2$ discrimination, displays small but significant short-term responses to CO_2 and irradiance in *Eucalyptus* seedlings. *Journal of Experimental Botany* 62, 5335–5346.

Douthe C., Dreyer E., Brendel O., Warren C.R. (2012) Is mesophyll conductance to CO_2 in leaves of three *Eucalyptus* species sensitive to short-term changes of irradiance under ambient as well as low O_2? *Functional Plant Biology* 39, 435–448.

Duan B., Li Y., Zhang X., Korpelainen H., Li C. (2009) Water deficit affects mesophyll limitation of leaves more strongly in sun than in shade in two contrasting *Picea aspera* populations. *Tree Physiology* 29, 1551–1561.

Dubois J.J.B., Fiscus E.L., Booker F.L., Flowers M.D., Reid C.D. (2008) Optimizing the statistical estimation of the parameters of the Farquhar-von Caemmerer-Berry model of photosynthesis. *New Phytologist* 177, 1034–1034.

Duckett, J.G. and Pressel, S. (2018) The evolution of the stomatal apparatus: intercellular spaces and sporophyte water relations in bryophytes – two ignored dimensions. *Philosophical Transactions of the Royal Society of London Series B: Biological Sciences* 373, 20160498.

Earles J.M., Théroux-Rancourt G., Roddy A.B., Gilbert M.E., McElrone A.J., Brodersen C.R. (2018) Beyond porosity: 3D leaf intercellular airspace traits that impact mesophyll conductance. *Plant Physiology* 178, 148–162.

Earles J.M., Buckley T.N., Brodersen C.R., Busch F.A., Cano F.J., Choat B., Evans J.R., Farquhar G.D., Harwood R., Huynh M., John G.P., Miller M.L., Rockwell F.E., Sack L., Scoffoni C., Struik P.C., Wu A., Yin X., Barbour M.M. (2019) Embracing 3D complexity in leaf carbon-water exchange. *Trends in Plant Science* 24, 15–24.

Eichelmann H., Oja V., Rasulov B., Padu E., Bichele I., Pettai H., Möls T., Kasparova I., Vapaavuori E., Laisk A. (2004) Photosynthetic parameters of birch (*Betula pendula* Roth) leaves growing in normal and in CO_2- and O_3- enriched atmospheres. *Plant, Cell and Environment* 27, 479–495.

Egea G., González-Real M.M., Baille A., Nortes P.A., Diaz-Espejo A. (2011) Disentangling the contributions of ontogeny and water stress to photosynthetic limitations in almond trees. *Plant Cell and Environment* 34, 962–979.

Ellsworth P.V., Ellsworth P.Z., Koteyeva N.R., Cousins A.B. (2018) Cell wall properties in *Oryza sativa* influence mesophyll CO_2 conductance. *New Phytologist* 19, 66–76.

Engelman D.M. (2005) Membranes are more mosaic than fluid. *Nature* 438, 578–580.

Ethier G.J., Livingston N.J. (2004) On the need to incorporate sensitivity to CO_2 transfer conductance into the Farquhar-von Caemmerer-Berry leaf photosynthesis model. Plant Cell Environ 27:137–153.

Evans J.R. (1989) Photosynthesis and nitrogen relationships in leaves of C_3 plants. *Oecologia* 78, 9–19.

Evans J.R., Kaldenhoff R., Genty B., Terashima I. (2009) Resistances along the CO_2 diffusion pathway inside leaves. *Journal of Experimental Botany* 60, 2235–2248.

Evans J.R., von Caemmerer S. (2013) Temperature response of carbon isotope discrimination and mesophyll conductance in tobacco. *Plant, Cell and Environment* 36, 745–756.

Fares S., Mahmood T., Liu S., Loreto F., Centritto M. (2011) Influence of growth temperature and measuring temperature on isoprene emission, diffusive limitations of photosynthesis and respiration in hybrid poplars. *Atmospheric Environment* 45, 155–161.

Farquhar G.D., Caemmerer S.V., Berry J.A. (1980) A biochemical model of photosynthetic CO_2 assimilation in leaves of C_3 species. Planta 149, 78–90.

Feng Z.Z., E.Z. H., Wang X.K., Jiang L.J., Liu X.J. (2015) Ground-level O_3 pollution and its impacts on food crops in China: a review. *Environmental Pollution* 199, 42–48.

Ferrio J.P., Pou A., Florez-Sarasa I., Gessler A., Kodama N., Flexas J., Ribas-Carbó M. (2012) The Peclet effect on leaf water enrichment correlates with leaf hydraulic conductance and mesophyll conductance for CO_2. *Plant, Cell and Environment* 35, 611–625.

Fini A., Loreto F., Tattini M., Giordano C., Ferrini F., Brunetti C., Centritto M. (2016) Mesophyll conductance plays a central role in leaf functioning of Oleaceae species exposed to contrasting sunlight irradiance. *Physiologia Plantarum* 157, 54–68.

Fitter A., Hay R. (2002) *Environmental Physiology of Plants*. Academic Press, San Diego, CA.

Flexas J., Ribas-Carbó M., Bota J., Galmés J., Henkle M., Martínez-Cañellas S., Medrano H. (2006) Decreased Rubisco activity during water stress is not induced by decreased relative water content but related to conditions of low stomatal conductance and chloroplast CO_2 concentration. *New Phytologist* 172, 73–82.

Flexas J., Díaz-Espejo A., Berry J., Cifre J., Galmés J., Kaldenhoff R., Medrano H., Ribas-Carbó M. (2007a) Analysis of leakage in IRGA's leaf chambers of open gas exchange systems: quantification and its effects in photosynthesis parameterization. *Journal of Experimental Botany* 58, 1533–1543.

Flexas J., Ortuño M.F., Ribas-Carbó M., Díaz-Espejo A., Flórez-Sarasa I.D., Medrano H., (2007b) Mesophyll conductance to CO_2 in *Arabidopsis thaliana*. *New Phytologist* 175, 501–511.

Flexas J., Ribas-Carbó M., Díaz-Espejo A., Galmés J., Medrano H. (2008) Mesophyll conductance to CO_2: current knowledge and future prospects. *Plant, Cell and Environment* 31, 602–621.

Flexas J., Baron M., Bota J., Ducruet J.M., Gallé A., Galmés J., Jiménez M., Pou A., Ribas-Carbó M., Sajnani C., Tomàs M., Medrano H. (2009) Photosynthesis limitations during water stress acclimation and recovery in the drought-adapted *Vitis* hybrid Richter-110 (*V. berlandieri* x *V. rupestris*). *Journal of Experimental Botany* 60, 2361–2377.

Flexas J., Barbour M.M., Brendel O., Cabrera H.M., Carriquí M., Díaz-Espejo A., Douthe C., Dreyer E., Ferrio J.P., Gago J., Gallé A., Galmés J., Kodama, N., Medrano H., Niinemets Ü., Peguero-Pina J.J., Pou A., Ribas-Carbó M., Tomás M., Tosens T., Warren C.R. (2012) Mesophyll diffusion conductance to CO_2: An unappreciated central player in photosynthesis. *Plant Science* 193–194, 70–84.

Flexas J., Keeley J.E. 2012. Evolution of photosynthesis I. Basic leaf morphological traits and diffusion and photosynthetic structures. In: Flexas J., Loreto F., Medrano H. (eds.) *Terrestrial photosynthesis in a changing environment: a molecular, physiological and ecological approach*. Cambridge, UK: Cambridge University Press, 373–385.

Flexas J., Díaz-Espejo A. (2015) Interspecific differences in temperature response of mesophyll conductance: food for thought on its origin and regulation. *Plant, Cell and Environment* 38, 625–628.

Flexas J., Cano F.J., Carriquí M., Coopman R.E., Mizokami Y., Tholen D., Xiong D. (2018) CO_2 diffusion inside photosynthetic organs. In: Adams W., Terashima I. (eds) *The leaf: A platform for performing photosynthesis. Advances in Photosynthesis and Respiration (including bioenergy and related processes)*, Vol. 44 pp. 163–208. Springer, Cham.

Flowers M.D., Fiscus E.L., Burkey K.O., Booker F.L., Dubois J.-J.B. (2007) Photosynthesis, chlorophyll fluorescence, and yield of snap bean (*Phaseolus vulgaris* L.) genotypes differing in sensitivity to ozone. *Environmental and Experimental Botany* 61, 190–198.

Franks P.J., Farquhar G.D. (2007) The mechanical diversity of stomata and its significance in gas-exchange control. *Plant Physiology* 143, 78–87.

Franks P.J., Beerling D.J. (2009) Maximum leaf conductance driven by CO_2 effects on stomatal size and density over geologic time. *Proceedings of the National Academy of Sciences of the United States of America* 106, 10343–10347.

Gago J., Coopman R.E., Cabrera H.M., Hermida C., Molins A., Conesa M.À., Galmés J., Ribas-Carbó M., Flexas J. (2013) Photosynthesis limitations in three fern species. *Physiologia Plantarum* 149, 599–611.

Gago J., Daloso D.M., Figueroa C.M., Flexas J., Fernie A.R., Nikoloski Z. (2016) Relationships of leaf net photosynthesis, stomatal conductance, and mesophyll conductance to primary metabolism: a multispecies meta-analysis approach. *Plant Physiology* 171, 1–15.

Gallé A., Florez-Sarasa I., Tomas M., Pou A., Medrano H., Ribas-Carbo M., Flexas J. (2009) The role of mesophyll conductance during water stress and recovery in tobacco (*Nicotiana sylvestris*): acclimation or limitation? *Journal of Experimental Botany* 60, 2379–2390.

Gallé A., Florez-Sarasa I., El Aououad H., Flexas J. (2011) The Mediterranean evergreen *Quercus ilex* and the semi-deciduous *Cistus albidus* differ in their leaf gas exchange regulation and acclimation to repeated drought and re-watering cycles. *Journal of Experimental Botany* 62, 5207–5216.

Galmés J., Medrano H., Flexas J. (2007) Photosynthetic limitations in response to water stress and recovery in Mediterranean plants with different growth forms. *New Phytologist* 175, 81–93.

Galmés J., Ochogavía J.M., Gago J., Roldán E.J., Cifre J., Conesa M.À. (2013) Leaf responses to drought stress in Mediterranean accessions of *Solanum lycopersicum*: anatomical adaptations in relation to gas Exchange parameters. *Plant, Cell and Environment* 36, 920–935.

Galmés J., Molins A., Flexas J., Conesa M.À. (2017) Coordination between leaf CO_2 diffusion and Rubisco properties allows maximizing photosynthetic efficiency in *Limonium* species. *Plant, Cell and Environment* 40, 2081–2094.

Gao F., Calatayud V., García-Breijo F., Reig-Armiñana J., Feng Z. (2016) Effects of elevated ozone on physiological, anatomical and ultrastructural characteristics of four common urban tree species in China. *Ecological Indicators* 67: 367–379.

Giuliani R., Koteyeva N., Voznesenskaya E., Evans M.A., Cousins A.B., Edwards G.E. (2013) Coordination of leat photosynthesis, transpiration, and structural traits in rice and wild relatives (genus *Oryza*). *Plant Physiology* 162, 1632–1651.

Gorton H.L., Herbert S.K., Vogelmann T.C. (2003) Photoacoustic analysis indicates that chloroplast movement does not alter liquid-phase CO_2 diffusion in leaves of *Alocasia brisbanensis*. *Plant Physiology* 132, 1529–1539.

Grassi G., Magnani F. (2005) Stomatal mesophyll conductance and biochemical limitations to photosynthesis as affected by drought and leaf ontogeny in ash and oak trees. *Plant, Cell and Environment* 28, 834–849.

Griffiths H., Helliker B.R. (2013) Mesophyll conductance: internal insights of leaf carbon exchange. *Plant, Cell and Environment* 36, 733–735.

Gu L., Sun Y. (2014) Artefactual responses of mesophyll conductance to CO_2 and irradiance estimated with the variable J and online isotope discrimination methods. *Plant, Cell and Environment* 37, 1231–1249.

Han Q. (2011) Height-related decreases in mesophyll conductance, leaf photosynthesis and compensating adjustments associated with leaf nitrogen concentrations in *Pinus densiflora*. *Tree Physiology* 31, 976–984.

Han J.M., Meng H.F., Wang S.Y., Jiang C.D., Liu F., Zhang W.F., Zhang Y.L. (2016) Variability of mesophyll conductance and its relationship with water use efficiency in cotton leaves under drought pretreatment. *Journal of Plant Physiology* 194, 61–71.

Han J., Lei Z., Flexas J., Zhang F., Carriquí M., Zhang W., Zhang Y. (2018) Mesophyll conductance in cotton bracts: anatomically determined internal CO_2 diffusion constraints on photosynthesis. *Journal of Experimental Botany* 69, 5433–5443.

Hanba Y.T., Miyazawa S.-I., Kogami H., Terashima I. (2001) Effects of leaf age on internal CO_2 transfer conductance and photosynthesis in tree species having different types of shoot phenology. *Australian Journal of Plant Physiology* 28, 1075–1084.

Hanba Y.T., Kogami H., Terashima I. (2002) The effect of growth irradiance on leaf anatomy and photosynthesis in *Acer* species differing in light demand. *Plant, Cell and Environment* 25, 1021–1030.

Hanba Y.T., Shibasaka M., Hayashi Y., Hayakawa T., Kasamo K., Terashima I., Katsuhara M. (2004) Overexpression of the barley aquaporin HvPIP2;1 increases internal CO_2 conductance and CO_2 assimillation in the leaves of transgenic rice plants. *Plant and Cell Physiology* 45, 521–529.

Hanson D.T., Renzaglia K., Villarreal J.C. (2014) Diffusion limitation and CO_2 concentrating mechanisms in bryophytes. In: Hanson D.T., Rice S.K. (eds) *Photosynthesis in bryophytes and early land plants, Advances in photosynthesis and respiration*, Vol. 37, pp. 95-111. Springer, Dordrecht.

Harley P.C., Loreto F., Marco G.D., Sharkey T.D. (1992) Theoretical considerations when estimating the mesophyll conductance to CO_2 flux by analysis of the response of photosynthesis to CO_2. *Plant Physiology* 98, 1429–1436.

Hassiotou F., Ludwig M., Renton M., Veneklaas E.J., Evans J.R. (2009) Influence of leaf dry mass per area, CO_2, and irradiance on mesophyll conductance in sclerophylls. *Journal of Experimental Botany* 60, 2303–2314.

Haworth M., Kingston C., McElwain J.C. (2011) Stomatal control as a driver of plant evolution. *Journal of Experimental Botany* 62, 2419–2423.

Hendrickson L., Ball M.C., Wood J.T., Chow W.S., Furbank R.T. (2004) Low temperature effects on photosynthesis and growth of grapevine. *Plant, Cell and Environment* 27, 795–809.

Hirose T., Bazzaz F.A. (1998) Trade-off between light- and nitrogen-use efficiency in canopy photosynthesis. *Annals of Botany* 82, 195–202.

Ho Q.T., Berghuijs H.N., Watté R., Verboven P., Herremans E., Yin X., Helfen L. (2016) Three-dimensional microscale modelling of CO_2 transport and light propagation in tomato leaves enlightens photosynthesis. *Plant, Cell and Environment* 39, 50–61.

Hommel R., Siegwolf R., Saurer M., Farquhar G.D., Kayler Z., Ferrio J.P., Gessler A. (2014) Drought response of mesophyll conductance in forest understory species – impact on water-use efficiency and interactions with leaf water movement. *Physiologia Plantarum* 152, 98–114.

Hu L., Wang Z., Huang B. (2010) Diffusional limitations and metabolic factors associated with inhibition and recovery of photosynthesis from drought stress in a C_3 perennial grass species. *Physiologia Plantarum* 139, 93–106.

Huang W., Tong Y.-G., Yu G.-Y., Yang W.-X. (2016) The sclerophyllous *Eucalyptus calmadulensis* and herbaceous *Nicotiana tabacum* have different mechanisms to maintain high rates of photosynthesis. *Frontiers in Plant Science* 7, 1769.

Itel F., Al-Samir S., Öberg F., Chami M., Kumar M., Supuran C.T., Deen P.M.T., Meier W., Hedfalk K., Gros G., Endeward V. (2012) CO_2 permeability of

cell membranes is regulated by membrane cholesterol and protein gas channels. *FASEB Journal* 26:5182–5191.

Ivanova L.A., Petrov M.S., Kadushnikov R.M. (2006) Determination of mesophyll diffusion resistance in *Chamaerion angustifolium* by the method of three dimensional reconstruction of the leaf cell packing. *Russian Journal of Plant Physiology* 53, 316–322.

Jaikumar N.S., Snapp S.S., Sharkey T.D. (2016) Older *Thinopyrum intermedium* (Poaceae) plants exhibit superior photosynthetic tolerance to cold stress and greater increases in two photosynthetic enzymes under freezing stress compared with young plants. *Journal of Experimental Botany* 67, 4743–4753.

Jin S.H., Huang X.Q., Li B.S., Zheng B.S., Wu J.S., Wang Z.J., Liu G.H., Chen M. (2011) Effects of potassium supply on limitations of photosynthesis by mesophyll conductance in *Carya cathayensis*. *Tree Physiology* 31, 1142–1151.

Joffre R., Rambal S., Damesin C. (2007) Functional attributes of Mediterranean-type ecosystems. In: Pugnaire F.I., Valladares F. (eds.) *Handbook of functional plant ecology. Boca Raton, FL, USA: CRC Press*, 285–312.

Kasahara M., Kagawa T., Oikawa K., Suetsugu N., Miyao M., Wada M. (2002) Chloroplast avoidance movement reduces photodamage in plants. *Nature* 420, 829–832.

Kitao M., Yazaki K., Kitaoka S., Fukatsu E., Tobita H., Komatsu M., Maruyama Y., Koike T. (2015) Mesophyll conductance in leaves of Japanese white birch (*Betula platyphylla* var. *japonica*) seedlings grown under elevated CO_2 concentration and low N availability. *Physiologia Plantarum* 155, 435–455.

Kobza J., Edwards G.E. (1987) Influences of leaf temperature on photosynthetic carbon metabolism in wheat. *Plant Physiology* 83, 69–74.

Koike T., Kitao M., Maruyama Y., Mori S., Lei T.T. 2001. Leaf morphology and photosynthetic adjustments among deciduous broad-leaved trees within the vertical canopy profile. *Tree Physiology* 21, 951–958.

Kok B. (1948) A critical consideration of the quantum yield of *Chlorella* photosynthesis. *Enzymologia* 1–56.

Kumarathunge D.P., Medlyn B.E., Drake J.E., Tjoelker M.G. (2019) Acclimation and adaptation components of the temperature dependence of plant photosynthesis at the global scale. *New Phytologist* 222, 768–784.

Kuusk V., Niinemets Ü., Valladares F. (2018) A major trade-off between structural and photosynthetic investments operative across plant and needle ages in three Mediterranean pines. *Tree Physiology* 38, 543–557.

Laisk A (1977) *Kinetics of photosynthesis and photorespiration of C_3 plants*. Nauka, Moscow (in Russian).

Laisk A., Eichelmann H., Oja V., Rasulov B., Padu E., Bichele I., Pettai H., Kull O. (2005) Adjustment of leaf photosynthesis to shade in a natural canopy: rate parameters. *Plant, Cell and Environment* 28, 375–388.

Lehmeier C., Pajor R., Lundgren M.R., Mathers A., Sloan J., Bauch M., Mitchell A., Bellasio C., Green A., Bouyer D., Schnittger A., Sturrock C., Osborne C.P., Rolfe S., Mooney S., Fleming A.J. (2017) Cell density and airspace patterning in the leaf can be manipulated to increase leaf photosynthetic capacity. *The Plant Journal* 92, 981–994.

Lewis J.D, Phillips N.G:, Logan B.A., Smith R.A., Aranjuelo I., Clarke S., Offord C.A:, Frith A., Barbour M.M., Huxman T., Tissue D.T. (2015) Rising temperature may negate the stimulatory effect of rising CO_2 on growth and physiology of Wollemi pine (*Wollemia nobilis*). *Functional Plant Biology* 42, 836–850.

Li Y., Gao Y.X., Xu X.M., Shen Q.R., Guo S.W. (2009) Light-saturated photosynthetic rate in high-nitrogen rice (*Oryza sativa* L.) leaves is related

to chloroplastic CO_2 concentration. *Journal of Experimental Botany* 60, 2351–2360.

Li, Y., Ren, B., Yang, X., Xu, G., Shen, Q., Guo, S., 2012. Chloroplast downsizing under nitrate nutrition restrained mesophyll conductance and photosynthesis in rice (*Oryza sativa* L.) under drought conditions. Plant and Cell Physiology 53 (5), 892e900.

Li P., Feng Z.Z., Calatayud V., Yuan X.Y., Xu Y.S., Paoletti E. (2017) A meta-analysis on growth, physiological, and biochemical responses of woody species to ground-level ozone highlights the role of plant functional types. *Plant, Cell and Environment* 40, 2369–2380.

Lima Nieto M.C., Martins M.d.O., Ferreira-Silva S.L. and Gomes Silveira J.A. (2015) *Jatropha curcas* and *Ricinus communis* display contrasting photosynthetic mechanisms in response to environmental conditions. *Scientia Agricola* 72, 260–269.

Lloyd J., Syvertsen J., Kriedermann P., Farquhar G. (1992) Low conductances for CO_2 diffusion from stomata to the sites of carboxylation in leaves of woody species. *Plant, Cell and Environment* 15: 873–899.

Long S.P., Ainsworth E.A., Rogers A., Ort D.R. (2004) Rising atmosphere carbon dioxide: Plants FACE the future. *Annual Review of Plant Biology* 55, 591.

Loreto F., Harley P.C., Di Marco G., Sharkey T.D. (1992) Estimation of mesophyll conductance to CO_2 flux by three different methods. *Plant Physiology* 98, 1437–1443.

Loreto F., Di Marco G., Tricoli D., Sharkey T.D. (1994) Measurements of mesophyll conductance, photosynthetic electron transport and alternative electron sinks of field grown wheat leaves. *Photosynthesis Research* 41, 397–403.

Loreto F., Tsonev T., Centritto M. (2009) The impact of blue light on leaf mesophyll conductance. *Journal of Experimental Botany* 60, 2283–2290.

Loriaux S.D., Avenson T.J., Welles J.M., McDermitt D.K., Eckles R.D., Riensche B., Genty B. (2013) Closing in on maximum yield of chlorophyll fluorescence using a single multiphase flash of sub-saturating intensity. *Plant, Cell and Environment* 36, 1755–1770.

Lu Z., Lu J., Pan Y., Lu P., Li X., Cong. R. and Ren T. (2016) Anatomical variability of mesophyll conductance under potassium deficiency has a vital role in determining leaf photosynthesis. *Plant, Cell and Environment* 39, 2428–2439.

Lu Z., Xie K., Pan Y., Ren T., Lu J., Wang M., Shen Q., Guo S. (2019) Potassium mediates coordination of leaf photosynthesis and hydraulic conductance by modifications of leaf anatomy. *Plant, Cell and Environment* doi, 10.1111/pce.13553.

Marchi, S., Tognetti, R., Minnocci, A., Borghi, M., Sebastiani, L. (2008) Variation in mesophyll anatomy and photosynthetic capacity during leaf development in a deciduous mesophyte fruit tree (*Prunus persica*) and an evergreen sclerophyllous Mediterranean shrub (*Olea europaea). Trees* 22: 559–571.

Martins S.C.V., Galmés J., Molins A., DaMatta F.M. (2013) Improving the estimation of mesophyll conductance to CO_2: on the role of electron transport rate correction and respiration. *Journal of Experimental Botany* 64, 3285–3298.

Martins S.C.V, Galmés J., Cavatte P.C., Pereira L.F., Ventrella M.C., DaMatta F.M. (2014) Understanding the low photosynthetic rates of sun and shade coffee leaves: bridging the cap on the relative roles of hydraulic, diffusive and biochemical constraints to photosynthesis. *PLoS ONE* 9, e95571.

Maurel C., Verdoucq L., Luu D.-T., Santoni V. (2008) Plant aquaporins: membrane channels with multiple integrated functions. *Annual Review of Plant Biology* 59, 595–624.

McGrath J.M., Betzelberger A.M., Wang S.W., Shook E., Zhu X.G., Long S.P., Ainsworth E.A. (2015) An analysis of ozone damage to historical maize

and soybean yields in the United States. *Proceedings of the National Academy of Sciences USA* 112, 14390–14395.

Medeiros D.B., Martins S.C.V., Cavalcanti J.H.F., Daloso D.M., Martinoia R., Nunes-Nesi A., DaMatta F.M., Fernie A.R. and Araújo W.L. (2016) Enhanced photosynthesis and growth in *atquac1* knockout mutants are due to altered organic acid accumulation and an increase in both stomatal and mesophyll conductance. *Plant Physiology* 170, 86–101.

Melzer E., O'Leary M.H. (1987) Anapleurotic CO_2 fixation by phosphoenolpyruvate carboxylase in C_3 plants. Plant Physiology 84:58–60.

Meyer H. (1899) Zur Theorie der Alkoholnarkose. *Naunyn-Schmiedeberg's Archives of Pharmacology* 42, 109–118.

Meyer M., Seibt U., Griffiths H. (2008) To concentrate or ventilate? Carbon acquisition, isotope discrimination and physiological ecology of early land plant life. *Philosophic Transactions of the Royal Society Series B* 363, 2767–2778.

Miyazawa S.-I., Satomi S., Terashima I. (1998) Slow leaf development of evergreen broad-leaved tree species in Japanese warm temperate forests. *Annals of Botany* 82, 859–869.

Miyazawa S.-I., Terashima I. (2001) Slow development of leaf photosynthesis in an evergreen broad-leaved tree, *Castanopsis sieboldii*: relationships between leaf anatomical characteristics and photosynthetic rate. *Plant, Cell and Environment* 24, 279–291.

Miyazawa, S.I., Makino, A., Terashima, I. (2003) Changes in mesophyll anatomy and sink-source relationships during leaf development in *Quercus glauca*, an evergreen tree showing delayed leaf greening. Plant Cell Environ 26, 745–755.

Miyazawa S.-I., Yoshimura S., Shinzaki Y., Maeshima M., Miyake C. (2008) Deactivation of aquaporins decreases internal conductance to CO_2

diffusion in tobacco leaves grown under long-term drought. *Functional Plant Biology* 35, 553–564.

Mizokami Y., Noguhi K., Kojima M., Sakakibara H., Terashima I. (2015) Mesophyll conductance decreases in the wild type but not in an ABA-deficient mutant (*aba1*) of *Nicotiana plumbaginifolia* under drought conditions. *Plant, Cell and Environment* 38, 388–398.

Mizokami Y., Terashima I. (2016) Cross-point of water and carbon in the leaf - CO_2 diffusion conductance-. *The Ecological Society of Japan* 66, 477–487.

Mizokami Y., Noguchi K., Kojima M., Sakakibara H., Terashima I. (2019) Effects of instantaneous and growth CO_2 levels, and ABA on stomatal and mesophyll conductances. *Plant, Cell and Environment* 42, 1257–1269.

Momayyezi M., Guy R. (2017) Substantial role for carbonic anhydrase in latitudinal variation in mesophyll conductance of *Populus trichocarpa* Torr. & Gray. *Plant, Cell and Environmenr* 40, 138–149.

Monti A., Bezzi G., Venturi G. (2009) Internal conductance under different light conditions along the plant profile of Ethiopian mustard (*Brassica carinata* A. Brown.). *Journal of Experimental Botany* 60, 2341–2350.

Montpied P., Granier A., Dreyer E. (2009) Seasonal time-course of gradients of photosynthetic capacity and mesophyll conductance to CO_2 across a beech (*Fagus sylvatica* L.) canopy. *Journal of Experimental Botany* 60, 24072418.

Morales L.V., Coopman R.E., Rojas R., Escandón A.B., Flexas J., Galmés J., García-Plazaola J.I., Gago J., Cabrera H.M., Corcuera L.J. (2014) Acclimation of leaf cohorts expanded under light and water stresses: an adaptive mechanism of *Eucryphia cordifolia* to face changes in climatic conditions? *Tree Physiology* 34, 1305–1320.

Muir C.D., Hangarter R.P., Moyle L.C., Davis P.A. (2014) Morphological and anatomical determinants of mesophyll conductance in wild relatives of

tomato (*Solanum lycopersicon*, sect. *Lycopersicoides*; Solanaceae). *Plant, Cell and Environment* 37, 1415–1426.

Nadal M., Flexas J., Gulías J. (2018) Possible link between photosynthesis and leaf modulus of elasticity among vascular plants: a new player in leaf traits relationships? *Ecology Letters* 21, 1372–1379.

Nicotra A.B., Atkin O.K., Bonser S.P., Davidson A.M., Finnegan E.J., Mathesius U., Poot P., Purugganan M.D., Richards C.L., Valladares F. (2010) Plant phenotypic plasticity in a changing climate. *Trends in Plant Science* 15, 684–692.

Niinemets Ü., Reichstein M. (2003) Controls on the emission of plant volatiles through stomata: differential sensitivity of emission rates to stomatal closure explained. *Journal of Geophysical Research* 108, 1–17.

Niinemets Ü., Sack L. (2006) Structural determinants of leaf light-harvesting capacity and photosynthetic potentials. In: Lüttge U., Matyssek R., Canovas Ramos F.M. (eds.) *Progress in Botany*, Vol. 67, pp. 385–429. Springer, Berlin.

Niinemets Ü., Anten N.P.R. (2009) Packing the photosynthesis machinery: from leaf to canopy. In: Laisk A., Nedbal L., Govindjee (eds.) *Photosynthesis in Silico: Understanding Complexity from Molecules to Ecosystems*. Springer Verlag, Berlin, pp. 363–399.

Niinemets Ü., Díaz-Espejo A., Flexas J., Galmés J., Warren C.R. (2009) Role of mesophyll conductance in constraining potential photosynthetic productivity in the field. *Journal of Experimental Botany* 60, 2249–2270.

Niinemets, Ü., García-Plazaola, J.I., Tosens, T. (2012) Photosynthesis during leaf development and ageing. In: Flexas, J., Loreto, F., Medrano, H. (eds) *Terrestrial photosynthesis in a changing environment. The molecular, physiological and ecological bases of photosynthesis driving its response to the environmental changes*. Cambridge University Press, Cambridge, pp 357–376.

Niinemets Ü., Keenan T.F., Hallik L. (2015) A worldwide analysis of within-canopy variations in leaf structural, chemical and physiological traits across plant functional types. *New Phytologist* 205, 973–993.

Niklas K.J., Tiffney B.H., Knoll A.H. 1983. Patterns in vascular land plant diversification. *Nature* 303, 614–616.

Nitta I., Ohsawa M. (1997) Leaf dynamics and shoot phenology of eleven warm-temperate evergreen broad-leaved trees near their northern limit in central Japan. *Plant Ecology* 130, 71–88.

Nobel P.S. (1999) *Physicochemical and environmental plant physiology*, 4th edn. San Diego, CA: Academic Press.

Ogren W. (1984) Photorespiration: pathways, regulation, and modification. *Annual Review of Plant Physiology* 35, 415–442.

Oguchi R., Hikosaka K., Hirose T. (2005) Leaf anatomy as a constraint for photosynthetic acclimation: differential responses in leaf anatomy to increasing growth irradiance among three deciduous trees. *Plant, Cell and Environment* 28, 916–927.

Oksanen E., Riikonen J., Kaakinen S., Holopainen T., Vapaavuori E. (2005) Structural characteristics and chemical composition of birch (*Betula pendula*) leaves are modified by increasing CO_2 and ozone. *Global Change Biology* 11, 732–748.

O'Leary M.H. (1982) Phosphoenolpyruvate carboxylase: an enzymologist's view. *Annual Review of Plant Physiology* 33:297–315.

Olsovska K., Kovar M., Brestic M., Zivcak M., Slamka P., Shao H.B. (2016) Genotypically identifying wheat mesophyll conductance regulation under progressive drought stress. *Frontiers in Plant Science* 7, 1111.

Onoda Y., Wright I.J., Evans J.R., Hikosaka K., Kitajima K., Niinemets Ü., Poorter H., Tosens T., Westoby M. (2017) Physiological and structural tradeoffs underlying the leaf economics spectrum. *New Phytologist* 214, 1447–1463.

Ort D.R., Mechant S.S., Alric J., Barkan A., Blankenship R.E., Bock R., Croce R., Hanson M.R., Hibberd J.M., Long S.P., Moore T.A., Moroney J., Niyogi K.K., Parry M.A., Peralta-Yahya P.P., Prince R.C., Redding K.E., Spalding M.H., van Wijk K.J., Vermaas W.F., von Caemmerer S., Weber A.P., Yeates T.O., Yuan J.S., Zhu X.G. (2015) Redesigning photosynthesis to sustainably meet global food and bioenergy demand. *Proceedings of the National Academy of Sciences of the United States of America* 112, 8529–8536.

Otto B., Uehlein N., Sdorra S., Fischer M., Ayaz M., Belastegui-Macadam X. (2010) Aquaporin tetramer composition modifies the function of tobacco aquaporins. *Journal of Biological Chemistry* 285, 31253–31260.

Overton C.E. (1901) *Studien über die Narkose zugleich ein Beitrag zur allgemeinen Pharmakologie*. Fischer, Jena,

Paoletti E., Contran N., Bernasconi P., Gunthardt-Goerg M.S., Vollenweider P. (2009) Structural and physiological responses to ozone in Manna ash (*Fraxinus ornus* L.) leaves of seedlings and mature trees under controlled and ambient conditions. *Science of the Total Environment* 407, 1631–1643.

Peguero-Pina J.J., Flexas J., Galmés J., Niinemets Ü., Sancho-Knapik D., Barredo G., Villarroya D., Gil-Pelegrín E. (2012) Leaf anatomical properties in relation to differences in mesophyll conductance to CO_2 and photosynthesis in two related Mediterranean *Abies* species. *Plant, Cell and Environment* 35, 2121–2129.

Peguero-Pina J.J., Sisó S., Sancho-Knapik D., Díaz-Espejo A., Flexas J., Galmés J. and Gil-Pelegrín E. (2016) Leaf morphological and physiological adaptations of a deciduous oak (*Quercus faginea* Lam.) to the Mediterranean climate: a comparison with a closely related temperate species (*Quercus robur* L.). *Tree Physiology* 36, 287–299.

Peguero-Pina J.J., Sisó S., Flexas J., Galmés J., García-Nogales A., Niinemets Ü, Sancho-Knapik D., Saz M.Á., Gil-Pelegrín E. (2017a) Cell-level

anatomical characteristics explain high mesophyll conductance and photosynthetic capacity in sclerophyllous Mediterranean oaks. *New Phytologist* 214, 585–596.

Peguero-Pina J.J., Sisó S., Flexas J., Galmés J., Niinemets Ü., Sancho-Knapik D., Gil-Pelegrín E. (2017b) Coordinated modifications in mesophyll conductance, photosynthetic potentials and leaf nitrogen contribute to explain the large variation in foliage net assimilation rates across Quercus ilex provenances. *Tree Physiology* 37, 1084–1094.

Pérez-Martin A., Flexas J., Ribas-Carbó M., Bota J., Tomás M., Infante J.M., Díaz-Espejo A. (2009) Interactive effects of soil water deficit and air vapour pressure deficit on mesophyll conductance to CO_2 in *Vitis vinifera* and *Olea europaea*. *Journal of Experimental Botany* 60, 2391–2405.

Pérez-Martin A., Michelazzo C., Torres-Ruiz J.M., Flexas J., Fernandez J.E., Sebastiani L., Díaz-Espejo A. (2014) Regulation of photosynthesis and stomatal and mesophyll conductance under water stress and recovery in olive trees: correlation with gene expression of carbonic anhydrase and aquaporins. *Journal of Experimental Botany* 65, 3143–3156.

Piel C., Frak E., Le Roux X., Genty B. (2002) Effect of local irradiance on CO_2 transfer conductance of mesophyll in walnut. *Journal of Experimental Botany* 53, 2423–2430.

Pons T.L., Flexas J., von Caemmerer S., Evans J.R., Genty B., Ribas-Carbó M., Brugnoli E. (2009) Estimating mesophyll conductance to CO_2: methodology, potential errors, and recommendations. *Journal of Experimental Botany* 60, 2217–2234.

Poorter H., Niinemets Ü., Poorter L., Wright I.J., Villar R. (2009) Causes and consequences of variation in leaf mass per area (LMA): a meta-analysis. *New Phytologist* 182, 565–588.

Poorter, H., Niinemets, Ü., Ntagkas, N., Siebenkäs, A., Mäenpää, M., Matusbara, S., Pons T.L. (2019) A meta-analysis of plant responses to light intensity

for 70 traits ranging from molecules to whole plant performance. *New Phytologist*, doi: 10.1111/nph.15754.

Portsmuth A., Niinemets Ü. (2007) Structural and physiological plasticity in response to light and nutrients in five temperate deciduous woody species of contrasting shade tolerance. *Functional Ecology* 21, 61–77.

Possell M., Hewitt C.N. (2009) Gas exchange and photosynthetic performance of the tropical tree *Acacia nigrescens* when grown in different CO_2 concentrations. *Planta* 229, 837–846.

Price G.D., von Caemmerer S., Evans J.R., Yu J.W., Lloyd J., Oja V. (1994) Specific reduction of chloroplast carbonic-anhydrase activity by antisense RNA in transgenic tobacco plants has a minor effect on photosynthetic CO_2 assimilation. *Planta* 193, 331–340.

Qiu C., Ethier G., Pepin S., Dubé P., Desjardins Y., Grosselin A. (2017) Persistent negative temperature response of mesophyll conductance in red raspberry (*Rubis idaeus* L.) leaves under both high and low vapour pressure deficits: a role for abscisic acid? *Plant, Cell and Environment* 40, 1940–1959.

Quinn P., Williams W. (1985) Environmentally induced changes in chloroplast membranes and their effects on photosynthetic function. In: *Photosynthetic Mechanisms and the Environment (Eds J. Barber and N. Baker)*, pp 1–47. Elsevier, Amsterdam.

Raich J.W., Lambers H., Oliver D.J. (2014) Respiration in terrestrial ecosystems. In: Karl D.M., Schlesinger W.H. (eds.) *Biogeochemistry, Treatise on geochemistry* (Vol. 10). Amsterdam, the Netherlands: Elsevier, 613–649.

Rambal S. (2001) Productivity of Mediterranean-type ecosystems. In: Mooney H.A., Saugier B., Roy J. (eds,) *Terrestrial global productivity: past, present, and future*. SanDiego, CA, USA: Academic Press, Inc, 315–344.

Raven J.A. (1997) CO_2-concentrating mechanisms: a direct role for thylakoid lumen acidification? *Plant, Cell and Environment* 20, 147–154.

Ren T., Weraduwage S.M., Sharkey T.D. (2019) Prospects for enhancing leaf photosynthetic capacity by manipulating mesophyll cell morphology. *Journal of Experimental Botany* 70, 1153–1165.

Renzaglia K. S., McFarland K. D., Smith D. K. (1997) Anatomy and ultrastructure of the sporophyte of *Takakia ceratophylla* (Bryophyta). *American Journal of Botany* 84, 1337–1350.

Resco V., Ewers B.E., Sun W., Huxman T.E., Weltzin J.F. and Williams D.G. (2008) Drought-induced hydraulic limitations constrain leaf gas exchange recovery after precipitation pulses in C_3 woody legume, *Prosopis velutina*. *New Phytologist* 181, 672–682.

Robertson E.J., Leech R.M. (1995) Significant changes in cell and chloroplast development in young wheat leaves (*Triticum aestivum* cv Hereward) grown in elevated CO_2. *Plant Physiology* 107: 63–71.

Ruiz-Vera U.M., De Souza A.P., Long S.P., Ort D.R. (2017) The role of sink strength and nitrogen availability in the down-regulation of photosynthetic capacity in field-grown *Nicotiana tabacum* L. at elevated CO_2 concentration. *Frontiers in Plant Science* 8, 998.

Scafaro A.P., von Caemmerer S., Evans J.R., Atwell B.J. (2011) Temperature response of mesophyll conductance in cultivated and wild *Oryza* species with contrasting mesophyll cell wall thickness. *Plant, Cell and Environment* 34, 1999–2008.

Sade N., Shatil-Cohen A., Attia Z., Maurel C., Boursiac Y., Kelly G., Granot D., Yaaran A., Lerner S., Moshelion M. (2014) The role of plasma membrane aquaporins in regulating the bundle sheath-mesophyll continuum and leaf hydraulics. *Plant Physiology* 166, 1609–1620.

Sáez P.L., Bravo L.A., Cavieres L.A., Vallejos V., Sanhueza C., Font-Carrascosa M., Gil-Pelegrín E., Peguero-Pina J.J., Galmés J. (2017) Photosynthetic limitations in two Antarctic vascular plants: importance of leaf anatomical traits and Rubisco kinetic parameters. *Journal of Experimental Botany* 68, 2871–2883.

Sáez P.L., Cavieres L.A., Galmés J., Gil-Pelegrín E., Peguero-Pina J.J., Sancho-Knapik D., Vivas M., Sanhueza C., Ramírez C.F., Rivera B.K., Corcuera L.J., Bravo L.A. (2018a) In situ warming in the Antarctic: effects on growth and photosynthesis in Antarctic vascular plants. New Phytologist 218: 1406–1418.

Sáez P.L., Galmés J., Ramírez C.F., Poblete L., Rivera B.K., Cavieres L.A., Clemente-Moreno M.J., Flexas J., Bravo L. (2018b) Mesophyll conductance to CO_2 is the most significant limitation to photosynthesis at different temperatures and water availabilities in Antarctic vascular plants. *Environmental and Experimental Botany* 156, 279–287.

Sage R.F., Kubien D.S. (2007) The temperature response of C_3 and C_4 photosynthesis. *Plant, Cell and Environment* 30, 1086–1106.

Saxe H., Ellsworth D.S., Heath J. (1998) Tree and forest functioning in an enriched CO_2 atmosphere. *New Phytologist* 139, 395–436.

Schuettpelz E., Pryer K.M. (2009) Evidence for a Cenozoic radiation of ferns in an angiosperm-dominated canopy. *Proceedings of the National Academy of Sciences of the United States of America* 106, 11200–11205.

Scaffaro A.P., von Caemmerer S., Evans J.R., Atwell B.J. (2011) Temperature response of mesophyll conductance in cultivated and wild *Oryza* species with contrasting mesophyll cell wall thickness. *Plant, Cell and Environment* 34, 1999–2008.

Sharkey TD, Loreto F, Delwiche C (1991) High carbon dioxide and sun/shade effects on isoprene emission from oak and aspen tree leaves. Plant Cell Environ 14:333–338

Sharkey T.D., Bernacchi C.J., Farquhar G.D., Singsaas E.L. (2007) Fitting photosynthetic carbon dioxide response curves for C_3 leaves. *Plant, Cell and Environment* 30, 1035–1040.

Shi Z., Haworth M., Feng Q., Cheng R., Centritto M. (2015) Growth habit and leaf economics determine gas exchange responses to high elevation in an

evergreen tree, a deciduous shrub and a herbaceous annual. *Annals of Botany Plants* 7, plv115.

Shrestha A., Buckley T.N., Lockhart E.L., Barbour M.M. (2018) The response of mesophyll conductance to short- and long-term environmental conditions in chickpea genotypes. *Annals of Botany Plants* 11, ply073.

Shrestha A., Dong X., Barbour M.M. (2019) The temperature response of mesophyll conductance, and its component conductances, varies between species and genotypes. *Photosynthesis Research* doi: 10.1007/s11120-019-00622-z.

Silim S.N., Ryan N., Kubien D.S. (2010) Temperature responses of photosynthesis and respiration in *Populus balsamifera* L.: acclimation versus adaptation. *Photosynthesis Research* 104: 19–30.

Silva E.N., Silveira J.A.G., Ribeiro R.V., Vieira S.A. (2015) Photoprotective function of energy dissipation by thermal processes and photorespiratory mechanisms in *Jatropha curcas* plants during different intensities of drought and after recovery. *Environmental and Experimental Botany* 110, 36–45.

Singh S.K., Badgujar G., Reddy V.R., Fleisher D.H., Bunce J.A. (2013) Carbon dioxide diffusion across stomata and mesophyll and photo-biochemical processes as affected by growth CO_2 and phosphorus nutrition in cotton. *Journal of Plant Physiology* 170, 801–813.

Singh S.K., Reddy V.R. (2016) Method of mesophyll conductance estimation: its impact on key biochemical parameters and photosynthetic limitations in phosphorus-stressed soybean across CO_2. *Physiologia Plantarum* 157, 234–254.

Singh S.K., Reddy V.R. (2018) Co-regulation of photosynthetic processes under potassium deficiency across CO_2 levels in soybean: mechanisms of limitations and adaptations. *Photosynthesis Research* 137, 183–200.

Singsaas E., Ort D., DeLucia E. (2004) Elevated CO_2 effects on mesophyll conductance and its consequences for interpreting photosynthetic physiology. *Plant, Cell and Environment* 27, 41–50.

Singsaas E.L., Ort D.R., De Lucia E.H. (2003) Elevated CO_2 effects on mesophyll conductance and its consequences for interpreting photosynthetic physiology. *Plant and Cell Environment* 27, 41–50.

Soolanayakanahally R.Y., Guy R.D., Silim S.N., Drewes E.C., Schroeder W.R. (2009) Enhanced assimilation rate and water use efficiency with latitude through increased photosynthetic capacity and internal conductance in balsam poplar (*Populus balsamifera* L.). *Plant, Cell and Environment* 32, 1821–1832.

Syversten J.P., Lloyd J., McConchie C., Kriedemann P.E., Farquhar G.D. (1995) On the relationship between leaf anatomy and CO_2 diffusion through the mesophyll of hypostomatous leaves. *Plant, Cell and Environment* 18, 149–157.

Tazoe Y., von Caemmerer S., Badger M.R., Evans J.R. (2009) Light and CO_2 do not affect the mesophyll conductance to CO_2 diffusion in wheat leaves. *Journal of Experimental Botany* 60, 2291–2301.

Tazoe Y., von Caemmerer S., Estavillo G.M., Evans J.R. (2011) Using tunable diode laser spectroscopy to measure carbon isotope discrimination and mesophyll conductance to CO_2 diffusion dynamically at different CO_2 concentrations. *Plant, Cell and Environment* 34, 580–591.

Teng, N., Wang, J., Chen, T., Wu, X., Wang, Y. and Lin, J. (2006) Elevated CO_2 induces physiological, biochemical and structural changes in leaves of *Arabidopsis thaliana*. *New Phytologist* 172: 92–103.

Terashima I., Miyazawa S.I., Hanba Y.T. (2001) Why are sun leaves thicker than shade leaves? Consideration based on analyses of CO_2 diffusion in the leaf. *Journal of Plant Research* 114, 93–105.

Terashima I., Ono K. (2002) Effects of $HgCl_2$ on CO_2 dependence of leaf photosynthesis: evidence indicating involvement of aquaporins in CO_2 diffusion across the plasma membrane. Plant and Cell Physiology 43:70–78.

Terashima I., Hanba Y.T., Tazoe Y., Vyas P., Yano S. (2006) Irradiance and phenotype: comparative ecodevelopment of sun and shade leaves in relation to photosynthetic CO_2 function. *Journal of Experimental Botany* 57, 343–354.

Terashima I., Hanba Y.T., Tholen D., Niinemets Ü. (2011) Leaf functional anatomy in relation to photosynthesis. *Plant Physiology* 155, 108–116.

Théroux-Rancourt G., Éthier G., Pepin S. (2014) Threshold response of mesophyll CO_2 conductance to leaf hydraulics in highly transpiring hybrid poplar clones exposed to soil drying. *Journal of Experimental Botany* 65, 741–753.

Théroux-Rancourt G., Éthier G., Pepin S. (2015) Greater efficiency of water use in poplar clones having a delayed response of mesophyll conductance to drought. *Tree Physiology* 35, 172–184.

Théroux-Rancourt G., Earles J.M., Gilbert M.E., Zwieniecki M.A:, Boyce K., McElrone A.J., Brodersen C.R. (2017) The bias of a two dimensional view: comparing two dimensional and three-dimensional mesophyll surface area estimates using noninvasive imaging. *New Phytologist* 215, 1609–1622.

Tholen D., Boom C., Noguchi K., Ueda S., Katase T., Terashima I. (2008) The chloroplast avoidance response decreases internal conductance to CO_2 diffusion in *Arabidopsis thaliana* leaves. *Plant, Cell and Environment* 31, 1688–1700.

Tholen D., Zhu X.-G. (2011) The mechanistic basis of internal conductance: a theoretical analysis of mesophyll cell photosynthesis and CO_2 diffusion. *Plant Physiology* 156, 90–105.

Tholen D., Éthier G., Genty B., Pepin S., Zhu X.-G. (2012) Variable mesophyll conductance revisited: theoretical background and experimental implications. *Plant, Cell and Environment* 35, 2087–2103.

Tomàs M., Flexas J., Copolovici L., Galmés J., Hallik L., Medrano H., Ribas-Carbó M., Tosens T., Vislap V., Niinemets Ü. (2013) Importance of leaf anatomy in determining mesophyll diffusion conductance to CO_2 across species: quantitative limitations and scaling up by models. *Journal of Experimental Botany* 64, 2269–2281.

Tomàs M., Medrano H., Brugnoli E., Escalona J.M., Martorell S., Pou A., Ribas-Carbó M., Flexas J. (2014) Variability of mesophyll conductance in grapevine cultivars under water stress conditions in relation to leaf anatomy and water use efficiency. *Australian Journal of Grape and Wine Research* 20, 272–280.

Tosens T., Niinemets Ü., Westoby M., Wright I.J. (2012a) Anatomical basis of variation in mesophyll resistance in eastern Australian sclerophylls: news of a long and winding path. *Journal of Experimental Botany* 63, 5105–5119.

Tosens T., Niinemets Ü., Vislap V., Eichelmann H., Castro-Díez P. (2012b) Developmental changes in mesophyll diffusion conductance and photosynthetic capacity under different light and water availabilities in *Populus tremula*: how structure constrains function. *Plant, Cell and Environment* 35, 839–856.

Tosens T., Nishida K., Gago J., Coopman R.E., Cabrera H.M., Carriquí M., Laanisto L., Morales L., Nadal M., Rojas R., Talts E., Tomas M., Hanba Y., Niinemets Ü., Flexas J. (2016) The photosynthetic capacity in 35 ferns and fern allies: mesophyll CO_2 diffusion as a key trait. *New Phytologist* 209, 1576–1590.

Tosens T., Laanisto L. (2018) Mesophyll conductance and accurate photosynthetic carbon gain calculations. *Journal of Experimental Botany* 69, 5315-5318.

Tremmel I., Kirchhoff H., Weis E., Farquhar G.D. (2003) Dependence of plastoquinol diffusion on the shape, size, and density of integral thylakoid proteins. *Biochimica et Biophysica Acta* 1607, 97–109.

Trojan A., Gabrys H. (1996) Distribution in *Arabidopsis thaliana* (L.) depends on light conditions during growth. *Plant Physiology* 111, 419–425.

Ubierna N., Cernusak L.A., Holloway-Phillips M., Busch F.A., Cousins A.B., Farquhar G.D. (2019) Critical review: incorporating the arrangement of mitochondria and chloroplasts into models of photosynthesis and carbon isotope discrimination. *Photosynthesis Research* doi: 10.1007/s111120-019-00635-8.

Uehlein N., Otto B., Hanson D.T., Fischer M., McDowell N., Kaldenhoff R. (2008) Function of *Nicotiana tabacum* aquaporins as chloroplast gas pores challenges the concept of membrane CO_2 permeability. *Plant Cell* 20, 648–657.

Uprety D.C., Dwivedi N., Mohan R., Paswan G. (2001) Effect of elevated CO_2 concentration on leaf structure of *Brassica juncea* under water stress. *Biologia Plantarum* 44, 149–152.

Valentini R., Epron D., Angelis P., Matteucci G., Dreyer E. (1995) In situ estimation of net CO_2 assimilation, photosynthetic electron flow and photorespiration in Turkey oak (*Q. cerris* L.) leaves: diurnal cycles under different levels of water supply. *Plant, Cell and Environment* 18, 631–640.

Valladares F., Wright S.J., Lasso E., Kitajima K., Pearcy R.W. (2000) Plastic phenotypic response to light of 16 congeneric shrubs from a Panamanian rainforest. *Ecology* 91, 1925–1936.

Valladares F., Hernández L.G., Dobarro I., García-Pérez C., Sanz R., Pugnaire F.I. (2003) The ratio of leaf to total photosynthetic area influences shade survival and plastic response to light of green-stemmed leguminous shrub seedlings. *Annals of Botany* 91, 577–584.

Varone L., Ribas-Carbó M., Cardona C., Gallé A., Medrano H., Gratani L. and Flexas J. (2012) Stomatal and non-stomatal limitations to photosynthesis in seedlings and saplings of Mediterranean species pre-conditioned and aged nurseries: Different response to water stress. *Environmental and Experimental Botany* 75, 235–247.

Velikova V., Tsonev T., Pinelli P., Alessio G.A., Loreto F. (2005) Localized ozone fumigation system for studying ozone effects on photosynthesis, respiration, electron transport rate and isoprene emission in field-grown Mediterranean oak species. *Tree Physiology* 25: 1523–1532.

Velikova V., Vitale M., Catoni R:, Gratani L. (2015) Physiological differences of five Holm oak (*Quecus ilex* L.) ecotypes growing under common growth conditions were related to native local climate. *Plant Species Biology* 31, 196–210.

Velikova V., Tsnoev T., Barta C., Centritto M., Koleva D., Stefanova M., Busheva M., Loreto F. (2009) BVOC emissions, photosynthetic characteristics and changes in chloroplast ultrastructure of *Platanus orientalis* L. exposed to elevated CO_2 and high temperature. *Environmental Pollution* 157, 2629–2637.

Veromann-Jürgenson L.-L., Tosens T., Laanisto L. and Niinemets Ü. (2017) Extremely thick cell walls and low mesophyll conductance: welcome to the world of ancient living! *Journal of Experimental Botany* 68, 1639–1653.

Vrabl D., Vaskova M., Hronkova M., Flexas J., Santrucek J. (2009) Mesophyll conductance to CO_2 transport estimated by two independent methods: effect of variable CO_2 concentration and abscisic acid. *Journal of Experimental Botany* 60, 2315–2323.

Waite M., Sack L. (2010) How does moss photosynthesis relate to leaf and canopy structure? Trait relationships for 10 Hawaiian species of contrasting light habitats. *New Phytologist* 185, 156–172.

Wang Z., Liu X., Bader M.Y., Feng D., Bao W. (2017) The ‘plant economic spectrum’ in bryophytes, a comparative study in subalpine forest. *American Journal of Botany* 104, 261–270.

Warren C.R., Dreyer E. (2006) Temperature responses of photosynthesis and internal conductance to CO_2: results from two independent approaches. *Journal of Experimental Botany* 57, 3057–3067.

Warren C.R., Löw M., Matyssek R., Tausz M. (2007) Internal conductance to CO_2 transfer of adult *Fagus sylvatica*: variation between sun and shade leaves and due to free-air ozone fumigation. *Environmental and Experimental Botany* 59, 130–138.

Warren C.R., Dreyer E. (2006) Temperature response of photosynthesis and internal conductance to CO_2: results from two independent approaches. *Journal of Experimental Botany* 57, 3057–3067.

Warren C.R. (2008) Soil water deficits decrease the internal conductance to CO_2 transfer but atmospheric water deficits do not. *Plant, Cell and Environment* 39, 327–334.

Warren C.R., Aranda I., Cano F.J. (2011) Responses to water stress of gas exchange and metabolites in *Eucalyptus* and *Acacia* spp. *Plant, Cell and Environment* 34, 1609–1629.

Watanabe M., Kamimaki Y., Mori M., Okabe S., Arakawa I., Kinose Y., Nakaba S., Izuta T. (2018) Mesophyll conductance to CO_2 in leaves of Siebold’s beech (*Fagus crenata*) seedlings under elevated ozone. *Journal of Plant Research* 131, 907–914.

Way D.A., Yamori W. (2014) Thermal acclimation of photosynthesis: on the importance of adjusting our definitions and accounting for thermal acclimation of respiration. *Photosynthesis Research* 119, 89–100.

Weis E. (1981) The temperature sensitivity of dark-inactivation and light-activation of the ribulose-1,5-bisphosphate carboxylase in spinach chloroplasts. *FEBS Letters* 129, 197–200.

Weissbach A., Horecker B.L., Hurwitz J. (1956) Enzymatic formation of phosphoglyceric acid from ribulose diphosphate and carbon dioxide. *Journal of Biological Chemistry* 218, 795–810.

Weraduwage S.M., Kim S.-J., Renna L., Anozie F.C., Sharkey T.D., Brandizzi F. (2016) Pectin methylesterification impacts the relationship between photosynthesis and plant growth. *Plant Physiology* 171, 833–848.

Weraduwage S.M., Campos M.L., Yoshida Y., Major I.T., Kim Y.-S., Kim S.-J., Renna L., Anozie F.C. (2018) Molecular mechanisms affecting cell wall properties and leaf architecture. In *The Leaf: A platform for performing photosynthesis, Advances in Photosynthesis and Respiration (including bioenergy and related processes)* (eds Adams W.W. and Terashima I.), Vol. 44 pp. 209-253. Springer, Cham.

Williams T.G., Flanagan L.B., Coleman J.R. (1996) Photosynthetic gas exchange and discrimination against $^{13}CO_2$ and $C^{18}O^{16}O$ in tobacco plants modified by an antisense construct to have low chloroplastic carbonic anhydrase. *Plant Physiology*, 112, 319–326.

Woodward F. I. (1998) Do plants really need stomata? *Journal of Experimental Botany* 49, 471–480.

Wright I.J., Reich P.B., Westoby M., Ackerly D.D., Baruch Z., Bongers F., Cavender-Bares J., Chapin T., Cornelissen J.H.C., Diemer M., Flexas J., Garnier E., Groom P.K., Gulias J., Hikosaka K., Lamont B.B., Lee T., Lee W., Lusk C., Midgley J.J., Navas M.L., Niinemets Ü., Oleksyn J., Osada N., Poorter H., Poot P., Prior L., Pyankov V.I., Roumet C., Thomas S.C., Tjoelker M.G., Veneklaas E.J., Villar R. (2004) The worldwide leaf economics spectrum. *Nature* 428: 821–827.

Xiao Y., Zhu X.-G. (2017) Components of mesophyll resistance and their environmental responses: A theoretical modelling analysis. *Plant, Cell and Environment* 40, 2729–2742.

Xiong D., Liu X., Liu L., Douthe C., Li Y., Peng S., Huang J. (2015) Rapid responses of mesophyll conductance to changes of CO_2 concentration,

temperature and irradiance are affected by N supplements in rice. *Plant, Cell and Environment* 12, 2541–2550.

Xiong D., Flexas J., Yu T., Peng S., Huang J. (2017a) Leaf anatomy mediates coordination of leaf hydraulic conductance and mesophyll conductance of CO_2 in *Oryza*. *New Phytologist* 213, 572–583.

Xiong D., Huang J., Peng S., Li Y. (2017b) A few enlarged chloroplasts are less efficient in photosynthesis than a large population of small chloroplasts in *Arabidopsis thaliana*. *Scientific Reports* 7, 5782.

Xiong D., Douthe C., Flexas J. (2018) Differential coordination of stomatal conductance, mesophyll conductance in response to changing light across species. *Plant, Cell and Environment* 41, 436–450.

Xu Z., Zhou G. (2011) Responses of photosynthetic capacity to soil moisture gradient in perennial rhizome grass and perennial bunchgrass. *BMC Plant Biology* 11, 21.

Xu G., Singh S.K., Reddy V.R., Barnaby J.Y., Sicher R.C., Li T. (2016) Soybean grown under elevated CO_2 benefits more under low temperature than high temperature stress: Varying response of photosynthetic limitations, leaf metabolites, growth, and seed yield. *Journal of Plant Physiology* 205, 20–32.

Xu Y., Feng Z., Shang B., Dai L., Uddling J., Tarvainen L. (2019) Mesophyll conductance limitation of photosynthesis in poplar under elevated ozone. *Science of the Total Environment* 657, 136–145.

Xue W., Otieno D., Ko J., Werner C., Tenhunen J. (2016) Conditional variations in temperature response of photosynthesis, mesophyll and stomatal control of water used in rice and winter wheat. *Field and Crop Research* 199, 77–88.

Yamori W., Noguchi K., Hanba Y.T., Terashima I. (2006) Effects of internal conductance on the temperature dependence of the photosynthetic rate in

spinach leaves from contrasting growth temperatures. *Plant and Cell Physiology* 47, 1069–1080.

Yamori W., Hikosaka K., Way D.A. (2014) Temperature response of photosynthesis in C_3, C_4 and CAM plants: temperature acclimation and temperature adaptation. *Photosynthesis Research* 119, 101–117.

Yang Z.H., Huang W., Yang Q.Y., Chang W., Zhang S.B. (2018) Anatomical and diffusional determinants inside leaves explain the difference in photosynthetic capacity between *Cypripedium* and *Paphiopedilum*, Orchidaceae. *Photosynthesis Research* 136, 315–328.

Yaneff A., Vitali V., Amodeo G. (2015) *PIP1* aquaporins: intrinsigc water channels or *PIP2* aquaporin modulators? *FEBS Letters* 589, 3508–3515.

Yin X., Struik P.C., Romero P., Harbinson J., Evers J.B., Van Der Puten P.E.L., Vos J. (2009) Using combined measurements of gas exchange and chlorophyll fluorescence to estimate parameters of a biochemical C_3 photosynthesis model: a critical appraisal and a new integrated approach applied to leaves in a wheat (*Triticum aestivum*) canopy. *Plant, Cell and Environment* 32, 448–464.

Yin X., Struik P.C. (2017) Simple generalization of a mesophyll resistance model for various intracellular arrangements of chloroplasts and mitochondria in C_3 leaves. *Photosynthesis Research* 132, 211–220.

Zait Y., Shtein I., Schwartz A. (2018) Long-term acclimation to drought, salinity and temperature in the thermophilic tree *Ziziphus spina-christi*: revealing different tradeoffs between mesophyll and stomatal conductance. Tree Physiology, doi: 10.1093/treephys/tpy133.

Zhou S.X., Medlyn B.E., Prentice I.C. (2016) Long-term water stress leads to acclimation of drought sensitivity of photosynthetic capacity in xeric but not riparian *Eucalyptus* species. *Annals of Botany* 117:133–144.

Zhu C., Ziska L., Zhu J., Zeng Q., Xie Z., Tang H., Jia X., Hasegawa T. (2012) The temporal and species dynamics of photosynthetic acclimation in flag

leaves of rice (*Oryza sativa*) and wheat (*Triticum aestivum*) under elevated carbon dioxide. *Physiologia Plantarum* 145, 395–405.